

M. Hanif Chaudhry

# Applied Hydraulic Transients

*Third Edition*

# Applied Hydraulic Transients



M. Hanif Chaudhry

# Applied Hydraulic Transients

Third Edition



Springer

M. Hanif Chaudhry  
College of Engineering and Computing  
University of South Carolina  
Columbia, SC, USA

ISBN 978-1-4614-8537-7      ISBN 978-1-4614-8538-4 (eBook)  
DOI 10.1007/978-1-4614-8538-4  
Springer New York Heidelberg Dordrecht London

Library of Congress Control Number: 2013947167

© Author 1979, 1987, 2014

This work is subject to copyright. All rights are reserved by the Publisher, whether the whole or part of the material is concerned, specifically the rights of translation, reprinting, reuse of illustrations, recitation, broadcasting, reproduction on microfilms or in any other physical way, and transmission or information storage and retrieval, electronic adaptation, computer software, or by similar or dissimilar methodology now known or hereafter developed. Exempted from this legal reservation are brief excerpts in connection with reviews or scholarly analysis or material supplied specifically for the purpose of being entered and executed on a computer system, for exclusive use by the purchaser of the work. Duplication of this publication or parts thereof is permitted only under the provisions of the Copyright Law of the Publisher's location, in its current version, and permission for use must always be obtained from Springer. Permissions for use may be obtained through RightsLink at the Copyright Clearance Center. Violations are liable to prosecution under the respective Copyright Law.

The use of general descriptive names, registered names, trademarks, service marks, etc. in this publication does not imply, even in the absence of a specific statement, that such names are exempt from the relevant protective laws and regulations and therefore free for general use.

While the advice and information in this book are believed to be true and accurate at the date of publication, neither the authors nor the editors nor the publisher can accept any legal responsibility for any errors or omissions that may be made. The publisher makes no warranty, express or implied, with respect to the material contained herein.

Printed on acid-free paper

Springer is part of Springer Science+Business Media ([www.springer.com](http://www.springer.com))

**To Shamim**



---

## Preface

*Applied Hydraulic Transients* covers transient flow in closed conduits and in open channels in a systematic and comprehensive manner from introduction to advanced level, with an emphasis on the presentation of efficient and robust computational procedures for analysis and simulation. These procedures, based on modern numerical methods, are suitable for machine computations, provide more accurate results as compared to the available traditional methods and allow the analysis of large and complex systems. The field of application is very broad and diverse and covers systems, such as hydroelectric power plants, pumped storage schemes, water-supply systems, oil pipelines, cooling-water and industrial piping systems. The book is suitable as a reference for practicing engineers and researchers and as a text for senior-level undergraduate and graduate students.

Because of diverse nature, the material in each chapter is presented more or less as stand-alone. Practical applications are emphasized throughout by including case studies of real-life projects, problems of applied nature and photographs and design criteria. Design charts and empirical formulas are presented in the appendix for approximate analyses and for comparing different alternatives for feasibility studies and preliminary design and for the selection of parameters for detailed analyses. Solved examples and sample computer programs are included to facilitate learning. SI units are used throughout. However, equivalent values of empirical constant in the Customary English units are provided which should allow the use of these units without much difficulty.

The general sequence of presentation in this third edition is similar to that in the earlier editions. However, revisions are made throughout for clarity and the references are updated. A new chapter on leak and partial blockage detection is added. In each chapter, a chapter-opener photograph is included as an illustrative introduction to the chapter. In Chapter 1, the historical background is updated and a section on wave reflection and transmission is added. A new section introduces the

inclusion of unsteady friction in the governing equations in Chapter 2 and the simulation of unsteady friction and the application of higher-order numerical methods are presented in Chapter 3. Coverage of the modeling of pump turbines is expanded in Chapter 5. A new section in Chapter 8 outlines the determination of the functional significance of stenosis in cardiovascular systems. The material in Chapters 10, 11, and 13 is revised and a new Chapter 12 discusses the detection of leaks and partial blockages in pipelines. Design charts and other data are presented in Appendix A and sample computer programs in FORTRAN along with sample input and output data are included in Appendices B through E.

I have used Chapters 1 through 5 and 10 as a textbook for a three-credit graduate course on hydraulic transients at Old Dominion University, Washington State University and University of South Carolina. Different chapters or parts thereof may be used for instructional material for advanced level, specialized courses and workshops.

Thanks are extended to British Columbia Hydro and Power Authority and California Department of Water Resources for data and prototype test results on their projects and to my former colleagues, R. E. Johnson for the instrumentation for the prototype tests and R. M. Rockwell and J. Gurney for [Figs. 5-11](#) and [5-29](#), and G. Vandenburg for [Fig. 10-4](#). Dr. Sam Martin generously provided technical advice, photographs, and figures. Assistance provided by my former graduate student, Dr. Elkholy, for the preparation of the manuscript, by Dr. Mohapatra for proofreading the final draft, and by Rebecca Wessinger for the preparation of the figures for inclusion in the manuscript is thankfully acknowledged. Several individuals from all over the globe were very kind in providing photographs and other material; these are acknowledged throughout the book. I am thankful to my family, especially our grandchildren, Aryaan, Amira, and Rohan, for many hours that should have been spent with them but were required by the preparation of this edition.

Columbia, SC, USA

M. Hanif Chaudhry

---

# Contents

|  |    |
|--|----|
| <b>1 BASIC CONCEPTS .....</b>                                | 1  |
| 1-1 Introduction .....                                       | 2  |
| 1-2 Terminology .....  | 2  |
| 1-3 Historical Background .....                              | 3  |
| 1-4 Basic Waterhammer Equations .....                        | 8  |
| 1-5 Wave Propagation .....                                   | 11 |
| 1-6 Wave Reflection and Transmission .....                   | 15 |
| 1-7 Transient Flow Analysis .....                            | 19 |
| 1-8 Causes of Transients .....                               | 19 |
| 1-9 System Design and Operation .....                        | 20 |
| 1-10 Accidents and Incidents .....                           | 20 |
| 1-11 Summary .....   | 26 |
| Problems .....   | 27 |
| References .....   | 29 |
| <b>2 TRANSIENT-FLOW EQUATIONS .....</b>                      | 35 |
| 2-1 Introduction .....                                       | 36 |
| 2-2 Reynolds Transport Theorem .....                         | 36 |
| 2-3 Continuity Equation .....                                | 39 |
| 2-4 Momentum Equation .....                                  | 43 |
| 2-5 General Remarks .....                                    | 45 |
| 2-6 Wave Velocity .....                                      | 49 |
| 2-7 Solution of Governing Equations .....                    | 54 |
| 2-8 Unsteady Friction .....                                  | 55 |
| 2-9 Summary .....  | 59 |
| Problems .....   | 59 |
| References .....   | 60 |
| <b>3 CHARACTERISTICS AND FINITE-DIFFERENCE METHODS .....</b> | 65 |
| 3-1 Introduction .....                                       | 66 |

|          |   |            |
|----------|---|------------|
| 3-2      | Characteristic Equations . . . . .                            | 66         |
| 3-3      | Boundary Conditions . . . . .                                 | 73         |
| 3-4      | Convergence and Stability . . . . .                           | 82         |
| 3-5      | Method of Specified Intervals . . . . .                       | 86         |
| 3-6      | Computational Time Interval . . . . .                         | 88         |
| 3-7      | Unsteady Friction . . . . .                                   | 88         |
| 3-8      | Explicit Finite-Difference Method . . . . .                   | 92         |
| 3-9      | General Remarks . . . . .                                     | 95         |
| 3-10     | Implicit Finite-Difference Method . . . . .                   | 98         |
| 3-11     | Comparison of Numerical Methods . . . . .                     | 100        |
| 3-12     | Analysis Procedure . . . . .                                  | 102        |
| 3-13     | Case Study . . . . .  | 104        |
| 3-14     | Summary . . . . .   | 108        |
|          | Problems . . . . .  | 109        |
|          | References . . . . .  | 110        |
| <b>4</b> | <b>TRANSIENTS IN PUMPING SYSTEMS . . . . .</b>                | <b>115</b> |
| 4-1      | Introduction . . . . .  | 116        |
| 4-2      | Pump Operations . . . . .                                     | 116        |
| 4-3      | Pump Characteristics . . . . .                                | 117        |
| 4-4      | Power Failure . . . . .                                       | 122        |
| 4-5      | Complex Systems . . . . .                                     | 133        |
| 4-6      | Pump Start-Up . . . . .                                       | 141        |
| 4-7      | Design Criteria . . . . .                                     | 142        |
| 4-8      | Case Study . . . . .  | 143        |
| 4-9      | Summary . . . . .   | 148        |
|          | Problems . . . . .  | 148        |
|          | References . . . . .  | 150        |
| <b>5</b> | <b>TRANSIENTS IN HYDROELECTRIC<br/>POWER PLANTS . . . . .</b> | <b>155</b> |
| 5-1      | Introduction . . . . .  | 156        |
| 5-2      | Hydroelectric Power Plant . . . . .                           | 156        |
| 5-3      | Conduit System . . . . .                                      | 158        |
| 5-4      | Hydraulic Turbine . . . . .                                   | 159        |
| 5-5      | Hydraulic Turbine Governor . . . . .                          | 166        |
| 5-6      | Mathematical Model . . . . .                                  | 175        |
| 5-7      | Design Criteria . . . . .                                     | 182        |
| 5-8      | Governing Stability . . . . .                                 | 186        |
| 5-9      | Stability Analysis . . . . .                                  | 192        |
| 5-10     | Pumped-Storage Projects . . . . .                             | 201        |
| 5-11     | Pump Turbine . . . . .  | 202        |
| 5-12     | Case Study . . . . .  | 207        |
| 5-13     | Summary . . . . .   | 214        |
|          | Problems . . . . .  | 214        |
|          | References . . . . .  | 216        |

|   |     |
|---|-----|
| <b>6 TRANSIENTS IN COOLING-WATER SYSTEMS . . . . .</b>    | 221 |
| 6-1 Introduction . . . . .                                | 222 |
| 6-2 Cooling-Water Systems . . . . .                       | 222 |
| 6-3 Causes of Transients . . . . .                        | 225 |
| 6-4 Analysis Procedures . . . . .                         | 227 |
| 6-5 Boundary Conditions . . . . .                         | 230 |
| 6-6 Summary . . . . .                                     | 234 |
| Problems . . . . .  | 234 |
| References . . . . .                                      | 234 |
| <b>7 TRANSIENTS IN LONG OIL PIPELINES . . . . .</b>       | 237 |
| 7-1 Introduction . . . . .                                | 238 |
| 7-2 Definitions . . . . .                                 | 238 |
| 7-3 Causes of Transients . . . . .                        | 241 |
| 7-4 Methods of Analysis . . . . .                         | 242 |
| 7-5 Design Considerations . . . . .                       | 244 |
| 7-6 Summary . . . . .                                     | 246 |
| Problems . . . . .  | 246 |
| References . . . . .                                      | 247 |
| <b>8 PERIODIC FLOWS AND RESONANCE . . . . .</b>           | 249 |
| 8-1 Introduction . . . . .                                | 250 |
| 8-2 Terminology . . . . .                                 | 250 |
| 8-3 Development of Periodic Flow . . . . .                | 255 |
| 8-4 Methods of Analysis . . . . .                         | 261 |
| 8-5 Block Diagram . . . . .                               | 266 |
| 8-6 Transfer Matrices . . . . .                           | 266 |
| 8-7 Frequency Response . . . . .                          | 285 |
| 8-8 Spatial Variation of Pressure and Discharge . . . . . | 296 |
| 8-9 Pressure Nodes and Antinodes . . . . .                | 298 |
| 8-10 Resonant Frequencies . . . . .                       | 299 |
| 8-11 Verification of Transfer-Matrix Method . . . . .     | 304 |
| 8-12 Variable-Characteristics Pipeline . . . . .          | 314 |
| 8-13 Stenosis in Human Cardiovascular System . . . . .    | 316 |
| 8-14 Case Study . . . . .                                 | 318 |
| 8-15 Summary . . . . .                                    | 321 |
| Problems . . . . .  | 322 |
| References . . . . .                                      | 323 |
| <b>9 CAVITATION AND COLUMN SEPARATION . . . . .</b>       | 327 |
| 9-1 Introduction . . . . .                                | 328 |
| 9-2 General Remarks . . . . .                             | 328 |
| 9-3 Causes of Column Separation . . . . .                 | 330 |
| 9-4 Energy Dissipation . . . . .                          | 330 |
| 9-5 Wave Velocity in a Gas-Liquid Mixture . . . . .       | 332 |

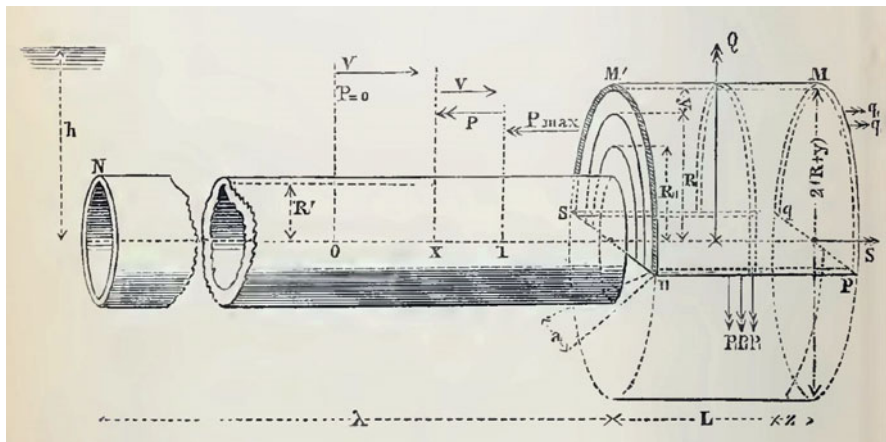
|           |  |            |
|-----------|--|------------|
| 9-6       | Analysis of Cavitation . . . . .                     | 335        |
| 9-7       | Design Considerations . . . . .                      | 336        |
| 9-8       | Case Study . . . . .                                 | 337        |
| 9-9       | Summary . . . . .                                    | 341        |
|           | Problems . . . . .                                   | 341        |
|           | References . . . . .                                 | 343        |
| <b>10</b> | <b>TRANSIENT CONTROL . . . . .</b>                   | <b>347</b> |
| 10-1      | Introduction . . . . .                               | 348        |
| 10-2      | Surge Tank . . . . .                                 | 349        |
| 10-3      | Air Chamber . . . . .                                | 351        |
| 10-4      | Valves . . . . .                                     | 354        |
| 10-5      | Optimal Transient Control . . . . .                  | 366        |
| 10-6      | Case Study . . . . .                                 | 367        |
| 10-7      | Summary . . . . .                                    | 370        |
|           | Problems . . . . .                                   | 371        |
|           | References . . . . .                                 | 373        |
| <b>11</b> | <b>SURGE TANKS . . . . .</b>                         | <b>377</b> |
| 11-1      | Introduction . . . . .                               | 378        |
| 11-2      | Types of Surge Tanks . . . . .                       | 378        |
| 11-3      | Governing Equations . . . . .                        | 379        |
| 11-4      | Solution of Governing Equations . . . . .            | 387        |
| 11-5      | Surge Oscillations in Frictionless System . . . . .  | 388        |
| 11-6      | Terminology . . . . .                                | 389        |
| 11-7      | Normalization of Equations . . . . .                 | 393        |
| 11-8      | Phase-Plane Method . . . . .                         | 393        |
| 11-9      | Stability of Simple Tank . . . . .                   | 395        |
| 11-10     | Stability of Closed Surge Tank . . . . .             | 401        |
| 11-11     | Multiple Surge Tanks . . . . .                       | 405        |
| 11-12     | Design Considerations . . . . .                      | 407        |
| 11-13     | Case Study . . . . .                                 | 410        |
| 11-14     | Summary . . . . .                                    | 414        |
|           | Problems . . . . .                                   | 414        |
|           | References . . . . .                                 | 418        |
| <b>12</b> | <b>LEAK AND PARTIAL BLOCKAGE DETECTION . . . . .</b> | <b>421</b> |
| 12-1      | Introduction . . . . .                               | 422        |
| 12-2      | Terminology . . . . .                                | 422        |
| 12-3      | Partial Blockage Detection . . . . .                 | 424        |
|           | Frequency Analysis . . . . .                         | 424        |
|           | System Parameters . . . . .                          | 425        |
|           | PPFR for Partial Blockage . . . . .                  | 426        |
| 12-4      | Leak Detection . . . . .                             | 428        |
|           | Frequency Response . . . . .                         | 430        |

|   |            |
|---|------------|
| Leak Detection Procedure .....                      | 430        |
| 12-5 Real-life Application .....                    | 433        |
| 12-6 Summary.....                                   | 433        |
| Problems .....                                      | 433        |
| References .....                                    | 434        |
| <b>13 TRANSIENT OPEN-CHANNEL FLOWS .....</b>        | <b>437</b> |
| 13-1 Introduction .....                             | 438        |
| 13-2 Terminology .....                              | 438        |
| 13-3 Examples of Transient Flows.....               | 440        |
| 13-4 Surge Height and Celerity .....                | 440        |
| 13-5 Governing Equations.....                       | 445        |
| 13-6 Methods of Solution .....                      | 450        |
| 13-7 Method of Characteristics .....                | 451        |
| 13-8 Explicit Finite-Difference Methods.....        | 454        |
| 13-9 Initial Conditions.....                        | 462        |
| 13-10 Implicit Finite-Difference Methods.....       | 465        |
| 13-11 Second-Order Explicit Schemes.....            | 470        |
| 13-12 Comparison of Finite-Difference Methods ..... | 473        |
| 13-13 Special Topics .....                          | 474        |
| 13-14 Case Study .....                              | 484        |
| 13-15 Summary.....                                  | 487        |
| Problems .....                                      | 487        |
| References .....                                    | 496        |
| <b>14 ERRATUM .....</b>                             | <b>E1</b>  |
| <b>A DESIGN CHARTS .....</b>                        | <b>503</b> |
| A-1 Equivalent Pipe .....                           | 503        |
| A-2 Valve Closure .....                             | 504        |
| A-3 Valve Opening .....                             | 504        |
| A-4 Power Failure to Centrifugal Pump .....         | 504        |
| A-5 Air Chamber .....                               | 506        |
| A-6 Simple Surge Tank .....                         | 511        |
| A-7 Surges in Open Channels .....                   | 514        |
| A-8 Data for Pumping Systems .....                  | 522        |
| References .....                                    | 525        |
| <b>B TRANSIENTS CAUSED BY OPENING OR CLOSING</b>    |            |
| <b>A VALVE .....</b>                                | <b>527</b> |
| B-1 Program isting.....                             | 527        |
| B-2 Input Data .....                                | 531        |
| B-3 Program Output .....                            | 531        |

|  |     |
|--|-----|
| <b>C TRANSIENTS CAUSED BY POWER FAILURE TO PUMPS .....</b>     | 535 |
| C-1 Program Listing.....                                       | 535 |
| C-2 Input Data .....   | 540 |
| C-3 Program Output .....                                       | 541 |
| <b>D FREQUENCY RESPONSE OF A SERIES PIPING SYSTEM .....</b>    | 545 |
| D-1 Program Listing.....                                       | 545 |
| D-2 Input Data .....   | 547 |
| D-3 Program Output .....                                       | 547 |
| <b>E WATER LEVEL OSCILLATIONS IN A SIMPLE SURGE TANK .....</b> | 549 |
| E-1 Program Listing.....                                       | 549 |
| E-2 Input Data .....   | 552 |
| E-3 Program Output .....                                       | 552 |
| <b>F SI AND ENGLISH UNITS AND CONVERSION FACTORS .....</b>     | 555 |
| F-1 SI Units .....   | 555 |
| F-2 Conversion Factors .....                                   | 556 |
| Author Index.....  | 557 |
| Subject Index .....  | 565 |

---

## BASIC CONCEPTS



Rigid metal pipe and elastic rubber section for  
Isebree Moens' experiments [1877].  
(Courtesy, Arris Tijsseling.)

## 1-1 Introduction

In this chapter, a number of common terms related to hydraulic transients are defined, and a brief history of the developments in hydraulic transients is presented. The basic waterhammer equations relating the change in pressure due to an instantaneous change in flow velocity and an expression for the velocity of pressure waves in a pipe are derived. The propagation and reflection of waves in a pipeline are discussed, followed by different approaches for the analysis of hydraulic transients. The chapter concludes with brief information on a number of accidents and incidents caused by hydraulic transients.

## 1-2 Terminology

A number of common terms are defined in this section.

**Steady and Unsteady Flow.** Flow is called steady if the flow conditions, such as pressure and velocity, at a point are constant with time. If the conditions change with time, the flow is termed unsteady. Strictly speaking, turbulent flows are always unsteady since the conditions at a point in these flows are changing continuously. However, these flows are considered steady if the temporal mean conditions over a short period do not change with time. When referring to the steady or unsteady turbulent flows herein, we will consider the temporal mean conditions for this designation.

**Transient Flow.** The intermediate-stage flow, when the flow conditions change from one steady-state to another steady state, is called transient flow.

**Uniform and Nonuniform Flow.** If the flow velocity is constant with respect to distance at any given time, the flow is called uniform flow, whereas if the velocity varies with distance, the flow is called nonuniform.

**Steady-Oscillatory or Periodic Flow.** If the flow conditions are varying with time and if they repeat after a fixed time interval, the flow is called periodic or steady-oscillatory flow. The time interval at which conditions are repeating is termed as the *period*. If  $T$  is the period in seconds, then the frequency of oscillations,  $f$ , in cycles/s and in rad/s is  $1/T$  and  $2\pi/T$ , respectively. Frequency expressed in rad/s is called *circular frequency* and is usually designated by  $\omega$ .

**Column Separation.** If the pressure in the flow drops to the vapor pressure of the liquid, then cavities are formed in the liquid and many times the liquid column may separate over the entire cross section.

**Waterhammer.** In the past, terms such as *waterhammer*, *oilhammer*, and *steamhammer* referred to the pressure fluctuations caused by a flow change depending upon the fluid involved. However, *hydraulic transients* has become common since the 1960s.

**Pressure Surge.** Transients involving slowly varying pressure oscillations are referred to as *pressure surges* or *surges* in North America. In Europe especially in the United Kingdom, however, the term *pressure surge* includes both rapid (i.e., waterhammer) and slow transients. In this book, we shall follow the North American practice.

To clarify the preceding definitions, let us discuss the flow conditions in a pipeline following instantaneous closure of the downstream valve (Fig. 1-1). Initially, the downstream valve is fully open, and the flow velocity throughout the pipeline is  $V_o$ . At time  $t = t_o$ , the valve is suddenly closed, reducing the flow through the valve instantly to zero. Because of the conversion of kinetic energy, pressure rises at the valve, and a pressure wave travels in the upstream direction. This wave is reflected from the reservoir and then travels back and forth between the closed valve and the reservoir. Due to losses in the system, this wave is dissipated as it travels in the pipeline. Finally, let us say at time  $t_1$ , the flow is completely stopped and the pressure in the entire pipeline is the same as the reservoir head.

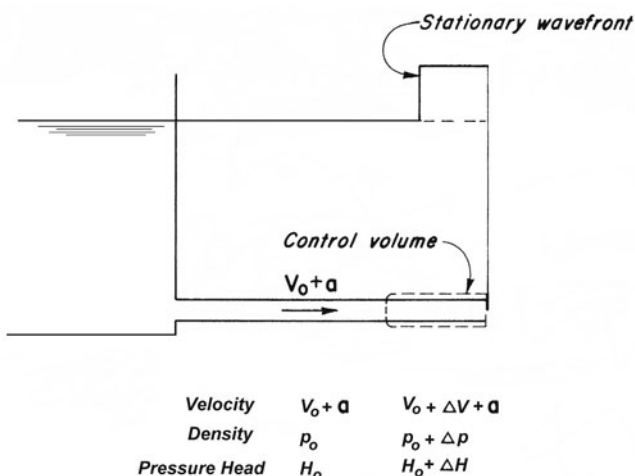
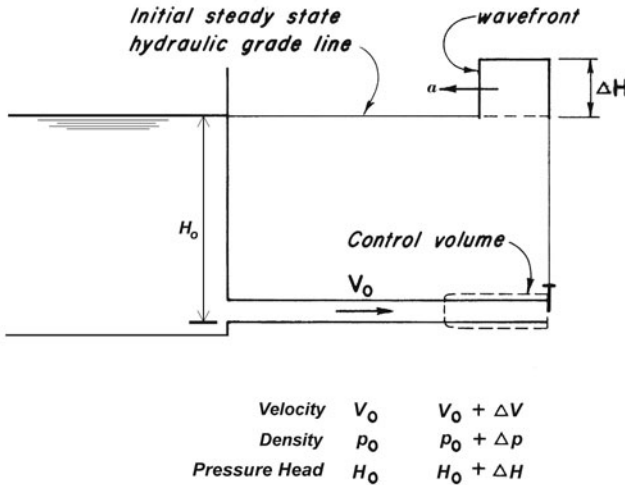
Based on the preceding definitions, the flow for  $t < t_o$  and  $t > t_1$  is steady when the conditions are constant with respect to time. However, the intermediate flow (i.e.,  $t_o \leq t \leq t_1$ ) when the flow conditions are changing from the initial steady state to the final steady state is called transient flow.

Now let us consider another flow situation in which the downstream valve is opened and closed periodically at frequency,  $\omega_f$ . After a number of cycles, the transient flow in the pipeline becomes periodic with the same period as that of the opening and closing valve. This flow is called *steady-oscillatory flow* or *periodic flow*.

## 1-3 Historical Background

A brief history of the developments in hydraulic transients is presented in this section (most of the material is based on Wood [1970]). Interested reader should see papers by Tijsseling and Anderson [2004, 2007, 2008, 2012].

The study of fluid transients began with the investigation of the propagation of sound waves in air, the propagation of waves in shallow water, and the flow of blood in arteries. Newton [1687] studied the propagation of sound waves in air and the propagation of water waves in canals. Both Newton and Lagrange obtained theoretically the velocity of sound in air as 298.4 m/s as compared to their experimental value of 348 m/s. Lagrange erroneously attributed this difference to experimental error, whereas Newton indicated that



(b) Unsteady flow converted to steady flow

Fig. 1-1. Propagation of pressure wave.

the theoretical velocity was incorrect and that this discrepancy was due to spacing of the solid particles of air and the presence of vapors in air. By comparing the oscillations of a liquid in a U-tube to that of a pendulum, Newton derived an incorrect expression for the celerity of water waves in a canal as  $\pi\sqrt{L/g}$ , where  $L$  = the wavelength and  $g$  = acceleration due to gravity. Euler [1759] derived the following partial differential equation for wave propagation:

$$\frac{\partial^2 y}{\partial t^2} = a^2 \frac{\partial^2 y}{\partial x^2} \quad (1-1)$$

in which  $a$  = wave speed. He developed a general solution of this equation as

$$y = F(x + at) + f(x - at) \quad (1-2)$$

in which  $F$  and  $f$  are the traveling waves. Euler [1775] tried, but failed, to obtain a solution for the flow of blood through arteries.

Lagrange [1788] analyzed the flow of compressible and incompressible fluids utilizing the concept of *velocity potential*. He also derived a correct expression for the celerity of waves in a canal as  $c = \sqrt{gd}$ , in which  $d$  = flow depth. Monge developed a graphical method for integrating the partial differential equations [1789] and introduced the term *method of characteristics*. Around 1808, Laplace explained the difference between the theoretical and measured values of the velocity of sound in air as follows: The relationships derived by Newton and Lagrange were based on Boyle's law. This law was not valid under varying pressures since the air temperature did not remain constant. He reasoned that the theoretical velocity would increase by about 20 percent if the adiabatic conditions were assumed instead of the isothermal conditions.

Young [1808] investigated the propagation of pressure waves in pipes. Helmholtz appears to be the first to point out that the velocity of pressure waves in water contained in a pipe was less than that in unconfined water. He correctly attributed this difference to the elasticity of pipe walls. In 1869, Riemann [1869] developed a three-dimensional equation of motion and applied its simplified one-dimensional form to analyze vibrating rods and sound waves. Weber [1866] studied the flow of an incompressible fluid in an elastic pipe and conducted experiments to determine the velocity of pressure waves. He also developed the dynamic and continuity equations. Marey [1875] conducted extensive tests to determine the velocity of pressure waves in water and in mercury and concluded that the wave velocity was independent of the amplitude of the pressure waves, was three times greater in mercury than in water, and was proportional to the elasticity of the tube. Resal [1876] developed the continuity and dynamic equations and a second-order wave equation and compared his analytical studies with Marey's experimental results. Lord Rayleigh published his book "Theory of Sound" in 1877.

Korteweg [1878] was the first to determine the wave velocity considering the elasticity of both the pipe wall and the fluid; earlier investigators had considered only one of the two at a time. Tijsseling and Anderson [2012] indicated that Korteweg gave Moens' smei-empirical expression for wave speed a mathematical basis and credited Moen [1877] for extensive experiments on metal pipes equipped with air pockets.

Although Wood lists Michaud [1878] as the first to study waterhammer, recent investigations by Anderson [1976] have shown that actually Menabrea [1858] was the first to do so. Michaud [1878] presented the design and use of

air chambers and safety valves. Gromeka [1883] included the friction losses in the waterhammer analysis for the first time, assuming the liquid to be incompressible and the friction losses to be directly proportional to the flow velocity.

Weston [1885] and Carpenter [1893-1894] conducted experiments to develop a theoretical relationship between the reduction of flow velocity in a pipe and the corresponding pressure rise. However, neither one succeeded because their pipelines were short. Frizell [1898] analyzed waterhammer in the Ogden hydroelectric development in Utah with a 9.45 km long penstock, developed expressions for the velocity of waterhammer waves and for the pressure rise due to instantaneous reduction of the flow. He stated that the wave velocity would be the same as that of sound in unconfined water if the modulus of elasticity of the pipe walls were infinite. He also discussed the effects of branch lines, wave reflections, and successive waves on speed regulation. Unfortunately, for some unknown reason, Frizell's work has not been recognized as much as that of his contemporaries, such as Joukowsky [1898] and Allievi [1903, 1913 and 1937].

In 1897, Joukowsky conducted extensive experiments in Moscow on 7.62 km long and 50 mm in diameter, 305 m long and 101.5 mm in diameter, and 305 m long and 152.5 mm in diameter pipelines. Based on his experimental and theoretical studies, he published his classic report [1898, 1900] on the basic theory of waterhammer. He developed a formula for the wave velocity, taking into consideration the elasticity of both the water and the pipe walls. He also developed the relationship between the reduction of flow velocity and the resulting pressure rise by using the conservation of energy and the continuity condition. He discussed the propagation of a pressure waves in a pipe and the wave reflection from the open end of a branch. He studied the utilization of air chambers, surge tanks, and safety valves to control waterhammer pressures. He found that the pressure rise was a maximum for closing times  $\leq 2L/a$ , in which  $L$  = length of the pipeline and  $a$  = wave speed.

Allievi published the general theory of waterhammer in 1903. His dynamic equation was more accurate than that of Korteweg. He showed that the term  $V(\partial V/\partial x)$  in the dynamic equation was not important as compared to the other terms and could be dropped. He introduced two dimensionless parameters:

$$\rho = \frac{aV_o}{2gH_o} \quad (1-3)$$

$$\theta = \frac{aT_c}{2L}$$

in which  $a$  = wave velocity;  $V_o$  = steady-state velocity;  $L$  = length of the pipeline;  $T_c$  = valve-closure time;  $\rho$  = one half of the ratio of the kinetic energy of the fluid to the potential energy stored in the fluid and the pipe walls at pressure head  $H_o$  and  $\theta$  = the valve-closure characteristics. For the valve-closure time,  $T_c$ , Allievi obtained an expression for the pressure rise at the valve and presented charts for the pressure rise and drop caused by a

uniformly closing or opening valve.

Braun [1909, 1910] presented equations similar to those presented by Allievi [1913]. In another publication, Braun [1939] claimed priority over Allievi, and it appears that the so-called Allievi constant,  $\rho$ , was actually introduced by Braun. However, Allievi is still considered to be the originator of the basic waterhammer theory. Allievi [1913, 1937] also studied the rhythmic movement of a valve and proved that the maximum pressure cannot exceed twice the static head.

Camichel et al. [1919] demonstrated that doubling of pressure head is not possible unless  $H_o > aV_o/g$ . Constantinescu [1919] described a mechanism to transmit mechanical energy by pressure waves. In World War I, British fighter planes were equipped with the Constantinescu gear for firing the machine guns. Based on Joukowski's theory, Gibson [1919-1920] included, for the first time, nonlinear friction losses in the analysis. He also invented an apparatus [Gibson, 1923] to measure the turbine discharge by using the pressure-time history following load rejection.

Strowger and Kerr [1926] presented a step-by-step procedure to compute the speed variation of a hydraulic turbine following load changes in which waterhammer pressures, changes in the turbine efficiency at various gate openings, and the uniform and nonuniform gate movements were considered. While discussing this paper, Wood [1926] introduced the graphical method for waterhammer analysis, Löwy independently developed and presented an identical graphical method in 1928. Schnyder [1929] included complete pump characteristics in his analysis of waterhammer in pipelines connected to centrifugal pumps. Bergeron [1931] extended the graphical method to determine the conditions at the intermediate sections of a pipeline, and Schnyder [1932] was the first to include the friction losses in the graphical analysis.

Two symposia on waterhammer were held in 1933 and 1937. Since then, several books [Rich, 1951; Parmakian, 1955; Gardel, 1956; Bergeron, 1961; Streeter and Wylie, 1967; Pickford, 1969; Tullis, 1970; Fox, 1977; Jaeger, 1977; Wylie and Streeter, 1978; Chaudhry, 1979; Webb and Gould, 1979; Sharp, 1981; Watters, 1983; Almeida and Koelle, 1992; and Ruus and Karney, 1997] have been published on the subject. In addition, a number of professional societies have organized conferences and symposia on fluid transients; a few of these are: conferences by British Hydromechanics Research Association [1972, ..., 2012], symposia by American Society of Mechanical Engineering [1965, 1983 and 1984] and by International Association for Hydraulic Research [1971, 1974, 1977, 1980 and 1981] and meetings by other organizations [1982 and 1993].

## 1-4 Basic Waterhammer Equations

In this section, we derive the basic waterhammer equations — expressions for the velocity of pressure waves in a conduit and for the change in pressure due to instantaneous change in the flow velocity.

Let us consider the flow in a frictionless pipe (Fig. 1-1) in which a slightly compressible fluid is flowing with velocity  $V_o$ , and the initial steady state pressure head upstream of the valve is  $H_o$ . Let the flow velocity  $V_o$  be changed instantaneously at time  $t = 0$  to  $V_o + \Delta V$ . An increase in the flow velocity  $\Delta V$  and an increase in pressure  $\Delta H$  are considered positive and a decrease, as negative. As a result of this change in the flow velocity, the pressure head  $H_o$  changes to  $H_o + \Delta H$ , the fluid density  $\rho_o$  changes to  $\rho_o + \Delta\rho$ , and a pressure wave of magnitude  $\Delta H$  travels in the upstream direction. Let us designate the velocity of the pressure wave (commonly called *wave velocity*) by  $a$ , and, to simplify the derivation, let us assume the pipe walls are rigid, i.e., the pipe area,  $A$ , does not change due to pressure changes. In the next chapter, an expression for the wave velocity is derived in which the fluid is slightly compressible and the pipe walls are slightly deformable.

The unsteady flow of Fig. 1-1a may be converted into steady flow by superimposing velocity  $a$  in the downstream direction. This is equivalent to an observer traveling in the upstream direction with velocity  $a$  to whom the moving wave front appears as stationary (Fig. 1-1b), and the inflow and outflow velocities from the control volume are  $(V_o + a)$  and  $(V_o + \Delta V + a)$ , respectively.

Let us consider distance,  $x$ , and velocity,  $V$ , in the downstream direction as positive. Referring to Fig. 1-1b, the time rate of change of momentum in the positive  $x$ -direction

$$\begin{aligned} &= \rho_o (V_o + a) A [(V_o + \Delta V + a) - (V_o + a)] \\ &= \rho_o (V_o + a) A \Delta V \end{aligned} \quad (1-4)$$

Neglecting friction, the resultant force,  $F$ , acting on the fluid in the control volume in the positive  $x$ -direction

$$F = \rho_o g H_o A - \rho_o g (H_o + \Delta H) A = -\rho_o g \Delta H A \quad (1-5)$$

According to Newton's second law of motion, the time rate of change of momentum is equal to the resultant force. Hence, it follows from Eqs. 1-4 and 1-5 that

$$\Delta H = -\frac{1}{g} (V_o + a) \Delta V \quad (1-6)$$

The wave velocity  $a$  in metal or concrete pipes or in the rock tunnels, is approximately 1000 m/s while typical flow velocity is about 10 m/s or less.

Therefore,  $V_o$  is significantly smaller than  $a$  and may thus be neglected. Then, Eq. 1-6 becomes

$$\Delta H = -\frac{a}{g} \Delta V \quad (1-7)$$

The negative sign on the right-hand side of Eq. 1-7 indicates that the pressure head increases (i.e.,  $\Delta H$  is positive) for a reduction in velocity (i.e., for negative  $\Delta V$ ) and vice versa. Also note that Eq. 1-7 is derived for an instantaneous velocity change at the downstream end of a pipe and for the wave front moving in the upstream direction. Proceeding similarly, it can be proven that for a velocity change at the upstream end and for the wave front to move in the downstream direction,

$$\Delta H = \frac{a}{g} \Delta V \quad (1-8)$$

Note that, unlike Eq. 1-7, there is no negative sign on the right-hand side of Eq. 1-8. This means that the pressure head in this case increases for an increase in velocity and decreases with a decrease in velocity.

If the fluid density change  $\Delta\rho$  is caused by the change in pressure,  $\Delta p$ , then referring to Fig. 1-1b,

$$\text{Rate of mass inflow} = \rho_o A (V_o + a) \quad (1-9)$$

$$\text{Rate of mass outflow} = (\rho_o + \Delta\rho) A (V_o + \Delta V + a) \quad (1-10)$$

If the fluid is slightly compressible, the increase in the mass of control volume due to the change in fluid density is small and may be neglected. Therefore, the rate of mass inflow is equal to the rate of mass outflow. Hence,

$$\rho_o A (V_o + a) = (\rho_o + \Delta\rho) A (V_o + \Delta V + a) \quad (1-11)$$

which upon simplification becomes

$$\Delta V = -\frac{\Delta\rho}{\rho_o} (V_o + \Delta V + a) \quad (1-12)$$

Since  $(V_o + \Delta V) \ll a$ , Eq. 1-12 may be written as

$$\Delta V = -\frac{\Delta\rho}{\rho_o} a \quad (1-13)$$

The bulk modulus of elasticity,  $K$ , of a fluid is defined as [Streeter, 1966]

$$K = \frac{\Delta p}{\Delta\rho/\rho_o} \quad (1-14)$$

Hence, it follows from Eqs. 1-13 and 1-14 that

$$a = -K \frac{\Delta V}{\Delta p} \quad (1-15)$$

By utilizing Eq. 1-7 and noting that  $\Delta p = \rho_o g \Delta H$ , we may write this equation as

$$a = \frac{K}{a \rho_o} \quad (1-16)$$

or

$$a = \sqrt{\frac{K}{\rho_o}} \quad (1-17)$$

Note that this expression for the wave velocity is for a slightly compressible fluid confined in a rigid pipe. In the next chapter, we will discuss how this expression is modified if the pipe walls are elastic.

### Example

*Compute the velocity of pressure waves in a 0.5-m-diameter pipe conveying oil. Determine the pressure rise if a steady flow of 0.4 m<sup>3</sup>/s is instantaneously stopped at the downstream end. Assume that the pipe walls are rigid, the density of the oil,  $\rho = 900 \text{ kg/m}^3$ , and the bulk modulus of elasticity of the oil,  $K = 1.5 \text{ GPa}$ .*

### Solution

$$\begin{aligned} A &= \frac{\pi}{4}(0.5)^2 = 0.196 \text{ m}^2 \\ V_o &= \frac{Q_o}{A} = \frac{0.4}{0.196} = 2.04 \text{ m/s} \\ a &= \sqrt{\frac{K}{\rho}} \\ &= \sqrt{\frac{1.5 \times 10^9}{900}} = 1291 \text{ m/s} \end{aligned}$$

Since the flow is completely stopped,  $\Delta V = 0 - 2.04 = -2.04 \text{ m/s}$ . Therefore,

$$\begin{aligned} \Delta H &= -\frac{a}{g} \Delta V \\ &= -\frac{1291}{9.81} (-2.04) = 268.5 \text{ m} \end{aligned}$$

A positive sign for  $\Delta H$  means the pressure rises as a result of this reduction in the flow velocity.

## 1-5 Wave Propagation

In this section, we discuss transient flow in a piping system with a constant-level reservoir at the upstream end and a valve at the downstream end (Fig. 1-2) to illustrate the propagation of a wave in a pipe and the reflections of the wave from a reservoir and from a closed valve. The pipe walls are considered elastic. Therefore, the pipe expands as the inside pressure increases and contracts as the pressure decreases.

Let the flow conditions in the piping system be steady prior to instantaneous closure of the downstream valve at time  $t = 0$ . If the system is assumed frictionless, then the initial steady-state pressure head along the length of the pipeline is  $H_o$ . Let us consider the distance  $x$  and the velocity  $V$  as positive in the downstream direction. The upstream and downstream directions are with respect to the initial steady flow.

The sequence of events following valve closure may be divided into four parts (Fig. 1-2) as follows:

### 1. $0 < t \leq L/a$

The flow velocity at the valve is reduced to zero as soon as the valve is completely closed. This increases the pressure at the valve by  $\Delta H = (a/g) V_o$ . Because of this increase in pressure, the pipe expands (the initial steady-state pipe diameter in the expanded or contracted parts of the pipe is shown by dotted lines in Fig. 1-2), the fluid is compressed which increases the fluid density, and a positive pressure wave propagates towards the reservoir. Behind this wave front, the flow velocity is zero, and the kinetic energy has been converted into elastic energy (Fig. 1-2a). If  $a$  is the velocity of the pressure wave and  $L$  is the length of the pipeline, then the wave front reaches the upstream reservoir at time  $t = L/a$ . At this time, along the entire length of the pipeline, the pipe is expanded, the flow velocity is zero, and the pressure head is  $H_o + \Delta H$  (Fig. 1-2b).

### 2. $L/a < t \leq 2L/a$

Just as the wave reaches the upstream reservoir, pressure at a section on the reservoir side is  $H_o$  while the pressure at an adjacent section in the pipe is  $H_o + \Delta H$ . Because of this difference in pressure, the fluid flows from the pipeline into the reservoir with velocity  $-V_o$ . Thus, the flow velocity at the pipe entrance is reduced from zero to  $-V_o$ . This causes the pressure to drop from  $H_o + \Delta H$  to  $H_o$  and a negative wave travels towards the valve (Fig. 1-2c). The pressure behind this wave front (i.e., on the reservoir side) is  $H_o$  and the fluid velocity is  $-V_o$ . At  $t = 2L/a$ , the wave front reaches the closed valve, and the pressure head in the entire pipeline is  $H_o$ , and the fluid velocity is  $-V_o$  (Fig. 1-2d).

### 3. $2L/a < t \leq 3L/a$

Since the valve is completely closed, a negative velocity cannot be maintained at the valve. Therefore, the velocity changes instantaneously from  $-V_o$  to 0, the pressure drops to  $H_o - \Delta H$ , and a negative wave propagates

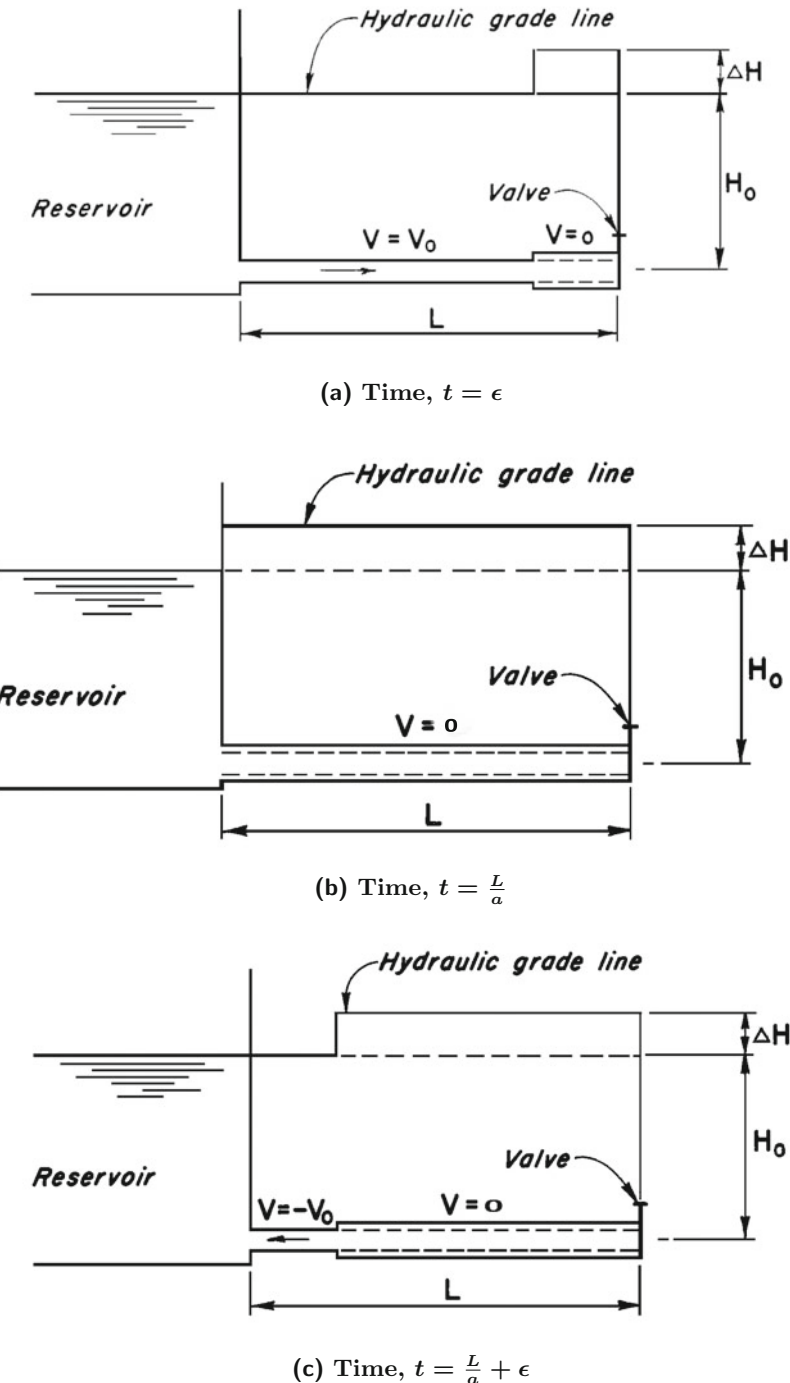
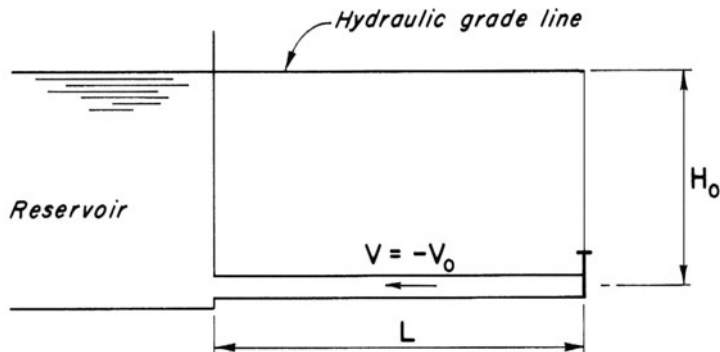
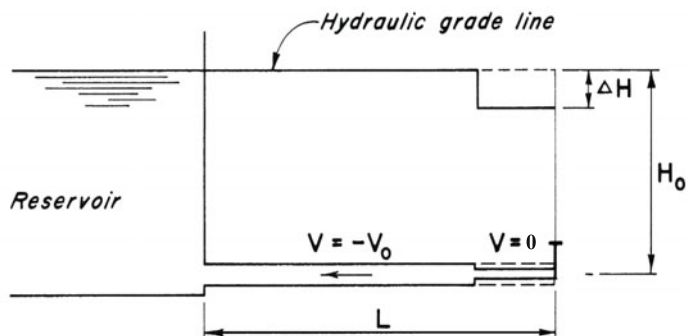


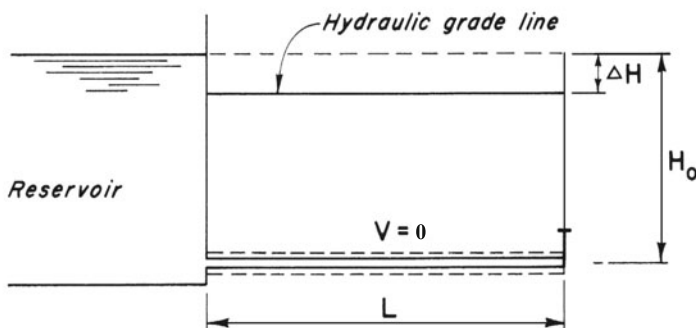
Fig. 1-2. Propagation and Reflection of pressure waves.



$$(d) \text{ Time, } t = \frac{2L}{a}$$



$$(e) \text{ Time, } t = \frac{2L}{a} + \epsilon$$



$$(f) \text{ Time, } t = \frac{3L}{a}$$

Fig. 1-2. (Continued)

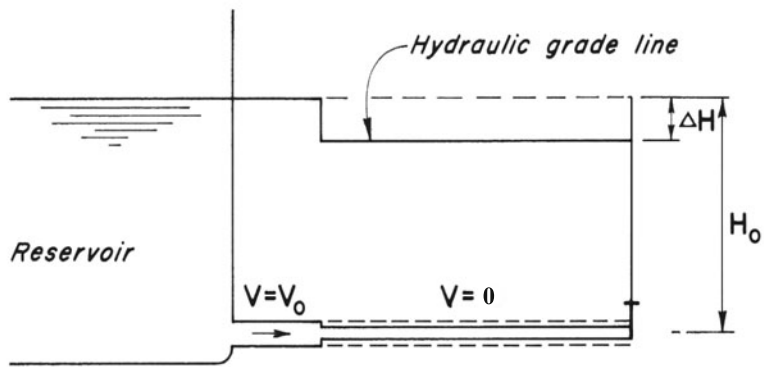
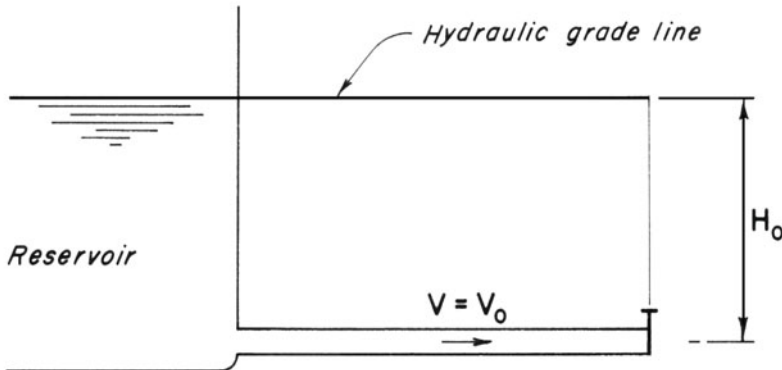
(g) Time,  $t = \frac{3L}{a} + \epsilon$ (h) Time,  $t = \frac{4L}{a}$ 

Fig. 1-2. (Continued)

towards the reservoir (Fig. 1-2e). Behind this wave front, the pressure is  $H_o - \Delta H$  and the fluid velocity is zero. The wave front reaches the upstream reservoir at time  $t = 3L/a$ , the pressure head in the entire pipeline is  $H_o - \Delta H$ , and the fluid velocity is zero (Fig. 1-2f).

4.  $3L/a < t \leq 4L/a$

As soon as this negative wave reaches the reservoir, an unbalanced condi-

tion is created again at the upstream end. Now the pressure is higher on the reservoir side than at an adjacent section in the pipeline. Therefore, the

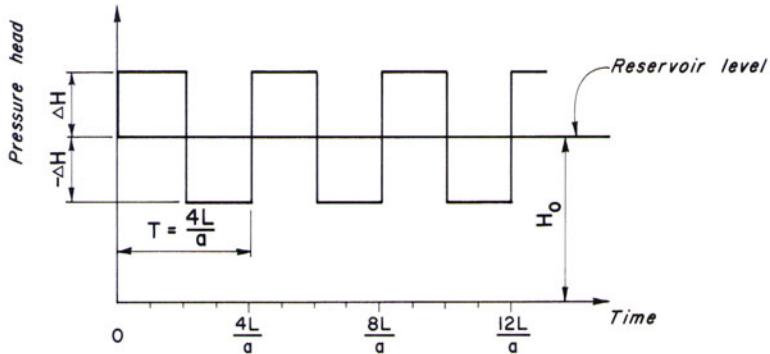


**Fig. 1-3.** Pressure variation at valve; friction losses neglected.

fluid now flows from the reservoir into the pipeline with velocity  $V_o$ , and the pressure head increases to  $H_o$  (Fig. 1-2g). At time  $t = 4L/a$  the wave front reaches the downstream valve, the pressure head in the entire pipeline is  $H_o$ , and the flow velocity is  $V_o$ . Thus, the conditions in the pipeline at this time are the same as those during the initial steady-state conditions except that the valve is now closed (Fig. 1-2h).

Since the valve is completely closed, the preceding sequence of events starts again at  $t = 4L/a$ . Figure 1-2 illustrates the sequence of events along the pipeline, while Fig. 1-3 shows the variation of pressure at the valve with time. Since we assumed the system to be frictionless, this process continues with the conditions repeating at an interval of  $4L/a$ . The interval at which conditions are repeated is termed the *theoretical period* of the pipeline. In a real system, however, pressure waves are dissipated due to energy losses as the waves propagate back and forth in the pipeline, and the fluid becomes stationary after some time. The variation of pressure at the valve with time is shown in Fig. 1-4 if the friction losses are taken into consideration.

## 1-6 Wave Reflection and Transmission

In the previous section we discussed the propagation of pressure waves in a pipe and the reflection of the wave from a reservoir and from a closed valve. In this section, we introduce the concept of reflection and transmission coefficients which defines the magnitude and the sign of reflected and transmitted

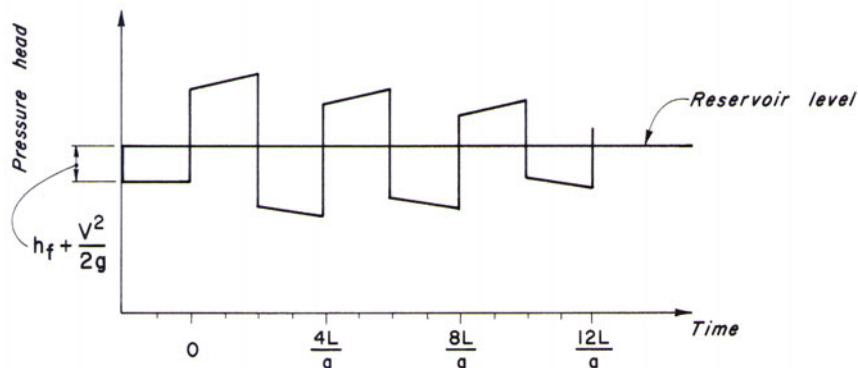


**Fig. 1-4.** Pressure variation at valve; friction losses considered.

waves from or at a boundary. For simplification, we assume no energy loss as a wave is reflected from or is transmitted at a boundary.

Let us designate an incident pressure wave approaching a boundary as  $F$  and the wave reflected from the boundary as  $f$ . Then, the reflection coefficient,  $r$ , is defined as  $r = f/F$ . The pressure in a positive pressure wave is higher behind the wave front than ahead of the wave front while the pressure in a negative wave is lower behind the wave front than ahead of the wave front.

### Constant-Level Reservoir

A large lake, reservoir, tank or other storage facility may be considered to have a constant level if its water surface level remains unchanged irrespective of the changes in the flow in the pipeline connected to the facility. The reflected pressure wave,  $f$ , from a constant-level reservoir is equal in magnitude to that of the incident wave,  $F$ , but is of the opposite sign. Therefore, the reflection coefficient for a constant-level reservoir,  $r = -1$  (Fig. 1-5). For example, a 10-m positive pressure wave is reflected from a reservoir as a 10-m negative pressure wave.

The reflection of a velocity wave at a reservoir has the same magnitude and the same sign as that of the incident wave.

### Dead End

At a dead end or at a fully closed valve, a reflected pressure wave has the same magnitude and the same sign as that of the incident wave (Fig. 1-6), i.e., the reflection coefficient,  $r = 1$ . Thus, if a 10-m pressure wave is approaching a dead end with the initial pressure head of 100 m, the pressure increases to

110 m as the wave arrives at the dead end and then increases to  $110+10 = 120$  m after the pressure wave is reflected from the dead end.

### Series Junction

A junction of two pipes having different diameters, wall thicknesses, wave velocities, and/or friction factors is called a series junction. A pressure wave  $F$  traveling in one of the series pipes, say pipe 1, is reflected back into pipe 1 and another wave,  $f_s$  is transmitted into the second pipe, say pipe 2 (Fig. 1-7). The reflection coefficient,  $r$  and transmission coefficient,  $s$ , for this junction are:

$$r = \frac{f}{F} = \frac{\frac{A_1}{a_1} - \frac{A_2}{a_2}}{\frac{A_1}{a_1} + \frac{A_2}{a_2}}$$

$$s = \frac{f_s}{F} = \frac{\frac{2A_1}{a_1}}{\frac{A_1}{a_1} + \frac{A_2}{a_2}} \quad (1-18)$$

in which  $A$  = pipe cross-sectional area;  $a$  = wave velocity; and subscripts 1 and 2 refer to the quantities for pipe 1 and 2, respectively. Note that  $f_s$  is a positive wave since the diameter of pipe 1 is larger than that of pipe 2. If the diameter of pipe 2 is larger than that of pipe 1, then  $f_s$  will be a negative wave.

### Branching Junction

At the junction, pipe 1 branches into pipe 2 and pipe 3. The incident wave,  $F$ , in pipe 1 is reflected back as  $f$  from the junction into pipe 1 and a transmitted wave  $f_s$  is transmitted into pipe 2 and pipe 3. The reflection and transmission coefficients for a branching junction are:

$$r = \frac{f}{F} = \frac{\frac{A_1}{a_1} - \frac{A_2}{a_2} - \frac{A_3}{a_3}}{\frac{A_1}{a_1} + \frac{A_2}{a_2} + \frac{A_3}{a_3}}$$

$$s = \frac{f_s}{F} = \frac{\frac{2A_1}{a_1}}{\frac{A_1}{a_1} + \frac{A_2}{a_2} + \frac{A_3}{a_3}} \quad (1-19)$$

Similar equations for  $r$  and  $s$  may be written for a branching junction of two incoming pipes and one outgoing pipe.

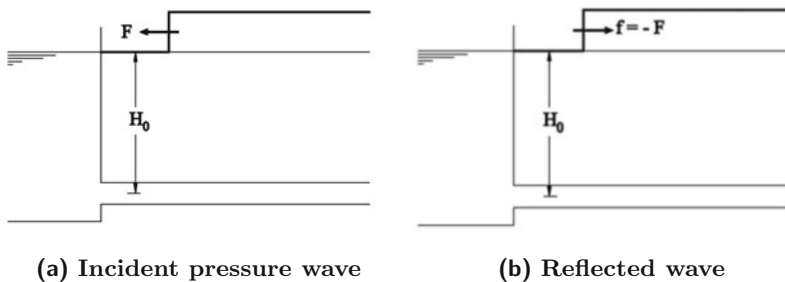


Fig. 1-5. Incident and reflected waves at a reservoir.

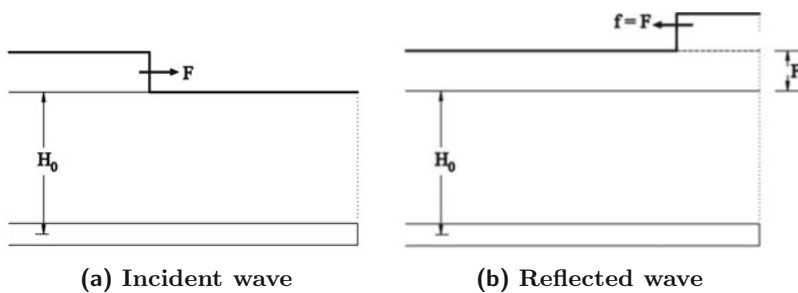


Fig. 1-6. Incident and reflected waves at a dead end.

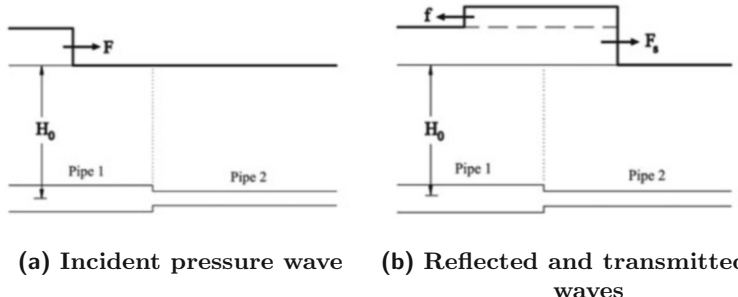


Fig. 1-7. Incident, reflected, and transmitted waves at a series junction.

## 1-7 Transient Flow Analysis

For analysis, transient flow may be classified as closed-conduit flow, open-channel or free-surface flow and combined free-surface-pressurized flow. We consider each of these flows in the following paragraphs.

The transient flow in closed-conduits may be analyzed by using the distributed-system or lumped-system approach. In the distributed-system approach, transient phenomenon is in the form of traveling waves. Examples are transients in water-supply pipes, in power plant conduits, and in gas-transmission lines. In the lumped-system approach, any change in the flow conditions is assumed to travel instantaneously throughout the system, i.e., the fluid is considered as a solid body. An example of such a system is the slow oscillations of water level in a surge tank following a load change on the turbines in a hydroelectric power plant.

Mathematically speaking, the transients in a distributed system are represented by partial differential equations, whereas the transients in a lumped system are described by ordinary differential equations. As discussed in Chapter 8, the system may be analyzed as a lumped system if  $\omega L/a$  is significantly less than 1, [Chaudhry, 1970]; otherwise, the system should be analyzed as a distributed system. In the preceding expression,  $\omega$  = frequency of the flow oscillations,  $L$  = length of the pipeline, and  $a$  = wave velocity.

Transients in an open channel may be classified based on the time rate at which they occur: gradual, such as flood waves in rivers, and rapid, such as surges in power canals. If the wave front in the rapidly varied flow is steep, it is referred to as a *bore*.

Free-surface flow may become pressurized due to priming of the conduit during the transient-state conditions. Such flows are called combined free-surface-pressurized flows. Examples of such flows are the flow in a sewer following a large rainstorm, and the flow in the tailrace tunnel of a hydroelectric power plant following rapid acceptance of load on turbines.

## 1-8 Causes of Transients

As defined previously, the intermediate-stage flow when the flow conditions change from one steady state to another, is termed *transient-state flow*. In other words, the transient conditions are initiated whenever the steady state conditions are disturbed. Such a disturbance may be caused by planned or accidental changes in the settings of the control equipment of a man-made system or by changes in the inflow or outflow of a natural system.

Common causes of transients in engineering systems are:

- Opening, closing, or “chattering” of valves in a pipeline;
- Starting or stopping the pumps in a pumping system;
- Starting-up a hydraulic turbine, accepting or rejecting load;

Vibrations of the vanes of a runner or an impeller;  
Sudden opening or closing the control gates of a canal;  
Failure of a dam, and  
Sudden increases in the river or sewer inflow due to a flash storm.

## 1-9 System Design and Operation

No generalized procedures are presently available to design a system directly that gives an acceptable transient response. Therefore, following trial-and-error approach is employed.

The system layout and parameters are first selected, and the system is analyzed for transients caused by various possible operating conditions. If the system response is unacceptable, e.g., the maximum and minimum pressures are not within the prescribed limits, then the system layout and/or parameters are changed, or various control devices are provided and the system is analyzed again. This procedure is repeated until a desired response is obtained. For a particular system, several different control devices may be suitable for transient control. If possible it may be economical in some cases to modify the operating conditions, or the acceptable response. However, the final objective is to have an *overall* economical system that yields an acceptable response.

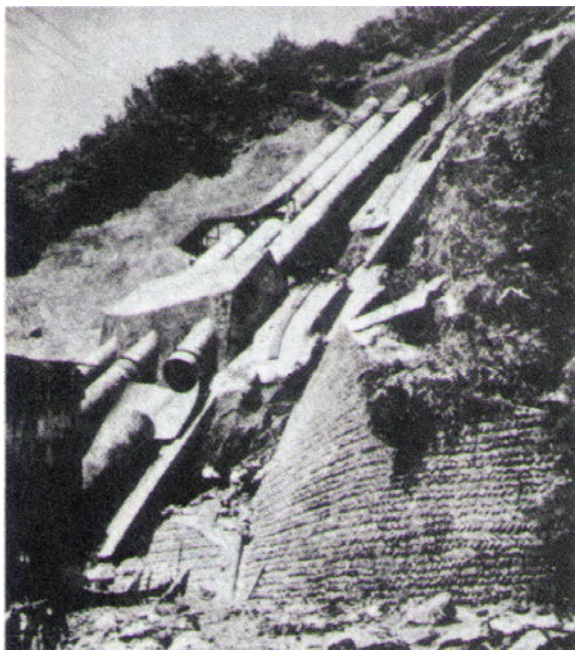
The system is designed for the normal operating conditions expected to occur during its life. And, similarly, it is essential that the system be operated strictly according to the operating guidelines. Failure to do so may cause spectacular accidents and result in extensive property damage and many times in loss of life [Rocard, 1937; Jaeger, 1948; Bonin, 1960; Jaeger, 1963; Kerensky, 1965-1966; Pulling, 1976; Trenkle, 1979; Serkiz, 1983].

If the data for a system are not precisely known, e.g., wave speed, friction factors, reservoir levels, etc., then the system should be analyzed for the expected range of various variables. This is usually referred to as sensitivity analysis. For example, such an analysis may be done by varying the variable by  $\pm 10\%$ .

During the commissioning of a newly built system or after major modifications have been completed on an existing project, the system should be tested for possible operating conditions. To avoid accidents and failures, it is usually advisable to conduct the tests in a progressive manner. For example, if there are four parallel pumping-sets on a pipeline, the tests for power failure should begin with one pumping-set and progressively increase to all four.

## 1-10 Accidents and Incidents

In this section, a number of photographs of failures caused by transients are presented.



(a)



(b)

**Fig. 1-8. Burst penstock of Oigawa Hydroelectric Power Plant, Japan.**  
(After Bonin [1960].)



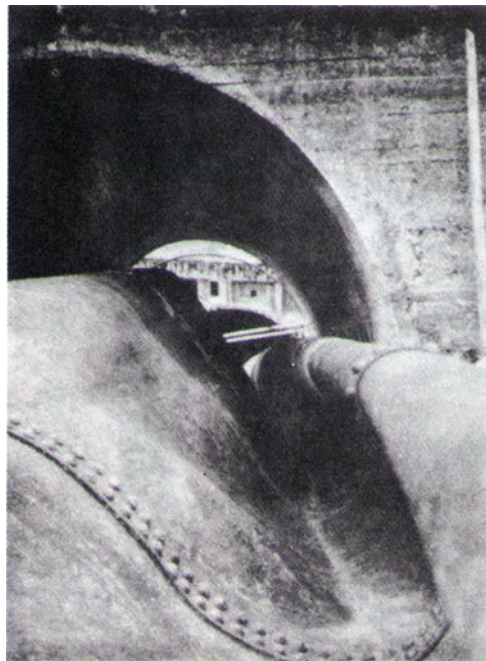
(a)

**Fig. 1-9.** Collapsed penstock of Oigawa Hydroelectric Power Plant, Japan. (After Bonin [1960].)

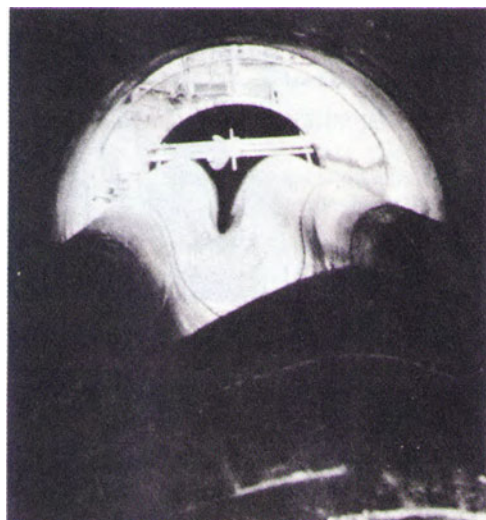
**Figure 1-8:** The burst penstock of Oigawa Power Station, Japan [Bonin, 1960] due to excessive pressures caused by operating errors and malfunctioning equipment resulting in the death of three service men and  $\frac{1}{2}$  million dollar in damage.

**Figure 1-9:** The collapsed penstock of Oigawa Power Plant due to vacuum upstream of the burst section [Bonin, 1960]. The uncontrolled flow through the burst section caused the hydraulic grade line to drop below the penstock, producing vacuum.

**Figure 1-10:** The burst turbine inlet valve of Big Creek No. 3 Hydropower Plant [Trenkle, 1979] U. S. A. The penstock of unit 2 failed at the manhole following closure of turbine shut-off valve in less than 3 sec. This happened while servicing the hydraulic operator of the valve; the unit was in operation. The crack was 3.7 m long and 76 mm at the widest point.



(b)

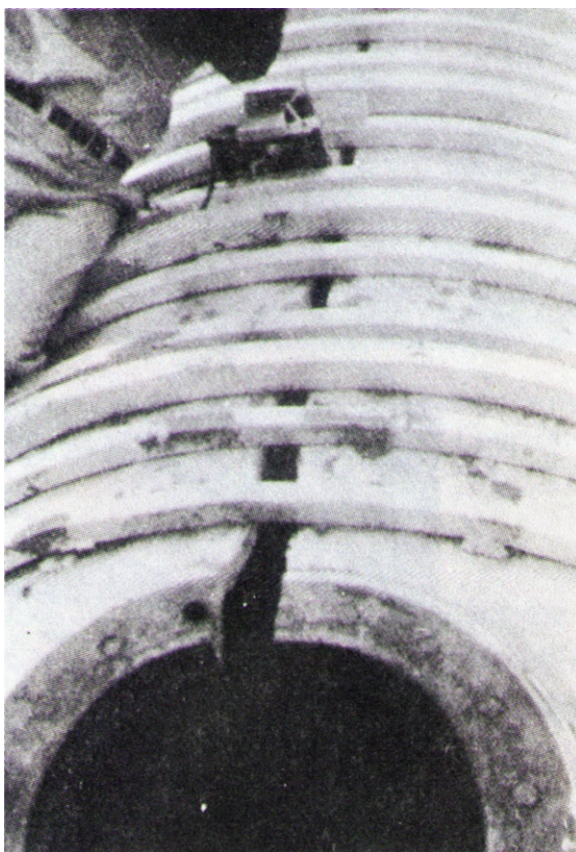


(c)

**Fig. 1-9. (Continued)**



(a)



(b)

**Fig. 1-10. Crack in the turbine inlet valve of Big Creek No. 3 Hydropower Plant, USA. (After Trenkle [1979].)**

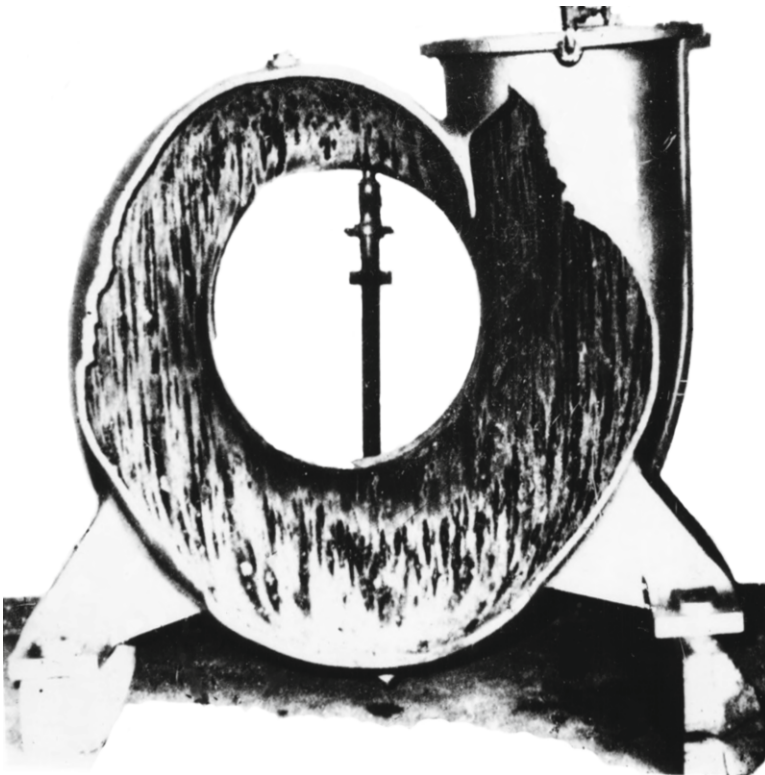


**Fig. 1-11.** The burst pump casing, Azambuja Pump Station, Portugal.  
(Courtesy of A. B. de Almeida.)

**Figure 1-11:** The burst pump casing of Azambuja Pump Station, Portugal due to rejoining of separated water columns following water column separation, not anticipated during design.

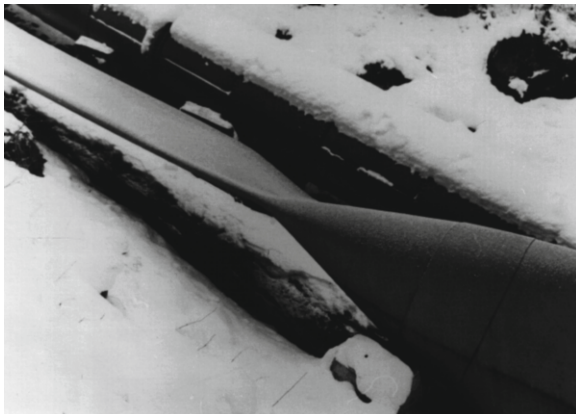
**Figure 1-12:** The collapsed penstock of Lütschinen Hydroelectric Power Plant, Switzerland, during draining with the frozen vent at the upstream end.

**Figure 1-13:** Damaged penstock of Arequipa Hydroelectric Power Plant, Peru. Pressure fluctuations caused by the clogging of the control system of the spherical valve resulted in the failure of the welding seams of the penstock due to fatigue.

**Figure 1-14:** The draft tube access doors of both units of Ok Menga Hydroelectric Power Plant, Papua New Guinea, were blown off due to failure of bolts caused by the high pressures following column separation, flooding the power house. Under-torquing of the wicket gates is considered to have caused rapid gate closure following load rejection resulting in column separation in the draft tube [Anonymous, 1991].



(a)



(b)

**Fig. 1-12.** Collapsed penstock of Lütschinen Hydroelectric Power Plant during draining with the upstream vent frozen, Switzerland.  
(Courtesy, M. Humbel, Colonco, Switzerland.)

## 1-11 Summary

In this chapter, commonly used terms are defined. A brief historical background on the developments in hydraulic transients is presented, and expressions for the pressure change due to an instantaneous change in the flow velocity and for the wave velocity are derived. The propagation of a pressure wave in a piping system and wave reflection at the boundaries are discussed and the concept of reflection and transmission coefficient is introduced. The chapter is concluded by a discussion of the causes and various approaches for the analysis of hydraulic transients.



**Fig. 1-13. Damaged penstock of Arequipa Hydroelectric Power Plant, Peru.** (Courtesy, M. H umbel, Colonco, Switzerland.)

## Problems

**1-1** Derive Eq. 1-8 from first principles.

**1-2** Derive Eq. 1-7 assuming that the pipe is inclined to the horizontal at an angle  $\theta$ .

**1-3** Compute the wave velocity in a 2-m-diameter pipe conveying seawater. Assume the pipe is rigid.

**1-4** Determine the pressure rise if an initial steady discharge of  $10 \text{ m}^3/\text{s}$  is stopped instantaneously at the downstream end of the pipeline of Problem 1.3.

**1-5** A valve is suddenly opened at the downstream end of a 1-m-diameter pipeline such that the flow velocity increases from 2 to 4 m/s. Compute the pressure drop due to the opening of the valve. Assume the liquid is water.



**Fig. 1-14.** Draft tube door, Ok Menga Hydroelectric Power Plant, Papua New Guinea. (Courtesy, E. A. Portfors, Klohn Crippen Berger, Canada and ok Tedi Mines, Papua New Guinea.)

**1-6** Prove that if the fluid is incompressible and the pipe walls are assumed rigid, then the pressure rise

$$\Delta H = -\frac{L}{g} \frac{dV}{dt}$$

in which  $L$  = length of the pipe and  $dV/dt$  = the rate of change of velocity with respect to time. (*Hint:* Apply Newton's second law of motion to the fluid volume.)

**1-7** Plot the pressure variation with time at the mid-length of the pipeline shown in Fig. 1-2 following an instantaneous closure of the valve. Assume the system is frictionless.

**1-8** A pipeline has a pump at the upstream end and a constant-level reservoir at the downstream end. If the pump instantaneously stops pumping water

at time  $t = 0$ , plot the pressure variation with respect to time at the upstream end, at the mid-length, and at quarter points. Assume the system is frictionless.

**1-9** A gate at the downstream end of a rigid pipeline is closed uniformly in  $T$  seconds, thereby changing the flow velocity from  $V_o$  to  $V_f$ . If the liquid in the pipeline is assumed to be rigid and frictionless and the coefficient of discharge of the gate remains constant during the transient conditions, prove that the maximum pressure rise  $(\Delta H)_{max}$  at the gate is given by the expression

$$(\Delta H)_{max} = H_o \left[ 0.5k + \sqrt{k + 0.25k^2} \right]$$

in which  $H_o$  = initial steady-state head at the gate,  $k = [LV_f / (gH_o T)]^2$ , and  $L$  = length of the pipeline. (*Hint:* Write an equation for the velocity through the gate in terms of the head on the gate. Solve this equation simultaneously with that of Problem 1.6 and note that when  $H$  is maximum,  $d(\Delta H)/dt = 0$ .)

## Answers

**1-3** 1488 m/s

**1-4** 482.81 m

**1-5** 301.86 m

## References

- Allievi, L., 1903, "Teoria generale del moto perturbato dell'acqua nei tubi in pressione," *Ann. Soc. Ing. Arch. italiana*, (French translalion by Allievi, Revue de Mechanique, 1904).
- Allievi, L., 1913, "Teoria del colpo d'ariete." *Atti Collegio Ing. Arch.* (English translation by E. E. Halmos, "The Theory of waterhammer," *Trans., Amer. Soc. Mech. Engrs.*, 1929.)
- Allievi, L., 1937, "Air Chambers for Discharge Pipes," *Trans., Amer. Soc. Mech. Engrs.*, vol. 59, Nov., pp. 651-659.
- Almeida, A. B., and Koelle, E., 1992, *Fluid Transients in Pipe Networks*, Computational Mechanics Publications, Southampton Boston (Co-published with) Elsevier Applied Science, London, New York, NY.
- Anderson, A., 1976, "Menabrea's Note on Waterhammer: 1858," *Jour., Hyd. Div.*, Amer. Soc. Civ. Engrs., vol. 102, Jan., pp. 29-39.
- Anonymous, 1991, "Ok Menga Hydro Failure Hydraulic Transient Study," Report prepared by Klohn Leonoff for Ok Tedi Mining Ltd., 67 pp.

- Bergeron, L., 1931, "Variations de regime dans les conduites d'eau," *Comptes Rendus des Travaux de la Soc. Hydrotech. de France*.
- Bergeron, L., 1961, *Waterhammer in Hydraulics and Wave Surges in Electricity*, (translated under the sponsorship of the ASME), John Wiley & Sons, Inc., New York, NY. (Original French Text, Dunod, Paris, 1950.)
- Bonin, C. C., 1960, "Water-Hammer Damage to Oigawa Power Station," *Jour. Engineering for Power*, Amer. Soc. Mech. Engrs., April, pp. 111-119.
- Braun, E., 1909, Druckschwankungen in Rohrleitungen, Wittwer. Stuttgart, Germany.
- Braun, E., 1910, *Die Turbine, Organ der turbinentechnischen Gesellschaft*, Berlin, Germany.
- Braun, E., 1939, "Bermerkungen zur Theorie der Druckschwankungen in Rohrleitungen." *Wasserkraft und Wasserwirtschaft*, vol. 29, no. 16, Munich, Germany, pp. 181-183.
- Cabrera, E., and Martinez, F., 1993, *Water Supply Systems, State of the art and future trends*, Computational Mechanics publications, Southampton Boston.
- Camichel, C., Eydoux, D., and Gariel, M., 1919, "Étude Théorique et Expérimentale des Coups de Bélier." Dunod, Paris, France.
- Carpenter, R. C., 1893-1894, "Experiments on Waterhammer," *Trans., Amer. Soc. of Mech. Engrs.*
- Chaudhry, M. H., 1970, "Resonance in Pressurized Piping Systems," *thesis* presented to the University of British Columbia, Vancouver, British Columbia, Canada, in partial fulfillment of the requirements for the degree of doctor of philosophy.
- Chaudhry, M. H., 1979, *Applied Hydraulic Transients*, First ed., Van Nostrand Reinhold Co., Princeton, NJ.
- Constantinescu, G., 1920, Ann. des Mines de Roumanie. Dec. 1919, Jan.
- ENEL, 1971, *Proc. Meeting on Water Column Separation*, Organized by ENEL, Milan, Italy, Oct.
- ENEL, 1980, *Proc. Fourth Round Table and International Assoc. for Hydraulic Research Working Group Meeting on Water Column Separation*, Report No. 382, Cagliari, Italy.
- Euler, L., 1759, "De la Propagation du Son," *Mémoires de l 'Acad. d. Wiss.*, Berlin, Germany.
- Euler, L., 1775, "Principia pro Motu Sanguinis per Arterias Determinando." Opera Postume Tomus Alter, XXXIII.
- Fox, J. A., 1977, *Hydraulic Analysis of Unsteady Flow in Pipe Networks*, John Wiley & Sons, Inc., New York, NY.
- Frizell, J. P., 1898, "Pressures Resulting from Changes of Velocity of Water in Pipes." *Trans., Amer. Soc. Civil Engrs.*, vol. 39, June, pp. 1-18.
- Gardel, A., 1956, *Chambres d'Equilibre*, Rouge et Cie, Lausanne, Switzerland.
- Gibson, N. R., 1919-1920, "Pressures in Penstocks Caused by Gradual Closing of Turbine Gates." *Trans., Amer. Soc. Civil Engrs.*, vol. 83, pp. 707-775.

- Gibson, N. R., 1923, "The Gibson Method and Apparatus for Measuring the Flow of Water in Closed Conduits," *Trans. Amer. Soc. Mech. Engrs.*, vol. 45, pp. 343-392.
- Gromeka, I. S., 1883, "Concerning the Propagation Velocity of Waterhammer Waves in Elastic Pipes." Scientific Soc. of Univ. of Kazan, Kazan, U.S.S.R., May.
- IAHR, 1981, *Proc. Fifth International Symp. and international Assoc. for Hydraulic Research Working Group Meeting on Water Column Separation*, Obemach. Universities of Hanover and Munich, Germany.
- Jaeger, C., 1948, "Water Hammer Effects in Power Conduits," *Civil Engineering Pub. Works Rev.*, London, vol. 23, nos. 500-503, Feb.- May.
- Jaeger, C., 1963, "The Theory of Resonance in Hydropower Systems. Discussion of Incidents Occurring in Pressure Systems," *Jour. Basic Engineering*, Amer. Soc. Mech. Engrs., vol. 85, Dec., pp. 631-640.
- Jaeger, C., 1977, *Fluid Transients in Hydroelectric Engineering Practice*, Blackie & Sons, Ltd., Glasgow and London, UK.
- Joukowski, N. E., 1898, 1900, *Mem. Imperial Academy Soc. of St. Petersburg*, vol. 9. no. 5, (in Russian. translated by O. Simin, *Proc. Amer. Water Works Assoc.*, vol. 24, 1904. pp. 341-424.)
- Kerensky, G., 1965-1966, Discussion of "The Velocity of Water Hammer Waves," by Pearsall, I. S., *Symposium on Surges in Pipelines, Inst. of Mech. Engrs.*, London, vol. 180, Pt 3E, p. 25.
- Koelle, E. and Chaudhry, M. H. (eds.), 1982, *Proc. International Seminar on Hydraulic Transients* (in English with Portuguese translation), vols. 1-3, Sao Paulo, Brazil.
- Korteweg, D. J., 1878, "Ueber die Fortpflanzungsgeschwindigkeit des Schalles in elastischen Rohren," *Annalen der Physik und Chemie*, Wiedemann, ed ., New Series, vol. 5, no. 12, pp. 525-542.
- Lagrange, I. L., 1788, *Mecanique Analytique*, Paris, Bertrund's ed., p. 192.
- Laplace, P. S., 1799, *Celestial Mechanics*, 4 volumes, Bowditch translation.
- Löwy, R., 1928, *Druckschwankungen in Druckrohrleitungen*, Springer.
- Marey, M., 1875, "Mouvement des Ondes Liquides pour Servir a la Théorie du Pouls." Travaux du Laboratoire de M. Marey.
- Menabrea, L. F., 1858, "Note sur les effects de choc de l'eau dans les conduites," *Comptes Rendus Hebdomadaires des Séances de L'Academie des Sciences*, Paris, France, vol. 47, July-Dec., pp. 221-224.
- Michaud, J., 1878, "Coups de bâlier dans les conduites. Étude des moyens employés pour en atténuer les effets," *Bulletin de la Société Vaudoise des Ingénieurs et des Architectes*, Lausanne, Switzerland. 4 année. nos. 3 and 4. Sept. and Dec., pp. 56-64,65-77.
- Moens, I A., 1877, "Over de Voortplantingssnelheid van den Pols," *Ph.D. Thesis*, Univ. of Leiden, Leiden, The Netherlands, (in Dutch), 76 pp.
- Monge, G., 1789, "Graphical integration." *Ann. des Ing. Sortis des Ecoles de Gand.*

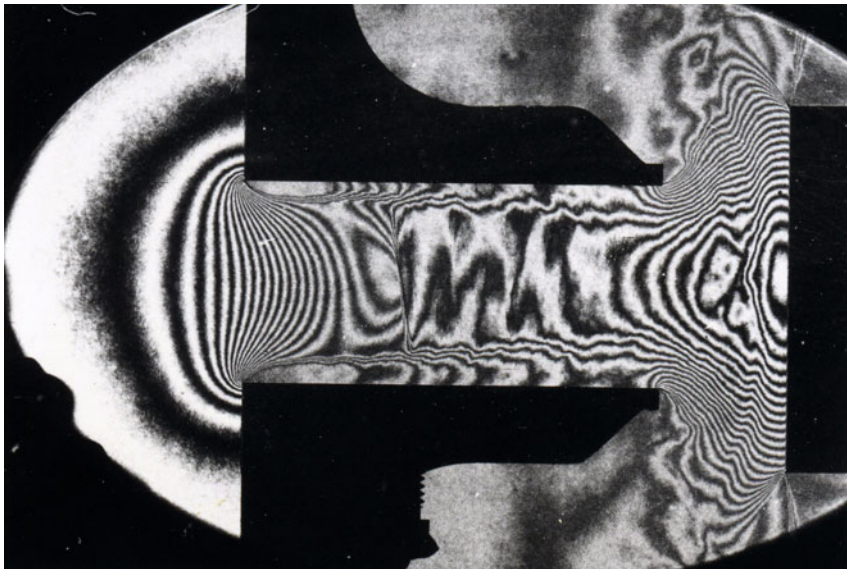
- Newton, I., 1687, *The Principia*, Royal Soc., London, Boole 2. Propositions 44-46.
- Parmakian, J., 1955, *Waterhammer Analysis*, Prentice-Hall, Inc., Englewood Cliffs, NJ, (Dover Reprint, 1963.)
- Pickford, J., 1969, *Analysis of Surge*, Macmillan, London, UK.
- Proc. Pressure Surge Conferences*, British Hydromechanics Research, First, 1972; Second, 1977; Third, 1980; Fourth, 1983; Fifth, 1986; Sixth, 1989; Seventh, 1992; Eighth, 1995; Ninth, 2004; Tenth, 2008; Eleventh, 2012.
- Proc. Second Round Table Meeting on Water Column Separation*, Vallombrosa. 1974, ENEL Report 290; also published in *L'Energia Elettrica*, No.4 1975, pp. 183-485, not inclusive.
- Proc. Third Round Table Meeting on Water Column Separation*, Royaumont, *Bulletin de la Direction des Études et Récherches*, Series A, No.2, 1977.
- Pulling, W. T., 1976, "Literature Survey of Water Hammer Incidents in Operating Nuclear Power Plants," Report No. WCAP-8799, *Westinghouse Electric Corporation*, Pittsburgh, Pennsylvania, Nov.
- Rayleigh, J. W. S., 1877, *Theory of Sound*.
- Resal, H., 1876, "Note sur les petits mouvements d'un fluide incompressible dans un tuyau élastique." *Journal de Mathématiques Pures et Appliquées*, Paris, France, 3rd Series, vol. 2, pp. 342-344.
- Rich, G. R., 1951, *Hydraulic Transients*, McGraw-Hill Book Co., New York, NY.
- Riemann, B., 1869, *Partielle Differentialgleichungen*, Braunschweig, Germany.
- Rocard, Y., 1937, "Les Phenomenes d'Auto-Oscillation dans les Installations Hydrauliques," Hermann, Paris, France.
- Rouse, H. and Ince, S., 1963, *History of Hydraulics*, Dover Publications, New York, NY.
- Ruus, E. and Karney, B., 1997, *Applied Hydraulic Transients*, Ruus Consulting Ltd., Kelowna, British Columbia, Canada.
- Schnyder, O., 1929, "Druckstöße in Pumpensteigleitungen," *Schweizerische Bauzeitung*, vol. 94, Nov.- Dec., pp. 271-273, 283-286.
- Schnyder, O., 1932, "Ueber Druckstöße in Rohrleitungen," *Wasserkraft u. Wasserwirtschaft*, vol. 27, Heft 5, pp. 49-54, 64-70.
- Serkiz, A. W., 1983, "Evaluation of Water Hammer Experience in Nuclear Power Plants," *Report NUREG-0927*, U.S. Nuclear Regulatory Commission, Washington, DC, May.
- Sharp, B. B., 1981, *Water Hammer, Problems and Solutions*, Edward Arnold Publishers, Ltd., London, UK.
- Streeter, V. L., 1966, *Fluid Mechanics*, 4th Ed., McGraw-Hill Book Co., New York, NY, p. 15.
- Streeter, V. L., and Wylie, E. B., 1967, *Hydraulic Transients*, McGraw-Hill Book Co., New York, NY.
- Strawger, E. B. and Kerr, S. L., 1926, "Speed Changes of Hydraulic Turbines for Sudden Changes of Load," *Trans., Amer. Soc. Mech. Engrs.*, vol. 48, pp. 209-262.

- Symposium on Waterhammer, *Amer. Soc. of Mech. Engrs. and Amer. Soc. of Civil Engrs.*, Chicago, Illinois, June, 1933.
- Symposium on Waterhammer, Annual Meeting, *Amer. Soc. of Mech. Engrs.*, Dec., 1937.
- Symposium, "Waterhammer in Pumped-Storage Projects," *Amer. Soc. of Mech. Engrs.*, 1965.
- Symposium, "Numerical Methods for Fluid Transient Analysis," Martin, C. S. and Chaudhry, M. H. eds., *Amer. Soc. of Mech. Engrs.*, 1983.
- Symposium, "Multi-dimensional Fluid Transients," Chaudhry, M. H. and Martin, C. S. eds., *Amer. Soc. of Mech. Engrs.*, 1984.
- Tijsseling, A. S., and Anderson, A., 2004, "A Precursor in Waterhammer Analysis –Rediscovering Johannes von Kries," *Proc. 9th International Conference on Pressure Surges*, BHR Group, Cranfield, UK., pp. 739-751.
- Tijsseling, A. S., and Anderson, A., 2007, "Johannes von Kries and the History of Water Hammer," *Jour. Hydraulic Engineering*, Amer. Soc. Civil Engrs., vol. 133, pp. 1-8.
- Tijsseling, A. S., and Anderson, A., 2008, "Thomas Young's Research On Fluid Transients: 200 Years On," *Proc. 10th International Conference on Pressure Surges*, BHR Group, Cranfield, UK., pp. 21-33.
- Tijsseling, A. S., and Anderson, A., 2012, "A. Isebree Moens and D. J. Korteweg: On the Speed of Propagation of Waves in Elastic Tubes," *Proc. 11th International Conference on Pressure Surges*, BHR Group, Cranfield, UK., Oct., pp. 227-245.
- Trenkle, C. J., 1979, "Failure of Riveted and Forge-Welded Penstock," *Jour. of Energy Div.*, Amer. Soc. Civ. Engrs., vol. 105, Jan., pp. 93-102.
- Tullis, J. P., 1970, *Control of Flow in Closed Conduits*, Proc. of the Institute held at Colorado State University, Colorado State University Press, Fort Collins, CO.
- Watters, G. Z., 1979, *Modern Analysis and Control of Unsteady Flow in Pipelines*, Ann Arbor Science Publications, Ann Arbor, MI; second Ed., Butterworth, Boston, London, UK, 1983.
- Webb, T. and B. W. Gould, 1979, *Waterhammer*, Books Australia.
- Weber, W., 1866, "Theorie der durch Wasser oder andere incompressible Flüssihkeiten in elastischen Rohren fortgepflanzten Wellen," *Berichte über die Verhandlungen der Königlichen Sachsischen Gesellschaft der Wissenschaften zu Leipzig*, Leipzig, Germany, MathematischPhysische Klasse, pp. 353-357.
- Weston, E. B., 1885, "Description of Some Experiments Made on the Providence. R.I., Water Works to Ascertain the Force of Water Ram in Pipes," *Trans., Amer. Soc. of Civil Engrs.*, vol. 14, p. 238.
- Wood, F. M., 1926, discussion of Strowger and Kerr [1926] *Trans., Amer. Soc. Mech. Engrs.*, vol. 48.
- Wood, F. M., 1970, "History of Waterhammer," *Report No. 65*. Department of Civil engineering, Queen's University at Kingston. Ontario, Canada, April.

- Wylie, E. B. and Streeter, V. L., 1983, *Fluid Transients*, McGraw-Hill Book Co., New York, NY, 1978; reprinted by FEB Press, Ann Arbor, MI.
- Young, T., 1808, "Hydraulic Investigations," *Phil. Trans., Royal Society*, London, pp. 164-186.

---

## TRANSIENT-FLOW EQUATIONS



Isovel lines of measured constant density for the calculated constant Mach Numbers (adiabatic isentropic flow) for a standing pressure wave in a safety valve for pressure ratio of 0.35. Flow pattern is at the limit of becoming unstable. (Courtesy, Föllmer, B. and Zeller, H. [1980].)

## 2-1 Introduction

Equations for the conservation of mass and momentum describe the transient flow in closed conduits. These equations are usually referred to as the continuity and momentum equations. Some authors call a simplified form of the latter, the equation of motion or the dynamic equation. These equations are a set of partial differential equations since the flow velocity and pressure in transient flow are functions of time as well as distance.

In this chapter, the continuity and momentum equations are derived by making a number of simplifying assumptions. A brief introduction to the Reynolds transport theorem, which is used to derive a generalized form of these equations, is first presented. A simplified version of these equations is then derived and various methods for their solution are discussed. Expressions for the wave velocity and a number of models to simulate unsteady friction are presented.

## 2-2 Reynolds Transport Theorem

A number of terms are defined first for the presentation of this theorem which relates the flow variables for a specified quantity of fluid mass, called a *system*, to that of a specified region, called a *control volume* [Roberson and Crowe, 1997]. Everything external to this system is called the *surroundings*, and the system *boundaries* separate the system from its surroundings. The boundary of a control volume is referred to as the *control surface*.

In fluid flow, the shape of a system may change as it travels from one location to another. A control volume usually remains fixed at a location; although in some applications, it may travel and/or deform in shape. For the application of this theorem in this chapter, the shape of the control volume changes with time due to variation in the internal pressure.

The basic conservation laws of mechanics, such as, conservation of mass, momentum and energy are valid for a system. These laws describe the interaction between the system and its surroundings and usually specify the time rate of change of some system property. For example, Newton's second law of motion relates the time rate of change of momentum of a system to the external forces exerted on the system by its surroundings. In the control-volume approach, the boundaries of the system and that of the control volume are the same at the instant a particular conservation law is applied. In other words, all of the system mass is contained in the control volume.

For the analysis of fluid flow, we do not follow the motion of a specified particle or of a specified quantity of mass. Instead, we are interested in the flow through a region. The basic laws, therefore, are written for the flow in a region. The Reynolds transport theorem is useful for this application.

Let  $B$  be an *extensive property* (momentum, energy) of a fluid, and let  $\beta$  be the corresponding intensive property. An *intensive property* is defined as

the amount of  $B$  per unit mass of a system, i.e.,  $\beta = \lim_{\Delta m \rightarrow 0} \Delta B / \Delta m$ . The total amount of  $B$  in a control volume,  $B_{cv}$ , is then

$$B_{cv} = \int_{cv} \beta \rho dV \quad (2-1)$$

in which  $m$  = mass,  $\rho$  = mass density, and  $dV$  = differential volume of the fluid.

Let us now discuss how the flow variables of a control volume are related to that of a system. To facilitate understanding, our discussion is confined to one-dimensional flow and we assume that the control volume is fixed in space. We are interested in relating the time rate of change of property  $B$  of the system to that of the control volume and the inflow and outflow of  $B$  across the control surface.

Let us consider a system at times  $t$  and  $t + \Delta t$ , as shown in Fig. 2-1. The dashed lines show the control surface, and the solid lines show the boundaries of the system. At time  $t$ , part of the system occupies the control volume while another part is about to move into the control volume. At time  $t + \Delta t$ , part of the system occupies the control volume while another part has moved out. Property  $B$  of the system at times  $t$  and  $t + \Delta t$  may be written as

$$\begin{aligned} B_{sys}(t) &= B_{cv}(t) + \Delta B_{in} \\ B_{sys}(t + \Delta t) &= B_{cv}(t + \Delta t) + \Delta B_{out} \end{aligned} \quad (2-2)$$

where the subscripts “sys” and “cv” refer to the system and the control volume, and the subscripts “in” and “out” refer to the inflow and outflow from the control volume respectively, and  $\Delta B_{in}$  and  $\Delta B_{out}$  are inflow and outflow of property  $B$  into or out of the control volume during time interval  $\Delta t$ .

The time rate of change of property  $B$  of the system is

$$\frac{dB_{sys}}{dt} = \lim_{\Delta t \rightarrow 0} \frac{B_{sys}(t + \Delta t) - B_{sys}(t)}{\Delta t} \quad (2-3)$$

By substituting the expressions for  $B_{sys}$  from Eq. 2-2 into Eq. 2-3 and rearranging the terms yield

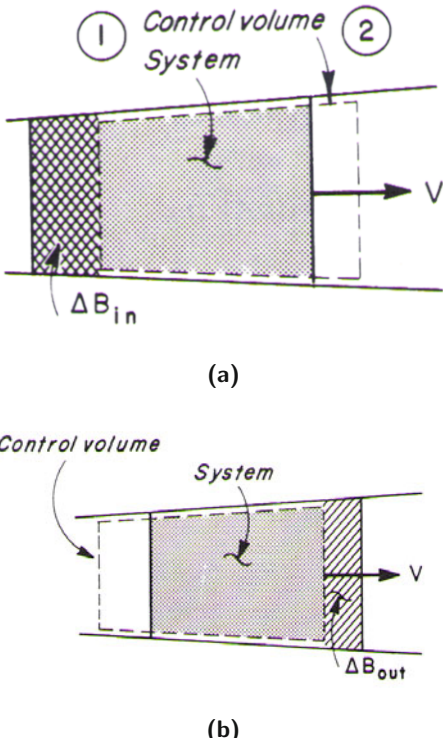
$$\frac{dB_{sys}}{dt} = \lim_{\Delta t \rightarrow 0} \frac{B_{cv}(t + \Delta t) - B_{cv}(t)}{\Delta t} + \lim_{\Delta t \rightarrow 0} \frac{\Delta B_{out}}{\Delta t} - \lim_{\Delta t \rightarrow 0} \frac{\Delta B_{in}}{\Delta t} \quad (2-4)$$

Now, as  $\Delta t$  approaches zero in the limit, the first term on the right-hand side of Eq. 2-4 represents the time rate of change of property  $B$  in the control volume, i.e.,

$$\lim_{\Delta t \rightarrow 0} \frac{B_{cv}(t + \Delta t) - B_{cv}(t)}{\Delta t} = \frac{dB_{cv}}{dt} \quad (2-5)$$

By substituting Eq. 2-1 into Eq. 2-5

$$\lim_{\Delta t \rightarrow 0} \frac{B_{cv}(t + \Delta t) - B_{cv}(t)}{\Delta t} = \frac{d}{dt} \int_{cv} \beta \rho dV \quad (2-6)$$

**Fig. 2-1.** System and control volume.

The second term on the right-hand side of Eq. 2-4 is the rate at which property  $B$  is leaving the control volume. Similarly, the third term of this equation represents the rate at which property  $B$  is entering the control volume. For one-dimensional flow, we may write

$$\lim_{\Delta t \rightarrow 0} \frac{\Delta B_{\text{out}}}{\Delta t} = (\beta \rho A V_s)_{\text{out}} \quad (2-7)$$

$$\lim_{\Delta t \rightarrow 0} \frac{\Delta B_{\text{in}}}{\Delta t} = (\beta \rho A V_s)_{\text{in}}$$

where  $A$  = cross-sectional area of the conduit and  $V_s$  = flow velocity measured relative to the control surface.

On the basis of Eqs. 2-6 and 2-7, Eq. 2-4 may be written as

$$\frac{dB_{\text{sys}}}{dt} = \frac{d}{dt} \int_{\text{cv}} \beta \rho dV + (\beta \rho A V_s)_{\text{out}} - (\beta \rho A V_s)_{\text{in}} \quad (2-8)$$

Note that the velocity,  $V$ , is with respect to the control surface, since it accounts for the inflow or outflow from the control volume. For a fixed control

volume,  $V_s$  = fluid flow velocity,  $V$ . However, if the control volume stretches or contracts with respect to time, then the control surface is not fixed and  $V_s$  in Eq. 2-8 is the relative flow velocity, i.e.,  $V_s = (V - W)$ , where  $W$  is the velocity of the control surface at section 1 for inflow and at section 2 for outflow. Both  $V$  and  $W$  are measured with respect to the coordinate axes. Hence, a general form of Eq. 2-8 for an expanding or contracting control volume in a one-dimensional flow may be written as

$$\frac{dB_{\text{sys}}}{dt} = \frac{d}{dt} \int_{\text{cv}} \beta \rho dV + [\beta \rho A(V - W)]_{\text{out}} - [\beta \rho A(V - W)]_{\text{in}} \quad (2-9)$$

This is the Reynolds transport theorem relating the properties of the system to those of the control volume.

## 2-3 Continuity Equation

To derive the continuity equation, we apply the law of conservation of mass to a control volume. We consider the flow of a slightly compressible fluid in a conduit having linearly elastic walls. Let the control surface be comprised of sections 1 and 2 and the inside surface of the conduit walls (Fig. 2-2). The control volume may shorten or elongate as pressure changes. Let the velocity (with respect to the coordinate axes) of sections 1 and 2 due to this contraction or expansion be  $W_1$  and  $W_2$ , respectively. Let us assume that the flow is one dimensional and the pressure at the end sections of the control volume is uniform. The radial velocity due to radial expansion and contraction is small and not included in the analysis. However, the effects of radial expansion and contraction are important and are taken into account. The distance  $x$ , flow velocity  $V$ , and discharge  $Q$  are considered positive in the downstream direction.

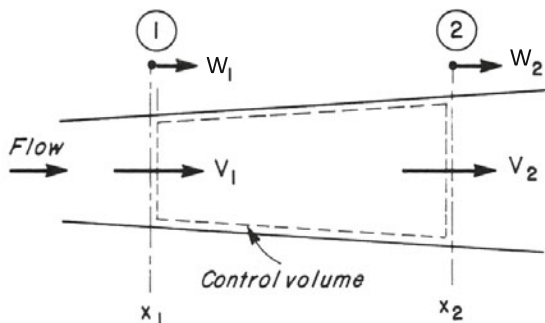


Fig. 2-2. Definition sketch.

To apply the Reynolds transport theorem for the conservation of mass, the intensive property of the fluid is mass/unit mass, i.e.,  $\beta = \lim_{\Delta m \rightarrow 0} \Delta m / \Delta m = 1$ . In addition, since the mass of a system remains constant,  $dM_{\text{sys}}/dt = 0$ . Hence, applying Eq. 2-9 to the control volume shown in Fig. 2-2 and substituting  $\beta = 1$ , we obtain

$$\frac{d}{dt} \int_{x_1}^{x_2} \rho A dx + \rho_2 A_2 (V_2 - W_2) - \rho_1 A_1 (V_1 - W_1) = 0 \quad (2-10)$$

The application of the Leibnitz's rule\* to the first term on the left-hand side gives

$$\begin{aligned} & \int_{x_1}^{x_2} \frac{\partial}{\partial t} (\rho A) dx + \rho_2 A_2 \frac{dx_2}{dt} - \rho_1 A_1 \frac{dx_1}{dt} \\ & + \rho_2 A_2 (V_2 - W_2) - \rho_1 A_1 (V_1 - W_1) = 0 \end{aligned} \quad (2-11)$$

Noting that  $dx_2/dt = W_2$  and  $dx_1/dt = W_1$ , this equation simplifies to

$$\int_{x_1}^{x_2} \frac{\partial}{\partial t} (\rho A) dx + (\rho AV)_2 - (\rho AV)_1 = 0 \quad (2-12)$$

Based on the mean value theorem†, this equation may be written as

$$\frac{\partial}{\partial t} (\rho A) \Delta x + (\rho AV)_2 - (\rho AV)_1 = 0 \quad (2-13)$$

where  $\Delta x = x_2 - x_1$ . Dividing throughout by  $\Delta x$  and letting  $\Delta x$  approach zero, Eq. 2-13 is simplified as

$$\frac{\partial}{\partial t} (\rho A) + \frac{\partial}{\partial x} (\rho AV) = 0 \quad (2-14)$$

Expansion of the terms inside the parentheses gives

$$A \frac{\partial \rho}{\partial t} + \rho \frac{\partial A}{\partial t} + \rho A \frac{\partial V}{\partial x} + \rho V \frac{\partial A}{\partial x} + AV \frac{\partial \rho}{\partial x} = 0 \quad (2-15)$$

By rearranging terms, using expressions for the total derivatives, and dividing throughout by  $\rho A$ , we obtain

\*Material presented in Sections 2-3 and 2-4 is based on the collaborative efforts of Professor Clayton Crowe and the author.

According to this rule [Wylie, 1967],

$$\frac{d}{dt} \int_{f_1(t)}^{f_2(t)} F(x, t) dx = \int_{f_1(t)}^{f_2(t)} \frac{\partial}{\partial t} F(x, t) dx + F(f_2(t), t) \frac{df_2}{dt} - F(f_1(t), t) \frac{df_1}{dt}$$

if  $f_1$  and  $f_2$  are differentiable functions of  $t$  and  $F(x, t)$  and  $\partial F/\partial t$  are continuous in  $x$  and  $t$ .

†According to this theorem,  $\int_{x_2}^{x_1} F(x) dx = (x_2 - x_1) F(\xi)$ , where  $x_1 < \xi < x_2$ .

$$\frac{1}{\rho} \frac{d\rho}{dt} + \frac{1}{A} \frac{dA}{dt} + \frac{\partial V}{\partial x} = 0 \quad (2-16)$$

Typically the variables of interest are the pressure intensity  $p$  and the flow velocity  $V$ . To write this equation in terms of these variables, we express the derivatives of  $\rho$  and  $A$  in terms of  $p$  and  $V$  as follows.

The bulk modulus of elasticity, of a fluid [Roberson and Crowe, 1997]

$$K = \frac{dp}{d\rho/\rho} \quad (2-17)$$

This equation may be written as

$$\frac{d\rho}{dt} = \frac{\rho}{K} \frac{dp}{dt} \quad (2-18)$$

Now, for a circular conduit having radius  $R$ ,

$$\frac{dA}{dt} = 2\pi R \frac{dR}{dt} \quad (2-19)$$

In terms of the strain,  $\epsilon$ , this equation may be written as

$$\frac{dA}{dt} = 2\pi R^2 \frac{1}{R} \frac{dR}{dt} \quad (2-20)$$

or

$$\frac{1}{A} \frac{dA}{dt} = 2 \frac{d\epsilon}{dt} \quad (2-21)$$

As indicated earlier, we assume that the conduit walls are linearly elastic [Timoshenko, 1941], i.e., stress is proportional to strain. This is true for most common pipe wall materials, e.g., metal, wood, concrete, etc. Then

$$\epsilon = \frac{\sigma_2 - \mu\sigma_1}{E} \quad (2-22)$$

where  $\sigma_2$  = hoop stress,  $\sigma_1$  = axial stress, and  $\mu$  = Poisson ratio. To simplify the derivation, we assume the conduit has expansion joints throughout its length. Therefore, the axial stress,  $\sigma_1 = 0$ . Hence, Eq. 2-22 becomes

$$\epsilon = \frac{\sigma_2}{E} \quad (2-23)$$

Now, the hoop stress in a thin-walled conduit

$$\sigma_2 = \frac{pD}{2e} \quad (2-24)$$

where  $p$  = inside pressure;  $e$  = thickness of the conduit walls and  $D$  = conduit diameter. By taking the time derivative of Eq. 2-24, we obtain

$$\frac{d\sigma_2}{dt} = \frac{p}{2e} \frac{dD}{dt} + \frac{D}{2e} \frac{dp}{dt} \quad (2-25)$$

Based on Eq. 2-23, we may write Eq. 2-25 as

$$E \frac{d\epsilon}{dt} = \frac{p}{2e} \frac{dD}{dt} + \frac{D}{2e} \frac{dp}{dt} \quad (2-26)$$

Using Eqs. 2-19 and 2-21, Eq. 2-26 becomes

$$E \frac{d\epsilon}{dt} = \frac{pD}{2e} \frac{d\epsilon}{dt} + \frac{D}{2e} \frac{dp}{dt} \quad (2-27)$$

which may be simplified as

$$\frac{d\epsilon}{dt} = \frac{\frac{D}{2e} \frac{dp}{dt}}{E - \frac{pD}{2e}} \quad (2-28)$$

It follows from Eqs. 2-21 and 2-28 that

$$\frac{1}{A} \frac{dA}{dt} = \frac{\frac{D}{e} \frac{dp}{dt}}{E - \frac{pD}{2e}} \quad (2-29)$$

Substituting Eqs. 2-18 and 2-29 into Eq. 2-16 and simplifying, the resulting equation becomes

$$\frac{\partial V}{\partial x} + \left( \frac{1}{K} + \frac{1}{eE - \frac{p}{2}} \right) \frac{dp}{dt} = 0 \quad (2-30)$$

Since  $p/2 \ll eE/D$  in typical engineering applications, this equation may be written as

$$\frac{\partial V}{\partial x} + \frac{1}{K} \left( 1 + \frac{1}{\frac{eE}{DK}} \right) \frac{dp}{dt} = 0 \quad (2-31)$$

Let us define

$$a^2 = \frac{\frac{K}{\rho}}{1 + \frac{DK}{eE}} \quad (2-32)$$

Note that this expression for the wave velocity is for a conduit with expansion joints. In Chapter 3, we show that  $a$  is the velocity of pressure wave in an elastic conduit filled with a slightly compressible fluid. For other types of support conditions, the expressions for the wave velocity are modified slightly. These expressions are presented in Section 2-6, with their derivation left as an exercise for the reader (Problem 2-6). Substituting Eq. 2-32 and the expression for the total derivative into Eq. 2-31 gives

$$\frac{\partial p}{\partial t} + V \frac{\partial p}{\partial x} + \rho a^2 \frac{\partial V}{\partial x} = 0 \quad (2-33)$$

This equation is called the continuity equation.

## 2-4 Momentum Equation

In this Section, we apply the Reynolds Transport Theorem to derive the momentum equation. The extensive property  $B$  for this application is the momentum of the fluid which is equal to  $mV$ . Therefore, the corresponding intensive property,

$$\beta = \lim_{\Delta m \rightarrow 0} V (\Delta m / \Delta m) = V$$

According to the Newton's second law of motion, the time rate of change of momentum of a system is equal to the resultant of the forces exerted on the system by its surroundings, i.e.,

$$\frac{dM_{\text{sys}}}{dt} = \sum F \quad (2-34)$$

By substituting  $\beta = V$  into Eq. 2-9 and using Eq. 2-34, we obtain

$$\frac{d}{dt} \int_{cv} V \rho dV + [\rho A (V - W) V]_2 - [\rho A (V - W) V]_1 = \sum F \quad (2-35)$$

By applying the Leibnitz rule to the first term on the left-hand side of this equation and noting that  $dx_1/dt = W_1$  and  $dx_2/dt = W_2$ , we obtain

$$\begin{aligned} & \int_{x_1}^{x_2} \frac{\partial}{\partial t} (\rho AV) dx + (\rho AV)_2 W_2 - (\rho AV)_1 W_1 + [\rho A (V - W) V]_2 \\ & - [\rho A (V - W) V]_1 = \sum F \end{aligned} \quad (2-36)$$

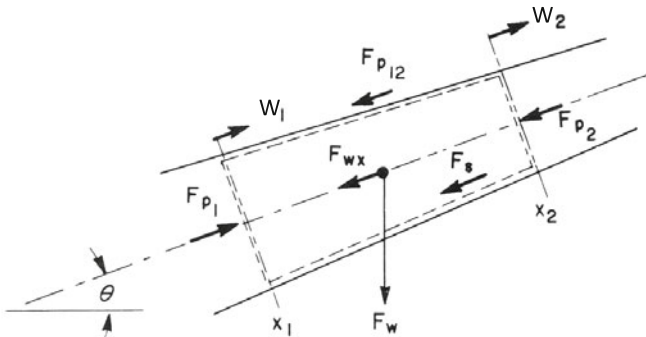


**Fig. 2-3.** Notation for momentum equation.

By simplifying this equation, applying the mean-value theorem to the first term, and dividing throughout by  $\Delta x$  give

$$\frac{d}{dt} (\rho A V) + \frac{(\rho A V^2)_2 - (\rho A V^2)_1}{\Delta x} = \frac{\sum F}{\Delta x} \quad (2-37)$$

Now let us consider the following forces acting on the control volume (Fig. 2-3):

$$\text{Pressure force at section 1, } F_{p_1} = p_1 A_1 \quad (2-38)$$

where  $p$  = pressure intensity, and the subscript 1 refers to cross section 1.

Similarly,

$$\text{Pressure force at section 2, } F_{p_2} = p_2 A_2 \quad (2-39)$$

Pressure force on the converging sides,

$$F_{p_{12}} = \frac{1}{2} (p_1 + p_2) (A_1 - A_2) \quad (2-40)$$

Component of the weight of fluid along the conduit centerline

$$F_{wx} = \rho g A (x_2 - x_1) \sin \theta \quad (2-41)$$

where  $\theta$  = angle the conduit makes with the horizontal, considered positive for conduit sloping upwards in the downstream direction. Now,

$$\text{Shear force, } F_s = \tau_o \pi D (x_2 - x_1) \quad (2-42)$$

where  $\tau_o$  = shear stress exerted by the conduit walls on the flowing fluid.

Considering the downstream flow direction as positive, it follows from Eqs. 2-38 to 2-42 that

$$\begin{aligned} \sum F &= p_1 A_1 - p_2 A_2 - \frac{1}{2} (p_1 + p_2) (A_1 - A_2) \\ &\quad - \rho g A (x_2 - x_1) \sin \theta - \tau_o \pi D (x_2 - x_1) \\ &= \frac{1}{2} (p_1 - p_2) (A_1 + A_2) - \rho g A (x_2 - x_1) \sin \theta \\ &\quad - \tau_o \pi D (x_2 - x_1) \end{aligned} \quad (2-43)$$

Dividing Eq. 2-43 by  $\Delta x = x_2 - x_1$  gives

$$\frac{\sum F}{\Delta x} = \frac{(p_1 - p_2) (A_1 + A_2)}{2 \Delta x} - \rho g A \sin \theta - \tau_o \pi D \quad (2-44)$$

By substituting Eq. 2-44 into Eq. 2-37 and letting  $\Delta x$  approach zero in the limit, we obtain

$$\frac{\partial}{\partial t} (\rho A V) + \frac{\partial}{\partial x} (\rho A V^2) + A \frac{\partial p}{\partial x} + \rho g A \sin \theta + \tau_o \pi D = 0 \quad (2-45)$$

Let us assume the energy losses for a given flow velocity during the transient state are the same as those for steady flows at that velocity (we will discuss unsteady friction in Section 2-8). If we use the Darcy-Weisbach friction equation for computing the friction losses, then the wall shear stress

$$\tau_o = \frac{1}{8} \rho f V |V| \quad (2-46)$$

where  $f$  = Darcy-Weisbach friction factor. Note that we are writing  $V^2$  as  $V|V|$  to allow for the reverse flow. The substitution of this expression into Eq. 2-45 and the expansion of the terms in parentheses yield

$$\begin{aligned} V \frac{\partial}{\partial t} (\rho A) + \rho A \frac{\partial V}{\partial t} + V \frac{\partial}{\partial x} (\rho AV) + \rho AV \frac{\partial V}{\partial x} \\ + A \frac{\partial p}{\partial x} + \rho g A \sin \theta + \frac{\rho A f V |V|}{2D} = 0 \end{aligned} \quad (2-47)$$

The rearrangement of the terms of this equation gives

$$\begin{aligned} V \left[ \frac{\partial}{\partial t} (\rho A) + \frac{\partial}{\partial x} (\rho AV) \right] + \rho A \frac{\partial V}{\partial t} + \rho AV \frac{\partial V}{\partial x} \\ + A \frac{\partial p}{\partial x} + \rho g A \sin \theta + \frac{\rho A f V |V|}{2D} = 0 \end{aligned} \quad (2-48)$$

Based on the continuity equation (Eq. 2-14), the sum of the two terms inside the brackets is zero. Hence, dropping the terms inside the brackets and dividing the resulting equation by  $pA$ , we obtain

$$\frac{\partial V}{\partial t} + V \frac{\partial V}{\partial x} + \frac{1}{\rho} \frac{\partial p}{\partial x} + g \sin \theta + \frac{f V |V|}{2D} = 0 \quad (2-49)$$

This equation is called the momentum equation.

## 2-5 General Remarks

In this section, we discuss various parameters of the governing equations and whether they are hyperbolic, parabolic or elliptic. Each type of these equations describes a particular physical process or phenomenon. For example, wave propagation in a fluid is described by a set of hyperbolic partial differential equations. In addition, once we know the type of the governing equations, suitable numerical methods can be selected for their solution.

The continuity and momentum equations (Eqs. 2-33 and 2-49) describe transient-flows in closed conduits. In these equations, distance  $x$  and time  $t$  are two independent variables and pressure  $p$  and flow velocity  $V$  are two dependent variables. The other variables,  $a$ ,  $\rho$ ,  $f$ , and  $D$ , are the system parameters and usually do not vary with time; these may, however, be functions

of  $x$ . Although wave velocity  $a$  depends on the characteristics of the conduit and on the fluid properties, laboratory tests [Streeter, 1972] show that it is significantly reduced by a reduction of pressure, even when the pressure remains above the liquid vapor pressure. The friction factor  $f$  usually varies with the Reynolds number. However, the effects of such a variation of  $f$  on transient conditions are usually small and may be neglected.

### Classification of Governing Equations

Equations 2-33 and 2-49 are a set of first-order, partial differential equations. We shall now determine the type of these equations, make some qualitative observations for their solution, and discuss methods for numerically integrating them. These equations may be written in the matrix form as

$$\frac{\partial}{\partial t} \begin{pmatrix} p \\ V \end{pmatrix} + \begin{bmatrix} V & \rho a^2 \\ \frac{1}{\rho} & V \end{bmatrix} \frac{\partial}{\partial x} \begin{pmatrix} p \\ V \end{pmatrix} = \begin{pmatrix} 0 \\ -g \sin \theta - \frac{fV|V|}{D} \end{pmatrix} \quad (2-50)$$

or

$$\frac{\partial \mathbf{U}}{\partial t} + \mathbf{B} \frac{\partial \mathbf{U}}{\partial \mathbf{x}} = \mathbf{E} \quad (2-51)$$

where

$$\mathbf{U} = \begin{pmatrix} p \\ V \end{pmatrix}; \quad \mathbf{B} = \begin{bmatrix} V & \rho a^2 \\ \frac{1}{\rho} & V \end{bmatrix}; \quad (2-52)$$

$$\mathbf{E} = \begin{pmatrix} 0 \\ -g \sin \theta - \frac{fV|V|}{D} \end{pmatrix}$$

The eigenvalues,  $\lambda$ , of matrix  $\mathbf{B}$  determine the type of the set of partial differential equations. The characteristic equation [Wylie, 1967] of matrix  $\mathbf{B}$  is

$$(V - \lambda)^2 = a^2 \quad (2-53)$$

Hence,

$$\lambda = V \pm a \quad (2-54)$$

Since both eigenvalues are real and distinct, Eqs. 2-33 and 2-49 are a set of hyperbolic partial differential equations. This type of equations describes the propagation of waves in a fluid.

## Initial Conditions

The initial conditions are needed to compute the transient conditions. Mostly the initial conditions correspond to the initial steady-state flows. In this section, we discuss how to specify the initial flow conditions that are compatible with the transient flow equations.

Equations 2-33 and 2-49 describe unsteady, nonuniform flow of a slightly compressible fluid in an elastic conduit. Steady flow may be considered a special case [Stuckenbruck and Wiggert, 1985] in which the time variation of flow velocity,  $\partial V/\partial t$  and of pressure,  $\partial p/\partial t$  are both zero. Hence the governing equations for steady flow may be derived from these two equations by dropping the terms representing the local variation of pressure and flow velocity with respect to time  $t$ ; i.e.,  $\partial p/\partial t$  and  $\partial V/\partial t$  of Eqs. 2-33 and 2-49 are both zero. Therefore, Eqs. 2-33 and 2-49 for *steady flow* become

$$V \frac{dp}{dx} + \rho a^2 \frac{dV}{dx} = 0 \quad (2-55)$$

$$V \frac{dV}{dx} + \frac{1}{\rho} \frac{dp}{dx} + g \sin \theta + \frac{fV|V|}{2D} = 0 \quad (2-56)$$

Note the total derivatives and not the partial derivatives in these equations since both  $p$  and  $V$  are functions of  $x$  only. It follows from Eq. 2-55 that

$$\frac{dV}{dx} = -\frac{V}{\rho a^2} \frac{dp}{dx} \quad (2-57)$$

Substitution of this expression into Eq. 2-56 and simplification of the resulting equation give

$$\frac{dp}{dx} = \frac{\rho [g \sin \theta + fV|V|/(2D)]}{M^2 - 1} \quad (2-58)$$

where  $M = V/a$  = Mach number. By substituting Eq. 2-58 into Eq. 2-57 and simplifying, we obtain

$$\frac{dV}{dx} = \frac{M^2}{V} \frac{(g \sin \theta + fV|V|/2D)}{1 - M^2} \quad (2-59)$$

For nonzero  $V$ , it is clear from Eq. 2-59 that the velocity gradient  $dV/dx$  is not zero and similarly it is clear from Eq. 2-58 that the pressure gradient  $dp/dx$  is not constant. This is due to the fact that the mass density of the fluid and the flow area of the conduit are functions of  $x$ .

If the initial conditions correspond to steady flow and all the terms of the governing equations have to be included in the analysis, then the initial conditions should be determined from Eqs. 2-58 and 2-59. However, in most of the engineering applications, a number of terms of the governing equations are small as compared to the other terms and may be neglected. This considerably simplifies the analysis without significantly affecting the accuracy of the computed results. These simplified equations are derived in the next section.

### Simplified Equations

In most of the engineering applications, the convective acceleration terms,  $V(\partial p/\partial x)$  and  $V(\partial V/\partial x)$ , are small as compared to the other terms. Similarly, the slope term is usually small and may be neglected. Therefore, dropping these terms from the governing equations, we obtain

$$\begin{aligned}\frac{\partial p}{\partial t} + \rho a^2 \frac{\partial V}{\partial x} &= 0 \\ \frac{\partial V}{\partial t} + \frac{1}{\rho} \frac{\partial p}{\partial x} + \frac{fV|V|}{2D} &= 0\end{aligned}\tag{2-60}$$

It is a common practice in hydraulic engineering to compute pressures in the pipeline in terms of the piezometric head,  $H$ , above a specified datum and use the discharge,  $Q$ , as the second variable instead of the flow velocity  $V$ . Now,  $Q = VA$  and the pressure intensity  $p$  may be written as

$$p = \rho g (H - z)\tag{2-61}$$

in which  $z$  = elevation of the pipe centerline above the specified datum.

We assumed in the derivation of the governing equations (Eqs. 2-33 and 2-49) that the fluid is slightly compressible, and the conduit walls are slightly deformable. Therefore, we may neglect the spatial variation of  $\rho$  and flow area  $A$  due to the variation of the inside pressure with  $x$ . However, the small variation of  $\rho$  and  $A$  is indirectly taken into account by considering the wave velocity  $a$  to have a finite value. Note that if the fluid is considered incompressible and the conduit walls are assumed rigid, then the wave velocity becomes infinite, and a pressure or velocity change is felt instantaneously throughout the system. For a horizontal pipe,  $dz/dx = 0$ . Hence, with these assumptions, it follows from Eq. 2-61 that  $\partial p/\partial t = \rho g (\partial H/\partial t)$  and  $\partial p/\partial x = \rho g (\partial H/\partial x)$ .

By substituting these relationships into Eqs. 2-60 and 2-61, we obtain

$$\frac{\partial H}{\partial t} + \frac{a^2}{gA} \frac{\partial Q}{\partial x} = 0\tag{2-62}$$

$$\frac{\partial Q}{\partial t} + gA \frac{\partial H}{\partial x} + \frac{fQ|Q|}{2DA} = 0\tag{2-63}$$

Steady-state equations corresponding to Eqs. 2-62 and 2-63 may be obtained by substituting  $\partial H/\partial t = 0$  and  $\partial Q/\partial t = 0$ . Hence, it follows from Eq. 2-62 that  $\partial Q/\partial x = 0$ ; i.e.,  $Q$  is constant along the pipe length. Substituting  $\partial Q/\partial t = 0$  into Eq. 2-63, simplifying the resulting equation, and writing it in a finite-difference form, we obtain

$$\Delta H = \frac{f \Delta x Q^2}{2g D A^2}\tag{2-64}$$

where  $\Delta H$  = head loss in pipe length  $\Delta x$  for a flow of  $Q$ . Note that this equation is the same as the Darcy-Weisbach friction equation.

To summarize, steady-state conditions should be computed from Eqs. 2-55 and 2-56 if Eqs. 2-33 and 2-49 are the governing equations. However, if a simplified form of the governing equations (i.e., Eqs. 2-62 and 2-63) is used, then  $Q$  is considered as constant along the pipe, and the piezometric head along the pipe length is computed from Eq. 2-64. However, if complete equations (Eqs. 2-33 and 2-49) are the governing equations, then assuming constant discharge for the initial steady-state conditions and computing the pressure head along the pipe length by using the Darcy-Weisbach equation give erroneous results.

In the above derivation, we used the Darcy-Weisbach equation to compute the friction losses. For a general exponential formula for these losses, the last term of Eq. 2-63 may be written as  $kQ|Q|^m/D^b$ , with the values of  $k$ ,  $m$ , and  $b$  depending on the formula employed. For example, for the Hazen-William formula,  $m = 0.85$  and  $b = 4.87$ . With correct values of  $m$  and  $b$ , the results are independent of the formula employed; i.e., the Darcy-Weisbach and the Hazen-William formulas give comparable results [Evangelisti, 1969]. For most of typical engineering applications, the above assumptions are valid and Eqs. 2-62 and 2-63 may be used. However, if any of the above assumptions are not valid, then the analysis should employ complete equations, Eqs. 2-33 and 2-49. From hereon, in our discussion, we will use Eqs. 2-62 and 2-63.

## 2-6 Wave Velocity

An expression for the wave velocity in a slightly compressible fluid confined in a rigid conduit was derived in Section 1-4. However, in addition to the bulk modulus of elasticity and mass density of the fluid, the wave velocity depends upon the elastic properties of the conduit as well as on the external constraints. Elastic properties include the conduit size, wall thickness, and wall material; and the external constraints include the type of supports and the freedom of conduit movement in the longitudinal direction. The bulk modulus of elasticity of a fluid depends upon its temperature, pressure, and the quantity of entrained gases. Pearsall [1965] showed that the wave velocity changes by about 1 percent per  $5^\circ\text{C}$ . The fluid compressibility increases by the presence of free gases, and it has been reported [Pearsall, 1965] that 1 part of air in 10,000 parts of water by volume reduces the wave velocity by about 50 percent. Figure 2-4 shows the variation of wave velocity in an air-water mixture with different air content [Kobori, et al., 1955]. An expression for the wave velocity in a gas-liquid mixture is derived in Section 9-5.

The presence of solids in liquids have less drastic influence on the wave velocity, unless they are compressible. Laboratory studies [Streeter, 1972] and prototype tests [Pearsall, 1965] show that the dissolved gases tend to come out of solution when the pressure is reduced, even when it remains above the liquid vapor pressure. This results in decreasing the wave velocity significantly.

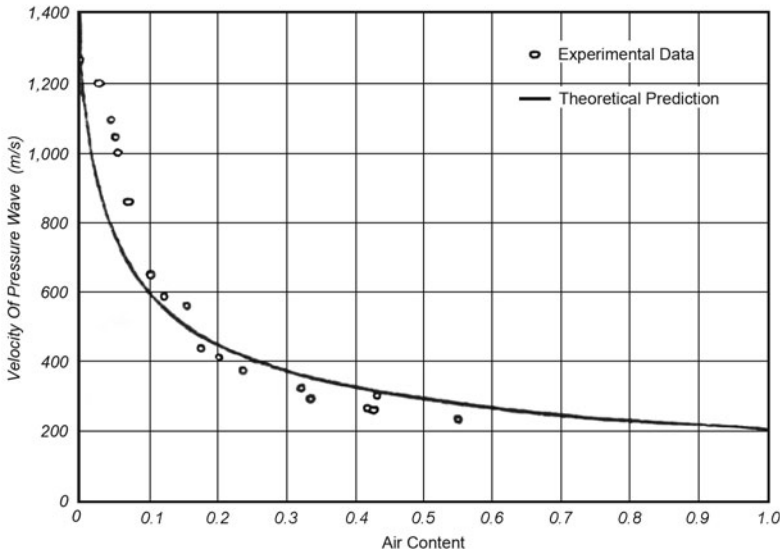


**Fig. 2-4.** Variation of wave velocity in an air-water mixture with air content. (After Kobori, et al. [1955].)

Therefore, the wave velocity of a positive pressure wave may be higher than that of a negative wave. Further prototype tests are needed to quantify the reduction in the wave velocity due to reduction of pressure.

Hallowell [1963] presented the following general expression for the wave velocity

$$a = \sqrt{\frac{K}{\rho [1 + (K/E) \psi]}} \quad (2-65)$$

in which  $\psi$  is a nondimensional parameter that depends on the elastic properties of the conduit;  $E$  = Young's modulus of elasticity of the conduit walls; and  $K$  and  $\rho$  are the bulk modulus of elasticity and density of the fluid, respectively. The moduli of elasticity of materials commonly used for conduit walls and the bulk moduli of elasticity and mass densities of various liquids are listed in Tables 2-1 and 2-2.

Expressions for  $\psi$  for various conditions are as follows:

### Rigid Conduit

$$\psi = 0 \quad (2-66)$$

### Thick-Walled Elastic Conduit

Three different cases for the anchoring of the conduit are as follows.

**Table 2-1. Young's modulus of elasticity and Poisson's ratio**

| Material                  | Modulus of Elasticity, $E^*$<br>(GPa) | Poisson's Ratio |
|---------------------------|---------------------------------------|-----------------|
| Aluminum alloys           | 68-73                                 | 0.33            |
| Asbestos cement, transite | 24                                    |                 |
| Brass                     | 78-110                                | 0.36            |
| Cast iron                 | 80-170                                | 0.25            |
| Concrete                  | 14-30                                 | 0.1-0.15        |
| Copper                    | 107-131                               | 0.34            |
| Glass                     | 46-73                                 | 0.24            |
| Lead                      | 4.8-17                                | 0.44            |
| Mild steel                | 200-212                               | 0.27            |
| Plastics                  |                                       |                 |
| ABS                       | 1.7                                   | 0.33            |
| Nylon                     | 1.4-2.75                              |                 |
| Perspex                   | 6.0                                   | 0.33            |
| Polyethylene              | 0.8                                   | 0.46            |
| Polystyrene               | 5.0                                   | 0.4             |
| PVC rigid                 | 2.4-2.75                              |                 |
| Rocks                     |                                       |                 |
| Granite                   | 50                                    | 0.28            |
| Limestone                 | 55                                    | 0.21            |
| Quartzite                 | 24.0-44.8                             |                 |
| Sandstone                 | 2.75-4.8                              | 0.28            |
| Schist                    | 6.5-18.6                              |                 |

Source: Compiled from Halliwell [1963]; Roark [1965] and Pickford [1969].

\* To convert  $E$  into lb/ft<sup>2</sup>, multiply the values in this column by 145.04 × 10<sup>3</sup>.

- i. Conduit anchored against longitudinal movement throughout its length

$$\psi = 2(1 + \nu) \left( \frac{R_o^2 + R_i^2}{R_o^2 - R_i^2} - \frac{2\nu R_i^2}{R_o^2 - R_i^2} \right) \quad (2-67)$$

in which  $\nu$  = the Poisson ratio and  $R_o$  and  $R_i$  = the external and internal radii of the conduit.

- ii. Conduit anchored against longitudinal movement at the upper end

$$\psi = 2 \left[ \frac{R_o^2 + 1.5R_i^2}{R_o^2 - R_i^2} + \frac{\nu(R_o^2 - 3R_i^2)}{R_o^2 - R_i^2} \right] \quad (2-68)$$

- iii. Conduit with frequent expansion joints

$$\psi = 2 \left( \frac{R_o^2 + R_i^2}{R_o^2 - R_i^2} + \nu \right) \quad (2-69)$$

### ***Thin-Walled Elastic Conduit***

Three different cases for the anchoring of the conduit against longitudinal movement are:

- i. Conduit anchored against longitudinal movement throughout its length

$$\psi = \frac{D}{e} (1 - \nu^2) \quad (2-70)$$

in which  $D$  = conduit diameter and  $e$  = wall thickness.

- ii. Conduit anchored against longitudinal movement at the upper end [Wylie and Streeter, 1983]

$$\psi = \frac{D}{e} (1 - 0.5\nu) \quad (2-71)$$

- iii. Conduit with frequent expansion joints

$$\psi = \frac{D}{e} \quad (2-72)$$

### ***Rock Tunnel***

Halliwell [1963] presented long expressions for  $\psi$  for the lined and unlined rock tunnels. Usually the rock characteristics are not known precisely because of nonhomogeneous rock conditions and because of the presence of fissures. Therefore, the following simplified expressions [Parmakian, 1963] may be used instead of Halliwell's expressions.

- i. Unlined tunnel

$$\begin{aligned} \psi &= 1 \\ E &= G \end{aligned} \quad (2-73)$$

in which  $G$  = modulus of rigidity of the rock.

- ii. Steel-lined tunnel

$$\psi = \frac{DE}{GD + Ee} \quad (2-74)$$

in which  $e$  = thickness of the steel-liner and  $E$  = modulus of elasticity of steel.

### ***Reinforced Concrete Pipe***

The reinforced concrete pipe is replaced by an equivalent steel pipe having equivalent thickness [Parmakian, 1963]

$$e_e = E_r e_c + \frac{A_s}{l_s} \quad (2-75)$$

in which  $e_c$  = thickness of the concrete pipe;  $A_s$  and  $l_s$  are the cross-sectional area and the spacing of steel bars, respectively; and  $E_r$  = ratio of the modulus of elasticity of concrete to that of steel. Usually the value of  $E_r$  varies from 0.06 to 0.1. However, to allow for any cracks in the concrete pipe, a value of 0.05 is suggested [Parmakian, 1963]. The wave velocity may then be determined from Eq. 2-65 for the equivalent thickness  $e_e$  and the modulus of elasticity of steel.

### **Wood-Stave Pipe**

The thickness of a uniform steel pipe equivalent to the wood-stave pipe is determined [Parmakian, 1963] from Eq. 2-75 by using  $E_r = \frac{1}{60}$ ,  $e_c$  = thickness of wood staves, and  $A_s$  and  $l_s$  are the cross-sectional area and the spacing of the steel bands, respectively. The wave velocity is then computed from Eq. 2-65.

### **Polyvinyl Chloride (PVC) and Reinforced Plastic Pipes**

Watters et al. [1976] show that Eq. 2-65 may be used to determine the wave velocity in the polyvinyl chloride (PVC) and in the reinforced plastic pipes, provided a proper value of the modulus of elasticity for the wall material is used.

### **Noncircular Conduits**

The following expression for  $\psi$  is obtained from the equation for the wave velocity in the thin-walled rectangular conduits presented by Jenkner [1971] by using the steady-state bending theory and by allowing the corners of the conduit to rotate:

$$\psi = \frac{\beta b^4}{15e^3 d} \quad (2-76)$$

in which  $\beta = 0.5(6 - 5\alpha) + 0.5(d/b)^3[6 - 5(b/d)^2]$ ,  $\alpha = [1 + (d/b)^3]/[1 + (d/b)]$ ,  $b$  = width of the conduit (longer side), and  $d$  = depth of the conduit (shorter side).

Thorley and Guymer [1976] included the influence of the shear force on the bending deflection of the thick-walled ( $l/e < 20$ ) rectangular conduits while deriving the equations for the wave velocity. From these equations, the following expression is obtained for a *thick-walled conduit* having a square cross section:

$$\psi = \frac{1}{15} \left( \frac{l}{e} \right)^3 + \frac{l}{e} \left( 1 + \frac{e}{2G} \right) \quad (2-77)$$

in which  $e$  = wall thickness,  $(l - e)$  = inside dimension of the conduit, and  $G$  = shear modulus of the wall material. Based on the equations presented by

Thorley and Twyman [1977], the following expression is obtained for  $\psi$  for a *thin-walled hexagonal conduit*:

$$\psi = 0.0385 \left( \frac{l}{e} \right)^3 \quad (2-78)$$

in which  $l$  = mean width of one of the flat sides of the hexagonal section.

**Table 2-2. Bulk modulus of elasticity and density of common liquids at atmospheric pressure**

| Liquid        | Temperature<br>(°C) | Density $\rho^*$<br>(kg/m <sup>3</sup> ) | Bulk Modulus of<br>Elasticity, $K^{**}$<br>(GPa) |
|---------------|---------------------|--|--|
| Benzene       | 15                  | 880                                      | 1.05   |
| Ethyl alcohol | 0                   | 790                                      | 1.32   |
| Glycerin      | 15                  | 1,260                                    | 4.43   |
| Kerosene      | 20                  | 804                                      | 1.32   |
| Mercury       | 20                  | 13,570                                   | 26.2   |
| Oil           | 15                  | 900                                      | 1.5  |
| Water, fresh  | 20                  | 999                                      | 2.19   |
| Water, sea    | 15                  | 1,025                                    | 2.27   |

Source: Compiled from Pearsall [1965]; Baumeister [1967] and Pickford [1969].

\* To convert the specific weight of the liquid into lb/ft<sup>3</sup>, multiply the values of this column by  $62.43 \times 10^{-3}$ .

\*\* To convert  $K$  into lb/in<sup>2</sup>, multiply the values of this column by  $145.04 \times 10^3$ .

## 2-7 Solution of Governing Equations

As demonstrated previously, the momentum and continuity equations are quasi-linear, hyperbolic, partial differential equations. A closed-form solution of these equations is not available. However, by neglecting or by linearizing the nonlinear terms, various graphical [Parmakian, 1963; Bergeron, 1961] and analytical [Rich, 1963; Wood, 1937] methods have been developed. These methods are approximate and cannot be used to analyze large systems or systems with complex boundary conditions.

The following methods, suitable for computer analyses, are available for numerically integrating the nonlinear, hyperbolic partial differential equations:

- Method of characteristics;
- Finite-difference methods;
- Finite-element method;

Spectral method, and  
Boundary-integral method.

The method of characteristics has become popular and is extensively used for the solution of one-dimensional, hydraulic transient problems, especially if the wave velocity is constant. This method has proven to be superior to other methods in several aspects, such as correct simulation of steep wave fronts, illustration of wave propagation, ease of programming, and efficiency of computations [Evangelisti, 1969; Wylie and Streeter, 1983; Lister, 1960; Abbott, 1966; Streeter and Lai, 1962]. Details of this method are presented in the next chapter; and its use and necessary boundary conditions are developed in Chapters 4 through 10.

The finite-difference methods [Perkins et al., 1964; Smith, 1978; Chaudhry and Yevjevich, 1981; Chaudhry, 1983; Chaudhry and Hussaini, 1983] may be classified into two categories: explicit and implicit. Both of these categories have several schemes. Implicit methods usually have the advantage that they allow larger time steps. However, if too large a time step is used, then the accuracy of the scheme is adversely affected and numerical oscillations may be produced in some cases that may yield totally incorrect results [Holloway and Chaudhry, 1985]. Both of these methods are briefly discussed in Chapter 3. The finite-element method [Chung, 1978; Baker, 1983] does not offer any significant advantage for the solution of one-dimensional problems. The spectral method [Gottlieb and Orszag, 1976-1977] is not suitable for nonperiodic boundary conditions and the boundary-integral method [Liggett, 1984] does not efficiently handle the time-dependent problems as compared to the other available methods, especially if shocks or bores are formed. Neither of these methods are discussed further herein.

## 2-8 Unsteady Friction

In the derivation of the governing equations in Sections 2-3 and 2-4, we assumed that the steady friction formulas may be used to compute the transient-state head losses. Although this approximation yields satisfactory results for computing the first peak of transient pressures, the computed pressure oscillations show very slow dissipation as compared to that measured in the laboratory experiments or that measured during field tests on actual projects. This does not pose serious limitations for determining the maximum or minimum pressures in a typical installations or typical operations. However, the computed results are not reliable for multiple operations, such as starting the pumps following a power failure, load acceptance on turbines following load rejection, or for sequential starting or stopping of turbo-machinery, etc.

Several methods have been proposed to account for the unsteady friction effects in transient flow computations. These methods may be classified into

three categories: Quasi-two-dimensional, convolution integral, and instantaneous, acceleration-based methods. Brief descriptions of the first two methods and details of the third method are presented in the following paragraphs. This discussion is based on the paper by Reddy, Silva, and Chaudhry [2012]. Literature review by Ghidaoui [2001] is a good source on the topic.

### **Quasi-two-dimensional models**

These models provide accurate simulation of the phenomenon [Vardy and Hwang 1991; Brunone et al. 1995; Silva-Araya and Chaudhry 1997; Pezzinga 1999; Zhao and Ghidaoui 2004]. However, they are computationally intensive, and thus have been used primarily for simple piping systems.

### **Convolution integral methods**

Zielke [1968] introduced these methods by developing an exact solution for the laminar unsteady friction. These methods, suitable for one-dimensional models, use past local accelerations and weighting functions. These solutions are time consuming and require large computer memory. Trikha [1975] proposed a less demanding version of Zielke's method, but with reduced accuracy. Similar versions were proposed by Kagawa et al. [1983], Suzuki et al. [1991], and Schohl [1993]. The convolution integral method was extended to turbulent flow by Vardy and Brown [1995, 2003, 2004] for smooth and for rough pipes. These solutions provide acceptable results at the expense of numerical accuracy, because of the approximation of the convolution integral by a limited number of weighted coefficients [Vitkovsky et al. 2006b].

### **Instantaneous acceleration-based (IAB) methods**

These models are based on the assumption that the damping attributable to unsteady friction is caused by instantaneous local and convective accelerations. The accelerations are computed from the average cross-sectional values without taking into consideration the velocity distribution at a cross section. Carsten and Roller [1959] introduced this concept. Since then several different formulations have been proposed [Brunone and Golia, 1990; Vitkovsky et al. 2006a, Brunone et al. 1991b; Bergant et al. 2001; Bughazem and Anderson, 2000; Vardy and Brown, 1995, and 2003; Ramos et al. 2004]. Of these formulations, one- and two-coefficient models appear to give satisfactory results and are presented herein.

The friction term in the momentum equation may be divided into steady and unsteady parts as

$$\frac{\partial H}{\partial x} + \frac{1}{g} \frac{\partial V}{\partial t} + J_s + J_u = 0 \quad (2-79)$$

in which  $J_s$  and  $J_u$  are the steady and unsteady friction terms, respectively. The steady friction may be expressed by the Darcy-Weisbach relation as

$$J_s = \frac{fV|V|}{2gD} \quad (2-80)$$

An expression for  $J_u$  for a one-coefficient model may be written as

$$J_u = \frac{k}{g} \left[ \frac{\partial V}{\partial t} + \text{Sign}(V)a \left| \frac{\partial V}{\partial x} \right| \right] \quad (2-81)$$

The expression for a two-coefficient model used by Loureiro and Ramos [2003], Ramos [2004] and Vitkovsky et al. [2000] are similar and are of the form

$$J_u = \frac{1}{g} \left[ K_{ut} \frac{\partial V}{\partial t} + K_{ux} \text{Sign}(V)a \left| \frac{\partial V}{\partial x} \right| \right] \quad (2-82)$$

in which  $K_{ut}$  and  $K_{ux}$  are two decay coefficients related to the local and convective accelerations, respectively. It has been shown numerically that the term  $K_{ut}\partial V/\partial t$  affects the phase shift of transient pressure waves and  $K_{ux}\partial V/\partial x$  affects the rate of damping [Ramos et al. 2004].

Reddy, Silva and Chaudhry [2012] presented an equation for the estimation of decay coefficients for IAB models. To develop this equation, a genetic algorithm (GA) was used to reproduce time-history of pressure oscillations recorded in 14 experiments, conducted in laboratories all over the world. The pipe material for these experiments includes steel, copper, and PVC, pipe diameter ranges from 0.012 m to 0.4 m and pipe length from 14 m to 160 m. Transients were produced by valve closure at the upstream or downstream ends of the piping systems.

The decay coefficients for one- and two-coefficient IAB models were determined for both methods of characteristics and finite-difference methods. The values that reproduced the time history of the experimental pressure oscillations range from 0.015 to 0.060 for  $K$  in the one-coefficient model and from 0.025 to 0.053 for  $K_{ux}$  and from 0.006 to 0.057 for  $K_{ut}$  in the two-coefficient model.

### Example

Compute the wave velocity in the steel penstock of the Kootenay Canal hydroelectric power plant, BC, Canada. The data for different segments of the penstock are listed in [Table 2-3](#). The values of  $E$  for steel,  $G$  for concrete, and  $K$  and  $\rho$  for water are 207 GPa, 20.7 GPa, 2.19 GPa, and 999 kg/m<sup>3</sup>, respectively.

### Solution

For transient analysis, the wave velocity in each segment of the penstock may be determined as follows.

**Table 2-3. Data for penstock**

| Pipe | Length<br>(m) | Diameter<br>(m) | Wall<br>Thickness,<br>(mm) | Remarks                       |
|------|---------------|-----------------|----------------------------|-------------------------------|
| 1    | 244.          | 6.771           | 19                         | Expansion coupling at one end |
| 2    | 36.5          | 5.55            | 22                         | Encased in concrete           |

**Pipe 1**

$$\frac{D}{e} = \frac{6.71}{0.019} = 353$$

As the pipe is anchored at one end,

$$\begin{aligned}\psi &= \frac{D}{e} (1 - 0.50\nu) \quad (\text{Eq. 2-71}) \\ &= 353 (1 - 0.15) \\ &= 300.05\end{aligned}$$

$$a = \sqrt{\frac{K}{\rho [1 + (K/E)\psi]}} \quad (\text{Eq. 2-65})$$

$$\frac{K}{E} = \frac{2.19}{207} = 0.0106$$

$$\begin{aligned}a &= \sqrt{\frac{2.19 \times 10^9}{999 (1 + 0.0106 \times 300.05)}} \\ &= 724 \text{ m/s}\end{aligned}$$

**Pipe 2**

Equations for a steel-lined tunnel (Eq. 2-74) may be used to compute the wave velocity in pipe 2.

$$\begin{aligned}\psi &= \frac{DE}{GD + Ee} \\ &= \frac{5.55 \times 207 \times 10^9}{20.7 \times 10^9 \times 5.55 + 207 \times 10^9 \times .022} \\ &= 9.62 \quad (\text{Eq. 2-74}) \\ a &= \sqrt{\frac{2.19 \times 10^9}{999 (1 + 0.0106 \times 9.62)}} \\ &= 1410 \text{ m/s}\end{aligned}$$

## 2-9 Summary

In this chapter, the momentum and continuity equations describing the transient flows in closed conduits are derived and the assumptions made in the derivations are discussed. It is demonstrated that these equations are quasi-linear, hyperbolic, partial differential equations. Various numerical methods available for their solution are discussed and a number of models to simulate unsteady friction and expressions for the wave velocity in the closed conduits are presented.

## Problems

**2-1** Derive the momentum equation considering the conduit walls are rigid and the fluid is compressible.

**2-2** Compute the wave velocity in a 3.05-m-diameter steel penstock having a wall thickness of 25 mm if it:

- i. is embedded in a concrete dam;
- ii. is anchored at the upstream end; and
- iii. has expansion joints throughout its length.

**2-3** Determine the wave velocity in a reinforced concrete pipe having 1.25-m diameter, 0.15-m wall thickness, and carrying water. The 20-mm reinforcing bars have a spacing of 0.5 m, and the pipe has expansion joints throughout its length.

**2-4** A 0.2-m-diameter copper pipe having a wall thickness of 25 mm is conveying kerosene oil at 20°C from a container to a valve. If the valve is closed instantly, at what velocity would the pressure waves propagate in the pipe? Assume the pipe is anchored at the upper end.

**2-5** [Figure 5-13](#) shows the power conduits of an underground hydroelectric power station. Compute the wave velocity in each segment of the conduit. Assume modulus of rigidity of rock is 5.24 GPa.

**2-6** Derive the continuity equation if the conduit is:

- i. anchored against longitudinal movement throughout its length; and
- ii. anchored against longitudinal movement at the upper end.

## Answers

**2-2**

- i. 1413 m/s
- ii. 992 m/s
- iii. 978 m/s

**2-3** 913 m/s

**2-4** 1232 m/s

## References

- Baker, A. J., 1983, *Finite Element Computational Fluid Mechanics*, McGraw-Hill, New York, NY.
- Baumeister, T. (ed.), *Standard Handbook for Mechanical Engineers*, 7th ed., McGraw-Hill Book Co., New York, NY.
- Bergant, A., Simpson, A. R. and Vitkovsky, J. P., 2001, "Developments in Unsteady Pipe Flow Friction Modelling." *Jour. Hydraulic Research*, vol. 39, no. 3, pp. 249-257.
- Bergeron, L., 1961, *Waterhammer in Hydraulics and Wave Surges in Electricity*, John Wiley & Sons, Inc., New York, NY.
- Brunone, B., Golia, U. M. 1990, "Improvements in Modelling of Water Hammer and Cavitating Flow in Pipes. Experimental verification." *Proc., 22nd Convegno Nazionale di Idraulica e Costuzioni Idrauliche*, Vol. 4, Italian Group of Hydraulics (GII), pp. 147-160 (in Italian).
- Brunone, B., Golia, U. M. and Greco, M., 1991b, "Some Remarks of the Momentum Equation for Fast Transients." *Proc., Int. Conf. on Hydraulic Transients with Water Column Separation, International Association for Hydro-Environment Engineering and Research*, (IAHR) Group, Madrid, Spain, pp. 201-209.
- Brunone, B., Golia, U. M. and Greco, M., 1995, "The Effects of Two Dimensionality on Pipe Transients Modeling." *Jour. Hydraulic Engineering*, vol. 121, no. 12, pp. 906-912.
- Bughazem, M. and Anderson, A. 1996, "Problems with simple models for damping in unsteady flow." *Proc., Int. Conf. on Pressure Surges*, Vol. 7, BHRA Group, Bedford, UK, pp. 483-498.
- Carstens, M. R. and Roller, J. E. 1959, "Boundary-shear Stress in Unsteady Turbulent Pipe Flow." *Jour. Hydraul Div.*, 95, pp. 67-81.
- Chaudhry, M. H. and Yevjevich, V., 1981, *Closed-Conduit Flow*, Water Resources Publications, Littleton, Co.
- Chaudhry, M. H., 1983, "Numerical Solution of Transient-Flow Equations," *Proc., Hydraulic Specialty Conf.*, Amer. Soc. Civ. Engrs., pp. 663-660.

- Chaudhry, M. H. and Hussaini, M. Y., 1983, "Second-Order Explicit Methods for Transient-Flow Analysis," in *Numerical Methods for Fluid Transients Analysis*, Martin, C. S. and Chaudhry, M. H. (eds.), Amer. Soc. Mech. Engrs., pp. 9-15.
- Chaudhry, M. H. and Hussaini, M. Y., 1985, "Second-Order Accurate Explicit Finite-Difference Schemes for Waterhammer Analysis," *Jour. Fluids Engineering*, Amer. Soc. Mech. Engrs., vol. 107, Dec., pp. 523-529.
- Evangelisti, G., 1969, "Waterhammer Analysis by the Method of Characteristics," *L'Energia Elettrica*, Nos. 10-12, pp. 673-692, 759-770, 839-858.
- Föllmer, B. and Zeller, H., 1980, "The Influence of Pressure Surges on the Functioning of Safety Valves," *Third International Conference on Pressure Surges*, Canterbury, England, March 25-27, pp. 429-444.
- Ghidaoui, M. S., and Kolyshkin, A. A. 2001, "Stability Analysis of Velocity Profiles in Waterhammer," *Journal of Hydraulic Engineering*, ASCE, vol. 127, no. 6, pp. 499-512.
- Ghidaoui, M. S., Axworthy, D., Zhao, M. and McInnis, D. 2001, "Closure to "Extended Thermodynamics Derivation of Energy Dissipation in Unsteady Pipe Flow." *Jour. Hydraulic Engineering*, vol. 127, no. 10, pp. 888-890.
- Halliwell, A. R., 1963, "Velocity of a Waterhammer Wave in an Elastic Pipe," *Jour., Hydraulics Div.*, Amer. Soc. Civil Engrs., vol. 89, No. HY4, July, pp. 1-21.
- Hirose, M., 1971, "Frequency-Dependent Wall Shear in Transient Fluid Flow Simulation of Unsteady Turbulent Flow," *Master's Thesis*, Massachusetts Institute of Technology , Mass..
- Holloway, M. B. and Chaudhry, M. H., 1985, "Stability and Accuracy of Waterhammer Analysis," *Advances in Water Resources*, vol. 8, Sept., pp. 121-128.
- Hydraulic Models*, Manual of Engineering Practice No. 25, Committee of Hyd. Div. on Hyd. Research, Amer. Soc. Civil Engrs., July.
- Jenkner, W. R., 1971, "Über die Druckstossgeschwindigkeit in Rohrleitungen mit quadratischen und rechteckigen Querschnitten," *Schweizerische Bauzeitung*, vol. 89, Feb., pp. 99-103.
- Joukowsky, N., 1904, "Waterhammer," Translated by O. Simin, *Proc. Amer. Water Works Assoc.*, vol. 24, pp. 341-424.
- Kagawa, T., Lee, I., Kitagawa, A. and Takenaka, T. 1983, "High Speed and Accurate Computing Method of Frequency-dependent Friction in Laminar Pipe Flow for Characteristic Method." *Nippon Kikai Gakkai Ronbunshu, A-hen*, 49(447), pp. 2638-2644 (in Japanese).
- Karam, J. T. and Leonard, R. G., 1973, "A Simple Yet Theoretically Based Time Domain Model for Fluid Transmission Line Systems," *Jour. Fluids Engineering, Trans.*, Amer. Soc. Mech. Engrs., vol. 95, Dec., pp. 498-504.
- Kennison, H. F., 1956, "Surge-Wave Velocity-Concrete Pressure Pipe," *Trans., Amer. Soc. Mech. Engrs.*, Aug., pp. 1323-1328.
- Kobori, T., Yokoyama, S., and Miyashiro, H., 1955, "Propagation Velocity of Pressure Wave in Pipeline," *Hitachi Hyoron (Hitachi Review)*, vol. 37, no.

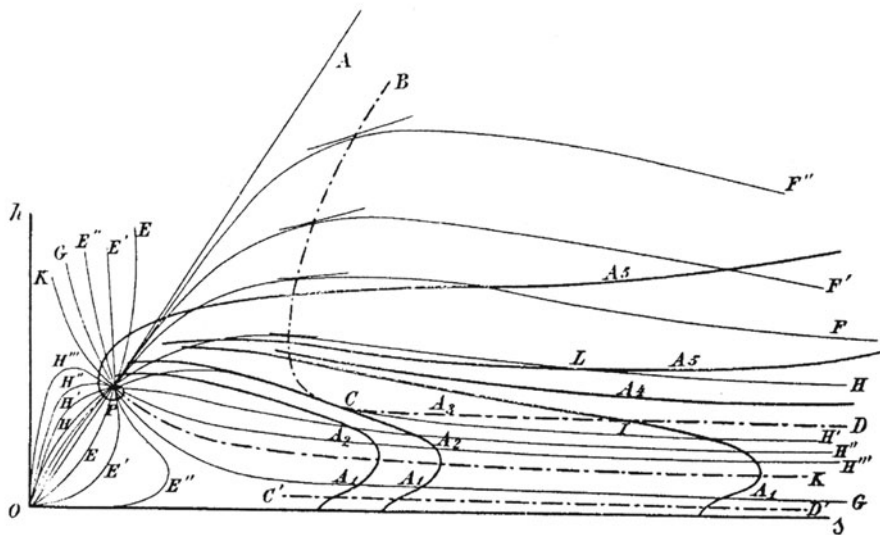
- 10, Oct., pp. 33-37 (translated by C. Lai, Sept. 1966, US Geological Survey Library, Dec. 1974.)
- Liggett, J. A., 1984, "The Boundary Element Method-Some Fluid Applications," in *Multi-Dimensional Fluid Transients*, Chaudhry, M. H. and Martin, C. S. (eds.), Amer. Soc. Mech. Engrs., Dec., pp. 1-8.
- Lister, M., 1960, "The Numerical Solution of Hyperbolic Partial Differential Equations by the Method of Characteristics," in Ralson, A., and Wilf, H. S. (eds.), *Mathematical Method for Digital Computers*, John Wiley & Sons, Inc., New York, pp. 165-179.
- Loureiro, D. and Ramos, H. 2003, "A Modified Formulation for Estimating the Dissipative Effect of 1-D Transient Pipe Flow." *Proc., Conf. on Pumps, Electromechanical Devices and Systems Applied to Urban Water Management*, International Water Association (IWA)/International Association on Hydraulic Engineering and Research (IAHR), Madrid, Spain, pp. 755-763.
- Parmakian, J., 1963, *Waterhammer Analysis*, Dover Publications, Inc., New York, NY.
- Pearsall, I. S., 1965, "The Velocity of Waterhammer Waves," *Proc. Symposium on Surges in Pipelines*, Inst. of Mech. Engrs., England, vol. 180, Part 3E, Nov., pp. 12-27.
- Perkins, F. E., Tedrow, A. C., Eagleson, P. S., and Ippen, A. T., 1964, "Hydro-power Plant Transients," *Report No. 71*, Part II and III, Dept. of Civil Engineering, Hydrodynamics Lab., Massachusetts Institute of Technology, Sept.
- Pezzinga, G., 1999, "Quasi-2D Model for Unsteady Flow in Pipe Networks." *Jour. Hydraulic Engineering*, vol. 125, no. 7, pp. 676-685.
- Pickford, J., 1969, *Analysis of Surge*, Macmillan, London, UK.
- Rahm, S. L. and Lindvall, G. K. E., 1963, "A Laboratory Investigation of Transient Pressure Waves in Pre-Stressed Concrete Pipes," *Proc. 10th International Assoc. for Hydraulic Research*, London, UK, pp. 47-53.
- Ramos, H., Covas, D., Borga, A. and Loureiro, D. 2004, "Surge Damping Analysis in Pipe Systems: Modeling and Experiments." *Jour. Hydraulic Research*, vol. 42, no. 4, pp. 413-425.
- Reddy, H. P., Silva-Araya, W. and Chaudhry, M. H., 2012, "Estimation of Decay Coefficients for Unsteady Friction for Instantaneous, Acceleration-Based Models" *Jour. Hydraulic Engineering*, vol. 138, no. 3, pp. 260-271.
- Rich, G. R., 1963, *Hydraulic Transients*, Dover Publications, Inc., New York, NY.
- Roark, R. J., 1965, *Formulas for Stress and Strain*, 4th ed., McGraw-Hill Book, New York, NY.
- Roberson, J. A. and Crowe, C. T., 1997, *Engineering Fluid Mechanics*, 6th ed., Wiley, New York, NY.
- Safwat, H. H., 1971, "Measurements of Transient Flow Velocities for Waterhammer Applications," Paper No. 71-FE-29, Amer. Soc. of Mech. Engrs., May, 8.

- Schohl, G. A., 1993, "Improved Approximate Method for Simulating Frequency-dependant Friction in Transient Laminar Flow." *Jour. Fluids Engineering*, vol. 115, no. 3, pp. 420-424.
- Silva-Araya, W. F. and Chaudhry, M. H. 1997, "Computation of Energy Dissipation in Transient Flow." *Jour. Hydraulic Engineering*, vol. 123, no. 2, pp. 108-115.
- Smith, G. D., 1978, *Numerical Solution of Partial Differential Equations*, Second Ed., Clarendon Press, Oxford, UK.
- Streeter, V. L. and Lai, C., 1962, "Waterhammer Analysis Including Fluid Friction," *Jour. Hydraulics Div.*, Amer. Soc. Civil Engrs., vol. 88, No. HY3, May, pp. 79-112.
- Stuckenbruck, S., and Wiggert, D. C., 1985, Discussion of "Fundamental Equations of Waterhammer, by E. B. Wylie," *Jour. Hydraulic Engineering*, Amer. Soc. Civil Engrs., vol. III, Aug., pp. 1195-1196. (See original paper Apr 1984 and other discussions and closure Aug 1985, pp. 1185-2000).
- Suzuki, K., Taketomi, T. and Sato, S. 1991 "Improving Zielkes Method of Simulating Frequency-dependent Friction in Laminar Liquid Pipe Flow." *Jour. Fluids Engineering*, vol. 113, no. 4, pp. 569-573.
- Swaffield, J. A., 1968-69, "The Influence of Bends on Fluid Transients Propagated in Incompressible Pipe Flow," *Proc. Institution of Mech. Engrs.*, vol. 183, Part I, no. 29, pp. 603-614.
- Swaminathan, K. V., 1965, "Waterhammer Wave Velocity in Concrete Tunnels," *Water Power*, March, 117-121.
- Thorley, A. R. D., 1968, "Pressure Transients in Hydraulics Pipelines," Paper No. 68-WA/FE-2, *Amer. Soc. Mech. Engrs.*, Dec., 8.
- Thorley, A. R. D. and Guymer, G., 1976, "Pressure Surge Propagation in Thick-Walled Conduits of Rectangular Cross Section," *Jour. Fluid Engineering*, Amer. Soc. Mech. Engrs., vol. 98, Sept., pp. 455-460.
- Thorley, A. R. D. and Twyman, J. W. R., 1977, "Propagation of Transient Pressure Waves in a Sodium-Cooled Fast Reactor," *Proc. Second Conf. on Pressure Surges*, London, UK, published by British Hydromechanics Research Assoc..
- Timoshenko, S., 1941, *Strength of Materials*, Second Edition, part 2, Van Nostrand Co. Inc New York.
- Trikha, A. K., 1975, "An Efficient Method for Simulating Frequency-Dependent Friction in Transient Liquid Flow," *Jour. Fluid Engineering*, Amer. Soc. Mech. Engrs., vol. 97, March, pp. 97-105.
- Vardy, A. E. and Brown, J. M. B., 1995, "Transient, turbulent, smooth pipe friction." *Jour. Hydraulic Research*, vol. 33, no. 4, pp. 435-456.
- Vardy, A. E. and Brown, J. M. B., 2003, "Transient Turbulent Friction in Smooth Pipe Flows." *Jour. Sound and Vib.*, vol. 259, no. 5, pp. 1011-1036.
- Vardy, A. E. and Brown, J. M. B., 2004, "Transient Turbulent Friction in Fully Rough Pipe Flows." *Jour. Sound and Vib.*, vol. 270, no 12, pp. 233-257.
- Vardy, A. B. and Hwang, K., 1991, "A Characteristics Model of Transient Friction." *Jour. Hydraulic Res.*, vol. 29, no. 5, pp. 669-684.

- Vitkovsky, J. P., Lambert, M. F. Simpson, A. R. and Bergant, A., 2000, "Advances in Unsteady Friction Modeling in Transient Pipe Flow." *Proc., 8th Int. Conf. on Pressure Surges*, BHR Group, Bedford, UK, pp. 471-482.
- Vitkovsky, J. P., Bergant, A., Simpson, A. R. and Lambert, M. F. 2006a, "Systematic Evaluation of One-dimensional Unsteady Friction Models in Simple Pipelines." *Jour. Hydraulic Engineering*, vol. 132, no. 7, pp. 696-708.
- Vitkovsky, J. P., Stephens, M., Bergant, A., Simpson, A. R. and Lambert, M. F. 2006b, "Numerical Error in Weighing Functionbased Unsteady Friction Models for Pipe Transients." *Jour. Hydraulic Engineering*, vol. 132, no. 7, pp. 709-721.
- Watters, G. Z., Jeppson, R. W., and Flammer, G. H., 1976, "Water Hammer in PVC and Reinforced Plastic Pipe," *Jour. Hyd. Div.*, Amer. Soc. Civil Engrs., vol. 102, July, pp. 831-843. (See also Discussion by Goldberg, D. E., and Stoner, M. A., June 1977.)
- Weyler, M. E., Streeter, V. L., and Larsen, P. S., 1971, "An Investigation of the Effect of Cavitation Bubble on the Momentum Loss in Transient Pipe Flow," *Jour. Basic Engineering*, Amer. Soc. Mech. Engrs., March, pp. 1-10.
- White, F. M., 1998, *Fluid Mechanics*, McGraw-Hill, New York.
- Wood, F. M., 1937, "The Application of Heavisides Operational Calculus to the Solution of Problems in Waterhammer," *Trans., Amer. Soc. Mech. Engrs.*, vol. 59, Nov., pp. 703-713.
- Wylie, C. R., 1967, *Advanced Engineering Mathematics*, Third Edition, McGraw-Hill Book Co., New York, NY.
- Wylie, E. B. and Streeter, V. L., 1983, *Fluid Transients*, FEB Press, Ann Arbor, MI.
- Zhao, M. and Ghidaoui, M. S. 2004, "Review and analysis of 1D and 2D energy dissipation models for transient flows." *Proc., Int. Conf. on Pressure Surges*, BHR Group, Bedford, UK, pp. 477-492.
- Zielke, W., 1968, "Frequency-Dependent Friction in Transient Pipe Flow," *Jour. Basic Engineering*, Amer. Soc. Mech. Engrs., March.

---

## CHARACTERISTICS AND FINITE-DIFFERENCE METHODS



Massau's integral curves for hydraulic problem, Massau 1878-1887,  
Livre VI, Planche XIII. (After Tournès, D. [2003].)

### 3-1 Introduction

We demonstrated in Chapter 2 that the equations describing the transient flow in closed conduits are hyperbolic, partial differential equations, and discussed a number of numerical methods available for their solution. The details of the method of characteristics [Lister, 1960; Streeter and Lai, 1962; Perkins et al. 1964; Abbott, 1966, Evangelisti, 1969; Gray, 1953] are presented in this chapter. The equations for simulating the transient flow in a conduit by this method are derived, a number of simple boundary conditions are developed and the stability and convergence criteria are discussed. Explicit and implicit finite-difference methods are briefly introduced. A computational procedure for the analysis of piping systems is then outlined. The chapter concludes with the presentation of a case study.

The material presented in this chapter is free of advanced mathematics and a reader having an elementary knowledge of partial differential equations should be able to follow the development of these equations; those interested in a rigorous treatment should refer to Lister [1960], Abbott [1966], and Evangelisti [1969].

### 3-2 Characteristic Equations

To facilitate discussion, let us rewrite the simplified form of momentum and continuity equations (Eqs. 2-64 and 2-63) derived in the last chapter as

$$L_1 = \frac{\partial Q}{\partial t} + gA \frac{\partial H}{\partial x} + RQ |Q| = 0 \quad (3-1)$$

$$L_2 = a^2 \frac{\partial Q}{\partial x} + gA \frac{\partial H}{\partial t} = 0 \quad (3-2)$$

in which  $R = f/(2DA)$ . Let us consider a linear combination of Eqs. 3-1 and 3-2, i.e.,  $L = L_1 + \lambda L_2$ , where  $\lambda$  is an unknown multiplier. By multiplying Eq. 3-2 by  $\lambda$ , adding to Eq. 3-1 and re-arranging the terms of the resulting equation, we obtain

$$\left( \frac{\partial Q}{\partial t} + \lambda a^2 \frac{\partial Q}{\partial x} \right) + \lambda gA \left( \frac{\partial H}{\partial t} + \frac{1}{\lambda} \frac{\partial H}{\partial x} \right) + RQ |Q| = 0 \quad (3-3)$$

If  $H = H(x, t)$  and  $Q = Q(x, t)$ , then the total derivative

$$\frac{dQ}{dt} = \frac{\partial Q}{\partial t} + \frac{\partial Q}{\partial x} \frac{dx}{dt} \quad (3-4)$$

and

$$\frac{dH}{dt} = \frac{\partial H}{\partial t} + \frac{\partial H}{\partial x} \frac{dx}{dt} \quad (3-5)$$

By defining the unknown multiplier  $\lambda$  as

$$\frac{1}{\lambda} = \frac{dx}{dt} = \lambda a^2 \quad (3-6)$$

i.e.,

$$\lambda = \pm \frac{1}{a} \quad (3-7)$$

and by using Eqs. 3-4 and 3-5, Eq. 3-3 may be written as

$$\frac{dQ}{dt} + \frac{gA}{a} \frac{dH}{dt} + RQ |Q| = 0 \quad (3-8)$$

if

$$\frac{dx}{dt} = a \quad (3-9)$$

and

$$\frac{dQ}{dt} - \frac{gA}{a} \frac{dH}{dt} + RQ |Q| = 0 \quad (3-10)$$

if

$$\frac{dx}{dt} = -a \quad (3-11)$$

Equations 3-8 and 3-10 are called compatibility equations. Note that Eq. 3-8 is valid if Eq. 3-9 is satisfied and that Eq. 3-10 is valid if Eq. 3-11 is satisfied. In other words, by imposing the relations given by Eqs. 3-9 and 3-11, we have eliminated independent variable  $x$ , and have converted the partial differential equations, Eqs. 3-1 and 3-2, into ordinary differential equations in the independent variable  $t$ . However, we have paid a price for this simplification: Eqs. 3-1 and 3-2 are valid everywhere in the  $x$ - $t$  plane; however, Eq. 3-8 is valid only along the straight line (if  $a$  is constant) given by Eq. 3-9, and Eq. 3-10 is valid only along the straight line described by Eq. 3-11.

In the  $x$ - $t$  plane, Eqs. 3-9 and 3-11 represent two straight lines having slopes  $\pm a$ . These are called characteristic lines. Mathematically, these lines divide the  $x$ - $t$  plane into two regions, which may be dominated by two different solutions, i.e., the solution may be discontinuous along these lines [Perkins et al., 1964]. Physically, these lines represent the path traversed by a disturbance in the  $x$ - $t$  plane. For example, a disturbance at point  $A$  ([Fig. 3-1](#)) at time  $t_o$  travels along line  $AP$  and reaches point  $P$  after time  $\Delta t$ .

Prior to presenting a procedure for solving Eqs. 3-8 and 3-10, let us first discuss the physical significance of characteristic lines in the  $x$ - $t$  plane. To facilitate discussion, let us consider the piping system shown in [Fig. 3-2](#). The piping system has a constant-head reservoir at the upper end (at  $x = 0$ ), and a valve at the downstream end (at  $x = L$ ), and the transient conditions are produced by closing the valve. The compatibility equations (Eqs. 3-8 and 3-10) are valid along the pipe length (i.e., for  $0 < x < L$ ) and special boundary conditions are required at the ends, i.e., at  $x = 0$  and at  $x = L$  ([Fig. 3-3](#)). Let us assume the flow is steady at time  $t = 0$  when the valve is instantaneously closed. This reduces the flow at the valve to zero which increases the pressure at the valve. Because of the pressure increase, a positive pressure wave (the

pressure is higher behind the wave front than that in front) travels in the upstream direction. Line  $BC$  is the path of this wave in the  $x-t$  plane, as shown in Fig. 3-4. It is clear from this figure that the conditions in Region I depend only on the initial conditions because the upstream boundary remains unchanged, whereas in Region II they depend upon the conditions imposed by the downstream boundary. Thus, the characteristic line  $BC$  separates the two regions with different solutions. If excitations are imposed simultaneously at points  $A$  and  $B$ , then the region influenced by the initial conditions is as shown in Fig. 3-5; the characteristic line  $AC$  separates the regions influenced by the upstream boundary and by the initial conditions, and the line  $BC$  separates the regions influenced by the downstream boundary and by the initial conditions. In other words, the characteristic lines on the  $x-t$  plane represent the traveling paths of perturbations initiated at various locations in the system.

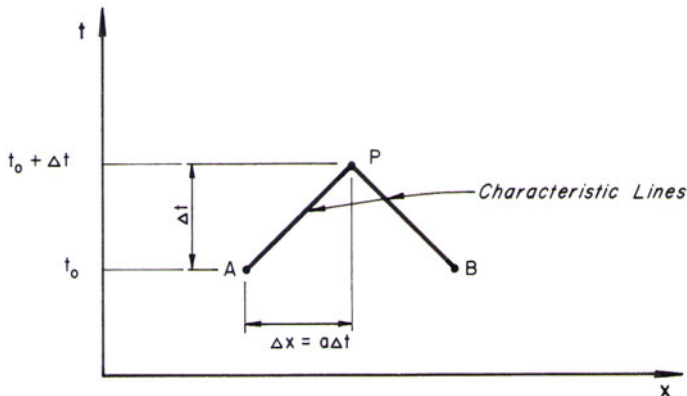


**Fig. 3-1. Characteristic lines in  $x-t$  plane.**

Let us now discuss how to compute transient pressures and discharges. Let us assume the head,  $H$ , and discharge,  $Q$  at time  $t = t_o$  are known. These may be either initially known (i.e., at  $t = 0$ , these are initial conditions), or they were calculated during the previous time step. We want to compute the unknown values of  $H$  and  $Q$  at time  $t = t_o + \Delta t$ . Referring to Fig. 3-1, let us say that we know the values of  $Q$  and  $H$  at points  $A$  and  $B$  and we want to determine their values at point  $P$ . This may be done by solving Eqs. 3-8 and 3-10 as follows: By multiplying the left-hand side of Eq. 3-8 by  $dt$  and integrating, we obtain

$$\int_A^P dQ + \frac{gA}{a} \int_A^P dH + R \int_A^P Q |Q| dt = 0 \quad (3-12)$$

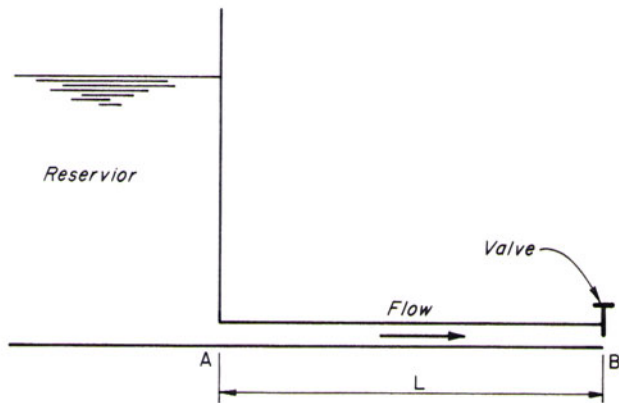


Fig. 3-2. Piping system.

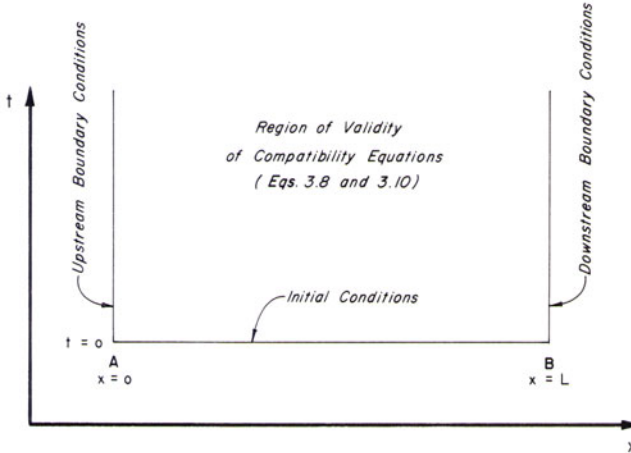


Fig. 3-3. Regions of validity for a single pipe.

We shall use subscripts  $A$  and  $P$  to indicate locations in the  $x$ - $t$  plane; e.g.,  $Q_P$  is the discharge at point  $P$ . Since Eq. 3-8 is valid only along the characteristic line  $AP$ , we have used the limits for integration from  $A$  to  $P$ .

We can easily evaluate the first two integral terms of Eq. 3-12. However, we cannot do so for the third term, which represents the friction losses, because we do not explicitly know the variation of  $Q$  with respect to  $t$ . By using a first-order approximation, we may evaluate the integral of the third term as

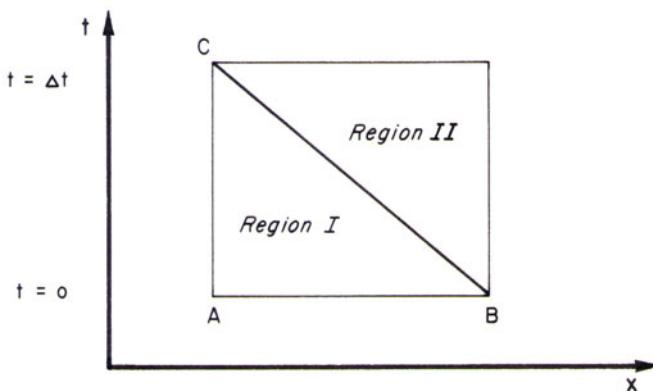


Fig. 3-4. Excitation at downstream end.

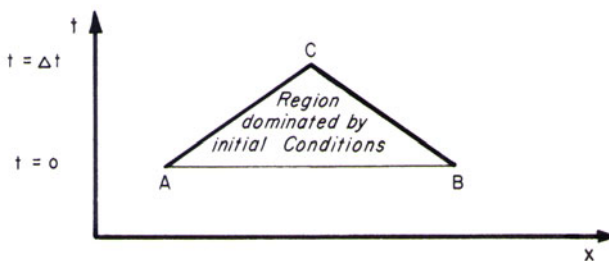


Fig. 3-5. Excitation at the upstream and downstream ends.

$$\begin{aligned} R \int_A^P Q |Q| dt &\simeq R Q_A |Q_A| (t_P - t_A) \\ &= R Q_A |Q_A| \Delta t \end{aligned} \quad (3-13)$$

In other words,  $Q$  remains constant from  $A$  to  $P$  for the evaluation of this term. Hence, Eq. 3-12 becomes

$$Q_P - Q_A + \frac{gA}{a} (H_P - H_A) + R \Delta t Q_A |Q_A| = 0 \quad (3-14)$$

Note that Eq. 3-14 is exact except for the approximation of the friction term. This first-order approximation usually yields satisfactory results for typical engineering applications. However, as discussed in Section 3-4, the first-order approximation may yield unstable results if the friction term becomes large. To avoid this, we may use a shorter computational interval  $\Delta t$  or use a higher-order approximation or an iterative procedure to evaluate the friction term.

For example, a second-order approximation of the integral of the third term of Eq. 3-12 is

$$R \int_A^P Q |Q| dt = 0.5 R \Delta t [Q_A |Q_A| + Q_P |Q_P|] \quad (3-15a)$$

This is commonly referred to as the trapezoidal rule. Two other approximations for the friction term are

$$R \int_A^P Q |Q| dt = R \Delta t \frac{Q_A + Q_P}{2} \left| \frac{Q_A + Q_P}{2} \right| \quad (3-15b)$$

and

$$R \int_A^P Q |Q| dt = R \Delta t |Q_A| Q_P \quad (3-15c)$$

Since the value of  $Q_P$  is unknown, an iterative procedure may be used for the approximations of Eqs. 3-15a and 3-15b. The approximation of Eq. 3.15c, however, results in a linear equation similar to Eq. 3-14 that may be solved directly [Wylie, 1983]. By proceeding similarly, we may write Eq. 3-10 as

$$Q_P - Q_B - \frac{gA}{a} (H_P - H_B) + R \Delta t Q_B |Q_B| = 0 \quad (3-16)$$

By combining the known variables together, Eq. 3-14 may be written as

$$Q_P = C_p - C_a H_P \quad (3-17)$$

and Eq. 3-16 as

$$Q_P = C_n + C_a H_P \quad (3-18)$$

where

$$C_p = Q_A + \frac{gA}{a} H_A - R \Delta t Q_A |Q_A| \quad (3-19)$$

$$C_n = Q_B - \frac{gA}{a} H_B - R \Delta t Q_B |Q_B| \quad (3-20)$$

and

$$C_a = \frac{gA}{a} \quad (3-21)$$

Note that Eq. 3-17 is valid along the positive characteristic line  $AP$  and Eq. 3-18, along the negative characteristic line  $BP$  (Fig. 3-1). The value of  $C_p$  and  $C_n$  are known and are constant for each time step although they may vary from one time interval to next, and  $C_a$  is a constant that depends upon the conduit properties. We will refer to Eq. 3-17 as the *positive characteristic equation* and Eq. 3-18 as the *negative characteristic equation*. In Eqs. 3-17 and 3-18, we have two unknowns, namely,  $H_P$  and  $Q_P$ . The values of these unknowns may be determined by simultaneously solving these two equations, i.e.,

$$Q_P = 0.5 (C_p + C_n) \quad (3-22)$$

Now the value of  $H_P$  may be determined either from Eq. 3-17 or Eq. 3-18. Thus, by using Eqs. 3-17 and 3-22,  $Q_P$  and  $H_P$  at all interior points at time  $t_o + \Delta t$  (i.e., the end of the time step) may be determined (see Fig. 3-6). However, at the boundaries, either Eq. 3-17 or 3-18 is available. Therefore, as discussed later, we need special boundary conditions to determine the conditions at the boundaries at time  $t_o + \Delta t$ .

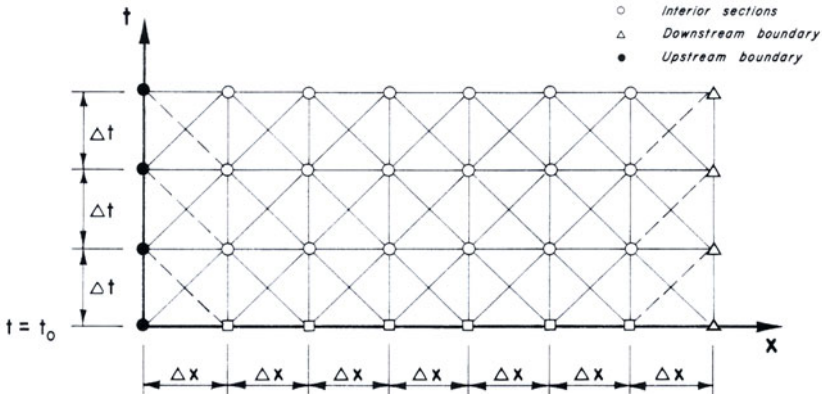


**Fig. 3-6.** Characteristic grid.

To illustrate the use of the above equations, let us consider the pipeline of Fig. 3-2. The pipeline is divided into  $n$  reaches (Fig. 3-6), each having length  $\Delta x$ . The ends of these reaches are called *sections*, *nodes*, or *grid points*. The end sections of each pipe are referred to as *boundaries*, and the sections excluding the boundaries are called *interior sections*, *interior nodes*, or *interior grid points*.

The steady-state conditions at  $t = t_o$  at all the grid points are first computed. Then, to determine the conditions at  $t = t_o + \Delta t$ , Eqs. 3-17 and 3-22 are used for the interior nodes, and special boundary conditions are used for the end nodes. A close look at Fig. 3-6 shows that the conditions at the boundaries at  $t = t_o + \Delta t$  must be known to calculate the conditions at  $t = t_o + 2\Delta t$  at the interior nodes adjacent to the boundaries. Now the discharge and head at time  $t_o + \Delta t$  being known at all the nodes,  $Q_P$  and  $H_P$  at  $t = t_o + 2\Delta t$  are computed by following the procedure just outlined. In this manner, the computations proceed step-by-step until transient conditions for the required time are determined.

### 3-3 Boundary Conditions

In the previous section we indicated that special boundary conditions are needed to determine the transient-state head and discharge at the boundaries. These are developed by solving Eqs. 3-17 or 3-18, or both, simultaneously with the conditions imposed by the boundary. These conditions describe special relationships that define the discharge or head at the boundary, or a relationship between the head and discharge at the boundary. Equation 3-17 is used for the downstream boundaries and Eq. 3-18, for the upstream boundaries.

Let us now discuss the notation we shall use. We designate the upstream and downstream ends with reference to the initial-flow direction even though the flow may reverse during the transient state. A section at the upstream end of a conduit is numbered as section 1 and the one at the downstream end as section  $n + 1$ , assuming the conduit is divided into  $n$  reaches. To specify variables at different sections, we use two subscripts: The first subscript designates the conduit number, and the second indicates the section number. For example,  $Q_{P_{i,j}}$  represents flow at the  $j$ th section of the  $i$ th conduit. For variables that have the same value at all sections of a conduit, only one subscript is used. For example,  $C_{a_i}$  refers to constant  $C_a$  (Eq. 3-21) for the  $i$ th conduit. Although  $C_p$  and  $C_n$  may have different values at different sections of a conduit, only one subscript is used to indicate the conduit number. This simplifies the presentation and does not result in any ambiguity, since each conduit has only one end section at a boundary. As discussed previously, the subscript  $P$  indicates unknown variables at the end of the time step.

A number of simple boundary conditions are developed in this section. Complex boundary conditions, such as for pumps and turbines, are derived in Chapters 4 and 5 and, for transient control devices, in Chapter 10.

#### Constant-Level, Upstream Reservoir

In this case, the water level in the reservoir (Fig. 3-7) is assumed to remain constant during the transient state. This is normally valid if the reservoir volume is large. In many situations (e.g., a large surge tank), the changes in the water level may be small during the period of interest. In such cases, the boundary may be analyzed as a constant-level reservoir instead of taking minor changes in the level into account. Such an approximation simplifies the analysis considerably without adversely affecting the accuracy of the computed results.

Let the entrance losses be given by the equation

$$h_e = \frac{k Q_{P_{i,1}}^2}{2g A_i^2} \quad (3-23)$$

in which  $k$  is the entrance loss coefficient. Then, referring to Fig. 3-7a, we may write

$$H_{P_{i,1}} = H_{res} - (1 + k) \frac{Q_{P_{i,1}}^2}{2gA_i^2} \quad (3-24)$$

in which  $H_{res}$  = height of the reservoir water surface above the datum.

This equation specifies the condition imposed by the reservoir boundary; i.e., the relationship between the head and the discharge at section 1 of the  $i$ th conduit and the water level in the reservoir. To develop the boundary condition, we solve this equation simultaneously with the negative characteristic equation (Eq. 3-18). Elimination of  $H_{P_{i,1}}$  from Eqs. 3-18 and 3-24 and simplification of the resulting equation yield

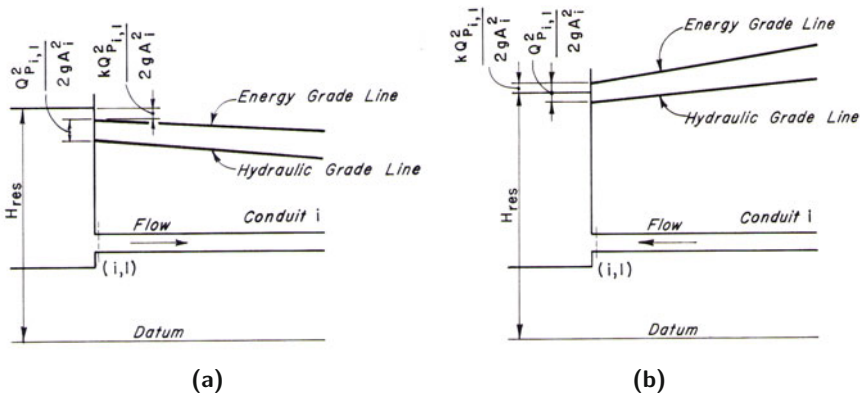


Fig. 3-7. Constant-level, upstream reservoir.

$$k_1 Q_{P_{i,1}}^2 + Q_{P_{i,1}} - (C_{n_i} + C_{a_i} H_{res}) = 0 \quad (3-25)$$

in which

$$k_1 = \frac{C_a (1 + k)}{2gA_i^2} \quad (3-26)$$

By solving Eq. 3-25 and neglecting the negative sign with the radical term, we obtain

$$Q_{P_{i,1}} = \frac{-1 + \sqrt{1 + 4k_1 (C_{n_i} + C_{a_i} H_{res})}}{2k_1} \quad (3-27)$$

Now,  $H_{P_{i,1}}$  may be determined from Eq. 3-18.

For the reverse flow,  $k$  is assigned a negative value in Eqs. 3-24 and 3-26 and the negative sign with the radical term is again neglected.

If the entrance losses as well as the velocity head at the entrance section are negligible, then

$$H_{P_{i,1}} = H_{res} \quad (3-28)$$

in which  $H_{res}$  = height of the reservoir water surface above the datum. Equation 3-18 for the upstream end thus becomes

$$Q_{P_i,1} = C_{n_i} + C_{a_i} H_{res} \quad (3-29)$$

Note that the boundary condition in this case is simplified significantly as compared to that in which the entrance losses and the velocity head are included.

### Constant-Level, Downstream Reservoir

The boundary condition for a downstream reservoir (Fig. 3-8) is developed similar to that for an upstream reservoir. We first write an equation defining the relationship between the piezometric head and discharge at the downstream end and the reservoir level, and then solve it simultaneously with the positive characteristic equation Eq. 3-17. Following derivation clarifies the procedure.

If the head losses at the entrance to the reservoir are

$$h_e = \frac{k Q_{P_i,n+1}^2}{2g A_i^2} \quad (3-30)$$

then referring to Fig. 3-8a

$$H_{P_i,n+1} = H_{res} - (1 - k) \frac{Q_{P_i,n+1}^2}{2g A_i^2} \quad (3-31)$$

Elimination of  $H_{P_i,n+1}$  from Eqs. 3-31 and 3-17 yields

$$k_2 Q_{P_i,n+1}^2 - Q_{P_i,n+1} + C_{p_i} - C_{a_i} H_{res} = 0 \quad (3-32)$$

in which

$$k_2 = \frac{C_{a_i} (1 - k)}{2g A_i^2} \quad (3-33)$$

By solving Eq. 3-32 and neglecting the positive sign with the radical term

$$Q_{P_i,n+1} = \frac{1 - \sqrt{1 - 4k_2 (C_{p_i} - C_{a_i} H_{res})}}{2k_2} \quad (3-34)$$

Now,  $H_{P_i,n+1}$  may be determined from Eq. 3-17. For the reverse flow,  $k$  in Eq. 3-33 is assigned a negative value.

If the exit loss and the velocity head at the reservoir end are negligible, then

$$H_{P_i,n+1} = H_{res} \quad (3-35)$$

Hence it follows from Eq. 3-17 that

$$Q_{P_i,n+1} = C_{p_i} - C_{a_i} H_{res} \quad (3-36)$$

In this case, the head at the boundary is specified. Note that similar to the upstream reservoir, the boundary condition for the downstream reservoir is simplified if the velocity head and the entrance losses at the reservoir are neglected.

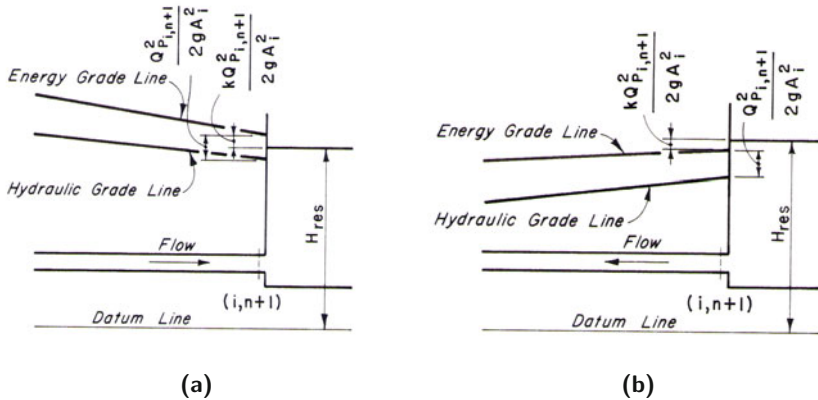


Fig. 3-8. Constant level, downstream reservoir.

### Dead End

At a dead end located at the downstream end of the  $i$ th conduit (Fig. 3-9),  $Q_{P_{i,n+1}} = 0$ . Hence, it follows from the positive characteristic equation (Eq. 3-17) that

$$H_{P_{i,n+1}} = \frac{C_{p_i}}{C_{a_i}} \quad (3-37)$$

### Downstream Valve

Unlike the previous three boundaries where either the head or the discharge were specified at the boundary, the condition imposed by a valve boundary is a relationship between the head and discharge through the valve.

Steady-state flow through a valve discharging into air may be written as

$$Q_{o_{i,n+1}} = (C_d A_v)_o \sqrt{2g H_{o_{i,n+1}}} \quad (3-38)$$

in which subscript  $o$  indicates steady-state conditions,  $C_d$  = coefficient of discharge,  $H_{o_{i,n+1}}$  = head upstream of the valve, and  $A_v$  = area of the valve opening. If we assume that the transient-state flow through a valve may be described by an equation similar to that for steady-flow equation, then

$$Q_{P_{i,n+1}} = (C_d A_v) \sqrt{2g H_{P_{i,n+1}}} \quad (3-39)$$

Dividing Eq. 3-39 by Eq. 3-38, taking square of both sides and defining relative valve opening  $\tau = (C_d A_v)/(C_d A_v)_o$ , we obtain

$$Q_{P_{i,n+1}}^2 = \frac{(Q_{o_{i,n+1}} \tau)^2}{H_{o_{i,n+1}}} H_{P_{i,n+1}} \quad (3-40)$$

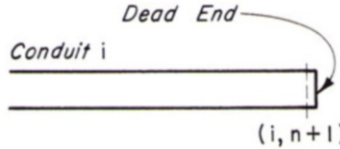


**Fig. 3-9. Dead end.**

Note that  $\tau$  includes the variation of discharge coefficient with valve opening. Substitution for  $H_P$  from the positive characteristic equation (Eq. 3-17) into Eq. 3-40 yields

$$Q_{P_{i,n+1}}^2 + C_v Q_{P_{i,n+1}} - C_{p_i} C_v = 0 \quad (3-41)$$

in which  $C_v = (\tau Q_{o_{i,n+1}})^2 / (C_a H_{o_{i,n+1}})$ . Solving for  $Q_{P_{i,n+1}}$  and neglecting the negative sign with the radical term

$$Q_{P_{i,n+1}} = 0.5 \left( -C_v + \sqrt{C_v^2 + 4C_{p_i} C_v} \right) \quad (3-42)$$

Now  $H_{P_{i,n+1}}$  may be determined from Eq. 3-17.

To compute the transient-state conditions for an opening or a closing valve,  $\tau$  versus  $t$  curve (Fig. 3-10b and c) may be specified either in a tabular form or by an algebraic expression. Note that  $\tau = 1$  corresponds to valve opening at which the flow through the valve is  $Q_{o_{i,n+1}}$  under a head of  $H_{o_{i,n+1}}$ .

For an orifice located at the downstream end of a pipe, the above equations may be used by substituting  $\tau = 1$  since orifice opening remains constant.

### Series Junction

A *series junction* is a junction of two conduits having different diameters, wall thicknesses, wall materials, and/or friction factors (Fig. 3-11). If the velocity head at section  $(i, n+1)$  and at  $(i+1, 1)$  is the same and the head loss at the junction is neglected, then it follows from the energy equation that

$$H_{P_{i,n+1}} = H_{P_{i+1,1}} \quad (3-43)$$

The positive and negative characteristic equations for sections  $(i, n+1)$  and  $(i+1, 1)$  are

$$Q_{P_{i,n+1}} = C_{p_i} - C_{a_i} H_{P_{i,n+1}} \quad (3-44)$$

$$Q_{P_{i+1,1}} = C_{n_{i+1}} + C_{a_{i+1}} H_{P_{i+1,1}} \quad (3-45)$$

The continuity equation at the junction is

$$Q_{P_{i,n+1}} = Q_{P_{i+1,1}} \quad (3-46)$$

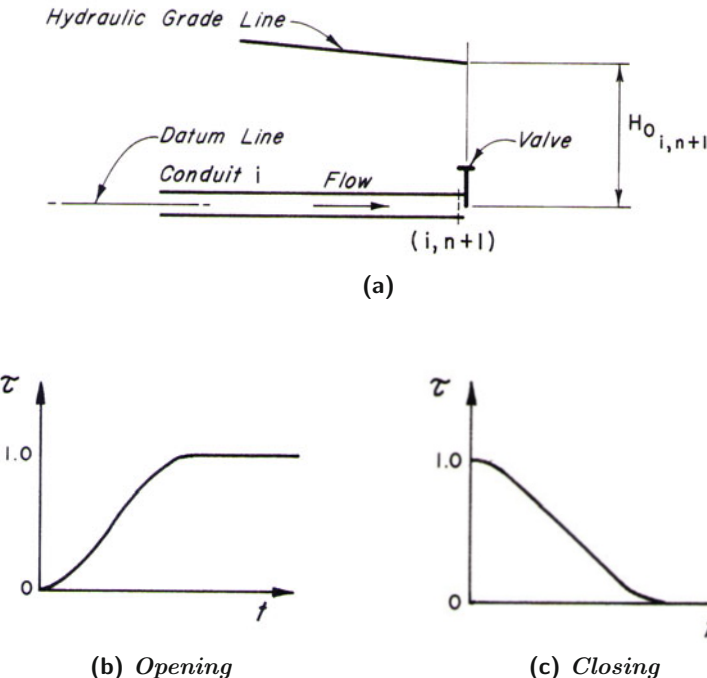


Fig. 3-10. Valve at downstream end.

It follows from Eqs. 3-43 through 3-46 that

$$H_{P_{i,n+1}} = \frac{C_{p_i} - C_{n_{i+1}}}{C_{a_i} + C_{a_{i+1}}} \quad (3-47)$$

Now  $H_{P_{i+1,1}}$ ,  $Q_{P_{i,n+1}}$  and  $Q_{P_{i+1,1}}$  may be determined from Eqs. 3-43 through 3-45.

### Branching Junction

For the branching junction shown in Fig. 3-12, the following equations may be written:

Continuity equation

$$Q_{P_{i,n+1}} = Q_{P_{i+1,1}} + Q_{P_{i+2,1}} \quad (3-48)$$

Characteristic equations

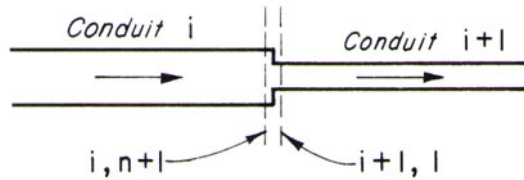


**Fig. 3-11. Series junction.**

$$Q_{P_{i,n+1}} = C_{p_i} - C_{a_i} H_{P_{i,n+1}} \quad (3-49)$$

$$Q_{P_{i+1,1}} = C_{n_{i+1}} + C_{a_{i+1}} H_{P_{i+1,1}} \quad (3-50)$$

$$Q_{P_{i+2,1}} = C_{n_{i+2}} + C_{a_{i+2}} H_{P_{i+2,1}} \quad (3-51)$$

Energy equation

If the head losses at the junction and the difference in the velocity heads in different conduits at the junction are neglected, then it follows from the energy equation that

$$H_{P_{i,n+1}} = H_{P_{i+1,1}} = H_{P_{i+2,1}} \quad (3-52)$$

Simultaneous solution of Eqs. 3-48 through 3-52 yields

$$H_{P_{i,n+1}} = \frac{C_{p_i} - C_{n_{i+1}} - C_{n_{i+2}}}{C_{a_i} + C_{a_{i+1}} + C_{a_{i+2}}} \quad (3-53)$$

Now  $H_{P_{i+1,1}}$  and  $H_{P_{i+2,1}}$  may be determined from Eq. 3-52; and then  $Q_{P_{i,n+1}}$ ,  $Q_{P_{i+1,1}}$  and  $Q_{P_{i+2,1}}$  may be determined from Eqs. 3-49 through 3-51.

Similar equations may be derived for a branching junction of more than three branching conduits.

### Centrifugal Pump

Let us develop the boundary condition for a centrifugal pump located at the upstream end of  $i$ th conduit and running at constant speed.

Fig. 3-13 shows a typical head-discharge curve for a centrifugal pump running at constant speed. This curve is referred to as *pump performance curve*. The head developed by the pump when there is no discharge is called the *shut-off head*,  $H_{sh}$ , and the head and discharge when the pump efficiency is maximum are called the *rated head*,  $H_r$  and *rated discharge*,  $Q_r$ .

The pump characteristic for a pump operating at constant speed may be approximated as

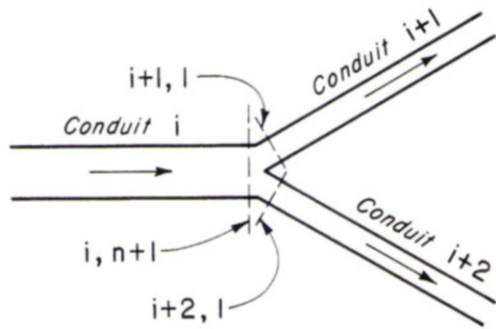


**Fig. 3-12.** Branching junction.

$$H_{P_{i,1}} = H_{sh} - C_8 Q_{P_{i,1}}^2 \quad (3-54)$$

in which  $C_8 = (H_{sh} - H_r)/Q_r^2$ . The relationship between the head and the discharge at the pump is described by Eq. 3-54. Solving this equation simultaneously with the negative characteristic equation (Eq. 3-18), we obtain

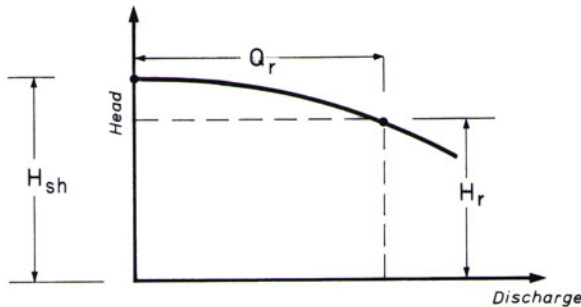


**Fig. 3-13.** Head-discharge curve for a centrifugal pump.

$$Q_{P_{i,1}} = \frac{-1 + \sqrt{1 + 4C_{a_i}C_8(C_{n_i} + C_{a_i}H_{sh})}}{2C_{a_i}C_8} \quad (3-55)$$

Now  $H_{P_{i,1}}$  may be determined from Eq. 3-54.

## Francis Turbine

Let us develop the boundary condition for a Francis turbine connected to a large grid (i.e., turbine speed is constant) with constant gate opening and a short draft tube which may be neglected in the analysis.

The head-discharge curve for a Francis turbine located at the downstream end of  $i$ th conduit and running at constant speed and at constant gate opening may be approximated as

$$H_{P_{i,n+1}} = C_9 + C_{10}Q_{P_{i,n+1}}^2 \quad (3-56)$$

Solving this equation simultaneously with the positive characteristic equation (Eq. 3-17) yields

$$Q_{P_{i,n+1}} = \frac{-1 + \sqrt{1 + 4C_{a_i}C_{10}(C_{p_i} - C_{a_i}C_9)}}{2C_{a_i}C_{10}} \quad (3-57)$$

Now  $H_{P_{i,n+1}}$  may be determined from Eq. 3-56.

## Non-Reflecting Boundary

Many times it is useful to replace part of a system, such as a very long pipe or a large network comprising of long pipes, by a non-reflecting boundary which acts like an infinite pipe, i.e., a wave arriving at this node is absorbed completely without any reflection back into the system.

To develop this boundary, we assume a fictitious node  $B$  located symmetrically to node  $A$  but outside the system, as shown in Fig. 3-14. Then, we specify the flow and head at  $B$  at the beginning of the time step have the same values as those at node  $A$ . In other words,  $H_B = H_A$  and  $Q_B = Q_A$ . Let us substitute these values for  $H_B$  and  $Q_B$  into Eq. 3-20 for  $C_n$ , i.e.,

$$C_n = Q_A - C_a H_A - R\Delta t Q_A |Q_A| \quad (3-58)$$

Now

$$Q_P = \frac{1}{2} (C_p + C_n) \quad (3-59)$$

Substituting for  $C_n$  from Eq. 3-58, we obtain

$$\begin{aligned} Q_P &= \frac{1}{2} (Q_A + C_a H_A - R\Delta t Q_A |Q_A| \\ &\quad + Q_A - C_a H_A - R\Delta t Q_A |Q_A|) \\ &= Q_A - R\Delta t Q_A |Q_A| \end{aligned} \quad (3-60)$$

It is clear from Eq. 3-60 that, for a frictionless system,  $Q_P = Q_A$ . Thus, the wave is transmitted totally to the outside of the system, but with no reflection back into the system from the boundary.

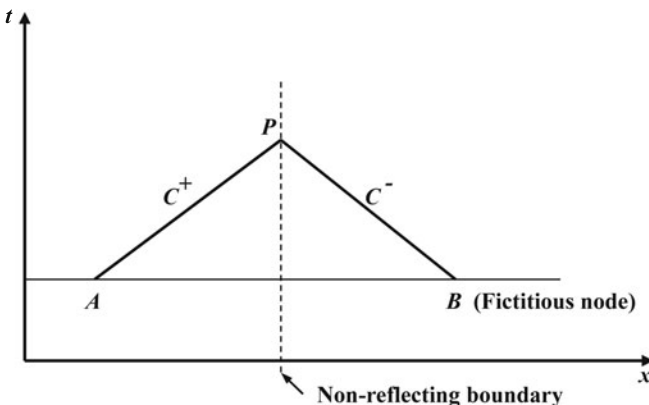


**Fig. 3-14.** Non-reflecting boundary.

### 3-4 Convergence and Stability

For an accurate numerical solution of a partial differential equation, the finite-difference approximations must satisfy the convergence and stability conditions [Smith, 1978]. In this section, we shall define some of the commonly used terms and present the stability criteria for the finite-difference scheme of Section 3-2.

#### Discretization Error

The error introduced due to approximation of the partial derivatives by finite-differences is referred to as the discretization error. Let  $U(x, t)$  be an exact solution of a partial differential equation with  $x$  and  $t$  as the independent variables, and that  $u(x, t)$  is an exact solution of the finite-difference equation approximating the partial differential equation. Then, the difference  $(U - u)$  is the *discretization error* [Smith, 1978].

#### Truncation Error

Let  $F_i^j(u) = 0$  represent the finite-difference equation at grid point  $i\Delta x$  and  $j\Delta t$ , in which  $i$  and  $j$  refer to the grid points in the  $x$  and  $t$  directions in the  $x$ - $t$  plane. Now, if we substitute the exact solution of the partial differential equation,  $U$ , into this finite-difference equation, then  $F_i^j(U)$  is called the *local truncation error* at grid point  $(i, j)$  [Smith, 1978].

## Consistency

If the truncation error tends to zero as both  $\Delta x$  and  $\Delta t$  tend to zero, then the finite-difference equation is said to be *consistent* with the partial differential equation [Smith, 1978].

## Convergence

A finite-difference scheme is said to be convergent if the exact solution,  $u$ , of the finite-difference equation tends to the exact solution,  $U$ , of the partial differential equation as both  $\Delta x$  and  $\Delta t$  tend to zero.

It may not be possible to develop the convergence conditions directly. However, the convergence of linear, hyperbolic, partial differential equations may be investigated through stability and consistency conditions. A finite-difference scheme is convergent if it is stable and consistent with the differential equation [Smith, 1978].

## Stability

An exact solution  $u(x, t)$  of a finite-difference equation is obtained only if computations are performed with an infinite number of significant digits. However, round-off errors are introduced at each time step since calculations are done with a finite number of digits, even on modern computers. Therefore, the numerical solution differs from the exact solution.

In step-by-step computations, the roundoff error introduced at any step may amplify, decrease or remain the same as the computations progress. A numerical scheme is said to be *stable* [Smith, 1978] if the amplification of the roundoff error for all sections ( $i = 1$  to  $n + 1$ ) remains bounded as time  $t$  tends to infinity. If the roundoff error grows as the solution progresses, then the scheme is called *unstable*. In the case of an unstable scheme, the error usually grows very rapidly in a few time steps and masks the actual solution, thereby making the computed results useless. Therefore, it is very important to know whether any *stability conditions* have to be satisfied for a particular numerical scheme. A scheme is said to be unconditionally stable if there is no such condition for stability.

Methods for determining the convergence or stability criteria for nonlinear partial differential equations are not presently available. The stability of a numerical scheme may be studied [Collatz, 1960] by examining the computed results obtained by numerically solving the equations for a number of  $\Delta x/\Delta t$  ratios. Analytical procedures are, however, available for determining the stability criteria for linear equations. Therefore, the stability criteria for nonlinear equations are usually determined by linearizing or by neglecting the nonlinear terms. It is reasonable to assume that the criteria developed by such a procedure is valid for the original nonlinear equations if the nonlinear

terms are relatively small as compared to the other terms of the governing equations.

The stability of a finite-difference scheme may be investigated by using a method developed by von Neumann. In this method, suitable only for linear equations, errors in the numerical solution at an instant of time are expressed in a Fourier series. Then it is determined whether these errors decay or grow as time increases. A scheme is said to be stable if the errors decay with time and *unstable* if the errors grow as time increases. By neglecting the nonlinear friction term of Eq. 3-1 and following a procedure developed by O'Brien et al. [1951], it can be shown that the finite-difference scheme of Section 3-2 is stable if

$$\Delta x \geq a\Delta t \quad (3-61)$$

This condition is called the *Courant-Friedrich-Lowy (CFL) stability condition*

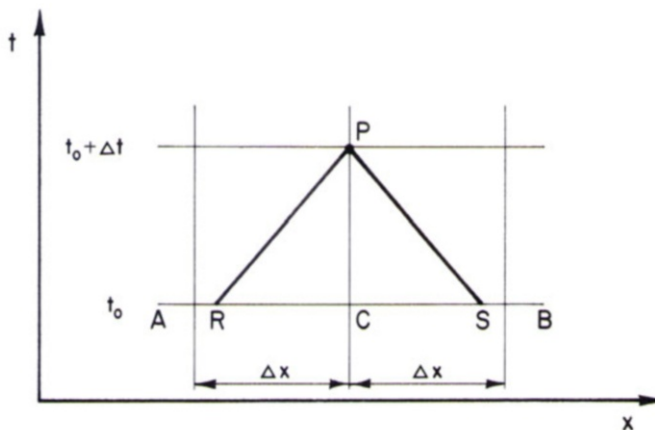


**Fig. 3-15. Notation for interpolation.**

or the *Courant condition*. It implies that the characteristic lines through  $P$  in Fig. 3-15 must intersect the line  $AB$  between  $A$  and  $C$  and between  $C$  and  $B$ .

The Courant number,  $C_N$ , is defined as the ratio of the actual wave speed,  $a$ , and the numerical wave speed,  $\Delta x/\Delta t$ ; i.e.,

$$C_N = \frac{a}{\Delta x/\Delta t} = \frac{a\Delta t}{\Delta x} \quad (3-62)$$

Thus, for the numerical scheme to be stable, the computational time step,  $\Delta t$ , and the reach length,  $\Delta x$ , must be selected such that  $C_N \leq 1$ . The first-order scheme of Section 3-2 yields acceptable results if this stability condition

is satisfied and the friction term is small since the above stability condition is developed by neglecting this term. However, if the friction term in a particular application is large due to a large friction factor, long  $\Delta t$ , large change in discharge  $\Delta Q$ , and/or small conduit diameter, then this scheme may become unstable even if  $\Delta x$  and  $\Delta t$  satisfy the CFL condition. Friction factors are usually large in slurry pipelines and in unlined rock tunnels, whereas small conduit diameters are encountered in industrial applications. For the analysis of transients in very long pipelines, longer  $\Delta t$  may be used to reduce computational time, or it may be necessitated by limited computer storage.

As discussed in the previous paragraphs, the CFL condition given by Eq. 3-61 is developed by neglecting the friction term. Similar stability conditions cannot be developed analytically if this nonlinear term is included. However, the effect of this term on stability was investigated empirically [Chaudhry and Holloway, 1984 and Holloway and Chaudhry, 1985] by analyzing a piping system with a constant-level reservoir at its upstream end and a valve at the downstream end for different wave speeds, friction factors, etc. The stability limits were determined by varying the discharge and by increasing  $\Delta x$  ( $C_N$  was always equal to unity) until the solution became unstable. Computations were done with different system parameters, e.g., conduit length and diameter, initial and final flows, wave speed, friction factor, and number of computational nodes, to assure the general applicability of the stability limits. Investigations were also done for instantaneously and slowly closing valves located at the upstream or at the downstream ends and for partial valve closures. The stability limits for these cases were the same as those for the instantaneous, closure of a downstream valve. The friction term was approximated as given by Eqs. 3-13 and 3-15. These studies yielded the following stability limits for various approximations of the friction term:

*First-Order Approximation (Eq. 3-13)*

$$C_R \leq 0.5 \quad (3-63)$$

*Second-Order Approximation (Eq. 3-15a)*

$$C_R \leq 0.79 \quad (3-64)$$

*Second-Order Approximation (Eq. 3-15b)*

$$C_R \leq 0.56 \quad (3-65)$$

in which  $C_R = f(\Delta Q)(\Delta t)/(4DA)$ . Von Neumann stability analysis shows that the linear approximation of the friction term given by Eq. 3-15c yields stable results for any value of  $C_R$  [Wylie, 1983]. Empirical investigations by Holloway and Chaudhry [1985] confirm this conclusion.

### 3-5 Method of Specified Intervals

The derivation of equations in Section 3-2 assumes that the characteristics through  $P$  pass through the grid points  $A$  and  $B$ , i.e.,  $\Delta x = a\Delta t$ . For a single pipe, the computational time interval and spatial grid spacing can be selected such that this condition is satisfied. However, if the wave speed depends on pressure (e.g., if the liquid has entrained gases), or if the system has more than one pipe, then we may not be able to satisfy this condition for each pipe without adjusting the wave speeds or the pipe lengths (see Section 3-6). Since it is advantageous to compute with specified time and space intervals, the following procedure may be used in these cases.

If  $\Delta x \neq a\Delta t$ , then the characteristics through  $P$  do not pass through  $A$  and  $B$ ; instead, let us say, they intersect at  $R$  and  $S$ , as shown in Fig. 3-15. Note that for stability, they have to intersect  $AC$  and  $CB$ , as discussed in the previous section. The values of  $H$  and  $Q$  at time  $t = t_o$  are known only at the grid points  $A$ ,  $B$ , and  $C$ . However, we need their values at  $R$  and  $S$  to determine  $H_P$  and  $Q_P$  at time  $t = t_o + \Delta t$ . The values at  $R$  and  $S$  may be determined from the known conditions at  $A$ ,  $B$ , and  $C$  by using linear or higher-order interpolations. A procedure for linear interpolations follows.

Since  $x_P$  and  $t_P$  in the method of specified time intervals are specified by the analyst, the coordinates of  $R$  and  $S$  may be determined from

$$x_R = x_P - a(t_P - t_R) = x_P - a\Delta t \quad (3-66)$$

and

$$x_S = x_P + a(t_P - t_S) = x_P + a\Delta t \quad (3-67)$$

For linear interpolations, we may write

$$\begin{aligned} Q_R &= Q_C - \frac{a\Delta t}{\Delta x} (Q_C - Q_A) \\ Q_S &= Q_C - \frac{a\Delta t}{\Delta x} (Q_C - Q_B) \\ H_R &= H_C - \frac{a\Delta t}{\Delta x} (H_C - H_A) \\ H_S &= H_C - \frac{a\Delta t}{\Delta x} (H_C - H_B) \end{aligned} \quad (3-68)$$

The values of  $Q_P$  and  $H_P$  may now be determined from Eqs. 3-17 and 3-18 by replacing  $Q_A$  and  $H_A$  in Eq. 3-19 by  $Q_R$  and  $H_R$ , and by replacing  $Q_B$  and  $H_B$  in Eq. 3-20 by  $Q_S$  and  $H_S$ . This is done because the characteristics through  $P$  now pass through  $R$  and  $S$  instead of through  $A$  and  $B$ , respectively.

These interpolations cause attenuation and dispersion of steep waves and result in the propagation of waves at faster-than-specified wave speeds, as discussed in the following paragraphs.

Let us consider the propagation of a steep wave front in a frictionless system and let the wave be at grid point  $B$  at time  $t_o$  (Fig. 3-16). Let us

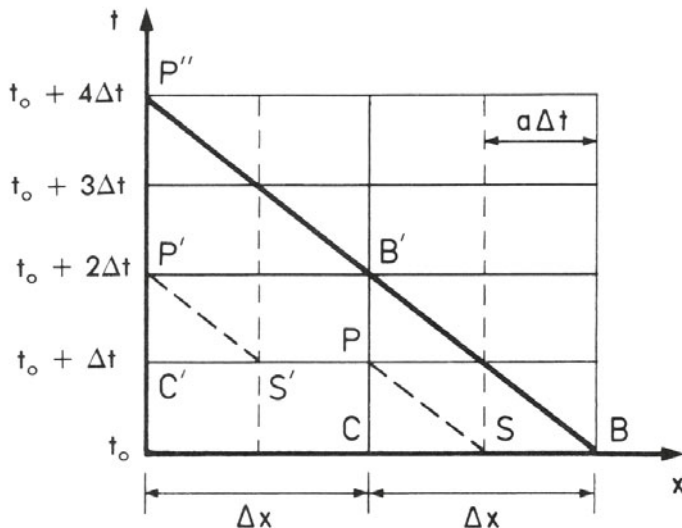


**Fig. 3-16.** Effects of interpolation on wave propagation.

assume we have selected  $\Delta x = 2a\Delta t$ . As discussed in Section 3-2, the path of this wave in the  $x$ - $t$  plane is plotted as shown by the full line  $BB'P''$  in the figure. However, if we are using the method of specified time intervals, then we have to interpolate the head at  $S$  to determine the head at  $P$ . By linearly interpolating the head between  $B$  and  $C$ , the wave height at  $S$  is one-half the wave height at  $B$ , although in reality there is no such wave front at  $S$ . Now, this wave of one-half height is propagated to point  $P$  while computing the conditions at time  $t_o + \Delta t$ . Similarly, while interpolating values between  $C'$  and  $P$  at time  $t_o + \Delta t$ , one quarter of the wave height is computed at  $S'$  which is then propagated to  $P'$  during the computations for conditions at time  $t_o + 2\Delta t$ . In other words, a wave of one-quarter height has arrived at point  $P'$  during time  $2\Delta t$ , rather than the wave of full height propagating to point  $B'$  during this time. Also, note that spurious waves have been generated during interpolation at each point whenever there are waves at the neighboring grid point. These waves and reflections from the boundaries usually result in smoothing the sharp peaks. In addition, the computed wave speed is faster than the actual speed, as illustrated by this example: The wave traveled to the upstream end (Point  $P'$ ) in  $2\Delta t$  instead of  $4\Delta t$  (Point  $P''$ ).

Figure 3-17 shows the smearing of a steep wave front due to interpolations. To avoid this dispersion and attenuation of steep waves, interpolations should be avoided and  $C_N$  should be as close to 1 as possible. In addition, since the wave speed is not precisely known in engineering applications, it may be adjusted slightly to eliminate interpolations [Portfors and Chaudhry, 1972].

Kaplan et al. [1972] presented a procedure to avoid interpolations in which  $\Delta t$  for longer pipes is an integer multiple of  $\Delta t$  for shorter pipes. To reduce errors due to interpolations, Vardy [1977] and Wiggert and Sundquist [1977] proposed to jump outside the interval but still satisfy the Courant condition. This procedure works well at the interior nodes but is somewhat awkward to apply at the boundaries. Goldberg and Wylie [1983] show that the interpolations in time rather than space produce less smearing of peaks. However, this requires more storage as compared to the procedure of the previous section.

### 3-6 Computational Time Interval

For a system of two or more conduits, the same computational time interval should be used for all conduits so that the conditions at the same time are computed at all the grid points at the junction. This time interval however, must satisfy Courant stability condition (Eq. 3-61).

If the time interval,  $\Delta t$ , is such that the reach length of any conduit in the system is not equal to  $a\Delta t$ , then  $\Delta x$  for that conduit must be greater than  $a\Delta t$  to satisfy the Courant stability criterion. However, as discussed in the previous section, the following equation should be satisfied to avoid interpolation:

$$\Delta t = \frac{L_i}{a_i n_i} \quad (i = 1 \text{ to } N) \quad (3-69)$$

in which  $n_i$  must be an integer and is equal to the number of reaches into which  $i$ th conduit is divided, and  $N$  = number of pipes in the system. As the wave velocity is not precisely known, its value may be adjusted slightly so that Courant number,  $C_N = 1$ . Because of the limitations imposed on  $\Delta t$  by the Courant stability condition, a large amount of computer time is required for analyzing systems having slowly varying transients. For the analysis of such systems, Yow [1972] presented a technique in which the inertial term of the momentum equation is multiplied by an arbitrary factor  $\alpha^2$  and the resulting equation and the continuity equation are then converted into characteristic form. This allows a time step as long as  $\alpha$  times the time step given by the Courant condition. The value of  $\alpha$  may be as large as 20 and may be different for different conduits. This technique, however, is suitable for systems with a small inertial term compared to the other terms, such as gas flow in pipes [Wylie et al., 1974], flow in porous media [Wylie, 1976], and floods in rivers. Since the original governing equations are altered arbitrarily, extreme caution must be exercised while using this technique (Rachford and Todd, 1974).

### 3-7 Unsteady Friction

In the development of the equations in Section 3-2, we included the transient-state head losses by a term based on an equation for the head losses in steady

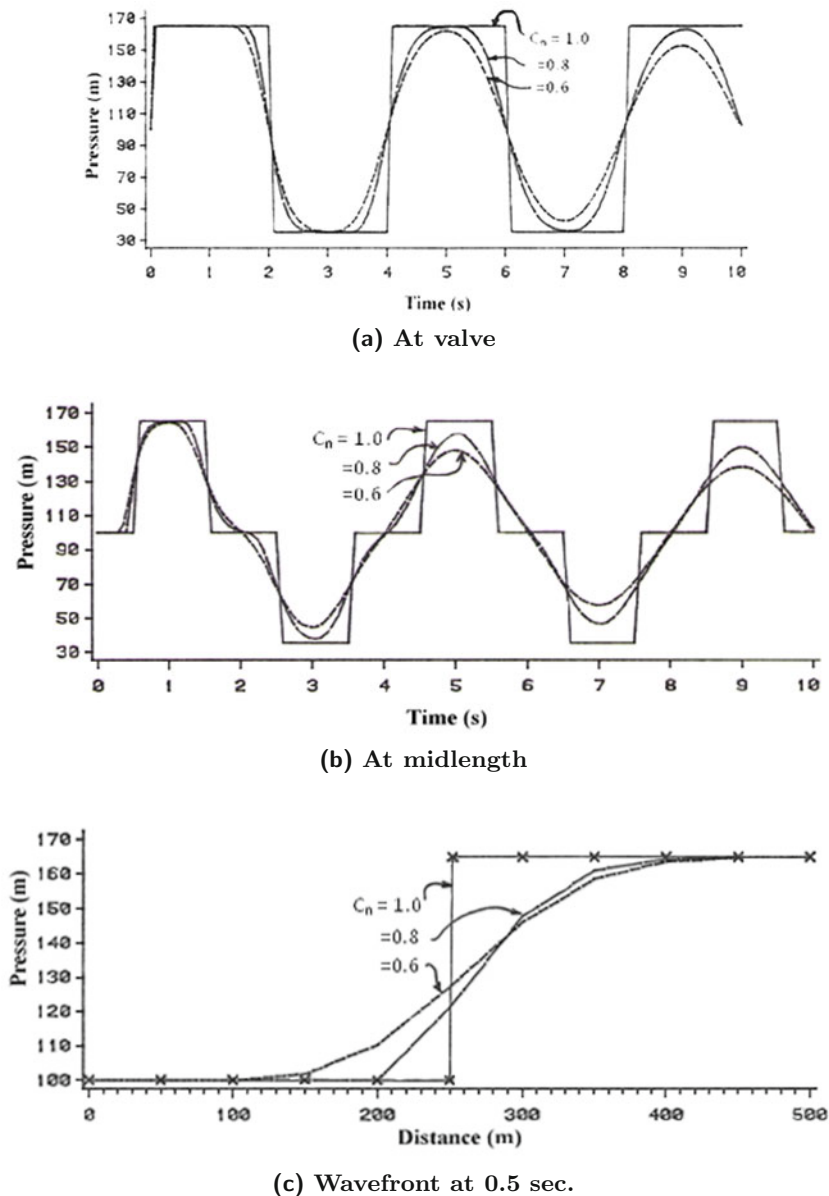


**Fig. 3-17.** Smearing of wave front due to interpolations in the method of characteristics. (Courtesy, O. Jimenez.)

flows. These equations are modified if the expressions for the unsteady friction presented in Chapter 2 are included. In the following paragraphs, we present the modified equations for the method of characteristics to include both one-coefficient and two-coefficient instantaneouss-acceleration-based (IAB) models for unsteady friction. This material follows Reddy, Silva, and Chaudhry [2012].

### One-Coefficient Model

Following Vitkovsky et al. (2006a), the positive compatibility equation for transient flow with the addition of the one-coefficient IAB model given by Eq. 2-81 is

$$dH + \frac{(1+k)}{\left[1 + \frac{1}{2}k(1 - \text{Sign}(V \frac{\partial V}{\partial x}))\right]} \frac{a}{g} dV + \frac{fV|V|}{2gD} dt = 0 \quad (3-70)$$

The corresponding characteristic equation is

$$\frac{dx}{dt} = \frac{a}{1 + \frac{1}{2}k \left[1 - \text{Sign}(V \frac{\partial V}{\partial x})\right]} \quad (3-71)$$

The negative compatibility equation is

$$dH - \frac{(1+k)}{\left[1 + \frac{1}{2}k(1 + \text{Sign}(V \frac{\partial V}{\partial x}))\right]} \frac{a}{g} dV - \frac{fV|V|}{2gD} dt = 0 \quad (3-72)$$

with the corresponding characteristic equation

$$\frac{dx}{dt} = -\frac{a}{1 + \frac{1}{2}k \left[1 + \text{Sign}(V \frac{\partial V}{\partial x})\right]} \quad (3-73)$$

Dividing by  $dt$  and rearranging the terms of Eqs. 3-70 and 3-72, the following differential equations are obtained:

Positive characteristic equation

$$\frac{dQ}{dt} + \frac{gA\alpha_P}{a} \frac{dH}{dt} + \frac{fQ|Q|}{2DA(1+k)} = 0 \quad (3-74)$$

where

$$\alpha_P = \frac{1 + \frac{1}{2}k \left[1 - \text{Sign}(V \frac{\partial V}{\partial x})\right]}{1 + k} \quad (3-75)$$

Negative characteristic equation

$$\frac{dQ}{dt} - \frac{gA\alpha_n}{a} \frac{dH}{dt} + \frac{fQ|Q|}{2DA(1+k)} = 0 \quad (3-76)$$

where

$$\alpha_n = \frac{1 + \frac{1}{2}k \left[1 + \text{Sign}(V \frac{\partial V}{\partial x})\right]}{1 + k} \quad (3-77)$$

These equations are similar to those presented in Section 3-2, except that the wave speed is multiplied by  $1/[\alpha_P(1+k)]$  and  $1/[\alpha_n(1+k)]$  for the positive and negative compatibility equations, respectively. These terms cause numerical attenuation and dispersion because of changes in the wave speed. They also introduce the need for interpolation during the computations, depending on the value of  $\text{Sign}(V\partial V/\partial x)$ . This may be done by using the procedures for the method of specified time intervals, discussed in the previous section.

## Two-Coefficient Model

Including the equation for the two-coefficient IAB model (Eq. 2-82) into Eqs. 3-1 and 3-2 and applying the method of characteristic, the following total differential equations are obtained:

Positive compatibility equation

$$\frac{dQ}{dt} + \frac{\lambda^+ g A}{(1 + K_{ut})} \frac{dH}{dt} + \frac{f Q |Q|}{2D(1 + K_{ut})} = 0 \quad (3-78)$$

Positive characteristic equation

$$\frac{dx}{dt} = \frac{1}{\lambda^+} = \alpha_P \quad (3-79)$$

in which

$$\alpha_P = \frac{2a(1 + K_{ut})}{-\text{Sign}(V\frac{\partial V}{\partial x}) K_{ux} + 2 + K_{ut}} \quad (3-80)$$

Negative compatibility equation

$$\frac{dQ}{dt} + \frac{\lambda^- g A}{(1 + K_{ut})} \frac{dH}{dt} + \frac{f Q |Q|}{2D(1 + K_{ut})} = 0 \quad (3-81)$$

Negative characteristic equation

$$\frac{dx}{dt} = \frac{1}{\lambda^-} = \alpha_n \quad (3-82)$$

in which

$$\alpha_n = \frac{2a(1 + K_{ut})}{-\text{Sign}(V\frac{\partial V}{\partial x}) K_{ux} - 2 - K_{ut}} \quad (3-83)$$

In the following discussion, subscripts  $i$ ,  $i+1$ , and  $i-1$  designate the spatial grid points and superscripts  $j$  and  $j+1$  indicate the time levels. Referring to Fig. 3-18, let us assume the conditions at time  $t_o$  (i.e.,  $j$  level) are known and we want to compute their values at time  $t_o + \Delta t$  (i.e.,  $j+1$  level). Thus the values of  $H$  and  $Q$  are known at the  $j$ -time level (either known initial conditions or computed during the previous time step) and their values at  $j+1$  time level are to be determined.

By integrating Eq. 3-78 along the characteristics and assuming the characteristics pass through the grid points, the following equations are obtained:

Positive compatibility equation

$$Q_i^{j+1} = C_p' - C_a' H_i^{j+1} \quad (3-84)$$

where

$$C_p' = Q_{i-1}^j + C_a' H_{i-1}^j - \frac{f Q_{i-1}^j |Q_{i-1}^j|}{2D(1+K_{ut})} \Delta t \quad (3-85)$$

$$C_a' = \frac{C_a}{\alpha_P} \quad (3-86)$$

and

$$C_a = \frac{gA}{a} \quad (3-87)$$

Negative compatibility equation

$$Q_i^{j+1} = C_n' + C_a' H_i^{j+1} \quad (3-88)$$

where

$$C_n' = Q_{i+1}^j + C_a' H_{i+1}^j - \frac{f Q_{i+1}^j |Q_{i+1}^j|}{2D(1+K_{ut})} \Delta t \quad (3-89)$$

and

$$C_a' = \frac{C_a}{\alpha_n} \quad (3-90)$$

Note that the slopes of the characteristic lines are variable due to the incorporation of the unsteady friction terms. To handle this, linear interpolation may be used in the method of specified intervals.

### 3-8 Explicit Finite-Difference Method

In the explicit finite-difference method, the partial derivatives are replaced by the finite-difference approximations such that the unknown conditions at a grid point at the end of time step are expressed in terms of the known conditions at the beginning of the time step. A number of explicit finite-difference schemes and their application in hydraulic transients have been reported in the literature [Chaudhry and Yevjevich, 1981; Chaudhry and Hussaini, 1985; Chaudhry and Mays, 1994 and Chaudhry, 2008]. Details of two of these schemes — Lax and MacCormack schemes — are presented in the following paragraphs.

## Lax Scheme

This scheme is first-order accurate, is easy to program and gives satisfactory results although sharp wave fronts are slightly smeared.

Referring to Fig. 3-18, let us assume the conditions at time  $t_o$  (i.e.,  $j$  level) are known and we want to compute their values at time  $t_o + \Delta t$  (i.e.,  $j + 1$  level). Thus the values of  $H$  and  $Q$  are known at the  $j$ -time level (either known initial conditions or computed during the previous time step) and their values at  $j + 1$  time level are to be determined.

We may approximate the partial derivatives as follows:

$$\frac{\partial H}{\partial t} = \frac{H_i^{j+1} - \bar{H}_i}{\Delta t} \quad (3-91)$$

$$\frac{\partial Q}{\partial t} = \frac{Q_i^{j+1} - \bar{Q}_i}{\Delta t} \quad (3-92)$$

$$\frac{\partial Q}{\partial x} = \frac{Q_{i+1}^j - Q_{i-1}^j}{2\Delta x} \quad (3-93)$$

$$\frac{\partial H}{\partial x} = \frac{H_{i+1}^j - H_{i-1}^j}{2\Delta x} \quad (3-94)$$

in which

$$\bar{H}_i = 0.5 (H_{i+1}^j + H_{i-1}^j) \quad (3-95)$$

and

$$\bar{Q}_i = 0.5 (Q_{i+1}^j + Q_{i-1}^j) \quad (3-96)$$

Substituting Eqs. 3-91 to 3-96 into Eqs. 3-1 and 3-2 and writing the friction-loss term in terms of  $\bar{Q}_i$ , we obtain

$$Q_i^{j+1} = \frac{1}{2} (Q_{i-1}^j + Q_{i+1}^j) - \frac{1}{2} gA \frac{\Delta t}{\Delta x} (H_{i+1}^j - H_{i-1}^j) - R\Delta t \bar{Q}_i |\bar{Q}_i| \quad (3-97)$$

and

$$H_i^{j+1} = \frac{1}{2} (H_{i-1}^j + H_{i+1}^j) - \frac{1}{2} \frac{\Delta t}{\Delta x} \frac{a^2}{gA} (Q_{i+1}^j - Q_{i-1}^j) \quad (3-98)$$

Thus we have expressed explicitly the unknown variables  $H_i^{j+1}$  and  $Q_i^{j+1}$  at grid point  $i$  in terms of the known values of  $Q$  and  $H$  at grid points  $i - 1$  and  $i + 1$ . Hence  $Q_i^{j+1}$  and  $H_i^{j+1}$  can be directly computed from Eqs. 3-97 and 3-98.

## MacCormack Scheme

The MacCormack scheme is second-order accurate in both space and time and is inherently dissipative. It comprises two steps: predictor and corrector. In each of these steps, one-sided finite-difference approximations are used. Depending upon the difference approximations for the spatial derivatives, two

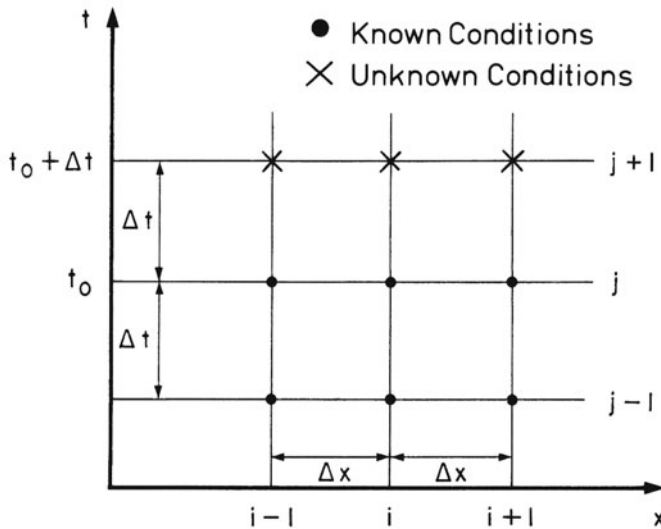


**Fig. 3-18. Definition sketch.**

alternatives are possible. In the first alternative, forward finite-difference approximations are used in the predictor part and backward finite-difference approximations in the corrector part; while in the second alternative, backward finite-difference approximations are used in the predictor part and forward finite-differences in the corrector part. MacCormack recommends using these alternatives in a sequence, i.e. the first alternative during one time step and the second alternative during the next time step, followed by the first alternative again.

In the following discussion, the notation of Section 3-8 is used and an asterisk (\*) denotes the predicted values.

For *Alternative 1*, Eqs. 3-1 and 3-2 may be written in the finite-difference form as

Predictor

$$\begin{aligned} H_i^* &= H_i^j - \frac{\Delta t}{\Delta x} \frac{a^2}{gA} (Q_{i+1}^j - Q_i^j) \\ Q_i^* &= Q_i^j - \frac{\Delta t}{\Delta x} gA (H_{i+1}^j - H_i^j) - RQ_i^j |Q_i^j| \end{aligned} \quad (3-99)$$

$(i = 1, 2, \dots, n)$

Corrector

$$\begin{aligned} H_i^{j+1} &= \frac{1}{2} \left\{ H_i^j + H_i^* - \frac{\Delta t}{\Delta x} \frac{a^2}{gA} (Q_i^* - Q_{i-1}^*) \right\} \\ Q_i^{j+1} &= \frac{1}{2} \left\{ Q_i^j + Q_i^* - \frac{\Delta t}{\Delta x} gA (H_i^* - H_{i-1}^*) - RQ_i^* |Q_i^*| \right\} \\ &\quad (i = 2, 3, \dots, n+1) \end{aligned} \quad (3-100)$$

For *Alternative 2*, the predictor and corrector parts are

Predictor

$$\begin{aligned} H_i^* &= H_i^j - \frac{\Delta t}{\Delta x} \frac{a^2}{gA} (Q_i^j - Q_{i-1}^j) \\ Q_i^* &= Q_i^j - \frac{\Delta t}{\Delta x} gA (H_i^j - H_{i-1}^j) - RQ_i^j |Q_i^j| \\ &\quad (i = 2, 3, \dots, n+1) \end{aligned} \quad (3-101)$$

Corrector

$$\begin{aligned} H_i^{j+1} &= \frac{1}{2} \left\{ H_i^j + H_i^* - \frac{\Delta t}{\Delta x} \frac{a^2}{gA} (Q_{i+1}^* - Q_i^*) \right\} \\ Q_i^{j+1} &= \frac{1}{2} \left\{ Q_i^j + Q_i^* - \frac{\Delta t}{\Delta x} gA (H_{i+1}^* - H_i^*) - RQ_i^* |Q_i^*| \right\} \\ &\quad (i = 1, 2, \dots, n) \end{aligned} \quad (3-102)$$

Both alternatives are stable if  $a\Delta t \leq \Delta x$ .

## Boundary Conditions

Equations 3-97 and 3-98 for the Lax scheme and Eqs. 3-99 to 3-102 for the MacCormack scheme are valid for the interior grid points. At the boundaries, however, we cannot write Eqs. 3-93 or 3-94 because the grid points are on only one side of the boundary. Therefore, to determine conditions at the boundaries, a number of computational procedures have been reported. Of these procedures, solving the characteristic equations (Eqs. 3-17 and 3-18) simultaneously with the conditions imposed by the boundary appears to be the most suitable. However, proper care should be taken so that the boundary conditions are neither under-specified nor over-specified.

## 3-9 General Remarks

For each time step, higher-order methods require more computational effort than that required for a first-order method. However, the same accuracy is

obtained by a higher-order method using fewer computational nodes than that required by a first-order method. Another advantage of the higher order methods is that they reproduce better and sharper discontinuities in the solution.

The derivatives of the flux function in a hyperbolic system determine the phase velocities. Phase or dispersion errors and damping or dissipative errors are introduced due to the errors in approximating this function and its derivatives, respectively.

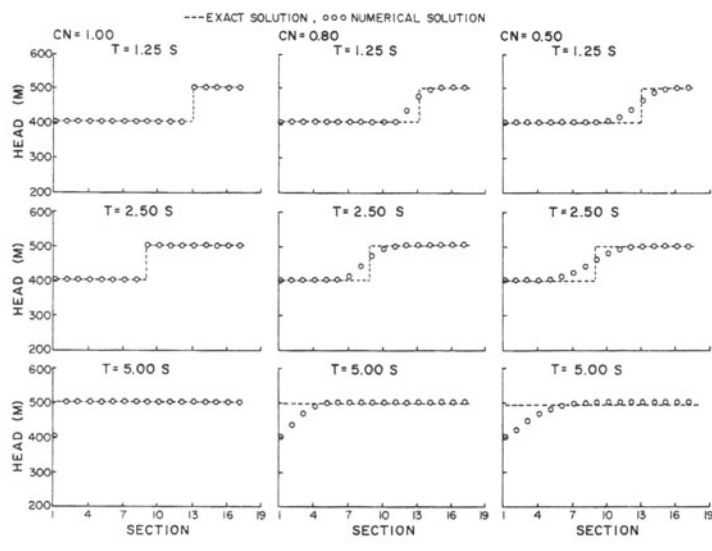
For illustration purposes, the piping system shown in [Figure 3-2](#) is analyzed using the above numerical schemes. In this system, pipe length = 5 km, wave velocity = 1000 m/s, pipe cross-sectional area = 1 m<sup>2</sup>, initial steady-state flow = 0.981 m<sup>3</sup>/s, and  $H_o = 400$  m. The transient conditions are produced by instantaneously closing the downstream valve at  $t = 0$ . This instantaneous closure produces a 100-m high pressure wave which travels in the upstream direction. If the system is assumed frictionless (i.e.,  $f = 0$ ), then this wave propagates to the reservoir, is reflected as a 100-m high negative wave and travels to the valve where it is reflected again.

In order to compare the computed results with the exact solution, the system is assumed frictionless. Computations are done using Courant numbers equal to 0.5, 0.8, and 1.0.

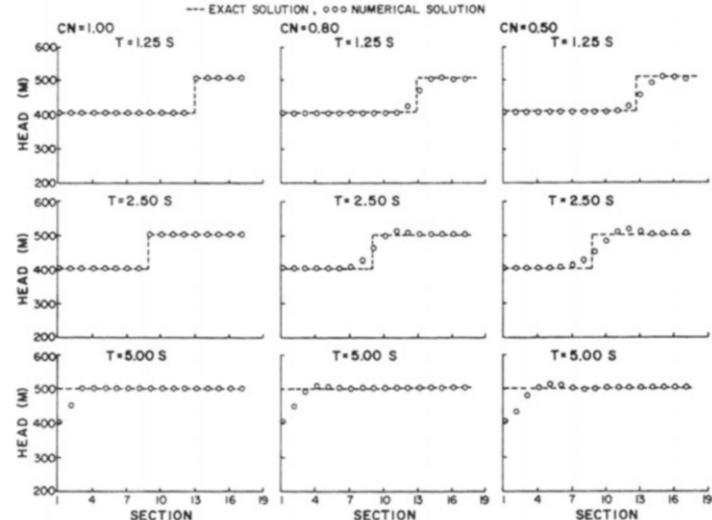
[Figures 3-19](#) show the computed results using the MacCormack scheme and the first-order characteristic method. For  $C_N = 1.0$ , the MacCormack and characteristic methods produce exact results. There is some smearing of the shock in the MacCormack scheme after the shock is reflected at the reservoir. However, for  $C_N < 1.0$ , the shock is smeared and propagates at a faster speed in the characteristic method. With the MacCormack scheme, the smearing of the shock is reduced although there are post-shock oscillations in the solution. To compare the accuracy of the above schemes,  $L_1$  and  $L_2$  errors at  $t = 2.5$  s are computed for  $C_N = 1.0$ , 0.8, and 0.5 and for several values of  $N$ . The expression for  $L_1$  and  $L_2$  are:

$$\begin{aligned} L_1 &= \frac{1}{N} \sum_{i=1}^N |H_{comp_i} - H_{exac_i}| \\ L_2 &= \frac{1}{N} \sum_{i=1}^N \{H_{comp_i} - H_{exac_i}\}^2 \end{aligned} \quad (3-103)$$

where  $N$  = number of computational nodes,  $H_{comp_i}$  = computed piezometric head at node  $i$  and  $H_{exac_i}$  = exact piezometric head at node  $i$ . To conserve space, only the results for  $C_N = 0.8$  are presented in [Figure 3-20](#). With  $C_N = 1.0$ ,  $L_1$  and  $L_2$  are both zero for the characteristic method as well as for the MacCormack scheme. However, for  $C_N < 1.0$ ,  $L_2$  error in the MacCormack scheme is much smaller than that in the first-order method. In other words, the number of computational nodes required to achieve a specified accuracy is considerably reduced for the MacCormack scheme. For example, in order



(a) Characteristic method



(b) MacCormack scheme

**Fig. 3-19.** Comparison of exact and numerical solution. (After Chaudhry and Hussaini [1985].)

to keep  $L_2$  error  $< 100$  and using  $C_N = 0.8$ , the required number of computational nodes is at least 52 in the characteristic method, and 35 in the MacCormack scheme (See Fig. 3-20).

To compare the computer time required by the above numerical methods, the piping system of Fig. 3-2 was analyzed from  $t = 0$  to time  $t = 5$  s using  $C_N = 0.8$ . The required computer time for the characteristic method was 180 percent of the time required by the MacCormack scheme.

To summarize, with Courant number equal to unity, there is little advantage in using the second-order accurate methods over the first-order methods for waterhammer analysis. For  $C_N < 1$ , however, higher-order methods have merit and should be preferred.

### 3-10 Implicit Finite-Difference Method

In the implicit finite-difference method, the unknown discharge and head at a grid point at the end of time step ( $j + 1$  time level) are expressed in terms of the unknown values of these variables (i.e., at the  $j + 1$  time level) at the neighboring sections. Therefore, equations for the entire system have to be solved simultaneously. Several implicit finite-difference methods have been reported in the literature, the details of only one of these schemes — the four-point-centered implicit scheme — are presented here.

Referring to Fig. 3-18, let us assume that the conditions at time  $t_o$  (i.e.,  $j$  level) have been computed and that we want to compute their values at time  $t_o + \Delta t$  (i.e.,  $j + 1$  level). Let us replace the partial derivatives of Eqs. 3-1 and 3-2 by the following finite-difference approximations:

$$\frac{\partial H}{\partial x} = \frac{(H_{i+1}^{j+1} + H_{i+1}^j) - (H_i^{j+1} + H_i^j)}{2\Delta x} \quad (3-104)$$

$$\frac{\partial H}{\partial t} = \frac{(H_{i+1}^{j+1} + H_i^{j+1}) - (H_{i+1}^j + H_i^j)}{2\Delta t} \quad (3-105)$$

$$\frac{\partial Q}{\partial x} = \frac{(Q_{i+1}^{j+1} + Q_{i+1}^j) - (Q_i^{j+1} + Q_i^j)}{2\Delta x} \quad (3-106)$$

$$\frac{\partial Q}{\partial t} = \frac{(Q_{i+1}^{j+1} + Q_i^{j+1}) - (Q_{i+1}^j + Q_i^j)}{2\Delta t} \quad (3-107)$$

$$RQ|Q| = \frac{R}{4} \left[ Q_{i+1}^{j+1} |Q_{i+1}^{j+1}| + Q_i^{j+1} |Q_i^{j+1}| + Q_{i+1}^j |Q_{i+1}^j| + Q_i^j |Q_i^j| \right] \quad (3-108)$$

Substituting Eqs. 3-104 to 3-108 into Eqs. 3-1 and 3-2 and simplifying, we obtain the following nonlinear algebraic equations for each interior node:

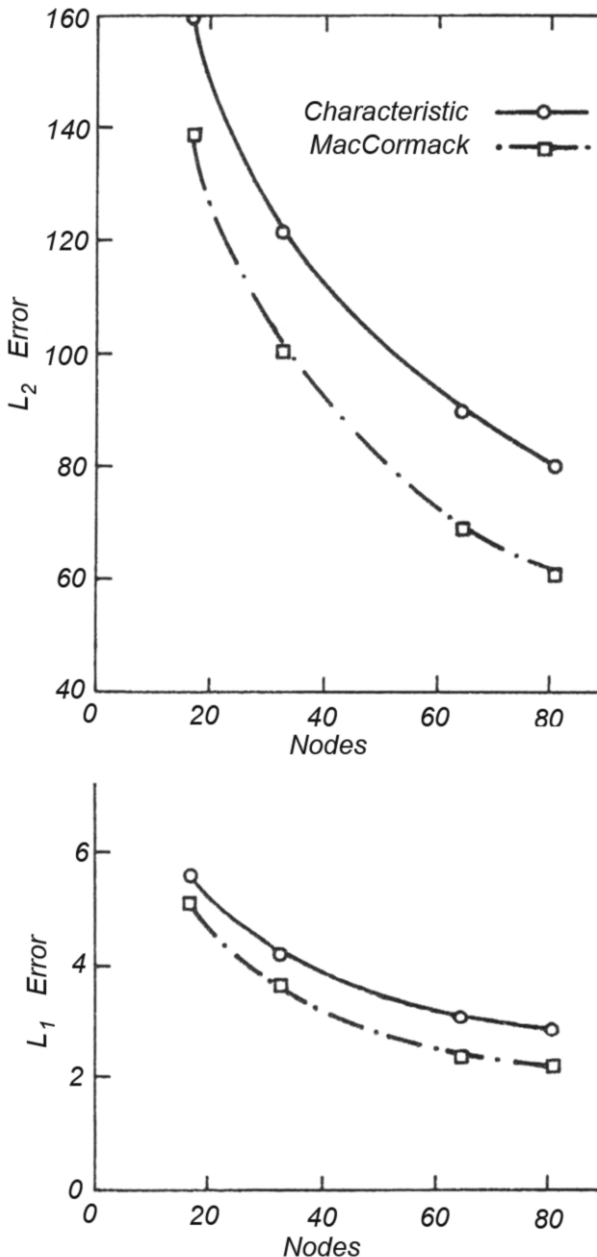


Fig. 3-20.  $L_1$  and  $L_2$  errors for  $C_N = 0.8$ . (After Chaudhry and Hussaini [1985].)

$$\begin{aligned}
C_1 [Q_{i+1}^{j+1} + Q_i^{j+1}] + C_2 [H_{i+1}^{j+1} - H_i^{j+1}] + \frac{R}{4} [Q_{i+1}^{j+1} |Q_{i+1}^{j+1}| + Q_i^{j+1} |Q_i^{j+1}|] \\
= C_1 [Q_{i+1}^j + Q_i^j] + C_2 [H_{i+1}^j - H_i^j] \\
+ \frac{R}{4} [Q_{i+1}^j |Q_{i+1}^j| + Q_i^j |Q_i^j|]
\end{aligned} \tag{3-109}$$

$$\begin{aligned}
C_1 [H_{i+1}^{j+1} + H_i^{j+1}] + C_3 [Q_{i+1}^{j+1} - Q_i^{j+1}] \\
= C_1 [H_{i+1}^j + H_i^j] + C_3 [Q_{i+1}^j - Q_i^j]
\end{aligned} \tag{3-110}$$

in which  $C_1 = 0.5\Delta t$ ;  $C_2 = gA/(2\Delta x)$ ; and  $C_3 = a^2/(2gA\Delta x)$ . Note that the terms on the left-hand sides of the preceding equations are functions of the variables at the unknown  $j+1$  time level, whereas the terms on the right-hand sides are functions of the variables at the known  $j$  time level. Equations 3-109 and 3-110 for each interior computational node along with the equations describing the end conditions are solved simultaneously for the entire system. In this method we use only the equations representing the boundaries and do not use the characteristic equations, as we did in the characteristics and explicit finite-difference methods. Due to nonlinear terms of the equations, an iterative procedure is employed for their solution.

### 3-11 Comparison of Numerical Methods

In the method of characteristics, each boundary and each conduit section are analyzed separately during a time step. Therefore, the method is particularly suitable for the analysis of systems having complex boundary conditions. The main limitation of the method is that the stability condition restricts the size of the computational time interval. In addition, interpolations may be necessary to analyze systems with more than one pipe or systems where the wave velocity is pressure dependent. As discussed earlier, these interpolations may cause numerical dispersion and attenuation.

In the implicit finite-difference method, the algebraic equations for the entire system are solved simultaneously. Since the friction term is nonlinear, this requires the solution of a larger number of nonlinear algebraic equations. In addition, the inclusion of complex boundary conditions in an iterative procedure may require a large amount of computing time because the entire system must be analyzed for each iteration. The main advantage of the method is that the time interval is not restricted for the scheme to be stable. However, the time interval cannot be increased arbitrarily so that the replacement of the partial derivatives by finite-difference approximations remains valid. To ensure the results computed by the implicit method are accurate, computational time step should be nearly equal to that required for the stability of the method of characteristics, i.e.,  $C_N \approx 1$ , despite the fact that the former

is unconditionally stable [Chaudhry and Holloway, 1984 and Holloway and Chaudhry, 1985]. It should be noted that  $C_N = 1$  reproduces the propagation of the waves correctly, as described by the physics of the problem. In addition, high-frequency oscillations [Holloway and Chaudhry, 1985] behind steep wave fronts are produced if  $C_N \neq 1$  (see Fig. 3-21). These oscillations are not real and are introduced by the numerical scheme. Because of these limitations, the implicit finite-difference method has not become popular for the analysis of transients in closed conduits.

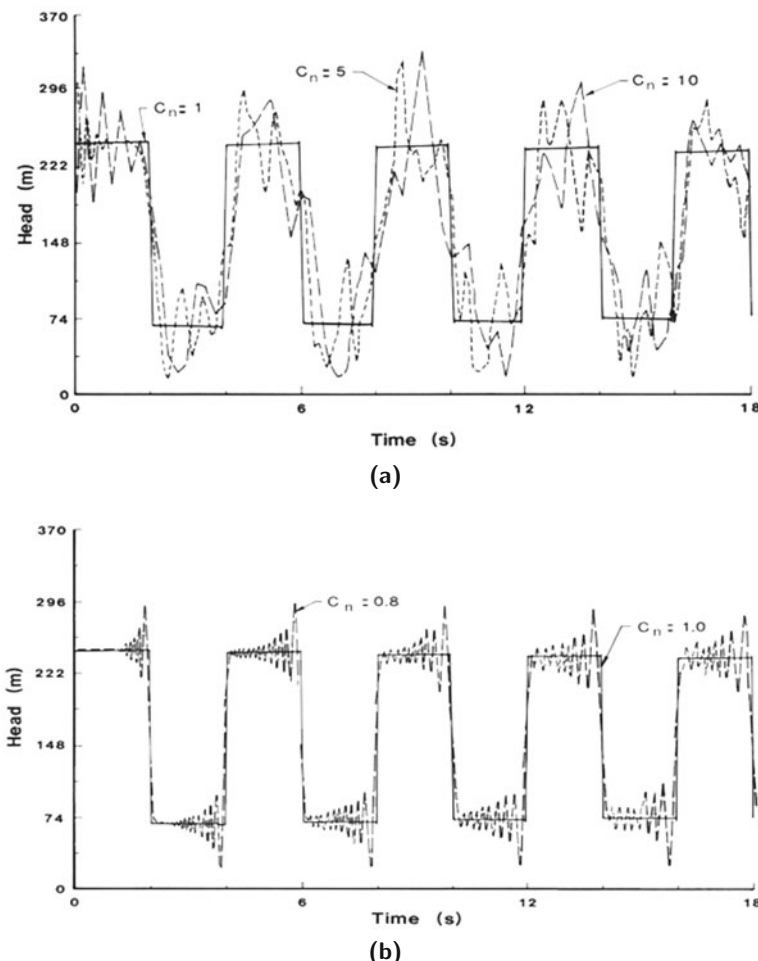


**Fig. 3-21.** Transient state pressures computed by implicit finite-difference method. (After Holloway and Chaudhry [1985].)

### 3-12 Analysis Procedure

In this section, we outline steps for the analysis of transient conditions in a piping system.

The shortest conduit in the system is divided into a number of reaches so that a desired computational time interval,  $\Delta t$ , is obtained. According to Evangelisti [1969], a time interval equal to 1/16 to 1/24 of the transit time, i.e., wave-travel time from one end of the system to the other, should give sufficiently accurate results. We recommend, however, to use this criterion as a rough guide only, and increase or decrease  $\Delta t$  depending upon the rate at which transients are produced.

For the selected-value of  $\Delta t$ , the remaining conduits in the system are divided into equal-length reaches by using the procedure outlined in Section 3-6. If necessary, the wave velocities are adjusted to satisfy Eq. 3-69 so that characteristics pass through the grid points (i.e.,  $C_N = 1$ ).

The steady-state discharge and pressure head at all the sections are then computed. The time is now incremented by  $\Delta t$ . The transient conditions at all the interior nodes are computed from Eqs. 3-22 and 3-18, and at the boundaries from the appropriate boundary conditions. The steps for increasing the time by  $\Delta t$  and computing the transient condition are repeated until transient conditions for the required time are computed. The flowchart of Fig. 3-22 shows the computational steps for determining the transient conditions in a series piping system.

To illustrate the above procedure, transient conditions produced by closing the downstream valve in the piping system shown in Fig. 3-23a are determined by using the computer program of Appendix B. The variation of effective valve opening,  $\tau$ , with time are as shown by the  $\tau$ - $t$  curve in Fig. 3-23b. Since the valve-closure time is long compared to the wave-transit time in the system, pipe no. 2 is divided into two reaches, thus giving  $\Delta t = 0.25$  s. Pipe no. 1 is also divided into two reaches to satisfy Eq. 3-69. The initial steady-state conditions are computed at all sections of pipes 1 and 2. Time is incremented by  $\Delta t$ , and the conditions at the interior sections are determined from Eqs. 3-22 and 3-18.

The boundary conditions for the upstream reservoir (Eqs. 3-28 and 3-29) are used to determine the conditions at the upstream end, and Eqs. 3-47, 3-43, 3-44, and 3-46 are used to determine conditions at the junction of pipes 1 and 2. Seven points on the  $\tau$ - $t$  curve are stored in the computer, and the values at the intermediate times are interpolated parabolically. The conditions at the valve are determined from Eqs. 3-42 and 3-17.

Conditions at  $t = \Delta t$  at all sections of the system are now known. These are stored as conditions at the beginning of the next time step. This procedure is repeated until transients for the desired duration are computed. The conditions are printed every second time step by specifying IPRINT = 2.

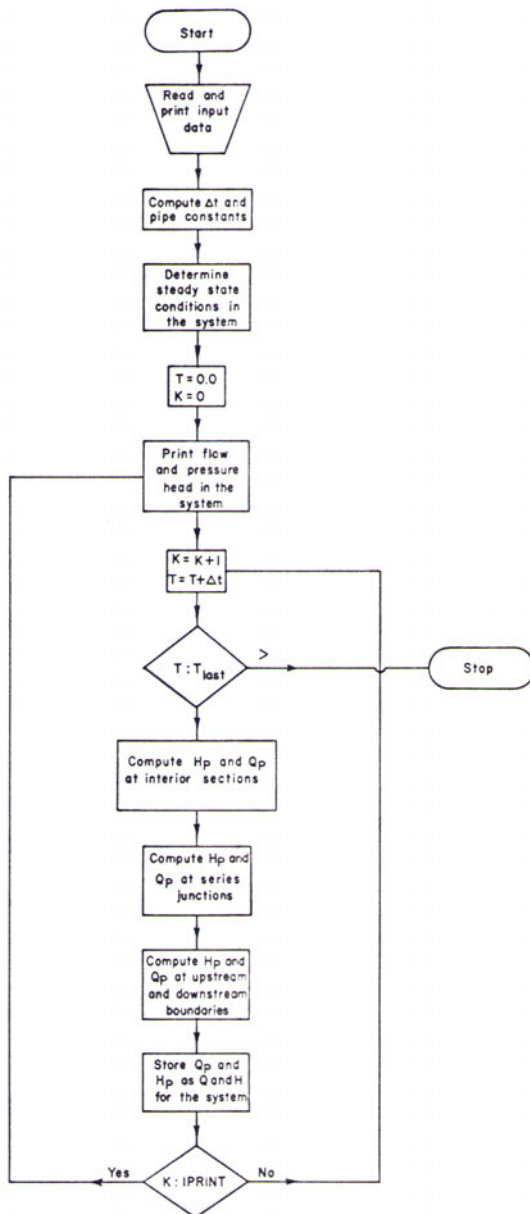
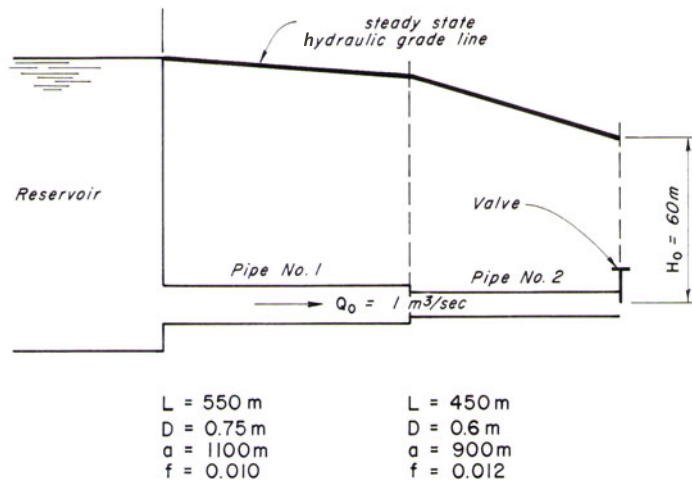
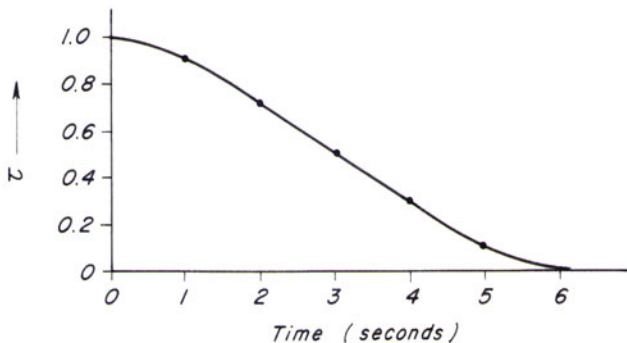


Fig. 3-22. Flowchart for a series piping system.



(a) Piping system



(b) Valve closure curve

Fig. 3-23. Series piping system.

### 3-13 Case Study

The computation of transient conditions in the upstream conduits of the Jordan River Redevelopment [Portfors and Chaudhry, 1972 and Chaudhry and Portfors, 1973] British Columbia, Canada, caused by closing the pressure reg-

ulating valve and their comparison with the prototype measurements are discussed in this section.

Figure 3-24 shows the longitudinal section of the upstream conduit, typical cross-sections and the schematic layout of the turbine and the bypass valve. The upstream conduit consists of a tunnel which has a 5.28-km-long, mainly D-shaped section; and 82-m-long, 3.96-m-diameter, and 451-m-long, 3.2-m-diameter sections; and a 1.4-km-long penstock, reducing in diameter from 3.2 to 2.7 m. The power plant, primarily used for peaking, has one Francis turbine rated at 154 MW and 265.5-m rated head. To reduce the maximum transient-state pressures, a pressure-regulating valve (PRV) is provided. The rating curve for the PRV, as determined from the prototype tests at the rated head  $H_r$  of 265.5 m, is shown in Fig. 3-25.

To compute the transient conditions caused by the opening or closing of PRV, a computer program is developed using the boundary conditions for the PRV derived in this section. (The analysis of transients caused by various turbine operations is discussed in Chapter 5 and the boundary conditions for the simultaneous operation of the PRV and wicket gates are developed in Section 10-6.) Points on the PRV rating curve (Fig. 3-25) are stored in the computer at 20 percent intervals of the valve stroke, and the discharge at the intermediate valve openings is determined by linear interpolation. Assuming the valve characteristics obtained under steady-state operation are valid during the transient state, the PRV discharge under net head  $H_n$  is given by the equation

$$Q_v = Q_r \sqrt{\frac{H_n}{H_r}} \quad (3-111)$$

in which  $Q_v$  = PRV discharge under a net head of  $H_n$ , and  $Q_r$  = discharge under rated net head  $H_r$ , both at valve opening  $\tau$ . Note that both  $H_r$  and  $H_n$  are total heads, i.e.,  $H_n = H_P + Q_v^2/(2gA^2)$ , in which  $A$  = cross-sectional area of the conduit just upstream of the PRV.

To develop the boundary condition for the PRV, Eqs. 3-17 and 3-111 are simultaneously solved. Noting that  $Q_P = Q_v$  and eliminating  $H_n$  from these equations,

$$Q_P = \frac{-C_{16} + \sqrt{C_{16}^2 + 4C_{15}C_{17}}}{2C_{15}} \quad (3-112)$$

in which

$$C_{15} = 1 - \frac{Q_r^2}{2gH_r A^2}$$

$$C_{16} = \frac{Q_r^2}{C_a H_r} \quad (3-113)$$

$$C_{17} = \frac{Q_r^2 C_p}{C_a H_r}$$

Now  $H_P$  may be determined from Eq. 3-17.

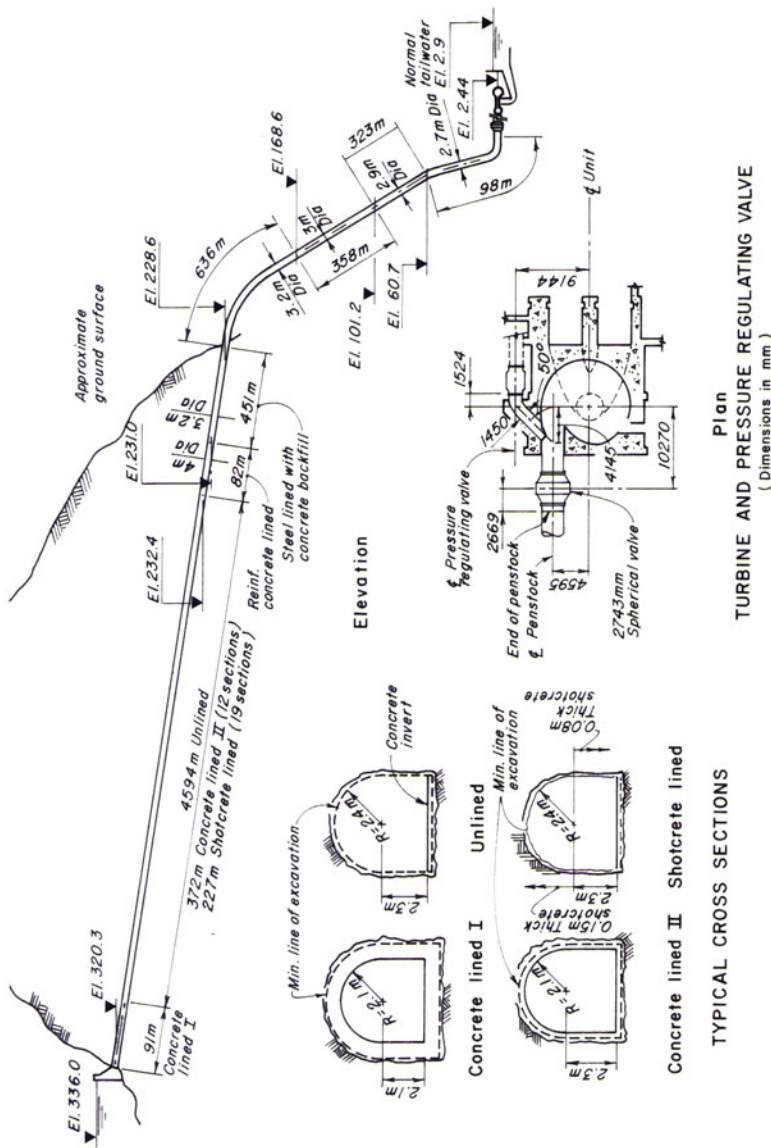


**Fig. 3-24.** Jordan River Power Plant: Profile of the upstream conduit.

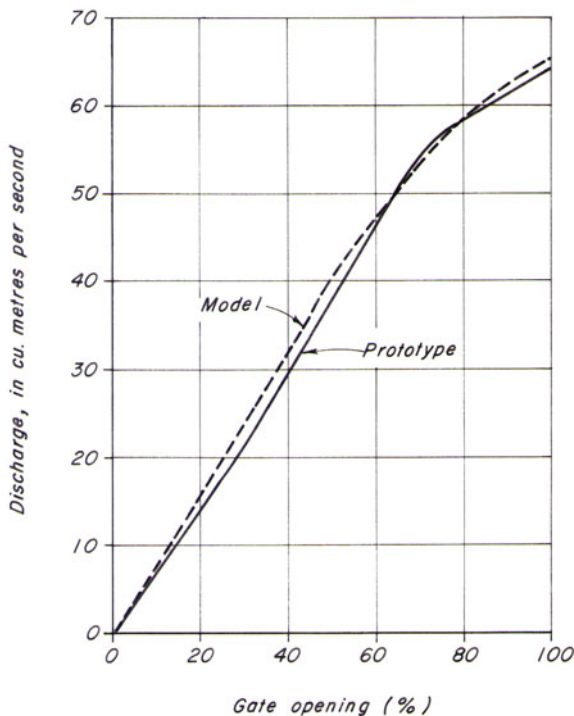
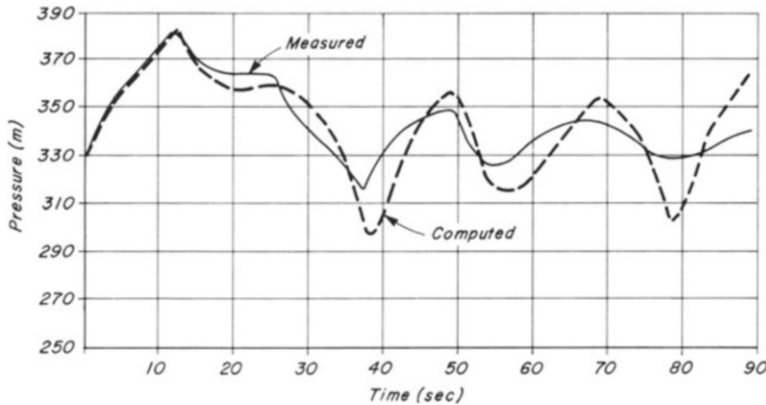


Fig. 3-25. Discharge characteristics of pressure-regulating valve.

In the computer analysis, the upstream conduit is represented by 11 pipes while the conduit downstream of the PRV is neglected because of its short length. Lined and unlined segments of the tunnel are combined into two lined and unlined conduits, and the D-shaped tunnel is replaced by a circular conduit having the same cross-sectional area. The wave velocity [Parmakian, 1963] is computed by assuming the modulus of rigidity of the rock as 5.24 GPa, and the penstock to be anchored at the lower end and free for longitudinal expansion at the upper end. The friction factor for various conduits are computed such that they include the friction and form losses, such as expansion, contraction, and bend losses. The computed head losses agree closely with those measured on the prototype.

A number of transient-state tests were conducted on the prototype. Initial steady-state pressure was measured by a Budenberg deadweight gauge, having a certified accuracy of 0.35 m. Transient-state pressures were measured with a strain-gauge-type pressure cell, with linear output within 0.6 percent over its entire range. The natural frequency of the cell was greater than 1000 Hz,

and it was calibrated against the deadweight gauge. A multturn potentiometer mechanically connected to the PRV-stroke mechanism recorded the PRV opening, and a Westinghouse leading-edge flowmeter [Fischer, 1973] was used to measure the transient-state flows.



**Fig. 3-26.** Comparison of computed and measured results.

In the prototype test, the PRV was first opened from 0 to 20 percent very slowly and was kept at this opening until steady flow was established in the upstream conduit. The PRV was then closed in 26.5 sec. The wicket gates were kept closed throughout the test. In the computer analysis, however, the PRV was not completely closed but was held at one percent opening to simulate the leakage through the wicket gates. The computed and measured transient-state pressures are shown in Fig. 3-26.

As can be seen from Fig. 3-26, the computed and measured transient pressures agree closely for about 18 s; afterward, there is good agreement between the shapes of the pressure curves but the measured pressure oscillations show a higher rate of dissipation than that indicated by the pressures computed by the mathematical model. In addition, the period of the measured pressure oscillations is less than that of the computed oscillations. These differences may be due to using the steady-state friction formula for computing the transient-state friction losses, as discussed in Section 2-8.

### 3-14 Summary

In this chapter, the details of the method of characteristics and a number of finite-difference methods are presented, and a number of simple boundary

conditions are developed. The stability and convergence conditions for a finite-difference scheme are discussed, and a procedure is outlined for the selection of time interval for a complex system. For illustration purposes, a computational procedure for analyzing the transient conditions caused by closing a valve in a series system is presented. The chapter concludes with a case study comparing the computed and measured transient conditions caused by the closure of a pressure-regulating valve in a hydroelectric power plant.

## Problems

**3-1** Prove that the equations of the characteristic curves are  $dx/dt = V \pm a$  if the term  $V(\partial V/\partial x)$  in the momentum equation and the term  $V(\partial H/\partial x)$  in the continuity equation are retained.

**3-2** Develop the boundary conditions for a centrifugal pump running at rated speed, taking into consideration transients in the suction line.

**3-3** Write a computer program for the piping system shown in Fig. 3-23a. Run the program for various values of  $\Delta t$  and plot a graph between the computed pressure at the valve and  $\Delta t$ .

**3-4** Develop the boundary conditions for an opening or closing valve located at the junction of two conduits (Fig. 3-27). (Hint: The following four equations are available: the positive characteristic equation for section  $i, n+1$ ; the negative characteristic equation for section  $i+1, 1$ ; the continuity equation, and the equation for flow through the valve. Solve these equations simultaneously to obtain an expression for  $Q_{P_{i,n+1}}$ .)

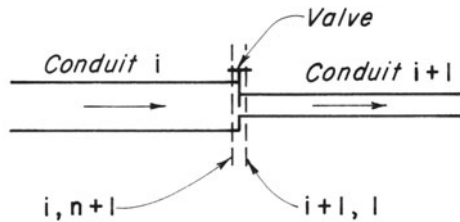


Fig. 3-27. Valve at series junction.

**3-5** Prove that if the valve in Fig. 3-27 is replaced by an orifice and the conduits  $i$  and  $i+1$  have the same diameter, wall thickness, and wall material, then

$$Q_{P_{i,n+1}} = Q_{P_{i+1,1}} = -C + \sqrt{C^2 + C(C_p + C_n)}$$

in which  $C = Q_o^2/(C_a \Delta H_o)$  and  $\Delta H_o$  is the orifice head loss for  $Q_o$ .

**3-6** Is the equation for  $Q_{P_{i,n+1}}$  given in Problem 3-5 valid for the reverse flow? If not, derive a similar equation for the reverse flow.

**3-7** Develop the boundary conditions for the pressure-regulating valve and the Francis turbine shown in Fig. 3-24. The transient conditions are caused by opening or closing the valve. Assume that the turbine speed and the wicket-gate opening remain constant during the transient state.

**3-8** Prepare a flowchart for programming the boundary conditions developed in Problem 3-7.

**3-9** A procedure called zooming is presented in Kaplan et al., [1972] in which the time step for the long pipes may be an integral multiple of that for the short pipes. However, the procedure requires extrapolation at the junction of pipes having different time steps. Investigate the effect of extrapolation on the pressure peaks for the piping system shown in Fig. 3-23a. Assume that pipe No.2 is 90-m-long instead of 450 m as shown. (Hint: Solve the system using the zooming procedure and then using the same  $\Delta t$  for the whole system as determined by Courant condition.)

**3-10** Investigate the effect of errors introduced by interpolation on the first pressure peak at the valve of the piping system of Fig. 3-23. The wave velocity in pipe 1 is 1000 m/s, and assume that the valve is instantaneously closed. (Hint: By using different values for the computational time interval, solve the system and compare the pressure history.)

**3-11** Develop the stability criterion for the finite-difference scheme of Section 3-2, including a linearized friction term in the analysis.

**3-12** For a typical system having two pipes in series, an instantaneously closing valve at the downstream end and a constant-level reservoir at the upper end, compare the procedures for reducing errors due to interpolation reported in Vardy [1977] and in Wiggert and Sundquist [1977].

**3-13** In the finite-difference scheme, the friction term may be approximated as given by Eqs. 3-13 and 3-15. Compare the accuracy of these approximations by solving a typical piping system.

## References

Abbott, M. B., 1966, *An Introduction to the Method of Characteristics*, American Elsevier, New York, NY.

- Chaudhry, M. H. and Portfors, E. A., 1973, "A Mathematical Model for Analyzing Hydraulic Transients in a Hydroelectric Power Plant," *Proc. First Canadian Hydraulic Conference*, published by the University of Alberta, Edmonton, Canada, May, pp. 298-314.
- Chaudhry, M. H. and Yevjevich, V. (eds.), *Closed-Conduit Flow*, Water Resources Publications, Littleton, Co.
- Chaudhry, M. H., 1982, "Numerical Solution of Transient-Flow Equations," *Proc. Hydraulic Specialty Conf.*, Amer. Soc. of Civil Engrs., Jackson, MS, Aug., pp. 633-656.
- Chaudhry, M. H. and Hussaini, M. Y., 1983, "Second-Order Explicit Methods for Transient-Flow Analysis," in *Numerical Methods for Fluid Transient Analysis*, C. S. Martin and M. H. Chaudhry (eds.), Amer. Soc. of Mech. Engrs., New York, pp. 9-15.
- Chaudhry, M. H. and Holloway, M. B., 1984, "Stability of Method of Characteristics," *Proc. Hydraulics Division Specialty Conf.*, Amer. Soc. Civil Engrs., Coeur d'Alene, Idaho, Aug., pp. 216-220.
- Chaudhry, M. H. and Hussaini, M. Y., 1985, "Second-Order Accurate Explicit Finite-difference Schemes for Waterhammer Analysis," *Jour. of Fluids Engineering*, vol. 107, Dec., pp. 523-529.
- Chaudhry, M. H. and Mays, L. W., 1994, (eds.), *Computer Modeling of Free-Surface and Pressurized Flows*, Kluwer, the Netherlands, 741 pp.
- Chaudhry, M. H., 2008, *Open-Channel Flow*, 2nd. ed., Springer, New York, NY, 523 pp.
- Collatz, L., 1960, *The Numerical Treatment of Differential Equations*, Third ed., Springer, Berlin, Germany.
- Evangelisti, G., 1969, "Waterhammer Analysis by the Method of Characteristics," *L'Energia Elettrica*, Nos. 10-12, pp. 673-692, 759-770, 839-858.
- Fischer, S. G., 1973, "The Westinghouse Leading Edge Ultrasonic Flow Measurement System," presented at the Spring Meeting, Amer. Soc. of Mech. Engrs., Boston, May.
- Goldberg, D. E. and Wylie, E. B., 1983, "Characteristics Method Using Time-Line Interpolation," *Jour. Hydraulic Engineering*, Amer. Soc. Civil Engrs., May, pp. 670-683.
- Gray, C. A. M., 1954, "Analysis of Water Hammer by Characteristics," *Trans. of Amer. Soc. of Civil Engrs.*, vol. 119, pp. 1176-1194.
- Holloway, M. B. and Chaudhry, M. H., 1985, "Stability and Accuracy of Waterhammer Analysis," *Advances in Water Resources*, vol. 8, Sept., pp. 121-128.
- Kaplan, M., Belonogoff, G. and Wentworth, R. C., 1972, "Economic Methods for Modelling Hydraulic Transient Simulation," *Proc. First International Conference on Pressure Surges*, Canterbury, England, published by British Hydromechanics Research Assoc., Sept., pp. A-33 - A4-38.
- Lister, M., 1960 "The Numerical Solution of Hyperbolic Partial Differential Equations by the Method of Characteristics," in *Mathematical Methods for*

- Digital Computers*, edited by Ralston, A. and Wiley, H. S. , John Wiley & Sons, New York, Chap. 15.
- O'Brien, G. G., Hyman, M. A. and Kaplan, S., 1951, "A Study of the Numerical Solution of Partial Differential Equations," *Jour. Math. and Physics*, No. 29, pp. 223-251.
- Parmakian, J., *Waterhammer Analysis*, Dover Publications, Inc., New York, NY.
- Perkins, F. E., Tedrow, A. C., Eagleson, P. S. and Ippen, A. T., 1964, *Hydro-Power Plant Transients*, Part II, Dept. of Civil Engineering, Hydrodynamics Lab. Report No. 71, Massachusetts Institute of Technology, Sept.
- Portfors, E. A. and Chaudhry, M. H., 1972, "Analysis and Prototype Verifications of Hydraulic Transients in Jordan River Power Plant," *Proc. First International Conference on Pressure Surges*, Canterbury, British Hydromechanics Research Assoc., September, pp. E4-57 to E4-72.
- Rachford, H. H. and Todd, D., 1974, "A Fast, Highly Accurate Means of Modeling Transient Flow in Gas Pipeline Systems by Variational Methods," *Jour. Soc. of Petroleum Engrs.*, April, pp. 165-175. (See also Discussion by Stoner, M. A., and Authors' Reply, pp. 175-178.)
- Reddy, H. P., Silva-Araya, W. and Chaudhry, M. H., 2012, "Estimation of Decay Coefficients for Unsteady Friction for Instantaneous, Acceleration-Based Models" *Jour. Hydraulic Engineering*, vol. 138, no. 3, pp. 260-271.
- Smith, G. D., 1978, *Numerical Solution of Partial Differential Equations*, Second ed., Clarendon Press, Oxford, England.
- Streeter, V. L. and Lai, C., 1962, "Waterhammer Analysis Including Fluid Friction," *Jour. Hyd. Div.*, Amer. Soc. of Civ. Engrs., May, pp. 79-112.
- Tournès, D., 2003, "Junius Massau et L'intégration Graphique," *Revue d'histoire des mathématiques*, vol. 9, pp. 181-252.
- Vardy, A. E., 1977, "On the Use of the Method of Characteristics for the Solution of Unsteady Flows in Networks," *Proc. Second International Conf. on Pressure Surges*, British Hydromechanics Research Assoc., Bedford, England.
- Wiggert, D. C. and Sundquist, M. J., 1977, "On the Use of Fixed Grid Characteristics for Pipeline Transients," *Jour. Hyd. Div.*, Amer. Soc. of Civil Engrs., vol. 103, Dec., pp. 1403-1416.
- Wylie, E. B., Streeter, V. L. and Stoner, M. A., 1974, "Unsteady-State Natural Gas Transient Calculations in Complex Pipe Systems," *Jour. Soc. of Petroleum Engrs.*, Feb., pp. 35-43.
- Wylie, E. B., 1976, "Transient Aquifer Flows by Characteristics Method," *Jour. Hyd. Div.*, Amer. Soc. of Civil Engrs., vol. 102, March, pp. 293-305.
- Wylie, E. B., 1983, "Advances in the Use of MOC in Unsteady Pipeline Flow," *Fourth International Conf. on Pressure Surges*, British Hydromechanics Research Assoc., Bath, England, Sept. 21-23, pp. 27-37.
- Wylie, E. B., 1983, "The Microcomputer and Pipeline Transients," *Jour. Hydraulic Engineering*, Amer. Soc. Civil Engrs. Proc. Paper No. 18453, Vol. 109, No. 12, Dec., pp. 1723-1739.

- Wylie, E. B., and Streeter, V. L. 1983, *Fluid Transients*, FEB Press, Ann Arbor, Mich..
- Yow, W., 1972, "Numerical Error on Natural Gas Transient Calculations," *Trans. Amer. Soc. of Mech. Engrs.*, vol. 94, Series D, no. 2, pp. 422-428.

### Additional References

- Brown, F. T., 1968, "A Quasi Method of Characteristics with Application to Fluid Lines with Frequency Dependent Wall Shear and Heat Transfer," Paper No. 68-WA/Aut.-7, Amer. Soc. of Mech. Engrs., Dec.
- Contractor, D. N., 1965, "The Reflection of Waterhammer Pressure Waves from Minor Losses," *Trans. Amer. Soc. Mech. Engrs.*, vol. 87, Series D, June.
- Evangelisti, G., 1966, "On the Numerical Solution of the Equation of Propagation by the Method of Characteristics," *Meccanica*, vol. 1, No. 1/2, pp. 29-36.
- Fox, J. A. and Henson, D. A., 1971, "The Prediction of the Magnitudes of Pressure Transients Generated by a Train Entering a Single Tunnel," *Proc.*, Institution of Civil Engrs., Paper 7365, vol. 49, May, pp. 53-69.
- Miyashiro, H., 1967, "Waterhammer Analysis of Pump System," *Bull. Japan Soc. of Mech. Engrs.*, vol. 10, No. 42, pp. 952-958.
- Proc. Pressure Surge Conferences*, Proceedings of British Hydromechanics Research, First, 1972; Second, 1977; Third, 1980; Fourth, 1983; Fifth, 1986; Sixth, 1989; Seventh, 1992; Eighth, 1995; Ninth, 2004; Tenth, 2008; Eleventh, 2012.
- Symposium 1965, Waterhammer in Pumped Storage Projects, Chicago, Nov., Amer. Soc. of Mech. Engrs.

---

## TRANSIENTS IN PUMPING SYSTEMS



**Wind Gap Pumping Plant with nine units, static head of 158 m and total discharge of 141.5 m<sup>3</sup>/s. Diameter of discharge line 1 is 2.9 m and of lines 2 through 4, 3.8 m.** (Courtesy, S. Loghmanpour, California Dept. of Water Resources.)

## 4-1 Introduction

The starting or stopping of pump produces transient flows in pumping systems. These flows may be analyzed by using the method of characteristics presented in Chapter 3. Since the pumping head, discharge and pump speed for a centrifugal pump, are inter-dependent, transient-state speed needs to be included in the analysis. This requires special boundary conditions. These conditions are developed in this chapter. Transients caused by various pump operations are first discussed. A procedure for including the pump characteristics is then outlined, boundary conditions for a centrifugal pump are developed, and a typical pumping system is analyzed. Design criteria for the pipelines are presented, and the chapter concludes with a case study.

## 4-2 Pump Operations

Typical pump operations, such as pump start-up, pump shut down, power failure to pump motors, etc., and the transient conditions produced by these operations are discussed in this section.

During a normal pump start-up, the discharge valve is kept closed to reduce the electrical load on the pump motor; and as the pump speed reaches the rated speed, the valve is opened gradually. However, if there is no discharge valve, then the rotational speed of the pump motors is increased slowly. Similarly for a normal pump shutdown, the discharge valve is first closed slowly or the motor speed is reduced slowly, and then the power supply to the pump motor is switched off. Thus, both normal pump start-up and shutdown are pre-planned and, by increasing the time of the operation as necessary, the severity of the transients can be controlled. Transients caused by both of these operations may be analyzed by using the boundary conditions developed in Chapter 3 if the pump speed may be assumed to be constant during these transients. However, if this is not the case, then procedures presented in this chapter should be used for the transient analysis.

Transients caused by sudden power failure to the pump motor are usually severe, and the pipeline is designed to withstand the resulting maximum and minimum pressures. Following power failure, the pump speed reduces since the pump inertia is usually small as compared to that of the liquid in the discharge line [Parmakian, 1963]. Because the flow and the pumping head at the pump end are reduced, negative pressure waves propagate in the downstream direction in the discharge line, and positive pressure waves propagate towards the upstream end of the suction line. Flow in the discharge line reduces rapidly to zero and then reverses through the pump even though the latter may still be rotating in the normal direction unless a check valve prevents reverse flow through the pump. A pump with reverse flow while it is rotating in the normal direction is said to be operating in the *zone of energy dissipation* [Stepanoff, 1957]. Because of reverse flow, the pump speed reduces

rapidly first to zero and, then becomes negative. The pump is now rotating in the reverse direction; i.e., it is operating as a turbine. The reverse pump speed keeps on increasing until it reaches the *runaway speed* when the available head is equal to the head loss in the pump. With the increased reverse speed, the reverse flow through the pump is reduced due to choking, resulting in positive and negative pressure waves in the discharge and suction lines, respectively.

Depending on the pipeline profile, the transient-state hydraulic grade line may drop below the pipeline and the pressure inside the pipe may become sub-atmospheric. If the pressure is reduced to the liquid vapor pressure, the liquid column in the pipeline may separate at that location. Excessive pressure is produced when the two separated columns later rejoin. During design, the possibility of water-column separation should be investigated, and, if necessary, protective devices may be provided to prevent column separation. This is discussed in detail in Chapters 9 and 10.

### 4-3 Pump Characteristics

As discussed in Chapter 3, the relationship between the pump discharge and the pumping head are needed to develop the boundary condition for a pump. Presently, very limited information is available on the dynamic behavior of pumps, such as reported by Tsukamoto and Ohashi, [1981], Ohashi, [1968] and Daigo and Ohashi, [1972]. Therefore, data from steady-state tests are utilized in the transient analysis even though the validity of these data during the transient state has not been demonstrated. Any reference to pump data in our discussions means data obtained by steady-state tests.

The discharge,  $Q$ , of a centrifugal pump is a function of the rotational speed,  $N$ , and the pumping head,  $H$ , whereas the transient-state speed changes depend upon the net torque,  $T$ , and the combined moment of inertia of the rotating parts of the pump and motor and liquid entrained in the impeller. Thus, four variables, namely  $Q$ ,  $H$ ,  $N$ , and  $T$  are needed for the mathematical representation of a pump. The curves showing the relationships between these variables are called the *pump characteristics* or *pump performance curves*.

The values of  $Q$ ,  $H$ ,  $N$ , and  $T$  at the point of best efficiency are referred to as the *rated conditions* [Stepanoff, 1957]. By using these values as a reference, we may define the following nondimensional variables:

$$v = \frac{Q}{Q_R}; \quad h = \frac{H}{H_R}; \quad \alpha = \frac{N}{N_R}; \quad \beta = \frac{T}{T_R} \quad (4-1)$$

The subscript  $R$  denotes rated conditions.

During normal pump operation,  $\alpha$ ,  $\beta$ ,  $v$ , and  $h$  are all positive. However, during the transient state, they may become negative individually or in groups. These conditions are called abnormal. (Some of these are considered as normal conditions for a pump turbine, as discussed in Section 5-11). In the

laboratory, all possible abnormal operations may be contrived by using two or more pumps as a “master” and the test pump as a “slave” [Martin, 1983].

Based on the signs of  $\alpha$  and  $v$ , the pump operation may be divided into four quadrants, I to IV, as shown in Fig. 4-1, in which  $v$  is abscissa and  $\alpha$  is ordinate. Some authors use  $\alpha$  as the abscissa and  $v$  as the ordinate. This should be taken into consideration for the pump characteristics data using this convention. Based on the signs of  $\alpha$ ,  $\beta$ ,  $v$ , and  $h$ , the pump operation may be divided into eight zones, as listed in Table 4-1 and as shown in Fig. 4-1. A brief description of these zones and quadrants, compiled from Martin [1983], is given in the following paragraphs.

### **Quadrant I**

The pump operation in Zone A (normal pumping) is called normal and  $\alpha$ ,  $\beta$ ,  $v$ , and  $h$  are all positive. In Zone B (energy dissipation), only  $h$  is negative while  $\alpha$ ,  $\beta$ , and  $v$  are positive. Such an operation is possible if the pump is being overpowered by another pump, by a reservoir during steady-state operation, or by a sudden drop in head following a power failure during the transient state. In Zone C (reverse turbine), both  $v$  and  $\alpha$  are positive and both  $h$  and  $\beta$  are negative.

### **Quadrant II**

Zone H (energy dissipation) is usually encountered following a power failure to the pump motor. The combined inertia of the rotating elements — motor, pump and the entrained liquid — keeps the rotational speed positive while the flow has reversed due to positive head on the pump.

### **Quadrant III**

If there is no mechanical ratchet to prevent reverse rotation, then following a power failure, pump enters Zone G (normal turbines) after passing through Zone H. In this turbines mode, both  $\alpha$  and  $v$  are negative, and the head and the torque are positive. After Zone G, the machine operation may enter Zone F (energy dissipation), in which torque also becomes negative, thus producing a braking effect. At the boundary between Zones F and G,  $\beta$  is equal to zero and the machine reaches the runaway condition.

### **Quadrant IV**

Zone D (energy dissipation) and Zone E (reverse pumping) are infrequent. Pump-turbines may operate in Zone E during transient state. If inadvertently rotated in the wrong direction due to improper wiring of the electric motor, a pump may operate in Zones D and E. Radial flow pump-turbines are known

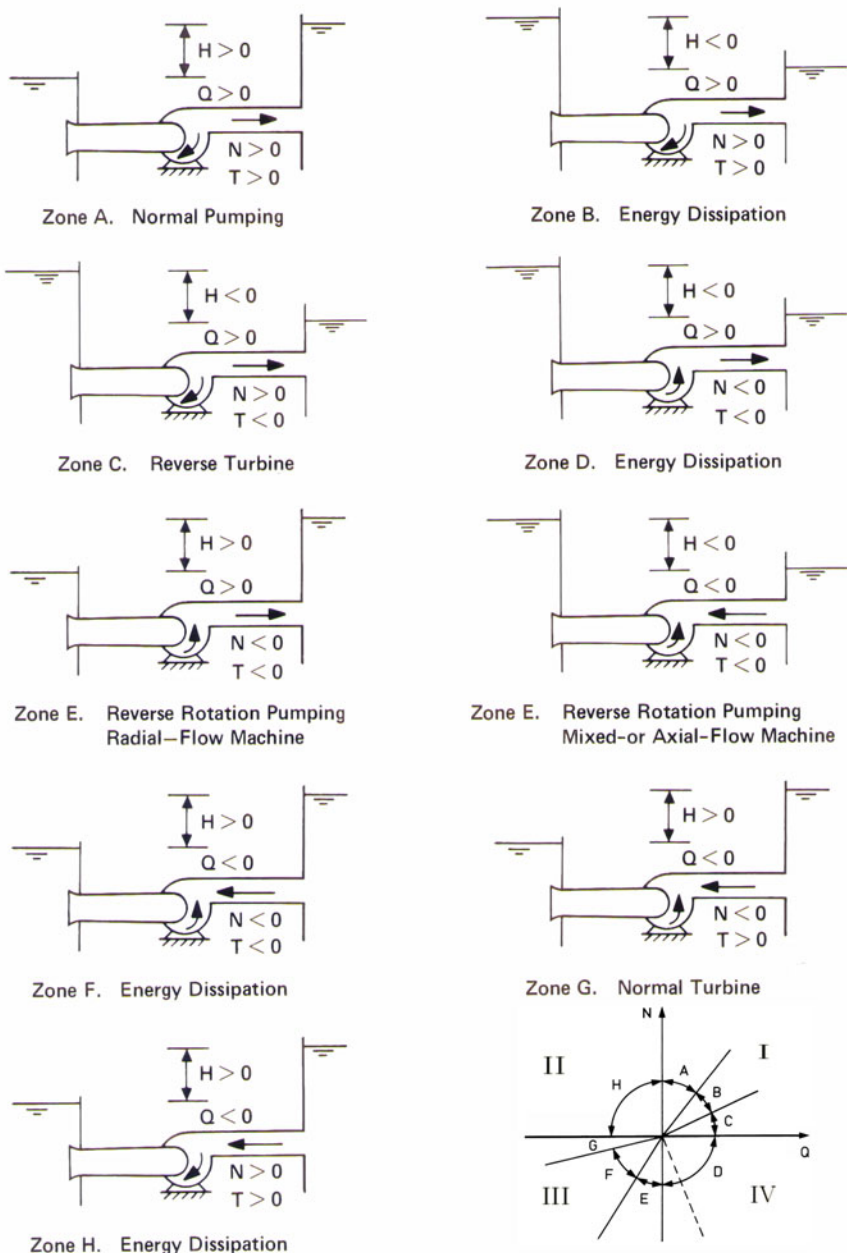


**Fig. 4-1. Different zones and quadrants of pump operation.** (After C. S. Martin [1983].)

**Table 4-1. Zones of pump operation**

| Zone | Definition               | Sign of |          |       |         | Quadrant |
|------|--------------------------|---------|----------|-------|---------|----------|
|      |                          | $v$     | $\alpha$ | $h$   | $\beta$ |          |
| A    | Normal pumping           | +       | +        | +     | +       | I        |
| B    | Energy dissipation       | +       | +        | -     | +       | I        |
| C    | Reverse turbine          | +       | +        | -     | -       | I        |
| D    | Energy dissipation       | +       | -        | -     | -       | IV       |
| E    | Reverse rotation pumping | $\pm$   | -        | $\pm$ | -       | III, IV  |
| F    | Energy dissipation       | -       | -        | +     | -       | III      |
| G    | Normal turbining         | -       | -        | +     | +       | III      |
| H    | Energy dissipation       | -       | +        | +     | +       | II       |

Source: Martin, C. S. [1983].

to pump in the reverse direction during the transient state, i.e., the machine rotates as a turbine but pumps the flow in the pump direction.

For transient analysis, various authors [Stepanoff, 1957; Parmakian, 1963; Martin, 1983 and Streeter, 1994] have presented the pump-characteristic data in different forms. Of the available methods for including the pump characteristics in the transient analysis by a computer, the method presented by Marchal et al. [1965] appears to be the most suitable and is outlined herein.

Prototype pump characteristics are obtained from the model test data by using homologous relationships [Stepanoff, 1957]. Two pumps (or turbines) are considered *homologous* if they are geometrically similar and the stream flow pattern through them is also similar. For homologous pumps, the following ratios are valid:

$$\frac{H}{N^2 D^2} = \text{Constant} \quad \text{and} \quad \frac{N}{Q D^3} = \text{Constant} \quad (4-2)$$

in which  $D$  = diameter of pump impeller. Since  $D$  is constant for a particular unit, it may be included in the constants of Eq. 4-2, i.e.,

$$\frac{H}{N^2} = \text{Constant} \quad \text{and} \quad \frac{N}{Q} = \text{Constant} \quad (4-3)$$

On the basis of Eq. 4-1, Eq. 4-3 may be written in nondimensional form as

$$\begin{aligned} \frac{h}{\alpha^2} &= \text{Constant} \\ \frac{\alpha}{v} &= \text{Constant} \end{aligned} \quad (4-4)$$

For  $\alpha = 0$  during the transient state,  $h/\alpha^2$  becomes infinite. To avoid this and to increase accuracy for smaller values of this parameter, Marchal et al.

[1965] suggest using  $\text{sgn}(h)\sqrt{|h| / (\alpha^2 + v^2)}$  in which  $\text{sgn}$  designates sign of  $h$ . However,  $h / (\alpha^2 + v^2)$  is used herein because it simplifies the derivation of the boundary conditions for a pump. (see Section 4-4)

The signs of  $v$  and  $\alpha$  depend upon the zones of operation. In addition to the need to define a different characteristic curve for each zone of operation,  $\alpha/v$  is infinite for  $v = 0$ . To avoid this, we define a new variable

$$\theta = \tan^{-1} \frac{\alpha}{v} \quad (4-5)$$

and prepare the characteristics between  $\theta$  and  $h / (\alpha^2 + v^2)$ . By definition,  $\theta$  is always finite and its value varies between  $-\pi/2$  and  $\pi/2$ . Thus, we can utilize it for all zones of operation by varying its value between  $0^\circ$  and  $360^\circ$ .

Similar to the head characteristics, the torque characteristic may be prepared between  $\beta / (\alpha^2 + v^2)$  and  $\theta$ .

Although the pump-characteristic data in the normal pumping zone are usually available, data for the abnormal operation are rather scarce. If complete characteristics for a pump are not available, then the characteristics of a pump with approximately the same specific speed<sup>†</sup> may be used as an approximation. However, note that the characteristics depend upon the type of pump (i.e., radial flow, mixed flow, or axial flow) and on other design features, such as impeller, diffuser, casing or volute, etc. Therefore, although specific speed is used to classify the pump type, two pumps having approximately the same specific speed but different design features may have different characteristics during abnormal operation.

The number of references in which pump data for three or four quadrants are reported [Martin, 1983] is limited. Of the available information, data on

<sup>†</sup>Several definitions of specific speed in terms of physical units are reported in the literature. Of these, we use the following equation [Martin, 1983], which yields the same values if a consistent set of units are used:

$$N_s = \frac{\omega_R \sqrt{Q_R}}{(gH_R)^{3/4}}$$

in which subscript  $R$  refers to the rated conditions. We call this an SI unit in which  $\omega$  is in radians/s,  $Q_R$  is in  $\text{m}^3/\text{s}$  and  $H_R$  is in m. In the metric and U.S. customary units [Stepanoff, 1957], specific speed is defined as

$$N_s = \frac{N_R Q_R}{H_R^{3/4}}$$

In metric units,  $N_R$  is in rpm,  $Q_R$  is in  $\text{m}^3/\text{s}$ , and  $H_R$  is m; in gpm units,  $N_R$  is in rpm,  $Q_R$  is in U.S. gal/min, and  $H_R$  is in ft. For a double-suction pump,  $Q_R$  is divided by 2 when computing the specific speed.

Conversion factors for specific speed are: 1 SI unit = 2733 gpm units and 1 Metric unit = 51.7 gpm units.

a double-suction, radial-flow ( $N_s = 0.5$  SI units),\* a mixed-flow pump ( $N_s = 2.8$  SI units), and an axial-flow pump ( $N_s = 4.9$  SI units) presented by Knapp [1937] and Swanson [1953] are complete and have been widely used. The characteristics for these three pumps are plotted in Fig. 4-2 and listed in Appendix F along with data for two more pumps with different specific speeds. In case the data for the pump characteristics are not available, the characteristics for a pump with approximately the same specific speed may be used as an approximation.

To include the characteristics in a mathematical model, discrete points on the characteristic curves may be stored at equal intervals of  $\theta$ , for  $\theta = 0^\circ$  to  $\theta = 360^\circ$ . Each segment of these curves between the two consecutive points stored in the computer may be approximated by a straight line (Fig. 4-3). The error introduced by approximating the curves by segmental straight lines is negligible if a sufficient number of points (e.g., 73) are stored.

For any value of  $\alpha$  and  $v$  (except when both  $\alpha$  and  $v$  are simultaneously zero), the value of  $\theta = \tan^{-1}(\alpha/v)$  may be determined by using the function ATAN2. However, this function computes the value of  $\theta$  between 0 and  $\pi$  and between 0 and  $-\pi$ , whereas our range of interest is between 0 and  $2\pi$ . This limitation may be easily circumvented by adding  $2\pi$  to the computed value of  $\theta$  if  $\theta < 0$ . For example, if  $\theta$  given by this function is  $-30^\circ$ , then the value of  $\theta$  to be used for determining the point on the pump characteristic curve is  $360^\circ - 30^\circ = 330^\circ$ .

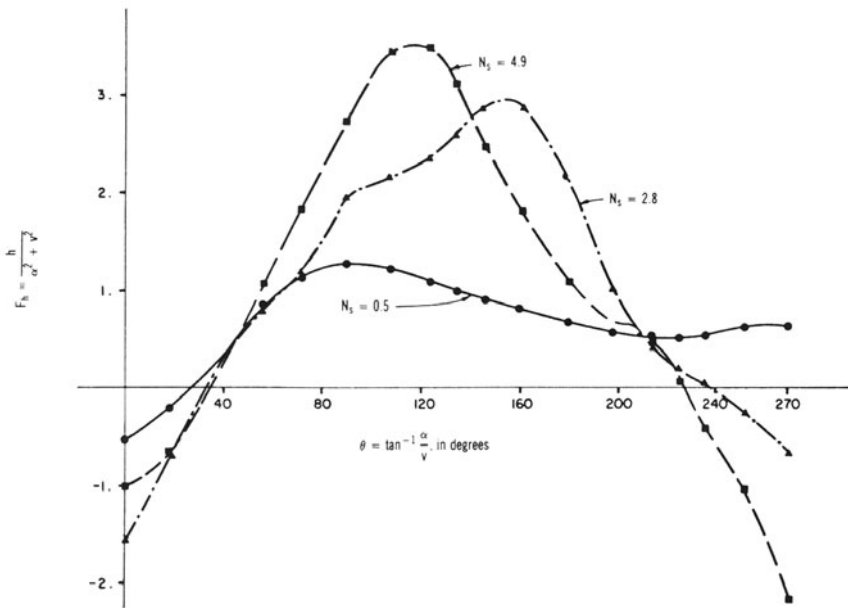
## 4-4 Power Failure

As discussed in Chapter 3, the characteristic equation (equations if the boundary has pipes on both the upstream and downstream sides) and the conditions imposed by the boundary are solved simultaneously to develop the boundary conditions. For the pump, the pump characteristics define the conditions imposed by the boundary, and a differential equation defines the variation of pump speed with time following power failure. These equations are solved simultaneously to develop the boundary conditions for the pump.

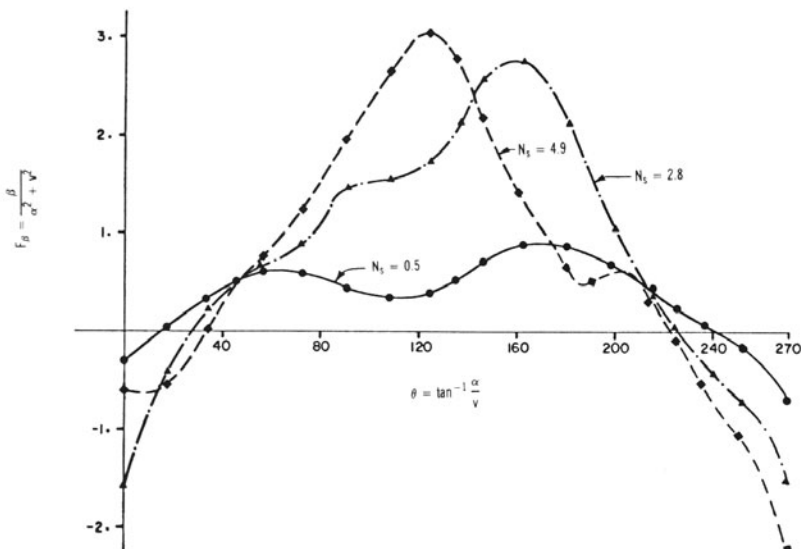
Let us first consider a simple system having only one pump with a short suction line which may be neglected. The boundary conditions for more complex cases are developed in the next section. The equations describing the pump, discharge valve, rotating masses and discharge pipe are presented first. Then a procedure is outlined for their solution numerically.

---

\*Some authors erroneously list a specific speed of 0.66 SI units (1800 gpm units) for this pump. Because of double suction, the rated discharge should be divided by 2 to compute the specific speed (see closure of Thomas [1972], pp. A-124 and A-127).



(a) Pressure



(b) Torque

**Fig. 4-2.** Characteristics of pumps of various specific speeds. ( $N_s$  is in SI units.)

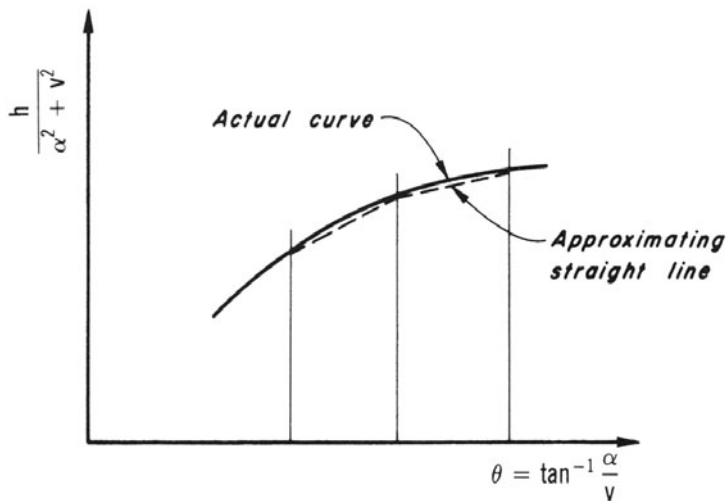


**Fig. 4-3.** Approximation of pump characteristic curve.

## Pump

Let us assume the calculations have progressed to the  $i$ th time step, the variables  $\alpha$ ,  $v$ ,  $h$ , and  $\beta$  at the beginning of the time step are known and we want to compute their values at the end of the time step. Following the notation of the previous chapter in which subscript "P" is used for the unknown variables at the end of time step, let us denote these unknown variables by  $\alpha_P$ ,  $v_P$ ,  $h_P$ , and  $\beta_P$ .

To compute these variables, we determine first the segments of head and torque characteristics corresponding to  $\alpha_P$  and  $v_P$ . For this purpose, since the values of these variables are initially unknown, we use the estimated values of these variables determined by extrapolation from the known values for the previous time steps, i.e.,

$$\begin{aligned}\alpha_e &= \alpha_i + \Delta\alpha_{i-1} \\ v_e &= v_i + \Delta v_{i-1}\end{aligned}\tag{4-6}$$

in which  $\alpha_e$  and  $v_e$  are the estimated values at the end of the  $i$ th time step,  $\alpha_i$  and  $v_i$  refer to the known values at the beginning of the  $i$ th time step, and  $\Delta\alpha_{i-1}$  and  $\Delta v_{i-1}$  are the variation of these variables during the  $(i - 1)$ th time step. Since the pump speed and the pump discharge vary gradually, the preceding linear extrapolation yield satisfactory estimates if the computational time step,  $\Delta t$ , is small. In addition, note that these estimated values are used only to determine the appropriate segment of the pump characteristics. Now, the grid points are searched on either side of  $\theta_e = \tan^{-1}(\alpha_e/v_e)$ , and the

ordinates  $h / (\alpha^2 + v^2)$  and  $\beta / (\alpha^2 + v^2)$  for these grid points are determined from the stored values. From these, the coefficients\*  $a_1$  and  $a_2$  of the equation of the segmental straight line (Fig. 4-3) are computed. Now, assuming that the points corresponding to  $\alpha_P$ ,  $v_P$ ,  $h_P$ , and  $\beta_P$  lie on these straight lines, we may write

$$\frac{h_P}{\alpha_P^2 + v_P^2} = a_1 + a_2 \tan^{-1} \frac{\alpha_P}{v_P} \quad (4-7)$$

$$\frac{\beta_P}{\alpha_P^2 + v_P^2} = a_3 + a_4 \tan^{-1} \frac{\alpha_P}{v_P} \quad (4-8)$$

in which  $a_1$  and  $a_2$ , and  $a_3$  and  $a_4$  are constants for the straight lines representing the head and torque characteristics, respectively.

Referring to Fig. 4-4, the following equation may be written for the head at the pump, i.e., at section ( $i, 1$ ):

$$H_{P_{i,1}} = H_{suc} + H_P - \Delta H_{P_v} \quad (4-9)$$

in which  $H_{suc}$  = height of the liquid surface in the suction reservoir above the datum,  $H_P$  = pumping head at the end of the time step, and  $\Delta H_{P_v}$  = head loss in the discharge valve for the pump discharge at the end of the time step. The valve head loss

$$\Delta H_{P_v} = C_v Q_{P_{i,1}}^2 = C_v Q_{P_{i,1}} |Q_{P_{i,1}}| \quad (4-10)$$

in which  $C_v$  = coefficient of valve head loss and  $Q_{P_{i,1}}^2$  is replaced by  $Q_{P_{i,1}} |Q_{P_{i,1}}|$  to account for the reverse flow. Note that the velocity head in the discharge pipe, which is usually small, is neglected in Eq. 4-9.

## Rotating Masses

The accelerating torque for a rotational system is equal to the product of the angular acceleration and the polar moment of inertia of the system. Since there is no external torque acting on the pump following power failure, the decelerating torque is the pump torque. Hence,

$$T = -I \frac{d\omega}{dt}$$

or

$$T = -I \frac{2\pi}{60} \frac{dN}{dt} \quad (4-11)$$

in which  $I$  = combined polar moment of inertia of the pump, motor, shaft, and liquid entrained in the pump impeller, and  $\omega$  and  $N$  are rotational speed

---

\*If  $y = a_1 + a_2 x$  is the equation of a straight line passing through the points  $(x_1, y_1)$  and  $(x_2, y_2)$ , then  $a_1 = (y_1 x_2 - y_2 x_1) / (x_2 - x_1)$  and  $a_2 = (y_2 - y_1) / (x_2 - x_1)$ .

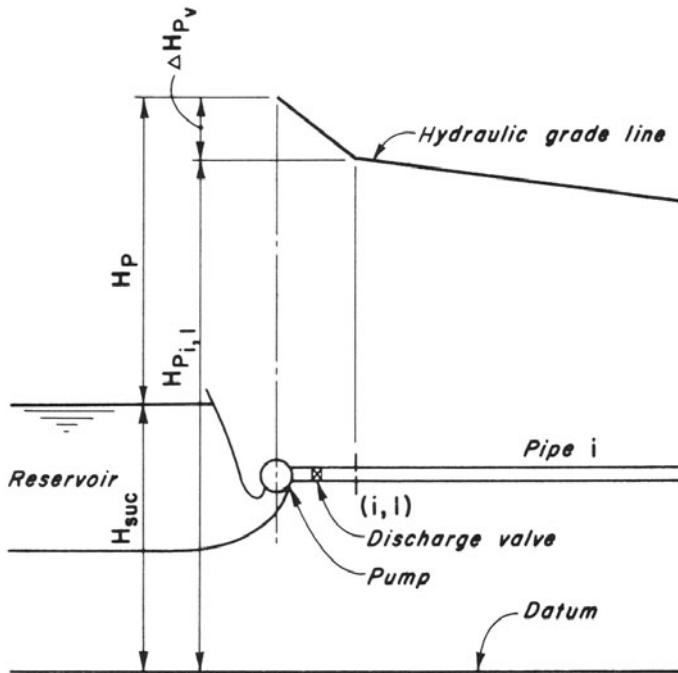


**Fig. 4-4. Notation for a pump boundary.**

of the pump, in rad/s and in rpm, respectively. On the basis of Eq. 4-1, Eq. 4-11 may be written as

$$\beta = -I \frac{2\pi}{60} \frac{N_R}{T_R} \frac{d\alpha}{dt} \quad (4-12)$$

In this equation,  $T_R = 60\gamma H_R Q_R / (2\pi N_R \eta_R)$  in which  $\gamma$  = specific weight of the liquid, and  $\eta_R$  = pump efficiency at the rated conditions. In the English units,  $I$  in Eqs. 4-11 and 4-12 is replaced by  $WR^2/g$ . In the SI units,  $I$  is in  $\text{kg m}^2$  and  $T_R$  is in Nm while in the English units,  $WR^2$  is in  $\text{lb}\cdot\text{ft}^2$ , and  $T_R$  is in lb-ft.  $N_R$  in both SI and English units is in revolutions/minute (rpm).

By using an average value of  $\beta$  during the time step, this equation may be written in a finite-difference form as

$$\frac{\alpha_P - \alpha}{\Delta t} = \frac{60T_R}{2\pi I N_R} \frac{\beta + \beta_P}{2} \quad (4-13)$$

which may be simplified as

$$\alpha_P - C_6 \beta_P = \alpha + C_6 \beta \quad (4-14)$$

in which

$$C_6 = \frac{-15T_R\Delta t}{\pi IN_R} \quad (4-15)$$

In the English Units,  $I$  in Eq. 4-15 is replaced by  $WR^2/g$ .

### Discharge Pipe

Since the suction line is short, it may be neglected in the analysis. Therefore, we need only the characteristic equation for the discharge line, i.e., for section  $(i, 1)$ ,

$$Q_{P_{i,1}} = C_n + C_a H_{P_{i,1}} \quad (4-16)$$

### Continuity Equation

Since there is no change in the volume stored between the suction reservoir and section  $(i, 1)$

$$Q_{P_{i,1}} = Q_P \quad (4-17)$$

in which  $Q_P$  = flow through the pump at the end of the time step.

### Solution of Governing Equations

As discussed earlier, the four unknowns at the end of the time step are  $\alpha_P$ ,  $v_P$ ,  $h_P$ , and  $\beta_P$ . Therefore, we need four equations for a unique solution. We will derive these equations in this section.

Equations 4-7 through 4-10, 4-14, 4-16, and 4-17 describe the boundary. Now, let us discuss how to solve these equations.

By eliminating  $H_{P_{i,1}}$ ,  $\Delta H_{P_v}$ , and  $Q_{P_{i,1}}$  from Eqs. 4-9, 4-10, 4-16, and 4-17 and by using  $Q_R$  and  $H_R$  as reference values, the resulting equation may be written as

$$Q_R v_P = C_n + C_a H_{suc} + C_a H_R h_P - C_a C_v Q_R^2 v_P |v_P| \quad (4-18)$$

We have four equations, i.e., Eqs. 4-7, 4-8, 4-14, and 4-18, in four unknowns:  $\alpha_P$ ,  $v_P$ ,  $h_P$ , and  $\beta_P$ . We may solve these equations by the Newton-Raphson method. To simplify the solution, we may first eliminate  $h_P$  and  $\beta_P$  from these equations as discussed in the following paragraphs and then solve the resulting two equations.

By substituting for  $h_P$  from Eq. 4-7 into Eq. 4-18 and for  $\beta_P$  from Eq. 4-8 into Eq. 4-14 and simplifying, we obtain

$$\begin{aligned} F_1 &= C_a H_R a_1 (\alpha_P^2 + v_P^2) + C_a H_R a_2 (\alpha_P^2 + v_P^2) \tan^{-1} \frac{\alpha_P}{v_P} - Q_R v_P \\ &\quad - C_a C_v Q_R^2 v_P |v_P| + C_n + C_a H_{suc} = 0 \end{aligned} \quad (4-19)$$

$$F_2 = \alpha_P - C_6 a_3 (\alpha_P^2 + v_P^2) - C_6 a_4 (\alpha_P^2 + v_P^2) \tan^{-1} \frac{\alpha_P}{v_P} - \alpha - C_6 \beta = 0 \quad (4-20)$$

Equations 4-19 and 4-20 are nonlinear equations in two unknowns,  $\alpha_P$  and  $v_P$ . These equations may be solved by using the Newton-Raphson method as follows. The values of  $\alpha_P$  and  $v_P$  are first estimated and then refined to a required degree of accuracy by successive iterations.

Let  $\alpha_P^{(1)}$  and  $v_P^{(1)}$  be the initial estimates for the solution in which the superscript indicates the number of the iteration, i.e., superscript (1) is the estimated value at the beginning of the first iteration and superscript (2) indicates values at the beginning of the second iteration. To start the procedure, these may be assumed equal to  $\alpha_e$  and  $v_e$ , as determined from Eq. 4-6. Then, a better estimate of the solution of Eqs. 4-19 and 4-20 is

$$\alpha_P^{(2)} = \alpha_P^{(1)} + \delta\alpha_P \quad (4-21)^{\dagger}$$

$$v_P^{(2)} = v_P^{(1)} + \delta v_P \quad (4-22)^{\dagger}$$

in which

$$\delta\alpha_P = \frac{F_2 \frac{\partial F_1}{\partial v_P} - F_1 \frac{\partial F_2}{\partial v_P}}{\frac{\partial F_1}{\partial \alpha_P} \frac{\partial F_2}{\partial v_P} - \frac{\partial F_1}{\partial v_P} \frac{\partial F_2}{\partial \alpha_P}} \quad (4-23)$$

$$\delta v_P = \frac{F_2 \frac{\partial F_1}{\partial \alpha_P} - F_1 \frac{\partial F_2}{\partial \alpha_P}}{\frac{\partial F_1}{\partial v_P} \frac{\partial F_2}{\partial \alpha_P} - \frac{\partial F_1}{\partial \alpha_P} \frac{\partial F_2}{\partial v_P}} \quad (4-24)$$

In Eqs. 4-23 and 4-24, functions  $F_1$  and  $F_2$  and their derivatives with respect to  $\alpha_P$  and  $v_P$  are computed by using  $\alpha_P^{(1)}$  and  $v_P^{(1)}$ . The following expressions for these derivatives are obtained by differentiating Eqs. 4-19 and 4-20:

$$\frac{\partial F_1}{\partial \alpha_P} = C_a H_R \left( 2a_1 \alpha_P + a_2 v_P + 2a_2 \alpha_P \tan^{-1} \frac{\alpha_P}{v_P} \right) \quad (4-25)$$

$$\begin{aligned} \frac{\partial F_1}{\partial v_P} &= C_a H_R \left( 2a_1 v_P - a_2 \alpha_P + 2a_2 v_P \tan^{-1} \frac{\alpha_P}{v_P} \right) \\ &\quad - Q_R - 2C_a C_v Q_R^2 |v_P| \end{aligned} \quad (4-26)$$

$$\frac{\partial F_2}{\partial \alpha_P} = 1 - C_6 \left( 2a_3 \alpha_P + a_4 v_P + 2a_4 \alpha_P \tan^{-1} \frac{\alpha_P}{v_P} \right) \quad (4-27)$$

$$\frac{\partial F_2}{\partial v_P} = C_6 \left( -2a_3 v_P + a_4 \alpha_P - 2a_4 v_P \tan^{-1} \frac{\alpha_P}{v_P} \right) \quad (4-28)$$

If  $|\delta\alpha_P|$  and  $|\delta v_P|$  are less than a specified tolerance (e.g., 0.001), then  $\alpha_P^{(2)}$  and  $v_P^{(2)}$  are solutions of Eqs. 4-19 and 4-20; otherwise,  $\alpha_P^{(1)}$  and  $v_P^{(1)}$  are assumed

---

<sup>†</sup>These equations may be deduced from the general derivation presented later in Section 4-5 or in Section 13-8.

equal to  $\alpha_P^{(2)}$  and  $v_P^{(2)}$  and the above procedure is repeated until a solution is obtained. Then, it is verified whether the segment of the pump characteristics used in the computations corresponds to  $\alpha_P$  and  $v_P$ . If it does not, then  $\alpha_e$  and  $v_e$  are assumed equal to  $\alpha_P$  and  $v_P$ , and the above-mentioned procedure is repeated.

However, if the correct segment is used, then  $h_P$  and  $\beta_P$  are determined from Eqs. 4-7 and 4-8;  $H_P$  and  $Q_P$  from Eq. 4-1; and  $H_{P_{i,1}}$  and  $Q_{P_{i,1}}$  from Eqs. 4-9 and 4-17. The values of  $\alpha$  and  $v$  are initialized for the next time step (i.e.,  $\alpha = \alpha_P$  and  $\beta = \beta_P$ ), and the solution progresses to the next time step. To avoid an unlimited number of iterations in the case of divergence of solution, a counter may be used so that the computations are stopped if the number of iterations exceeds a specified value (e.g., 30). The flowchart of Fig. 4-5 and the following example illustrates the application of this procedure.

### Example

Analyze the pumping system shown in [Fig. 4-6](#). The pipe and pump data are listed in [Table 4-2](#). Initially, both pumps are operating at rated conditions, and the transient conditions are caused by simultaneous power failure to both pumps. The suction line and the pipe between the pump and the discharge manifold are short.

### Solution

The discharge of both pumps is lumped together and considered as the inflow at the upstream end of the system. The suction lines being short are not included in the analysis.

A computer program is developed using the boundary conditions for parallel pumps derived in this section. The method of characteristics and the boundary conditions for the reservoir and for the series junction presented in Chapter 3 are used to analyze the transient conditions in the discharge line. The wave velocity for various sections of the discharge line is determined using the equations presented in Section 2-6. The pump-characteristics data for  $N_s = 0.46$  SI units (1276 gpm units) tabulated in Appendix F are used in the analysis. At rated discharge and rated pump speed, the pressure head at the upstream end of the discharge line is equal to the rated head. Starting with this flow and pressure head at the upstream end, the steady-state conditions in the discharge line are determined. Then, the power is assumed to fail, and the resulting transient conditions are computed. The computer program and the computed results are presented in Appendix C.

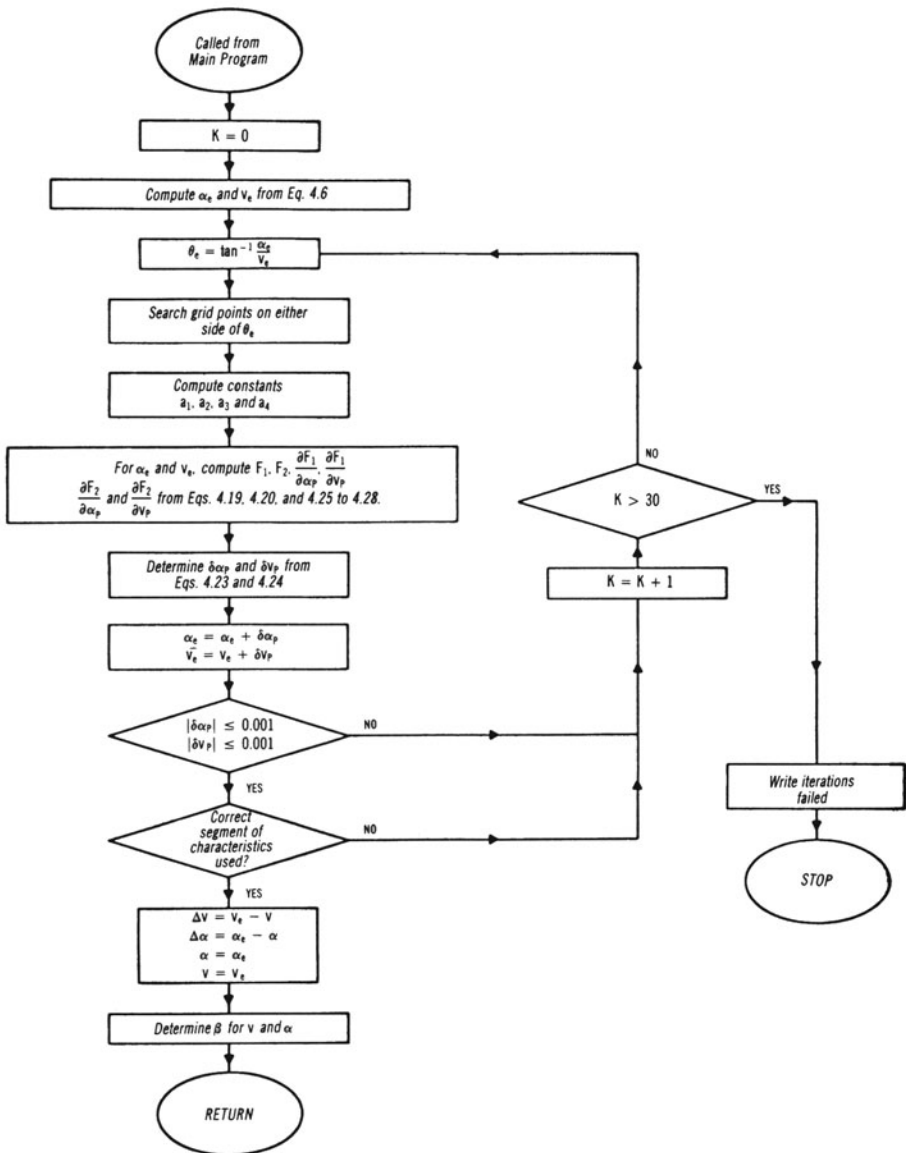
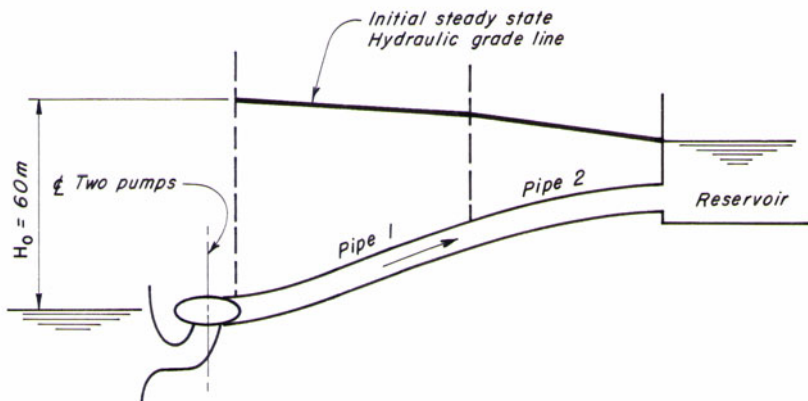


Fig. 4-5. Flowchart for a pump boundary.



**Fig. 4-6.** Piping system.

**Table 4-2**

| Pipeline                        | Pipe 1 | Pipe 2 |
|---------------------------------|--------|--------|
| Length (m)                      | 450    | 550    |
| Diameter (m)                    | 0.75   | 0.75   |
| Wave speed (m/s)                | 900    | 1100   |
| Friction factor, $f$            | 0.01   | 0.012  |
| Discharge $\text{m}^3/\text{s}$ | 0.5    | 0.5    |

*Pump*

$$Q_R = 0.25 \text{ m}^3/\text{s}$$

$$H_R = 60 \text{ m}$$

$$N_R = 1100 \text{ rpm}$$

$$WR^2 = 16.85 \text{ kg-m}^2 \text{ per pump}$$

Pump efficiency at rated conditions = 0.84

### Verification of Mathematical Model

The prototype test data obtained during power failure tests on the Wind Gap Pumping Plant by the Department of Water Resources, State of California are compared with the computed results. The plant data are first presented; the tests, instrumentation, and mathematical model are then briefly described. This is followed by a comparison of the computed and measured results.

## Plant Data

The Wind Gap Pumping Plant has five pumping units: three small units (Nos. 1 to 3) and two large units (Nos. 4 and 5). Only test results and data for the large units and their discharge line are presented here.

The large units are manifolded together into a 3.81-m-diameter pipe. Each unit has a combined pump-motor moment of inertia of  $99,366 \text{ kg m}^2$ , and is rated at  $17.84 \text{ m}^3/\text{s}$  at a total head of 159.7 m and at a rotational speed of 360 rpm. The specific speed of the pump is 0.64 (SI units). The pipeline is 628 m long and varies in thickness from 11 to 27 mm. There is a discharge valve on the downstream side of each pumping unit. This valve closes in  $22 \pm 2 \text{ s}$  following power failure to the unit. The minimum and maximum total pumping heads are 159.06 and 160.03 m, respectively, and the head losses in the pipeline corresponding to a flow of both units is 1.8 m. To prevent backflow from the downstream canal, a siphon is provided near the downstream end of the pipeline. The siphon has an air valve at its top which opens as soon as power fails to the pump-motors.

## Tests and Instrumentation

Single- and multiple-unit tests were conducted on both the small and large units. Runaway tests were conducted by subjecting the units to simulated power failure, with the discharge-valve closure delayed until after the units had reached the runaway speed.

The strain-gauge-type pressure transducers were used to measure the transient-state pressures on the upstream and downstream sides of the discharge valve. A valve position transducer (displacement) and an rpm (analog) transducer were installed on all units tested to record the discharge-valve closure and the unit speed.

## Mathematical Model

A computer program is developed based on the boundary conditions derived in this section and the computational procedure shown in flowchart of [Fig. 4-5](#). The pumping station may have several parallel pumps and the pumps may have long or short suction lines. The closure of the discharge valve following power failure may be included in the analysis. To compute the transient conditions in the pipeline, the method of characteristics and the boundary conditions for the downstream and upstream reservoirs and for the series junction of Chapter 3 are used in the program.

## Comparison of Computed and Measured Results

The computed and measured results are compared for the tests simulating power failure on Unit Nos. 4 or 5, with and without closure of the discharge

valve. The results for only one pump operating initially are presented. The discharge valve remained open following power failure for the results shown in Fig. 4-7a and the valve closed gradually in 22 s following power failure for the results shown in Fig. 4-7b. As can be seen from the figure, the agreement between the computed and measured results is satisfactory. However, the computed minimum pressure is lower than the measured minimum pressure. This difference is most probably due to the operation of the siphon valve, which is not simulated in the mathematical model.

## 4-5 Complex Systems

In the previous section, we developed boundary conditions for power failure in a system having only one pump and a short suction line. Because of short length, the suction line was neglected in the derivation. In this section, we develop boundary conditions for a number of complex systems, such as parallel and series pumps; boundary conditions for the other systems may be developed similarly.

The terms parallel and series pumps are borrowed from electrical engineering: The flow in the discharge line of parallel pumps is the sum of the discharge of individual pumps while the flow in each of the series pump and in the discharge line is the same (Fig. 4-8). For both cases, we briefly describe the system configuration first and then present the governing equations and the expressions for  $F_1$ ,  $F_2$ ,  $\partial F_1 / \partial \alpha_P$ ,  $\partial F_1 / \partial v_P$ ,  $\partial F_2 / \partial \alpha_P$ , and  $\partial F_2 / \partial v_P$ . Using these expressions, the transient flow conditions may be computed, as outlined in Section 4-4.

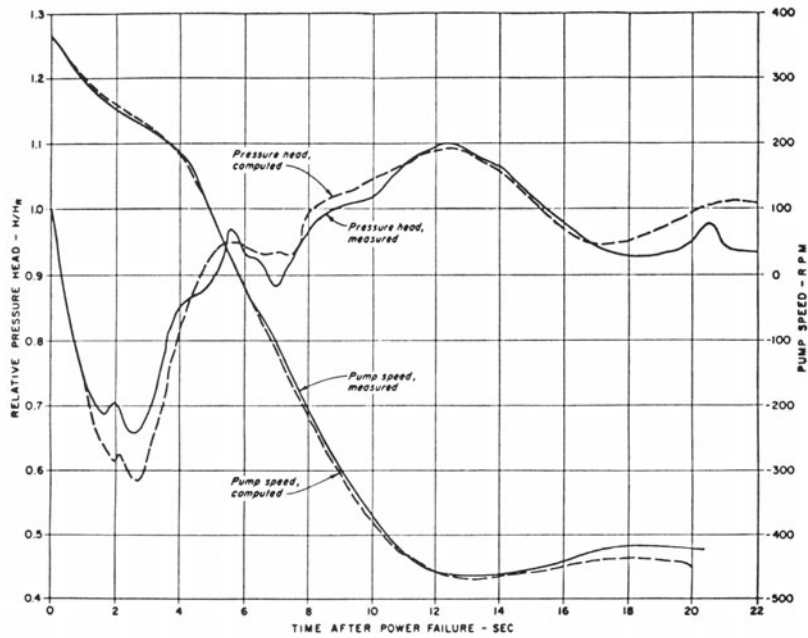
### Parallel Pumps

A system having parallel pumps to which power fails simultaneously may be analyzed by considering each pump individually, if the pipes between the pumps and the discharge manifold are long. In this case, the boundary conditions presented in Chapter 3 and in Section 4-4 are used and the discharge manifold is included as a branching junction of two or more pipes. However, if the pipe length between each pump and the discharge manifold is short, then this pipe may be neglected in the analysis, and the combined discharge of all pumps may be considered as the flow at the upstream end of the discharge line. Boundary conditions for the latter case are developed in this section.

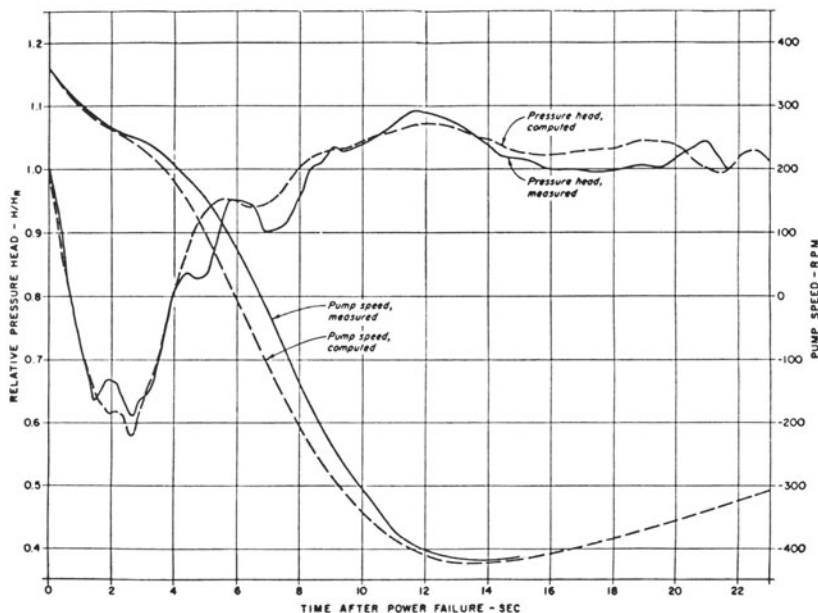
The discharge at the upstream end of the discharge line, i.e., at section  $(i, 1)$  may be written as

$$Q_{P_{i,1}} = n_P Q_P \quad (4-29)$$

in which  $n_P$  = number of parallel pumps. Depending upon the length of the suction line as compared to the other pipes in the system, the boundary conditions for the parallel pumps may be divided into the following two cases:



(a) Discharge valve remained open



(b) Discharge valve closed gradually in 22 seconds

Fig. 4-7. Wind Gap Pumping Plant. Comparison of computed and measured results.

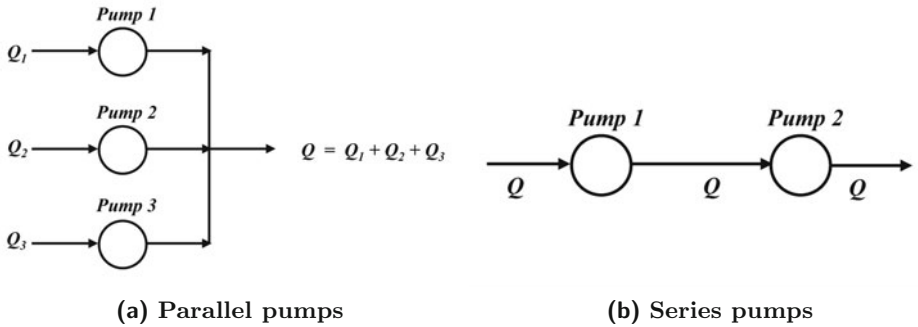


Fig. 4-8. Parallel and series pumps.

### Short suction line

If the suction line is short, then this line may be neglected. On the basis of Eq. 4-29, Eq. 4-18 becomes

$$n_P Q_R v_P = C_n + C_a H_{suc} + C_a H_R h_P - C_a C_v Q_R^2 |v_P| \quad (4-30)$$

Equations 4-7, 4-8, and 4-14 are valid for this case as well. Proceeding similarly as in Section 4-4, the following expressions are obtained:

$$\begin{aligned} F_1 &= C_a H_R a_1 (\alpha_P^2 + v_P^2) + C_a H_R a_2 (\alpha_P^2 + v_P^2) \tan^{-1} \frac{\alpha_P}{v_P} - n_P Q_R v_P \\ &\quad - C_a C_v Q_R^2 |v_P| + C_n + C_a H_{suc} = 0 \end{aligned} \quad (4-31)$$

$$\frac{\partial F_1}{\partial v_P} = C_a H_R \left( 2a_1 v_P - a_2 \alpha_P + 2a_2 v_P \tan^{-1} \frac{\alpha_P}{v_P} \right) - n_P Q_R - 2C_a C_v Q_R^2 |v_P| \quad (4-32)$$

Expression for  $F_2$ ,  $\partial F_1 / \partial \alpha_P$ ,  $\partial F_2 / \partial \alpha_P$ , and  $\partial F_2 / \partial v_P$  are given by Eqs. 4-20, 4-25, 4-27, and 4-28, respectively.

### Long suction line

A suction line that is similar in length or longer as compared to the discharge line is considered in the analysis. This is done by including the characteristic equation for the suction line in addition to Eqs. 4-7, 4-8, and 4-14. Referring to Fig. 4-9,

$$H_P = H_{P_{i+1,1}} - H_{P_{i,n+1}} \quad (4-33)$$

$$Q_{P_{i,n+1}} = C_p - C_{a_i} H_{P_{i,n+1}} \quad (4-34)$$

$$Q_{P_{i+1,1}} = C_n + C_{a_{i+1}} H_{P_{i+1,1}} \quad (4-35)$$

$$Q_{P_{i,n+1}} = Q_{P_{i+1,1}} = n_P Q_P \quad (4-36)$$

By multiplying Eq. 4-34 by  $C_{a_{i+1}}$ , Eq. 4-35 by  $C_{a_i}$ , substituting for  $Q_{P_{i,n+1}}$  and  $Q_{P_{i+1,1}}$  from Eq. 4-36, and adding the resulting equations, we obtain

$$n_P Q_P (C_{a_i} + C_{a_{i+1}}) = C_n C_{a_i} + C_p C_{a_{i+1}} + C_{a_i} C_{a_{i+1}} H_P \quad (4-37)$$

By using the rated conditions  $Q_R$  and  $H_R$  as reference values, Eq. 4-37 may be written as

$$h_P = \frac{n_P (C_{a_i} + C_{a_{i+1}}) Q_R v_P - C_n C_{a_i} - C_p C_{a_{i+1}}}{C_{a_i} C_{a_{i+1}} H_R} \quad (4-38)$$

Elimination of  $h_P$  from Eqs. 4-7 and 4-38 yields

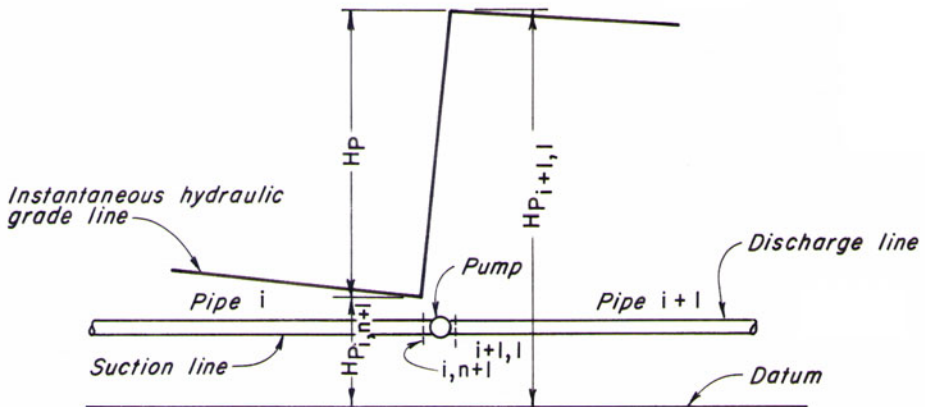


Fig. 4-9. Pump with long suction line.

$$F_1 = a_1 (\alpha_P^2 + v_P^2) + a_2 (\alpha_P^2 + v_P^2) \tan^{-1} \frac{\alpha_P}{v_P} - C_7 v_P + C_8 = 0 \quad (4-39)$$

in which

$$C_7 = \frac{n_P (C_{a_i} + C_{a_{i+1}}) Q_R}{C_{a_i} C_{a_{i+1}} H_R} \quad (4-40)$$

$$C_8 = \frac{C_n C_{a_i} + C_p C_{a_{i+1}}}{C_{a_i} C_{a_{i+1}} H_R} \quad (4-41)$$

By differentiating Eq. 4-39 with respect to  $\alpha_P$  and  $v_P$ , we obtain

$$\frac{\partial F_1}{\partial \alpha_P} = 2a_1\alpha_P + 2a_2\alpha_P \tan^{-1} \frac{\alpha_P}{v_P} + a_2 v_P \quad (4-42)$$

$$\frac{\partial F_1}{\partial v_P} = 2a_1 v_P + 2a_2 v_P \tan^{-1} \frac{\alpha_P}{v_P} - a_2 \alpha_P - C_7 \quad (4-43)$$

Equations 4-20, 4-27, and 4-28 define the expressions for  $F_2$ ,  $\partial F_2/\partial \alpha_P$ , and  $\partial F_2/\partial v_P$ .

### Series Pumps

Two pumping-sets with a long pipe between them may be analyzed by considering each set individually and the downstream pumps with a long suction line. However, if the pipe length between the pumps is short, then this pipe may be neglected in the analysis, and both pumping units may be lumped together as a boundary of series pumps (Fig. 4-10). The upstream pump in this case is called booster pump and the downstream pump as the main pump.

The boundary conditions for the series pumps may be developed as follows. Referring to Fig. 4-10, the following equations may be written [Miyashiro, 1965] for the system in which subscripts  $b$ ,  $m$ , and  $v$  refer to the booster and main pump and to the valve, respectively;  $n_P$  = number of pumping-sets connected in parallel; and  $C_v$  = coefficient of head loss in the valve.

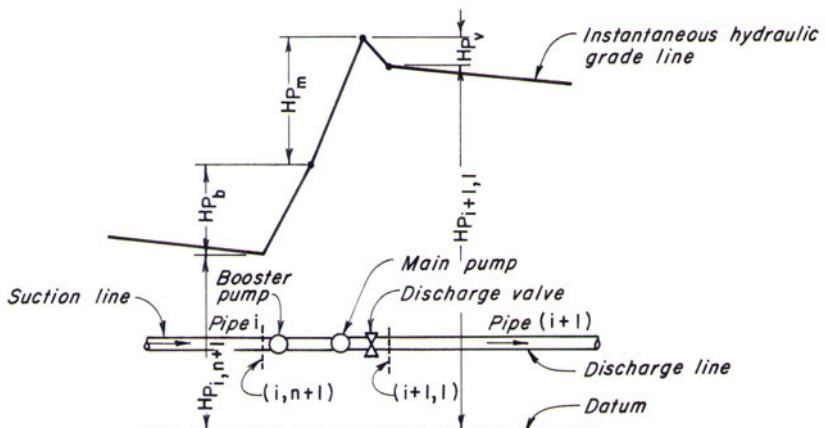


**Fig. 4-10.** Notation for series pumps.

Pumping head

$$H_{P_{i+1,1}} = H_{P_{i,n+1}} + H_{P_b} + H_{P_m} - \Delta H_{P_v} \quad (4-44)$$

Continuity equations

$$Q_{P_{i,n+1}} = n_P Q_{P_b} \quad (4-45)$$

$$Q_{P_b} = Q_{P_m} \quad (4-46)$$

$$Q_{P_{i+1,1}} = n_P Q_{P_m} \quad (4-47)$$

Positive characteristic equation for the suction line

$$Q_{P_{i,n+1}} = C_p - C_{a_i} H_{P_{i,n+1}} \quad (4-48)$$

Negative characteristic equation for the discharge line

$$Q_{P_{i+1,1}} = C_n + C_{a_{i+1}} H_{P_{i+1,1}} \quad (4-49)$$

Equation for head loss in the valve

$$\Delta H_{P_v} = C_v Q_{P_{i+1,1}} |Q_{P_{i+1,1}}| \quad (4-50)$$

Equations for the pump characteristics

$$h_{P_m} = a_{1m} (\alpha_{P_m}^2 + v_{P_m}^2) + a_{2m} (\alpha_{P_m}^2 + v_{P_m}^2) \tan^{-1} \frac{\alpha_{P_m}}{v_{P_m}} \quad (4-51)$$

$$h_{P_b} = a_{1b} (\alpha_{P_b}^2 + v_{P_b}^2) + a_{2b} (\alpha_{P_b}^2 + v_{P_b}^2) \tan^{-1} \frac{\alpha_{P_b}}{v_{P_b}} \quad (4-52)$$

$$\beta_{P_m} = a_{3m} (\alpha_{P_m}^2 + v_{P_m}^2) + a_{4m} (\alpha_{P_m}^2 + v_{P_m}^2) \tan^{-1} \frac{\alpha_{P_m}}{v_{P_m}} \quad (4-53)$$

$$\beta_{P_b} = a_{3b} (\alpha_{P_b}^2 + v_{P_b}^2) + a_{4b} (\alpha_{P_b}^2 + v_{P_b}^2) \tan^{-1} \frac{\alpha_{P_b}}{v_{P_b}} \quad (4-54)$$

Equation for the rotating masses (i.e., equations similar to Eq. 4-14)

$$\alpha_{P_m} - C_{6m} \beta_{P_m} = \alpha_m + C_{6m} \beta_m \quad (4-55)$$

$$\alpha_{P_b} - C_{6b} \beta_{P_b} = \alpha_b + C_{6b} \beta_b \quad (4-56)$$

To simplify the solution of these equations, let us first reduce the number of unknowns from 13 to three as follows. Elimination of  $H_{P_{i,n+1}}$ ,  $Q_{P_{i,n+1}}$ ,  $H_{P_{i+1,1}}$ ,  $Q_{P_{i+1,1}}$ ,  $Q_{P_b}$  and  $H_{P_v}$  from Eqs. 4-44 to 4-50 yields

$$H_{P_m} + H_{P_b} = \frac{n_P Q_{P_m} - C_n}{C_{a_{i+1}}} - \frac{C_p - n_P Q_{P_m}}{C_{a_i}} + C_v n_P Q_{P_m} |Q_{P_m}| \quad (4-57)$$

By using the rated conditions  $H_{R_m}$ ,  $H_{R_b}$ , and  $Q_{R_m}$  as reference values, Eq. 4-57 may be written as

$$\begin{aligned} h_{P_m} H_{R_m} + h_{P_b} H_{R_b} &= \frac{n_P Q_{R_m}}{C_{a_{i+1}}} v_{P_m} + \frac{n_P Q_{R_m}}{C_{a_i}} v_{P_m} \\ &\quad + n_P C_v Q_{R_m}^2 v_{P_m} |v_{P_m}| - \frac{C_n}{C_{a_{i+1}}} - \frac{C_p}{C_{a_i}} \end{aligned} \quad (4-58)$$

By substituting expressions for  $h_{P_m}$  and  $h_{P_b}$  from Eqs. 4-51 and 4-52 into Eq. 4-58 and simplifying the resulting equation, we obtain

$$\begin{aligned} F_1 = & a_{1m} H_{R_m} (\alpha_{P_m}^2 + v_{P_m}^2) + a_{2m} H_{R_m} (\alpha_{P_m}^2 + v_{P_m}^2) \tan^{-1} \frac{\alpha_{P_m}}{v_{P_m}} \\ & + a_{1b} H_{R_b} (\alpha_{P_m}^2 + v_{P_m}^2) + a_{2b} H_{R_b} (\alpha_{P_b}^2 + v_{P_m}^2) \tan^{-1} \frac{\alpha_{P_b}}{v_{P_m}} \\ & - n_P C_v Q_{R_m}^2 v_{P_m} |v_{P_m}| - \frac{n_P Q_{R_m}}{C_{a_{i+1}}} v_{P_m} - \frac{n_P Q_{R_m}}{C_{a_i}} v_{P_m} \\ & + \frac{C_n}{C_{a_{i+1}}} + \frac{C_p}{C_{a_i}} = 0 \end{aligned} \quad (4-59)$$

Note that we have replaced  $v_{P_b}$  in Eq. 4-59 by  $v_{P_m}$  since both are equal for the same number of main and booster pumping-sets.

By eliminating  $\beta_{P_m}$  from Eqs. 4-53 and 4-55 and  $\beta_{P_b}$  from Eqs. 4-54 and 4-56, we obtain

$$\begin{aligned} F_2 = & \alpha_{P_m} - C_{6m} \left[ a_{3m} (\alpha_{P_m}^2 + v_{P_m}^2) + a_{4m} (\alpha_{P_m}^2 + v_{P_m}^2) \tan^{-1} \frac{\alpha_{P_m}}{v_{P_m}} \right] \\ & - \alpha_m - C_{6m} \beta_m \end{aligned} \quad (4-60)$$

$$\begin{aligned} F_3 = & \alpha_{P_b} - C_{6b} \left[ a_{3b} (\alpha_{P_b}^2 + v_{P_m}^2) + a_{4b} (\alpha_{P_b}^2 + v_{P_m}^2) \tan^{-1} \frac{\alpha_{P_b}}{v_{P_m}} \right] \\ & - \alpha_b - C_{6b} \beta_b \end{aligned} \quad (4-61)$$

Now we have three nonlinear equations (Eqs. 4-59 to 4-61) in three unknowns,  $\alpha_{P_m}$ ,  $v_{P_m}$  and  $\alpha_{P_b}$ . We solve these equations by the Newton-Raphson method, as follows

$$\left( \frac{\partial F_1}{\partial \alpha_{P_m}} \delta \alpha_{P_m} + \frac{\partial F_1}{\partial v_{P_m}} \delta v_{P_m} + \frac{\partial F_1}{\partial \alpha_{P_b}} \delta \alpha_{P_b} \right)^{(1)} = -F_1^{(1)} \quad (4-62)$$

$$\left( \frac{\partial F_2}{\partial \alpha_{P_m}} \delta \alpha_{P_m} + \frac{\partial F_2}{\partial v_{P_m}} \delta v_{P_m} + \frac{\partial F_2}{\partial \alpha_{P_b}} \delta \alpha_{P_b} \right)^{(1)} = -F_2^{(1)} \quad (4-63)$$

$$\left( \frac{\partial F_3}{\partial \alpha_{P_m}} \delta \alpha_{P_m} + \frac{\partial F_3}{\partial v_{P_m}} \delta v_{P_m} + \frac{\partial F_3}{\partial \alpha_{P_b}} \delta \alpha_{P_b} \right)^{(1)} = -F_3^{(1)} \quad (4-64)$$

The values of  $\alpha_{P_m}^{(1)}$ ,  $v_{P_m}^{(1)}$  and  $\alpha_{P_b}^{(1)}$  are first estimated and the functions  $F_1$ ,  $F_2$ , and  $F_3$ , and their derivatives in these equations are evaluated for the estimated values of these variables. Then, a better estimate of the solution is determined from the following equations:

$$\alpha_{P_m}^{(2)} = \alpha_{P_m}^{(1)} + \delta \alpha_{P_m} \quad (4-65)$$

$$v_{P_m}^{(2)} = v_{P_m}^{(1)} + \delta v_{P_m} \quad (4-66)$$

$$\alpha_{P_b}^{(2)} = \alpha_{P_b}^{(1)} + \delta \alpha_{P_b} \quad (4-67)$$

As indicated previously, the superscript in the parentheses refers to the number of the iteration. The expressions for the derivatives obtained by differentiating Eqs. 4-59 through 4-61 are

$$\frac{\partial F_1}{\partial \alpha_{P_m}} = 2a_{1_m} H_{R_m} \alpha_{P_m} + 2a_{2_m} H_{R_m} \alpha_{P_m} \tan^{-1} \frac{\alpha_{P_m}}{v_{P_m}} + a_{2_m} H_{R_m} v_{P_m} \quad (4-68)$$

$$\begin{aligned} \frac{\partial F_1}{\partial v_{P_m}} &= 2a_{1_m} H_{R_m} v_{P_m} + 2a_{2_m} H_{R_m} v_{P_m} \tan^{-1} \frac{\alpha_{P_m}}{v_{P_m}} - a_{2_m} H_{R_m} \alpha_{P_m} \\ &\quad + 2a_{1_b} H_{R_b} v_{P_m} + 2a_{2_b} H_{R_b} v_{P_m} \tan^{-1} \frac{\alpha_{P_b}}{v_{P_m}} - a_{2_b} H_{R_b} \alpha_{P_b} \\ &\quad - 2n_P C_v Q_{R_m}^2 |v_{P_m}| - \frac{n_P Q_{R_m}}{C_{a_{i+1}}} - \frac{n_P Q_{R_m}}{C_{a_i}} \end{aligned} \quad (4-69)$$

$$\frac{\partial F_1}{\partial \alpha_{P_b}} = 2a_{1_b} H_{R_b} \alpha_{P_b} + 2a_{2_b} H_{R_b} \alpha_{P_b} \tan^{-1} \frac{\alpha_{P_b}}{v_{P_m}} + a_{2_b} H_{R_b} v_{P_m} \quad (4-70)$$

$$\frac{\partial F_2}{\partial \alpha_{P_b}} = 0 \quad (4-71)$$

$$\begin{aligned} \frac{\partial F_2}{\partial \alpha_{P_m}} &= 1 - 2C_{6_m} a_{3_m} \alpha_{P_m} - 2C_{6_m} a_{4_m} \alpha_{P_m} \tan^{-1} \frac{\alpha_{P_m}}{v_{P_m}} - C_{6_m} a_{4_m} v_{P_m} \\ &\quad \end{aligned} \quad (4-72)$$

$$\frac{\partial F_2}{\partial v_{P_m}} = -2C_{6_m} a_{3_m} v_{P_m} - 2C_{6_m} a_{4_m} v_{P_m} \tan^{-1} \frac{\alpha_{P_m}}{v_{P_m}} + C_{6_m} a_{4_m} \alpha_{P_m} \quad (4-73)$$

$$\frac{\partial F_3}{\partial \alpha_{P_m}} = 0 \quad (4-74)$$

$$\frac{\partial F_3}{\partial \alpha_{P_b}} = 1 - 2C_{6_b} a_{3_b} \alpha_{P_b} - 2C_{6_b} a_{4_b} \alpha_{P_b} \tan^{-1} \frac{\alpha_{P_b}}{v_{P_m}} - C_{6_b} a_{4_b} v_{P_m} \quad (4-75)$$

$$\frac{\partial F_3}{\partial v_{P_m}} = -2C_{6_b} a_{3_b} v_{P_m} - 2C_{6_b} a_{4_b} v_{P_m} \tan^{-1} \frac{\alpha_{P_b}}{v_{P_m}} + C_{6_b} a_{4_b} \alpha_{P_b} \quad (4-76)$$

If  $|\delta\alpha_{P_m}|$ ,  $|\delta\alpha_{P_b}|$ , and  $|\delta v_{P_m}|$ , obtained by simultaneously solving Eqs. 4-62 through 4-64, are less than a specified tolerance (e.g., 0.001), then  $\alpha_{P_m}^{(2)}$ ,  $v_{P_m}^{(2)}$ , and  $\alpha_{P_b}^{(2)}$  are solutions of Eqs. 4-59 through 4-61; otherwise,  $\alpha_{P_m}^{(1)}$ ,  $v_{P_m}^{(1)}$  and  $\alpha_{P_b}^{(1)}$  are assumed equal to  $\alpha_{P_m}^{(2)}$ ,  $v_{P_m}^{(2)}$  and  $\alpha_{P_b}^{(2)}$ , and the above procedure is repeated until a solution is obtained. Then, it is verified whether the segment of pump characteristics used in the computations corresponds to  $\alpha_P$  and  $v_P$ . If it does not, then  $\alpha_{e_m}$ ,  $\alpha_{e_b}$  and  $v_{e_m}$  are assumed equal to  $\alpha_{P_m}^{(2)}$ ,  $\alpha_{P_b}^{(2)}$  and  $v_{P_m}^{(2)}$  respectively, and the above procedure is repeated; otherwise, the values of the remaining variables are obtained from Eqs. 4-44 through 4-56, and the solution progresses to the next time step.

To avoid an unlimited number of iterations in the case of divergence of iterations, a counter should be used so that the computations are stopped if the number of iterations exceeds a specified value, e.g., 30.

## 4-6 Pump Start-Up

The start-up procedure outlined in Section 4-2 cannot be used for pumping systems without a control valve downstream of the pump since very high pressures may be produced. This is especially the case if the motor is of the induction type and is started across the line, i.e., without reducing the voltage.

A simplified procedure for computing the transient-state conditions produced by pump start-up is presented in this section. The motor manufacturer can provide the time needed for the pump to reach its rated speed from zero under selected start-up procedures. To allow for a factor of safety, the pump start-up time,  $T_s$ , is assumed to be 70 percent [Joseph and Hamill, 1972] of the time given by the manufacturer. The pump speed is assumed to increase linearly from zero to the rated speed  $N_R$  during time,  $T_s$ . Thus the time variation of the pump speed is known. This simplifies the computations considerably since now we do not have to determine  $\alpha$  at different times from the torque characteristics and the polar moment of inertia.

Let the pump speed at the end of the time step be  $\alpha^*$ , which may be determined from the known variation of pump speed with time. As discussed in Section 4-4, we may estimate  $v_e$  by extrapolation of the computed values of  $v$  during the previous time steps. Then for these values of  $\alpha^*$  and  $v_e$ , determine the relevant segment of the pump characteristics. Let the equation of the straight line representing this segment (Fig. 4-3) be

$$\frac{h_P}{\alpha^{*2} + v_P^2} = a_1 + a_2 \tan^{-1} \frac{\alpha^*}{v_P} \quad (4-77)$$

in which  $a_1$  and  $a_2$  may be determined from the stored pump characteristic data.

The following procedure is for a system having a short suction line. Proceeding similarly, we may include a suction line in the analysis. The negative characteristic equation for the pump end in a normalized form using  $H_R$  and  $Q_R$  as reference may be written as

$$Q_R v_P = C_n + C_a H_R h_P \quad (4-78)$$

Eliminating  $h_P$  from Eqs. 4-77 and 4-78 and simplifying the resulting equation yield

$$C_a H_R \left( a_1 + a_2 \tan^{-1} \frac{\alpha^*}{v_P} \right) v_P^2 + C_a H_R a_2 \alpha^{*2} \tan^{-1} \frac{\alpha^*}{v_P} - Q_R v_P + C_n + C_a H_R \alpha^{*2} a_1 = 0 \quad (4-79)$$

This equation may be solved by the Newton-Raphson method and the values of  $h_P$ ,  $H_{P_{i,1}}$  and  $Q_{P_{1,1}}$  may then be determined.

If the discharge line is under a static head prior to the pump start-up, then there will be no flow into the discharge line until the pumping head exceeds

this static head. This condition may be included in the above analysis by assuming that  $Q_{P_{1,1}} = 0.0$  until  $H_{P_{1,1}}$  exceeds the static head.

The pressure rise during a start-up may be reduced by increasing the start-up time  $T_s$ . This may be done by increasing the moment of inertia of the pump motor, by reducing voltage, or by having a part-winding start. The overall economy of decreasing the maximum pressure to reduce the pipe-wall thickness by these methods should be investigated prior to their selection.

## 4-7 Design Criteria

Once the layout and parameters of a piping system have been selected, the maximum and minimum pressures for various operating conditions may be determined by using the procedures outlined in Sections 4-4 and 4-5. In the safest design, all components of the system are designed for the possible maximum and minimum pressures with a liberal factor of safety. Such a design, however, is very uneconomical. Therefore, a factor of safety is chosen depending upon the risks and the probability of occurrence of a particular operating condition during the life of the project, i.e., the higher the probability of occurrence, the higher is the factor of safety.

Based upon the frequency of occurrence, operating conditions may be classified as *normal*, *emergency*, or *exceptional*. Various professional societies and organizations such as, American Society of Mechanical Engineers, American Water-Works Association, etc. have their own standards and recommended factor of safety. The designer should check these for their applicability for the particular jurisdiction. The following discussion on the operating conditions of each of these categories and the recommended factors of safety [Chaudhry et al., 1978] should be considered as a guide only.

### Normal

All operations that are likely to occur several times during the life of a system are termed *normal*. Appurtenances or devices (e.g., surge tank, surge suppressor, air chamber, and air valve) provided in the system to reduce severe transients are assumed to be properly designed and to function as planned during these operations.

The following are considered normal operating conditions:

- Automatic or manual starting or tripping of pumps throughout the entire range of pumping head. If there are multiple pumps on the line, all are tripped simultaneously; however, only one may be started at a time.
- If a check valve is present near the pump, it closes instantly upon flow reversal.
- A surge tank does not drain and thus admit air into the pipeline, and it does not overflow unless an overflow spillway is provided.

- An air chamber is assumed to have minimum air volume during a power failure.

As a result of any of these operations, the water column does not separate at any point in the pipeline. However, if the water-column separation does occur, then appurtenances such as air chamber, surge tank, etc. may be provided to prevent it. But, if it is impractical or too costly to do so, then special devices may be provided to minimize the transient pressures when the columns subsequently rejoin or the pipeline is designed to withstand these pressures.

A factor of safety of three based on the ultimate bursting strength of the member and a suitable factor of safety against collapse are recommended for the transient pressures caused by the normal operations.

### **Emergency**

The emergency operating conditions in pumping systems are those in which one of the transient-control devices malfunctions. These conditions include:

- One of the surge suppressors, surge tanks, or relief valves is inoperative.
- Closure of one of the check valves provided for shutting off return flow through the pumps is delayed and occurs at the time of maximum reverse flow.
- Air-inlet valves, if present in the system, are inoperative.

Since the probability of occurrence of these conditions is rather small, a factor of safety of *two* based on the ultimate bursting or collapsing strength is recommended.

### **Exceptional**

Exceptional conditions are those in which the protective equipment malfunctions in the most unfavorable manner, such as loss of all air in the air chamber, very rapid abnormal opening or closing of a valve or a gate, and pump-shaft failure. Because the probability of occurrence of any of these conditions is extremely remote, a factor of safety of *slightly more than one*, based on the ultimate bursting or collapsing strength, may be used.

## **4-8 Case Study**

The hydraulic transient studies [Chaudhry et al., 1978] during the preliminary design of the makeup and cooling-water supply system for the Hat Creek Project are presented in this section.

## Water-Supply System

The water-supply system (see Fig. 4-11) for pumping water from the Thompson River to the plant reservoir comprises of an 800-mm-diameter buried pipeline, approximately 23 km long; a pumping station with five pumping units at the river intake; two booster stations, each with four pumps and a free-surface suction tank; and a reservoir near the power plant. The maximum and average discharge is 0.725 and 0.60 m<sup>3</sup>/s, respectively, and the maximum total static lift from the river intake to the plant reservoir is 1083 m.

Both booster stations have three-stage pumps, each rated at 0.4 m<sup>3</sup>/s, 670 m, and 3580 rpm. The specific speed of each pump is 0.74 (SI units), and the moment of inertia of the pump, motor, shaft, and entrained water in the impeller is 62 kg m<sup>2</sup>. If required, total inertia for each unit may be increased to 420 kg m<sup>2</sup> without exceeding the limits set for the pump start-up. The pump manufacturer supplied the pump characteristics for the normal zone of pump operation only. Since no data were available for the other zones and since these characteristics agreed closely with those of Appendix F for  $N_s = 0.46$  (SI units), the characteristics of Appendix A were used for all zones of operation.

## Analysis

A computer program was used for analyzing the transient conditions in a pipeline caused by power failure and/or valve operation, incorporating the boundary conditions and solution procedures presented in Chapters 3, 4, and 10. To avoid interpolation errors in the method of characteristics, wave velocities were adjusted slightly, if necessary, so that the characteristics passed through the grid points. Because of a free-surface tank on the suction side of each booster station, transients in the discharge line were analyzed neglecting the suction line. The program was verified by comparing the computed results with those recorded during tests at Wind Gap Pumping Plant (see Section 4-4).

### *Selection of Control Devices*

Appropriate waterhammer control devices were selected as follows:

*Column separation.* The system was analyzed for simultaneous power failure to all pumps, assuming there were no control devices. Water-column separation occurred in the pipeline between Booster Stations Nos. 1 and 2, and in the pipeline downstream of Booster Station No. 2. The provision of additional inertia at the pumps and one-way surge tanks prevented column separation. The data for these devices are listed subsequently.

**Maximum pressure.** It was assumed during the initial design of the pipeline that, with appropriate control devices, the maximum pressure rise (Pressure rise = maximum transient state pressure – Steady-state pressure.) at the pump end could be limited to 10 percent of the rated head. With check valves located downstream of the pumps, the pressure rise following power failure exceeded 10 percent. However, it could be reduced to less than 5 percent by slowly closing the pump-discharge valves.

## Results

The maximum and minimum hydraulic grade lines following power failure are shown on [Fig. 4-11](#) for the system with suitable control equipment.

**Column Separation** The following control devices would successfully prevent column separation in the pipeline:

### Pipeline from Booster Station No. 1 to 2

Two alternatives are available:

- Increase the moment of inertia of each pump motor to  $115 \text{ kg m}^2$ , and provide a 4-m-diameter one-way surge tank at the top of Elephant Hill with the steady-state water level in the tank at El. 627 (10 m above the ground surface);
- Increase the moment of inertia of each pump motor to  $390 \text{ kg m}^2$ .

With these controls, the minimum pressures in the pipelines remain above atmospheric pressure.

### Pipeline Downstream of Booster Station No.2

- Increase the moment of inertia of each pump motor to  $370 \text{ kg m}^2$ ; provide a 4-m-diameter one-way surge tank at Station 11 + 175 with steady-state water level in the tank at El. 1252 (10 m above ground level); and provide a 4-m-diameter one-way surge tank at Station 17 + 480 with steady-state water level in the tank at El. 1345 (25 m above ground level).

With these measures, the minimum pressure along the pipeline was above atmospheric pressure.

**Maximum Pressures** The pressure rise following power failure could be reduced by slowly closing the pump-discharge valves. With the closing times of about 100 s, the pressure rise at the pump following power failure was less than 5 percent of the rated head. A single rate closure was assumed in these computations. The maximum reverse pump speed following power failure with

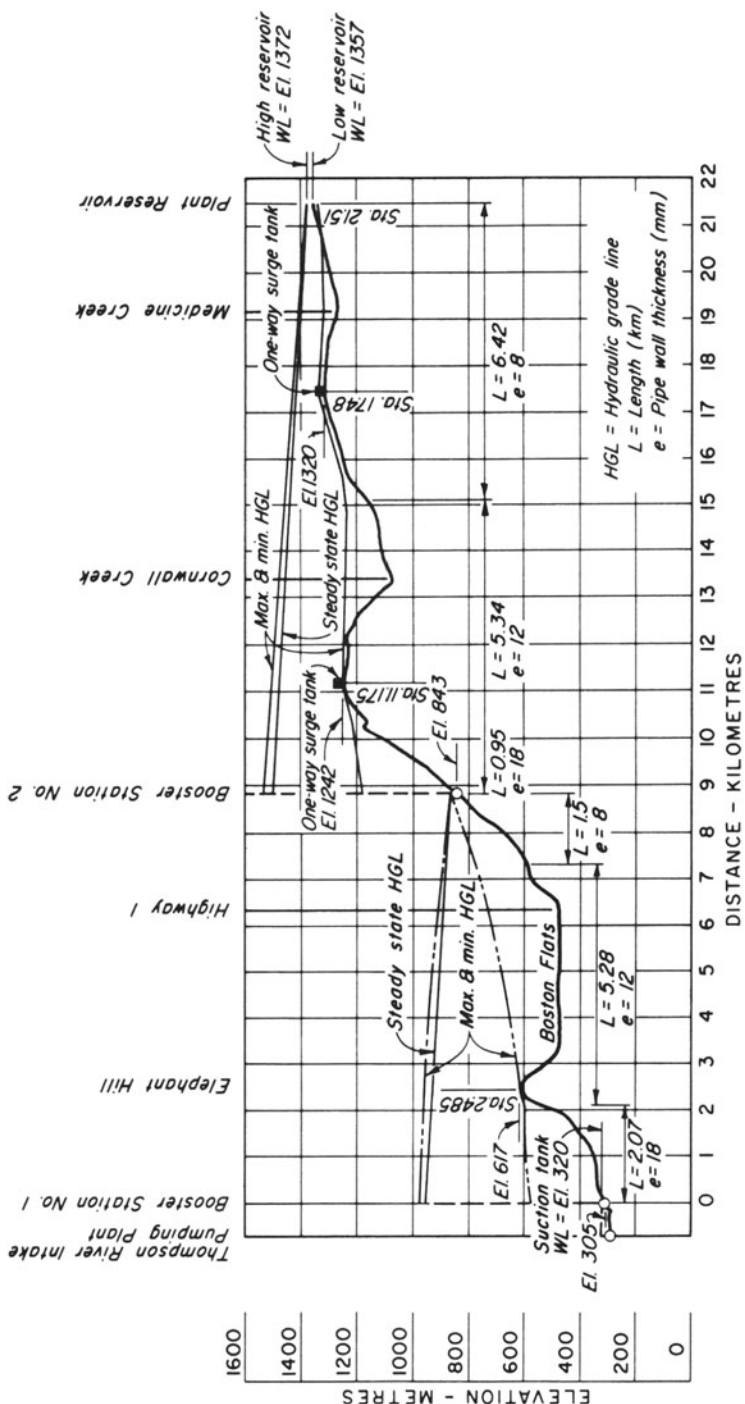


Fig. 4-11. Hat Creek Thermal Power Plant: pipeline profile of makeup cooling-water.

the discharge valve remaining open or with the discharge valve closed was less than the maximum permissible limits specified by the pump manufacturer: 130 percent of rated speed for less than 30 s and 120 percent of rated speed for longer periods.

***Emergency Conditions*** As an emergency condition, the discharge valves were assumed to remain open following power failure. Because of the higher than normal inertia, the maximum pressure at the pump in all cases remained less than the steady-state pressure.

## Discussion

The above results were obtained using assumed friction factors and assumed pump characteristics. In addition, both the topographic information and the data for discharge valves were not precisely known. Test runs using different pump characteristics showed that variation in the pump characteristics and/or in the data for the discharge valve could substantially change the computed maximum and minimum pressures. Similarly, significant changes in the ground topography would change the hydraulic grade line relative to the pipeline, thus possibly resulting in situations where column separation could occur. A difference in the head losses could also affect the maximum and minimum pressures.

With the available data, the maximum pressures at the pump could be kept below 5 percent of the rated head. However, as discussed, the pressure rise may be higher due to significant variations in the data for the system. If necessary, the pressure rise may be decreased by increasing the discharge-valve closing time, which increased the time period for which the pump runs in the reverse direction. Although the maximum reverse pump speed was within the limits specified by the pump manufacturer, reverse flow through the pumps for an extended period may partially drain the pipeline at high points. Therefore, it was recommended that, until better data are available and a sensitivity analysis of the effects of changes in the variables affecting pressure rise was done, the maximum pressure rise at the pump end should be taken equal to 10 percent of the rated head, and the elevation of the maximum hydraulic grade line shown in Fig. 4-11 should be adjusted proportionately.

With the specified control measures, the minimum hydraulic grade line was always above the pipeline. At Elephant Ridge and at the summits downstream of Booster Station 2, the minimum hydraulic grade line was less than 5 m above the pipeline. During the final design, however, when better data should be available, this should be investigated in detail; and if necessary, the safety margin may be increased.

Air valves should be provided at high points along the pipeline. These are helpful during filling and draining of the line and prevent collapse of a long length of the pipeline should a break occur in the pipeline at a lower elevation. In addition, valves may be provided along the line to isolate and

drain segments of the line for inspection, repair, etc. Transients caused by the operation of these valves, if provided, should be studied during the final design.

The one-way surge tanks should have two pipes for water outflow. This should considerably reduce the possibility of a tank becoming inoperative due to the failure of a check valve to open.

Two alternatives are available to prevent column separation in the pipeline between Booster Stations Nos. 1 and 2. The alternative with increased inertia only is better from an operational point of view because the one-way surge tank is not as foolproof and in addition requires continuous maintenance.

The inertia of the pump motors could be increased by adding flywheels or by a custom design of the electric motors. In order to provide operational flexibility and ease in exchanging spare parts, etc., it was decided that all units at both the booster stations should be identical and that each would have a moment of inertia equal to  $400 \text{ kg m}^2$ .

## 4-9 Summary

In this chapter, a procedure for utilizing the pump characteristics in a computer analysis is presented, an iterative procedure for analyzing transients in piping systems caused by various pump operations is outlined, and boundary conditions for a number of cases usually found in practice are developed. Criteria for the design of pipelines are presented, and the chapter is concluded by a case study.

## Problems

**4-1** Write a general-purpose computer program to determine the transient-state pressures in a discharge line caused by power failure. Using the pump characteristic of Appendix F, investigate the effect of increasing the value of moment of inertia on the maximum and minimum pressures.

**4-2** Using the program of Problem 4-1, prove that the maximum pressure at the pump does not exceed [Stephenson, 1976] the pumping head if the friction losses are greater than  $0.7aV_o/g$ , in which  $a$  = waterhammer wave velocity,  $V_o$  = steady-state flow velocity, and  $g$  = acceleration due to gravity.

**4-3** Develop the boundary conditions for a system having  $n$  parallel pumps, in which power fails to  $n_f$  pumps and  $n_o$  pumps keep operating.

**4-4** Draw a flowchart for the boundary condition derived in Problem 4-3, and develop a computer program.

**4-5** To reduce maximum pressures following a power failure, a pressure-regulating valve is provided just downstream of the pump. This valve opens as the power fails and is closed slowly later. Develop the boundary conditions for such a system; write a computer program and investigate the effect of various rates of opening and closure of the pressure-regulating valve.

**4-6** A check valve is provided in a discharge line to prevent reverse flow through the pumps. When power fails to the pump, water in the discharge line decelerates, and the check valve closes. A check valve having no dashpot and having negligible bearing friction losses closes [Parmley, 1965] according to the equation

$$I \frac{d^2\theta}{dt^2} - W_s \bar{r} \sin \theta + \left( \frac{BV}{K_f} + \frac{C}{K_d} + \frac{d\theta}{dt} \right)^2 + \left( \frac{G}{K_d} \frac{d\theta}{dt} \right)^2 + \left( \frac{FV}{K_f} \right)^2 = 0$$

in which  $\theta$  = angle between the center of gravity of disk and vertical;  $I$  = moment of inertia of the disk;  $W_s$  = weight of disk in water;  $\bar{r}$  = distance from pivot to weight-center of gravity of disk;  $V$  = mean pipeline velocity;  $K_f$  = flow coefficient of stationary disk in moving water (function of  $\theta$ );  $K_d$  = flow coefficient for moving disk in still water (function of  $\theta$ ); and  $B$ ,  $C$ ,  $G$ , and  $F$  are constants. Expression for these constants are

$$\begin{aligned} B &= \left( \frac{AR}{P^3} \right)^{0.25} \\ C &= J \left( \frac{A^2 P^3}{R} \right)^{0.25} \\ F &= \left( AR - J^2 \sqrt{\frac{A^2 R}{P^3}} \right)^{0.5} \\ G &= \left( AP^3 - J^2 \sqrt{\frac{A^2 P^3}{R}} \right)^{0.5} \end{aligned}$$

in which  $A$  = area of disk;  $R$  = distance from pivot to center of disk;  $P$  = distance from pivot to the point of concentration of  $\int r^3 dA$ ;  $J$  = distance from pivot to point of concentration of moment of inertia of disk area; and  $r$  = moment arm measured from disk pivot.

Develop the boundary conditions for the check valve, assuming that  $K_f$  and  $K_d$  are given in a tabular form.

**4-7** Write a computer program for a check valve, and run it for the following data:  $I = 0.235 \text{ lb-ft-sec}^2$ ;  $B = 0.548$ ;  $C = 0.357$ ;  $F = 0.11$ ;  $G = 0.07$ ;  $W_s \bar{r} = 10.74 \text{ lb-ft}$ ;  $\theta = 16.1^\circ + \alpha$ ; initial steady-state  $\theta$  and  $\alpha$  are  $60.1^\circ$  and  $44^\circ$ , respectively.  $K_f$  and  $K_d$  are listed in the following:

| $\alpha$<br>(degrees) | $K_f$ | $K_d$ |
|-----------------------|-------|-------|
| 0                     | 0.    | 0.0   |
| 4                     | 0.16  | 0.23  |
| 8                     | 0.28  | 0.40  |
| 12                    | 0.40  | 0.49  |
| 16                    | 0.49  | 0.55  |
| 20                    | 0.56  | 0.58  |
| 24                    | 0.62  | 0.54  |
| 28                    | 0.67  | 0.49  |
| 32                    | 0.71  | 0.44  |
| 36                    | 0.77  | 0.38  |
| 40                    | 0.84  | 0.27  |
| 44                    | 0.95  | 0.09  |

Use the pipeline and pump data given in [Fig. 4-6](#) and [Table 4-2](#) with the diameter of the pipelines changed to 9 in.

**4-8** Write a computer program for analyzing the transient conditions caused by pump start-up. By using this program, investigate the effect of starting time,  $T_s$ , on the maximum and minimum pressures.

## References

- Brown, R. J. and Rogers, D. C., 1980, "Development of Pump Characteristics from Field Tests," *Jour. Mechanical Design*, Amer. Soc. of Mech. Engrs., vol. 102, pp. 807-817.
- Chaudhry, M. H., Cass, D. E., and Bell, P. W. W., 1978, "Hat Creek Project: Hydraulic Transient Analysis of Make-up Cooling Water Supply System," *Report No. DD 108*, Hydroelectric Design Division, British Columbia Hydro and Power Authority, Vancouver, Canada, Feb.
- Curtis, E. M., 1983, "Four-Quadrant Characteristics of a Vaned Diffuser, End Suction, Pump," *Sixth International Symp. on Hydraulic Transients in Power Stations*, International Assoc. Hydraulic Research, Gloucester, England, September 18-20.
- Daigo, H. and Ohashi, H., 1972, "Experimental Study on Transient Characteristics of a Centrifugal Pump During Rapid Acceleration of Rotational Speed," *Proc. 2nd. International Symp. Fluid Machinery and Fluidics*, vol. 2, Jap. Soc. Mech. Engrs., Sept., pp. 175-182.
- Donsky, B., 1961, "Complete Pump Characteristics and the Effect of Specific Speeds on Hydraulic Transients," *Jour. Basic Engineering*, Amer. Soc. of Mech. Engrs., Dec., pp. 685-699.
- Joseph, I. and Hamill, F., 1972, "Start-Up Pressures in Short Pump Discharge Lines," *Jour. Hydraulics Div.*, Amer. Soc. of Civ. Engrs., vol. 98, July, pp. 1117-1125.

- Kamath, P. S. and Swift, W. L., 1982, "Two-Phase Performance of Scale Models of a Primary Coolant Pump," *Final Report*, NP-2578, September.
- Kennedy, W. G., , Jacob, M. C., , Whitehouse, J. C., , Fishburn J. D., , and Kanupka, G. J., 1980, "Pump Two-Phase Performance Program," *Final Report*, NP-1556, vols. 2, 5, September.
- Kittredge, C. P. and Thoma, D., 1931, "Centrifugal Pumps Operated Under Abnormal Conditions," *Power*, vol. 73, pp. 881-884.
- Kittredge, C. P., 1933, "Vorgange bei Zentrifugalkumpenlagen nach plötzlichem Ausfallen des Antriebes," *Mitteilungen des Hydraulischen Instituts der Technischen Hochschule München*, vol. 7, pp. 53-73.
- Kittredge, C. P., 1956, "Hydraulic Transients in Centrifugal Pump Systems," *Trans.*, Amer. Soc. of Mech. Engrs., vol. 78, pp. 1307-1322.
- Knapp, R. T., 1937, "Complete Characteristics of Centrifugal Pumps and Their Use in Prediction of Transient Behaviour," *Trans.*, Amer. Soc. of Mech. Engrs., vol. 59, pp. 683-689.
- Kobori, T., 1954, "Experimental Research on Water Hammer in the Pumping Plant of the Numazawanuma Pumped Storage Power Station," *Hitachi Review*, pp. 65-74.
- Marchal, M., , Flesch, G., , and Suter, P., 1965, "The Calculation of Waterhammer Problems by Means of the Digital Computer," *Proc. International Symp. on Waterhammer in Pumped Storage Projects*, Amer. Soc. of Mech. Engrs., pp. 168-188.
- Martin, C. S., 1983, "Representation of Pump Characteristics for Transient Analysis," *Proc. Symp. on Performance Characteristics of Hydraulic Turbines and Pumps.*, Amer. Soc. Mech. Engrs., Nov.
- Miyashiro, H., 1965, "Waterhammer Analysis for Pumps Installed in Series," *Marchal et al. Proc. International Symp. on Waterhammer in Pumped Storage Projects*, Amer. Soc. of Mech. Engrs., pp. 123-133.
- Miyashiro, H. and Kondo, M., 1969, "Model Tests of Pumps for Snake Creek Pumping Plant No. 1, USA," *Hitachi Review*, vol. 18, no. 7, pp. 286-292.
- Miyashiro, H. and Kondo, M., 1970, "Model Tests of Centrifugal Pumps for Santa Ines Pumping Plant, Brazil," *Hitachi Review*, vol. 19, no. 11, pp. 386-394.
- Ohashi, H., 1968, "Analytical and Experimental Study of Dynamic Characteristics of Turbopumps," *NASA TN D-4298*, April.
- Olson, D. J., 1974, "Single and Two-Phase Performance Characteristics of the MOD-1 Semiscale Pump Under Steady State and Transient Fluid Conditions," ANCR-1165, Aerojet Nuclear Company, Oct.
- Parmakian, J., 1957, "Waterhammer Design Criteria," *Jour. Power Div.*, Amer. Soc. of Civ. Engrs., April, pp. 1216-1 to 1216-8.
- Parmakian, J., 1963, *Waterhammer Analysis*, Dover Publications, pp. 78-81.
- Parmley, L. J., 1965, "The Behaviour of Check Valves During Closure," *Research Report*, Glenfield and Kennedy Ltd., Kilmarnock, England, Oct.

- Paynter, H. M., 1972, "The Dynamics and Control of Eulerian Turbomachines," *Jour., Dynamic Systems, Measurement, and Controll*, Amer. Soc. Mech. Engrs., Sept., pp. 198-205.
- Paynter, H. M., 1979, "An Algebraic Model of a PumpITurbine," *Proc. Symp. on Pump Turbine Schemes*, Amer. Soc. of Mech. Engrs., June, pp. 113-115.
- Sprecher, J., 1951, "The Hydraulic Power Storage Pumps of the Etzel Hydro-Electric Power Scheme," *Sulzer Technical Review*, No.3, pp. 1-14.
- Stepanoff, A. J., 1957, *Centrifugal and Axial Flow Pumps*, John Wiley & Sons, New York, NY.
- Stephenson, D., 1976, *Pipeline Design for Water Engineers*, Elsevier Scientific Publishing Co., Amsterdam, The Netherlands, p. 58.
- Streeter, V. L., 1964, "Waterhammer Analysis of Pipelines," *Jour. Hydraulics Div.*, Amer. Soc. of Civ. Engrs., July, pp. 151-171.
- Suter, P., 1966, "Representation of Pump Characteristics for Calculation of Waterhammer," *Sulzer Technical Review*, No. 66, pp. 45-48.
- Swanson, W. M., 1953, "Complete Characteristic Circle Diagrams for Turbo-Machinery," *Trans. Amer. Soc. of Mech. Engrs.*, vol. 75, pp. 819-826.
- Thoma, D., 1931, "Vorgange beim Ausfallen des Antriebes von Kreiselpumpen," *Mitteilungen des Hydraulischen Instituts der Technischen Hochschule Munchen*, vol. 4, pp. 102-104.
- Thomas, G., 1972, "Determination of Pump Characteristics for a Computerized Transient Analysis," *Proc. First International Conf. on Pressure Surges*, British Hydromechanics Research Assoc. Canterbury, England, Sept., pp. A3-21-A3-32.
- Tognola, S., 1960, "Further Development of High Head Storage Pumps," *Escher-Wyss News*, vol. 33, Nos. 1-3, pp. 58-66.
- Tsukamoto, H. and Ohashi, H., 1981, "Transient Characteristics of a Centrifugal Pump During Starting Period," *Paper No. 81-WA/FE-16*, presented at Winter Annual Meeting, Amer. Soc. Mech. Engrs., Nov.
- Winks, R. W., 1977, "One-Third Scale Air-Water Pump Test Program and Performance," EPRI NP-135, July.
- Wylie, E. B. and Streeter, V. L., 1981, *Fluid Transients*, FEB Publishers, Ann Arbor, Mich.

### Additional References

- Cooper, P., 1982, "Performance of a Vertical Circulating Pump in the Turbine Mode," *Symp. on Small Hydro Power Fluid Machines*, Amer. Soc. Mech. Engrs., Phoenix, Nov.
- Donsky, B., , Byrne, R. M., , and Barlett, P. E., 1979, "Upsurge and Speed-Rise Charts Due to Pump Shutdown," *Jour. Hydraulics Div.*, Amer. Soc. Civ. Engrs., vol. 105, HY6, June, pp. 661-674.
- Jaeger, C., 1959, *Engineering Fluid Mechanics*, Blackie and Sons, London, UK.

- Jaeger, C., 1959, "Waterhammer Caused by Pumps," *Water Power*, London, July, pp. 259-266.
- Kinno, H. and Kennedy, J. F., 1965, "Waterhammer Charts for Centrifugal Pump Systems," *Jour. Hydraulics Div.*, Amer. Soc. Civ. Engrs., vol. 91, pp. 247-270.
- Koelle, E. and Chaudhry, M. H. (eds.), 1982, *Proc. International Seminar on Hydraulic Transients* (in English with Portuguese translation), vols. 1-3, Sao Paulo, Brazil.
- Kovats, A., 1970, "Fluid Transient Conditions in Condenser Cooling Water Systems," *Paper 70-WA/FE 25*, Amer. Soc. Mech. Engrs.
- Linton, P., 1950, "Pressure Surges on Starting Pumps with Empty Delivery Pipes," British Hydromechanic Research Assoc., TN402.
- Miyashiro, H., 1962, "Waterhammer Analysis of Pumps in Parallel Operation," *Bull.*, Japan Soc. of Mech. Engrs., vol. 5, no. 19, pp. 479-484.
- Miyashiro, H., 1963, "Water Level Oscillations in a Surge Tank When Starting a Pump in a Pumped Storage Power Station," *Proc.*, International Assoc. for Hydraulic Research, London, pp. 133-140.
- Parmakian, J., 1953, "Pressure Surges at Large Pump Installations," *Trans.*, Amer. Soc. of Mech. Engrs., vol. 75, Aug., pp. 995-1006.
- Parmakian J., 1953, "Pressure Surge Control at Tracy Pumping Plant," *Proc.* Amer. Soc. of Civil Engrs., vol. 79, Separate no. 361, Dec.
- Paynter, H. M. and Free, J. G., 1966, "Discussion of Water-Hammer Charts for Centrifugal Pump System, by Kinno and Kennedy," *Jour. Hydraulics Div.*, Amer. Soc. Civ. Engrs., vol. 92, March, pp. 379-382.
- Rich, G. R., 1951, *Hydraulic Transients*, McGraw-Hili Book Co., New York.
- Ritter, H. K. and Rohling, T. A., 1972, "Starting Large Custom Pumps Against Reverse Flow," *Allis-Chalmers Engineering Review*, vol. 37, no. 2.
- Schnyder, O., 1937, "Comparison Between Calculated and Test Results on Waterhammer in Pumping Plant," *Trans.*, Amer. Soc. of Mech. Engrs., vol. 59, pp. 695-700.

## TRANSIENTS IN HYDROELECTRIC POWER PLANTS



**Castaic Powerplant with six pump turbines (65 m<sup>3</sup>/s pumping, 98.3 m<sup>3</sup>/s generating) and one Pelton (22.7 m<sup>3</sup>/s), 328.6 m static head, 732 m long penstocks varying in diameter from 4.1 to 2.7 m, and a 36.6 m dia 116.7 high surge tank.** (Courtesy, S. Loghmanpour, California Department of Water Resources.)

## 5-1 Introduction

Various turbine operations, such as start-up, shut-down, load acceptance and rejection, produce transients in hydroelectric power plants. This chapter deals with the analysis of these transients. In this analysis, the conduits and related boundaries may be simulated utilizing the computational procedures and boundary conditions presented in Chapter 3. For a hydraulic turbine, however, special boundary conditions are needed to account for the inter-dependance of turbine head, discharge, rotational speed and gate opening. The inclusion of the governor for a turbine under governor control adds another complexity to the boundary.

The rotational speed of a turbo-generator remains constant if it is connected to a large grid. The boundary conditions for a reaction turbine operating at constant speed and at constant gate opening derived in Chapter 3 may be used in this case. However, if the unit is isolated, then the speed changes during transients caused by various turbine operations have to be included in the boundary condition.

In this chapter, typical layouts of hydroelectric power plants are first presented. Details of the mathematical simulation of the conduit system, turbo-generator, and governor are then outlined. Various turbine operations that produce transients in the water passages of a power plant are discussed. Prototype test results used to verify the mathematical model are then presented, followed by a discussion of the governing stability of hydro-turbines, and the selection of generator inertia and optimum governor settings. The chapter concludes with the case study of the governing stability studies carried out for a 500-MW hydroelectric power plant.

## 5-2 Hydroelectric Power Plant

Typical hydropower-plant layouts are shown in [Figure 5-1](#). An upstream conduit conveys water from the upstream reservoir, lake, or canal, to the turbine and the turbine outflow is carried downstream through the tailrace conduits. A generator is mechanically coupled to the turbine, and the electrical output is carried by transmission lines to the load centers. A governor is provided to keep system frequency constant by opening or closing the wicket gates as the turbine speed changes.

The components of a mathematical model for the analysis of transients in a hydroelectric power plant are:

- Upstream and downstream water conduits, including any surge tanks;
- Turbine and generator; and
- Governor.

Details of the simulation of these components are presented in the following sections.

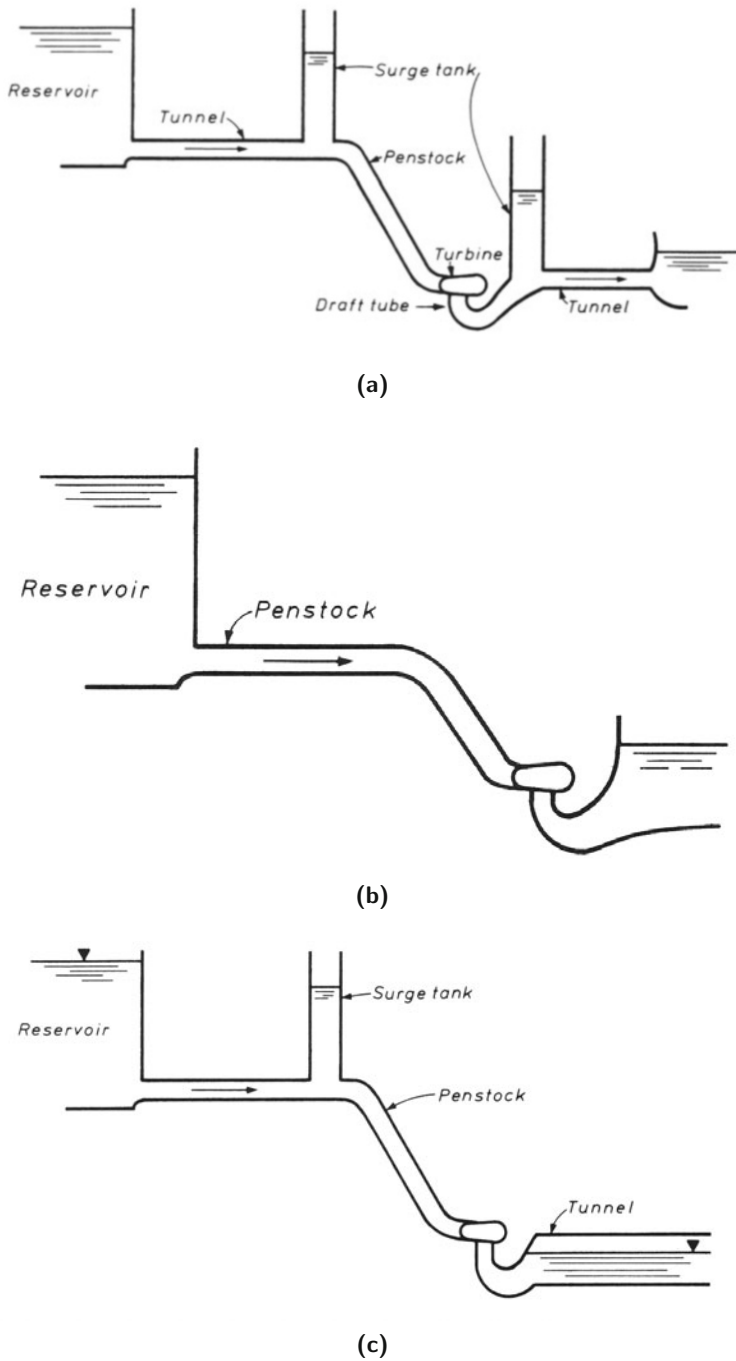
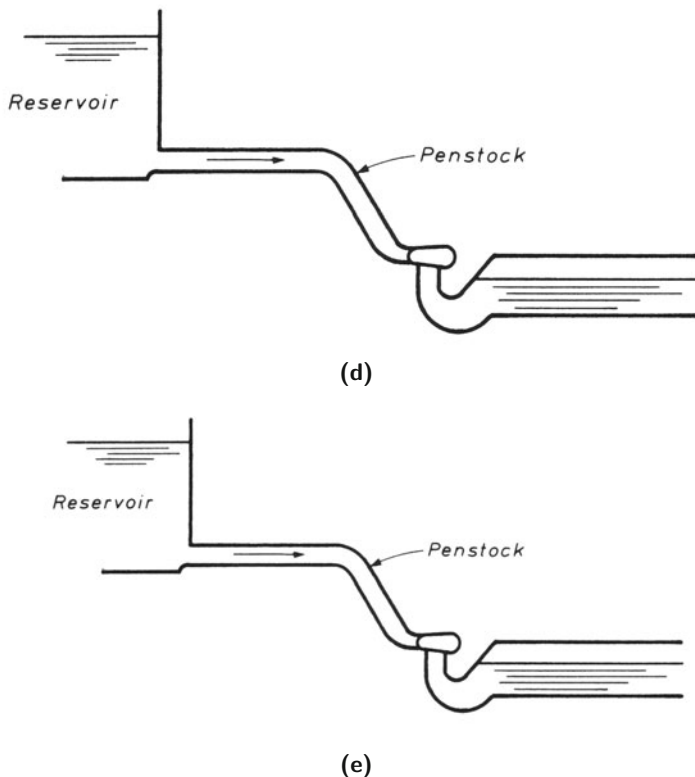


Fig. 5-1. Typical hydroelectric power plant layouts.



**Fig. 5-1. (Continued)**

### 5-3 Conduit System

As shown in Fig. 5-1, water is conveyed from the upstream reservoir or canal to the turbine scroll case through a tunnel and/or a penstock, and the outflow from the turbine is discharged through the draft tube to the downstream water passages. These passages may consist of a free-surface flow tunnel, a pressurized conduit, a tailrace canal, a river, or a downstream reservoir. Depending upon the length of conduits, surge tanks may be provided to control the maximum and minimum pressures and for regulation and governing stability.

The method of characteristics and the boundary conditions presented in Chapters 3 and 10 are used to simulate the upstream and downstream conduits and other boundaries. Tailrace system comprising of a free-surface-flow tunnel,

a canal, or a short draft tube and a short pressurized conduit may be neglected to simplify the analysis.

Boundary conditions for a turbine are developed in the following section.

## 5-4 Hydraulic Turbine

The relationship between the net head and discharge is specified to develop the turbine boundary conditions (Net head = Pressure head at turbine inlet + velocity head – pressure head at the downstream end of the draft tube). The flow through an impulse turbine depends on the pressure head and the nozzle opening. The boundary condition for a valve developed in Chapter 3 may be used for simulating this type of turbine. However, the flow through a Francis turbine depends upon the net head, rotational speed of the turbine, and wicket-gate opening, while the flow through a Kaplan turbine depends upon these variables as well as the runner-blade angle. Special boundary conditions for a Francis turbine are developed in this section.

### Turbine Characteristics

The curves between different turbine parameters — net head, discharge, power output, rotational speed, gate opening, runner blade angle — are called turbine characteristics. Limited information is available for the transient-state turbine characteristics [Krivehenko et al. 1971]. Therefore, turbine characteristics, based on the steady-state model tests, are assumed to be valid during the transient state. As shown by Perkins et al. [1964], this appears to be a valid assumption.

The data for turbine flow and power output, obtained from the steady model tests, are presented in a graphical form, known as *hill charts* (Fig. 5-2). The prototype efficiency is usually higher than that determined from model tests because of scale effects. Therefore, prototype output is computed by stepping up the model efficiency. Of the several empirical formulas available for this, Moody formula [Streeter, 1966] is widely used.

Usually no characteristics data are available for small wicket-gate openings. Therefore, the characteristic curves are extrapolated to cover this range. To do this, the flow for zero turbine rotational speed, and the windage and friction losses for wicket-gate openings less than the speed-no-load gate (SNL) should be known. SNL gate is the lowest gate opening at which turbine rotates at synchronous speed with zero output.

Typical characteristics for a Francis turbine provided by the turbine manufacturer are shown in Fig. 5-3. In this figure, the abscissa is the unit speed,  $\phi$ , and the ordinates are the unit flow,  $q$ , and the unit power,  $p$ . The expressions for  $\phi$ ,  $p$ , and  $q$  are given in Table 5-1, in which  $D$  = diameter of the runner;  $N$  = rotational speed;  $H_n$  = net head;  $Q$  = turbine discharge; and  $P$  = power output. In the English units,  $D$  and  $H_n$  are expressed in ft,  $N$  in rpm,  $Q$  in

$\text{ft}^3/\text{sec}$ , and  $P$  in hp. In the SI units,  $H_n$  and  $D$  are in m,  $N$  in rpm,  $P$  in kW, and  $Q$  in  $\text{m}^3/\text{s}$ .

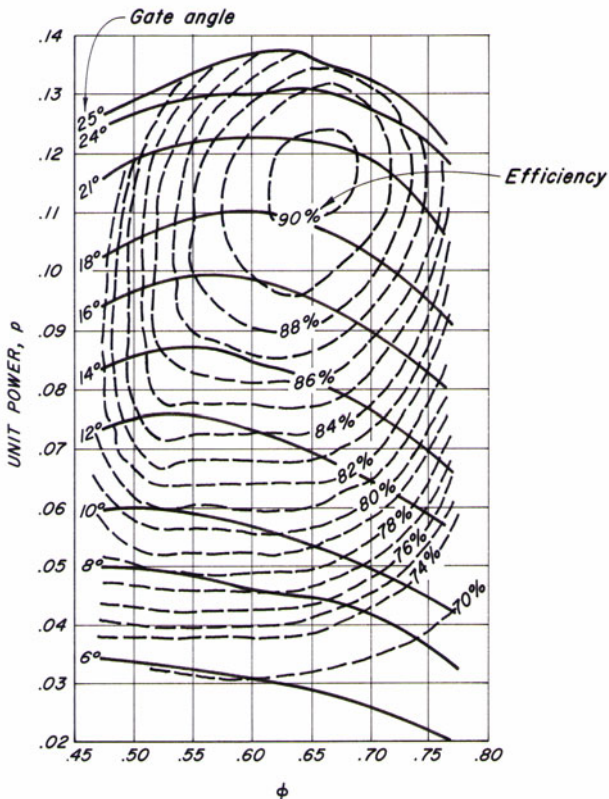
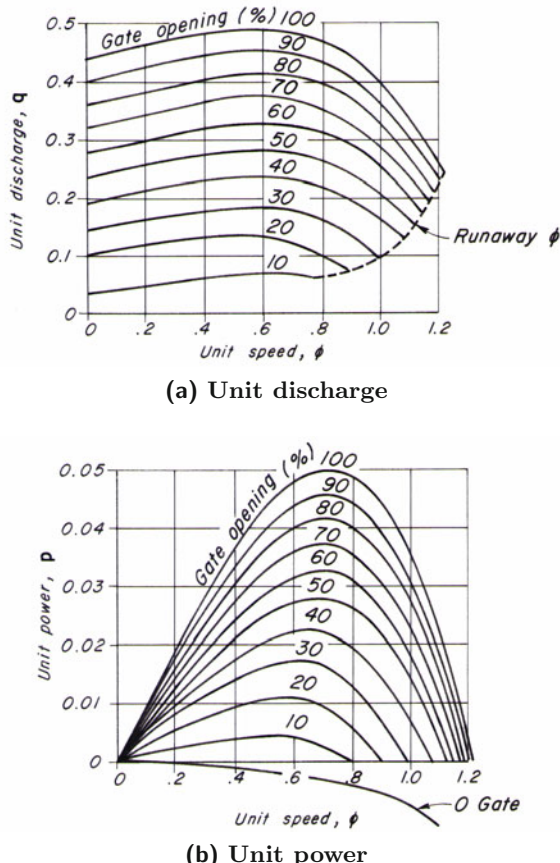


Fig. 5-2. Hill chart for a Francis turbine (in ft-lb-sec units).

At SNL gate, the turbine output is equal to the turbogenerator windage and friction losses at the synchronous speed. Therefore, if the wicket gates are kept open at the SNL gate opening, the unit rotates at the synchronous speed, and the net turbine output is zero. The abscissa axis on the unit power curves (Fig. 5-3b) represents the conditions at SNL gate. It is clear from this figure that the SNL gate varies with the net head. To keep the unit running at the synchronous speed when the wicket gates are open less than the SNL gate opening, power is supplied to the unit from an outside source because the windage and friction losses are greater than the turbine output. This is called *motoring* of the unit.

During steady-state model tests, unit speed does not exceed the runaway speed for a particular net head and gate opening. Therefore, model data are not available for  $\phi$  greater than  $\phi_{run}$  at runaway conditions ( $\phi_{run}$ ). However, during the transient state, the prototype speed may exceed the runaway speed for a short period. To account for this, the curves are extended for  $\phi$  values greater than  $\phi_{run}$  assuming that they follow the same trend as that for  $\phi$  values less than  $\phi_{run}$ .



**Fig. 5-3.** Francis turbine characteristics (in ft-lb-sec units).

The boundary conditions for a Francis turbine [Chaudhry and Portfors, 1973] are derived in this section. For a Kaplan turbine, the variation of the turbine characteristics with the runner-blade angle have to be included in the boundary conditions unless the blade movement is blocked under governor

**Table 5-1.** Definition of unit values

|        | English<br>Units              | SI Units                     |
|--------|-------------------------------|------------------------------|
| $\phi$ | $\frac{DN}{153.16\sqrt{H_n}}$ | $\frac{DN}{84.59\sqrt{H_n}}$ |
| $q$    | $\frac{Q}{D^2\sqrt{H_n}}$     | $\frac{Q}{D^2\sqrt{H_n}}$    |
| $p$    | $\frac{P}{(D^2H_n^{3/2})}$    | $\frac{P}{D^2H_n^{3/2}}$     |

control following load rejection. For a Pelton turbine, however, the boundary conditions for a valve developed in Chapter 3 may be used.

### Turbine Boundary Condition

Now, let us discuss the inclusion of turbine characteristics in the turbine boundary conditions. The unit discharge,  $q$ , and unit power,  $p$ , on the characteristic curves for various gate openings at an equally spaced grid of  $\phi$  are stored in the computer and then  $q$  and  $p$  at the intermediate gate openings are determined by interpolation.

Referring to Fig. 5-4

$$H_P = H_n + H_{tail} - \frac{Q_P^2}{2gA^2} \quad (5-1)$$

in which  $H_P$  = instantaneous piezometric head at the scroll-case entrance;  $H_n$  = instantaneous net head;  $H_{tail}$  = tailwater level above datum;  $Q_P$  = instantaneous flow at the scroll case entrance; and  $A$  = cross-sectional area of the pressure conduit at the turbine inlet. Note that, for computing the net head, the velocity head at the draft-tube exit is neglected in Eq. 5-1. This is usually a valid assumption since the exit-velocity head is negligible. However, if the velocity head is not small as compared to  $H_n$ , it should be included in the analysis.

Let us assume the transient conditions have been computed until time,  $t_o$  (beginning of time interval) and we want to determine their values at time  $t_o + \Delta t$  (end of the time interval). Thus, the piezometric head,  $H$ , turbine flow,  $Q$ , turbine speed,  $N$ , and wicket-gate opening,  $\tau$ , are known at  $t_o$  and we want to determine their values at  $t_o + \Delta t$ . Let us designate these unknown variables by  $H_P$ ,  $Q_P$ ,  $N_P$ , and  $\tau_P$ , respectively, and the net head at the end of the time step by  $H_{nP}$ . For a general boundary condition, let us consider the turbine is under governor control. Therefore,  $\tau_P$  is also unknown. However, if

the time variation of wicket-gate opening or closing is specified in the form of a curve or a table, then  $\tau_P$  may be determined from this specified data.

Four unknown variables, namely  $Q_P$ ,  $H_P$ ,  $\tau_P$ , and  $N_P$ , may be determined by the following iterative procedure. Because the transient-state turbine speed and gate opening vary gradually, their values at the end of the time step may be estimated, as a first approximation, by parabolic extrapolation from the computed results for the previous time intervals. To determine the range of  $\phi$  for the segment of the turbine characteristics to be used during the time step,  $Q_P$  is first extrapolated, and  $H_P$  is determined from the characteristic equation, and  $H_n$  is then computed from Eq. 5-1. Let the values of  $\tau_P$  and  $N_P$  estimated by extrapolation be  $\tau_e$  and  $N_e$ , the estimated value of  $H_n$  computed by using the above procedure be  $H_{n_e}$ , and  $\phi$  computed from the expression given in Table 5-1 by using these estimated values be  $\phi_e$ . Now, we may search the stored turbine characteristic data to determine the grid values  $\phi_1$  and  $\phi_2$  such that  $\phi_1 < \phi_e < \phi_2$ . The turbine characteristic curve for the gate opening  $\tau_e$  between  $\phi_1$  and  $\phi_2$  may be approximated by the straight line  $EF$ , as shown in Fig. 5-5. The value at  $E$  is interpolated from the known values at the grid points  $A$  and  $B$ , and the value at  $F$  is interpolated from the known values at points  $C$  and  $D$ .

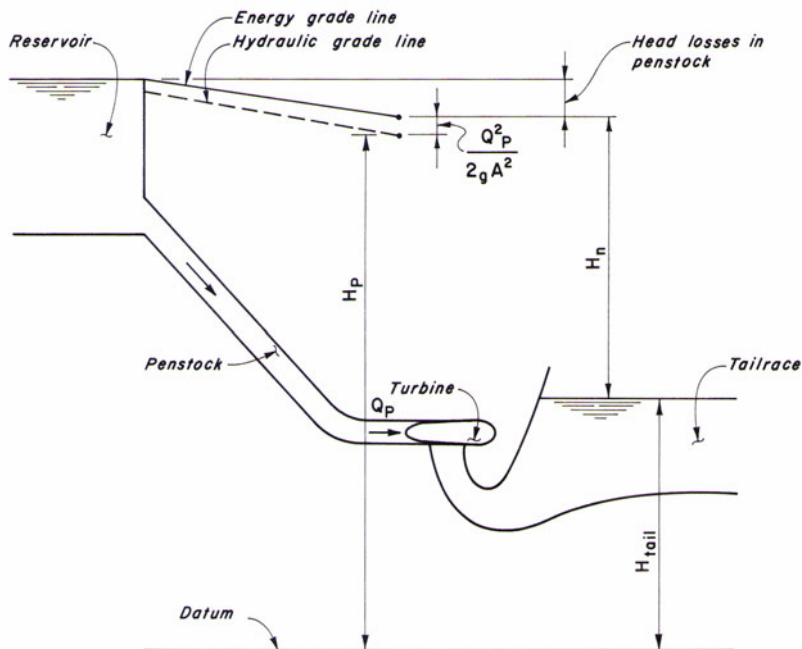
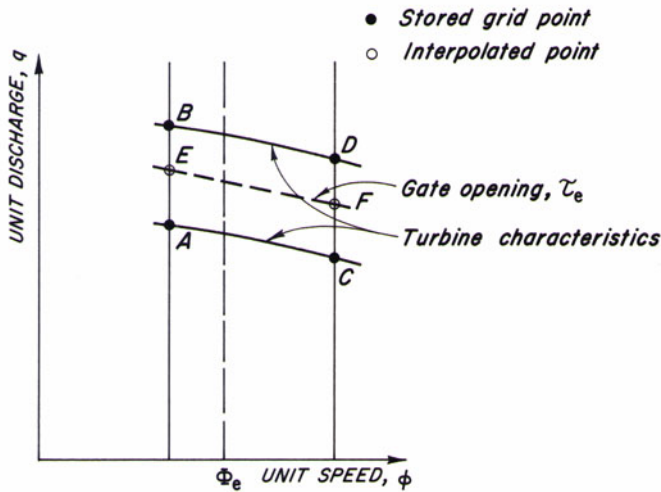


Fig. 5-4. Notation for boundary conditions for a Francis turbine.



**Fig. 5-5.** Interpolation of turbine characteristics.

The equation of straight line  $EF$  may be written as

$$q = a_o + a_1\phi \quad (5-2)$$

in which  $a_o$  and  $a_1$  are determined from the known coordinates of  $E$  and  $F$ .

Substituting the expressions for  $q$  and  $\phi$  in the SI units ([Table 5-1](#)) into Eq. 5-2 and simplifying

$$a_2 H_{nP}^{1/2} = Q_P - a_3 \quad (5-3)$$

in which  $a_2 = a_o D^2$  and  $a_3 = N_e D^3 a_1 / 84.59$ . In the English units,  $a_2 = a_o D^2$ , and  $a_3 = N_e D^3 a_1 / 153.16$ .

Combining Eqs. 3-17 and 5-1,

$$Q_P = (C_p - C_a H_{tail}) + \frac{C_a Q_P^2}{2gA^2} - C_a H_{nP} \quad (5-4)$$

Squaring both sides of Eq. 5-3, eliminating  $H_{nP}$  from the resulting equation and Eq. 5-4, and simplifying,

$$a_4 Q_P^2 + a_5 Q_P + a_6 = 0 \quad (5-5)$$

in which

$$a_4 = \frac{C_a}{2gA^2} - \frac{C_a}{a_2^2} \quad (5-6)$$

$$a_5 = \frac{2a_3 C_a}{a_2^2} - 1 \quad (5-7)$$

$$a_6 = C_p - C_a H_{tail} - \frac{C_a a_3^2}{a_2^2} \quad (5-8)$$

Solution of Eq. 5-5 yields

$$Q_P = \frac{-a_5 - \sqrt{a_5^2 - 4a_4 a_6}}{2a_4} \quad (5-9)$$

Note that the positive sign with the radical term is neglected. Now  $H_{nP}$  is determined from Eq. 5-3 and  $H_P$ , from Eq. 5-1.

Because of the instantaneous unbalanced torque,  $T_u = T_{tur} - T_{gen}$ , the variation of the speed of the turbogenerator-set is given by the equation

$$T_u = I \frac{d\omega}{dt} \quad (5-10)$$

or

$$T_{tur} - T_{gen} = I \frac{2\pi}{60} \frac{dN}{dt} \quad (5-11)$$

in which  $T_{tur}$  = instantaneous turbine torque;  $T_{gen}$  = instantaneous generator torque;  $\omega$  = rotational speed of the turbogenerator, in rad/s;  $N$  = rotational speed, in rpm; and  $I$  = total polar moment of inertia of the turbine and generator, in kg m<sup>2</sup>. (In the English units, replace  $I$  in Eqs. 5-10 and 5-11 by  $WR^2/g$ , in which the moment of inertia  $WR^2$  is in lb-ft<sup>2</sup>.)

For a resistive load, Eq. 5-11 may be written as

$$P_{tur} - \frac{P_{gen}}{\eta_{gen}} = \left( \frac{2\pi}{60} \right)^2 \times 10^{-3} I N \frac{dN}{dt} \quad (5-12)$$

in which  $\eta_{gen}$  = generator efficiency,  $P_{gen}$  = generator load, and  $P_{tur}$  = power developed by the turbine, both in kW.

Integrating both sides of Eq. 5-12,

$$\int_{t_1}^{t_P} \left( P_{tur} - \frac{P_{gen}}{\eta_{gen}} \right) dt = 1.097 \times 10^{-5} I \int_{N_1}^{N_P} N dN \quad (5-13)$$

Simplifying and replacing the generator load by its average value during the time step, we obtain

$$\left( \frac{P_{tur_1} + P_{tur_P}}{2} - \frac{P_{gen_1} + P_{gen_P}}{2\eta_{gen}} \right) \Delta t = 0.548 \times 10^{-5} I (N_P^2 - N_1^2) \quad (5-14)$$

in which subscripts 1 and  $P$  indicate the values of the variables at the beginning and at the end of time step. (In the English units, the moment of inertia

is in lb-ft<sup>2</sup> and both  $P_{tur}$  and  $P_{gen}$  are in horsepower. In this case, replace  $I$  of Eq. 5-12 by  $WR^2/g$ ; divide the right-hand side of Eq. 5-12 by 550, and replace  $1.097 \times 10^{-5}$  of Eq. 5-13 and  $0.548 \times 10^{-5}$  of Eq. 5-14 by  $0.619 \times 10^{-6}$  and  $0.3096 \times 10^{-6}$ , respectively.)

Solving for  $N_P$ , we obtain

$$N_P = \left\{ N_1^2 + 0.182 \times 10^6 \frac{\Delta t}{I} \left[ 0.5 (P_{tur_1} + P_{tur_P}) - \frac{0.5}{\eta_{gen}} (P_{gen_1} + P_{gen_P}) \right] \right\}^{0.5} \quad (5-15)$$

Eqs. 5-14 and 5-15 are for a gradual variation of the generator load. For a step change in the generator load, Eq. 5-15 is simplified as

$$N_P = \left\{ N_1^2 + 0.182 \times 10^6 \frac{\Delta t}{I} \left[ 0.5 (P_{tur_1} + P_{tur_P}) - \frac{P_{gen_f}}{\eta_{gen}} \right] \right\}^{0.5} \quad (5-16)$$

in which  $P_{gen_f}$  = final generator load. If the moment of inertia is in lb-ft<sup>2</sup>, and  $P_{tur}$  and  $P_{gen}$  are both in hp, then replace 0.182 in Eqs. 5-15 and 5-16 by 3.23.

A computational procedure for using Eqs. 5-9 and 5-16 is presented later in Section 5-6.

## 5-5 Hydraulic Turbine Governor

To keep the frequency of generated power constant, the rotational speed of the turbo-generator set should be same as the synchronous or reference speed. However, the turbine rotational speed changes following a change in the generator load. To minimize the amplitude and duration of the deviation of the turbine speed from the reference speed, an hydraulic governor is provided which opens the wicket gates if the speed drops and closes the gates if the speed rises above the reference speed.

In this section, we discuss various components of a hydraulic governor, terminology, types of governors and their operations. Then, equations are presented to introduce the basic concepts of feedback control and stability, followed by the block diagram and governing equations for a dashpot governor.

### Components

The main components of a governor are a speed-sensing device and a servomechanism for opening or closing the wicket gates. For speed-sensing, various mechanical and electrical devices have been used. Of the mechanical devices, a centrifugal ballhead in various configurations has been popular because of its simplicity, sensitivity, and ruggedness. The electrical speed sensors include a dc generator with permanent magnetic field, a permanent magnet alternator, a permanent magnet alternator feeding into a frequency-sensitive

network, and a speed-signal generator. The output of these speed sensors is the deviation from the reference speed. This output is usually small and is amplified by means of pilot and distributing valves before feeding it into the servomechanism for opening or closing the wicket gates. Since a large force is required to move the wicket gates, a hydraulic servo is provided for this purpose.

### Terminology

*Effective gate opening and closing times* are defined as twice the time taken by the wicket gates to open or close between 25 and 75 percent openings.

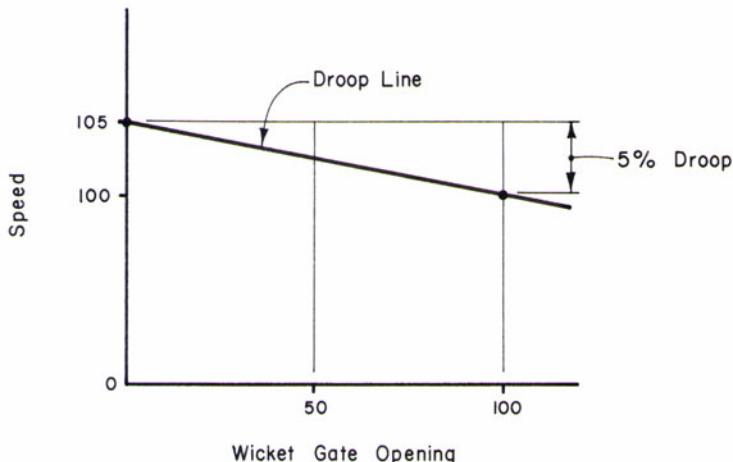


Fig. 5-6. Speed droop.

The *speed droop* is a governor characteristic [Anonymous, 1973] that requires a decrease in the turbine speed to produce an increase in the turbine gate opening (Fig. 5-6), i.e.,

$$\text{Droop} = \frac{-\Delta n}{\Delta \tau} \times 100 \quad (5-17)$$

in which  $n$  = relative turbine speed =  $N/N_r$ ,  $N_r$  = reference or synchronous speed,  $\tau$  = relative gate opening =  $G/G_r$ ,  $G$  = gate opening,  $G_r$  = reference gate opening, and  $\Delta$  indicates change in these variables.

Speed droop may be classified as permanent or temporary. *Permanent speed droop* is the speed droop that remains in the steady state after the decay action of the damping device has been completed [Anonymous, 1977].

This droop, also called *primary compensation*, is used to share the load on units operating in parallel. It is usually about 5 percent.

The permanent droop is not sufficient [Hovey, 1960] on hydraulic turbines to stabilize the system because of large inertia of water in the water passages. Therefore, a *temporary speed droop*, also called *secondary compensation*, is provided. This is the droop that would occur if the decay action of the damping device were blocked and the permanent speed droop were made inactive.

**Dashpot Time Constant.** The dashpot characteristic is such that if the turbine gate is suddenly opened, then point A (Fig. 5-7) moves up proportional to the gate movement and then moves down at an exponential rate that is a function of the spring constant and of the needle valve opening.

Let  $y$  = normalized distance of point A from the equilibrium position. Then the differential equation for the motion of point A is

$$\frac{dy}{dt} = -ky \quad (5-18)$$

in which  $k$  is a constant. Integrating Eq. 5-18 and noting that  $y = 1$  when  $t = 0$ , we obtain

$$\ln y = -kt$$

or

$$y = e^{-kt} \quad (5-19)$$

in which  $e$  = base of natural logarithms. The exponential decay of  $y$  is shown

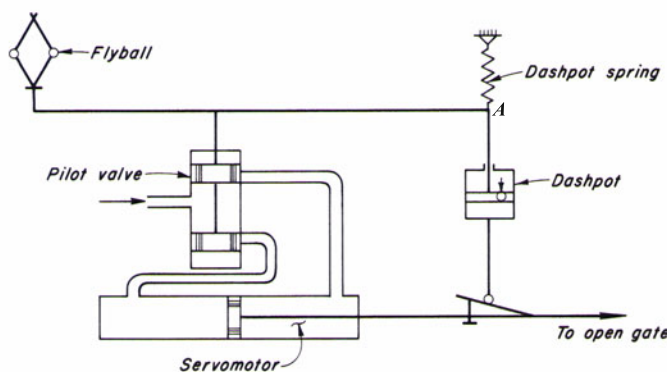
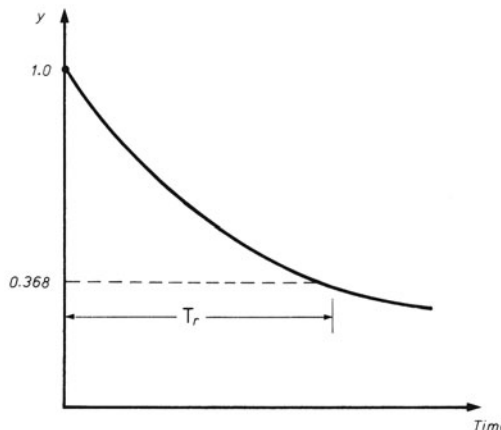


Fig. 5-7. Dashpot governor (permanent speed droop not shown).

in Fig. 5-8. The *dashpot time constant*,  $T_r$ , is defined as the time required for  $y$  to decrease from 1 to  $1/e = 0.368$ .



**Fig. 5-8.** Definition sketch for dashpot time constant.

## Types

Based on the criteria for the corrective action, a hydraulic governor may be classified as:

- Temporary-droop governor;
- Accelerometric governor; and
- Proportional-integral-derivative (PID) governor.

The corrective action of a temporary-droop governor is proportional to the speed deviation,  $n$ , and its integral with time; it is proportional to  $dn/dt$  for an accelerometric governor, and it is proportional to  $n$ ,  $dn/dt$ , and the integral of the speed deviation with time for a PID governor. In the past, temporary-droop governors were used mainly in North America and accelerometric governors, mainly in Europe. The PID governors were introduced in the early seventies. These are now used extensively all over the globe in new hydropower plants, and in rehabilitated projects and redevelopments.

## Operation

Figure 5-7 shows the schematic diagram of a dashpot governor. For simplicity, the permanent droop is not shown. The following description of events after a load increase should help in understanding the governor operation.

Following an increase in load, the turbine speed decreases, and the flyballs move inward. This displaces the piston of the pilot valve downwards, admitting oil into the hydraulic servo that opens the wicket gates. As a result of the wicket-gate movement, the dashpot spring is compressed, which changes the position of the pilot valve. Because of oil flow at a slow rate through the small

orifice in the dashpot, the dashpot spring returns to its original position after some time, even though the servo and the wicket gates are now at different positions.

### Stability

To illustrate the stabilizing influence of speed droop, let us first consider a very simple hydraulic governor in which the gates are opened or closed, depending upon the speed deviation [Chaudhry, 1979]. A block diagram for this governor is shown in Fig. 5-9. In this figure, the transfer function listed in the block is the relationship between the input and output variables, and the Laplace variable,  $s$ , is equivalent to time derivative  $d/dt$  if the initial conditions are zero [D'Azzo and Houpis, 1966; Lathi, 1965]. To simplify the analysis, let us neglect changes due to waterhammer in the water passages.

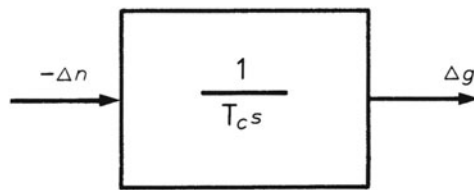


**Fig. 5-9.** Block diagram of a simple governor.

Referring to Fig. 5-9, an equation for this governor may be written as

$$T_c \frac{d(\Delta g)}{dt} + \Delta n = 0 \quad (5-20)$$

in which  $T_c$  = gate closing time,  $\Delta g$  = relative wicket gate deviation =  $(G - G_o)/G_o$ ,  $G$  = instantaneous wicket gate opening,  $G_o$  = reference wicket gate opening,  $\Delta n$  = relative speed deviation =  $(N - N_r)/N_r$ ,  $N$  = instantaneous rotational speed, and  $N_r$  = synchronous speed.

The equation for machine acceleration is

$$T_m \frac{d(\Delta n)}{dt} = \Delta g - \Delta m \quad (5-21)$$

in which  $T_m$  = mechanical starting time, which is a function of the moment of inertia, synchronous speed, and rated output of the turbogenerator set (an expression for  $T_m$  is derived in Section 5-8),  $\Delta m$  = relative load-torque change

$= \Delta M/M_o$ ,  $\Delta M$  = step load-torque change (negative for load rejection), and  $M_o$  = reference load torque.

Elimination of  $\Delta g$  from Eqs. 5-20 and 5-21 yields

$$\frac{d^2\Delta n}{dt^2} + \frac{\Delta n}{T_c T_m} = 0 \quad (5-22)$$

A general solution of Eq. 5-22 may be written as

$$\Delta n = A \sin \frac{t}{\sqrt{T_c T_m}} + B \cos \frac{t}{\sqrt{T_c T_m}} \quad (5-23)$$

in which  $A$  and  $B$  are arbitrary constants. This equation describes a simple harmonic motion. Hence, such a governor is unsuitable for practical applications.

Now, let us add a feedback, as shown in Fig. 5-10. This feedback represents the permanent speed droop,  $\sigma$ . Referring to Fig. 5-10, the equation for this governor may be written as

$$\frac{d\Delta g}{dt} = -\frac{1}{T_c} (\Delta n + \sigma \Delta g) \quad (5-24)$$

Elimination of  $\Delta g$  from Eqs. 5-21 and 5-24 yields

$$\frac{d^2\Delta n}{dt^2} + \frac{\sigma}{T_c} \frac{d\Delta n}{dt} + \frac{1}{T_c T_m} \Delta n = -\frac{\sigma \Delta m}{T_c T_m} \quad (5-25)$$

This equation describes a damped simple harmonic motion, with the degree of damping depending upon  $\sigma/T_c$ . Also, note that because of the term  $(\sigma \Delta m) / (T_c T_m)$  on the right-hand side of Eq. 5-25, the final steady-state turbine speed is different from the initial steady-state reference speed  $N_r$ . Therefore, for such a governor, the speed has to be manually adjusted back to the reference speed. Proceeding similarly, it can be shown that the damping rate for a temporary-droop governor is higher, and that the final steady-state speed settles down to the reference speed, i.e., synchronous speed.

## Governing Equations

The governing equations for different components of a governor may be written based on its block diagram [D'Azzo and Houpis, 1966; Lathi, 1965 and Chaudhry, 1980] which is provided by the governor manufacturer along with the values of different time constants. The equations for a dashpot governor are derived in this section; proceeding similarly, equations for other types of governors may be derived (see Problem 5-3 for a PID governor).

Figure 5-11 shows the block diagram for a dashpot governor in which conventional notation of control systems is used. In this notation, a block represents a component of the governor; the input and output of a block are

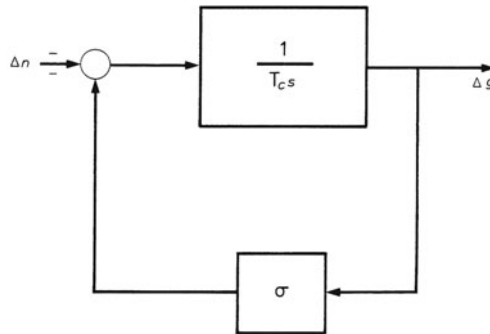


**Fig. 5-10.** Block diagram for a governor with permanent droop.

shown by means of arrows, and the transfer functions are listed in the blocks to show the relationship between the input and output of various components. The output of a summer, shown by a circle in the block diagram along with the positive and negative signs marked with each input, is determined by an algebraic sum of all the input signals.

The variables of the block diagram of Fig. 5-11 are as follows with a typical range listed in parentheses:  $T_a$  = actuator time constant (0.05 to 0.1 s);  $T_r$  = dashpot time constant;  $\delta$  = temporary speed droop;  $\sigma$  = permanent speed droop (0.03 to 0.05);  $T_d$  = distributing valve time constant (0.05 to 0.1 s);  $k_d$  = distributing valve gain (10 to 15);  $k_s$  = gate-servomotor gain (0.2); and  $e_{t_{max}}$  = dashpot saturation limit (0.2 to 0.5). The values of  $T_r$  and  $\delta$  are selected so that the speed oscillations are stable following a load change.

The synchronous speed of the turbogenerator set,  $N_r$ , is used as a reference speed to normalize the turbine speed, i.e.,  $n = N/N_r$ . If  $\tau_o$  = initial steady-state wicket-gate opening, then  $n_{ref} = 1.0 + \sigma\tau_o$ . The outputs of various governor components and their saturation limits are shown in Fig. 5-11. The optimum values of  $\delta$  and  $T_r$  for a power plant may be determined by using the procedures outlined in Section 5-9.

Now, let us write the equations for different components of the governor. The transfer function of the component is first listed from which the equation for the component is then derived. The saturation limits, where appropriate, are also included.

### Actuator

$$v_a = \frac{1}{T_a s} e$$

or

$$e = T_a \frac{dv_a}{dt} \quad 0 \leq v_a \leq 1.0 \quad (5-26)$$

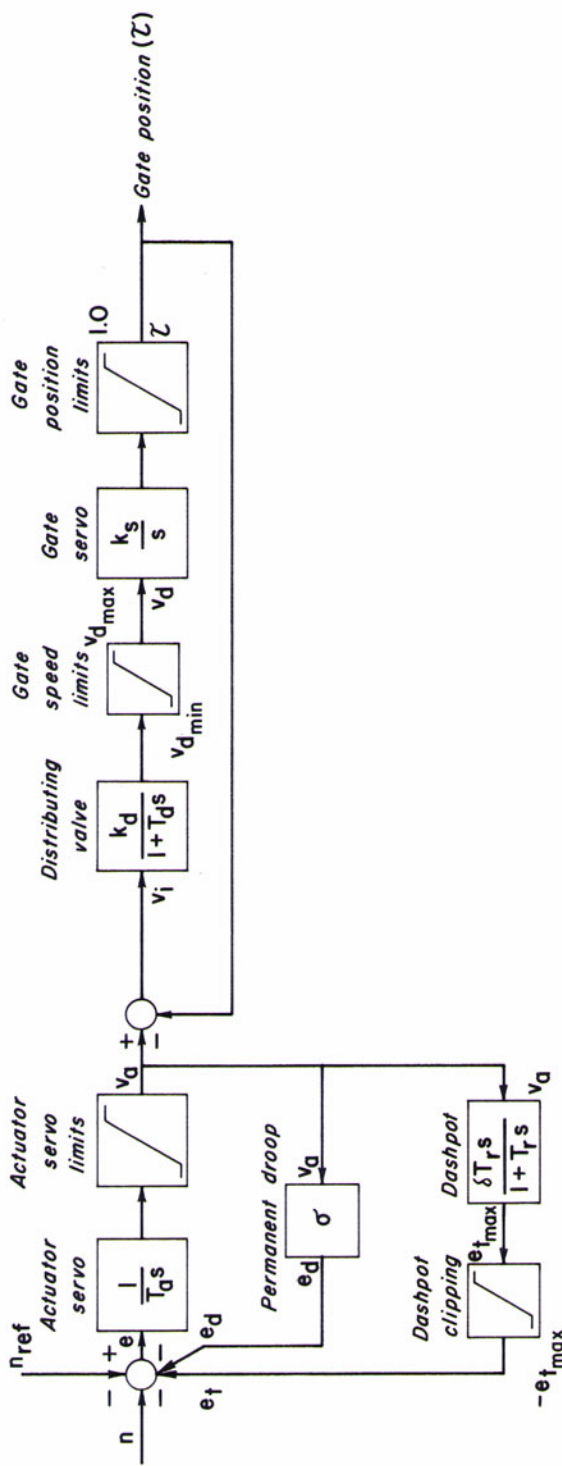


Fig. 5-11. Block diagram of a dashpot governor.

**Dashpot**

$$e_t = \frac{\delta T_r s}{1 + T_r s} v_a$$

or

$$e_t + T_r \frac{de_t}{dt} - \delta T_r \frac{dv_a}{dt} = 0 \quad -e_{t_{max}} \leq e_t \leq e_{t_{max}} \quad (5-27)$$

**Permanent Droop**

$$e_d - \sigma v_a = 0 \quad (5-28)$$

**Distributing Valve**

$$v_d = \frac{k_d}{1 + T_d s} v_i$$

or

$$T_d \frac{dv_d}{dt} + v_d - k_d v_i = 0 \quad v_{d_{min}} \leq v_d \leq v_{d_{max}} \quad (5-29)$$

The rate limits of a gate-servomotor are often applied by restricting the maximum travel of the distributing valve in the positive and negative directions. Therefore, in the above inequality

$$v_{d_{max}} = \frac{1}{k_s T_o}$$

and

$$v_{d_{min}} = \frac{-1}{k_s T_c}$$

in which  $T_o$  and  $T_c$  are the effective gate opening and closing times, which are defined as twice the time taken by the wicket gates to open or close between 25 and 75 percent openings.

**Gate Servomotor**

$$\tau = \frac{k_s}{s} v_d$$

or

$$\frac{d\tau}{dt} - k_s v_d = 0 \quad 0 \leq \tau \leq 1.0 \quad (5-30)$$

The equations for the two feedbacks may be written as

$$e = n_{ref} - e_d - e_t - n \quad (5-31)$$

and

$$v_i = v_a - \tau \quad (5-32)$$

Note that the output of various components may saturate during transient-state conditions. These saturation limits must be taken into consideration for the analysis of large load changes.

By eliminating  $e$  and  $e_d$  from Eqs. 5-26, 5-28, and 5-31, eliminating  $v_i$  from Eqs. 5-29 and 5-32, and rearranging Eqs. 5-29 and 5-30, we obtain

$$\begin{aligned} \frac{dv_a}{dt} &= \frac{1}{T_a} (n_{ref} - n - e_t - \sigma v_a) \\ \frac{de_t}{dt} &= \frac{1}{T_r} \left( \delta T_r \frac{dv_a}{dt} - e_t \right) \\ \frac{dv_d}{dt} &= \frac{1}{T_d} [k_d (v_a - \tau) - v_d] \\ \frac{d\tau}{dt} &= k_s v_d \end{aligned} \quad (5-33)$$

A closed-form solution of the preceding four differential equations in four variables, namely,  $v_a$ ,  $e_t$ ,  $v_d$ , and  $\tau$ , is not possible because of nonlinearities introduced by the saturation of various variables. These equations may be integrated by any standard numerical technique. We employ the fourth-order Runge-Kutta method [McCracken and Dorn, 1964] for this purpose in our analysis, as discussed in the next section.

## 5-6 Mathematical Model

In this section, we outline a computational procedure for utilizing the boundary conditions developed earlier in this chapter and compare the computed results with those measured during prototype tests for the verification of the model. Typical turbine operations that produce transient conditions are also listed.

### Computational Procedure

Boundary conditions for a Francis turbine and equations for a dashpot governor were derived in Section 5-4 and 5-5, respectively. A computational procedure for using these conditions is presented in the following paragraphs.

Let us assume the transient-state conditions have been computed for  $(i-1)$  time steps. The values of  $N_e$ ,  $\tau_e$ , and  $H_{ne}$  at the end of the  $i$ th time step may

be estimated from the computed values for the previous three time steps  $i - 1$ ,  $i - 2$ , and  $i - 3$  by parabolic extrapolation from the equation

$$y_i = 3y_{i-1} - 3y_{i-2} + y_{i-3} \quad (5-34)$$

in which  $y$  is the variable to be extrapolated and the subscript indicates the time step. Note that this equation is valid only if the time steps are equal. Since there are no previous time steps at  $t = 0$ , the initial values may be used for the previous time steps for extrapolation. For the estimated values of  $H_{ne}$ ,  $N_e$ , and  $\tau_e$ , the grid points  $A$  through  $D$  (Fig. 5-5) are searched from the stored characteristic data. The coefficients  $a_0$  and  $a_1$  are computed, and the values of coefficients  $a_4$  to  $a_6$  are determined from Eqs. 5-6 through 5-8. Now  $Q_P$  is computed from Eq. 5-9 and  $H_{nP}$ , from Eq. 5-3. The value of  $\phi_e$  is determined using the estimated value of  $N_e$  and the computed value of  $H_{nP}$ . The turbine output,  $P_{turb_P}$ , is then determined from the turbine characteristic data for  $\phi_e$  and  $\tau_e$ . The generator load,  $P_{gen_P}$  and  $P_{turb_P}$  now being known, the value of  $N_P$  is determined from Eq. 5-15 or 5-16. If  $|N_P - N_e| > 0.001N_r$ , then  $N_e$  is assumed equal to  $N_P$ , and the above procedure is repeated; otherwise, the governor equations (Eqs. 5-33) are solved for  $\tau_P$  by the fourth-order Runge-Kutta method. If  $|\tau_P - \tau_e| > 0.005$ ,  $\tau_e$  is assumed equal to  $\tau_P$ , and the above procedure is repeated; otherwise, time is incremented, and the transient conditions are computed for the rest of the system. To avoid unlimited number of iterations in the case of divergence of solution, a counter is included in both the iterative loops.

The flowchart of Fig. 5-12 illustrates the preceding computational procedure.

## Turbine Operations

Turbine operations that produce transient-state conditions in the water conduits of a hydroelectric power plant may be classified into two categories:

### *Unit synchronized to a large grid*

Load acceptance

Load reduction or total load rejection

### *Isolated unit*

Unit start-up

Load acceptance

Load reduction or total load rejection.

The speed of a unit connected to a large grid remains constant at the synchronous speed during load acceptance or rejection because of the large inertia of the grid. However, the speed of an isolated unit increases following load rejection and decreases following load acceptance. Due to choking caused by turbine overspeed, the discharge of a Francis turbine decreases. The magnitude of this decrease depends upon the specific speed of the turbine (see

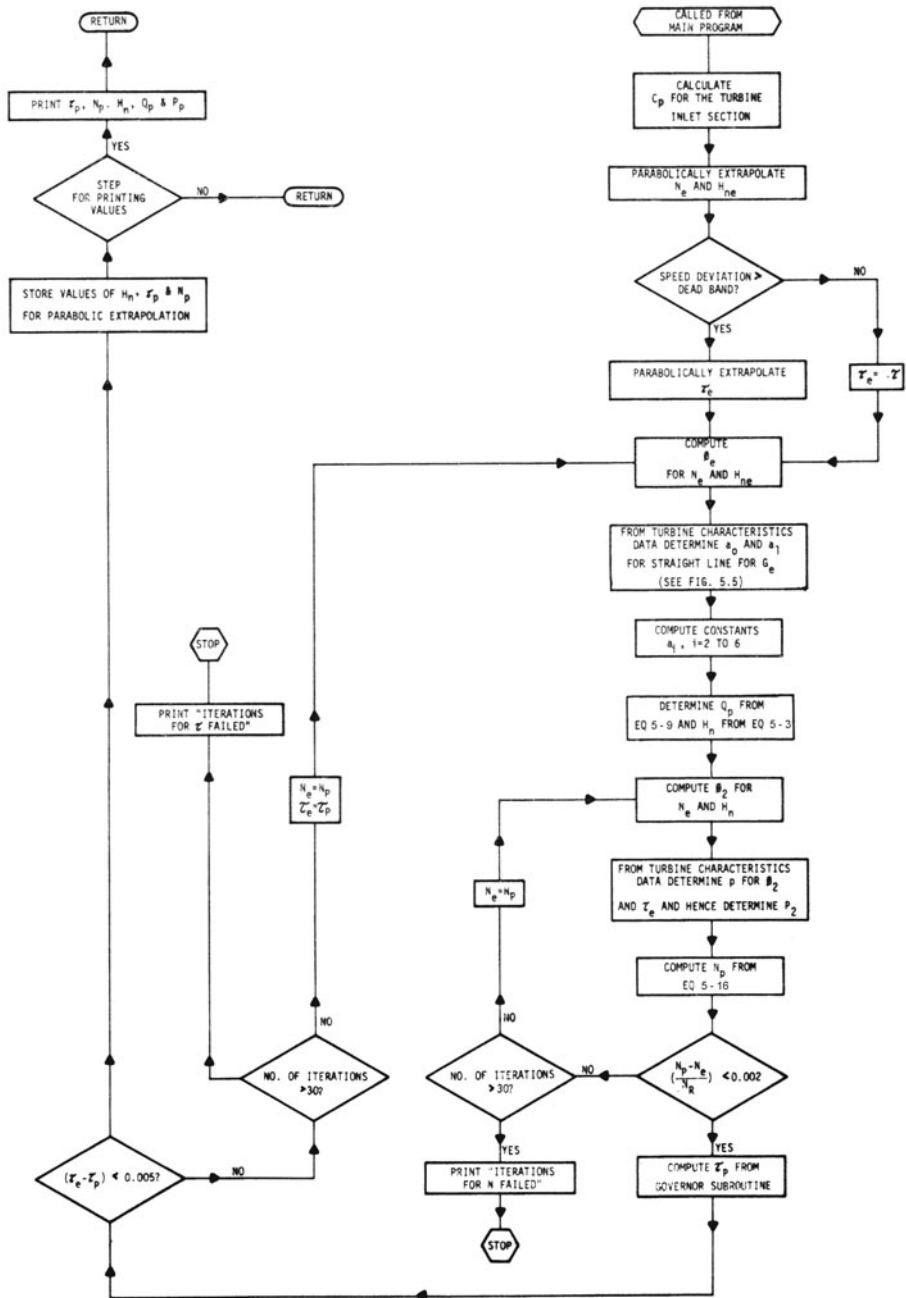
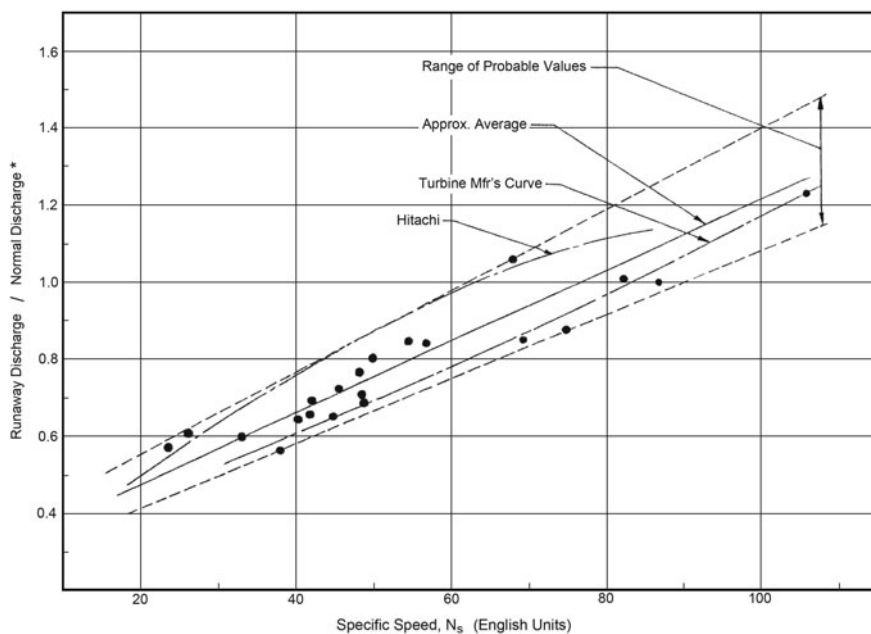


Fig. 5-12. Flowchart for boundary conditions for a governed Francis turbine.

**Fig. 5-13).** For a Kaplan turbine, however, the flow increases at runaway. For example, the discharge of a low-specific-speed Francis turbine at runaway may be reduced by as much as 40 per cent due to overspeed and that of a high-specific-speed Kaplan turbine may be increased at runaway similarly. These changes in the turbine discharge are as if the wicket gates are closed or opened although in reality the wicket gates are constant for runaway conditions. The flow changes at speeds higher than the rated speed but less than that at runaway are similar. Therefore, changes in the turbine speed and the resulting change in the discharge due to overspeed should be taken into consideration while computing the transient pressures produced by turbine operations and a valve boundary for the simulation of a turbine may result in inaccurate results.



**Fig. 5-13. Discharge of reaction turbines at runaway speed. (After Parmakian [1986].)**

The boundary conditions and the computational procedure described in Sections 5-4 through 5-6 are for an isolated unit only. These conditions may be used for a unit connected to a large system by keeping the speed constant by bypassing the loop for computing the speed changes.

To start a unit from stationary condition, the wicket gates are opened to the breakaway gate opening to give the unit a "kick" to overcome static friction. Gates are usually kept at this opening until the unit speed is about

60 percent of the rated speed; then the gates are closed to the speed-no-load gate, and the unit is allowed to run at the synchronous speed for a short period of time. It is then synchronized to the system and is ready for load acceptance.

For load acceptance, the wicket gates are opened at the prescribed rate to the opening at which turbine output is equal to the final output. Similarly, the gates are closed from one opening to another for load reduction. The wicket-gate opening following total load rejection, however, depends upon whether the unit remains connected to the grid or not after load rejection.

## Verification

The computed transient pressures and turbine speed are compared with those measured during tests at G. M. Shrum Generating Station, British Columbia, Canada to verify the preceding mathematical model.

## Project Description

The power plant has 10 Francis units, each with individual intake and penstock. Five units discharge into a tailrace manifold and then free-flow tailrace tunnel conveys water from each manifold to the tailrace channel. A schematic of the upstream water passages is shown in [Fig. 5-14](#), and of the downstream water passages in [Fig. 13-21](#).

Data for Unit No.4, on which tests were conducted, are listed in [Table 5-2](#).

## Tests

For the load-rejection tests, the unit was loaded to the specific load and was kept at this load until the pressure and flow at the turbine inlet became steady. Then, to simulate an isolated load rejection, the speed-no-load solenoid was blocked, and the load was rejected. The upstream reservoir level during the tests was at El. 671.0 m, and the downstream manifold level was at El. 503.2 m.

A Westinghouse leading-edge flowmeter [Fischer, 1973] was used to measure the steady as well as the transient-state flows. The locations of the flow transducers are shown in [Fig. 5-14](#). The flowmeter display exhibited average flow every 2.1 s. The flowmeter display along with a time clock were recorded on a videotape.

The speed of the turbogenerator was measured by a dc tachometer generator. A rubber-faced drive wheel was fastened to the shaft of the tachometer. The tachometer was mounted on a horizontal arm, which was free to turn about a vertical pivot anchored to the upper bearing of the turbine. A tensioning device held the drive wheel of the tachometer in contact with the turbogenerator shaft. The voltage output of the tachometer, which was proportional to the turbogenerator speed, was recorded on a Sanborn recorder.

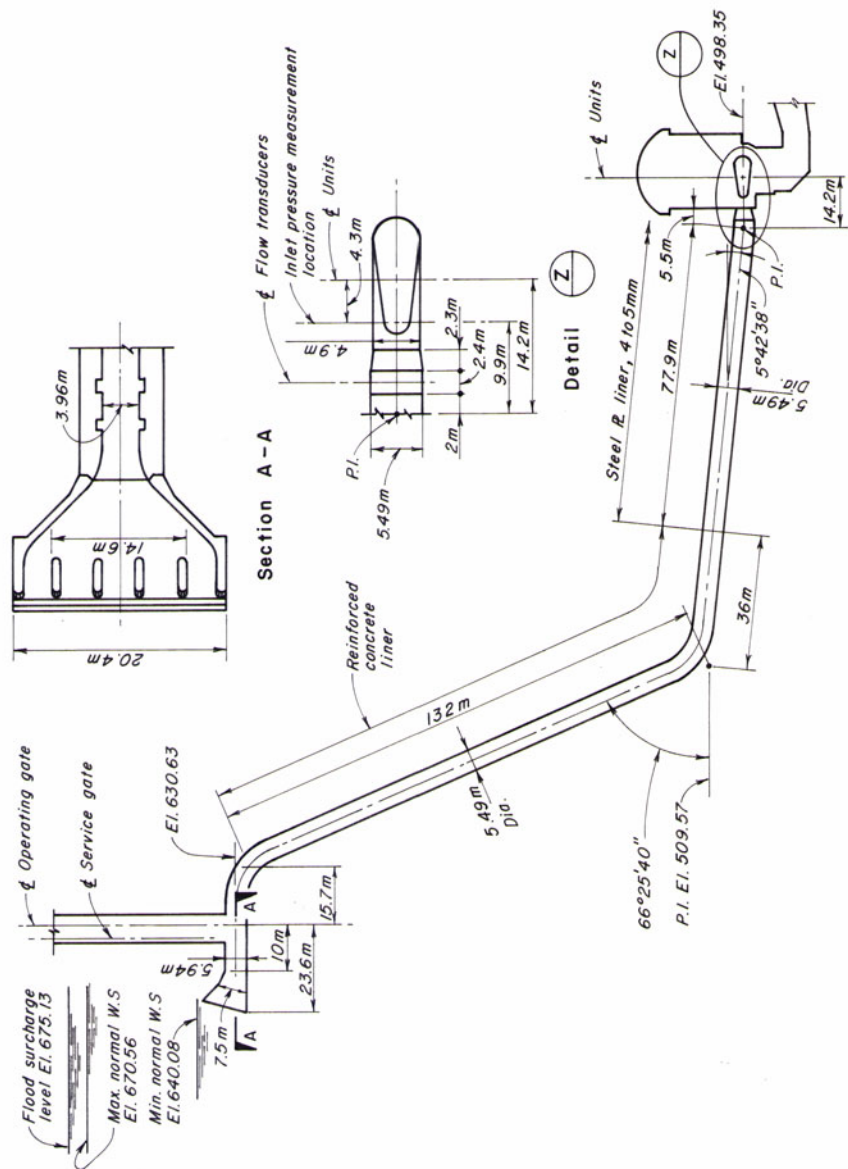


Fig. 5-14. Profile and details of G. M. Shrum Generating Station.

The transient-state pressures were measured by a strain-gauge pressure cell attached to the turbine-inlet piezometer manifold. The output of the transducer, when appropriately conditioned through its strain-gauge amplifier, was recorded on a chart recorder.

For recording the wicket-gate opening, the motion of one of the servomotors of the wicket-gate moving mechanism activated a precision voltage divider (potentiometer). The change in voltage was then recorded on an oscillograph, which was calibrated against 0 and 100 percent gate openings.

## Simulation

The conduit between the trashrack and the downstream end of the transition from a rectangular to a circular cross section was replaced by an equivalent 5.49-m-diameter pipe (See Appendix A for the expression for the equivalent pipe). The length of the scroll case was taken as one-half of the actual length to account for the reduction of flow along its length.

The draft tube was not included in the analysis because of its short length. The downstream manifold, being a free-surface area, was assumed as a constant-level reservoir. Wave velocities were computed using the equations presented in Section 2-6. The friction factors were calculated such that the form losses were included in the friction losses.

A computer program based on the preceding mathematical model was developed. The flow in the conduit was analyzed using the method of characteristics of Chapter 3, and the turbogenerator and governor were simulated using the equations derived in Sections 5-4 and 5-5.

Pipe No. 3 was divided into two reaches. To satisfy the Courant condition for the stability of the finite-difference scheme, i.e.,  $\Delta t \leq \Delta x/a$ , a time interval of 0.014 s was used. The wave velocities in the upper pipes were slightly adjusted to avoid interpolations. Static head and an estimated initial steady-state gate opening were the input data to the program. Corresponding flow and turbine output were computed from the turbine characteristics and the initial steady-state gate opening for the required turbine output was determined by trial and error.

Load was rejected at time,  $t = 0$ . As the unit was assumed to be isolated from the system following load rejection, it was allowed to overspeed, and the wicket gates were closed under governor control. Computed turbine speed, flow, gate opening, and pressure in each pipe were printed after every 35 time intervals, i.e., after every 0.5 s of prototype time.

## Comparison of Computed and Measured Results

The computed and measured results are plotted in Figs. 5-15 and 5-16. As can be seen, the computed and measured pressures agree closely. The computed and measured maximum unit speed agree closely; however, the computed speed reduction is faster than that measured. It should be noted that this

**Table 5-2. Data for Unit 4, G. M. Shrum Generating Station**

| <b>Turbine and Generator</b>            |              |            |  |                 |  |
|---|--------------|------------|--|-----------------|--|
| Rated turbine output                    |              |            | 231 MW                                   |                 |  |
| Rated head                              |              |            | 152.4 m                                  |                 |  |
| Synchronous speed                       |              |            | 150 rpm                                  |                 |  |
| Flow at rated head for rated output     |              |            | 164 m <sup>3</sup> /s                    |                 |  |
| Turbine and generator inertia           |              |            | 9.27 × 10 <sup>6</sup> kg m <sup>2</sup> |                 |  |
| Runner diameter                         |              |            | 4.86 m                                   |                 |  |
| <b>Governor Settings</b>                |              |            |  |                 |  |
| Dashpot time constant, $T_r$            |              |            | 8.0 s                                    |                 |  |
| Temporary droop, $\delta$               |              |            | 0.4                                      |                 |  |
| Permanent droop, $\sigma$               |              |            | 0.05                                     |                 |  |
| Dashpot saturation limit, $e_{t_{max}}$ |              |            | 0.25                                     |                 |  |
| Self-regulation constant, $\alpha$      |              |            | 0.15                                     |                 |  |
| <b>Conduits</b>                         |              |            |  |                 |  |
| Pipe No.                                | Diameter (m) | Length (m) | Wave Velocity (m/s)                      | Friction Factor |  |
| 1                                       | 5.49         | 207        | 1244                                     | 0.016           |  |
| 2                                       | 5.49         | 78         | 1290                                     | 0.010           |  |
| 3                                       | 4.9          | 36.5       | 1300                                     | 0.009           |  |

deviation starts when the wicket-gate opening is small. This difference may be due to an error in the estimation of the windage and friction losses and/or due to lack of data for the turbine characteristics at small wicket-gate openings. The computed pressures show some oscillations that were not recorded during field measurements. The cause of this difference has not been explained satisfactorily.

## 5-7 Design Criteria

As discussed in Section 4-7, the factor of safety depends upon the risks involved and the probability of occurrence of a particular operation during the life of the project. Various professional societies and organizations, such as the American Society of Mechanical Engineers, American Water-Works Association, etc. have their own standards and recommended factors of safety. The designer should check their applicability for a particular jurisdiction. Based on the frequency of occurrence, various operating conditions may be classified as *normal*, *emergency*, or *exceptional*. A discussion of the operating conditions included in each of these categories and recommended factors of safety [Parmakian, 1957] follows.

## Normal

All operations that are likely to occur several times during the life of the project are termed normal. During these operations, the appurtenances or devices such as surge tanks, pressure-regulating valves, and cushioning stroke devices, provided for reducing excessive pressure rise or pressure drop are assumed to function properly as designed. The surge tanks do not overflow, unless an overflow weir is provided, nor do they drain. The following are typical normal operations:

Full-load rejection and closure of the wicket gates in effective gate-closing time (Effective gate closing time is twice the time for the gates to close from 75 to 25 percent) with the maximum static head on the turbine.

Opening of the wicket gates from the speed-no-load to full opening in effective gate-opening time (Effective gate opening time is twice the time for the gate to open from 25 to 75 percent), with the static head on the turbine as low as its minimum value.

The penstock and spiral case are designed to withstand the maximum and minimum pressures produced by the preceding operations with a minimum factor of safety of *four*, based on the ultimate bursting and collapsing strength.

## Emergency

The *emergency* conditions are those in which one of the transient-control equipment malfunctions. These conditions include:

The pressure-regulating valve is inoperative on one unit.

The cushioning stroke device is inoperative on one unit.

A factor of safety of two, based on the ultimate collapsing or bursting strength, is recommended for pressures produced by emergency operations.

## Catastrophic

Those conditions in which various control devices malfunction in the most unfavorable manner are called catastrophic. For example, if a pressure-regulating valve is provided, then the wicket-gate closing mechanism is designed to close the wicket gates at a very slow rate in case the pressure-regulating valve is inoperative following a load rejection. However, if the pressure-regulating valve malfunctions and the wicket gates do not close at a slow rate following load rejection, then this operation is considered catastrophic [Parmakian, 1957].

Because of very low probability of occurrence, a factor of safety of *slightly more than one*, based on the ultimate bursting or collapsing strength, is suggested.

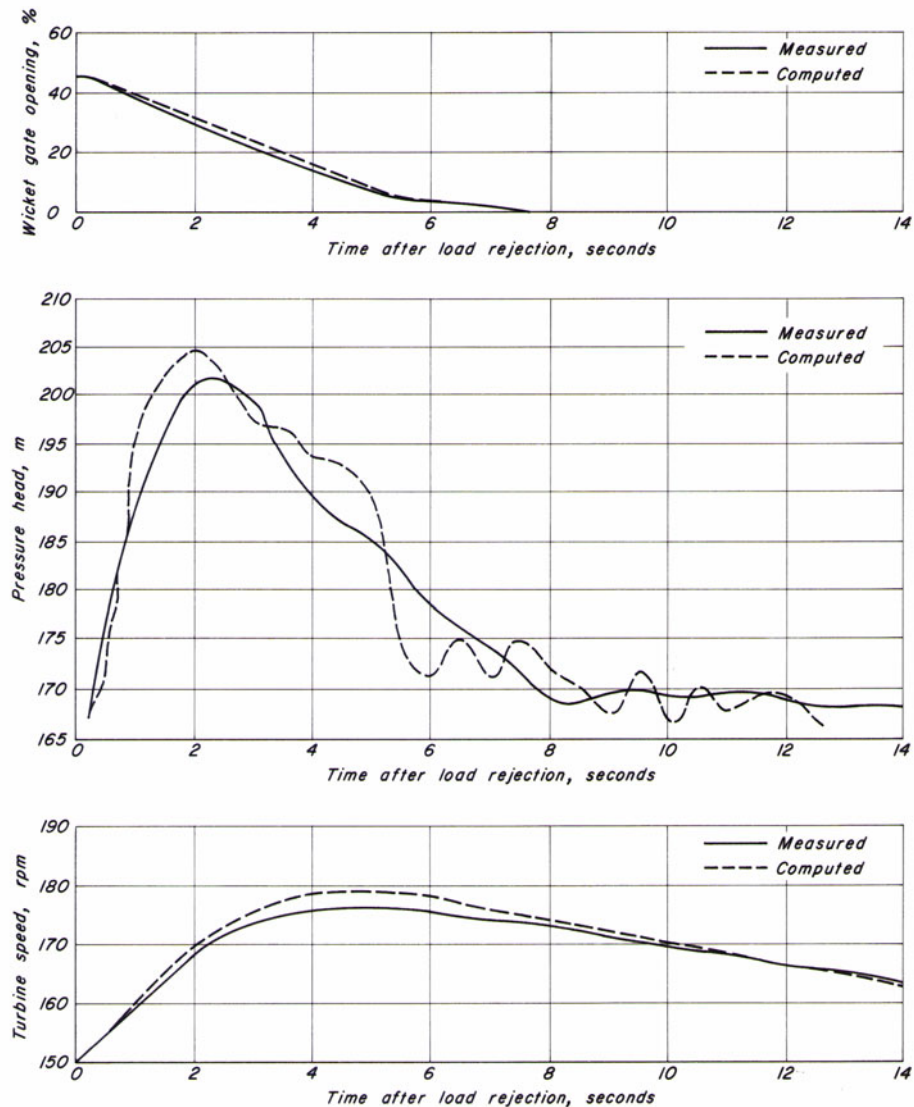
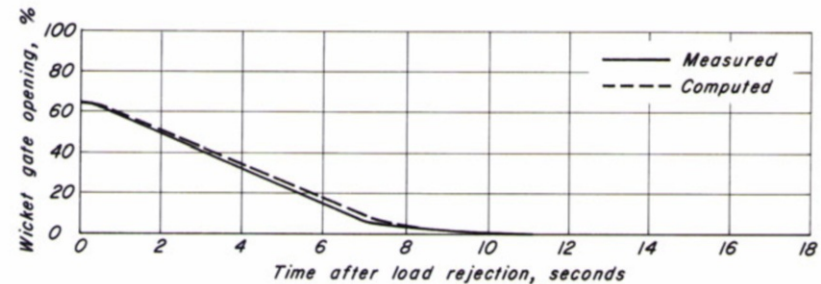
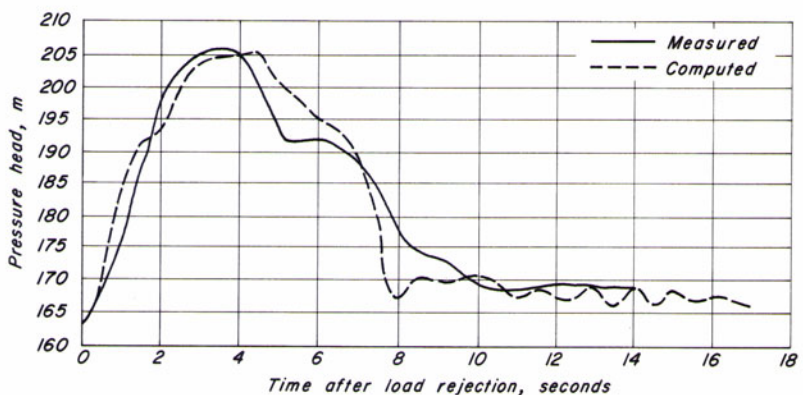


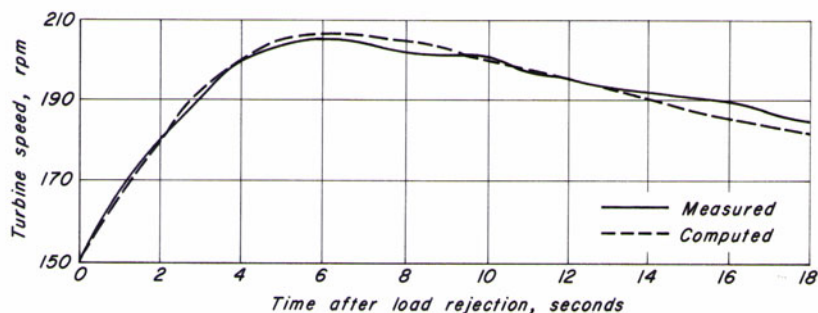
Fig. 5-15. 150-MW load rejection: comparison of computed and measured results.



(a) Turbine gate opening



(b) Penstock pressure



(c) Turbine speed

Fig. 5-16. Comparison of computed and measured results for 250-MW load rejection.

## 5-8 Governing Stability

The rotational speed of an isolated turbogenerator set, and hence the system frequency, varies with time following a load change. It is usually desirable, and in some industries imperative (e.g., textile, paper, etc.), that the deviation of the transient-state frequency from its reference value be as small as possible and that the frequency settles to its steady-state value within a reasonable time. As discussed earlier, a governor is provided on hydraulic turbines to control speed deviation, and the governor settings are selected to obtain a stable, and preferably an optimum unit response.

In this section, commonly used terms are defined, the general concepts of water starting time and mechanical starting time are introduced and procedures to determine generator inertia are discussed. Equations describing the system components, stability criteria, and optimum governor settings are presented in the following section.

### Terminology

In this section, common terms are defined and expressions for the water starting and mechanical starting times are developed.

**Stability.** A turbogenerator system is said to be *stable* if the speed oscillations following a load change are damped within a reasonable time (Fig. 5-17a); it is said to be *unstable* if the amplitude of the speed oscillations grows with time (Fig. 5-17b).

**Speed Deviation.** The difference between the instantaneous turbine speed and the reference speed is called speed deviation. It may be written in a nondimensional form as

$$n = \frac{N - N_r}{N_r} \quad (5-35)$$

in which  $n$  = per unit or normalized speed deviation,  $N_r$  = reference speed, and  $N$  = instantaneous speed. For brevity, only  $n$  is used in this section for the relative speed deviation, instead of  $\Delta n$  used in the previous sections.

**Water Starting Time.** Water starting time,  $T_w$ , is the time required to accelerate flow in a penstock from zero to velocity  $V_o$  under a pressure head of  $H_o$ . An expression for  $T_w$  may be derived as follows.

Let the water inside a penstock of length  $L$  and cross-sectional area  $A$  be stationary, and let the gates at the downstream end be opened instantly at time  $t = 0$  (Fig. 5-18). Assuming the penstock walls and the water inside the penstock are rigid and frictionless and applying Newton's second law of motion

$$\frac{\gamma A L}{g} \frac{dV}{dt} = \gamma A H_o \quad (5-36)$$

in which  $g$  = acceleration due to gravity,  $\gamma$  = specific weight of water,  $V$  = instantaneous flow velocity (positive in the downstream direction), and  $H_o$  =

pressure head acting on the upstream end. Eq. 5-36 simplifies as

$$\frac{L}{g} \frac{dV}{dt} = H_o \quad (5-37)$$

Integrating this equation and noting that, according to the definition of  $T_w$ , the flow velocity becomes  $V_o$  at  $t = T_w$ , we obtain

$$\frac{L}{g} \int_o^{V_o} dV = \int_o^{T_w} H_o dt \quad (5-38)$$

which may be simplified as

$$T_w = \frac{LV_o}{gH_o} \quad (5-39)$$

For a penstock with stepwise changes in diameter along its length, Eq. 5-39 may be written as

$$T_w = \sum_{i=1}^m \frac{L_i V_{oi}}{gH_o} \quad (5-40)$$

or

$$T_w = \frac{Q_o}{gH_o} \sum_{i=1}^m \frac{L_i}{A_i} \quad (5-41)$$

in which  $Q_o$  = discharge and  $m$  = total number of penstock segments. For the governing stability studies,  $T_w$  is computed using rated values for  $H_o$  and  $Q_o$  for the turbine and  $\sum(L/A)$  is computed from the upstream intake or upstream surge tank to a free surface on the downstream side of the turbine. The free surface may be a reservoir, a surge tank, a river, a free-flow tunnel, or a channel.

**Mechanical Starting Time.** Mechanical starting time is the time in which the unit is accelerated from zero to rated speed when rated torque is applied. The unit is assumed to be disconnected from the electrical grid. An expression for the mechanical starting time,  $T_m$ , may be derived as follows.

The equation for the acceleration of the rotating masses is

$$T = I \frac{d\omega}{dt} \quad (5-42)$$

in which  $T$  = torque,  $I$  = moment of inertia, and  $\omega$  = rotational speed, in rad/s =  $2\pi N/60$ . Equation 5-42 may be written as

$$T dt = I \frac{2\pi}{60} dN \quad (5-43)$$

Integrating both sides and noting that  $t = T_m$  when  $N = N_r$ ,

$$\int_o^{T_m} T dt = I \frac{2\pi}{60} \int_o^{N_r} dN \quad (5-44)$$

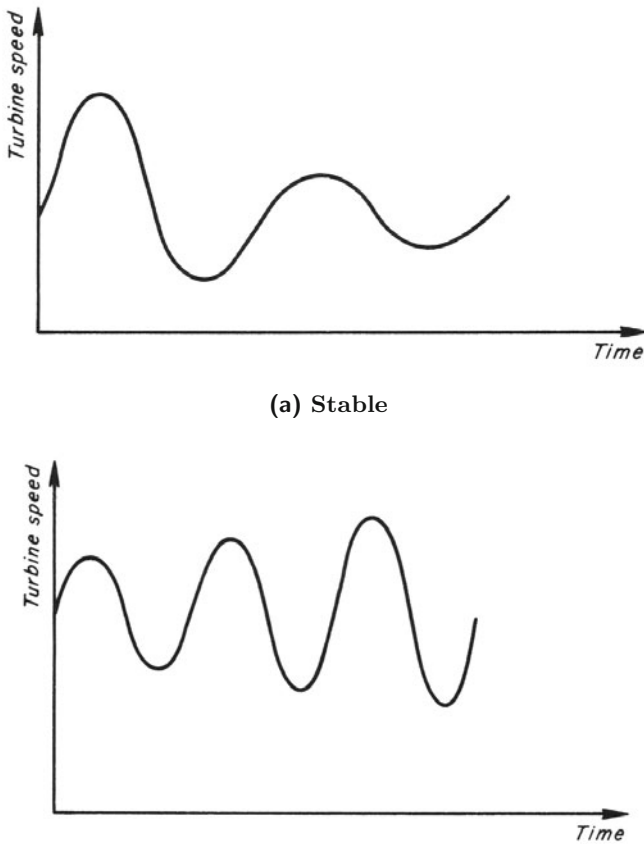


**Fig. 5-17.** Stable and unstable speed oscillations.

Simplifying, this equation becomes

$$T_m = \frac{2\pi}{60} \frac{IN_r}{T_R} \quad (5-45)$$

Now the rated torque

$$T_R = \frac{P_R}{\omega} = \frac{60}{2\pi} \frac{P_R}{N_r} \quad (5-46)$$

in which  $P_R$  = generator power output at rated conditions. Substituting for  $P_R$  from Eq. 5-46 into Eq. 5-45 and simplifying, we obtain

$$T_m = \frac{IN_r^2}{91.2 \times 10^6 P_R} \quad (5-47)$$

in which  $P_R$  is the rated output in MW. In the English units, replace 91.2 by 1.61 for  $I$  in lb-ft<sup>2</sup> and  $P_R$  in hp.

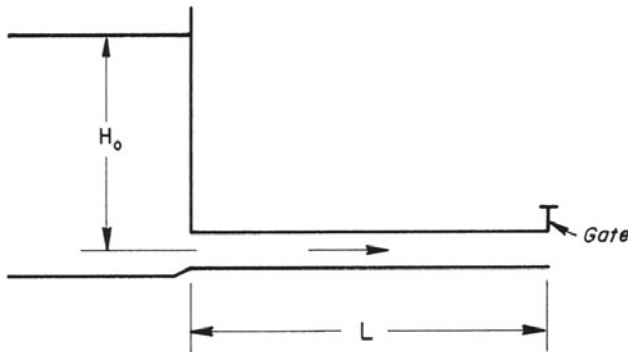


**Fig. 5-18.** Notation for water starting time.

**Self-regulation Coefficients.** The turbine self-regulation coefficient,  $\alpha_{tur}$ , is defined as the slope of the curve relating the per-unit deviation of the turbine torque to the per-unit deviation of the turbine speed at the rated conditions.

The load *self-regulation coefficient*,  $\alpha_l$ , is defined as the slope of the curve relating the per-unit deviation of the torque of the electrical load to the per-unit deviation of the frequency of the electrical load at the rated conditions (Fig. 5-19).

The *self-regulation coefficient*,  $\alpha$ , is defined as the algebraic difference between the load self-regulation coefficient and the turbine self-regulation coefficient, i.e.,

$$\alpha = \alpha_l - \alpha_{tur} \quad (5-48)$$

Typical values of  $\alpha$ ,  $\alpha_l$  and  $\alpha_{tur}$  are listed in Table 5-3.

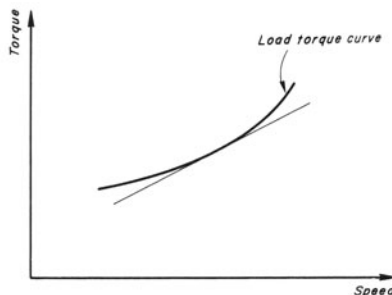


**Fig. 5-19.** Definition sketch for load self-regulation coefficient.

## Generator Inertia

For stable governing and for keeping the speed rise of the unit within permissible limits following load rejection, it is necessary that an adequate amount of generator and turbine (unit) inertia be provided. Turbine inertia is usually small compared to the generator inertia; and, if necessary, only the latter is increased. Although increasing the generator inertia does not increase the generator cost significantly, other associated costs, such as increasing the crane capacity or increasing the powerhouse dimensions, may be high. Therefore, the generator inertia is kept as small as possible while still maintaining acceptable governing characteristics.

**Table 5-3. Self-regulation coefficient<sup>†</sup>**

|   | $\alpha_l$ | $\alpha_{turb}$ | $\alpha = \alpha_l - \alpha_{turb}$ |
|---|------------|-----------------|-------------------------------------|
| Turbine                                       |            |                 |                                     |
| In general                                    | —          | about -1        | —                                   |
| High specific speed                           | —          | up to -1        | —                                   |
| Load  |            |                 |                                     |
| Grid loading: Motors only (constant torque)   | 0          | —               | +1                                  |
| Ohmic resistance only with voltage regulation | -1         | —               | 0.0                                 |
| Ohmic resistance without voltage regulation   | 1 to 4     | —               | 2 to 5                              |

<sup>†</sup> Taken from Stein [1947].

The following factors are considered in selecting the generator inertia:

### Allowable frequency fluctuation.

The allowable frequency fluctuation depends upon the type of load. For example, a frequency deviation of 0.1 percent is not permissible for paper mills, while deviation of as large as 5 percent may be acceptable for mining equipment.

### Size of the system.

A unit should be designed to be stable in isolated operation if it is supplying 40 percent or more of the system load, or if there are possibilities of the unit becoming isolated because of failure of the transmission line. The overall stability of the system is increased if the majority of the units in the system are stable in isolated operation.

### Type of load.

Periodic load changes, such as electric trams and mining shovels, contribute to system instability. Therefore, more inertia should be provided if such loads are present in the system.

### Water passages.

One of the major factors in the selection of the generator inertia is the size, length, and layout of the water passages of the power plant. By increasing the size of the water passages, the required generator inertia may be decreased. However, the former is usually more costly. Therefore, the size of the water passages is first selected based on the costs and benefits of reducing the head losses, and the required generator inertia is then determined.

### Governor times.

By decreasing the governor opening and closing times, the stability of the system can be improved. However, these times cannot be arbitrarily decreased since they are selected so that the waterhammer pressures are within the design limits and the water column does not separate at high points of the penstock, or in the draft tube.

Analytical methods are not presently available for determining directly the generator inertia required for a given set of plant parameters. Therefore, a number of empirical formulas and experience curves [Tennessee Valley Authority Projects, 1960 Gordon, 1961 and Krueger, 1980] have been proposed.

The *normal or standard generator* inertia depends upon the unit rating [Krueger, 1980] and is given by the equation,

$$\text{Normal generator inertia, } I = 15,000 \left( \frac{kva}{N_r^{1.5}} \right)^{1.25} \quad (5-49)$$

in which  $N_r$  = the synchronous speed, in rpm;  $kva$  = the generator output; and  $I$  = polar moment of inertia, in  $\text{kg m}^2$ . In the English units, the generator inertia is in  $\text{lb}\cdot\text{ft}^2$  and the constant 15,000 is replaced by 379,000.

Depending upon the factors just outlined, the inertia may be increased or decreased. For good regulation, the United States Bureau of Reclamation recommends [Krueger, 1980] that the ratio  $T_m/T_w^2$  be greater than 2. Units with  $T_m/T_w^2$  less than 2 may be integrated into a system but it may be necessary to compensate this deficiency on the other units of the system.

Experience curves proposed by the Tennessee Valley Authority relate  $T_m$  and  $T_w$  and show stability limits for various ratios of the unit size to that of the system. Gordon [1961] included the effect of the governor times while plotting his curves (see Fig. 5-20), which are based on experience with 40 Kaplan, Francis, and propeller turbine installations. These experience curves may be used for the preliminary design. During the final design, however, a mathematical model, such as developed in Sections 5-4 through 5-6, should be used to confirm the results of the preliminary analysis. To use these curves, the wicket-gate opening time,  $T_g$ , is computed by adding the time of the cushioning stroke (about 1.5 s) to the effective gate-opening time,  $T_o$ .

## 5-9 Stability Analysis

In the previous section, we discussed the stability of speed oscillations following load changes. In this section, the governing equations for small oscillations are presented and procedures for the selection of optimum governor parameters are outlined.

### General Remarks

The speed oscillations following a load change are stable or unstable depending upon the values of the parameters of the hydro-unit, penstock, and governor [Stein, 1947; Paynter, 1955; Hovey, 1961 and 1962; Chaudhry, 1970; and Chaudhry and Ruus, 1970]. Paynter [1955] presented a stability limit curve and suggested optimum governor settings based on the simulations on an analog computer. Hovey [1960 and 1962] derived a similar stability curve theoretically. However, both Paynter and Hovey neglected the permanent speed droop of the governor and the self-regulation of the turbine and of the load. In most cases, permanent speed droop  $\sigma$  is not zero while the self-regulation coefficient,  $\alpha$  [Stein, 1947] may or may not be zero depending on the type of load. (For values of  $\alpha$ , see [Table 5-3](#).) Chaudhry [1970] presented stability criteria in which the permanent speed droop and the self-regulation constant were included. Investigations conducted by Paynter [1955], Hovey [1960; 1961 and 1962] and Chaudhry [1970] are for a dashpot governor. Similar studies for a PID governor are reported in Thorne and Hill [1974], Thorne and Hill [1975] and Hagihara et al. [1979].

### Governing Equations

The following *assumptions* are made to develop the governing equations:

1. The changes in the turbine speed, head, and gate opening are small; thus, nonlinear relationships can be assumed linear.
2. A single hydro-unit supplies power to an isolated load.
3. The governor has no dead band, backlash, or hysteresis.
4. The walls of the penstock, and the water in the penstock and scroll case are rigid. Thus, waterhammer pressure caused by changes in the gate opening can be computed by using the rigid water-column theory.

By making these assumptions, the following differential equations [Stein, 1947; Paynter, 1955; Hovey, 1960; Hovey, 1962; and Chaudhry, 1970] may be written for the components of a hydroelectric power plant, shown in [Fig. 5-1b](#).

Turbo-generator

$$T_m \frac{dn}{dt} = g + 1.5h - \alpha n - \Delta m \quad (5-50)$$

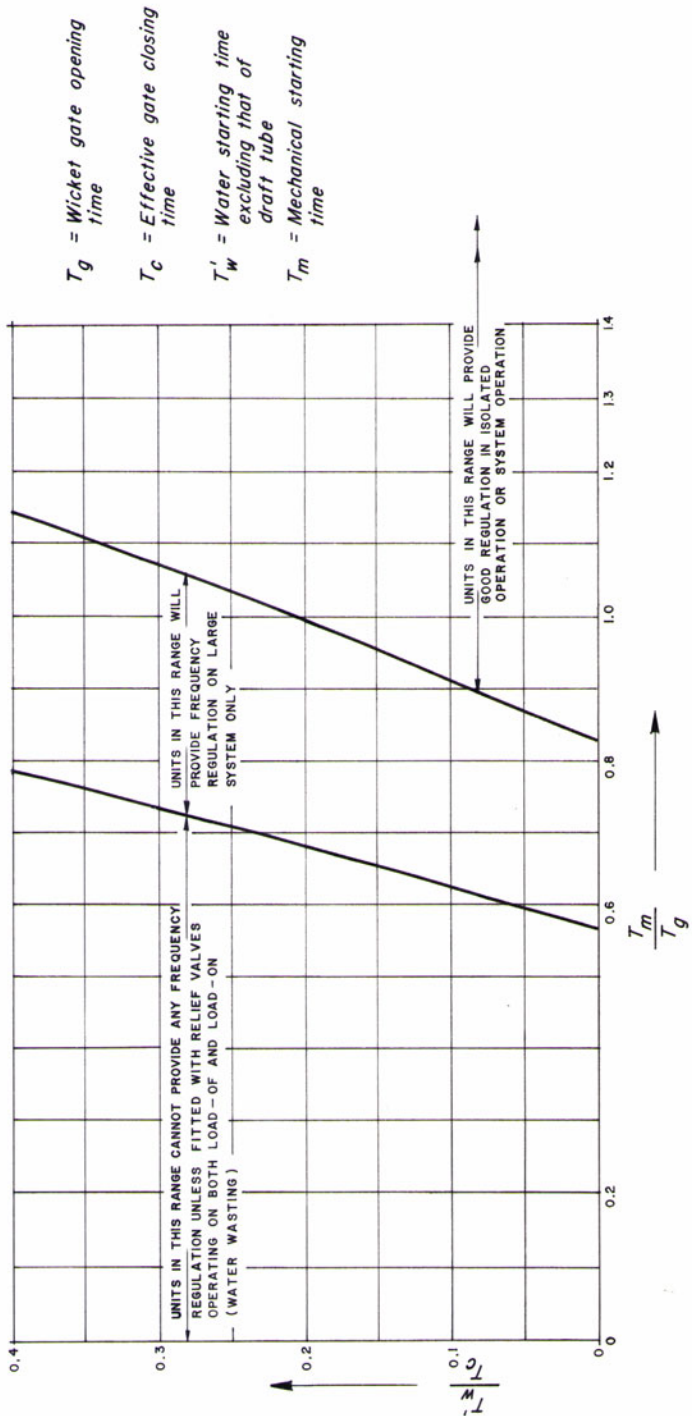


Fig. 5-20. Gordon stability curves. (After Gordon [1961].)

Water passages

$$-0.5T_w \frac{dh}{dt} = T_w \frac{dg}{dt} + h \quad (5-51)$$

Governor

$$(\sigma + \delta) T_r \frac{dg}{dt} + \sigma g = -T_r \frac{dn}{dt} - n \quad (5-52)$$

in which  $n$  = relative speed deviation  $= (N - N_o) / N_o$ ;  $h$  = relative pressure-head rise  $= (H - H_o) / H_o$ ;  $g$  = relative gate-opening change  $= (G - G_o) / G_o$ ;  $\Delta m$  = relative load-torque change  $= \Delta M / M_o$ ;  $\Delta M$  = step-load torque change (negative for load rejection);  $M_o$  = initial steady-state load torque;  $G$  = transient-state instantaneous gate opening; and  $N$  = transient-state instantaneous speed of the turbine, in rpm. The subscript  $o$  refers to the initial steady-state.

Let  $s = d/dt$ . Then Eq. 5-52 may be written as

$$g = \frac{-(T_r s + 1) n}{(\sigma + \delta) T_r s + \sigma} \quad (5-53)$$

It follows from Eq. 5-51 that

$$h = \frac{T_w s (T_r s + 1) n}{[(\sigma + \delta) T_r s + \sigma] (0.5T_w s + 1)} \quad (5-54)$$

Substituting Eqs. 5-53 and 5-54 into Eq. 5-50, simplifying, and replacing  $s^3$  by  $d^3/dt^3$ ,  $s^2$  by  $d^2/dt^2$ , and  $s$  by  $d/dt$ , we obtain

$$\begin{aligned} & 0.5 T_w T_m T_r (\sigma + \delta) \frac{d^3 n}{dt^3} \\ & + [0.5\sigma T_w T_m + (\sigma + \delta) T_m T_r - T_w T_r + 0.5\alpha T_w T_r (\sigma + \delta)] \frac{d^2 n}{dt^2} \\ & + [\sigma T_m + T_r - T_w + 0.5\sigma\alpha T_w + (\sigma + \delta) \alpha T_r] \frac{dn}{dt} \\ & + (1 + \sigma\alpha) n = -\sigma \Delta m \end{aligned} \quad (5-55)$$

### Stability Criteria

According to the Routh-Hurwitz criteria [Hovey, 1962], the oscillations represented by the third-order differential equation (Eq. 5-55) are stable if

$$0.5T_w T_m T_r (\sigma + \delta) > 0 \quad (5-56)$$

$$[0.5\sigma T_w T_m + (\sigma + \delta) T_m T_r - T_w T_r + 0.5\alpha T_w T_r (\sigma + \delta)] > 0 \quad (5-57)$$

$$[\sigma T_m + T_r - T_w + 0.5\alpha\sigma T_w + (\sigma + \delta) \alpha T_r] > 0 \quad (5-58)$$

$$(1 + \alpha\sigma) > 0 \quad (5-59)$$

$$\begin{aligned} & [\sigma T_m + T_r - T_w + 0.5\sigma\alpha T_w + (\sigma + \delta) \alpha T_r] [0.5\sigma T_w T_m + (\sigma + \delta) T_m T_r \\ & - T_w T_r + 0.5\alpha T_w T_r (\sigma + \delta)] > [0.5T_w T_m T_r (\sigma + \delta)] (1 + \sigma\alpha) \end{aligned} \quad (5-60)$$

The inequalities 5-56 and 5-59 are always satisfied. To plot the stability-limit curves, we have to consider the expressions given by inequalities 5-57, 5-58, and 5-60. There are six parameters in these expressions, namely,  $\sigma$ ,  $\delta$ ,  $\alpha$ ,  $T_w$ ,  $T_m$ , and  $T_r$ . To reduce the number of parameters and to present the criteria in a nondimensional form, the following nondimensional parameters [Chaudhry, 1970] are introduced:

$$\begin{aligned}\lambda_1 &= \frac{T_w}{\delta T_m} \\ \lambda_2 &= \frac{T_w}{T_r} \\ \lambda_3 &= \frac{\alpha T_w}{T_m} \\ \lambda_4 &= \frac{\sigma T_m}{T_w}\end{aligned}\tag{5-61}$$

By substituting the above parameters into inequalities 5-57, 5-58, and 5-60 and simplifying the resulting expressions, we obtain the following equations for the limits of stability:

$$0.5\lambda_1\lambda_2\lambda_4 + 0.5\lambda_1\lambda_3\lambda_4 + \lambda_1\lambda_4 + 0.5\lambda_3 - \lambda_1 + 1 = 0\tag{5-62}$$

$$0.5\lambda_1\lambda_2\lambda_3\lambda_4 + \lambda_1\lambda_3\lambda_4 + \lambda_1\lambda_2\lambda_4 - \lambda_1\lambda_2 + \lambda_1 + \lambda_3 = 0\tag{5-63}$$

$$\begin{aligned}&\lambda_1^2(\lambda_4 + 0.5\lambda_2^2\lambda_4^2 - 0.5\lambda_2^2\lambda_4 - 1 + \lambda_2 - 2\lambda_2\lambda_4 - 0.5\lambda_3\lambda_4 \\&\quad - \lambda_2\lambda_3\lambda_4 + \lambda_3\lambda_4^2 + \lambda_2\lambda_3\lambda_4^2 + 0.5\lambda_3^2\lambda_4^2 + 0.25\lambda_2\lambda_3^2\lambda_4^2 \\&\quad + 0.25\lambda_2^2\lambda_3\lambda_4^2 + \lambda_2\lambda_4^2) + \lambda_1(1 - 1.5\lambda_2 + \lambda_2\lambda_4 + 2\lambda_3\lambda_4 \\&\quad + \lambda_2\lambda_3\lambda_4 - 0.5\lambda_3 - 0.5\lambda_2\lambda_3 + \lambda_3^2\lambda_4 + 0.25\lambda_2\lambda_3^2\lambda_4) \\&\quad + (\lambda_3 + 0.5\lambda_3^2) = 0\end{aligned}\tag{5-64}$$

Equations 5-62 through 5-64 represent the stability criteria. Based on these equations, the stability limit curves for different values of  $\lambda_1$ ,  $\lambda_2$ ,  $\lambda_3$ , and  $\lambda_4$  are plotted in Fig. 5-21. Speed oscillations corresponding to those values of  $\lambda_1$  and  $\lambda_2$ , which lie in the region enclosed by the stability limit curve and the positive coordinate axes, are stable. For  $\lambda_3 = 0$  and  $\lambda_4 = 0$ , Hovey stability curve is obtained. This is shown as a dotted curve in Fig. 5-21.

### Example 5-1

For Kelsey Hydroelectric Plant,  $T_w = 1.24$  s and  $T_m = 9.05$  s. Hovey [1961] reported that, according to his criteria, the speed oscillations caused by a step load change are unstable for  $\delta = 0.28$  and  $T_r = 2.25$  s. Show that the oscillations are stable for these values of  $\delta$  and  $T_r$  if the permanent speed droop and the self-regulation are taken into consideration.

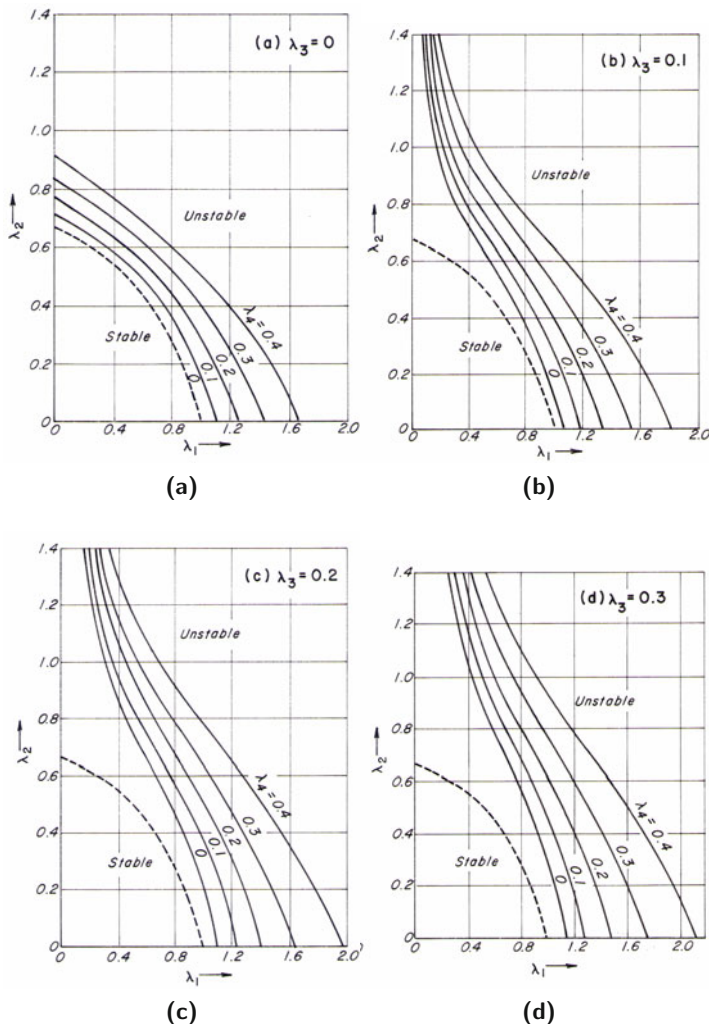


Fig. 5-21. Stability limit curves.

**Solution**

Kelsey plant supplies power to an isolated load consisting of furnaces, blowers, and compressors [Hovey, 1962]. Thus,  $\alpha$  is equal to 1 (see Table 5-3). As reported by Hovey [1962] in another paper,  $\sigma = 0.035$ . Stability calculations may be done as follows.

$$\begin{aligned}\lambda_1 &= \frac{T_w}{\delta T_m} = \frac{1.24}{0.28 \times 9.05} = 0.49 \\ \lambda_2 &= \frac{T_w}{T_r} = \frac{1.24}{2.25} = 0.55 \\ \lambda_3 &= \frac{\alpha T_w}{T_m} = \frac{1 \times 1.24}{9.05} = 0.137 \\ \lambda_4 &= \frac{\sigma T_m}{T_w} = \frac{0.035 \times 9.05}{1.24} = 0.255\end{aligned}$$

It follows from Fig. 5-21 that for  $\lambda_1 = 0.49$ ,  $\lambda_2 = 0.55$  and

- $\lambda_3 = 0.0$  and  $\lambda_4 = 0.0$ , the speed oscillations are unstable (Hovey's criteria);
- $\lambda_3 = 0.0$  and  $\lambda_4 = 0.255$ , the speed oscillations are stable;
- $\lambda_3 = 0.1$  and  $\lambda_4 = 0.0$ , the speed oscillations are stable; and
- $\lambda_3 = 0.1$  and  $\lambda_4 = 0.255$ , the speed oscillations are stable.

To check the validity of these results, Eqs. 5-50 through 5-52 are numerically integrated and the computed results are presented in Fig. 5-22. It is clear from Fig. 5-22a that the oscillations are unstable as indicated by the first case above. For the remaining three cases, the computed results confirm that the oscillations are stable, as shown in Fig. 5-22b through Fig. 5-22d.

### Transient Speed

For the initial conditions,  $N = N_o$ ,  $G = G_o$ , and  $H = H_o$  at time  $t = 0$  (i.e.,  $n|_{t=0} = 0$ ,  $g|_{t=0} = 0$ ,  $h|_{t=0} = 0$ ), the following solution of Eq. 5-55 is obtained:

$$n = A e^{\alpha' t} + e^{\beta t} (B \sin \gamma t + C \cos \gamma t) - \frac{\sigma \delta m}{(1 + \sigma \alpha)} \quad (5-65)$$

in which

$$A = \frac{\frac{-2\beta}{T_m} + \frac{2 - (\sigma + \delta)\alpha}{(\sigma + \delta)T_m^2} - \frac{\sigma}{(1 + \sigma\alpha)} (\gamma^2 + \beta^2)}{(\alpha' - \beta)^2 + \gamma^2} (-\Delta m)$$

$$B = \left[ \frac{-\Delta m}{T_m} - (\alpha' - \beta) A - \frac{\sigma \beta \Delta m}{1 + \sigma \alpha} \right] \frac{1}{\gamma} \quad (5-66)$$

$$C = \frac{\sigma \Delta m}{1 + \sigma \alpha} - A$$

and  $\alpha'$ , and  $\beta \pm i\gamma$  are the roots of the characteristic equation for Eq. 5-55.

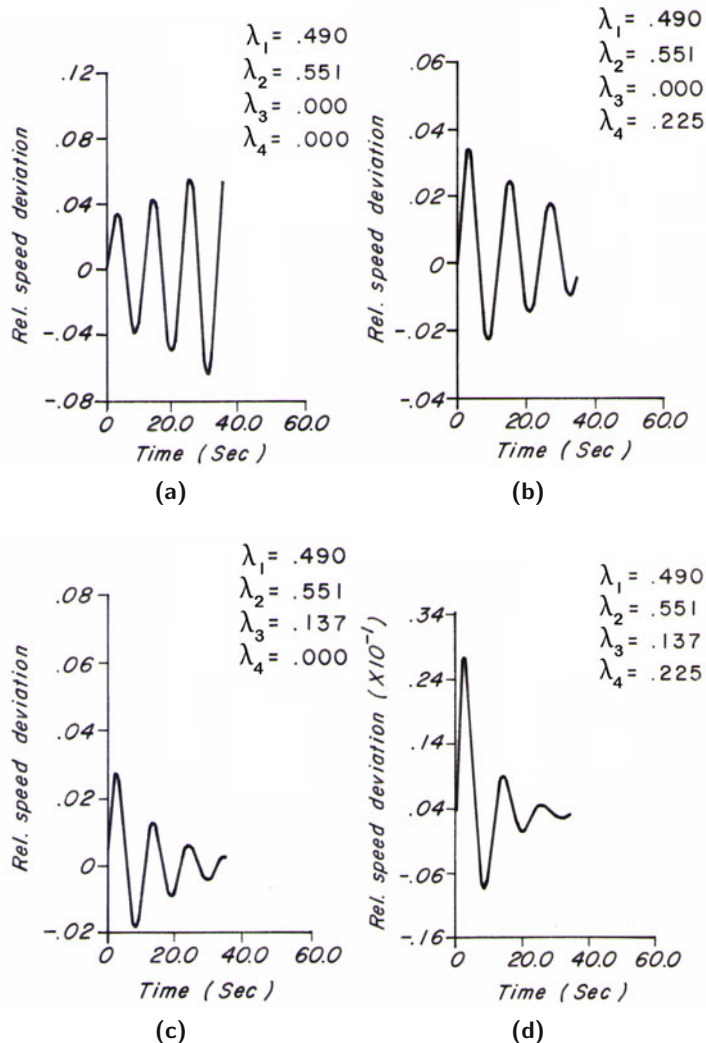


Fig. 5-22. Unstable and stable speed oscillations.

### Optimum Governor Settings

For specific values of  $\lambda_3$  and  $\lambda_4$ , Eqs. 5-50 through 5-52 are solved for different values of  $\lambda_1$  and  $\lambda_2$ . Those values of  $\lambda_1$  and  $\lambda_2$  which give the shortest settling time, but slightly underdamped response, are considered optimum. This procedure is repeated for  $\lambda_3 = 0.0$  and  $0.25$ , and  $\lambda_4 = 0.0$  to  $0.4$ . The curves for optimum values of  $\lambda_1$  and  $\lambda_2$  for different values of  $\lambda_3$  and  $\lambda_4$  are presented in Fig. 5-23.

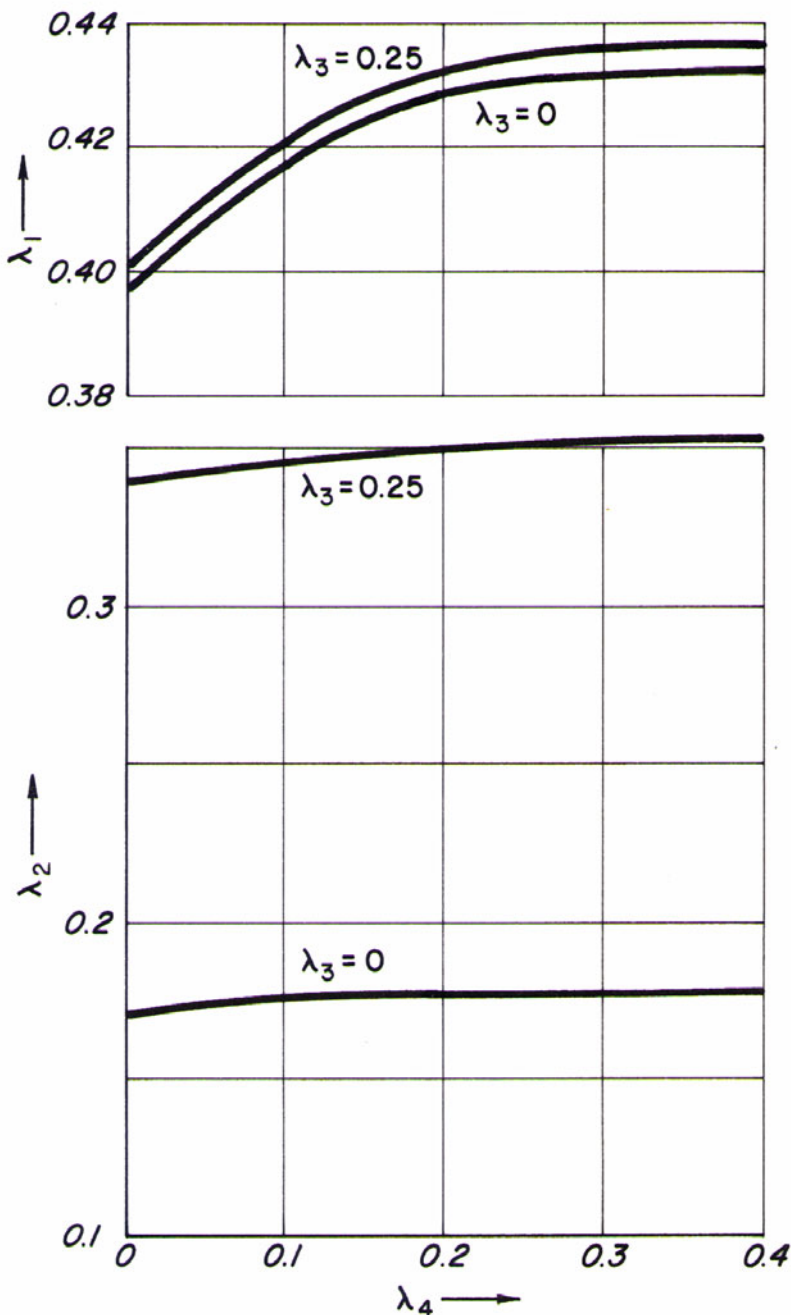


Fig. 5-23. Optimum governor settings.

The *optimum governor settings* for a particular power plant may be determined as follows:

1. Determine  $T_w$  for the given conduit dimensions and the specified rated head and flow for the turbine.
2. Compute  $T_m$  for the selected value of the moment of inertia of the generator and the turbine.
3. For the specific type of load, select a value of  $\alpha$  from [Table 5-3](#) and compute  $\lambda_3$  and  $\lambda_4$ . Assume  $\sigma = 0.05$ , if it is not specified.
4. For the computed values of  $\lambda_3$  and  $\lambda_4$ , determine the optimum values of  $\lambda_1$  and  $\lambda_2$  from [Fig. 5-23](#) and then determine  $\delta$  and  $T_r$  from Eqs. 5-61.

The following example illustrates this procedure.

### Example 5-2

Determine the optimum values of  $\delta$  and  $T_r$  for Kelsey Hydroelectric Power Plant having the following values of different parameters:  $T_w = 1.24\text{ s}$  (computed from the dimensions and geometry of the power conduit);  $T_m = 9.05\text{ s}$  (computed from the known value of polar moment of inertia and rated conditions of the turbine and the generator);  $\alpha = 1.0$  (determined from [Table 5-3](#) for the type of load) and  $\sigma = 0.035$ .

### Solution

- a. The optimum values of  $\delta$  and  $T_r$  as suggested by the author [Chaudhry, 1970] may be determined as follows:
1. Compute  $\lambda_3$  and  $\lambda_4$ .

$$\lambda_3 = \frac{\alpha T_w}{T_m} = \frac{1.0 \times 1.24}{9.05} = 0.137$$

$$\lambda_4 = \frac{\sigma T_m}{T_w} = \frac{0.035 \times 9.05}{1.24} = 0.255$$

2. From [Fig. 5-23](#), the following optimum values of  $\lambda_1$  and  $\lambda_2$  are obtained for  $\lambda_3 = 0.137$  and  $\lambda_4 = 0.255$ :  $\lambda_1 = 0.430$  and  $\lambda_2 = 0.27$ .
3. Compute  $\delta$  and  $T_r$  from the values of  $\lambda_1$  and  $\lambda_2$  determined in step 2.

$$\delta = \frac{T_w}{\lambda_1 T_m} = \frac{1.24}{0.430 \times 9.05} = 0.319$$

$$T_r = \frac{T_w}{\lambda_2} = \frac{1.24}{0.27} = 4.6 \text{ s}$$

- b. Hovey's optimum settings:

$$\delta = \frac{2T_w}{T_m} = \frac{2 \times 1.24}{9.05} = 0.274$$

$$T_r = 4T_w = 4 \times 1.24 = 4.96 \text{ s}$$

c. Paynter's optimum settings:

$$\delta = \frac{T_w}{0.4T_m} = \frac{1.24}{0.4 \times 9.05} = 0.342$$

$$T_r = \frac{T_w}{0.17} = \frac{1.24}{0.17} = 7.3 \text{ s}$$

For the above three cases,  $n \sim t$  curves for  $\Delta m = -0.1$  are presented in Fig. 5-24. It is clear that the author's optimum settings in which both  $\sigma$  and  $\alpha$  are taken into consideration give a better transient response than that by either Paynter's or Hovey's settings.

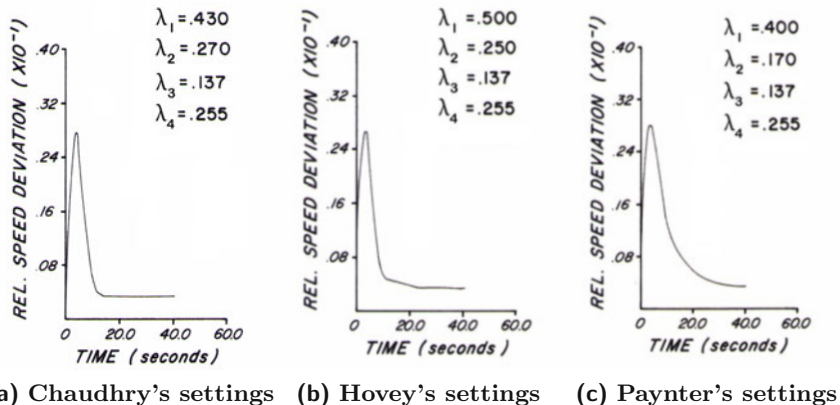


Fig. 5-24. Speed deviation for various governor settings.

## 5-10 Pumped-Storage Projects

Figure 5-25 shows the layout of a typical pumped-storage project. In the generation mode, water flows from the upper reservoir to the lower reservoir, and the turbo-machine acts as a turbine. In the pumping mode, the water is pumped from the lower reservoir to the upper reservoir, and the turbo-machine acts as a pump.

Transient flows are produced in the flow passages by the following operations:

Loading or unloading of turbines;

Tripping of pumps;

Switching from the generation mode to the pumping mode and vice versa;

Turbine shutdown following disconnection from the grid system; and  
Closure of the main shutoff valve against the water flow.

Transient conditions generated by these or other operations may be analyzed by using the method of characteristics. Most of the typical boundary conditions encountered in pumped-storage projects are presented in Chapters 3 and 5, and a few more are developed in Chapter 10. However, the simulation of a pump-turbine requires special treatment; this is discussed in the following section.

## 5-11 Pump Turbine

The following convention is used for the turbining and for the pumping modes:

*Normal turbining:* Positive rotational speed and positive flow.

*Normal pumping:* Negative rotational speed and negative flow.

Therefore, for a machine operating as a turbine during the initial steady state, the initial conduit flow and the machine rotational speed are positive. However, for a machine running as a pump during the initial steady state, the initial flow in the conduits and in the pump as well as the initial pump speed are all negative.

The *machine characteristics* of a pump turbine covering the four quadrants are presented in the form of unit discharge,  $q$ , vs unit speed,  $\phi$ , and unit torque,  $m$  vs unit speed. (Some manufacturers use  $Q_{11}$ ,  $T_{11}$ , and  $N_{11}$  for  $q$ ,  $m$  and  $\phi$ .) The head is positive during normal pumping, energy dissipation, normal turbining, and turbine energy dissipation.

The characteristics for a typical pump turbine are presented in Fig. 5-26. The abscissa in this figure is the unit speed,  $\phi$ ; and the ordinates are unit discharge,  $q$ , and unit torque,  $m$ . These quantities are defined as follows:

$$\begin{aligned} \text{Unit speed, } \phi &= ND/\sqrt{H_n} \\ \text{Unit discharge, } q &= Q/(D^2\sqrt{H_n}) \\ \text{Unit torque, } m &= M/(D^3 H_n) \end{aligned}$$

The following SI units are used for various parameters, with the the Customary English units listed in parentheses:

$$\begin{aligned} \text{Unit speed: rpm (rpm),} \\ \text{Unit flow: m}^3/\text{s (ft}^3/\text{s),} \\ \text{Unit torque: N-m (ft-lb).} \end{aligned}$$

The machine characteristics are a set of curves for different wicket gate openings. The wicket gate or guide vane openings may be specified as a percentage of the servomotor stroke, angle of the guide vanes, or distance between the vanes, etc. The specified gate opening vs time curve should be consistent with the parameter used for the wicket gate openings for the machine characteristics. Note that the relationship between the servomotor stroke (the value

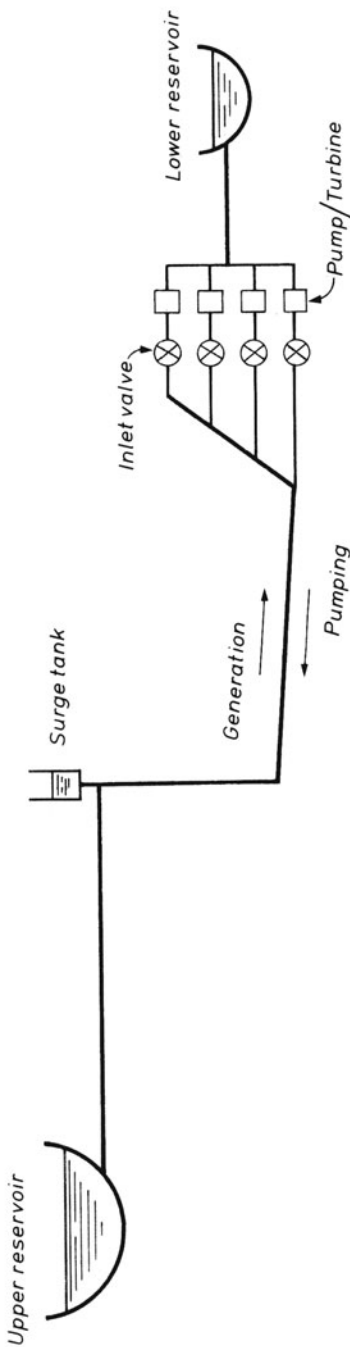


Fig. 5-25. Schematic layout of a pumped-storage project.

normally set or known before hand) and the guide vane opening is not always linear. This relationship depends on the particular parameter used to indicate the gate opening and the geometry of the linkage mechanism between the gate servomotor and the wicket gates. (For example, in Fig. 5-26, the wicket gate openings are given as the clear distance between the gates, in mm.) This same parameter should be used while specifying the the wicket gate opening at different times.

The characteristics data should cover all four quadrants, including the zones of energy dissipation both in the turbine mode (i.e., for gate opening smaller than the speed-no-load gate) and in the pumping mode. The characteristics data for zero gate opening (unit discharge characteristics is the zero line) is also included.

It is clear from Fig. 5-26 that the characteristics for various gate openings overlap, and more than one value of  $q$  and  $m$  is possible for a given gate opening and for a given unit speed. Because of these factors, the linear interpolation procedure discussed in Section 5-4 for a Francis turbine is not very satisfactory. To overcome this limitation, various procedures have been employed in the mathematical models [Paynter, 1972; Wozniak, 1976; Paynter, 1979; Boldy and Walmsley, 1982; Martin, 1982 and Boldy and Walmsley, 1983]. However, each of these representations has merits and limitations. We discuss two of these procedures in the following paragraphs.

## 1. S-Curves

Since the characteristic curves in many cases become multi-valued, the so-called S-curves may be used to store the data on these curves and to interpolate the intermediate values from the stored data. The S-curves are a set of *orthogonal lines* placed over each of the characteristics diagram for the unit discharge and for the unit torque. Figure 5-26 shows an example of the pump-turbine characteristics with a set of S-curves superimposed. Linear interpolation may be used between the S-lines; hence, these curves should be spaced more closely where the characteristics have sharp curvatures.

Normally 20 to 30 S-curves are sufficient. For example, there are 27 S-curves in Fig. 5-26 for both the unit torque and unit discharge diagrams. Note that the S-curves should connect or cross each of the gate openings from 0 to the maximum gate opening. These curves are numbered in an ascending order from the left to the right (i.e., from pumping to turbines) in both the unit discharge and unit torque diagrams. The extension of these curves from the maximum opening towards zero gate opening should be done carefully because sometimes there is a reversion in the order of the curves (see Fig. 5-27).

If for any reason during the computation of the transient conditions the point of operation falls outside the stored characteristics data, then a linear extrapolation from the nearest stored points may be used, and the following message may be printed in the general output file to warn the designer about

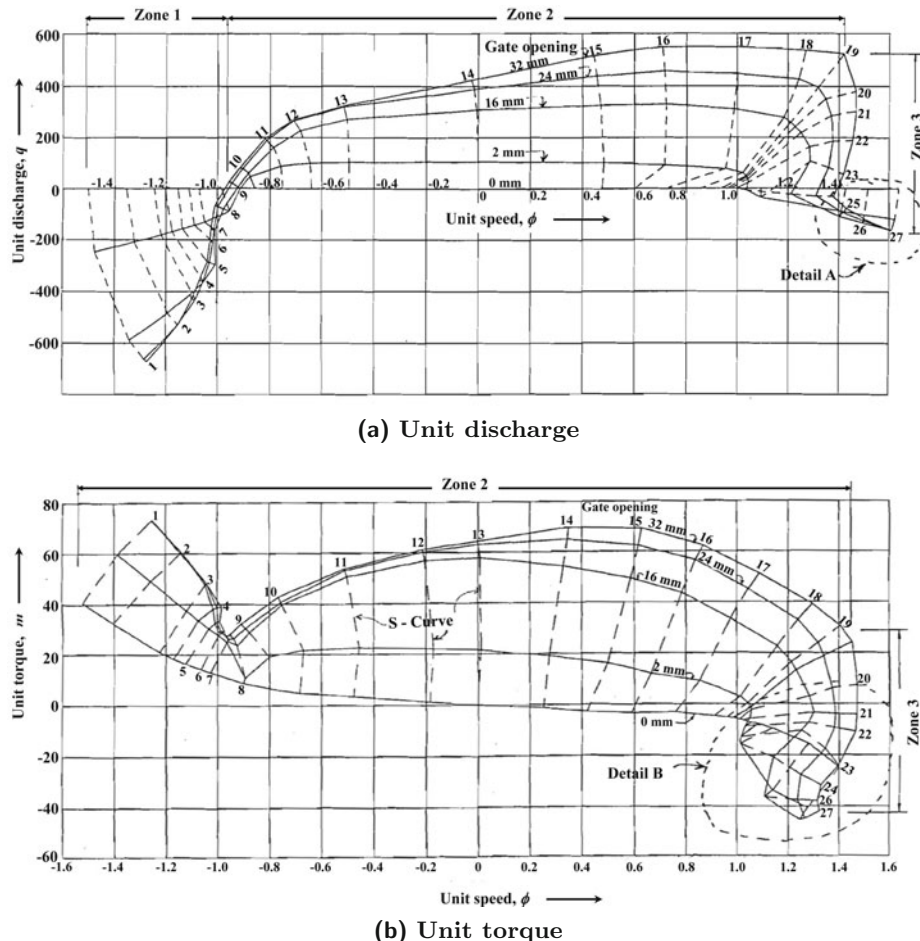


**Fig. 5-26. Pump-turbine characteristics.** (Courtesy, Computer Applications [2013].)

the limitation of the computed results: “POINT OUTSIDE THE CHARACTERISTICS.”

Once the S-curves are set, each characteristics diagram is divided into three zones depending on the slope of the characteristics curves. Zones 1 and 3 cover the range where the curves are steep. In these zones, it is impossible to interpolate for a given unit speed and gate opening because the ordinate may have multiple values. Therefore, the interpolation is carried out inversely. We call this as *inverse interpolation*.

Zone 2 includes the range where the curves are not steep or are not multi-valued so that normal interpolation may be employed. The limits of the three zones are specified by the following parameters: NSQT, MQLIM1, and

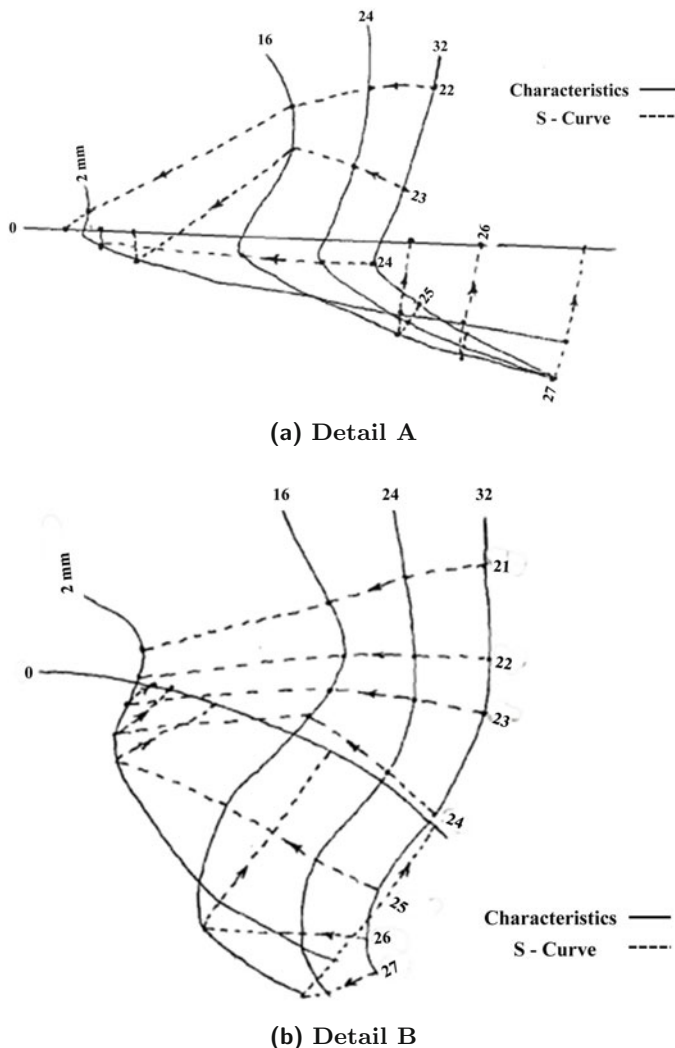


**Fig. 5-27.** Details of pump-turbine characteristics of Fig. 5-26.

MQLIM2 for the unit discharge diagram; and NSPT, NPLIM1, and NPLIM2 for the unit torque diagram. Zone 1 for the unit discharge diagram is from S-curve number 1 to S-curve number NQLIM1, Zone 2 is from NQLIM1 to NQLIM2, and Zone 3 is from NQLIM2 to NSQT where NSQT is the total number of S-curves in the unit discharge diagram. Similarly, for the unit torque diagram, the zones are from 1 to NPLIM1, from NPLIM1 to NPLIM2, and from NPLIM2 to NSPT, respectively. Note that depending on the actual machine characteristics, either Zone 1 or 3 or both may not be necessary. For

example, Zone 1 is not necessary in the unit torque diagram of Fig. 5-26 because the curves are not very steep and do not have multi-valued ordinates. The values of different parameters for this example are:

$$\begin{aligned} \text{NSPT} &= 27, \text{NPLIM1} = 1 \text{ and } \text{NPLIM2} = 20 \\ \text{NSQT} &= 27, \text{NQLIM1} = 9 \text{ and } \text{NQLIM2} = 19 \end{aligned}$$

If Zone 1 is not required in the unit discharge diagram, then NQLIM1 = 1; if Zone 3 is not required in this diagram, then NQLIM2 = NSQT. Similar is the case for the unit torque diagram.

Note that even in the areas of inverse interpolation in Fig. 5-26, the curves flatten when the gate opening is close to zero; therefore, it is not necessary to use inverse interpolation. This may be handled automatically by applying normal interpolation whenever the gate opening becomes less than one-half of the second gate opening for which characteristics are specified (2 mm in the example of Fig. 5-26).

## 2. Transformed Coordinates

Another procedure, developed by Martin [1982], appears to have some desirable features. In this procedure, the following transformed coordinates (Fig. 5-28) are used. The abscissa is  $\tan^{-1}(z_P/z)(v/\alpha)$ , and the ordinates are  $h/\left[\alpha^2 + (z_P/z)^2(v\alpha)^2\right]$  and  $\beta/\left[\alpha^2 + (zv^2/z_P)\right]$ , in which  $z$  = gate opening,  $z_P$  = full gate opening,  $v = Q/Q_R$ ,  $\alpha = N/N_R$ ,  $h = H/H_R$ , and  $\beta = M/M_R$ . The subscript  $R$  refers to the rated conditions. This procedure opens the individual guide vane curves, reduces the numerical range of various quantities for the maximum and minimum guide vane openings, and the curves are single valued throughout. The main limitation is that the zero guide vane opening is undefined, and special treatment is required during the final closure. If a curvilinear mesh, suggested by Boldy [1982 and 1983] is used, this representation of characteristics yields acceptable results.

## 5-12 Case Study

For illustration purposes, governing stability studies carried out for the Koote-  
nay Canal Hydroelectric Power Plant of British Columbia Hydro and Power Authority are presented in this section. This is a 500-MW hydroelectric power plant with each of the four units having its own power intake and penstock. Data for the turbine, generator, and penstock follow:

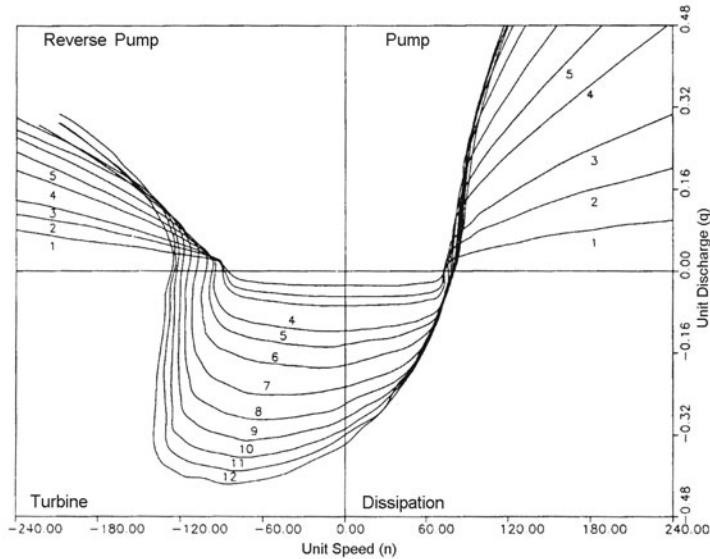
*Turbine*

Type: Francis

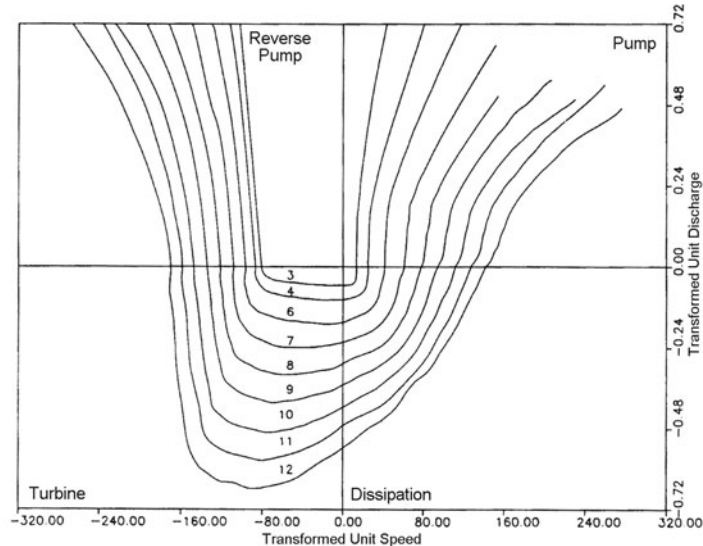
Specific speed:<sup>\*</sup> 55 (English units), 209 (Metric units)

---

<sup>\*</sup>Specific speed =  $N\sqrt{P}/H^{1.25}$ . In the English units,  $P$  is in hp,  $H$  in ft, and  $N$  in rpm; in the Metric units,  $P$  is in kW,  $H$  in m, and  $N$  in rpm.



(a) Original Model Test Data in Unit Plane



(b) Model Date in Transformed Unit Plane (opened and stretched mode)

**Fig. 5-28.** Transformed characteristics of a pump turbine. (Courtesy, Martin, C. S.)

Rated turbine output: 127.5 MW  
 Rated head : 74.6 m  
 Synchronous speed: 128.6 rpm  
 Flow at rated conditions: 191 m<sup>3</sup>/s  
 Runner-throat diameter: 4.95 m

*Generator*

Rated output: 125 MW

*Penstock*

The penstock diameter was determined by an economic analysis so that the incremental benefits from the decreased head losses were more than the increase in the penstock costs. The length, diameter, and wall thickness for the penstock are listed in Example 2-1.

Computations were done as follows:

***Mechanical starting time, T<sub>m</sub>***

$$kva = \frac{\text{MW} \times 10^3}{\text{Power factor}}$$

$$kva = 125 \times 10^3 / 0.95 = 131,579$$

$$\begin{aligned} \text{Normal generator inertia} &= 15,000 \left( \frac{kva}{N_r^{1.5}} \right)^{1.25} \quad (\text{Eq. 5-49}) \\ &= 15,000 \left( \frac{131,579}{(128.6)^{1.5}} \right)^{1.25} \\ &= 4.17 \text{ Gg m}^2 \end{aligned}$$

$$\begin{aligned} \text{Turbine inertia} &= 1446 \left( \frac{kW}{N_r^{1.5}} \right)^{1.25} \\ &= 1446 \left( \frac{127,500}{(128.6)^{1.5}} \right)^{1.25} \\ &= 0.39 \text{ Gg m}^2 \end{aligned}$$

$$\text{Total inertia, } I = 4.17 + 0.39 = 4.56 \text{ Gg m}^2$$

$$\begin{aligned} T_m &= \frac{I \times N_r^2}{91.2 \times 10^6 \text{ MW}} \\ &= \frac{4.56 \times 10^6 \times (128.6)^2}{91.2 \times 10^6 \times 127.5} \\ &= 6.49 \text{ s} \end{aligned}$$

### **Water starting time, $T_w$**

For different segments of the water passages,  $\Sigma L/A$  is computed in [Table 5-4](#).

$$\begin{aligned} T_w &= \frac{Q}{gH_R} \sum \frac{L}{A} \\ &= \frac{191 \times 10.54}{9.81 \times 74.6} \\ &= 2.75 \text{ s} \end{aligned}$$

### **Experience Criteria and Curves**

Since there is a strong possibility of this power plant being isolated from the system, the generator inertia was selected such that the units would be stable in isolated operation. For this purpose, the following empirical relationships and curves were used.

**Table 5-4. Computations for  $T_w$**

| Conduit     | Length $L$<br>(m) | Cross-sectional Area $A$<br>( $m^2$ ) | $\sum \frac{L}{A}$<br>( $m^{-1}$ )             | Remarks                             |
|-------------|-------------------|---------------------------------------|--|-------------------------------------|
| Intake      | 7.6               | $9.1 \times 9.1 = 82.8$               | 0.091  | Total length of spiral case = 29 m. |
|             | 12.8              | $4.9 \times 7.3 = 35.8$               | 0.357  |                                     |
| Penstock    | 244.              | $\frac{\pi}{4}(6.71)^2 = 35.4$        | 6.89   |                                     |
|             | 36.5              | $\frac{\pi}{4}(5.55)^2 = 24.2$        | 1.51   |                                     |
| Spiral case | 14.5              | $\frac{\pi}{4}(5.55)^2 = 24.2$        | 0.6  |                                     |
| Draft tube  | 15.2              | $\frac{\pi}{4}(4.88)^2 = 18.7$        | 0.81   |                                     |
|             | 13.7              | $0.5(18.7 + 14.6 \times 5.33) = 48.3$ | 0.28   |                                     |
|             |                   |                                       | $\sum \frac{L}{A} = 10.54;$                    |                                     |
|             |                   |                                       | $\sum \frac{L}{A}$ excluding draft tube = 9.45 |                                     |

- a. *U.S. Bureau of Reclamation Criteria (USBR)* For the normal inertia of the generator and turbine and for the selected conduit sizes, the values of  $T_m$  and  $T_w$  were computed as 6.49 and 2.75 s, respectively. Hence,

$$\frac{T_m}{T_w^2} = \frac{6.49}{(2.75)^2} = 0.86$$

As this ratio is less than 2, the unit would be unstable in isolated operation according to USBR criteria [Krueger, 1980].

- b. *Tennessee Valley Authority Curves.* The values of  $T_m$  and  $T_w$  computed in (a) were plotted on the TVA experience curves. It was found that the units would be unstable in isolated operation.
- c. *Gordon Curves [1961].* As both the USBR criteria and the TVA experience curves indicated that the units would be unstable in isolated operation with the normal inertia, total inertia of 7.2 and 8 Gg m<sup>2</sup> were considered in addition to the normal inertia of 4.56 Gg m<sup>2</sup>.  $T_m$  for inertia of 7.2 and 8.0 Gg m<sup>2</sup> is 10.2 and 11.4 s, respectively. By using  $\Sigma L/A$  computed in [Table 5-4](#), the water starting time, excluding the draft tube,

$$T'_w = \frac{191 \times 9.45}{9.81 \times 74.6} = 2.46 \text{ s}$$

Let us assume the wicket-gate opening and closing times are equal. Then, allowing 1 sec for the cushioning stroke,  $T_g = T_c + 1.0$ , in which  $T_c$  = effective gate-closing time and  $T_g$  = total opening time. Now, points for different values of  $T_c$  and for total inertia of 4.56, 7.2, and 8.0 Gg m<sup>2</sup> were plotted on the Gordon curves [1960]. Of these three curves, the curve for 4.56 Gg m<sup>2</sup> did not intersect the curve dividing the stable regions for the isolated and for the system operation. The values of  $T_c$ , which would result in stable isolated operation for inertia = 7.2 and 8.0 Gg m<sup>2</sup>, were determined from the intersection of the other two curves. These values were 8.6 and 10.2 s, respectively.

### **Speed Rise**

Using the procedure outlined in Krueger [1980], speed rise for full-load rejection was computed for various values of  $T_c$  and  $T_m$ . These values are listed in [Table 5-5](#).

### **Waterhammer Pressure**

Waterhammer wave velocities in the penstock were computed in Example 2-1. Wave velocity and cross-sectional area for an equivalent 295-m-long (including half the length of spiral case) pipe were computed as follows [Parmakian, 1963]:

$$\frac{L}{a_e} = \sum \frac{L}{a}$$

$$a_e = \frac{295}{(244/694) + (51/1410) + (20/1244)} = 730 \text{ m/s}$$

$$\frac{2L}{a_e} = \frac{295}{730} = 0.81 \text{ s}$$

$$A_e = \frac{L}{\sum(L/A)}$$

$$= \frac{295}{9.45}$$

$$= 31.22 \text{ m}^2$$

$$V_o = \frac{191}{31.22} = 6.12 \text{ m/s}$$

$$\text{Allievi parameter, } \rho = \frac{aV_o}{2gH_R}$$

$$= \frac{730 \times 6.12}{2 \times 9.81 \times 74.6} = 3.05$$

The waterhammer pressures for various values of  $T_c$  were computed from the charts presented in Appendix A. The computed values are listed in [Table 5-6](#):

**Table 5-5. Speed rise**

| $T_c$ (s) | Speed rise, percent |                |                |
|-----------|---------------------|----------------|----------------|
|           | $T_m = 6.49$ s      | $T_m = 10.2$ s | $T_m = 11.4$ s |
| 6         | 54.7                | 38.4           | 35.4           |
| 8         | 62.5                | 43.9           | 40.5           |
| 10        | 69.5                | 49.3           | 45.4           |

**Table 5-6. Pressure rise**

| $T_c$<br>(s) | Pressure rise, $\Delta H/H_R$ |
|--------------|-------------------------------|
| 6            | 0.48                          |
| 8            | 0.36                          |
| 10           | 0.27                          |

### ***Generator Inertia and Governor Times***

From the preceding computations, the values of inertia and governor times were selected as follows:

The maximum effective governor time was selected as the minimum of

- i. The governor time required for isolated stable governing from Gordon's stability curves.
- ii. The governor time so that the speed rise following total load rejection does not exceed 60 percent.

The minimum value of the effective governor time is the maximum of

- i. The gate-opening time such that negative pressures do not occur in the penstock for the minimum forebay water level.
- ii. The waterhammer pressure rise following total load rejection does not exceed 50 percent of static head.

Based on these criteria, the following values were selected:

Total inertia of generator and turbine = 7.2 Gg m<sup>2</sup>

Turbine inertia = 0.2 Gg m<sup>2</sup> (specified by the turbine manufacturer)

Generator inertia = 7.2 - 0.2 = 7.0 Gg m<sup>2</sup>

Governor closing time = 8 s

### ***Governor Settings***

For the selected conduit sizes and generator inertia,  $T_w = 2.75$  s and  $T_m = 10.18$  s. Assuming the permanent speed droop,  $\sigma = 5$  percent and the self-regulation constant,  $\alpha = 0.5$ ,

$$\lambda_3 = \frac{\alpha T_w}{T_m} = \frac{0.5 \times 2.75}{10.18} = 0.135$$

$$\lambda_4 = \frac{\sigma T_m}{T_w} = \frac{0.05 \times 10.18}{2.75} = 0.185$$

For these values of  $\lambda_3$  and  $\lambda_4$ , optimum governor settings as determined from Fig. 5-23 are

$$\lambda_1 = 0.43$$

and

$$\lambda_2 = 0.27$$

Hence,

$$\begin{aligned}\text{Temporary speed droop, } \delta &= \frac{T_w}{\lambda_1 T_m} \\ &= \frac{2.75}{0.43 \times 10.18} = 0.63 \\ \text{Dashpot time constant, } T_r &= \frac{T_w}{\lambda_2} \\ &= \frac{2.75}{0.27} = 10 \text{ s}\end{aligned}$$

*Final check.* During the final design, the turbine characteristics were available from the model tests conducted by the turbine manufacturer. The mathematical model presented in Section 5-6 was used to compute the maximum and minimum transient-state pressures, maximum speed rise following total load rejection, and the speed deviation following large load changes. The maximum and minimum pressures and speed rise were found to be within the design limits, and the unit was stable following large load changes.

### 5-13 Summary

In this chapter, the details of the mathematical simulation of the conduit system, hydraulic turbine, and governor are outlined. Various turbine operations that produce the hydraulic transients are discussed. Prototype test results to verify the mathematical model are presented. Procedures for the selection of the generator inertia and for determining the optimum governor settings are then described. The chapter is concluded by the presentation of a case study.

## Problems

**5-1** Develop the boundary conditions for a Francis turbine having a long pressurized downstream conduit.

**5-2** How are the boundary conditions of Problem 5-1 be modified if there is a downstream surge tank?

**5-3** The block diagram for a proportional-integral-derivative (PID) governor is shown in Fig. 5-29. Proceeding similarly as in Section 5-5, derive the differential equations for this governor.

**5-4** Figure 3-24 shows the layout for the Jordan River Power Plant in which a pressure-regulating valve (PRV) is provided to reduce the transient pressures. In a load-rejection test on the prototype, the wicket gates closed, and the PRV opened as shown in Fig. 10-11. Develop a mathematical model to analyze the transients caused by a load rejection, and compare the computed results with

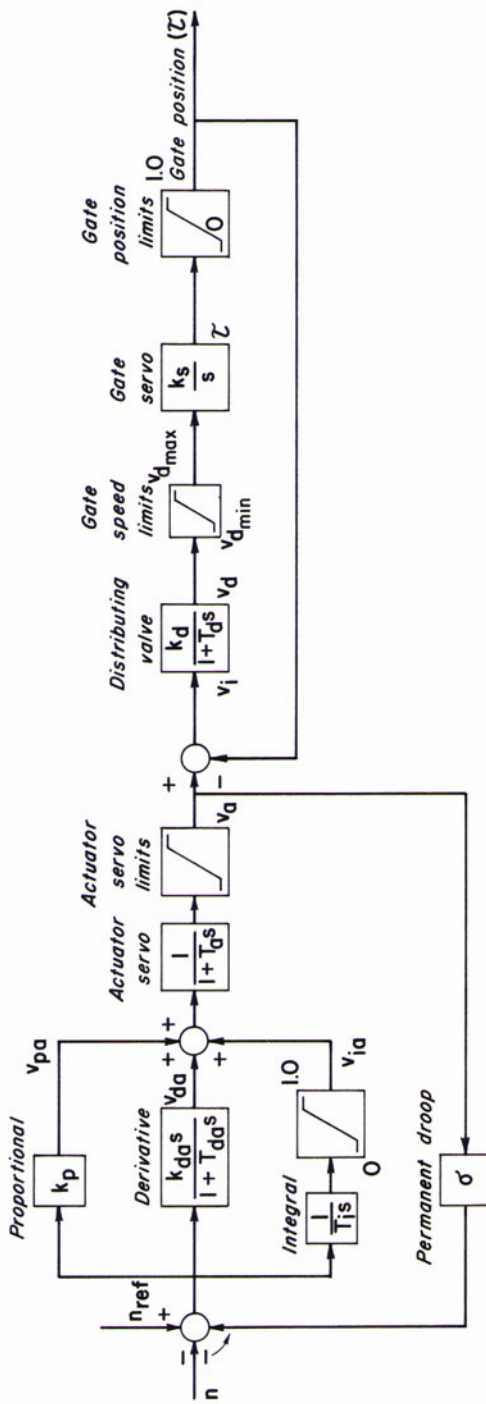


Fig. 5-29. Block diagram for a PID governor.

those measured on the prototype (Fig. 10-12). Assume the unit is isolated from the system and there is a delay of 0.4 s between the opening of the PRV and the closure of the wicket gates. Use the turbine characteristics of Fig. 5-3.

**5-5** Develop the boundary conditions for a Kaplan turbine taking into consideration the variation of the blade angle.

**5-6** Determine the required moment of inertia of the turbogenerator set for the stable governing of a hydroelectric power plant in isolated operation. The data for the power plant follow:

Rated output = 39 MW

Synchronous speed = 500 rpm

Rated head = 240 m

Turbine discharge at rated conditions = 38 m<sup>3</sup>/s

Length of the penstock = 640 m

Length of the scroll case = 36 m

Cross-sectional areas of the penstock, and the scroll case at the upstream end = 7.9 m<sup>2</sup>

Governor opening and closing time = 5 s

Neglect the length of the draft tube and assume a power factor of 0.95 while computing the *kva* of the unit.

**5-7** What are the optimum governor settings for the unit of Problem 5-6?

## References

- Anonymous, 1973, "Speed Governor Fundamentals," *Bulletin 25031*, Woodward Governor Company, Rockford, IL.
- Anonymous, 1977, "IEEE Recommended Practice for Preparation of Equipment Specifications for Speed Governing of Hydraulic Turbines Intended to Drive Electric Generators," Amer. Inst. of Elect. and Electronics Engrs., April.
- Boldy, A. P. and Walmsley, N., 1982, "Performance Characteristics of Reversible Pump Turbines," *Proc. Symp. on Operating Problems of Pump Stations and Power Plants*, International Association for Hydraulic Research, vol. 3, Sept.
- Boldy, A. P. and Walmsley, N., 1983, "Representation of the Characteristics of Reversible Pump Turbines For Use in Waterhammer Simulations." *Proc. Fourth International Conf. on Pressure Surges*, British Hydromechanics Research Association, Sept., pp. 287-296.
- Chaudhry, M. H., 1970, "Governing Stability of a Hydroelectric Power Plant," *Water Power*, London, April, pp. 131-136.

- Chaudhry, M. H. and Ruus, E., 1970, "Analysis of Governing Stability of Hydroelectric Power Plants," *Trans.*, Engineering Inst. of Canada, vol. 13, June, pp. I-V.
- Chaudhry, M. H. and Portfors, E. A., 1973, "A Mathematical Model for Analyzing Hydraulic Transients In a Hydroelectric Powerplant," *Proc. First Canadian Hydraulic Conf.*, University of Alberta, Edmonton, Canada, May 1973, p. 298-314.
- Chaudhry, M. H., 1979, "Governing Stability of Hydraulic Turbines," in *Transient Flow and Hydromachinery*, edited by Shen, H. T., Lecture Notes for Short Course, Colorado State Univ., Chap. 6.
- Chaudhry, M. H., 1980, "A Nonlinear Mathematical Model for Analysis of Transients Caused by a Governed Francis Turbine," *Proc. Third International Conf. on Pressure Surges*, British Hydromechanics Research Assoc., England, March, pp. 301-310.
- Computer Applications, 2013, "A computer Program for Analyzing Water hammer in Pumping systems and Hydroelectric Powerplants," (WH version 6.0), *User's Manual*, 83 pp.
- D'Azzo, J. J. and Houpis, C. H., 1966, *Feedback Control System Analysis and Synthesis*, Second ed., McGraw-Hill Book Co., New York, NY.
- Enever, K. J. and Hassan, J. M., 1983, "Transients Caused by Changes in Load on a Turbogenerator Set Governed by a PID Governor," *Proc. Fourth International Conf. on Pressure Suges*, British Hydromechanics Research Association, Sept., pp. 313-324.
- Fischer, S. G., 1973, "The Westinghouse Leading Edge Ultrasonic Flow Measuremenl System," Presented at the Spring Meeting, Amer. Soc. of Mech. Engineers, Boston, Mass., May 15-16.
- Gordon, J. L., 1961, "Determination of Generator Inertia," Presented to the Canadian Electrical Association, Halifax, Jan.
- Hagihara, S., Yokota, H., Goda, K., and Isobe, K., 1979, "Stability of a Hydraulic Turbine Generating Unit Controlled by PID Governor," Presented at Inst. of Elect. and Electronics Engrs., PES Winter Meeting, New York, Feb.
- Hovey, L. M., 1960, "Optimum Adjustment of Governors in Hydro Generating Stations," *Engineering Journal*, Engineering Inst. of Canada, Nov., pp. 64-71.
- Hovey, L. M., 1961, "The Use of an Electronic Analog Computer for Determining Optimum Settings of Speed Governors for Hydro Generating Units," *Annual General Meeting*, Eng. Inst. of Canada,Paper No.7, pp. 1-40.
- Hovey, L. M., 1962, "Speed Regulation Tests on a Hydrostation Supplying an Isolated Load," *Trans. Amer. Inst. of Elect. Engrs.*, pp. 364-368.
- Hovey, L. M., 1962, "Optimum Adjustment of Hydro Governors on Manitoba Hydro System," *Trans. Amer. Inst. of Elect. Engrs.*, Dec., pp. 581-486.
- Krivehenko, G. I., Zolotov, L. A., and Klabukov, V. M., 1971, "Moment Characteristics of Cascades under NOn-stationary Flow Conditions," *Proc. Annual Meeting*, International Association for Hydraulic Research, vol. 2, Paris, pp. B11-1 - B11-9.

- Krueger, R. E., 1980, "Selecting Hydraulic Reaction Turbines," *Engineering Monograph No. 20*, United States Bureau of Reclamation, Denver, CO.
- Lathi, B. P., 1965, *Signals, Systems and Communications*, John Wiley & Sons, New York, NY.
- Martin, C. S., 1982, "Transformation of Pump-Turbine Characteristics for Hydraulic Transient Analysis," *Proc. Symp. on Operating Problems of Pump Stations and Power Plants*, International Association for Hydraulic Research, vol. 2, Sept.
- McCracken, D. D. and Dorn, W. S., 1964, *Numerical Methods and Fortran Programming*, John Wiley & Sons, New York, NY.
- Parmakian, J., 1957, "Water Hammer Design Criteria," *Jour. Power Div.*, Amer. Soc. of Civ. Engrs., April, pp. 1216-1-1216-8.
- Parmakian, J., 1963, *Waterhammer Analysis*, Dover Publications, New York, NY.
- Parmakian, J., 1986, Private communication with M. H. Chaudhry.
- Paynter, H. M., 1955, "A Palimpsest on the Electronic Analogue Art," A. Philbrick Researches, Inc., Boston, MA.
- Paynter, H. M., 1972, "The Dynamics and Control of Eulerian Turbomachines," *Jour. of Dynamic Systems, Measurement, and Control*, Amer. Soc. of Mech. Engrs., vol. 94, pp. 198-205.
- Paynter, H. M., 1979, "An Algebraic Model of a Pump Turbine," *Proc. Symp. on Pump Turbine Schemes*, Amer. Soc. of Mech. Engrs, June, p. 75-94.
- Perkins, F. E., et al., 1964, "Hydropower Plant Transients," *Report 71, Parts II and III*, Hydrodynamics Lab., Department of Civil Engineering, Massachusetts Inst. of Tech., Cambridge, MA., Sept. 1964.
- Portfors, E. A. and Chaudhry, M. H., 1972, "Analysis and Prototype Verification of Hydraulic Transients in Jordan River Powerplant," *Proc. First International Conf. on Pressure Surges*, Canterbury, England, British Hydromechanics Research Association, Sept., pp. E4-57 - E4-72.
- Stein, T., 1947, "The Influence of Self-Regulation and of the Damping Period on the  $WR^2$  Value of Hydroelectric Power Plant," *The Engineers' Digest*, May-June 1948 (Translated from *Schweizerische Bauzeitung*, vol. 5, no. 4, Sept.-Oct.
- Streeter, V. L., 1966, *Fluid Mechanics*, Fourth ed., McGraw-Hill Book Co., New York, NY.
- "Mechanical Design of Hydro Plants," *Technical Report No. 24*, Tennessee Valley Authority Projects, vol. 3, 1960.
- Thorne, D. H. and Hill, E. F., 1974, "Field Testing and Simulation of Hydraulic Turbine Governor Performance," *Trans.*, Inst. of Elect. and Electronics Engrs., Power Apparatus and Systems, July/Aug., pp. 1183-1191.
- Thorne, D. H. and Hill, E. F., 1975, "Extension of Stability Boundaries of a Hydraulic Turbine Generating Unit," *Trans.*, Inst. of Elect. and Electronics Engrs., vol. PAS-94, July / Aug., pp. 1401-1409.

Wozniak, L., 1976, "Discussion of Transient Analysis of Variable Pitch Pump Turbines," *Jour. of Engineering for Power*, Amer. Soc. of Mech. Engrs., vol. 89, pp. 547-557.

### Additional References

- Almeras, P., 1947, "Influence of Water Inertia on the Stability of Operation of a Hydroelectric System," *Engineer's Digest*, vol. 4, Jan. 1947, pp. 9-12, Feb., pp. 55-61.
- Araki, M. and Kuwabara, T., "Water Column Effect on Speed Control of Hydraulic Turbines and Governor Improvement," *Hitachi Review*, vol. 22, no. 2, pp. SO-55.
- Blair, P. and Wozniak, L., 1976, "Nonlinear Simulation of Hydraulic Turbine Governor Systems," *Water Power and Dam Construction*, Sept.
- Brekke, H., 1974, "Stability Studies for a Governed Turbine Operating under Isolated Load Conditions," *Water Power*, London, Sept., pp. 333-341.
- Concordia, C. and Kirchmayer, L. K., "Tie-Line Power and Frequency Control of Electric Power Systems," Parts I and II, *Trans.*, Amer. Inst. of Elect. Engrs., June 1953, pp. 562-572; Apr. 1954, pp. 1-14. (See also discussion by H. M. Paynter.)
- Dennis, N. G., 1953, "Water-Turbine Governors and the Stability of Hydroelectric Plant," *Water Power*, Feb., pp. 65-76; Mar., pp. 104-109; Apr., pp. 151-154; May, pp. 191-196.
- Goldwag, E., 1971, "On the Influence of Water Turbine Characteristic on Stability and Response," *Jour. Basic Engineering*, Amer. Soc. of Mech. Engrs., Dec., pp. 480-493.
- Lein, G. and Parzany, K., 1967, "Frequency Response Measurements at Vianden," *Water Power*, July, pp. 283-286, Aug., pp. 323-328.
- Newey, R. A., 1967, "Speed Regulation Study for Bay D'Espoir Hydroelectric Generating Station," *Paper No. 67-WA/FE-17*, Presented at Winter Annual Meeting, Amer. Soc. of Mech. Engrs., Dec.
- Oldenburger, R., 1964, "Hydraulic Speed Governor with Major Governor Problems Solved," *Jour. Basic Engineering*, Amer. Soc. of Mech. Engrs., Paper No. 63-WA-15, pp. 1-8.
- Petry, B. and Jensen, P., 1982, "Transients in Hydroelectric Developments: Design and Analysis Considerations on Recent Projects in Brazil," *Proc., Seminar on Hydraulic Transients*, Koelle, E. and Chaudhry, M. H. (eds.), in English with Portuguese translation, vol. 2, Sao Paulo, Brazil, pp. HI-1 to I-60.
- Schleif, F. R. and Bates, C. G., 1971, "Governing Characteristics for 820,000 Horsepower Units for Grand Coulee Third Powerplant," *Trans.*, Inst. of Elect. and Electronics Engrs., Power Apparatus and Systems, Mar./Apr., pp. 882-890.
- Stein, T., 1970, "Frequency Control under Isolated Network Conditions," *Water Power*, Sept.

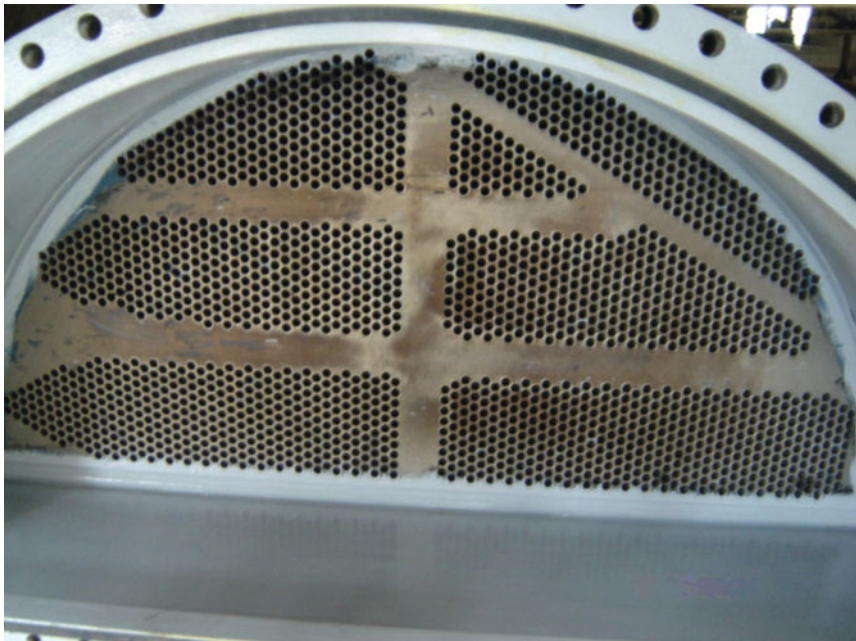
Vaughan, D. R., 1962, "Speed Control in Hydroelectric Power Systems," Thesis submitted to Massachusetts Institute of Technology in partial fulfillment of the requirements for the degree of doctor of philosophy.

Wozniak, L. and Fett, G. H., 1972, "Conduit Representation in Closed Loop Simulation of Hydroelectric Systems," *Jour. Basic Engineering*, Amer. Soc. of Mech. Engrs., Sept., pp. 599-604. (See also discussion by Chaudhry, M. H., pp. 604-605).

"Waterhammer in Pumped Storage Projects," *International Symp.*, Amer. Soc. Mech. Engrs., Nov. 1965.

International Code of Testing of Speed Governing Systems for Hydraulic Turbines, Technical Committee No.4, Hydraulic Turbines, International Electrotechnical Commission, Feb. 1965.

## TRANSIENTS IN COOLING-WATER SYSTEMS



Cooling-water condenser, 4.2-m diameter, 14.63-long, has 4.27-m high and 1.83-m wide water boxes and 25-mm diameter, 11-m long, titanium tubes. The coolant is seawater. (Courtesy, Abu Morshedi, M. A. Power Corporation, Canada.)

## 6-1 Introduction

Cooling-water systems are utilized in thermal and nuclear power plants to condense steam after it leaves the turbine. The condensed water is then used in the steam generators. For this purpose, steam is passed around a large number of small-diameter tubes through which cooling water, or coolant, is pumped. These tubes are contained in a large chamber, known as a *condenser*. The temperature of the cooling water rises as it passes through the tubes. The heated coolant is either discharged into a large body of water, such as a river, lake, estuary, etc., or it is cooled for re-use by passing it through a cooling tower, a cooling pond, etc.

Transient-state conditions in the cooling-water systems may be produced by several operations. It is necessary to analyze these conditions for the design of these systems. This chapter outlines such analyses. A brief description of cooling-water systems is first presented; several operations that may produce transients are then discussed. Typical boundary conditions are developed for the analysis of these systems by the method of characteristics.

## 6-2 Cooling-Water Systems

In this section, we discuss different types of cooling-water systems, typical layouts, and components.

### Classification

The cooling-water systems may be classified as: a once-through system, recirculating system, or a combination of once-through and recirculating systems [Jones, 1977; DeClemente et al., 1978; Martin and Chaudhry, 1981 and Martin and Wiggert, 1986]. A brief description of each follows.

### Once-through System

In a once-through system (Fig. 6-1), water is drawn from a large body of water, e.g., river, lake, reservoir, estuary, ocean, etc., and is pumped through the condenser tubes. The heated cooling water is then returned to the original source. Since environmental considerations do not allow significant increase in the temperature of the coolant, large volumes of cooling water become necessary. This type of system is usually a low-head system with sub-atmospheric pressures in the condensers during the steady-state conditions. A seal-well weir or a diffuser may be provided at the outfall.

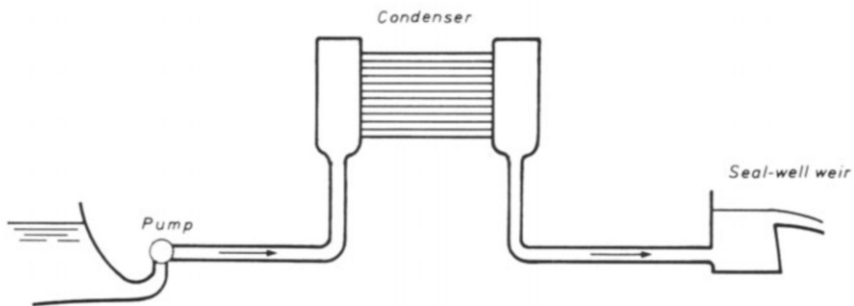


**Fig. 6-1.** Once-through cooling-water system.

### Recirculating System

A cooling facility, such as a cooling tower, a cooling pond, a spray pond, etc., is used in recirculating systems (Fig. 6-2) to cool the heated coolant so that it may be reused in the condensers. Systems with cooling towers are high-head systems in which the condensers are pressurized. If the condensers are lower than the cooling towers, then the pumps may be located downstream from the condensers.

### Combined Once-through Recirculating System

As the name implies, a combined system has both the once-through and the recirculating systems. This type of system is employed for retrofitting or backfitting (Fig. 6-3). This may be required to increase the capacity of an existing system to meet environmental requirements, or to utilize them during periods of low flows or higher water temperatures in the original source of water.

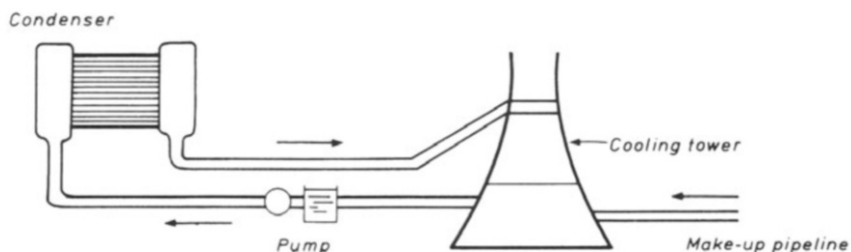


**Fig. 6-2.** Recirculating cooling-water system.

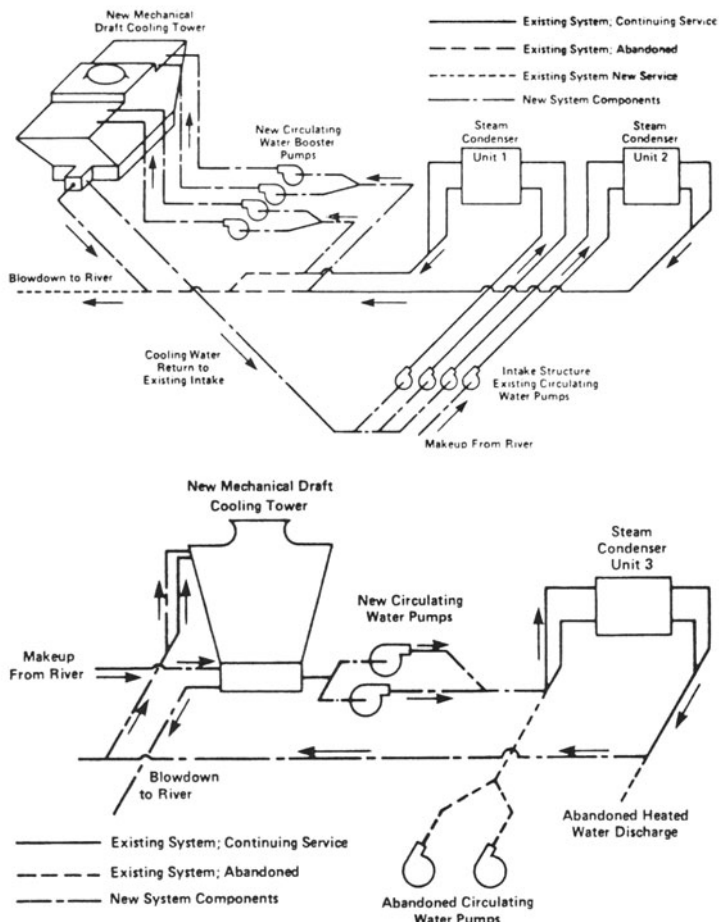


Fig. 6-3. Backfit cooling-water systems. (After DeClemente et al. [1978].)

### Layout

The layout and configuration of cooling-water systems vary from one installation to another. The layout of the inlet and outlet conduit systems, interconnection of various conduits, and the number of pumps and condensers per tunnel may vary significantly. Cooling towers, cooling ponds, spray ponds, seal-well weirs, submerged diffusers, etc., may be provided, depending upon the site conditions.

A number of typical arrangements [Martin and Wiggert, 1986] for cooling-water systems are presented in Fig. 6-4. Arrangement A is the most widely used. Each tunnel in this arrangement may have two or more pumps. Because of interconnection, Arrangement B provides more flexibility of operation as

compared to Arrangement A. For the once-through systems requiring long diffusers, either Arrangement C or Arrangement D may be used.

## Components

The main components of a cooling-water system are: intake; inlet conduit; pumps; valves; condensers; and outlet conduits. Seal-well weir, outfall diffuser, cooling towers, cooling ponds, etc., may be provided on some systems.

The intakes are designed so that no vortices are formed at the entrance. Typically, two or more pumps are installed in parallel, although sometimes a single pump is used. A system with multiple pumps provides more flexible and efficient operation for servicing or for running the plant at partial capacity or following breakdown. For multiple parallel pumps, a discharge valve is installed downstream of each pump. This valve allows isolation of the inoperative pump to prevent backflow through the pump.

There are several types of condensers [Langley, 1981], as shown in [Fig. 6-5](#). Once-through systems are usually designed so that the pressure in the outlet water box or at the highest point of the outlet conduit system is subatmospheric during the steady-state conditions. Vacuum breakers or air admission valves are commonly used on the outlet water box for surge protection. These valves are activated by a signal triggered by a pump trip or when the water level in the water box falls below a specified level. The use of minimum water level for triggering the vacuum breakers should be preferred. Since the siphoning action of the condenser may result in the accumulation of air in the water boxes and in the upper part of the condenser tubes, vacuum pumps are usually employed to purge air from the system.

Seal-well weirs are provided to keep the outlet conduit system primed during the steady-state conditions. The weir level is selected such that design vacuum pressure is obtained in the outlet box of the condenser or at the highest point of the outlet conduit system.

Environmental concerns may dictate provision of submerged diffusers at the outfall in once-through systems.

## 6-3 Causes of Transients

Transient conditions in the cooling-water systems may be produced by the following operations [Richards, 1956; Richards, 1959; Scarborough and Webb, 1968; Sheer, 1972]:

- Power failure to the pumps;
- Opening or closing of valves;
- Planned tripping of one or more pumps;
- Pump start-up; and
- Filling or emptying of the system.

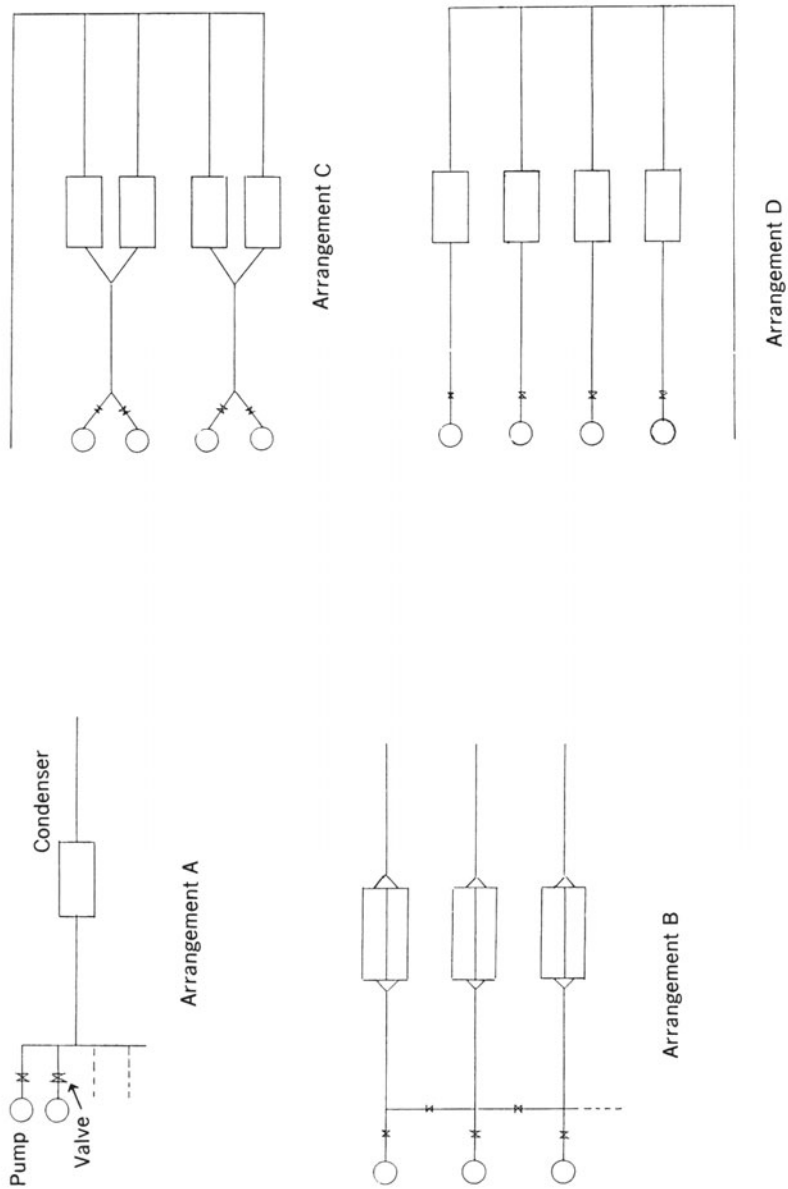
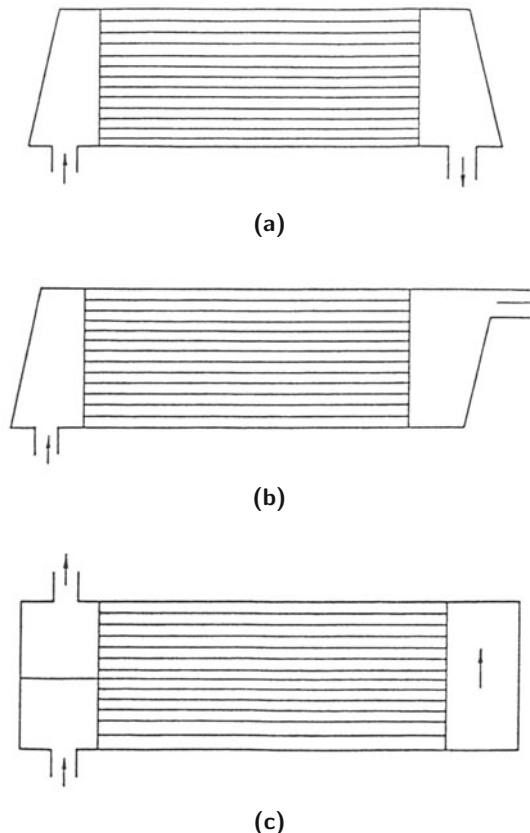


Fig. 6-4. Different layouts for cooling-water systems. (After Martin and Wiggert [1986].)



**Fig. 6-5. Types of condensers.** (After Langley [1981].)

Power failure appears to be the most critical operation, especially since the pump inertia is usually small. Therefore, following a power failure, water is decelerated very rapidly, and the risk of water-column separation is increased. Similarly, due to subatmospheric steady-state pressures, the probability of water-column separation increases. The most vulnerable location for severe negative pressure transients is usually the downstream condenser water box.

## 6-4 Analysis Procedures

Normally the components of a cooling-water system are the same as those of a typical piping system, except for the condensers and the diffusers. However, the presence of air in the cooling-water systems makes an accurate prediction of transient pressures in these systems very difficult [Sheer, 1972; Papadakis and Hollingshead, 1976 and Martin and Wiggert, 1986].

Free air may be present [Martin and Wiggert, 1986] in a cooling-water system as entrapped or entrained air in the form of small bubbles, slugs, or large masses. Entrapped air is stationary and remains at high points, bends, etc. The entrained air is, however, transported through the system in the form of bubbles and slugs. Free air may be introduced into a cooling-water system at the intake, through leaking seals, gas release during the steady state due to low pressures and high temperatures, and air remaining in the system from initial filling.

A comparison of computed results including the effects of free air in the analysis shows poor agreement with prototype measurements. Mathematical models that include free air and/or air release during the transient conditions range from simple waterhammer codes with lumped air at specified locations in the system to sophisticated models in which the air-water mixture is considered as a pseudo-fluid [Wiggert et al., 1983]. As shown by Martin and Wiggert [1986], the level of sophistication used in handling the free air is not as important as an accurate estimation of the quantity of free air in the system. Unfortunately, analytical or empirical procedures are presently unavailable for determining the quantity of air in a system precisely.

The flow in a cooling-water condenser is very complex. However, condensers have been included in a number of computer codes in a very simplified manner. A few typical simplified procedures for the simulation of a condensers are:

- i. A fixed orifice including the head losses, but excluding the effects of inertia of water and the passage of pressure waves.
- ii. An equivalent pipe including the water inertia and friction, but excluding the passage of pressure waves.
- iii. An equivalent pipe including the friction losses, water inertia, and the passage of pressure waves.

These simplified models do not allow the simulation of dewatering and refilling of condensers. However, this may be done by considering a number of equivalent pipes located at different levels [Zielke, 1979].

For modeling the water boxes, it is necessary to incorporate the variable-area geometry, air masses, and vacuum breakers. The elastic properties of water boxes include the compressibility of air mass, compressibility of water, and the elasticity of the box material. If air is present, then the compressibility of water and the elasticity of the box material are small compared to the compressibility of the air. Therefore, the compressibility of water and the elasticity of the box material may be neglected.

The water level in the outlet water boxes should be modeled accurately to simulate proper hydraulic gradient in the outlet conduit. This allows correct deceleration and reversal of the water column in the downstream conduit.

Outfall diffusers may be modeled by a number of equivalent orifices, say four or five, placed along the length of the diffuser [Zielke, 1979].

Since a large amount of free air is usually present in the cooling-water systems during the steady-state conditions, the amount of air released during the transient conditions due to depressurization is negligible. The latter may, therefore, be safely neglected during the analysis of real-life situations.

Martin and Wiggert [1986] show that if the majority of air is concentrated at the condenser, then standard waterhammer codes with a lumped-air boundary condition are adequate for engineering calculations. However, if air is distributed throughout the length of the downstream tunnel, then homogeneous, two-phase flow models [Wiggert et al., 1983] may become necessary.

The method of characteristics presented in Chapter 3 is satisfactory for the analysis of single-phase flows. A reduced wave velocity (see Sections 2-6 and 9-5) may be used in the analysis to account for a small amount of gaseous phase in the liquid,

The transients caused by opening or closing of valves, by starting or stopping of pumps, or by power failure to the pump-motors may be analyzed by using the method of characteristics. A number of commonly used boundary conditions are derived in Chapter 3 and 4, and a few more are developed in the next section and in Chapter 10.

Two-phase flows may be analyzed by considering them as homogeneous or separated flows. The liquid mixture may be treated as a pseudofluid in homogeneous flow using the averaged values of various variables, such as pressure, flow velocity, and void fraction over a cross section. The spatial variation of void fraction may be included in the analysis.

In the analysis of separated flows, each phase is treated separately, and the transfer of mass, momentum, and energy between each phase is taken into consideration. Analysis of these flows are beyond the scope of this book.

The following numerical methods have been used for the analysis of homogeneous two-phase flows: method of characteristics; Lax-Wendroff finite-difference method; explicit finite-difference methods; and implicit finite-difference methods.

In the method of characteristics, the discontinuities in the derivatives can be handled, and the boundary conditions are properly posed. The method, however, fails because of the convergence of characteristics if the wave velocity depends highly on pressure, and a shock is formed in the solution. In addition, if an explicit finite-difference scheme is used to solve the total differential equations obtained by this method, the Courant-Fredrich-Levy condition for the stability of the numerical scheme has to be satisfied. This condition requires small computational time steps, thus making the method unsuitable for solving large real-life systems. The method may, however, be used to verify other numerical schemes by analyzing small, simple systems.

The Lax-Wendroff finite-difference scheme [Lax and Wendroff, 1960] or other higher-order schemes [Chaudhry and Hussaini, 1983, 1985] may be used for analyzing systems in which a shock forms. However, these schemes produce spurious oscillations in the solution near the wave front, and a smoothening procedure has to be utilized. This introduces numerical damping, which is not

present in the actual system and which, if not properly taken care of, may smoothen the transient peaks.

Explicit finite-difference methods are easy to program. However, as the step size is limited by the Courant stability condition, a large amount of computer time is required. Thus, the method is not attractive for analyzing large systems.

The time step in the implicit finite-difference methods is governed by the accuracy considerations and not by the stability requirements. These methods are, therefore, useful for the analysis of large systems.

## 6-5 Boundary Conditions

To analyze a cooling-water system by the method of characteristics, the boundary conditions for a condenser and for a volume of entrapped air are derived in this section. Note that these conditions are suitable only for single-phase flows.

### Condenser

A condenser is comprised of a large number of tubes with a water box at each end (Fig. 6-6). To derive the boundary condition, the cluster of tubes may be replaced by an equivalent pipe having a cross-sectional area,  $A_e$ , equal to the combined area of all the tubes, i.e.,  $A_e = n_t A_t$  in which  $A_t$  = cross-sectional area of a tube and  $n_t$  = number of tubes in the condenser. The head loss in the equivalent pipe is, however, assumed equal to the head loss in an individual tube. The water boxes may be considered as lumped capacitances, and the compressibility of water and the elasticity of the walls of the boxes may be taken into consideration.

Equations for the upstream water box are derived in the following paragraphs; equations for the downstream box may be derived in a similar manner.

Let the volume of water in the box be  $\nabla$ , and let the combined effective bulk modulus of water inside the box and the vessel walls be  $K$ . Then, by definition,

$$K = \frac{\Delta p}{\frac{\Delta \nabla}{\nabla}} \quad (6-1)$$

in which  $\Delta \nabla$  is the change in volume due to change in pressure,  $\Delta p$ . For the pressure changes usually encountered in practice, the change in volume is small and may be neglected. The change in volume,  $\Delta \nabla$ , due to time variation of inflow and outflow from the water box during a time step,  $\Delta t$ , may be determined from the continuity equation

$$\Delta \nabla = \frac{1}{2} \Delta t [(Q_{P_{i,n+1}} + Q_{i,n+1}) - (Q_{P_{i+1,1}} + Q_{i+1,1})] \quad (6-2)$$

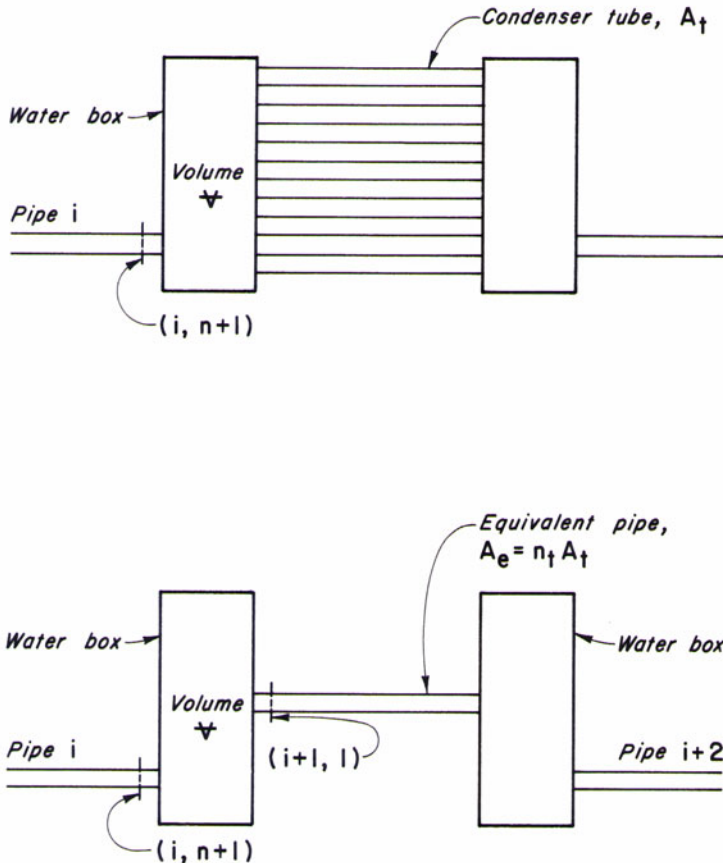


Fig. 6-6. Condenser.

in which  $Q$  and  $Q_P$  are discharges at the beginning and at the end of the time step, and subscripts  $(i, n + 1)$  and  $(i + 1, 1)$  refer to the section numbers (see Fig. 6-6). Assuming the pressure to be same throughout the box

$$H_{P_{i,n+1}} = H_{P_{i+1,1}} \quad (6-3)$$

in which  $H_P$  = piezometric head above the datum at the end of time step. Now, the change in pressure during the time step

$$\Delta p = \gamma \Delta H = \gamma (H_{P_{i,n+1}} - H_{i,n+1}) \quad (6-4)$$

in which  $\gamma$  = specific weight of water.

By substituting Eqs. 6-2 and 6-4 into Eq. 6-1 and simplifying the resulting equation, we obtain

$$H_{P_{i,n+1}} = H_{i,n+1} + \frac{K\Delta t}{2\gamma V} [(Q_{i,n+1} - Q_{i+1,1}) + (Q_{P_{i,n+1}} - Q_{P_{i+1,1}})] \quad (6-5)$$

The positive and negative characteristic equations (Eqs. 3-17 and 3-18 for sections  $(i, n+1)$  and  $(i+1, 1)$ ) are

$$Q_{P_{i,n+1}} = C_p - C_{a_i} H_{P_{i,n+1}} \quad (6-6)$$

$$Q_{P_{i+1,1}} = C_n + C_{a_{i+1}} H_{P_{i+1,1}} \quad (6-7)$$

in which  $C_p$ ,  $C_n$  and  $C_a$  are as defined by Eqs. 3-19 through 3-21. Substitution of Eqs. 6-3, 6-6, and 6-7 into Eq. 6-5 yields

$$\begin{aligned} H_{P_{i,n+1}} &= H_{i,n+1} + \frac{K\Delta t}{2\gamma V} [(Q_{i,n+1} - Q_{i+1,1}) + (C_p - C_n)] \\ &\quad - \frac{K\Delta t}{2\gamma V} (C_{a_i} + C_{a_{i+1}}) H_{P_{i,n+1}} \end{aligned} \quad (6-8)$$

Hence,

$$\begin{aligned} H_{P_{i,n+1}} &= \frac{2\gamma V}{2\gamma V + K\Delta t (C_{a_i} + C_{a_{i+1}})} \left\{ H_{i,n+1} \right. \\ &\quad \left. + \frac{K\Delta t}{2\gamma V} [(Q_{i,n+1} - Q_{i+1,1}) + (C_p - C_n)] \right\} \end{aligned} \quad (6-9)$$

Now,  $H_{P_{i+1,1}}$ ,  $Q_{P_{i,n+1}}$  and  $Q_{P_{i+1,1}}$  may be determined from Eqs. 6-3, 6-6, and 6-7, respectively.

### Entrapped Air

This boundary may be utilized for a node where air may be entrapped or where there is a possibility of liquid-column separation. The following boundary conditions is for an interior node with conduits on both the upstream and downstream sides. Proceeding similarly, the boundary conditions for a node at the upstream or at the downstream end of the conduit may be developed.

Let us consider a volume of air entrapped in a pipe having liquid on either side, as shown in Fig. 6-7. If the entrapped air follows the polytropic law for a perfect gas, then

$$H_{P_{\text{air}}}^* \nabla_{P_{\text{air}}}^* = C \quad (6-10)$$

in which  $H_{P_{\text{air}}}^*$  and  $\nabla_{P_{\text{air}}}^*$  are the absolute pressure head and volume of the entrapped air, respectively;  $m$  = exponent in the polytropic gas law, and constant  $C$  is determined from the initial steady-state conditions.

The following equation for the air volume may be written based on the continuity equation:

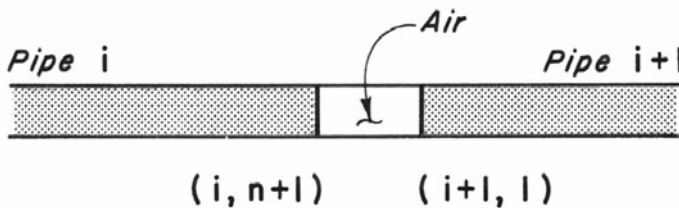


**Fig. 6-7. Entrapped air.**

$$\forall_{P_{\text{air}}}^* = \forall_{\text{air}} + \frac{1}{2} \Delta t \{ (Q_{i+1,1} + Q_{P_{i+1,1}}) - (Q_{i,n+1} + Q_{P_{i,n+1}}) \} \quad (6-11)$$

The positive and negative characteristic equations (Eqs. 3-17 and 3-18) for sections  $(i, n+1)$  and  $(i+1, 1)$  are

$$Q_{P_{i,n+1}} = C_p - C_{a_i} H_{P_{i,n+1}} \quad (6-12)$$

$$Q_{P_{i+1,1}} = C_n + C_{a_{i+1}} H_{P_{i+1,1}} \quad (6-13)$$

in which  $C_p$ ,  $C_n$ ,  $C_{a_i}$  and  $C_{a_{i+1}}$  are as defined by Eqs. 3-19 through 3-21. If the air pressure at any instant is assumed to be same throughout its volume, then

$$H_{P_{i,n+1}} = H_{P_{i+1,1}} \quad (6-14)$$

In addition,

$$\forall_{P_{\text{air}}}^* = H_b + H_{P_{i,n+1}} - z \quad (6-15)$$

in which  $H_b$  = barometric head, and  $z$  = height of the pipeline above the datum.

Now we have six equations (Eqs. 6-10 to 6-15) in six unknowns, namely,  $H_{P_{\text{air}}}^*$ ,  $\forall_{P_{\text{air}}}$ ,  $Q_{P_{i+1,1}}$ ,  $Q_{P_{i+1,1}}$ ,  $H_{P_{i+1,1}}$  and  $H_{P_{i,n+1}}$ . Elimination of the first five unknowns from these equations yields

$$(H_{P_{i,n+1}} + H_b - z) \left[ C_{\text{air}} + \frac{1}{2} \Delta t (C_{a_i} + C_{a_{i+1}}) H_{P_{i,n+1}} \right]^m = C \quad (6-16)$$

in which

$$C_{\text{air}} = \forall_{\text{air}} + \frac{1}{2} \Delta t (Q_{i+1,1} - Q_{i,n+1} + C_n - C_p) \quad (6-17)$$

Equation 6-16 may be solved for  $H_{P_{i,n+1}}$  by an iterative technique, such as the bisection or Newton-Raphson methods. The values of the remaining unknowns may then be determined from Eqs. 6-10 through 6-15.

## 6-6 Summary

In this chapter, a brief description of the cooling-water systems is presented. Various operations that produce transient conditions are then outlined. This is followed by a discussion of procedures for the analysis of transients in the cooling water systems. Typical boundary conditions of these systems are then developed.

## Problems

**6-1** Derive the boundary conditions for an air pocket entrapped in a pipeline. Assume the air is released slowly through an air valve as the air pressure increases.

**6-2** Develop the boundary conditions for a condenser in which the condenser tubes at higher level are unsubmerged as the water level in the condenser falls. (*Hint:* Replace the condenser tubes with a number of parallel pipes located at different levels. Consider the flow through only those pipes that are submerged.)

**6-3** Compare the computed pressures in a pipeline carrying an air-water mixture assuming: (i) the mixture as a pseudo-fluid and (ii) the air is lumped at discrete locations. Assume a typical value for the void fraction in the calculations.

**6-4** Develop the boundary for air entrapped at the upstream or at the downstream end of a conduit.

## References

- Anonymous, 1981, "The La Casella Thermal Power Station: Results of Unsteady Flow Regime Tests on Cooling Water Circuits of Condenser Groups 3 and 4," *ENEL Report 2995*, Sept.
- Chaudhry, M. H. and Hussaini, M. Y., 1983, "Second-Order Explicit Methods for Transient-Flow Analysis," in *Numerical Methods for Fluid Transients Analysis*, Martin, C. S. and Chaudhry, M. H. (eds.), Amer. Soc. Mech. Engrs., pp. 9-15.
- Chaudhry, M. H. and Hussaini, M. Y., 1985, "Second-Order Accurate Explicit Finite-difference Schemes for Waterhammer Analysis," *Jour. of Fluids Engineering*, vol. 107, Dec., pp. 523-529.
- Davison, B. and Hooker, D. G., 1979, "Grain Power Station: CW System Site Surge Tests," *Central Electricity Generating Board Report No. 715/34/12/EMB/80*, Nov.

- DeClemente, T. J., Caves, J. L., and Wahanik, R. J., 1978, "Hydraulics of Cooling System Backfits," *Proc., Symp. on Design and Operation of Fluid Machinery*, International Association for Hydraulic Research, Amer. Soc. Civ. Engrs. and Amer. Soc. Mech. Engrs., Fort Collins, June, pp. 475-487.
- De Vries, A. H., 1974, "Research on Cavitation due to Waterhammer in the Netherlands", *Proc., Second Round Table Meeting on Water Column Separation*, Vallomrosa, pp. 478-485.
- Hooker, D. G., 1980, "Grain Power Station: CW System Site Surge Tests," *Report No. 715/34/3/EMB/80*, Central Electricity Generating Board, June.
- Jolas, C., 1981, "Hydraulic Transients in Closed Cooling Water Systems," *Proc. Fifth International Symp. and IAHR Working Group Meeting on Water Column Separation*, Obemach, Universities of Hanover and Munich, pp. 381-399.
- Jones, W. G., 1977, "Cooling Water for Power Stations," *Proc., Inst. Civ. Engrs., Part I*, vol. 62, Aug., pp. 373-398.
- Kohara, I., Ogawa, Y., Iwakiri, T., and Shiraishi, T., 1973, "Transient Phenomena of Circulating Water System for Thermal and Nuclear Power Plants," *Technical Review*, Mitsubishi Heavy Industries, Oct., pp. 9-20.
- Langley, P., 1981, "Susceptibility of Once-Through, Siphonic Cooling Water Systems of Excessive Transient Pressures," *Proc. Fifth International Symp. and International Association for Hydraulic Research Working Group Meeting on Water Column Separation*, Obernach, University of Hanover and Munich, pp. 285-305.
- Lax, P. D. and Wendroff, B., 1960, "System of Conservation Laws," *Comm. on Pure and Applied Math.*, vol. 13, pp. 217-227.
- Martin, C. S. and Chaudhry, M. H., 1981, "Cooling-Water Systems," in *Closed-Conduit Flows*, Chaudhry, M. H. and Yevjevich, V., (eds.), Water Resources Publications, Littleton, CO, pp. 255-277.
- Martin, C. S. and Wiggert, D. C., "Critique of Hydraulic Transient Simulation in Cooling Water Systems," presented at Winter Annual Meeting, Amer. Soc. Mech. Eng., Dec.
- Martin, C. S. and Wiggert, D. C., 1986, "Hydraulic Transients in Circulating Cooling Water Systems," *Final Report*, vol. I, Prepared for Electric Power Research Institute, Georgia Institute of Technology and Michigan State University.
- Papadakis, C. N. and Hollingshead, D. F., 1976, "Air Release in the Transient Analysis of Condensers," *Proc., Second International Conf on Pressure Surges*, London, British Hydromechanics Research Association.
- Richards, R. T., 1956, "Water-Column Separation in Pump Discharge Lines," *Trans., Amer. Soc. Mech. Engrs.*, vol. 78, pp. 1297-1306.
- Richards, R. T., 1959, "Some Neglected Design Problems of Circulating Water Systems," *Consulting Engineer*, July, pp. 94-101.
- Scarborough, E. C. and Webb, K. A., 1968, "Cooling Water System for Torens Island Power Station-Operating Characteristics at Pump Startup and

- Shutdown: Waterhammer," *Mechanical and Chemical Engineering Trans.* (Australia), May, pp. 71-77.
- Sheer, T. J., 1972, "Computer Analysis of Water Hammer in Power Station Cooling Water Systems," Paper DI, *Proc. First International Conf on Pressure Surge*, British Hydromechanics Research Association, Canterbury.
- Siccardi, F., 1980, "The Problems of the Numerical Modeling of the Transients in Cooling Water Circuits with Liquid Column Separation," *Proc. Fourth Round Table and IAHR Working Group Meeting on Water Column Separation*, Cagliari, ENEL Report No. 383, pp. 300-312.
- Wahanik, R. J., 1972, "Circulating Water Systems Without Valves," *Proc. Jour. Power. Div.*, Amer. Soc. Civ. Engrs., vol. 98, Oct., pp. 187-199.
- Wiggert, D. C., 1968, "Unsteady Flows in Lines with Distributed Leakage," *Jour. Hydraulics Div.*, Amer. Soc. of Civ. Engrs., vol. 94, Jan., pp. 143-162.
- Wiggert, D. C., Lesmez, M., Martin, C. S., and Naghash, M., 1983, "Modeling of Two-Component Flows in Cooling Water Condenser Systems," *Proc. Sixth International Symp. and IAHR Working Group Meeting on Transients in Cooling Water Systems*, Bamwood, Gloucester, CEGB, England.
- Yow, W., Faibes, O. N., and Shiers, P. F., 1978, "Mathematical Modeling of Vacuum Breaker Valve Operation in a Cooling Water System," *Proc. Joint ASME-IAHRASCE Conf.*, Fort Collins, June, vol. I, pp. 463-473.
- Zielke, W., 1979, "StrOmungsschwankungen in Kiihwasserkreislaiifen und ihre numerische Simulation," *Wasserwirtschaft*, vol. 69, pp. 159-162.

### Additional References

- Almeida, A. B., 1982, "Cooling-Water Systems: Typical Circuits and Their Analysis," *Proc. International Seminar on Hydraulic Transients*, Koeller, E. and Chaudhry, M. H. (eds.), in English with Portuguese translation, vol. I, Sao Paulo, Brazil, pp. D1-D77.
- Proc. First Round Table Meeting on Water Column Separation*, Milan 1971.
- Proc. Second Round Table Meeting on Water Column Separation*, Vallombrosa 1974, ENEL Report 290; also published in L'Energia Elellrica, No.4 1975, pp. 183-485, not inclusive.
- Proc. Third Round Table Meeting on Water Column Separation*, Royaumont, Bulletin de la Direction des Etudes et Recherches, Series A, No.2 1977.
- Proc. Fourth Round Table and IAHR Working Group Meeting on Water Column Separation*, Cagliari, ENEL, Report No. 382 1980.
- Proc. Fifth International Symp. and IAHR Working Group Meeting on Water Column Separation*, Obemach, Univesities of Hanover and Munich 1981.
- Proc. Sixth International Symp. and IAHR Working Group Meeting on Transients in Cooling Water Systems*, Bamwood, Gloucester 1983, CEGB.
- Wylie, E. B., 1983, "Simulation of Vaporous and Gaseous Cavitation," *Proc. Symp. on Numerical Methods for Fluid Transient Analysis*, Amer. Soc. of Mech. Engrs., Houston, June, pp. 47-52.

## TRANSIENTS IN LONG OIL PIPELINES



**Alaska Pipeline**, 1.22-m diameter steel pipeline, carries freshly pumped crude oil from the largest American oil deposit at Prudhoe Bay, Alaska, 1315 km south to the ice-free port of Valdez, with maximum average daily throughput of about 2 million barrels/day during 1988. (Courtesy, M. Levshakoff, Alyeska Pipeline.)

## 7-1 Introduction

Cross-country pipelines transporting crude oil or refined products are usually hundreds of kilometers long with several pumping stations located along their length (Fig. 7-1). The pumping head of these stations mainly covers the friction losses in the pipeline. In a mountainous terrain, however, gravity lift may be required in addition to the friction losses.

The analysis of transients in oil pipelines, sometimes called oil-hammer analysis or surge analysis, is rather complex because the pipeline friction losses are large compared to the instantaneous pressure changes caused by sudden changes in the flow velocity. Prior to the availability of high-speed digital computers, these analyses were approximate. Therefore, a large factor of safety was used to allow for uncertainties in the computed results. Since the mid-sixties, the transient pressures for various operating conditions can be accurately predicted, thus allowing a reduction in the factor of safety.

In this chapter, a number of terms commonly used in the oil industry are first defined. Different operations and control devices that may produce transient conditions in the pipeline are discussed. A computational procedure to analyze the transient conditions in long pipelines by the method of characteristics is then presented.

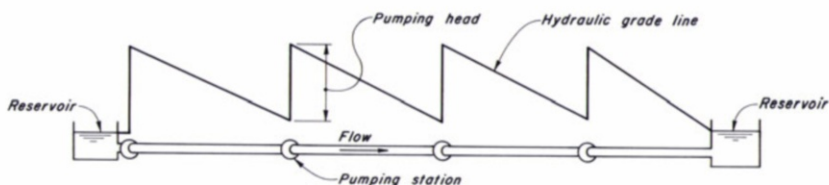


**Fig. 7-1. Schematic of a long oil pipeline.**

## 7-2 Definitions

The following terms [Ludwig and Johnson, 1950; Kaplan et al., 1967, Wylie and Streeter, 1971] are commonly used in the oil industry:

**Potential Surge.** The instantaneous pressure rise caused by instantaneously stopping the flow (i.e., reducing the flow velocity to zero) is defined as *potential surge*. The amplitude of the potential surge,  $Z$ , may be computed by utilizing the basic waterhammer equation of Chapter 1, Eq. 1-7. If  $V_o$  is the

initial steady-state velocity, then  $\Delta V = 0 - V_o = -V_o$ . Substituting this into Eq. 1-7, we obtain

$$Z = \Delta H = -\frac{a}{g} \Delta V = \frac{a}{g} V_o \quad (7-1)$$

in which  $\Delta H$  = instantaneous pressure rise due to the reduction of flow velocity  $V_o$  to zero;  $a$  = wave velocity; and  $g$  = acceleration due to gravity. If  $V_o$  and  $a$  are in m/s,  $g$  is in m/s<sup>2</sup>, then  $Z$  is in m.

**Line Packing.** The increase in the storage capacity of a pipeline due to an increase in pressure is called *line packing*. The following analogy should help in the understanding of this phenomenon.

Let us assume the flow velocity at the downstream end of the canal shown in Fig. 7-2 is suddenly reduced from  $V_o$  to zero by closing a sluice gate. This sudden reduction in the flow velocity produces a surge, which travels in the upstream direction. To simplify our discussion, let us assume the surge height remain constant as it travels in the upstream direction. If the rise in the water surface behind the wave front is the same as the surge, then the water surface is higher but parallel to the initial steady-state water surface (line cd in Fig. 7-2). Because the water surface is sloping in the downstream direction, water keeps on flowing toward the sluice gate even though the surge has passed a particular point in the canal. This process continues until the water level behind the wave front is horizontal. Since the velocity at the sluice gate is zero, the water flowing behind the surge is stored between the surge location and the sluice gate. Due to this storage, the water surface downstream of the

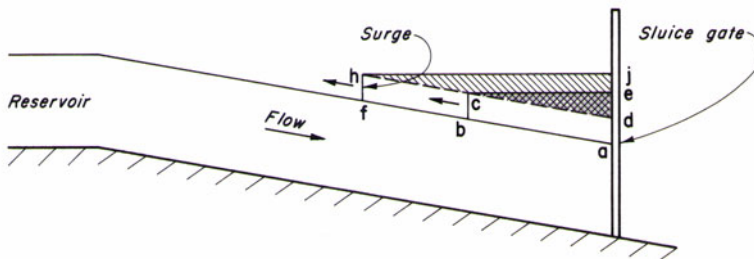


Fig. 7-2. Propagation of surge in a canal.

wave is almost horizontal. With further upstream travel of the surge from  $bc$  to  $fh$ , more water flows behind the surge, and the water level at the sluice gate rises from  $e$  to  $j$ . Thus, the shaded area in Fig. 7-2 is due to storage of water flowing downstream of the surge. At the downstream end, the water level rise from  $a$  to  $d$  is due to initial or potential surge, whereas the rise first

from  $d$  to  $e$  and then from  $e$  to  $j$  are due to storage of water between the surge location and the sluice gate.

Conditions are analogous in a long pipeline. Due to sudden closure of a downstream valve (Fig. 7-3), pressure rises instantaneously at the downstream end, and a wave having amplitude equal to the potential surge travels in the upstream direction. Just like the flow behind the surge in the canal, oil flows downstream of the wave front, pressure rises gradually at the downstream end, the hydraulic grade line becomes almost horizontal, and more oil is stored between the wave front and the valve. This increase in storage is called line packing. Referring to Fig. 7-3, the pressure rise at the valve is made up of two parts: potential surge,  $Z$ , produced due to instantaneous closure of the valve, and change in pressure,  $\Delta p$ , due to line packing.

Depending upon the length of the pipeline, the pressure rise due to line packing may be several times greater than the potential surge.

**Attenuation.** As discussed previously, oil keeps on flowing toward the valve even though the wave front has passed a particular location in the pipeline. In other words, the velocity differential ( $\Delta V$ ) across the wave front is reduced as the wave propagates in the upstream direction. Hence, it follows from Eq. 7-1 that the amplitude of the surge is reduced as it propagates along the pipeline due to reduction in the velocity differential across the wave front. This reduction in the surge amplitude is referred to as *attenuation*.

The surge amplitude is also reduced due to friction losses. However, this reduction is usually small as compared to that due to decrease in the velocity differential across the wave front.

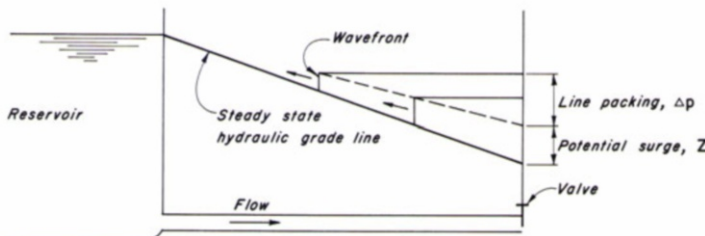


Fig. 7-3. Potential surge and line packing.

**Pyramidal Effect.** The superposition of one transient-state pressure upon another is referred to as *pyramidal effect*. For example, if a line were packed due to closure of a downstream valve or due to power failure to the pumps of

a downstream pumping station, and the pumps of an upstream station were started, then the pressure rise due to pump start-up is superimposed on the pressure due to line packing.

**Put-and-Take Operation.** In a put-and-take station operation, each station pumps oil from a tank on its suction side into a tank located on the suction side of the next station.

**Float-Tank Operation.** Float-tank operation is similar to the put-and-take station operation except that a float tank is open to the suction line of each station. The size of the float tank is usually smaller than that in the put-and-take operation.

**Tight-Line Operation.** In a tight-line station operation, each station pumps directly into the suction manifold of the downstream station, and no tanks are provided on the suction side. Such a system is called a *tight-line system* or a *closed system*.

**Station Regulation.** Maintenance of the pressures within the safe limits of the pipe and equipment by means of pressure controllers at each pumping station is called *station regulation*.

**Line Regulation.** The maintenance of an identical pumping rate at each pump station of a tight-line or closed system is referred to as *line regulation*.

**Rarefaction Control.** The planned reduction of flow at an upstream station to reduce pressure rise in the pipeline following a sudden accidental flow reduction at the downstream station is called *rarefaction control*. The flow at the pumping stations may be reduced by shutting down a pump or by closing a valve. A flow reduction at an upstream station produces a negative wave, which travels toward the downstream station. This wave nullifies part of the pressure rise caused by the upset at the downstream station.

## 7-3 Causes of Transients

The following operations and control devices [Ludwig and Johanson, 1950; Lundberg, 1966, Bagwell and Phillips, 1969] produce transient conditions in oil pipelines:

- Opening or closing the control valves;
- Starting or stopping the pumps;
- Power failure to the electric motors of pumping units;
- Change in the pumping rate and discharge pressure of pumping stations;
- Operation of the reciprocating pumps; and

Pipeline rupture.

Starting a pump or opening a valve at an intermediate station produces a pressure rise on the downstream side and a pressure drop on the upstream side, whereas a pump shutdown or closure of a valve produces a pressure rise on the upstream side and a pressure drop on the downstream side.

The flow and pressure on the suction and discharge sides of a reciprocating pump are periodic. If the period of the flow oscillations matches the natural period of the piping system, resonance develops (see Chapter 8). This may result in high-amplitude pressure fluctuations, which may damage the pipeline.

Air entrapped during filling or following major repairs may produce surges of high magnitude [Ludwig, 1956]. In addition, if air is present in the pipeline, there is a danger of an explosion, which may rupture the pipeline.

## 7-4 Methods of Analysis

The momentum and continuity equations derived in Chapter 2 describe the transient-state flow in an oil pipeline. Note that these equations are not valid for a simultaneous flow of gas and oil in a pipeline for which equations for a two-phase or two-component flow should be used.

To compute the transient conditions in a pipeline, the momentum and continuity equations are solved subject to appropriate boundary conditions. As discussed in Chapter 2, these equations can be integrated only by numerical methods since a closed-form solution is not possible because of the presence of nonlinear terms. The method of characteristics presented in Chapter 3 may be used for this purpose. However, as the friction losses in long oil pipelines are usually high, just satisfying the Courant stability condition for selected  $\Delta x$ , and  $\Delta t$ , does not ensure accurate and stable results [Holloway and Chaudhry, 1985]. In this case, in addition to the CFL condition, the stability conditions presented in Section 3-4 for different approximations of the friction-loss term,  $RQ|Q|$  of Eqs. 3-8 and 3-10 should be satisfied.

Since oil pipelines are usually very long, small time steps require an excessive amount of computer time. To avoid this, second-order approximations listed in Section 3-2 or a predictor-corrector scheme may be used. Both of these allow longer computational time intervals at the expense of slightly more computational effort.

In a second-order approximation [Holloway and Chaudhry, 1985], an average value of the friction term computed at points  $P$  and  $A$  ([Fig. 3-1](#)) is used for Eq. 3-8, and an average value of the friction term computed at points  $P$  and  $B$  is used for Eq. 3-10. This results in two nonlinear algebraic equations in  $Q_P$  and  $H_P$ . These equations may be solved by the Newton-Raphson method. In the predictor-corrector scheme, presented by Evangelisti [1969], a first-order approximation is used to determine the discharge at the end of the

time step. This predicted value of the discharge is then used in the corrector part to compute the friction term.

The predictor-corrector scheme is easy to program, and yields sufficiently accurate results. Details of this scheme follow.

Referring to [Fig. 3-1](#), the pressure and flow are known at time  $t_o$  and we want to determine their values at point  $P$ . At  $t_o = 0$ , these are initial steady-state conditions, and for  $t_o > 0$ , these are computed values for the previous time step.

For the predictor part, the integration of Eqs. 3-8 and 3-10 by a first-order approximation yields

$$Q_P^* - Q_A + C_a (H_P^* - H_A) + RQ_A |Q_A| = 0 \quad (7-2)$$

$$Q_P^* - Q_B - C_a (H_P^* - H_B) + RQ_B |Q_B| = 0 \quad (7-3)$$

in which the notation of Section 3-2 is used except that an asterisk is used to designate the predicted values of various variables,  $R = f\Delta t/(2DA)$ , and  $\int_{x_o}^{x_1} f(x)dx \approx f(x_o)(x_1 - x_o)$  is a *first-order approximation*.

Equations 7-2 and 7-3 may be written as

$$Q_P^* = C_p^* - C_a H_P^* \quad (7-4)$$

and

$$Q_P^* = C_n^* + C_a H_P^* \quad (7-5)$$

in which  $C_p^*$  and  $C_n^*$  are computed from Eqs. 3-19 and 3-20, respectively. Elimination of  $H_P^*$  from Eqs. 7-4 and 7-5 yields

$$Q_P^* = 0.5 (C_p^* + C_n^*) \quad (7-6)$$

Now this value of  $Q_P^*$  may be used in the corrector part to calculate the friction term. Integration of Eqs. 3-8 and 3-10 by using a second-order approximation ( $\int_{x_o}^{x_1} f(x)dx \approx \frac{1}{2} [f(x_o) + f(x_1)](x_1 - x_o)$  is a *second-order approximation*). and by using  $Q_P^*$  for computing the friction term yields

$$Q_P - Q_A + C_a (H_P - H_A) + 0.5R (Q_A |Q_A| + Q_P^* |Q_P^*|) = 0 \quad (7-7)$$

$$Q_P - Q_B - C_a (H_P - H_B) + 0.5R (Q_B |Q_B| + Q_P^* |Q_P^*|) = 0 \quad (7-8)$$

Equations 7-7 and 7-8 may be written as

$$Q_P = C_p - C_a H_P \quad (7-9)$$

and

$$Q_P = C_n + C_a H_P \quad (7-10)$$

in which

$$C_p = Q_A + C_a H_A - 0.5R (Q_A |Q_A| + Q_P^* |Q_P^*|) \quad (7-11)$$

$$C_n = Q_B - C_a H_A - 0.5R (Q_B |Q_B| + Q_P^* |Q_P^*|) \quad (7-12)$$

By eliminating  $H_P$  from Eqs. 7-9 and 7-10, we obtain

$$Q_P = 0.5(C_p + C_n) \quad (7-13)$$

Now  $H_P$  may be determined from either Eq. 7-9 or 7-10.

To determine the flow and the pressure at the boundaries, the boundary conditions derived in Chapters 3 and 10 are first used to compute  $Q_P^*$  for the predictor part. Then, this value of  $Q_P^*$  is used to compute  $C_p$  and  $C_n$  from Eqs. 7-11 and 7-12, and the same boundary conditions are used again to determine  $Q_P$  and  $H_P$  in the corrector part before proceeding to the next time step. The other computational steps are the same as described in Section 3-2.

## 7-5 Design Considerations

In this section, we discuss various operational issues and suggestions for handling them during design.

### General Remarks

During the design of a pipeline, the maximum and minimum pressures are computed to select the pipe-wall thickness necessary to withstand these pressures. A small reduction in the pipe-wall thickness results in significant savings in the initial cost of the project. Therefore, a detailed analysis of the transients caused by various possible operating conditions is necessary for an economic design. A detailed analysis of an existing pipeline may indicate the possibility of increasing its throughput by increasing the normal working pressures, which in the original design might have been set too low to allow for uncertainties in the prediction of the maximum and minimum pressures.

The friction factor,  $f$  is a very important parameter in the design of an oil pipeline. This should be precisely known to determine the initial steady-state pressures along the pipeline and hence the required pumping heads of the pumping units. In addition to  $f$ , the values of the bulk modulus of elasticity,  $K$ , and the mass density,  $\rho$ , of the oil should be known to compute the wave velocity. The friction factors can usually be estimated closely during the design stages; the values of  $K$  and  $\rho$ , however, are unknown and may vary from one oil batch to another. Therefore, a range of the expected values of  $K$  and  $\rho$  should be used in the analysis during design, and the values that yield worst conditions should be selected. As soon as the pipeline is commissioned, the value of these variables should be determined by conducting prototype tests. Based on the results of these tests, guidelines should be prepared for a safe operation of the pipeline.

With proper design and provision of automatic-control and protective devices, such as pressure controllers, pump-shutdown switches, and pressure relief valves, a pipeline can be operated safely to its maximum capacity. These

devices are designed to detect a severe upset in the system and to take appropriate corrective action so that the pipeline pressures remain within the design limits. The time lag between the detection of an upset and the corrective action should be as short as possible. In addition, the action of the protective devices should be rapid.

The maximum steady state pressure in a blocked line having a centrifugal pump is equal to the shutoff head. However, there is no such upper limit on the maximum pressure in a blocked line with a reciprocating pump; the pressure in this case keeps on increasing until either the pipeline ruptures or the pump fails.

Power failure to the electric motors of a pumping station shuts down all pumping units simultaneously. Since this condition may occur a number of times during the life of a project, it should be considered a normal operation during design. In an engine-powered pumping station, however, the probability of simultaneous shutdown of all pumping units is small under normal conditions although it is possible if some control equipment malfunctions.

While analyzing the controlling action of a valve, proper flow versus valve-opening curve should be used since the flow in certain types of valves does not change until the valve has been opened or closed by approximately 20 to 30 percent. Assuming the flow changes as soon as the valve starts to open or close may yield inaccurate results.

Since normal transient operating conditions are likely to occur several times during the life of a project, a factor of safety is selected that is larger than that for the emergency conditions, whose probability of occurrence is rather small. Malfunctioning of the control equipment in the most unfavorable manner may be considered as a catastrophic condition.

## Control and Surge Protective Devices

A discharge-pressure controller and a pump-shutdown switch are commonly provided in a pumping station having centrifugal pumps. A pressure controller regulates the discharge pressure by reducing the pump speed or by reducing the opening of the control valve. If the pressure exceeds the limits set on the controller, the pump shut-down switch shuts down the entire station.

In pumping stations having reciprocating pumps, a pressure controller is also used to operate a bypass valve or to change the pump stroke or the pump speed. As an added protection, a relief valve with a capacity equal to the pump discharge should be installed. To prevent resonance conditions in a pumping station with two or three pumps operating at 20 cycles/s or less and having a discharge pressure of less than 6 MPa, tying the discharge lines a short distance from the pump headers or providing an air chamber has been successful in reducing the pressure fluctuation by about 90 percent [Lundberg, 1966]. On high-speed, multiplex pumps operating at more than 20 cycles/s or having discharge pressures more than 6 MPa, the provision of air chambers does not adequately suppress the pressure fluctuations. In such

cases, pulsation dampeners of special design have been found to be satisfactory [Ludwig, 1956].

The pressure caused by line packing in a closed system may be several times greater than the potential surge, and it may stress the entire pipeline to the full discharge pressure of the upstream station. These pressures may be kept low by an advance action or by rarefaction control as follows: Pressure monitors on the suction side of the pump station detect any excessive pressure rise and transmit a signal to the supervisory control, which reduces the discharge pressure and/or outflow of the upstream station. A negative wave due to this reduction in the discharge pressure or flow of the upstream station travels in the downstream direction and reduces pressure built up in the pipeline. Another method for reducing the pressure rise is to provide a relief valve at the downstream station.

Upon power failure to the pumping units of an intermediate pumping station, pressure rises on the suction side and decreases on the discharge side. Excessive pressure rise or drop may be prevented by providing a check valve in the pump bypass. As soon as the rising pressure on the suction side exceeds the falling pressure on the discharge side, oil begins to flow from the suction side to the discharge side of the pump. This flow through the check valve prevents further increase in the pressure on the suction side and further decrease on the discharge side.

In a mountainous terrain, a surge tank may be provided at the peaks to avoid column separation following pump failure at an upstream station.

## 7-6 Summary

In this chapter, a number of terms commonly used in the oil industry are defined and different causes of transient conditions in oil pipelines are outlined. A computational procedure is presented to analyze transients in long pipelines by the method of characteristics. The chapter conclude with a discussion of various protective and control devices to keep the pressures within the design limits.

## Problems

**7-1** Write a computer program to analyze a long pipeline having a reservoir at the upstream end and a valve at the downstream end. Include the friction term of Eqs. 3-8 and 3-10 by using (i) a first-order finite-difference approximation outlined in Chapter 3 and (ii) a predictor-corrector scheme of Section 7-4.

**7-2** Use the computer program of Problem 7-1 to compute the potential surge, and the maximum transient-state pressures at the valve and at midlength of a 32-km-long, 0.2-m-diameter pipeline carrying  $0.314 \text{ m}^3/\text{s}$  of crude oil. Assume the downstream valve is instantaneously closed.

**7-3** Compare the maximum pressures of Problem 7-2, obtained by including the friction term, by using: (i) a first-order, finite-difference approximation and (ii) a predictor-corrector scheme.

**7-4** Develop the boundary conditions for a pumping station having a bypass line fitted with a check valve. The check valve opens as soon as the pressure on the suction side exceeds the pressure on the discharge side.

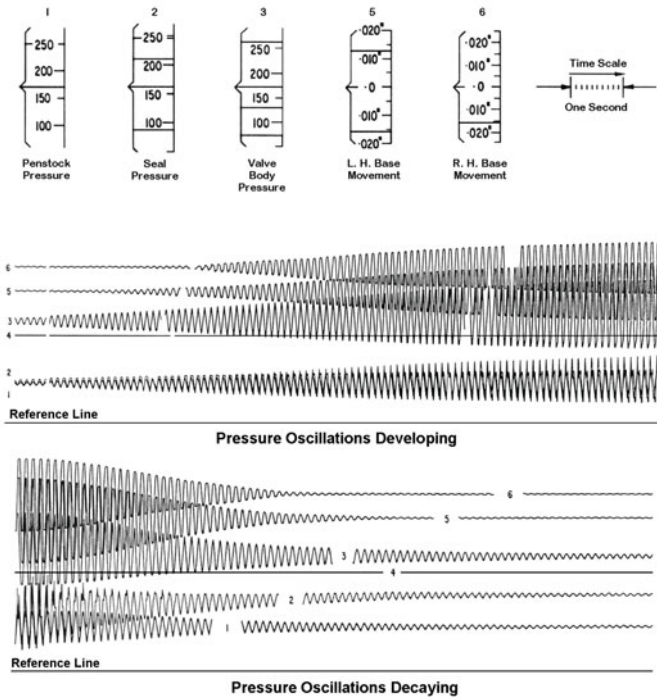
## References

- Bagwell, M. U. and Phillips, R. D., 1969, "Pipeline Surge: How It is Controlled," *Oil and Gas Jour., U.S.A.*, May 5, pp. 115-120.
- Bagwell, M. U. and Phillips, R. D., 1969, "Liquid Petroleum Pipe Line Surge Problems (Real and Imaginary)," Transportation Div., Amer. Petrol. Inst., April.
- Burnett, R. R., 1960, "Predicting and Controlling Transient Pressures in Long Pipelines," *Oil and Gas Jour., U.S.A.*, vol. 58, no. 10, May, pp. 153-160.
- Evangelisti, G., 1969, "Waterhammer Analysis by the Method of Characteristics," *L' Energia Elettrica*, nos. 10 11, and 12, pp. 673-692, 759-771, and 839-858.
- Evangelisti, G., Boari, M., Guerrini, P., and Rossi, R., "Some Applications of Waterhammer Analysis by the Method of Characteristics," *L' Energia Elettrica*, nos. 1 and 6, pp. 1-12, 309-324.
- Holloway, M. B. and Chaudhry, M. H., 1985, "Stability and Accuracy of Waterhammer Analysis," *Advances in Water Resources*, vol. 8, Sept., pp. 121-128.
- Kaplan, M., Streeter, V. L., and Wylie, E. B., 1967, "Computation of Oil Pipeline Transients," *Jour., Pipeline Div.*, Amer. Soc. of Civil Engrs., Nov., pp. 59-72.
- Ludwig, M. and Johnson, S. P., 1950, "Prediction of Surge Pressure in Long Oil Transmission Line," *Proc. Amer. Petroleum Inst.*, Annual Meeting, New York, NY, Nov.
- Ludwig, M., 1956, "Design of Pulsation Dampeners for High Speed Reciprocating Pumps," *Conference of the Transportation Div.*, Amer. Petroleum Inst., Houston, TX, May.
- Lundberg, G. A., 1966, "Control of Surges in Liquid Pipelines," *Pipeline Engineer*, March, pp. 84-88.
- Oil Pipeline Transportation Practices*, issued by Univ. of Texas in cooperation with Amer. Petroleum Inst., Division of Transportation, vol. 1 and 2 1975.
- Streeter, V. L., 1971, "Transients in Pipelines Carrying Liquids or Gases," *Jour., Transportation Engineering Div.*, Amer. Soc. of Civil Engrs., Feb., pp. 15-29.
- Wylie, E. B. and Streeter, V. L., 1983 *Fluid Transients*, FEB Press, Ann Arbor, Mich.

### Additional References

- Binnie, A. M., 1951, "The Effect of Friction on Surges in Long Pipelines," *Jour. Mechanics and Applied Mathematics*, vol. IV, Part 3.
- Green, J. E., 1945, "Pressure Surge Tests on Oil Pipelines," *Proc., Amer. Petroleum Inst.*, vol. 29, Section 5.
- Kaplan, M., 1968, "Analyzing Pipeline Transients by Method of Characteristics," *Oil and Gas Journal*, Jan. 15, pp. 105-108.
- Kersten, R. D. and Waller, E. J., 1957, "Prediction of Surge Pressures in Oil Pipelines," *Jour., Pipeline Div.*, Amer. Soc. of Civil Engrs., vol. 83, no. PL 1, March, pp. 1195-1-1195-22.
- Kerr, S. L., 1950, "Surges in Pipelines, Oil and Water," *Trans.. Amer. Soc. of Mech. Engrs.*, p. 667.
- Techo, R., 1976, "Pipeline Hydraulic Surges are Shown in Computer Simulations," *Oil and Gas Jour.*, November 22, pp. 103-111.
- Wostl, W. J. and Dresser, T., 1970, "Velocimeter Measures Bulk Moduli," *Oil and Gas Jour.*, Dec. 7, pp. 57-62.
- Wylie, E. B., Streeter, V. L., and Bagwell, M. U., 1973, "Flying Switching on Long Oil Pipelines," *Symposium Series*, Amer. Inst. Chem. Engrs., vol. 135, no. 69, pp. 193-194.

## PERIODIC FLOWS AND RESONANCE



Bersimis No. 2 Hydroelectric Powerplant: Recorded development and dissipation of pressure oscillations and vibrations with inadequate and normal inflation of valve service seal. (After Abbott et al. [1963].)

## 8-1 Introduction

In Chapters 1 through 7, we considered transient flows that represented the intermediate flow conditions when the flow is changed from one steady state to another. However, depending upon the characteristics of the system and of the excitation, a disturbance in a piping system may be amplified with time instead of decaying and may result in severe pressure and flow oscillations. This condition is called *resonance*. A periodic forcing function or excitation causes the pressure and flow in the entire system to oscillate at the period of the excitation. This flow is called *periodic* or *steady-oscillatory* flow.

In this chapter, the development of resonance and the analysis of periodic flows are discussed. The terminology is introduced first, the details of the transfer matrix method, derivation of the field and point matrices, and procedures for determining the natural frequencies and frequency response of piping systems are then presented. To verify the transfer matrix method, its results are compared with those of the characteristics method and with those measured in the laboratory and on the real-life projects.

## 8-2 Terminology

A number of common terms related to resonance and periodic flows are defined in this section.

### Steady-oscillatory or Periodic Flows

If the flow conditions, e.g., pressure, discharge, etc., vary with time and repeat after a fixed time interval, then the flow is called *steady-oscillatory or periodic flow* [Camichel, 1919; Jaeger, 1948; Paynter, 1953], and the time interval at which conditions are repeated is referred to as the *period* of oscillations. For example,  $T$  is the period of flow oscillations, as shown in Fig. 8-1.

In the theory of vibrations [Thomson, 1965], steady oscillations refer to the oscillations that have constant amplitude. However, the term *steady-oscillatory* is used herein for the fluid systems to avoid confusion with the steady flow in which the flow conditions at a point are constant with respect to time.

### Instantaneous and Mean Discharge and Pressure Head

In steady-oscillatory flow, the instantaneous discharge,  $Q$ , and the instantaneous pressure head,  $H$ , may be divided into two parts:

$$Q = Q_o + q^* \quad (8-1)$$

$$H = H_o + h^* \quad (8-2)$$

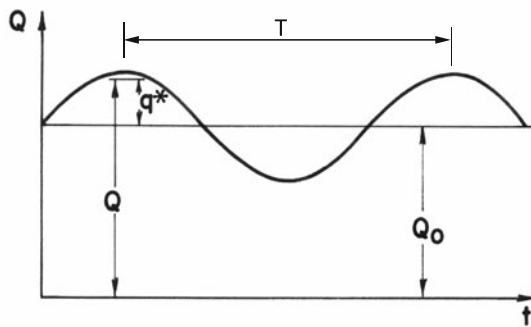


**Fig. 8-1.** Instantaneous, mean, and oscillatory discharge.

in which  $Q_o$  = mean discharge;  $q^*$  = discharge deviation from the mean (see Fig. 8-1);  $H_o$  = mean pressure head; and  $h^*$  = pressure head deviation from the mean. Both  $h^*$  and  $q^*$  are functions of time,  $t$ , and distance,  $x$ . It is assumed that  $h^*$  and  $q^*$  are sinusoidal in time which, in practice, is often true or is a satisfactory approximation [Jaeger, 1948]. Hence, by using complex algebra [Wylie, 1965], we can write

$$q^* = \operatorname{Re} (q(x)e^{j\omega t}) \quad (8-3)$$

$$h^* = \operatorname{Re} (h(x)e^{j\omega t}) \quad (8-4)$$

in which  $\omega$  = frequency in rad/s;  $j = \sqrt{-1}$ ;  $h$  and  $q$  are complex variables and are functions of  $x$  only; and “Re” stands for the real part of the complex variable.

### Theoretical Period

For a pipeline having constant diameter, constant wall thickness, and the same wall material throughout its length,  $L$ , the theoretical period,  $T_{th}$ , is given by the equation

$$T_{th} = \frac{4L}{a} \quad (8-5a)$$

in which  $a$  = the wave velocity,  $T_{th}$  = the fundamental period of the system, and the integral fractions of this period are referred to as the periods of higher harmonics. For example,  $\frac{1}{2}T_{th}$  is the period of the second harmonic, and  $T_{th}/10$  is the period of the tenth harmonic.

In a series piping system having stepwise changes in the diameter, wall thickness, and/or wall material, the theoretical period may be defined as

$$T_{th} = 4 \sum_{i=1}^n \frac{L_i}{a_i} \quad (8-5b)$$

in which the subscript  $i$  refers to the quantities for the  $i$ th pipe and  $n$  is the total number of pipes in series. Because of partial reflections at the changes in the geometry and/or properties of the pipeline, the period of the fundamental may not be equal to  $T_{th}$  given by Eq. 8-5b, and the period of the higher harmonics may not be integral fractions of  $T_{th}$ . The theoretical period may, however, be used to prepare the frequency-response diagram in a normalized or nondimensional form. Although the concept is not valid for a branching system,  $\sum L/a$  computed along the main line may be used to determine  $T_{th}$  for normalization purposes.

### Resonant Frequencies

The frequencies corresponding to the fundamental and higher harmonics are referred to as the *resonant frequencies*. If  $T$  is the period, then the corresponding frequency,  $\omega$ , in rad/s is

$$\omega = \frac{2\pi}{T} \quad (8-6a)$$

and the corresponding circular frequency,  $f$ , in cycles/s is

$$f = \frac{1}{T} \quad (8-6b)$$

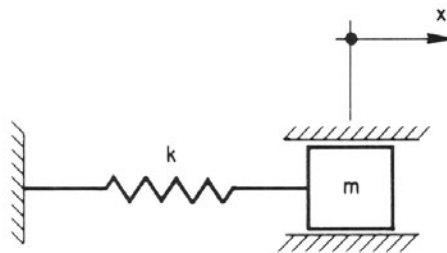
### Degree of Freedom

The number of coordinates required to define the motion of a system is said to be the *degree of freedom* of the system. The following examples should help in the understanding of this definition.

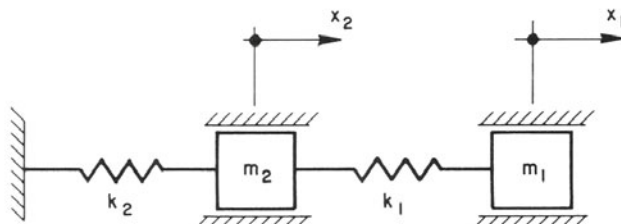
The motion of the spring-mass system shown in Fig. 8-2a may be described by only specifying the position of mass  $m$ . The system is, therefore, said to have a single degree of freedom. Two coordinates,  $x_1$ , and  $x_2$ , are required to completely define the position of masses  $m_1$  and  $m_2$  of Fig. 8-2b. This system is, therefore, said to have two degrees of freedom. Extending this reasoning, a system having  $n$  masses and springs connected in series has  $n$  degrees of freedom. In a hydraulic system, the liquid may be assumed to be composed of an infinite numbers of masses and springs connected in series, with the springs representing the compressibility of water (the analogy of a train is usually used to illustrate the propagation of pressure waves in a pipe). Hence, the hydraulic system has an infinite number of degrees of freedom.

Mathematically speaking, the differential equations describing the system behavior define the degree of freedom of the system: If an ordinary differential equation describes the system, then the number of degrees of freedom is finite and is equal to the order of the differential equation. However, if a partial

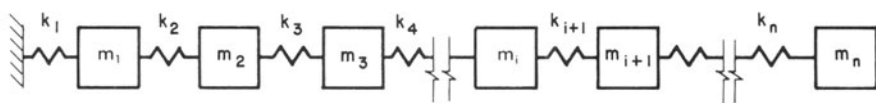
differential equation describes the system, then the system has an infinite number of degrees of freedom. Note that an ordinary differential equation defines the motion of a lumped system, whereas a partial differential equation describes the motion of a distributed system. Although distributed systems have an infinite number of degrees of freedom, only the first 10 to 15 are usually of practical importance.



(a) Single degrees of freedom



(b) Two degrees of freedom



(c) n degrees of freedom

**Fig. 8-2.** Degrees of freedom.

A system having  $n$  degrees of freedom has  $n$  natural frequencies, and corresponding to each natural frequency the system vibrates according to a definite shape, which is called the *normal mode*. Hence, the number of normal modes is equal to the number of degrees of freedom. Mathematically speaking, eigenval-

ues are the natural frequencies, and the corresponding eigenvectors represent the mode shapes.

## Forced Oscillations

Steady-oscillatory flows in a piping system may be produced by a boundary that acts as a periodic forcing function or by a self-excited excitation. The system oscillates at the frequency of the forcing function during forced oscillations and at one of the natural frequencies of the system during self-excited oscillations.

There are three common types of forcing functions in hydraulic systems: periodic variation of the pressure, flow, and the relationship between the pressure and the flow.

A typical example of the periodic pressure variation is a standing wave on the reservoir water surface at a pipe intake. If the period of the surface wave corresponds to one of the natural periods of the piping system, steady-oscillatory conditions are developed in the system in just a few cycles.

A reciprocating pump has periodic inflow and outflow. If the period of a predominant harmonic of either the inflow or of the outflow corresponds to a natural period of the suction or discharge lines, severe flow oscillations are developed.

A periodically opening and closing valve is an example of periodic variation of the relationship between the pressure and the flow. The development of steady-oscillatory flows by a periodic valve operation are discussed in Section 8-4.

## Self-Excited Oscillations

In the *self-excited* or *auto-oscillations*, a component of the system acts as an exciter, which causes the system energy to increase following a small disturbance in the system. Resonance develops when the net energy influx to the system per cycle is more than the energy dissipated per cycle.

A typical example of an exciter is a leaking valve or a leaking seal [Jaeger, 1963]. Let us examine how the oscillations develop in such a system.

[Figure 8-3](#) shows the valve characteristics of a normal and of a leaking valve. For a normal valve, the flow increases as the pressure increases; for a leaking valve, the flow decreases as the pressure increases. In Chapter 1, we derived the following equation for the change in pressure caused by an instantaneous change in flow velocity, i.e.,

$$\Delta H = -\frac{a}{g} \Delta V \quad (1-7)$$

On  $H \sim V$  diagram, this equation plots as a straight line having slope  $a/g$  for a decrease in the flow velocity and  $-a/g$  for an increase in the flow velocity.

Let us assume the initial steady-state velocity is  $V_o$  and that a disturbance decreases it to  $V_1$ . The decay or amplification of this disturbance for a normal or for a leaking valve by using the graphical waterhammer analysis [Allievi, 1925; Bergeron, 1935; Abbott et al., 1963 and Parmakian, 1963] is shown in Fig. 8-3. It is clear that the pressure oscillations decay in a few cycles for a normal valve whereas it amplifies for a leaking valve. As the flow through a leaking valve cannot be less than zero and it cannot increase infinitely, the amplification of the pressure oscillations in this case is therefore finite. This is discussed in detail in Section 8-3.

Den Hartog [1929] reported self-excited penstock vibrations caused by the disturbance produced by the runner-blades passing the guide vanes of a Francis turbine. Based on a simplified theoretical analysis, which was confirmed by observations on eight hydroelectric installations, he concluded that such vibrations are to be expected if the number of the runner blades is one less than the number of the guide vanes. Self-excited vibrations of the guide vanes of a centrifugal pump is considered to be the cause of the accident at the Lac Blanc-Lac Noir pumped storage plant [Rocard, 1937], in which several testing personnel died.

The possibility of the self-excited vibrations in a liquid rocket-engine-propellant feed system were determined by a computer analysis [Fashbaugh and Streeter, 1965]; experimental determination of such a possibility in the piping system of a control system is described by Saito [1962].

Improper settings of a hydraulic turbine governor can result in self-excited oscillations, called *governor hunting*.

Abbott et al. [1963] measured self-excited vibrations in Bersimiss II power plant. A slight leak in a 3.7-m-diameter penstock valve due to a reduction of seal pressure resulted in the vibrations of the valve. The valve vibrations and pressure oscillations were sinusoidal and were eliminated by opening a bypass valve.

McCaig and Gibson [1963] reported vibrations in a pump-discharge line caused by a leak in a 0.25-m-diameter spring-cushioned check valve under static conditions. Measurements showed that the pressure oscillations were approximately sinusoidal with sharp impulses of large magnitude every third cycle. The vibrations were prevented by installing a weaker cushioning spring in the check valve and removing the air valves from the pipeline.

## 8-3 Development of Periodic Flow

To illustrate the development of periodic or steady-oscillatory flow in a piping system, we describe first the development of steady vibrations in a spring-mass system by a periodic force.

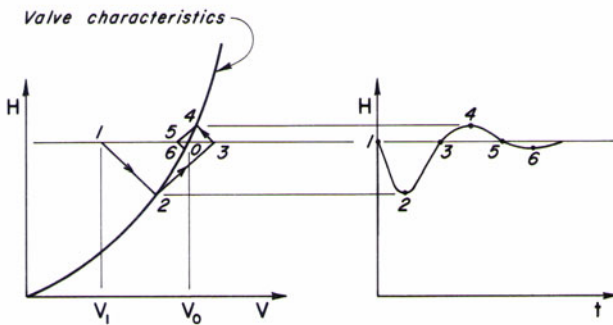
The natural frequency,  $\omega_n$ , of the spring-mass system [Thompson, 1965] shown in Fig. 8-4 is  $\sqrt{k/m}$ , in which  $\omega_n$  = natural frequency of the system in rad/s,  $m$  = mass, and  $k$  = spring constant. If a sinusoidal force having

frequency  $\omega_f$  (Fig. 8-4b) is applied to the mass, initially a beat develops (transient state) and then the system starts to oscillate (Fig. 8-4c) with a constant amplitude at the forcing frequency  $\omega_f$ . These oscillations with a constant amplitude are called *steady vibrations*. The amplitude of the vibrations depends upon the ratio  $\omega_r = \omega_f/\omega_n$ . If the forcing frequency  $\omega_f$  is equal to the natural frequency  $\omega_n$  and the system is frictionless, then the amplitude of steady vibrations becomes infinite because the total energy of the system keeps on increasing with each cycle since there is no energy dissipation in the system. Hence, the oscillations are amplified without any upper bound. However, in a real system with friction losses, the amplitude of the oscillations grows until the energy input and energy dissipation during a cycle are equal. In that case there is no additional energy input per cycle and thus the system oscillates with a finite amplitude. Now let us consider a piping system with an upstream reservoir and a downstream valve (Fig. 8-5a), which is initially closed. At time  $t_o$ , we start to open and close the valve sinusoidally at frequency  $\omega_f$  (Fig. 8-5b). Similar to the spring-mass system, a beat develops first (transient state), and then the flow and pressure oscillate at a constant amplitude but with frequency  $\omega_f$  (Fig. 8-5c). This flow is termed *periodic* or *steady-oscillatory flow*.

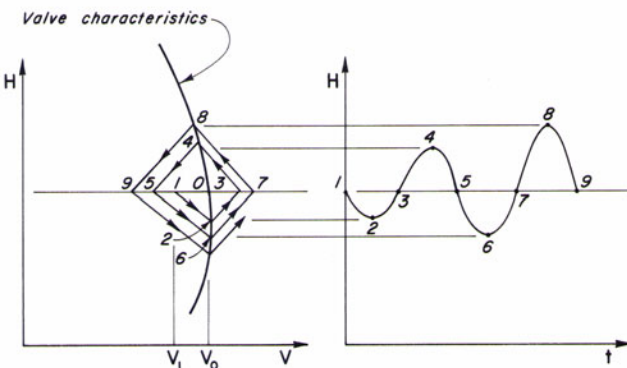
Let us consider the similarities, differences and characteristics of the steady-oscillatory flow in the piping system with the steady vibrations of the spring-mass system. The spring is fixed at one end in our spring-mass system where the displacement is zero. The water level in the upstream reservoir of the piping system being constant, the amplitude of pressure oscillations at the reservoir end is zero. In other words, there is a pressure node at the reservoir end. In the spring-mass system, there is only one mass and one spring. Therefore, the system has only one mode of vibrations or one degree of freedom, and thus only one natural frequency or natural period. If the compressibility of the fluid is taken into consideration, the fluid in the piping system is comprised of an infinite number of inter-connected masses and springs. Therefore, the piping system has infinite modes of oscillations or degrees of freedom and hence has infinite natural periods. The first period is called *fundamental*, and the others are called *higher harmonics*.

Figure 8-6 shows the amplitude of the pressure oscillations at various harmonics along the piping system of Fig. 8-5. Since the reservoir level is constant, a pressure node always exists at the reservoir end. At the valve, however, there is a pressure node during even harmonics and an antinode during odd harmonics. The location of the nodes and antinodes along a pipeline depends upon the harmonic at which the system is oscillating.

Let us now consider another significant difference between the spring-mass, and the piping system. In the former, the source of energy is the external periodic force acting on the mass. In the piping system, although the downstream valve is the forcing function, it is not the source of energy. The valve is just controlling the efflux of energy from the system, whereas the upstream reservoir is the source of energy. Since the volume of the fluid in the pipeline is



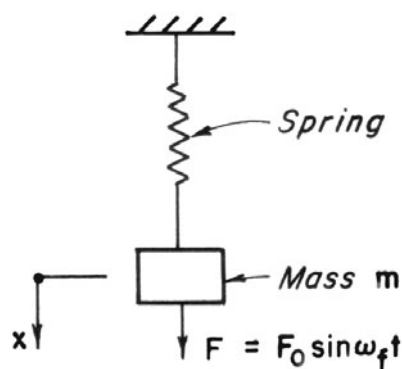
(a) Normal valve



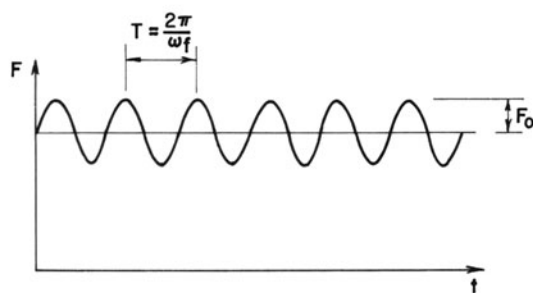
(b) Leaking valve

**Fig. 8-3.** Self-excited oscillations.

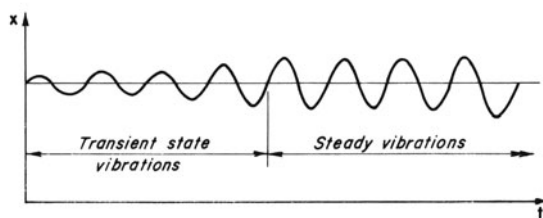
constant, the outflow per cycle at the valve must be equal to the inflow per cycle at the reservoir. The reservoir level being constant, the energy input into the system is at a constant head. However, there is no such restriction on the energy efflux at the valve. If the valve operation is such that there is outflow when the pressure at the valve is low and there is little or no outflow when the pressure is high, then there is net influx of energy during each cycle. This causes the amplitude of pressure oscillations to grow. When the steady-oscillatory flow is fully developed, a discharge node exists at the valve during oscillations at odd harmonics, if the head losses in the system are neglected. Once a discharge node is formed at the valve, opening or closing the valve has no effect on the energy efflux, and the amplitude of the pressure oscillations



(a) Spring - mass system



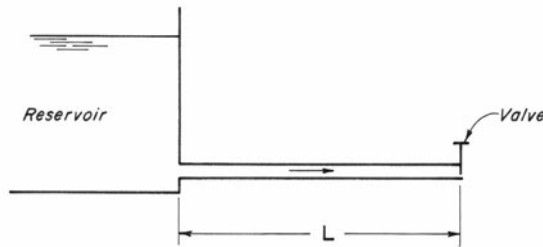
(b) Periodic force



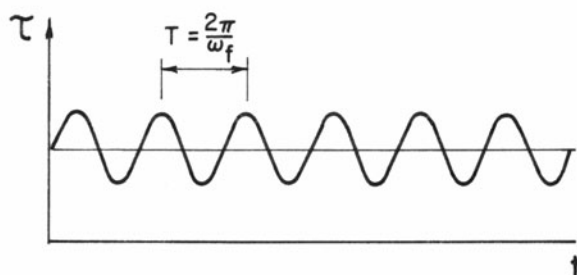
(c) Vibration of mass

Fig. 8-4. Vibrations of a spring-mass system.

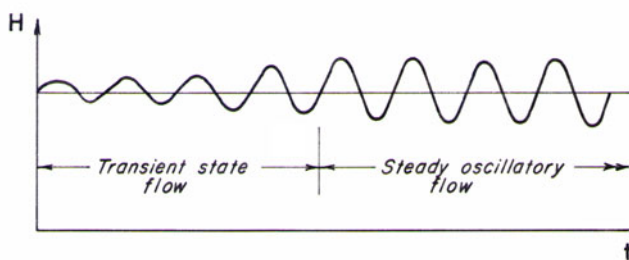
does not increase further even though it is assumed that there is no energy dissipation in the system.



(a) Single pipeline



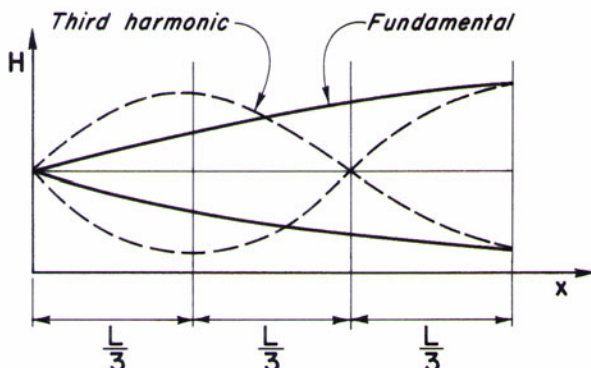
(b) Periodic valve operation



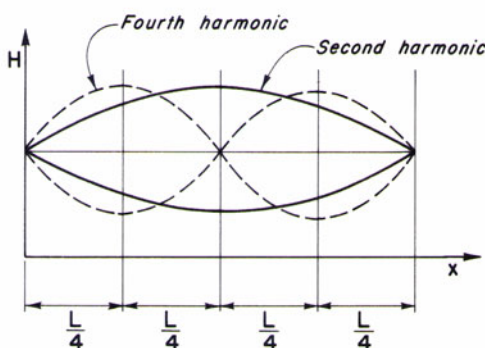
(c) Pressure oscillations at valve

**Fig. 8-5.** Development of steady-oscillatory flow in a single pipeline.

Allievi [1925] was the first to prove that the maximum possible amplitude of the pressure oscillations at the valve is equal to the static head. However, later on, Bergeron [1935] proved graphically that, for large values of Allievi constant,  $\rho = (aV_o) / (2gH_o)$ , it is possible to have amplitude greater than the static head. Also, Camichel [1919] demonstrated that doubling of the pressure head is not possible unless  $H_o > (aV_o) / g$ . In the preceding expressions,  $a$  = wave velocity;  $g$  = acceleration due to gravity;  $H_o$  = static head; and  $V_o$  = steady-state flow velocity.



(a) Odd harmonics



(b) Even harmonics

Fig. 8-6. Pressure oscillations along pipelines at various harmonics.

## 8-4 Methods of Analysis

The periodic or steady-oscillatory flows in a piping system may be analyzed either in the time domain or in the frequency domain [Hovanessian, 1969]. Several methods are available for each of these approaches. The advantages and disadvantages of each approach are discussed in the following paragraphs.

### Time Domain

In this approach, the partial differential equations describing the unsteady flow are solved numerically and the nonlinear friction losses and the nonlinear boundary conditions may be included in the analysis.

Methods for the analysis in the time domain include: method of characteristics, finite-difference, finite-element and spectral methods. The application of these methods was discussed briefly in Chapter 2 and 3.

To analyze the steady-oscillatory flows, the initial steady-state discharge and pressure head in the piping system are assumed equal to their mean values or equal to zero-flow conditions. The specified forcing function is then imposed as a boundary condition, and the system is analyzed by considering one frequency at a time. When the initial transients are vanished and a steady-oscillatory regime is established, the amplitudes of the pressure and discharge fluctuation are determined. The process of convergence to the steady-oscillatory conditions is slow (it may take about 150 cycles) and requires a considerable amount of computer time, thus making the approach uneconomical for general studies. The main advantage is that the nonlinear relationships can be included in the analysis.

### Frequency Domain

By assuming the pressure head and flow variations as sinusoidal, the momentum and continuity equations describing the unsteady flow in the time domain are converted into the frequency domain. The friction term and the nonlinear boundary conditions are linearized for solution by these methods. If the amplitude of oscillations is small, the error introduced by linearization is negligible.

Any periodic forcing function can be handled by these methods. The forcing function is decomposed into different harmonics by Fourier analysis [Blackwall, 1968], and each harmonic is analyzed separately. Because all the equations and relationships are linear, the system response is determined by superposition of the individual responses [Lathi, 1968].

Since the frequency response is determined directly, the computer time required for the analysis is small. Therefore, these methods are suitable for general studies. Two methods available for analysis in the frequency domain are: Impedance method and transfer matrix method. In the following paragraphs, general remarks on these methods are presented.

The concept of impedance was introduced by Rocard [1937] and was used later by Paynter [1953], Waller [1958], and Wylie [1965 and 1983]. In this method, the *terminal impedance*,  $Z_s$ , which is the ratio of the oscillatory pressure head and the discharge, is computed by using the known boundary conditions. An impedance diagram between  $\omega_f$  and  $|Z_s|$  is plotted. The frequencies at which  $|Z_s|$  is maximum are the resonant frequencies of the system.

Lengthy algebraic equations are involved in the application of this method. For a parallel piping system, a procedure is suggested that requires the solution of a large number of simultaneous equations. This becomes cumbersome if the system has many parallel pipes. For example, eight simultaneous equations have to be solved for a system having only two parallel pipes.

The transfer matrix method has been used extensively for the analysis of structural and mechanical vibrations [Molloy, 1957 and Pestel and Lackie, 1963] and electrical systems [Reed, 1955]. This method was introduced by the author for the analysis of steady-oscillatory flows and for determining the frequency response of hydraulic systems [Chaudhry, 1970, 1970a, 1970b, 1972, and 1972a].

Similar to the impedance method, the transfer matrix method is based on the linearized equations and on sinusoidal flow and pressure fluctuations. However, the transfer matrix method is simpler and more systematic than the impedance method, the analysis of the parallel systems does not require any special treatment; the method is suitable for both hand and digital computations; the stability of a system can be checked by the root locus technique [Thorley, 1972], and systems having oscillations of more than two variables (e.g., pressure, flow, density, temperature) can be analyzed.

Details of the transfer matrix method are presented herein. An elementary knowledge of the matrix algebra and complex variables should suffice to follow the derivation of matrices and their application. Block diagrams are used to achieve an orderly and concise formulation and the analysis of complex systems. In this section, state vector and various types of transfer matrices are introduced.

### State Vectors and Transfer Matrices

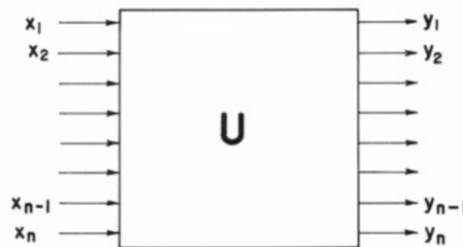
Let us consider a general system ([Fig. 8-7](#)) whose input variables  $x_1, x_2, \dots, x_n$  and output variables  $y_1, y_2, \dots, y_n$  are related by the following  $n$  simultaneous equations:

$$\begin{aligned} y_1 &= u_{11}x_1 + u_{12}x_2 + \dots + u_{1n}x_n \\ y_2 &= u_{21}x_1 + u_{22}x_2 + \dots + u_{2n}x_n \\ &\vdots \\ y_n &= u_{n1}x_1 + u_{n2}x_2 + \dots + u_{nn}x_n \end{aligned} \tag{8-7}$$

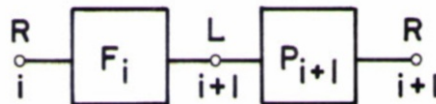
In the matrix notation, these equations may be written as

$$\mathbf{y} = \mathbf{U}\mathbf{x} \quad (8-8)$$

in which the input variables are combined into a single column vector,  $\mathbf{x}$ , and the output variables are combined into a column vector,  $\mathbf{y}$ . In other words the system converts, or transfers, the input variables  $\mathbf{x}$  into the output variables  $\mathbf{y}$ , and the transfer takes place in accordance with Eq. 8-8. The matrix  $\mathbf{U}$  in Eq. 8-8 is called the transfer matrix, and  $\mathbf{x}$  and  $\mathbf{y}$  are called the *state vectors*.



(a) Single component



(b) Two components

**Fig. 8-7. Block diagram.**

In the previous example, the system has only one component. The physical systems, however, are usually made up of several subsystems or components. In such cases, each component is represented by a transfer matrix, and the overall transfer matrix for the system is obtained by multiplying the individual transfer matrices in the proper sequence, as discussed at the end of this section.

The general system of Fig. 8-7 has  $n$  input and output variables. In hydraulic systems, however, the quantities of interest at section  $i$  of a pipe are  $q$  and  $h$ , which can be combined in the matrix notation as

$$\mathbf{z}_i = \begin{Bmatrix} q \\ h \end{Bmatrix}_i \quad (8-9)$$

The column vector  $\mathbf{z}_i$  is called the *state vector* at section  $i$ . The state vectors just to the left and to the right of a section are designated by the superscript  $L$  and  $R$ , respectively. For example,  $\mathbf{z}_i^L$  refers to the state vector just to the left of the  $i$ th section (Fig. 8-8). To combine the matrix terms in some cases,

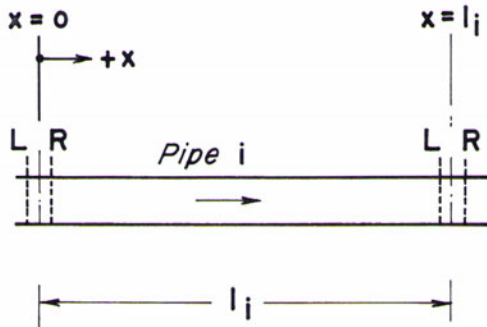


**Fig. 8-8.** Single conduit.

the state vector is defined as

$$\mathbf{z}'_i = \begin{Bmatrix} q \\ h \\ 1 \end{Bmatrix}_i \quad (8-10)$$

Because of the additional element with unit value, the column vector  $\mathbf{z}'_i$  is called *extended state vector*. A prime is used herein to designate an extended state vector.

A matrix relating two state vectors is called a *transfer matrix*. The upper case letters  $\mathbf{F}$ ,  $\mathbf{P}$ , and  $\mathbf{U}$  are used to designate the transfer matrices; the corresponding lower case letters with the double subscripts refer to the elements of the matrix: the first subscript represents the row, and the second subscript represents the column of the element. For example, the element in the second row and the first column of the matrix  $\mathbf{U}$  is represented by  $u_{21}$ .

Transfer matrices may be classified as field, point, and overall transfer matrices. A brief description of each follows.

*Field transfer matrix, or field matrix*,  $\mathbf{F}$ . A field transfer matrix relates the state vectors at the upstream and downstream end sections of a length of pipe. For example, in Fig. 8-8,

$$\mathbf{z}_{i+1}^L = \mathbf{F}_i \mathbf{z}_i^R \quad (8-11)$$

in which  $\mathbf{F}_i$  = field matrix for the  $i$ th pipe.

*Point transfer matrix, or point matrix,  $\mathbf{P}$ .* The state vectors just to the left and to the right of a boundary, junction, device or appurtenance, such as a series junction (Fig. 8-9) or a valve, are related by a point transfer matrix. The type of the boundary is designated by a subscript with the letter  $P$ . For example, in Fig. 8-9,

$$\mathbf{z}_{i+1}^R = \mathbf{P}_{sc}\mathbf{z}_{i+1}^L \quad (8-12)$$

in which  $\mathbf{P}_{sc}$  = point matrix for a series junction. Thus, the pipe length between the two sections is negligible for a point matrix but not for a field matrix.

*Overall transfer matrix,  $\mathbf{U}$ .* The overall transfer matrix for a piping system relates the state vector at one end of the system to that at the other end. Similarly, an overall transfer matrix for a branch relates the state vectors at one end of the branch to that at the other end. For example if  $n + 1$  is the last section, then

$$\mathbf{z}_{n+1}^L = \mathbf{U}\mathbf{z}_1^R \quad (8-13)$$

in which  $\mathbf{U}$  = overall transfer matrix. This is obtained by an ordered multiplication of all the intermediate field and point matrices as follows:

The intermediate field and point matrices are:

$$\begin{aligned} \mathbf{z}_2^L &= \mathbf{F}_1\mathbf{z}_1^R \\ \mathbf{z}_2^R &= \mathbf{P}_2\mathbf{z}_2^L \\ \mathbf{z}_3^L &= \mathbf{F}_2\mathbf{z}_2^R \\ &\dots \\ &\dots \\ &\dots \\ \mathbf{z}_i^L &= \mathbf{F}_{i-1}\mathbf{z}_{i-1}^R \\ \mathbf{z}_i^R &= \mathbf{P}_i\mathbf{z}_i^L \\ &\dots \\ &\dots \\ \mathbf{z}_n^R &= \mathbf{P}_n\mathbf{z}_n^L \\ \mathbf{z}_{n+1}^L &= \mathbf{F}_n\mathbf{z}_n^R \end{aligned} \quad (8-14)$$

Elimination of  $\mathbf{z}_2^L$ ,  $\mathbf{z}_2^R$ , ...,  $\mathbf{z}_n^L$ , and  $\mathbf{z}_n^R$  from Eq. 8-14 yields

$$\mathbf{z}_{n+1}^L = (\mathbf{F}_n\mathbf{P}_n \dots \mathbf{F}_i\mathbf{P}_i \dots \mathbf{F}_3\mathbf{P}_3\mathbf{F}_2\mathbf{P}_2\mathbf{F}_1)\mathbf{z}_1^R \quad (8-15)$$

Hence, it follows from Eqs. 8-13 and 8-15 that

$$\mathbf{U} = \mathbf{F}_n\mathbf{P}_n \dots \mathbf{F}_i\mathbf{P}_i \dots \mathbf{F}_3\mathbf{P}_3\mathbf{F}_2\mathbf{P}_2\mathbf{F}_1 \quad (8-16)$$

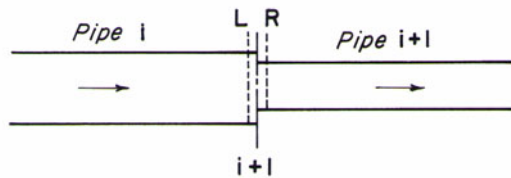


**Fig. 8-9.** Series junction.

## 8-5 Block Diagram

A block diagram is a schematic representation of a system in which each component, or a combination of components, of the system is represented by a “black box.” The box representing a pipeline of constant cross-sectional area, wall thickness, and wall material is characterized by a field matrix, while that for a boundary, junction or device in the system geometry is represented by a point matrix. The block diagram for a system may be simplified by representing a block of individual boxes by a single box. This is illustrated in the following sections by a number of typical examples.

A section on a block diagram is shown by a small circle on the line joining the two boxes. The number of the section is written below the circle and the left- and right-hand sides of the section are designated by the letters L and R above the circle. For example, in Fig. 8-7b,  $i$  and  $i + 1$  denote the number of the sections, and  $L$  and  $R$  denote the left- and right-hand sides of the section. In the case of a branch pipe, the number of the section is written to the right of the circle, and the left- and right-hand sides of the sections are identified by writing the letters  $BL$  and  $BR$  to the left of the circle (see Fig. 8-13b).

The block diagrams are helpful for a concise and orderly formulation and analysis of problems involving complex systems, for an easy understanding of the interaction of different parts of the system, and for determining the sequence of multiplication of transfer matrices for hand calculations or for developing a computer program for this purpose.

## 8-6 Transfer Matrices

To analyze the steady-oscillatory flows and to determine the resonating characteristics of a piping system by the method presented herein, it is necessary to know the transfer matrices of the system components. In this section, field matrices for a single conduit and for a system of parallel pipes are derived. A numerical procedure is presented to determine the field matrix for a pipe

having variable characteristics along its length. The point matrices for a series junction, a valve, an orifice, and for the junction of a branch (branch with various end conditions) and the main are developed.

## Field Matrices

Field matrix for a single conduit is first derived assuming it as a distributed system. Then, its simplified form for a lumped system is developed. This is followed by the field matrices for a conduit with variable characteristics along its length and for a system of parallel pipes.

### *Single Conduit*

The field matrix for a conduit having constant cross-sectional area, constant wall thickness, and the same wall material is derived in this section. In the derivation, the system is considered as distributed, and the friction-loss term is linearized.

Let us re-write the continuity and momentum equations describing the transient flow through closed conduits derived in Chapter 2 to facilitate discussion as

*Continuity equation*

$$\frac{\partial Q}{\partial x} + \frac{gA}{a^2} \frac{\partial H}{\partial t} = 0 \quad (8-17)$$

*Dynamic equation*

$$\frac{\partial H}{\partial x} + \frac{1}{gA} \frac{\partial Q}{\partial t} + \frac{fQ^n}{2gDA^n} = 0 \quad (8-18)$$

in which  $A$  = cross-sectional area of the pipeline;  $g$  = acceleration due to gravity;  $D$  = inside diameter of the pipeline;  $f$  = Darcy-Weisbach friction factor;  $n$  = exponent of velocity in the friction-loss term;  $x$  = distance along the pipeline, measured positive in the downstream direction (see Fig. 8-8); and  $t$  = time.

Since the mean flow and pressure head are time-invariant and the mean flow is constant along the pipe length,  $\partial Q_o/\partial x$ ,  $\partial Q_o/\partial t$ , and  $\partial H_o/\partial t$  are all zero. Hence, it follows from Eqs. 8-1 and 8-2 that

$$\begin{aligned} \frac{\partial Q}{\partial x} &= \frac{\partial q^*}{\partial x} & \frac{\partial Q}{\partial t} &= \frac{\partial q^*}{\partial t} \\ \frac{\partial H}{\partial t} &= \frac{\partial h^*}{\partial t} & \frac{\partial H}{\partial x} &= \frac{\partial H_o}{\partial x} + \frac{\partial h^*}{\partial x} \end{aligned} \quad (8-19)$$

However,  $\partial H_o/\partial x$  is not zero since we are considering the friction losses. For turbulent flow,

$$\frac{\partial H_o}{\partial x} = -\frac{fQ_o^n}{2gDA^n} \quad (8-20)$$

and for laminar flow

$$\frac{\partial H_o}{\partial x} = -\frac{32\nu Q_o}{gAD^2} \quad (8-21)$$

in which  $\nu$  = kinematic viscosity of the fluid. If  $q^* \ll Q_o$ , then

$$Q^n = (Q_o + q^*)^n \simeq Q_o^n + nQ_o^{n-1}q^* \quad (8-22)$$

in which higher-order terms are neglected. It follows from Eqs. 8-17 through 8-22 that

$$\frac{\partial q^*}{\partial x} + \frac{gA}{a^2} \frac{\partial h^*}{\partial t} = 0 \quad (8-23)$$

$$\frac{\partial h^*}{\partial x} + \frac{1}{gA} \frac{\partial q^*}{\partial t} + Rq^* = 0 \quad (8-24)$$

in which  $R = (nfQ_o^{n-1}) / (2gDA^n)$  for turbulent flow and  $R = (32\nu) / (gAD^2)$  for laminar flow.

The field matrix for a pipe may be derived by using the separation-of-variable technique [Wylie, 1965] or by using the Cayley-Hamilton theorem [Pestel and Lackie, 1963]. The former is used herein because of its simplicity; for the derivation using the Cayley-Hamilton theorem, interested readers should see Chaudhry [1970].

Elimination of  $h^*$  from Eqs. 8-23 and 8-24 yields

$$\frac{\partial^2 q^*}{\partial x^2} = \frac{1}{a^2} \frac{\partial^2 q^*}{\partial t^2} + \frac{gAR}{a^2} \frac{\partial q^*}{\partial t} \quad (8-25)$$

Now, if the variation of  $q^*$  is assumed sinusoidal in  $t$ , then on the basis of Eq. 8-3, Eq. 8-25 takes the form

$$\frac{d^2 q}{dx^2} = \left( -\frac{\omega^2}{a^2} + \frac{jgA\omega R}{a^2} \right) q \quad (8-26)$$

or

$$\frac{d^2 q}{dx^2} - \mu^2 q = 0 \quad (8-27)$$

in which

$$\mu^2 = -\frac{\omega^2}{a^2} + \frac{jgA\omega R}{a^2} \quad (8-28)$$

The solution of Eq. 8-27 may be written as

$$q = c_1 \sinh \mu x + c_2 \cosh \mu x \quad (8-29)$$

in which  $c_1$  and  $c_2$  are arbitrary constants.

If  $h^*$  is also assumed sinusoidal in  $t$ , then by substituting Eqs. 8-29 and 8-4 into Eq. 8-23 and solving for  $h$ , we obtain

$$h = -\frac{a^2 \mu}{jgA\omega} (c_1 \cosh \mu x + c_2 \sinh \mu x) \quad (8-30)$$

The field matrix for pipe  $i$  of length  $l_i$  relates the state vectors at the  $i$ th and at the  $(i+1)$ th section (see Fig. 8-8). It is known that at the  $i$ th section (i.e., at  $x = 0$ ),  $h = h_i^R$  and  $q = q_i^R$ . Hence, it follows from Eqs. 8-29 and 8-30 that

$$c_1 = -\frac{jgA_i\omega}{a_i^2\mu_i} h_i^R \quad (8-31)$$

$$c_2 = q_i^R$$

In addition, at the  $(i+1)$ th section (i.e., at  $x = l_i$ ),  $h = h_{i+1}^L$  and  $q = q_{i+1}^L$ . The substitution of these values of  $h$  and  $q$ , and  $c_1$  and  $c_2$  from Eq. 8-31 into Eqs. 8-29 and 8-30 yields

$$q_{i+1}^L = (\cosh \mu_i l_i) q_i^R - \frac{1}{Z_c} (\sinh \mu_i l_i) h_i^R \quad (8-32)$$

$$h_{i+1}^L = -Z_c (\sinh \mu_i l_i) q_i^R + (\cosh \mu_i l_i) h_i^R \quad (8-33)$$

in which *characteristic impedance* [Wylie, 1965a] for pipe  $i$ ,  $Z_c = (\mu_i a_i^2) / (j\omega g A_i)$ .

Equations 8-32 and 8-33 may be written in the matrix notation as

$$\begin{Bmatrix} q \\ h \end{Bmatrix}_{i+1}^L = \begin{bmatrix} \cosh \mu_i l_i & -\frac{1}{Z_c} \sinh \mu_i l_i \\ -Z_c \sinh \mu_i l_i & \cosh \mu_i l_i \end{bmatrix} \begin{Bmatrix} q \\ h \end{Bmatrix}_i^R \quad (8-34)$$

or

$$\mathbf{z}_{i+1}^L = \mathbf{F}_i \mathbf{z}_i^R \quad (8-35)$$

Hence, the field matrix for the  $i$ th pipe is

$$\mathbf{F}_i = \begin{bmatrix} \cosh \mu_i l_i & -\frac{1}{Z_c} \sinh \mu_i l_i \\ -Z_c \sinh \mu_i l_i & \cosh \mu_i l_i \end{bmatrix} \quad (8-36)$$

If friction is neglected, i.e.,  $R_i = 0$ , then  $\mathbf{F}_i$  becomes

$$\mathbf{F}_i = \begin{bmatrix} \cos b_i \omega & \frac{-j}{C_i} \sin b_i \omega \\ -jC_i \sin b_i \omega & \cos b_i \omega \end{bmatrix} \quad (8-37)$$

in which  $b_i = l_i/a_i$  and  $C_i = a_i/(gA_i)$ . Note that  $b_i$  and  $C_i$  are constants for a pipe and are not functions of  $\omega$ , and  $C_i$  is the characteristic impedance for the  $i$ th pipe if friction is neglected.

If  $\omega l_i/a_i \ll 1$ , then the system may be analyzed as a *lumped system*. In this case, the field matrix  $\mathbf{F}_i$  for a frictionless system becomes

$$\mathbf{F}_i = \begin{bmatrix} 1 & \frac{-gA_il_i\omega j}{a_i^2} \\ -\frac{l_i\omega j}{gA_i} & 1 \end{bmatrix} \quad (8-38)$$

which follows from Eq. 8-37 since, for small values of  $\omega l_i/a_i$ ,  $\cos(\omega l_i/a_i) \approx 1$  and  $\sin(\omega l_i/a_i) \approx \omega l_i/a_i$ .

For the analysis of a piping system, the elements of the field matrix for each pipe are first computed. It is clear from the field matrices of Eqs. 8-37 and 8-38 that the idealization of a distributed system as a lumped system does not simplify the computations significantly.

### Example 8-1

Compute the elements of the field matrix for a pipe for  $\omega = 2.0 \text{ rad/s}$ . The pipe is 400 m long, has a diameter of 0.5 m and the wave velocity in the pipe is 1000 m/s. Assume

- i. The liquid inside the pipe is a lumped mass.
- ii. The liquid inside the pipe is distributed, and the system is frictionless.

### Solution

- i. Lumped System

$$A = \frac{\pi}{4}(0.5)^2 = 0.196 \text{ m}^2$$

From Eq. 8-38,

$$\begin{aligned} f_{12} &= -\frac{gAl\omega j}{a^2} \\ &= -\frac{9.81 \times 0.196 \times 400 \times 2j}{(1000)^2} \\ &= -0.00154j \\ f_{21} &= -\frac{l\omega}{gA}j \\ &= -\frac{400 \times 2}{9.81 \times 0.196}j \\ &= -416.07j \end{aligned}$$

ii. *Distributed System*

$$\begin{aligned} b &= l/a = 400/1000 = 0.4 \text{ s} \\ C &= \frac{a}{gA} \\ &= \frac{1000}{9.81 \times 0.196} = 520.08 \text{ s m}^{-2} \\ b\omega &= 0.4 \times 2 = 0.8 \end{aligned}$$

Substituting these values into Eq. 8-37,

$$\begin{aligned} f_{11} &= f_{22} = \cos b\omega \\ &= \cos 0.8 = 0.697 \\ f_{12} &= -\frac{j}{C} \sin b\omega \\ &= -\frac{j}{520.08} \sin 0.8 = -0.0014j \\ f_{21} &= -jC \sin b\omega \\ &= -j \times 520.08 \times \sin 0.8 = 373.08j \end{aligned}$$

**Conduit Having Variable Characteristics**

A conduit has variable characteristics if  $A$ ,  $a$ , wall thickness, or wall material vary along its length [Chaudhry, 1972]. Equations 8-17 and 8-18 describe the transient flow through such conduits; the only difference is that  $A$  and/or  $a$  are functions of  $x$  instead of being constants, i.e.,

$$\frac{\partial Q}{\partial x} + \frac{gA(x)}{a^2(x)} \frac{\partial H}{\partial t} = 0 \quad (8-39)$$

$$\frac{\partial H}{\partial x} + \frac{1}{gA(x)} \frac{\partial Q}{\partial t} = 0 \quad (8-40)$$

in which  $A(x)$  and  $a^2(x)$  denote that  $A$  and  $a^2$  are functions of  $x$ . In these equations, higher-order nonlinear terms and friction are neglected. By substituting Eqs. 8-1 through 8-4 into the preceding equations and simplifying, we obtain

$$\frac{\partial q}{\partial x} + \frac{jgA(x)\omega}{a^2(x)} h = 0 \quad (8-41)$$

$$\frac{\partial h}{\partial x} + \frac{j\omega}{gA(x)} q = 0 \quad (8-42)$$

These equations may be expressed in the matrix notation as

$$\frac{d\mathbf{z}}{dx} = \mathbf{B}\mathbf{z} \quad (8-43)$$

in which  $\mathbf{z}$  is the column vector as defined in Eq. 8-9 and

$$\mathbf{B} = \begin{bmatrix} 0 & -\frac{jgA(x)\omega}{a^2(x)} \\ -\frac{j\omega}{gA(x)} & 0 \end{bmatrix} \quad (8-44)$$

Since the elements of matrix  $\mathbf{B}$  are functions of  $x$ , the field matrix for conduit having variable characteristics cannot be developed by using the procedure outlined earlier. In this case, either of the following procedures [Pestel and Lackie, 1963] may be employed for developing this matrix:

1. The actual pipeline is replaced by a number of substitute pipes having piecewise constant elements (see Fig. 8-10), and the system is analyzed using field matrices given by Eq. 8-37. This procedure gives satisfactory results at low frequencies [Chaudhry, 1972].
2. A numerical procedure is utilized to determine the elements of the field matrix. The determination of the field matrix for a pipeline having variable characteristics is equivalent to integrating the differential equation, Eq. 8-43. This may be done by the Runge-Kutta method [McCracken and Dorn, 1964] as follows.

The pipe is divided into  $n$  reaches, as shown in Fig. 8-10. First, the field matrix for each reach is computed, and then the field matrix for the entire pipe is determined by multiplying these matrices in a proper sequence. If  $s$  is the reach length between sections  $i$  and  $i + 1$ , then the fourth-order Runge-Kutta method gives [McCracken and Dorn, 1964]

$$\mathbf{z}_{i+1} = \mathbf{z}_i + \frac{1}{6} (\mathbf{k}_0 + 2\mathbf{k}_1 + 2\mathbf{k}_2 + \mathbf{k}_3) \quad (8-45)$$

in which

$$\begin{aligned} \mathbf{k}_0 &= s\mathbf{B}(x_i)\mathbf{z}_i \\ \mathbf{k}_1 &= s\mathbf{B}\left(x_i + \frac{1}{2}s\right)(\mathbf{z}_i + \frac{1}{2}\mathbf{k}_0) \\ \mathbf{k}_2 &= s\mathbf{B}\left(x_i + \frac{1}{2}s\right)(\mathbf{z}_i + \frac{1}{2}\mathbf{k}_1) \\ \mathbf{k}_3 &= s\mathbf{B}(x_{i+1})(\mathbf{z}_i + \mathbf{k}_2) \end{aligned} \quad (8-46)$$

The matrices  $\mathbf{B}(\mathbf{x}_i)$ ,  $\mathbf{B}(\mathbf{x}_{i+1})$ , and  $\mathbf{B}\left(\mathbf{x}_i + \frac{1}{2}\mathbf{s}\right)$  are, respectively, the values of the matrix  $\mathbf{B}(\mathbf{x})$  at section  $i$ , at  $i + 1$ , and at the middle of sections  $i$  and  $i + 1$ . By substituting Eqs. 8-46 into Eq. 8-45, we obtain

$$\mathbf{z}_{i+1} = \mathbf{F}_{vc}\mathbf{z}_i \quad (8-47)$$

in which the field matrix for a pipe having variable characteristics along its length is

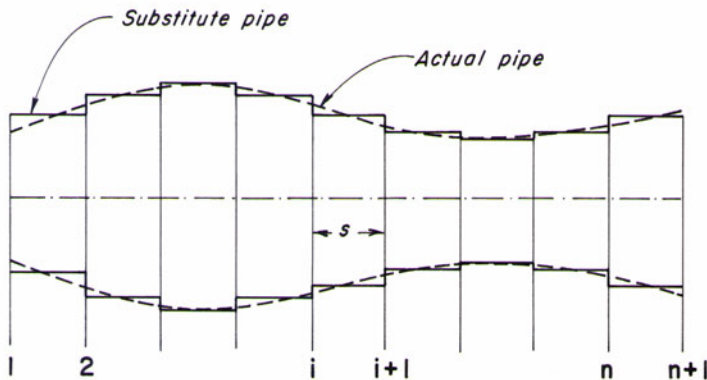


**Fig. 8-10.** Actual and substitute pipe for a pipe having variable characteristics along its length.

$$\begin{aligned}
 \mathbf{F}_{vc} = & \mathbf{I} + \frac{s}{6} [\mathbf{B}(x_i) + 4\mathbf{B}(x_i + \frac{1}{2}s) + \mathbf{B}(x_{i+1})] \\
 & + \frac{s^2}{6} [\mathbf{B}(x_i + \frac{1}{2}s)\mathbf{B}(x_i) + \mathbf{B}(x_{i+1})\mathbf{B}(x_i + \frac{1}{2}s) + \mathbf{B}^2(x_i + \frac{1}{2}s)] \\
 & + \frac{s^3}{12} [\mathbf{B}^2(x_i + \frac{1}{2}s)\mathbf{B}(x_i) + \mathbf{B}(x_{i+1})\mathbf{B}^2(x_i + \frac{1}{2}s)] \\
 & + \frac{s^4}{24} [\mathbf{B}(x_{i+1})\mathbf{B}^2(x_i + \frac{1}{2}s)\mathbf{B}(x_i)]
 \end{aligned} \quad (8-48)$$

in which  $I$  = identity or unit matrix

### Parallel System

We developed earlier the field matrix for a single conduit with constant characteristics and then, for a conduit with variable characteristics. In this section, we present the field matrix for a system of parallel loops.

Let there be  $n$  loops in parallel (Fig. 8-11) whose overall transfer matrices are

$$\mathbf{U}^{(m)} = \mathbf{F}_{n'_m}^{(m)} \mathbf{P}_{n'_m}^{(m)} \dots \mathbf{P}_{2'_m}^{(m)} \mathbf{F}_{1'_m}^{(m)} \quad m = 1, 2, \dots, n \quad (8-49)$$

The superscript in the parentheses refers to the number of the loop. The matrix  $\mathbf{U}^m$  relates the state vectors at the  $1'_m$  and at the  $(n'_m + 1)$ th section of the  $m$ th loop (see Fig. 8-11b), i.e.,

$$\mathbf{z}_{n'_m+1}^{(m)L} = \mathbf{U}^{(m)} \mathbf{z}_{1'_m}^{(m)R} \quad (8-50)$$

A prime on the subscript denotes a section on the conduit in the parallel loop.

The elements of the field matrix,  $\mathbf{F}_p$ , for the system of parallel loops relating the state vectors  $\mathbf{z}_{i+1}^R$  and  $\mathbf{z}_i^L$  (Fig. 8-11b) may be determined from the following equations [Molloy, 1957]:

$$\begin{aligned} f_{11} &= \frac{\xi}{\eta} \\ f_{12} &= \frac{\xi\zeta}{\eta} - \eta \\ f_{21} &= \frac{1}{\eta} \\ f_{22} &= \frac{\zeta}{\eta} \end{aligned} \quad (8-51)$$

in which

$$\xi = \sum_{m=1}^n \frac{u_{11}^{(m)}}{u_{21}^{(m)}}$$

$$\eta = \sum_{m=1}^n \frac{1}{u_{21}^{(m)}} \quad (8-52)$$

$$\zeta = \sum_{m=1}^n \frac{u_{22}^{(m)}}{u_{21}^{(m)}}$$

In deriving the above expressions, it is assumed that

$$|\mathbf{U}^{(m)}| = 1 \quad m = 1, 2, \dots, n \quad (8-53)$$

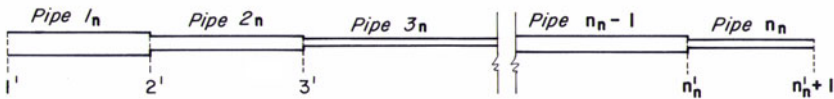
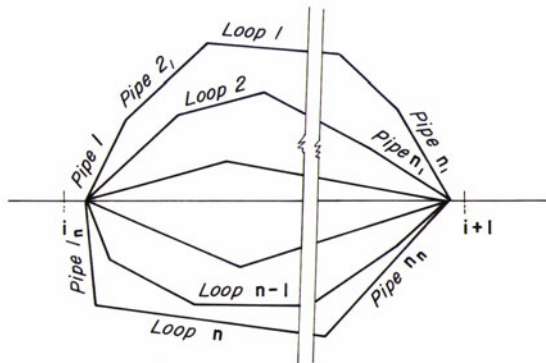
i.e.,

$$u_{11}^{(m)} u_{22}^{(m)} - u_{12}^{(m)} u_{21}^{(m)} = 1 \quad m = 1, 2, \dots, n. \quad (8-54)$$

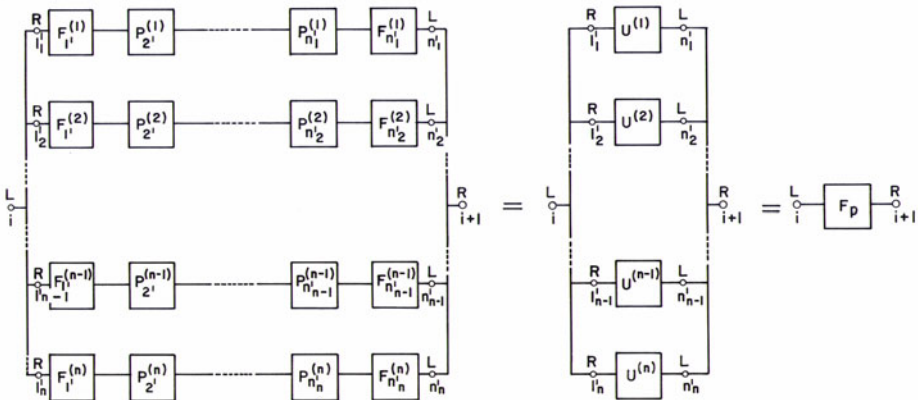
Note that Eq. 8-51 is valid only if the elements of the overall transfer matrix for each parallel loop satisfy Eq. 8-54. It is known from the theory of matrices that, for square matrices, the determinant of the product of matrices is equal to the product of the determinants of matrices. Hence, if  $|\mathbf{P}_k^{(m)}| = 1$ ,  $k = 2, 3, \dots, n_m$ , and  $|\mathbf{F}_k^{(m)}| = 1$ ,  $k = 1, 2, \dots, n_m$ , for  $m = 1, 2, \dots, n$ , then  $|\mathbf{U}^{(m)}| = 1$ . It is clear from Eqs. 8-36 and 8-37 that  $|\mathbf{F}| = 1$ . Furthermore, the determinants of the point matrices for a series junction, for a valve and for an orifice are also unity (see the point matrices derived in the following paragraphs). Thus, for any boundary other than a series junction, valve, or orifice in any of the parallel loops, the determinant of the point matrix for the boundary should be checked to ensure that it has unit value prior to using Eq. 8-51.

## Point Matrices

For any device, appurtenance, junction or boundary in a piping system such as a series junction, orifice, valve, branch junction, etc., a point matrix relates

Longitudinal section of  $n^{\text{th}}$  loop

(a) Piping system



(b) Block diagram

Fig. 8-11. Parallel system.

the state vector to the left of the boundary with that to the right. This point matrix is needed for the calculation of the overall transfer matrix for the system.

Point matrices for various common boundaries are derived in the following paragraphs.

### ***Series Junction***

A junction of two pipes having different diameters (see Fig. 8-9), wall thicknesses, wall materials, or any combination of these variables is called a *series junction*.

It follows from the continuity equation that

$$q_i^R = q_i^L \quad (8-55)$$

In addition

$$h_i^R = h_i^L \quad (8-56)$$

if the losses at the junction are neglected. These two equations may be expressed in the matrix notation as

$$\mathbf{z}_i^R = \mathbf{P}_{sc} \mathbf{z}_i^L \quad (8-57)$$

in which the point matrix for a series junction is

$$\mathbf{P}_{sc} = \begin{bmatrix} 1 & 0 \\ 0 & 1 \end{bmatrix} \quad (8-58)$$

Since  $\mathbf{P}_{sc}$  is a unit matrix, it may be incorporated into the field matrix while doing the calculations.

### ***Valve and Orifice***

The point matrix for a valve or for an orifice may be derived by linearizing the valve equation. This linearization does not introduce large errors if the pressure rise at the valve is small as compared to the static head. For an oscillating valve, a sinusoidal valve motion is assumed. It is possible, however, to analyze non-sinusoidal periodic valve motion by this method as follows. The periodic motion is decomposed into a set of harmonics by Fourier analysis [Wylie, 1965], and the system response is determined for each harmonic. The individual responses are then superimposed to determine the total response for the given valve motion. Since all the equations are linear, the principle of superposition [Wylie, 1965 and Lathi, 1968] can be applied.

*Oscillating Valve.* The instantaneous and mean discharge through a valve discharging into atmosphere (Fig. 8-12a) are given by the equations

$$Q_{n+1}^L = C_d A_v (2g H_{n+1}^L)^{1/2} \quad (8-59)$$

$$Q_o = (C_d A_v)_o (2g H_o)^{1/2} \quad (8-60)$$

in which  $C_d$  = coefficient of discharge,  $A_v$  = area of the valve opening, and subscript "o" refers to the mean values. Division of Eq. 8-59 by Eq. 8-60 yields

$$\frac{Q_{n+1}^L}{Q_o} = \frac{\tau}{\tau_o} \left( \frac{H_{n+1}^L}{H_o} \right)^{1/2} \quad (8-61)$$

in which the instantaneous relative gate opening  $\tau = (C_d A_v)_o / (C_d A_v)_s$ , and the mean relative gate opening  $\tau_o = (C_d A_v)_o / (C_d A_v)_s$ . The subscript  $s$  denotes steady-state reference, or index, value. The relative gate opening may be divided into two parts, i.e.,

$$\tau = \tau_o + \tau^* \quad (8-62)$$

in which  $\tau^*$  = deviation of the relative gate opening from the mean (Fig. 8-12b). Substitution of Eqs. 8-1, 8-2, and 8-62 into Eq. 8-61 yields

$$\left( 1 + \frac{q_{n+1}^{*L}}{Q_o} \right) = \left( 1 + \frac{\tau^*}{\tau_o} \right) \left( 1 + \frac{h_{n+1}^{*L}}{H_o} \right)^{1/2} \quad (8-63)$$

For a sinusoidal valve motion

$$\tau^* = \operatorname{Re} (k e^{j\omega t}) \quad (8-64)$$

in which  $k$  = amplitude of the valve motion. The phase angle between any other forcing function in the system and the oscillating valve may be taken into consideration by making  $k$  a complex number; otherwise,  $k$  is real.

By expanding Eq. 8-63, neglecting terms of higher order (this is valid only if  $|h_{n+1}^{*L}| \ll H_o$ ), and substituting Eqs. 8-3, 8-4, and 8-64 into the resulting equation, we obtain

$$h_{n+1}^L = \frac{2H_o}{Q_o} q_{n+1}^L - \frac{2H_o k}{\tau_o} \quad (8-65)$$

Since  $h_{n+1}^R = 0$ , on the basis of Eq. 8-65, we may write

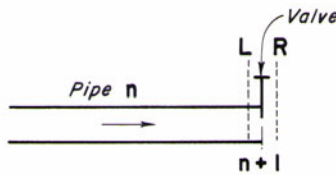
$$h_{n+1}^R = h_{n+1}^L + \frac{2H_o k}{\tau_o} - \frac{2H_o}{Q_o} q_{n+1}^L \quad (8-66)$$

In addition, it follows from the continuity equation that

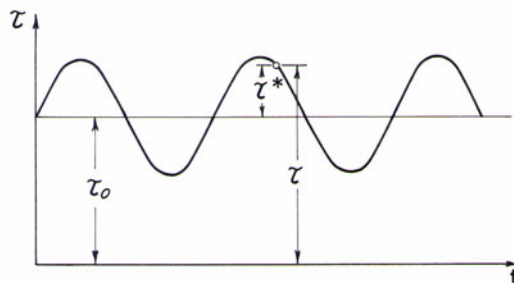
$$q_{n+1}^R = q_{n+1}^L \quad (8-67)$$

Equations 8-66 and 8-67 may be expressed in the matrix notation as

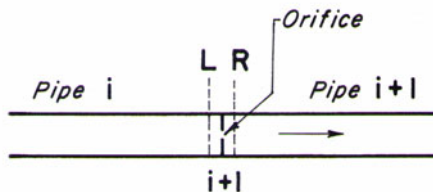
$$\begin{Bmatrix} q \\ h \end{Bmatrix}_{n+1}^R = \begin{bmatrix} 1 & 0 \\ -\frac{2H_o}{Q_o} & 1 \end{bmatrix} \begin{Bmatrix} q \\ h \end{Bmatrix}_{n+1}^L + \begin{Bmatrix} 0 \\ \frac{2H_o k}{\tau_o} \end{Bmatrix} \quad (8-68)$$



(a) Valve at downstream end



(b) Sinusoidal valve motion



(c) Orifice at intermediate section

**Fig. 8-12.** Oscillating valve and orifice.

By adding an additional element 1 in the column vector, the two matrix terms on the right-hand side of Eq. 8-68 may be combined as follows:

$$\begin{Bmatrix} q \\ h \\ 1 \end{Bmatrix}_{n+1}^R = \begin{bmatrix} 1 & 0 & 0 \\ -\frac{2H_o}{Q_o} & 1 & \frac{2H_0k}{\tau_o} \\ 0 & 0 & 1 \end{bmatrix} \begin{Bmatrix} q \\ h \\ 1 \end{Bmatrix}_{n+1}^L \quad (8-69)$$

Note that the expansion of Eq. 8-69 yields Eqs. 8-66 and 8-67, and  $1 = 1$ . Thus, the additional element 1 in the column vector aids in writing the right-hand side of Eq. 8-68 in a compact form. As defined in Section 8-4 (Eq. 8-10), the column vector with 1 as an additional element is called an *extended state vector*,  $\mathbf{z}'$ . The extended-state vectors and extended transfer matrices are denoted by a prime.

On the basis of Eq. 8-10, Eq. 8-69 may be written as

$$\mathbf{z}'^R_{n+1} = \mathbf{P}'_{ov} \mathbf{z}'^L_{n+1} \quad (8-70)$$

in which  $\mathbf{P}'_{ov}$  = the extended point matrix for an oscillating valve and is given by

$$\mathbf{P}'_{ov} = \begin{bmatrix} 1 & 0 & 0 \\ -\frac{2H_o}{Q_o} & 1 & \frac{2H_0k}{\tau_o} \\ 0 & 0 & 1 \end{bmatrix} \quad (8-71)$$

*Valve Having Constant Opening.* For a valve with constant opening,  $k = 0$ . Hence, Eq. 8-68 for a valve discharging into atmosphere becomes

$$\begin{Bmatrix} q \\ h \end{Bmatrix}_{n+1}^R = \begin{bmatrix} 1 & 0 \\ -\frac{2H_o}{Q_o} & 1 \end{bmatrix} \begin{Bmatrix} q \\ h \end{Bmatrix}_{n+1}^L \quad (8-72)$$

or

$$\mathbf{z}_n^R = \mathbf{P}_v \mathbf{z}_{n+1}^L \quad (8-73)$$

in which  $\mathbf{P}_v$  = point matrix for a valve or orifice discharging into atmosphere, and is given by

$$\mathbf{P}_v = \begin{bmatrix} 1 & 0 \\ -\frac{2H_o}{Q_o} & 1 \end{bmatrix} \quad (8-74)$$

Note that  $\mathbf{P}_v$  is not an extended point matrix.

If a valve with constant opening, or an orifice, is located at an intermediate section (Fig. 8-12c), then Eq. 8-74 becomes

$$\mathbf{P}_{vi} = \begin{bmatrix} 1 & 0 \\ -\frac{2\Delta H_o}{Q_o} & 1 \end{bmatrix} \quad (8-75)$$

in which  $\Delta H_o$  = the mean head loss across the valve corresponding to the mean discharge,  $Q_o$ .

### Branching Junction

In the branching system shown in Fig. 8-13a, pipeline  $abc$  is the main line, and  $bd$  is the side branch. The transfer matrix for the pipeline  $ab$  can be computed by using the field and point matrices derived previously. To calculate the overall transfer matrix for  $abc$ , the point matrix at junction  $b$ , relating the state vector on the left side and to that on the right side of the junction is needed. This matrix may be derived if the boundary conditions at point  $d$  are specified.

Point matrices for the junction of the main and the branch having various end conditions are derived in this section.

Let  $\tilde{\mathbf{U}}$  be the overall transfer matrix for the branch (refer to Fig. 8-13b), i.e.,

$$\tilde{\mathbf{z}}_{n+1}^L = \tilde{\mathbf{U}} \tilde{\mathbf{z}}_1^R \quad (8-76)$$

or

$$\begin{Bmatrix} \tilde{q} \\ \tilde{h} \end{Bmatrix}_{n+1}^L = \begin{bmatrix} \tilde{u}_{11} & \tilde{u}_{12} \\ \tilde{u}_{21} & \tilde{u}_{22} \end{bmatrix} \begin{Bmatrix} \tilde{q} \\ \tilde{h} \end{Bmatrix}_1^R \quad (8-77)$$

in which  $\tilde{\mathbf{U}} = \tilde{\mathbf{F}}_n \tilde{\mathbf{P}}_n \dots \tilde{\mathbf{P}}_3 \tilde{\mathbf{F}}_2 \tilde{\mathbf{P}}_2 \tilde{\mathbf{F}}_1$  and the quantities relating to the branch are designated by a tilde ( $\sim$ ).

Expansion of Eq. 8-77 yields

$$\tilde{q}_{n+1}^L = \tilde{u}_{11} \tilde{q}_1^R + \tilde{u}_{12} \tilde{h}_1^R \quad (8-78)$$

$$\tilde{h}_{n+1}^L = \tilde{u}_{21} \tilde{q}_1^R + \tilde{u}_{22} \tilde{h}_1^R \quad (8-79)$$

Considering the flow direction as shown in Fig. 8-13a as positive and neglecting the losses at the junction, the following equations may be written

$$q_i^L = q_i^R + \tilde{q}_1^R \quad (8-80)$$

$$h_i^L = h_i^R = \tilde{h}_1^R \quad (8-81)$$

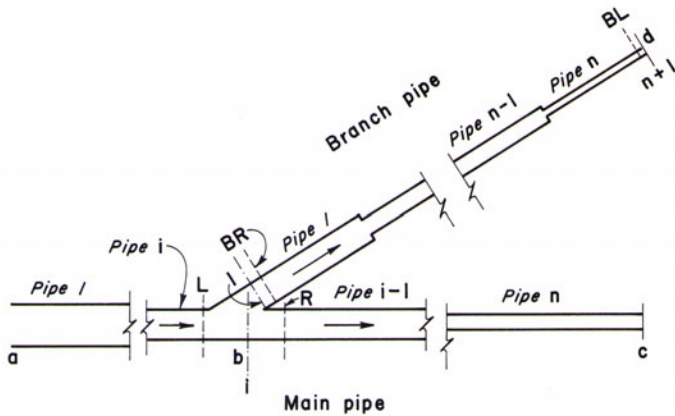
By substituting appropriate end conditions for the branch into Eqs. 8-78 and 8-79 and making use of Eqs. 8-80 and 8-81, the point matrices at the junction of the main and the branch can be derived. The following examples illustrate the procedure.

*Dead-End Branch.* For a branch with a dead end,  $\tilde{q}_{n+1}^L = 0$ . Hence, it follows from Eqs. 8-78 and 8-81 that

$$\tilde{q}_1^R = -\frac{\tilde{u}_{12}}{\tilde{u}_{11}} h_i^L \quad (8-82)$$

Substitution of this equation into Eq. 8-80 yields

$$q_i^R = q_i^L + \frac{\tilde{u}_{12}}{\tilde{u}_{11}} h_i^L \quad (8-83)$$



(a) Piping system

Fig. 8-13. Branch system.

Equation 8-81 may be written as

$$h_i^R = 0 \quad q_i^L + h_i^L \quad (8-84)$$

Equations 8-83 and 8-84 may be expressed in the matrix notation as

$$\begin{Bmatrix} q \\ h \end{Bmatrix}_i^R = \begin{bmatrix} 1 & \tilde{u}_{12} \\ 0 & \tilde{u}_{11} \end{bmatrix} \begin{Bmatrix} q \\ h \end{Bmatrix}_i^L \quad (8-85)$$

or

$$\mathbf{z}_i^R = \mathbf{P}_{\text{bde}} \mathbf{z}_i^L \quad (8-86)$$

in which  $\mathbf{P}_{\text{bde}}$  = point matrix for the branch with a dead end and is given by

$$\mathbf{P}_{\text{bde}} = \begin{bmatrix} 1 & \tilde{u}_{12} \\ 0 & \tilde{u}_{11} \end{bmatrix} \quad (8-87)$$

*Branch with Downstream Reservoir.* For a branch with a constant-head at the downstream end,  $\tilde{h}_{n+1}^L = 0$ . Hence, it follows from Eqs. 8-78 through 8-81 that

$$q_i^R = q_i^L + \frac{\tilde{u}_{22}}{\tilde{u}_{21}} h_i^L \quad (8-88)$$

Equations 8-88 and 8-84 may be expressed in the matrix notation as

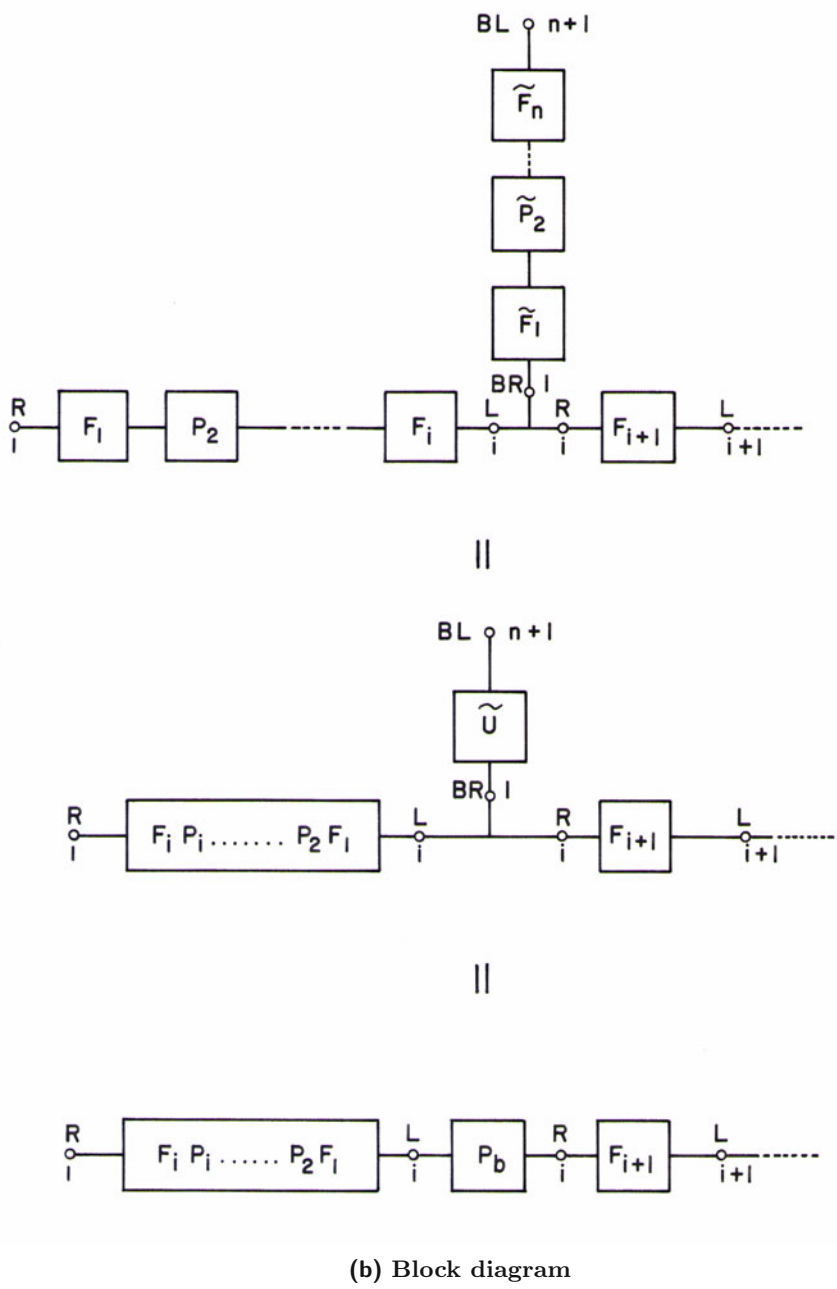


Fig. 8-13. (Continued)

$$\begin{Bmatrix} q \\ h \end{Bmatrix}_i^R = \begin{bmatrix} 1 & \tilde{u}_{22} \\ 0 & \tilde{u}_{21} \end{bmatrix} \begin{Bmatrix} q \\ h \end{Bmatrix}_i^L \quad (8-89)$$

or

$$\mathbf{z}_i^R = \mathbf{P}_{\text{bres}} \mathbf{z}_i^L \quad (8-90)$$

in which  $\mathbf{P}_{\text{bres}}$  = point matrix for the branch with a constant-head reservoir and is given by

$$\mathbf{P}_{\text{bres}} = \begin{bmatrix} 1 & \tilde{u}_{22} \\ 0 & \tilde{u}_{21} \end{bmatrix} \quad (8-91)$$

*Branch with Downstream Oscillating Valve.* To develop the point matrix for the junction of a branch with an oscillating valve, we have to use extended transfer matrices to include the forcing function on the branch. If the frequency of the oscillating valve on the branch is the same as that of the forcing function on the main (these may not be in phase) then the entire system may be analyzed for this forcing frequency. However, if the frequencies of the forcing functions are different, then the system is analyzed considering each forcing function at a time and the results are then superimposed to determine the total response. The superposition is valid because all governing equations are linear.

As discussed previously, we have to use an extended overall transfer matrix relating the state vector at the first and at the last section of the branch and the extended transfer matrices for all the components of the main line have to be used. Let the extended overall transfer matrix for the branch be

$$\tilde{\mathbf{U}}' = \begin{bmatrix} \tilde{u}_{11} & \tilde{u}_{12} & 0 \\ \tilde{u}_{21} & \tilde{u}_{22} & 0 \\ 0 & 0 & 1 \end{bmatrix} \quad (8-92)$$

Note that  $\tilde{\mathbf{U}}'$  in Eq. 8-92 is for a branch with an oscillating valve at its downstream end but with no other forcing boundary on the branch. If there is one or more forcing boundaries on the branch other than the one at its downstream end, then at least one of the elements  $\tilde{u}_{13}$ ,  $\tilde{u}_{23}$ ,  $\tilde{u}_{31}$ , and  $\tilde{u}_{32}$  is not equal to zero, and the point matrix derived in this section is modified accordingly.

For the branch pipeline,

$$\tilde{\mathbf{z}}_{n+1}^{R'} = \tilde{\mathbf{P}}'_{\text{ov}} \tilde{\mathbf{z}}_1^L \quad (8-93)$$

and

$$\tilde{\mathbf{z}}_{n+1}^L = \tilde{\mathbf{U}}' \tilde{\mathbf{z}}_1^R \quad (8-94)$$

By substituting  $\tilde{\mathbf{P}}'_{\text{ov}}$  from Eq. 8-71 and  $\tilde{\mathbf{z}}_{n+1}^L$  from Eq. 8-94 into Eq. 8-93 and expanding the resulting equation, we obtain

$$\tilde{q}_{n+1}^R = \tilde{u}_{11}\tilde{q}_1^R + \tilde{u}_{12}\tilde{h}_1^R \quad (8-95)$$

$$\tilde{h}_{n+1}^R = \left( \tilde{u}_{21} - \frac{2\tilde{H}_o}{\tilde{Q}_o}\tilde{u}_{11} \right) \tilde{q}_1^R + \left( \tilde{u}_{22} - \frac{2\tilde{H}_o}{\tilde{Q}_o}\tilde{u}_{12} \right) \tilde{h}_1^R + \frac{2\tilde{H}_o\tilde{k}}{\tilde{\tau}_o} \quad (8-96)$$

All the notations defined in the previous sections apply except that a tilde ( $\sim$ ) refers to the branch. For example,  $\tilde{\tau}_o$  = the mean relative valve opening of the valve on the branch line. Any phase shift between the valve on the branch and the forcing function on the main can be taken into consideration by making  $\tilde{k}$  a complex number; otherwise,  $\tilde{k}$  is real.

Since  $\tilde{h}_{n+1}^R = 0$ , and  $\tilde{h}_1^R = h_i^L$ , it follows from Eq. 8-96 that

$$\tilde{q}_1^R = -p_{12}h_i^L - p_{13} \quad (8-97)$$

in which

$$p_{12} = \frac{\tilde{u}_{22} - \frac{2\tilde{H}_o\tilde{u}_{12}}{\tilde{Q}_o}}{\tilde{u}_{21} - \frac{2\tilde{H}_o\tilde{u}_{11}}{\tilde{Q}_o}} \quad (8-98)$$

and

$$p_{13} = \frac{2\tilde{H}_o\tilde{k}/\tilde{\tau}_o}{\tilde{u}_{21} - \frac{2\tilde{H}_o\tilde{u}_{11}}{\tilde{Q}_o}} \quad (8-99)$$

By substituting  $\tilde{q}_1^R$  from Eq. 8-97 into Eq. 8-80, we obtain

$$q_i^R = q_i^L + p_{12}h_i^L + p_{13} \quad (8-100)$$

Moreover, we can write

$$1 = 0 \quad q_i^L + 0h_i^L + 1 \quad (8-101)$$

Equations 8-84, 8-100, and 8-101 can be expressed in the matrix notation as

$$\begin{Bmatrix} q \\ h \\ 1 \end{Bmatrix}_i^R = \begin{bmatrix} 1 & p_{12} & p_{13} \\ 0 & 1 & 0 \\ 0 & 0 & 1 \end{bmatrix} \begin{Bmatrix} q \\ h \\ 1 \end{Bmatrix}_i^L \quad (8-102)$$

or

$$\mathbf{z}'_i^R = \mathbf{P}'_{\text{bov}} \mathbf{z}'_i^L \quad (8-103)$$

in which  $\mathbf{P}'_{\text{bov}}$  = transfer matrix at the junction of the side branch having an oscillating valve and is given by

$$\mathbf{P}'_{\text{bov}} = \begin{bmatrix} 1 & p_{12} & p_{13} \\ 0 & 1 & 0 \\ 0 & 0 & 1 \end{bmatrix} \quad (8-104)$$

If there is an orifice, or a valve having constant valve opening at the downstream end of the branch, then  $k = 0$ . Hence,  $p_{13} = 0$ , and the point matrix for the branch may be written as

$$\mathbf{P}_{\text{borf}} = \begin{bmatrix} 1 & p_{12} \\ 0 & 1 \end{bmatrix} \quad (8-105)$$

Note that this is not an extended point matrix.

## 8-7 Frequency Response

The transfer matrix method may be used to determine the frequency response of a system having one or more periodic forcing boundaries, components or devices. The equations derived in this section may be used directly if the forcing functions are sinusoidal. Non-harmonic periodic functions are decomposed into different harmonics by Fourier analysis [Wylie, 1965] and by considering each harmonic one at a time at its frequency, the system response is determined. The results are then superimposed to determine the total response.

Systems having more than one exciter may be analyzed as follows: If all the exciters have the same frequency, then the system oscillates at this frequency. To analyze such a system, the extended transfer matrices are used, which allow all the exciters to be considered simultaneously. The concept of extending the matrices facilitates the development of a point matrix, including the forcing function. If, however, the forcing functions have different frequencies, then the system response for each forcing function is computed separately and the results are superimposed to determine the total response. The following explanation further clarifies this point.

Systems having more than one exciter may be classified into three categories, as shown in Fig. 8-14, and analyzed as follows:

- i. *All exciters have the same frequency* (Fig. 8-14a). In this case, the system may be analyzed considering all the exciters simultaneously by using the extended transfer matrices with frequency  $\omega_1$ .
- ii. *Group of exciters have the same frequency* (Fig. 8-14b). For this system, exciters are divided into groups, with each group comprised of exciters having the same frequency. Considering one group of exciters at a time, the system is analyzed by using the extended-transfer matrices with the frequency of the group. The results are then superimposed to determine the total response of the system.

- iii. *Each exciter with different frequency* (Fig. 8-14c). In this case, the system response for each exciter is determined separately, and the total response is then calculated by superposition. Since only one forcing function is considered at a time, ordinary matrices (i.e., 2 x 2) are used in this case.

Expressions to determine the frequency response of typical piping systems having the following exciters are derived in this section: fluctuating pressure head, oscillating valve, and fluctuating discharge. By proceeding in a similar manner, expression for other exciters may be derived.

A step-by-step procedure is outlined to determine the frequency response of piping systems.

### Fluctuating Pressure Head

A wave at the surface of a reservoir at the entrance of a piping system is a typical example of a boundary with fluctuating pressure head. To illustrate the application of the transfer matrix method to determine the frequency response, let us consider a system (Fig. 8-15), with a dead end at the right end and a wave on the reservoir surface. Due to the wave, the pressure head at section 1 fluctuates sinusoidally about the mean-pressure head. Let this pressure-head variation be given by

$$h_1^{*R} = \operatorname{Re}(h_1^R e^{j\omega t}) = K \cos \omega t = \operatorname{Re}(K e^{j\omega t}) \quad (8-106)$$

In addition, let  $\mathbf{U}$  be the transfer matrix relating the state vectors at the 1st and  $(n+1)$ th section, i.e.,

$$\mathbf{z}_{n+1}^L = \mathbf{U} \mathbf{z}_1^R \quad (8-107)$$

It is assumed that there is no other forcing function in the system; otherwise, an extended-transfer matrix,  $\mathbf{U}'$ , is used. Expansion of Eq. 8-107 yields

$$q_{n+1}^L = u_{11} q_1^R + u_{12} h_1^R \quad (8-108)$$

$$h_{n+1}^L = u_{21} q_1^R + u_{22} h_1^R \quad (8-109)$$

Since at the dead end,  $q_{n+1}^L = 0$ , it follows from Eq. 8-108 that

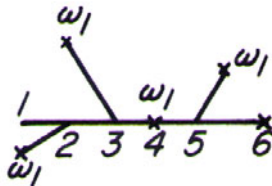
$$q_1^R = -\frac{u_{12}}{u_{11}} h_1^R \quad (8-110)$$

which on the basis of Eq. 8-106 becomes

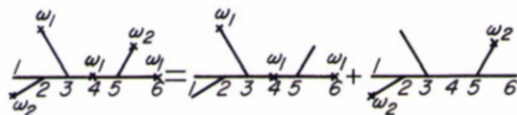
$$q_1^R = -\frac{u_{12} K}{u_{11}} \quad (8-111)$$

Substitution of Eq. 8-111 into Eq. 8-109 and simplification of the resulting equation gives

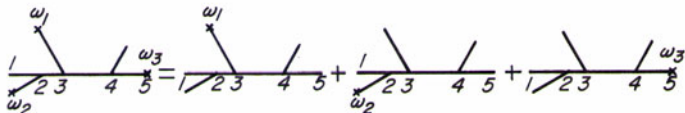
$$h_{n+1}^L = \left( u_{22} - \frac{u_{12} u_{21}}{u_{11}} \right) K \quad (8-112)$$



(a) All exciters have same frequency



(b) Exciters divided into two groups, according to frequency



(c) Each exciter has a different frequency

**Fig. 8-14.** Systems having more than one exciter.

Hence, the amplitude of the pressure-head fluctuation at the dead end is

$$h_a = |h_{n+1}^L| = \left| \left( u_{22} - \frac{u_{12}u_{21}}{u_{11}} \right) K \right| \quad (8-113)$$

The amplitude of the pressure head at the dead end may be nondimensionalized by dividing it by the amplitude of the pressure fluctuations at the reservoir end, i.e.,

$$h_r = \left| \frac{h_a}{K} \right| = \left| u_{22} - \frac{u_{12}u_{21}}{u_{11}} \right| \quad (8-114)$$

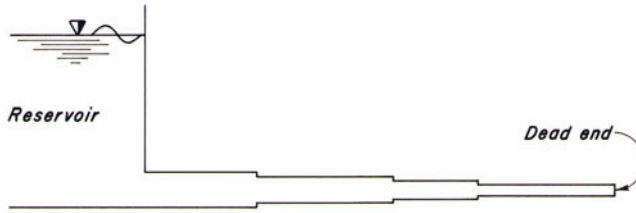


**Fig. 8-15.** Series system with dead end.

### Fluctuating Discharge

Flows of a reciprocating pump on the suction and on the discharge side are periodic. These fluctuations may be decomposed into a set of harmonics. Severe pressure oscillations are developed if any of these harmonics has a period equal to one of the natural periods of either the suction or discharge pipeline.

Expressions are derived in this section to determine, by the transfer matrix method, the frequency response of systems having a reciprocating pump. The suction and the discharge lines may have stepwise changes in diameter and/or wall thickness and may have branches with reservoirs, dead ends, or orifices but no boundary with a periodic forcing function.

### Suction Line

Let the transfer matrix relating the state vectors at the 1st and  $(n + 1)$ th section of the suction line (Fig. 8-16) be  $\mathbf{U}$ , i.e.,

$$\mathbf{z}_{n+1}^L = \mathbf{U} \mathbf{z}_1^R \quad (8-115)$$

By expanding Eq. 8-115 and noting that  $h_1^R = 0$ , we obtain

$$q_{n+1}^L = u_{11} q_1^R \quad (8-116)$$

and

$$h_{n+1}^L = u_{21} q_1^R \quad (8-117)$$

Hence,

$$h_{n+1}^L = \frac{u_{21}}{u_{11}} q_{n+1}^L \quad (8-118)$$

### Pump

The variation of inflow with time for one period is decomposed into a set of harmonics by Fourier analysis [Wylie, 1965]. Let the discharge for the  $m$ th harmonic be

$$q_{n+1}^L = A'_m \sin(m\omega t + \psi_m) \quad (8-119)$$

or

$$q_{n+1}^L = \operatorname{Re}(A_m e^{jm\omega t}) \quad (8-120)$$

in which  $A_m = A'_m \exp[j(\psi_m - \frac{1}{2}\pi)]$ ;  $A'_m$  and  $\psi_m$  are the amplitude and the phase angle, respectively, for the  $m$ th harmonic; and  $\omega$  = frequency of the fundamental. It follows from Eqs. 8-3 and 8-120 that  $q_{n+1}^L = A_m$  in which  $A_m$  is a complex constant. Substitution of this relationship into Eq. 8-118 yields

$$h_{n+1}^L = \frac{u_{21}}{u_{11}} A_m \quad (8-121)$$

Hence, the amplitude of pressure-head fluctuation at the suction flange is

$$h_m = |(h_{n+1}^L)_m| = \left| \frac{u_{21} A_m}{u_{11}} \right| \quad (8-122)$$

and the phase angle for the pressure head is

$$\phi_m = \tan^{-1} \left[ \frac{\operatorname{Im}(h_{n+1}^L)_m}{\operatorname{Re}(h_{n+1}^L)_m} \right] \quad (8-123)$$

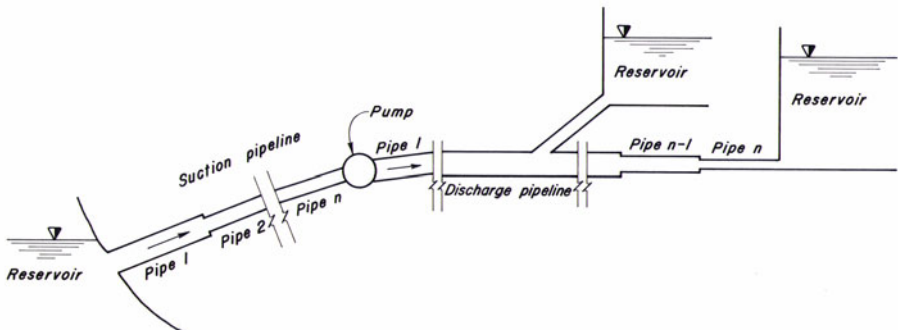


**Fig. 8-16. Suction and discharge lines.**

The head-versus-time curve may be obtained by vectorially adding the head-versus-time curve for each harmonic. For the  $m$ th harmonic,

$$h_{n+1}^{*L} = \operatorname{Re} \left[ h_m e^{j(m\omega t + \phi_m)} \right] \quad (8-124)$$

or

$$h_{n+1}^{*L} = h_m \cos (m\omega t + \phi_m) \quad (8-125)$$

Hence, the pressure-head-versus-time curve may be computed from the equation

$$h_{n+1}^{*L} = \sum_{m=1}^M h_m \cos (m\omega t + \phi_m) \quad (8-126)$$

in which  $M$  = number of harmonics into which the inflow-versus-time curve for the pump is decomposed.

### *Discharge Line*

By proceeding in a similar manner and noting that  $h_{n+1}^L = 0$  for a downstream reservoir, the following equation is obtained for the variation of pressure-head with time at the discharge side of the pump:

$$h_1^{*R} = \sum_{m=1}^M h'_m \cos (m\omega t + \phi'_m) \quad (8-127)$$

in which

$$h'_m = |(h_1^R)_m| = \frac{|u_{21}A_m|}{|u_{12}u_{21} - u_{11}u_{22}|} \quad (8-128)$$

$$\phi'_m = \tan^{-1} \left[ \frac{\operatorname{Im}(h_m^R)}{\operatorname{Re}(h_m^R)} \right] \quad (8-129)$$

and  $A_m$  = complex amplitude of  $m$ th harmonic of the variation of the pump discharge with time.

### *Oscillating Valve*

The flow area of an oscillating valve varies periodically. Since the equation (Eq. 8-59) relating the head, discharge, and the valve flow area is nonlinear, this case is more difficult to analyze than the preceding ones. However, as discussed in Section 8-7, this equation may be linearized if  $h \ll H_o$ . In the derivation of expressions in this section, the point matrix of Eq. 8-71 is used. This matrix is derived for a sinusoidal valve movement and by linearizing the valve equation. Thus, to use the expression for the nonharmonic periodic valve movement derived herein, the valve motion is decomposed into a set of harmonics by Fourier analysis, the system response is determined individually for each harmonic at its frequency, and then the total system response is calculated by superimposing the individual responses.

Let  $\mathbf{U}'$  be the extended overall transfer matrix relating the state vectors at the 1st and the  $(n + 1)$ th section of the system, i.e.,

$$\mathbf{z}'_{n+1}^L = \mathbf{U}' \mathbf{z}'_1^R \quad (8-130)$$

In addition,

$$\mathbf{z}'_{n+1}^R = \mathbf{P}'_{ov} \mathbf{z}'_{n+1}^L \quad (8-131)$$

Hence,

$$\mathbf{z}'_{n+1}^R = \mathbf{P}'_{ov} \mathbf{U}' \mathbf{z}'_1^R \quad (8-132)$$

By substituting  $\mathbf{P}'_{ov}$  from Eq. 8-71, multiplying the matrices  $\mathbf{P}'_{ov}$  and  $\mathbf{U}'$ , expanding and noting that  $h_1^R = 0$ ,  $h_{n+1}^R = 0$ , and  $q_{n+1}^L = q_{n+1}^R$ , we obtain

$$q_1^R = -\frac{u_{23} - \frac{2H_o}{Q_o}u_{13} + \frac{2H_0k}{\tau_o}u_{33}}{u_{21} - \frac{2H_o}{Q_o}u_{11} + \frac{2H_0k}{\tau_o}u_{13}} \quad (8-133)$$

$$q_{n+1}^L = u_{11}q_1^R + u_{13} \quad (8-134)$$

in which  $u_{11}, u_{12}, \dots, u_{33}$  are the elements of the matrix,  $\mathbf{U}'$ . By expanding Eq. 8-130 and noting that  $h_1^R = 0$ , we obtain

$$h_{n+1}^L = u_{21}q_1^R + u_{23} \quad (8-135)$$

To determine the frequency response, the extended field and point matrices are first computed. Then, the extended overall transfer matrix is determined by multiplying the field and point matrices starting at the downstream end, i.e.,

$$\mathbf{U}' = \mathbf{F}'_n \mathbf{P}'_n \dots \mathbf{P}'_2 \mathbf{F}'_1 \quad (8-136)$$

The value of  $q_1^R$  is determined from Eq. 8-133, and  $q_{n+1}^L$  and  $h_{n+1}^L$  are computed from Eqs. 8-134 and 8-135. The absolute values of  $h_{n+1}^L$  and  $q_{n+1}^L$  are the amplitudes of pressure head and discharge fluctuations at the valve, and their arguments are, respectively, the phase angles between head and  $\tau^*$  and between discharge and  $\tau^*$ .

If there is no other forcing function in the system except the oscillating valve at the downstream end of the system, then ordinary field and point matrices are used instead of the extended matrices. In this case,  $u_{13} = u_{23} = u_{31} = 0$  and  $u_{33} = 1$  in Eqs. 8-133 through 8-135.

### Computational Procedure

The frequency response of a piping system may be determined as follows:

1. Draw the general block diagram of the system and then prepare its simplified version. For simple systems, this step may be omitted.

2. If the forcing function is nonharmonic, decompose it into a set of harmonics by Fourier analysis. Then, consider one harmonic at its specified frequency at a time, and compute the point and field matrices. For an extended transfer matrix, add the following elements to the corresponding transfer matrix derived in Section 8-7:  $u_{13} = u_{23} = u_{31} = u_{32} = 0$  and  $u_{33} = 1$ . Note that extended transfer matrices are used only if there is more than one exciter in the system and each has the same frequency.
3. Calculate the overall transfer matrix by an ordered multiplication of the point and field matrices, starting at the downstream end. For this calculation, the block diagram of step 1 is very helpful. For the multiplication of matrices, the scheme outlined in Example 8-2 may be followed for hand calculations. This scheme reduces the amount of computations.
4. Use the expressions developed in this section to determine the frequency response.
5. For preparing a frequency-response diagram, repeat steps 3 and 4 for different frequencies, one frequency at a time.

The following example illustrates the preceding procedure for determining the frequency response at the downstream end of a system having a dead-end branch and an oscillating valve at the downstream end.

### Example 8-2

*Plot a frequency-response diagram for a section at the valve end of the branch system shown in Fig. 8-17a. Other data for the system are:  $Q_o = 0.314 \text{ m}^3/\text{s}$ ;  $T_{th} = 3.0 \text{ s}$ ;  $R = 0.0$ ;  $k = 0.2$ ;  $\tau_o = 1.0$ ; and  $H_o = 100 \text{ m}$ .*

*Set up a computational procedure suitable for hand calculations.*

### Solution

Computations for  $\omega_r = 2.0$  are presented in the following paragraphs. Proceeding similarly for different values of  $\omega_r$ , the frequency-response diagram shown in Fig. 8-17c may be plotted.

#### *Components of Transfer Matrices*

$$\omega_{th} = 2\pi/3 = 2.094 \text{ rad/s}$$

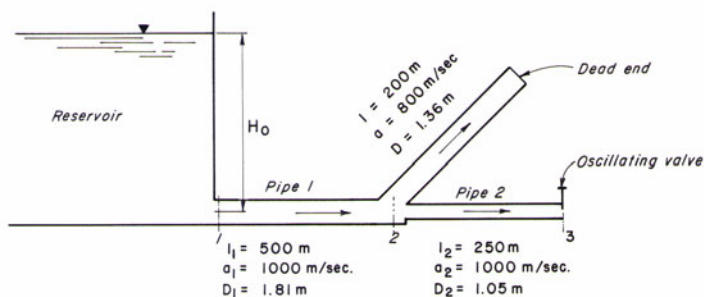
$$\omega = \omega_r \omega_{th} = 2 \times 2.094 = 4.189 \text{ rad/s}$$

Pipe 1:

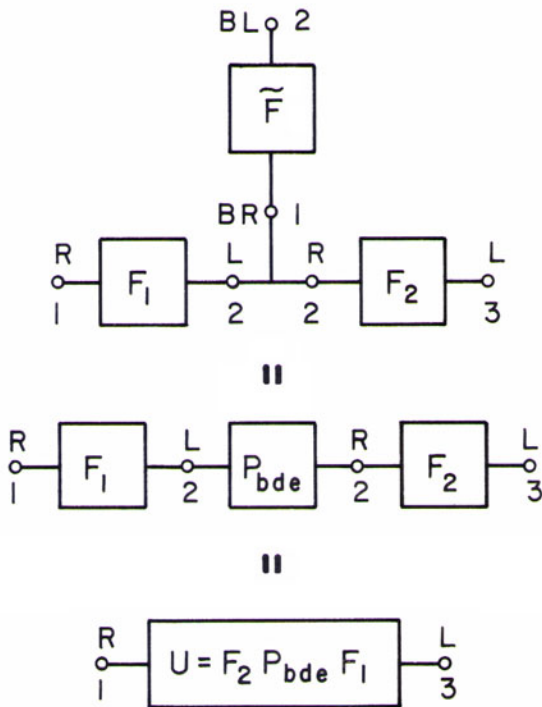
$$b_1 = l_1/a_1 = 500/1000 = 0.5 \text{ s}$$

$$A_1 = \pi D_1^2/4 = \pi(1.81)^2/4 = 2.578 \text{ m}^2$$

$$C_1 = a_1/(gA_1) = 1000/(9.81 \times 2.578) = 39.542 \text{ s m}^{-2}$$

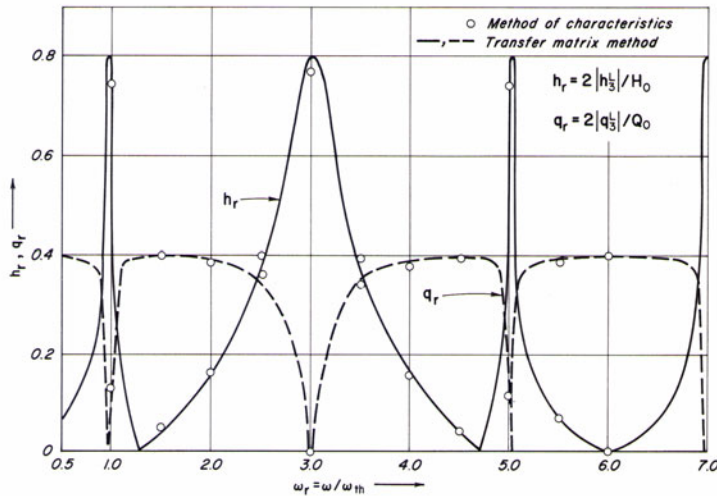


(a) Piping system



(b) Block diagram

Fig. 8-17. Frequency response of a branching system with a dead-end.



(c) Frequency response diagram

Fig. 8-17. (Continued)

Substitution of these values into Eq. 8-37 yields

$$f_{11} = f_{22} = \cos(0.5 \times 4.189) = -0.5$$

$$f_{21} = -39.542 \sin(0.5 \times 4.189)j = -34.244j$$

$$f_{12} = -j \sin(0.5 \times 4.189)/39.542 = -0.022j$$

Proceeding similarly, the field matrix for pipe 2,  $\mathbf{F}_2$ , is obtained.

$$\mathbf{F}_2 = \begin{bmatrix} 0.500 & -0.007j \\ -102.732j & 0.500 \end{bmatrix}$$

Branch pipe:

Since the branch line comprises a single pipe,  $\tilde{\mathbf{U}} = \tilde{\mathbf{F}}$ . Proceeding similarly as for pipe 1, the following values of the elements of the field matrix for the branch are obtained:

$$\tilde{u}_{11} = 0.5$$

$$\tilde{u}_{12} = -0.0154j$$

Substitution of these values into Eq. 8-87 yields the following point matrix for the junction of the branch and the main lines.

$$\mathbf{F}_2 = \begin{bmatrix} 1.0 & -0.0308j \\ 0.0 & 1.0 \end{bmatrix}$$

It is clear from the block diagram shown in Fig. 8-17b that

$$\mathbf{U} = \mathbf{F}_2 \mathbf{P}_{\text{bde}} \mathbf{F}_1$$

These matrices may be multiplied systematically as shown in Table 9-8. Since  $h_1^R = 0$  (constant-head reservoir), the second column in the matrices  $\mathbf{F}_1$ ,  $\mathbf{P}_{\text{bde}} \mathbf{F}_1$ , and  $\mathbf{F}_2 \mathbf{P}_{\text{bde}} \mathbf{F}_1$ , is multiplied by zero. Thus, the elements in the second column of these matrices are unnecessary and may be dropped. The unnecessary elements in Table 9-8 are indicated by a horizontal dash.

**Table 8-1.** Scheme for multiplication of transfer matrices

|                             |   |   |
|-----------------------------|---|---|
|                             | $\begin{bmatrix} -0.500 & - \\ -34.244j & - \end{bmatrix}$            | $\begin{Bmatrix} q \\ 0 \end{Bmatrix}_1^R = \mathbf{z}_2^L$   |
| $\mathbf{P}_{\text{bde}} =$ | $\begin{bmatrix} 1.000 & -0.031j \\ 0.000 & 1.000 \end{bmatrix}$      | $\begin{bmatrix} -1.555 & - \\ -34.244j & - \end{bmatrix} \quad \begin{Bmatrix} q \\ h \end{Bmatrix}_1^R = \mathbf{z}_2^R$  |
| $\mathbf{F}_2 =$            | $\begin{bmatrix} 0.500 & -0.0073j \\ -102.732j & 0.500 \end{bmatrix}$ | $\begin{bmatrix} -1.0273 & - \\ 142.595j & - \end{bmatrix} \quad \begin{Bmatrix} q \\ h \end{Bmatrix}_1^R = \mathbf{z}_3^L$ |

Note that ordinary transfer matrices are used because there is only one forcing function. Hence,  $u_{13}$ ,  $u_{23}$ , and  $u_{31}$  are zero, and  $u_{33}$  is unity in Eqs. 8-133 through 8-135. Substitution of these values and those for  $u_{11}$  and  $u_{21}$  calculated in Table 9-8 into Eq. 8-133 yields

$$q_1^R = -0.584 + 0.0127j$$

It follows from Eqs. 8-134 and 8-135 that

$$q_3^L = 0.0600 - 0.0131j$$

and

$$h_3^L = -1.8134 - 8.3215j$$

Hence,

$$h_r = 2 |h_3^L| / H_o = 0.170$$

$$q_r = 2 |q_3^L| / Q_o = 0.390$$

The phase angle between the pressure head and the relative gate opening

$$\begin{aligned} &= \tan^{-1} \left[ \frac{-8.3215}{-1.8134} \right] \\ &= -102.29^\circ \end{aligned}$$

The phase angle between the discharge and the relative gate opening

$$\begin{aligned} &= \tan^{-1} \left[ \frac{-0.0131}{0.0600} \right] \\ &= -12.29^\circ \end{aligned}$$

## 8-8 Spatial Variation of Pressure and Discharge

The previous sections dealt with the computation of the pressure and discharge oscillations at the end sections of a system. However, sometimes it is necessary to determine the amplitudes of these fluctuations along the length of the pipeline. A procedure for this is outlined in this section.

To analyze a piping system, two of the four quantities — discharge and pressure or their relationship at either end of the system — should be known. The other two are then calculated by using the equations derived in the previous section. The amplitudes of the discharge and pressure fluctuations at the upstream end being known, their amplitudes along the pipeline may then be determined. The procedure is illustrated for a system with an upstream reservoir and an oscillating valve at the downstream end. Proceeding similarly, the equations for other systems having different boundary conditions may be developed.

The following discussion is for determining the amplitudes of the discharge and pressure oscillations at the  $k$ th section of the  $i$ th pipe (see Fig. 8-18a). Let  $\mathbf{W}$  be the transfer matrix relating the state vectors at section 1 of the first pipe and section 1 of the  $i$ th pipe, i.e.,

$$(\mathbf{z}_1^R)_i = \mathbf{W} (\mathbf{z}_1^R)_1 \quad (8-137)$$

and the field matrix  $\mathbf{F}_x$  relating the state vectors at section 1 and the  $k$ th section of the  $i$ th pipe, i.e.,

$$(\mathbf{z}_k^L)_i = \mathbf{F}_x (\mathbf{z}_1^R)_i \quad (8-138)$$

In these equations, the subscript with the parentheses refers to the pipe number. The matrix  $\mathbf{W}$  is computed by multiplying the point and field matrices for the first  $(i - 1)$  pipes (see the block diagram of Fig. 8-18b), i.e.,

$$\mathbf{W} = \mathbf{P}_i \mathbf{F}_{i-1} \mathbf{P}_{i-1} \dots \mathbf{F}_1 \quad (8-139)$$

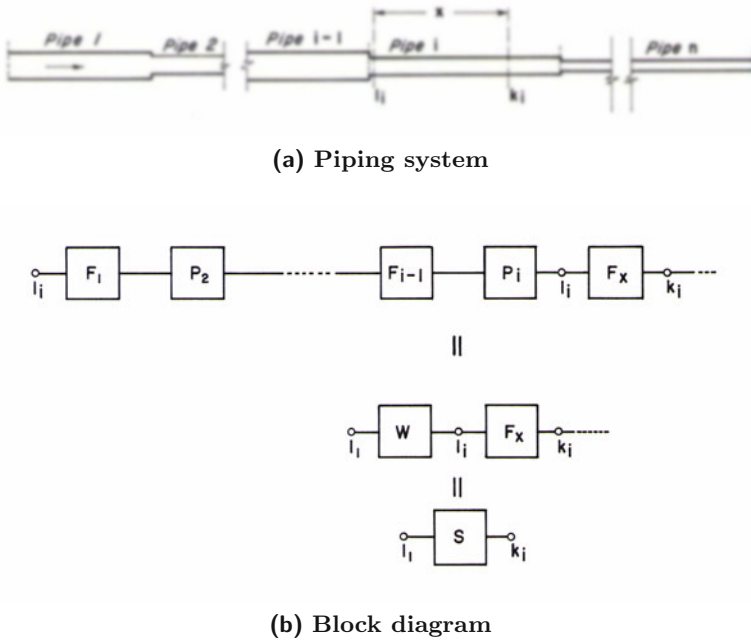


**Fig. 8-18.** Designation of  $k$ th section on  $i$ th pipe.

and the matrix  $\mathbf{F}_x$  is calculated by replacing 1 with  $x$  in Eq. 8-36. Note that the elements of the matrix  $\mathbf{W}$  for a specified frequency are constants, while those of the matrix  $\mathbf{F}_x$  depend upon the value of  $x$  as well.

It follows from Eqs. 8-137 and 8-138 that

$$(\mathbf{z}_k^L)_i = \mathbf{S} (\mathbf{z}_1^R)_1 \quad (8-140)$$

in which

$$\mathbf{S} = \mathbf{F}_x \mathbf{W} = \mathbf{F}_x \mathbf{P}_i \mathbf{F}_{i-1} \mathbf{P}_{i-1} \dots \mathbf{F}_1 \quad (8-141)$$

The value of  $(q_1^R)_1$  is calculated from Eq. 8-133. Furthermore, for the upstream reservoir,  $(h_1^R)_1 = 0$ . Substitution of these values into the expanded form of Eq. 8-140 yields

$$(q_k^L)_i = s_{11} (q_1^R)_1 \quad (8-142)$$

and

$$(h_k^L)_i = s_{21} (q_1^R)_1 \quad (8-143)$$

The amplitudes of the discharge and pressure fluctuations at any other section may be determined by proceeding in a similar manner.

## 8-9 Pressure Nodes and Antinodes

The location of pressure nodes and antinodes is an important aspect of the analysis of resonance in pipelines at higher harmonics. The amplitude of the pressure fluctuation is minimum at a node and, maximum at an antinode. For a frictionless system, the amplitude of the pressure fluctuation at a node is zero.

Severe pressure fluctuations at the antinodes may burst the pipe due to pressure in excess of the design pressure or may collapse the pipe due to sub-atmospheric pressure. A surge tank is not effective in preventing the transmission of pressure waves from one side of the tank to the other if a node is formed at its base. Jaeger explained the development of fissures in the Kandergrund tunnel [Jaeger, 1963 and 1977] due to the establishment of a pressure node at the tank. This made the tank ineffective in preventing the pressure oscillations from the penstock into the tunnel even though it was overdesigned.

The locations of the nodes and antinodes in a pipeline may be determined as follows: The amplitude of the pressure fluctuation at a section may be determined from Eq. 8-143. Since the amplitude of the pressure fluctuations at a node is zero and  $q_1^R \neq 0$  for a nontrivial solution, it follows from this equation that for a frictionless system

$$s_{21}(x) = 0 \quad (8-144)$$

The solution of this equation for  $x$  gives the location of the nodes on the  $i$ th pipe.

The amplitude of the pressure fluctuation is maximum at the antinodes. Hence, the location of the antinodes in a pipeline may be determined by differentiating Eq. 8-144 with respect to  $x$ , equating the result to zero, and then solving for  $x$ , i.e., the roots of the equation

$$\frac{d}{dx} s_{21}(x) = 0 \quad (8-145)$$

are the location of the antinodes.

The expressions for the location of nodes and antinodes in simple systems may be derived from Eqs. 8-144 and 8-145 as follows. The procedure is illustrated by deriving expressions for a single pipe and for two pipes in series. Expressions for other systems may be derived in a similar manner. For complex systems, however, it is better to solve Eqs. 8-144 and 8-145 numerically rather than to derive the expressions and then solve them.

### Single Pipe

For a frictionless single pipe having constant cross-sectional area, it follows from Eqs. 8-37 and 8-144 that

$$-jC_1 \sin(\omega x/a_i) = 0 \quad (8-146)$$

or

$$\sin(\omega x/a_i) = 0 \quad (8-147)$$

This equation is satisfied for

$$x = n\pi a_i/\omega \quad (n = 0, 1, 2, \dots) \quad (8-148)$$

The values of  $x > l_i$  represent the locations of the imaginary nodes, which are discarded. For the antinodes, it follows from Eqs. 8-145 and 8-147 that

$$\cos(\omega x/a_i) = 0 \quad (8-149)$$

The solution of this equation gives the locations of the antinodes, i.e.,

$$x = \left(n + \frac{1}{2}\right) \frac{\pi a_i}{\omega} \quad (n = 0, 1, 2, \dots) \quad (8-150)$$

Again, the values of  $x > l_i$  are the locations of the imaginary nodes and are discarded.

Equations 8-147 and 8-149 show that a standing wave is formed along the pipe length.

## Series System

In a two-pipe series system (Fig. 8-9), the locations of nodes and antinodes in the pipe leading from the reservoir are given by Eqs. 8-147 and 8-149. However, their location in the second pipe may be determined by using Eqs. 8-144 and 8-145.

By substituting the expressions for  $\mathbf{F}_x$ ,  $\mathbf{F}_1$ , and  $\mathbf{P}_2$  into Eq. 8-139, multiplying the matrices, and using Eq. 8-144, we obtain

$$-C_2 \sin\left(\frac{\omega x}{a_2}\right) \cos\left(\frac{\omega l_1}{a_1}\right) - C_1 \cos\left(\frac{\omega x}{a_2}\right) \sin\left(\frac{\omega l_1}{a_1}\right) = 0 \quad (8-151)$$

which upon simplification becomes

$$\tan \frac{\omega x}{a_2} = -\frac{a_1 A_2}{a_2 A_1} \tan \frac{\omega l_1}{a_1} \quad (8-152)$$

Note that Eqs. 8-151 and 8-152 are valid for a frictionless system only. Solution of Eq. 8-152 for  $x$  gives the location of the nodes.

## 8-10 Resonant Frequencies

To prevent resonance in a piping system, it is important to know its resonant frequencies so that possible forcing functions or excitors having similar

frequencies may be avoided. However, if it is not possible to avoid these frequencies, then remedial measures may be adopted. Since the forcing function of self-excited systems is usually unknown, the frequency response of the system cannot be determined. The resonant frequencies of such a system may be calculated by using a procedure presented by Zielke and Rösl, [1971] or by the application of the transfer matrix method, as discussed in the following paragraphs.

The transfer matrices for the system components are written for the free-damped oscillations by replacing  $j\omega$  in the transfer matrices presented in Section 8-7 by the complex frequency  $s = \sigma + j\omega$ . The overall-transfer matrix is obtained by multiplying these matrices. Then, two homogeneous equations in two unknowns are obtained by applying the free-end conditions, e.g., constant-head reservoir, dead end, orifice, etc. For a nontrivial solution, the determinant of the coefficients of these equations should be zero. A trial-and-error technique is used to solve the determinant equation to determine the resonant frequencies of the system.

The following example of a dead-end system having a constant-head reservoir at the upper end is presented for illustration purposes; systems with other end conditions may be analyzed in a similar manner.

Let  $\mathbf{U}$  be the overall transfer matrix for the system, i.e.,

$$\mathbf{z}_{n+1}^R = \mathbf{U}\mathbf{z}_1^R \quad (8-153)$$

By substituting the end conditions, i.e.,  $h_1^R = 0$  and  $q_{n+1}^L = 0$ , Eq. 8-153 becomes

$$u_{11}q_1^R = 0 \quad (8-154)$$

Note that both  $u_{11}$  and  $q_1^R$  are complex variables. By representing the real and imaginary parts of a complex variable by superscripts  $r$  and  $i$  respectively, i.e.,  $u_{11} = u_{11}^r + ju_{11}^i$  and simplifying, Eq. 8-154 takes the form

$$(u_{11}^r q_1^{rR} - u_{11}^i q_1^{iR}) + j(u_{11}^i q_1^{rR} + u_{11}^r q_1^{iR}) = 0 \quad (8-155)$$

For a complex number to be zero, both the real and imaginary parts must be zero. Hence,

$$u_{11}^r q_1^{rR} - u_{11}^i q_1^{iR} = 0 \quad (8-156)$$

$$u_{11}^i q_1^{rR} + u_{11}^r q_1^{iR} = 0 \quad (8-157)$$

For a nontrivial solution of Eqs. 8-156 and 8-157,

$$\begin{vmatrix} u_{11}^r & -u_{11}^i \\ u_{11}^i & u_{11}^r \end{vmatrix} = 0 \quad (8-158)$$

which upon simplification becomes

$$(u_{11}^r)^2 + (u_{11}^i)^2 = 0 \quad (8-159)$$

Equation 8-159 is satisfied if and only if

$$u_{11}^r = 0 \quad (8-160)$$

and

$$u_{11}^i = 0 \quad (8-161)$$

The values of  $\sigma$  and  $\omega$  may be determined by solving Eqs. 8-160 and 8-161 by the Newton-Raphson method [McCracken and Dorn, 1964]. If  $\sigma_k$  and  $\omega_k$  are the values after the  $k$ th iteration, then a better estimate of the solution,  $\sigma_{k+1}$  and  $\omega_{k+1}$ , of Eqs. 8-160 and 8-161 is

$$\sigma_{k+1} = \sigma_k - \frac{u_{11}^r \frac{\partial u_{11}^i}{\partial \omega} - u_{11}^i \frac{\partial u_{11}^r}{\partial \omega}}{\frac{\partial u_{11}^r}{\partial \sigma} \frac{\partial u_{11}^i}{\partial \omega} - \frac{\partial u_{11}^r}{\partial \omega} \frac{\partial u_{11}^i}{\partial \sigma}} \quad (8-162)$$

$$\omega_{k+1} = \omega_k - \frac{u_{11}^r \frac{\partial u_{11}^i}{\partial \sigma} - u_{11}^i \frac{\partial u_{11}^r}{\partial \sigma}}{\frac{\partial u_{11}^r}{\partial \omega} \frac{\partial u_{11}^i}{\partial \sigma} - \frac{\partial u_{11}^r}{\partial \sigma} \frac{\partial u_{11}^i}{\partial \omega}} \quad (8-163)$$

In Eqs. 8-162 and 8-163,  $u_{11}^r$  and  $u_{11}^i$  and their partial derivatives are computed for  $\sigma_k$  and  $\omega_k$ . If  $|\sigma_{k+1} - \sigma_k|$  and  $|\omega_{k+1} - \omega_k|$  are less than a specified tolerance, then  $\sigma_{k+1}$  and  $\omega_{k+1}$  are the solutions of Eqs. 8-160 and 8-161; otherwise,  $\sigma_k$  and  $\omega_k$  are assumed equal to  $\sigma_{k+1}$  and  $\omega_{k+1}$  and this process is repeated until the difference between the two successive values of  $\sigma$  and  $\omega$  is less than the specified tolerance.

This procedure is general and is not limited to simple and frictionless systems. Also, note that the intermediate state vectors are eliminated by multiplying the transfer matrices, and only a second-order determinant is solved as compared to an  $n \times n$  determinant (value of  $n$  depends upon the number of pipes and appurtenances in the system) in the procedure presented by Zielke and Rösl [1971].

The above procedure is simplified considerably for a frictionless system since  $u$  is a function of  $\omega$  only. In a frictionless system having a constant-head reservoir at the upstream end and an oscillating valve at the downstream end, the amplitude of the discharge fluctuation at the valve is zero during resonating conditions at the fundamental or at one of the higher odd harmonics. This was observed by Camichel et al. [1919] and reported to be true by Jaeger [1948 and 1963]. The frequency-response diagrams of a number of series, parallel, and branch systems (a branch system with a side branch having an orifice or an oscillating valve being an exception) presented by Wylie [1965-a, 1983]; and by Chaudhry [1970, 1970-a] confirm this result. Expressions for the resonant frequencies of the simple frictionless systems and their numerical values for the simple or complex systems may be determined by using this results as follows.

Let  $\mathbf{U}$  be the overall transfer matrix for a system having a constant-head reservoir at the upstream end (section 1) and an oscillating valve at the downstream end (section  $n + 1$ ), i.e.,

$$\mathbf{z}_{n+1}^L = \mathbf{U}\mathbf{z}_1^R \quad (8-164)$$

By expanding Eq. 8-164 and noting that  $h_1^R = 0$  (constant-head reservoir), and  $q_{n+1}^L = 0$  (discharge node) at a resonant frequency, we obtain

$$u_{11}q_1^R = 0 \quad (8-165)$$

Recall that  $u_{11}$  is the element in the first row and the first column of matrix  $\mathbf{U}$ . For a nontrivial solution,  $q_1^R \neq 0$ ; therefore,

$$u_{11} = 0 \quad (8-166)$$

Eq. 8-166 is solved to determine the resonant frequencies. To do this,  $u_{11}$  is computed for different trial values of  $\omega$ , and the  $u_{11}$ -versus- $\omega$  curve is plotted. If the selected value of  $\omega$  is equal to one of the resonant frequencies, then  $u_{11} = 0$ . This is not usually the case for the first guess for  $\omega$ , and the resulting numerical value of  $u_{11}$  is referred to as the residual. The points of intersection of the  $u_{11}$ -versus- $\omega$  curve and the  $\omega$ -axis are the resonant frequencies.

### Normal Modes

As discussed previously, the system vibrates according to a definite shape corresponding to each natural frequency. Once the real part  $\sigma$  and the imaginary part  $\omega$  of the natural frequency are determined, it is easy to determine the normal mode corresponding to this frequency.

Let us illustrate the procedure by considering again the series dead-end system with a constant-level reservoir at the upstream end.

By expanding the first of Eqs. 8-14 and substituting  $h_1^R = 0$ , we obtain

$$\begin{aligned} q_2^L &= f_{11}q_1^R \\ h_2^L &= f_{21}q_1^R \end{aligned} \quad (8-167)$$

If we arbitrarily assume  $q_1^R = 1$ , then we can determine both  $q_2^L$  and  $h_2^L$  from Eqs. 8-167. Then using Eqs. 8-14 successively,  $q$  and  $h$  along the entire pipeline may be determined. The amplitude of oscillation at any location is equal to the absolute value of the complex variables  $q$  and  $h$ .

### Example 8-3

*Derive an expression for the frequencies of the fundamental and odd harmonics of the system shown in Fig. 8-19. Assume the system is frictionless.*

### Solution

For the series system shown in Fig. 8-19,

$$\mathbf{U} = \mathbf{F}_2 \mathbf{P}_2 \mathbf{F}_1$$

By substituting  $\mathbf{F}_2$  and  $\mathbf{F}_1$ , from Eq. 8-37 and  $\mathbf{P}_2$  from Eq. 8-58, multiplying

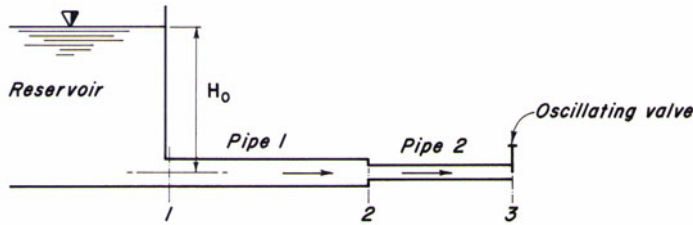


**Fig. 8-19.** Series piping system.

the matrices, and using Eq. 8-166, we obtain

$$\cos b_1\omega \cos b_2\omega - \frac{a_1}{a_2} \left( \frac{D_2}{D_1} \right)^2 \sin b_1\omega \sin b_2\omega = 0 \quad (8-168)$$

in which  $b_1$  and  $b_2$  are constants for pipe 1 and 2, respectively, as defined in Eq. 8-37.

### Example 8-4

Determine the frequencies of the fundamental and odd harmonics of the Toulouse pipeline shown in Fig. 8-20.

### Solution

The overall transfer matrix,  $\mathbf{U}$ , for the system of Fig. 8-20 is given by Eq. 8-167. For the selected value of  $\omega$ , the elements of the matrices  $\mathbf{F}_2$ ,  $\mathbf{P}_2$ , and  $\mathbf{F}_1$  are computed from Eqs. 8-37 and 8-58 for the system dimensions shown in Fig. 8-20, and these matrices are multiplied to compute the elements of  $\mathbf{U}$  matrix. As discussed earlier, the value of  $u_{11}$  is the residual. For different values of  $\omega$ , the values of the residual are computed, and the residual-versus- $\omega$  curve is plotted as shown in Fig. 8-21. The intersection of this curve with the  $\omega$ -axis yields the following frequencies, in rad/s:

- Fundamental: 8.863;
- Third harmonic: 20.14; and
- Fifth harmonic: 31.6.



(a) Toulouse pipeline



(b) Fully pipeline

**Fig. 8-20.** Longitudinal profile. (After Camichel et al. [1919].)

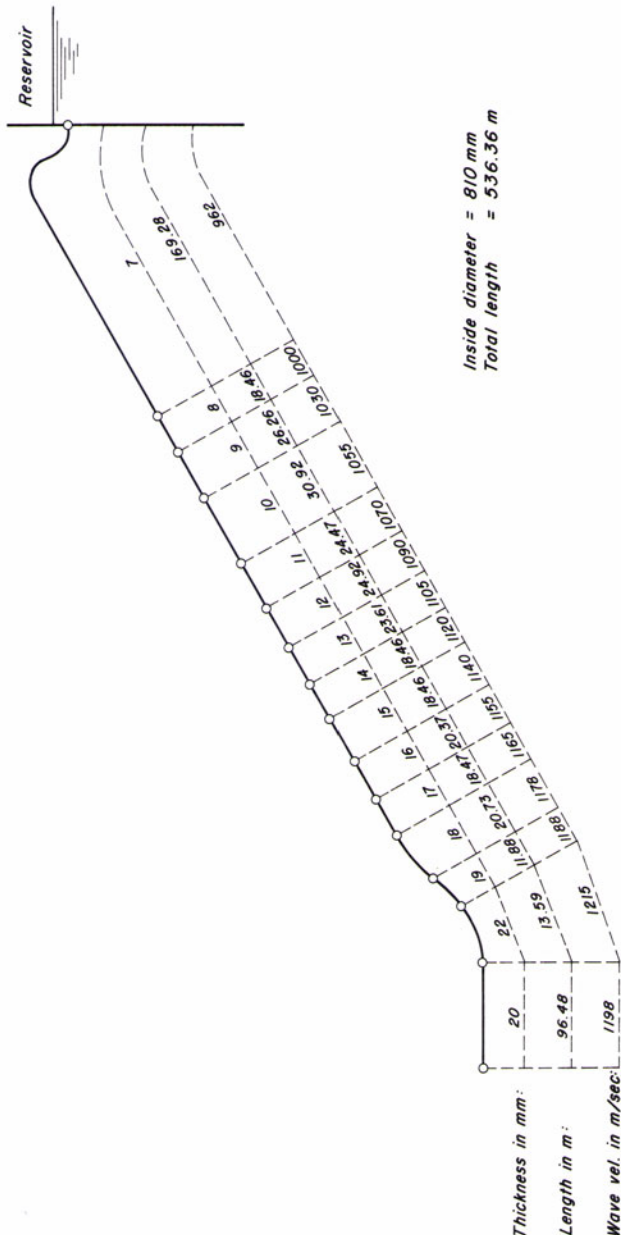
## 8-11 Verification of Transfer-Matrix Method

To demonstrate the validity of the method, the results computed by using the transfer matrix method are compared with the experimental values and with those determined by the method of characteristics and by energy concepts.

### Experimental Results

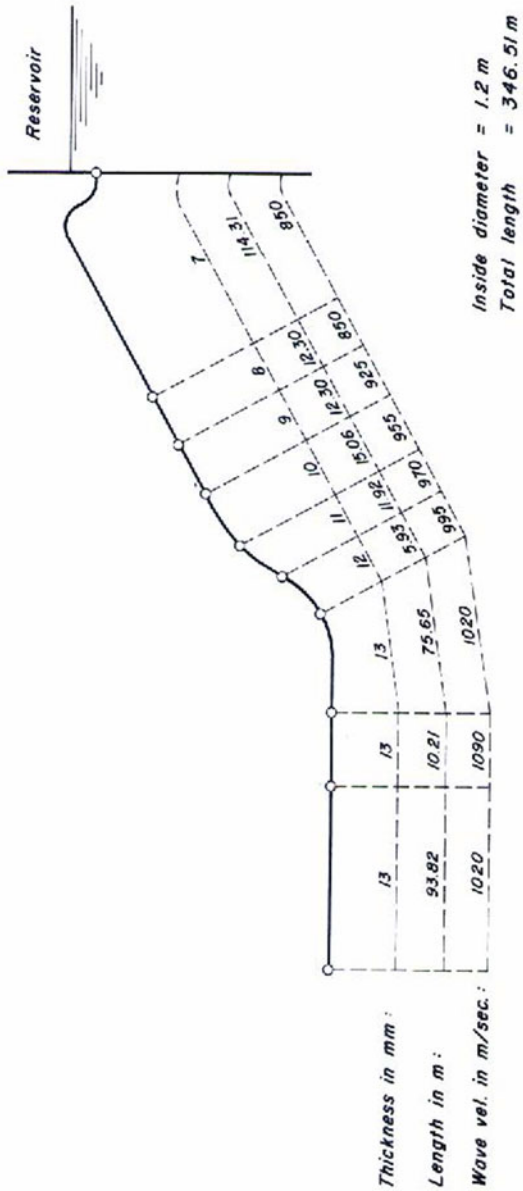
Except for the laboratory and field tests reported by Camichel et al. [1919], few experimental results on the resonating characteristics of pipes are available in the literature. In the tests reported by Camichel et al., the resonating conditions in series pipes were established by a rotating cock located at the downstream end of the pipeline. Each system had a constant-head reservoir at the upstream end. The data for these systems are given in [Fig. 8-20](#).

The periods of the fundamental and the higher harmonics determined experimentally and by the procedure outlined in the previous section are listed in [Table 8-2](#). There is close agreement between the experimental values and those determined by the transfer matrix method.



(c) Pipeline C4

Fig. 8-20. (Continued)



(d) Pipeline P3

Fig. 8-20. (*Continued*)

## Method of Characteristics

A number of series, parallel, and branching systems with the side branch having various boundary conditions were analyzed using the transfer-matrix method and the method of characteristics. The data for four of these systems and the frequency-response diagrams are presented in Figs. 8-22 through 8-25.

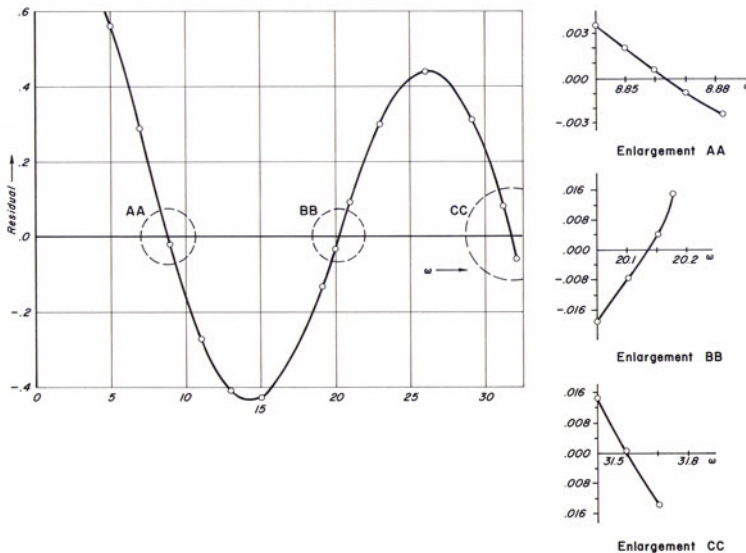


**Fig. 8-21.** Plot of residual versus  $\omega$  for Toulouse pipeline.

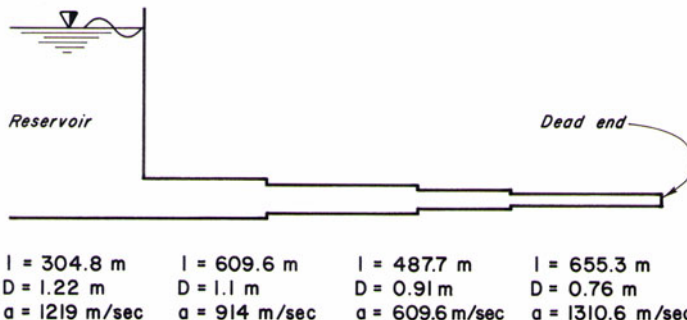
The frequency-response diagrams are presented in a nondimensional form. The frequency ratio,  $\omega_r$  is defined as  $\omega/\omega_{th}$ ; the pressure head ratio,  $h_r$  as  $2|h_{n+1}^L|/H_o$ ; and the discharge ratio,  $q_r$  as  $2|q_{n+1}^L|/Q_o$ . The values of  $h_r$  and  $q_r$  determined by the method of characteristics represent the amplitude of the swing from the minimum to the maximum value. The frequency of the forcing function is designated by  $\omega$ .

The oscillating valves are the excitors in all the systems except the dead-end series system of Fig. 8-22 in which the fluctuating pressure head at the upstream end is the exciter. The valve movement is sinusoidal with  $\tau_o = 1.0$  and  $k = 0.2$ . The fluctuating pressure head in Fig. 8-22 is also sinusoidal with  $K = 1.0$ . In the branch systems of Fig. 8-25,  $\tau_o = 1.0$  and  $k = 0.2$ .

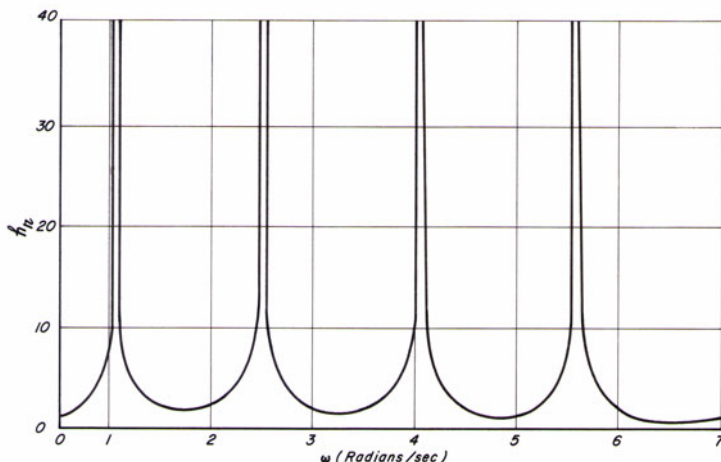
If the friction losses are taken into consideration, the analysis of various systems by the method of characteristics show that the amplitudes of the positive swing of pressure head and negative swing of the discharge are larger

Table 8-2. Calculated and measured periods

| System<br>No.  | Pipes | Theoretical<br>Period<br>(s) | Period (s)  |                 |                 |                 |                 |                  |
|----------------|-------|------------------------------|-------------|-----------------|-----------------|-----------------|-----------------|------------------|
|                |       |                              | Fundamental | 3rd<br>Harmonic | 5th<br>Harmonic | 7th<br>Harmonic | 9th<br>Harmonic | 11th<br>Harmonic |
|                |       |                              | Calc.       | Meas.           | Calc.           | Meas.           | Calc.           | Meas.            |
| Toulouse       | 2     | 0.932                        | 0.708       | 0.69            | 0.311           | 0.31            | 0.198           | —                |
| Fully          | 2     | 15.96                        | 13.719      | 13.50           | —               | —               | —               | —                |
| C <sub>4</sub> | 15    | 2.008                        | 1.887       | 1.882           | —               | —               | —               | —                |
| F <sub>3</sub> | 9     | 1.464                        | 1.405       | 1.368           | 0.502           | 0.505           | 0.296           | 0.310            |
|                |       |                              |             |                 |                 |                 | 0.2117          | 0.2150           |
|                |       |                              |             |                 |                 |                 | 0.1650          | 0.1667           |
|                |       |                              |             |                 |                 |                 | 0.1338          | 0.1420           |



(a) Piping system

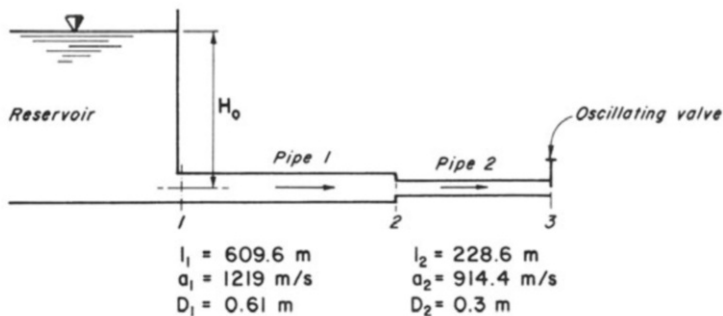


(b) Frequency response diagram

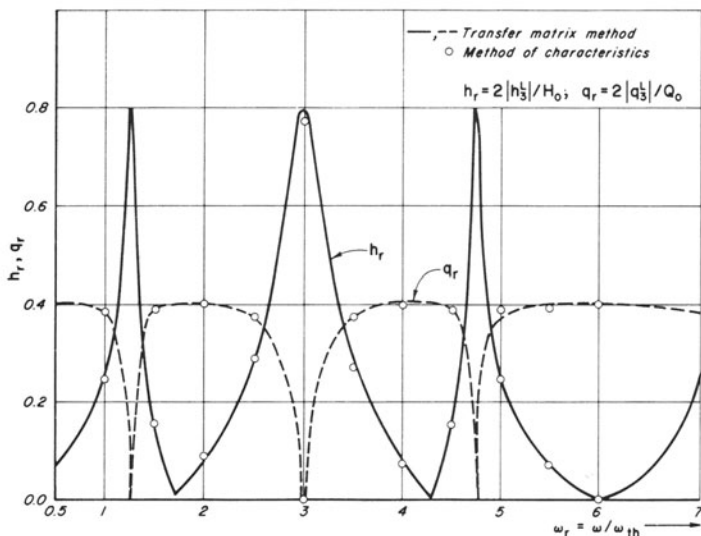
Fig. 8-22. Frequency response of a series piping system with dead end.

than the corresponding negative and positive swings. This is caused by the nonlinear friction term of the governing differential equations. In the transfer matrix method, however, the amplitudes of the positive and negative oscillations are equal because a sinusoidal solution is assumed and the equations are linearized.

To check the values of the phase angles between different quantities of interest, the oscillatory discharge and pressure head at the valve are computed by using the method of characteristics. The  $q_r^* \sim t$ ,  $h_r^* \sim t$ , and  $\tau^* \sim t$  curves are plotted in Fig. 8-26. In this diagram,  $h_r^* = h^*/H_o$  and  $q_r^* = q^*/Q_o$ . The phase angles determined by the transfer matrix method and by the method



(a) Piping system



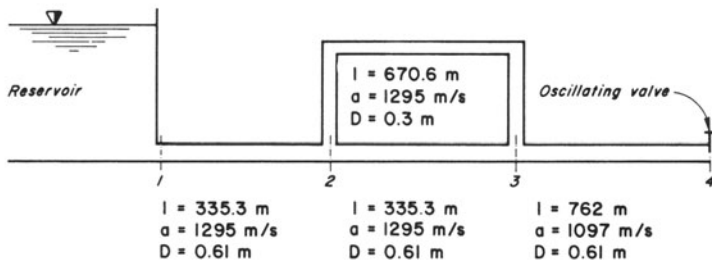
(b) Frequency response diagram

Fig. 8-23. Frequency response of a series piping system.

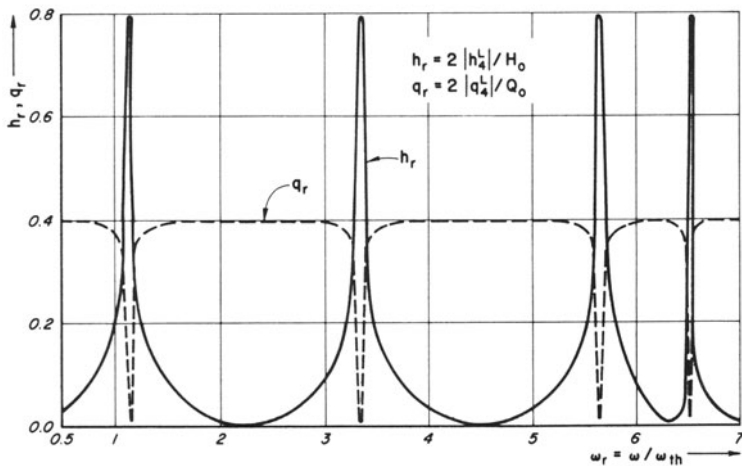
of characteristics are listed in [Table 8-3](#). It is clear that the results of the two methods agree closely.

### Energy Concepts

In the steady-oscillatory flow in a piping system, the energy input during a cycle is equal to the energy output plus the losses in the system. If the losses in the system are neglected, then the energy input is equal to the energy output during a period. This result may be used as follows to verify the numerical



(a) Piping system



(b) Frequency response diagram

Fig. 8-24. Frequency response of a parallel piping system.

values of the amplitudes of the pressure head and discharge oscillations, and of the phase angles obtained by the transfer matrix method.

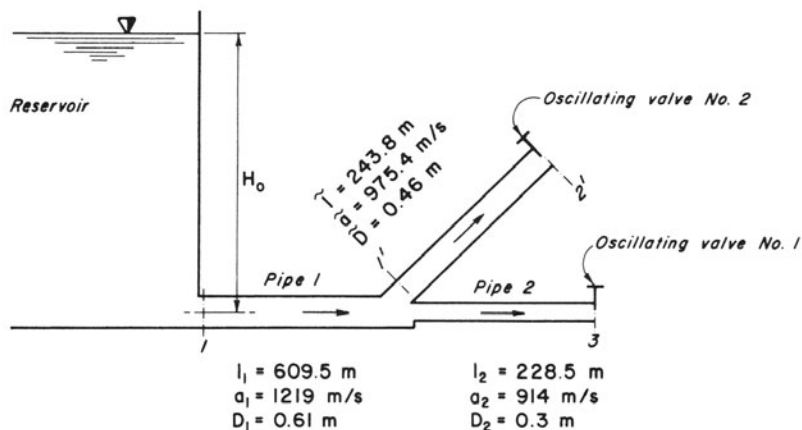
The energy entering the system during time interval  $\Delta t$  is

$$E_{in} = \gamma Q H \Delta t \quad (8-169)$$

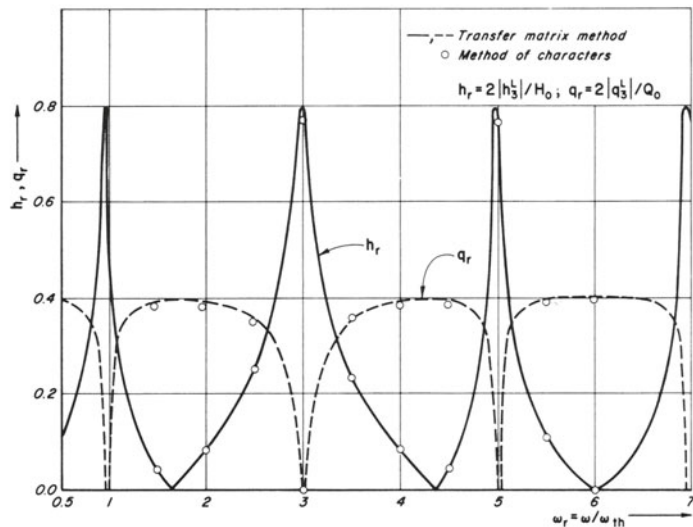
in which  $\gamma$  = specific weight of the fluid and the subscript "in" refers to the input quantities. Substitution of Eqs. 8-1 and 8-2 into Eq. 8-169 and expansion of the resulting equation yield

$$E_{in} = \gamma (Q_o H_o + q_{in}^* H_o + h_{in}^* Q_o + q_{in}^* h_{in}^*) \Delta t \quad (8-170)$$

Let  $q_{in}^*$  and  $h_{in}^*$  be sinusoidal, i.e.,



(a) Piping system



(b) Frequency response diagram (valves No. 1 and No. 2 are in phase)

Fig. 8-25. Frequency response of a branching system; branch with oscillating valve.

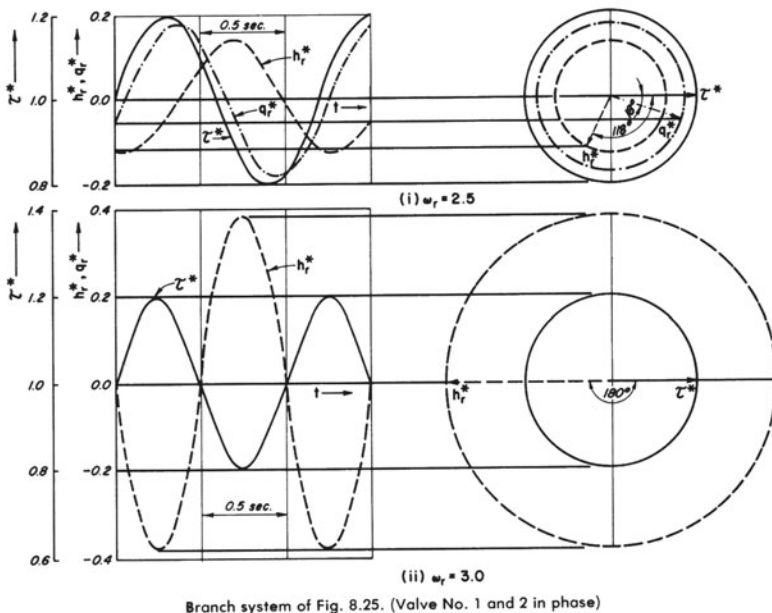
Fig. 8-26. Time history of  $h_r^*$ ,  $q_r^*$ , and  $\tau^*$ .

Table 8-3. Phase angles.

| System   | Frequency Ratio, $\omega_r$ | Phase Angles, $\phi$ (in degrees) |                    |                          |                    |
|--|-----------------------------|-----------------------------------|--------------------|--------------------------|--------------------|
|  |                             | Between $h$ and $\tau^*$          |                    | Between $q$ and $\tau^*$ |                    |
|  |                             | Transfer Matrix Method            | Method of Charact. | Transfer Matrix Method   | Method of Charact. |
| Series (Fig. 8-23a)                                | 2.5                         | -110.99                           | -110.50            | -20.99                   | -20.5              |
|  | 3.0                         | -180.01                           | -180.00            | -270.01                  | —                  |
| Branch (Fig. 8-17a, dead-end branch)               | 2.5                         | -117.90                           | -119.00            | -27.90                   | -29.50             |
| Branch (Fig. 8-25a, branch with oscillating valve) | 2.5                         | -117.13                           | -118.00            | -18.17                   | -18.00             |
|  | 3.0                         | -180.01                           | -180.00            | -270.01                  | —                  |

$$h_{in}^* = h'_{in} \cos \omega t \quad (8-171)$$

$$q_{in}^* = q'_{in} \cos (\omega t - \phi_{in}) \quad (8-172)$$

in which  $\phi_{in}$  = phase angle between  $q_{in}^*$  and  $h_{in}^*$  and  $h'_{in}$  and  $q'_{in}$  are the amplitudes of the pressure and discharge fluctuations. Note that both  $h'_{in}$  and  $q'_{in}$  are real quantities. The energy input during one cycle may be calculated by substituting Eqs. 8-171 and 8-172 into Eq. 8-170 and by integrating the resulting equation over period,  $T$ . This process gives

$$E_{in} = \gamma Q_o H_o T + \gamma q'_{in} h'_{in} \int_0^T \cos \omega t \cos (\omega t - \phi_{in}) dt \quad (8-173)$$

For a constant-level reservoir at the upstream end,  $h'_{in} = 0$ . Hence, Eq. 8-173 becomes

$$E_{in} = \gamma Q_o H_o T \quad (8-174)$$

By proceeding in a similar manner,

$$E_{out} = \gamma Q_o H_o T + \gamma q'_{out} h'_{out} \int_0^T \cos \omega t \cos (\omega t - \phi_{out}) dt \quad (8-175)$$

The subscript "out" designates output quantities.

If the losses in the system are neglected, then  $E_{in} = E_{out}$ . Hence, it follows from Eqs. 8-174 and 8-175 that

$$\int_0^T \cos \omega t \cos (\omega t - \phi_{out}) dt = 0 \quad (8-176)$$

which yields

$$\phi_{out} = 90^\circ \quad (8-177)$$

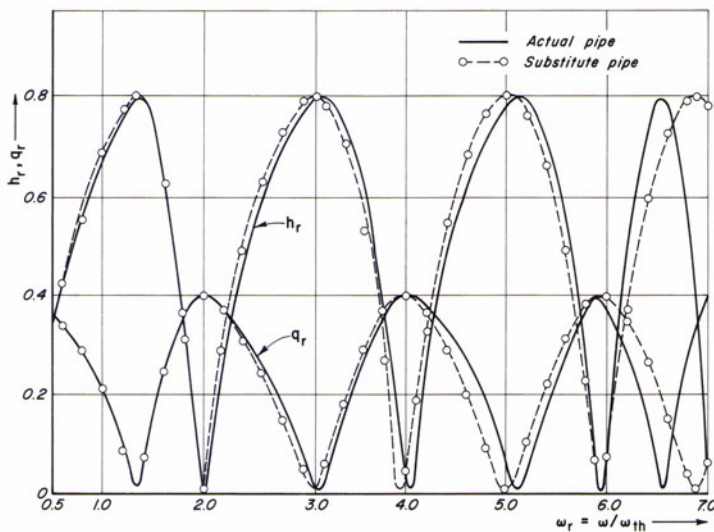
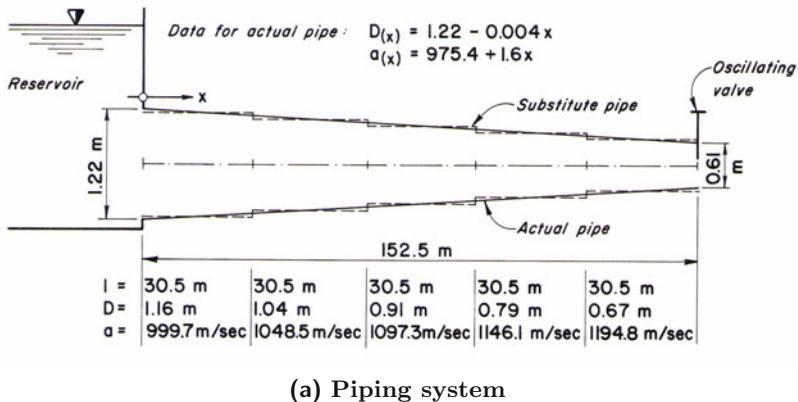
For all the systems analyzed by Chaudhry [1970],  $\phi_{out}$  is  $90^\circ$ . The only exceptions are the branch systems in which the side branch had an orifice or an oscillating valve. Equations 8-176 and 8-177 are not applicable in these cases because of energy outflow at more than one location (see Problem 8-6).

## 8-12 Variable-Characteristics Pipeline

The resonating characteristics of a pipeline with linearly variable characteristics, i.e., area  $A$  and wave velocity  $a$  along its length, a constant-head reservoir at the upstream end, and an oscillating valve at the downstream end (Fig. 8-27) are studied by using the transfer matrix method. Frequency response is determined by using the field matrix given by Eq. 8-48. Then the actual pipe is replaced by a substitute pipe having stepwise changes in characteristics, as shown in Fig. 8-27a. The expressions presented in Section 8-7 are used to determine the frequency response. To compute  $\omega_r$ , the theoretical period is calculated from the equation

$$T_{th} = \frac{4l}{a_m} \quad (8-178)$$

in which  $a_m$  = wave velocity at the midlength of the pipeline, and  $l$  = length of the pipeline. The results for both of these cases are presented in Fig. 8-27b.



(b) Frequency response diagram

Fig. 8-27. Frequency response of pipeline having variable characteristics.

Resonant frequencies for the system of Fig. 8-27a are determined by considering the pipe *per se* and then replacing it with a substitute pipe (shown by dotted lines in Fig. 8-27a), and by using the following expression for the resonant frequencies of a pipeline having linearly variable characteristics [Favre, 1942]:

$$\tan \frac{\omega l}{a_m} = -\frac{\omega l}{a_m \sigma} \quad (8-179)$$

in which  $\sigma = (1 + \psi/2) [\mu(1 + \psi/2) + \psi]$ ;  $\psi = (a_o - a_m)/a_m$ , and  $\mu = (D_A - D_o)/D_o$ . The subscripts  $o$ ,  $m$ , and  $A$  refer to the values at the valve, at the midlength, and at the reservoir end of the pipe, respectively. The computed results are listed in Table 8-4. There is satisfactory agreement between the results obtained in these cases up to the fifth harmonic. The higher harmonics may be predicted to a reasonable degree of accuracy by increasing the number of reaches into which the pipeline is divided.

**Table 8-4.** Resonant frequencies.

| Mode        | Resonant Frequencies (rad/s) |             |                 |
|-------------|------------------------------|-------------|-----------------|
|             | Transfer Matrix Method       |             |                 |
|             | Favre's Expression           | Actual Pipe | Substitute Pipe |
| Fundamental | 15.127                       | 15.075      | 14.905          |
| Third       | 35.683                       | 35.702      | 35.001          |
| Fifth       | 57.647                       | 57.856      | 56.375          |
| Seventh     | 79.963                       | 74.130      | 77.749          |

## 8-13 Stenosis in Human Cardiovascular System

The flow in a normal cardiovascular system is periodic. A stenosis (partial blockage) in an artery modifies the flow field and hence its frequency response. Therefore, the resulting change in the system frequency response may be utilized to assess the functional significance of a stenosis, i.e., whether the stenosis is affecting the blood flow significantly and therefore a treatment is necessary.

Blood flow may be considered as Newtonian flow if the artery size is 100  $\mu\text{m}$  or larger (O'Hesn, et al., 2004). The arteries clogged (Fig. 8-28) due to plaque build-up may block the blood flow completely, resulting in a heart attack. To open the partially blocked arteries, angio-plasty and the placement of stents have become routine. Present practice is to take no action if the

blockage is less than 50% (based on diameter), while a stent is placed at the blockage location after opening the artery by inflating a balloon if the blockage is more than 75%. However, for a blockage between 50% and 75%, called intermediate-grade stenosis, the decision to stent or not is not straightforward. In this case, the proximal and distal pressures at the blockage location,  $P_p$  and  $P_d$  respectively in Fig. 8-29, are measured by passing the pressure wire through the stenosis, and the ratio of the distal pressure,  $P_d$ , and proximal pressure,  $P_p$ , called *fractional flow reserve* (FFR), is computed. If FFR is less than 0.75, then the blockage is opened up with a balloon, and a stent is placed. Since passing the pressure wire through the blockage could result in serious patient complications, it will be very helpful if the decision criteria for stent placement could be developed in terms of only the proximal pressures. Following attempt for such a development using the frequency analysis is in an early stage. The results of the preliminary studies are reported herein to demonstrate the application of the method.

Transient flow in a piping system may be analyzed by using the frequency response method. Mohapatra, et al. [2006] applied the methodology to detect partial blockage in a piping system. The methodology is used herein to compare systems with and without stenosis.

Real-life proximal pressure measurements in systems with stenosis (three sets) and without stenosis (three sets), are used. To facilitate presentation, the data sets are designated as S-1, S-2 and S-3, and NS-1 and NS-2 where S indicates “stenosis” and NS indicates “No stenosis.” NS-3 is adapted from Reczuch, et al. [2002] and the others are from Moloo [2002]. The time scale is missing in all of the data sets, and it is estimated from the given pulse rates. Although both the proximal and distal pressures are available in the data sets, only the proximal values are used here to conserve space. It is important to note here that S-1 and NS-1 and S-2 and NS-2 are for the same patients with and without stenosis; however, S-3 and NS-3 are from different persons.

The discrete values are read from the acquired data sets by digitizing the traces. In all the cases, only eight peaks consisting of 64 points at equal intervals are considered to maintain consistency in the method. For the stenosed cases, the pressures after the administration of Adenosin are considered. An algorithm for discrete Fast Fourier Transform (FFT) is used to convert the data from the time domain into the frequency domain [Press, et al. 1993].

The recorded proximal pressures for the first patient are shown in the time domain in Fig. 8-30a, and the respective transformed series in the frequency domain are shown in Figs. 8-30b. The frequency response diagrams are presented in a non-dimensional form. The abscissa in this figure represents the non-dimensional frequency,  $\omega_r = \omega/\omega_c$ , where  $\omega$  is the frequency in radians/s;  $\omega_c = 2\pi/T_c$ ; and  $T_c = 60/72$  s refers to the time period between peaks for a normal human being with a pulse rate of 72 beats/minute. The ordinate in the frequency response diagram indicates the amplitude of fluctuation of pressure in a non-dimensional form,  $h_r = h/h_c$  where  $h$  is the amplitude of the pressure fluctuation, in mm of hg and  $h_c = 120$  mm of hg represents the

pressure under normal conditions. It may be noted that the fluctuation corresponding to zero frequency has been neglected. The frequency diagram has three prominent peaks and then gradually reduces to zero pressure amplitude at higher frequencies. The results are summarized in [Table 8-5](#).

The fractional flow reserve (FFR), which is the ratio of average distal pressure to average proximal pressure, is used extensively in present clinical practice to evaluate the significance of a stenosis. S-1 represents a 70 percent complex lesion in the proximal segment of the left circumflex artery with a corresponding FFR of 0.69. FFR for S-2 and S-3 are 0.59 and 0.55, respectively. A new indication parameter,  $I = P_1 P_3 / P_2^2$ , is proposed to signify the functionality of the stenosis.  $P_1$ ,  $P_2$  and  $P_3$  are the three peaks in the frequency response diagram for the proximal pressures. As seen from [Table 8-5](#), a value of  $I \geq 0.7$  indicates a functionally insignificant stenosis. Similarly,  $I \leq 0.6$  indicates that the stenosis is functionally significant. It may be assumed that the intermediate values of  $I$  indicate the presence of an insignificant stenosis.

It is clear from [Table 8-5](#) that the results of the proposed methodology are similar to that of FFR. However, it should be noted that the methodology is in an early stage and that the criteria developed herein needs additional verification with data from a large number of patients.

**Table 8-5. Indication Parameter and Fractional Flow Reserve**

| Data Set         | $P_1$ | $P_2$ | $P_3$ | $I = P_1 P_3 / P_2^2$ | FFR  |
|------------------|-------|-------|-------|-----------------------|------|
| No Stenosis NS-1 | 5.6   | 2.9   | 1.2   | 0.80                  | 1.00 |
| No Stenosis NS-2 | 2.8   | 1.1   | 0.3   | 0.69                  | 0.96 |
| No Stenosis NS-3 | 6.0   | 2.1   | 0.6   | 0.82                  | 1.00 |
| Stenosis S-1     | 6.9   | 3.4   | 0.9   | 0.54                  | 0.69 |
| Stenosis S-2     | 2.9   | 1.2   | 0.2   | 0.40                  | 0.59 |
| Stenosis S-3     | 3.9   | 1.8   | 0.3   | 0.37                  | 0.55 |

## 8-14 Case Study

The details of a resonance incident in the penstock of Jordan River Redevelopment, British Columbia, Canada, are presented in this section.

Project data for this powerplant is presented in Section 3-11. To keep the maximum transient-state pressures within the design limits, a bypass pressure-regulating valve (PRV) is provided. The turbine inlet valve (TIV), a 2.74-m-diameter plug valve, is located just upstream from the junction of the conduits

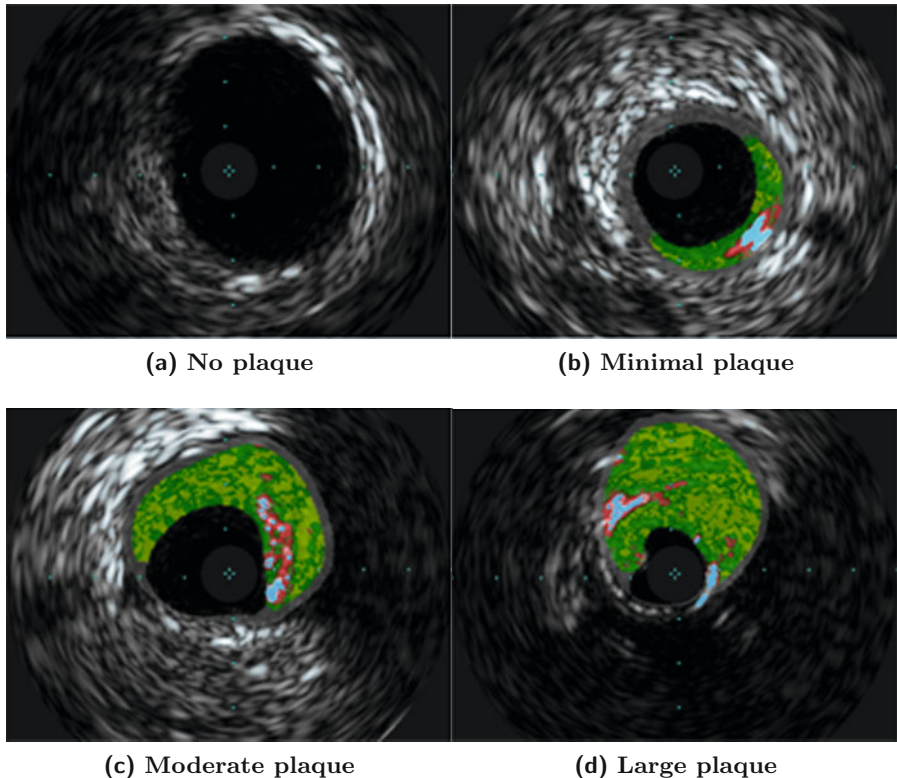


**Fig. 8-28.** Intravascular ultrasound images of coronary arteries with varying levels of plaque. In the color images, computer assisted to identify different types of plaque composition, calcification is shown as light blue, harder plaque as red, and softer plaque as green; the plaque is different shades of gray in the black and white images. (Courtesy, J. Penn and J. Moloo, University of Colorado, Aurora, CO.)

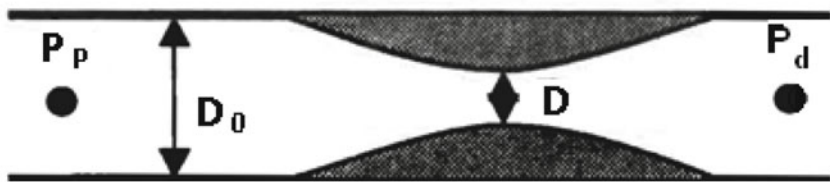


**Fig. 8-29.** Schematic of Stenosis

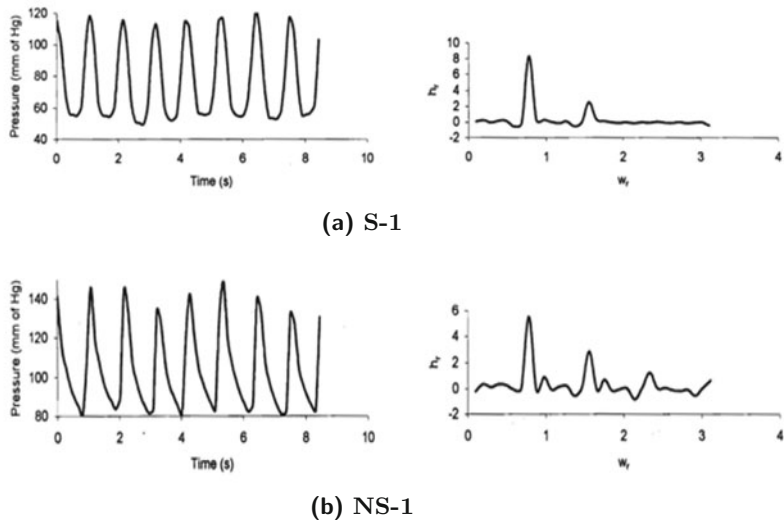


**Fig. 8-30.** Proximal Pressures with and without stenosis.

leading to the PRV and to the turbine. This valve has an upstream service seal that is applied manually and a downstream operating seal that is applied automatically (Fig. 8-31). The upstream service seal is used for isolating the TIV for minor repairs, etc.

To prevent resonance conditions due to leakage of TIV, an antiresonance device (ARD) is provided that, when activated, opens a 0.2-m bypass valve. Normally this valve is closed after the TIV is fully closed following unit shutdown. However, if resonance develops when the TIV is in the closed position and the pressure inside the penstock exceeds a specified limit, then this valve is opened automatically to eliminate the resonating conditions. The normal maximum penstock design pressure of 373 m was selected for the activation setting on the antiresonance device. During the first few years of operation, the penstock pressures exceeded the 373-m limit set on the antiresonance device following unit shutdown and during start-up and the antiresonance device was activated a few times. Once the device is activated, the unit cannot be started until the device is manually reset. Since the powerplant is operated under remote control, a service man had to drive about 75 km, a few times after midnight, to reset the device. The field staff, considering this device a “nuisance,” changed the activation setting to 430 m. It was learned later that the device had been disconnected completely for an extended period of time.

The downstream seal of TIV was damaged in September 1978, and the amount of leakage through the valve increased considerably. To replace the seal, the turbine would have to be taken out of service for several days. This was not done because of winter load peaks.

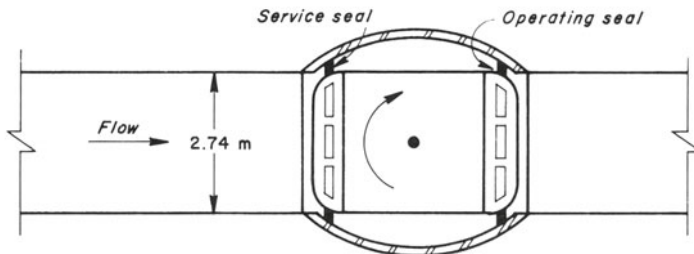


**Fig. 8-31. Schematic diagram of turbine inlet valve.**

On January 5, 1979, the unit was shut down at 12:16 hrs. At about 13:00 hrs, periodic noises were heard. Fortunately, a service man was present in the powerhouse at the time. After consultation with the field engineer, the upstream seal was applied manually and the resonance conditions stopped. During resonance, the amplitude of the pressure fluctuations was about 47 m, with the maximum and minimum pressures about 385 and 291 m, respectively. The resonance occurred for about 15 minutes before it was stopped. Since the time scale of the station recorder is 16 min/cm, the period of the oscillations could not be determined.

The activation limit on the antiresonance device was now set at 373 m, and the control circuitry was modified so that ARD would not operate during unit start-up and unit shutdown. On March 20, 1979, resonance developed again after the unit was shut down at 13:20 hrs. A person present in the plant described the development of resonance as follows: "Following closure of TIV and 0.2-m bypass valve, the loud noise associated with the TIV-downstream-seal leakage built up to its usual level but pulsated rather than a steady roar. Observed penstock pressure gauge oscillating at TIV cabinet, loud noise swings appeared to alternate but not completely. Oscillation period appeared to start lengthening and pressure swing began increasing in amplitude. Antiresonance device (set at 373 m) tripped, 0.2-m bypass valve opened and pressure swings died down."

## 8-15 Summary

In this chapter, the development of resonating conditions in piping systems is discussed; available methods for determining the frequency response and the resonant frequencies are presented; and the details of the transfer matrix method are outlined. The transfer matrix method is verified by comparing its results with those of the characteristics method and with those measured in the laboratory and on the prototype installations. Preliminary studies to

assess the functional significance of stenosis in human cardiovascular system are presented. The chapter concludes with a case study.

## Problems

**8-1** Prove that if  $(\omega l/a) \ll 1$ , the system may be analyzed as a lumped system. Assume the system is frictionless. (*Hint:* Compute and compare the elements of the field matrix for a lumped system [Eq. 8-38] and for a distributed system [Eq. 8-37] for  $\omega l/a \approx 0.01$ .)

**8-2** Derive the point matrix for an orifice located at the junction of  $i$ th and  $(i+1)$ th pipe (Fig. 8-12c). The mean head loss,  $\Delta H_o$ , across the orifice corresponds to the mean discharge,  $Q_o$ .

**8-3** Compute the elements of the field matrices for the pipes of the system shown in Fig. 8-22 for  $\omega_r = 2.0$ , and compute the overall transfer matrix.

**8-4** Derive expressions for the location of the nodes and antinodes for a system having three pipes in series, a constant-level reservoir at the upstream end, and an oscillating valve at the downstream end. Assume the system to be frictionless. (*Hint:* Proceed as in Section 8-9.)

**8-5** Derive an expression for the natural frequencies corresponding to the odd harmonics of a frictionless system having three pipes in series, a constant-level reservoir at the upstream end, and an oscillating valve at the downstream end.

**8-6** Prove that for a branching system having an oscillating valve or an orifice on the branch line

$$h'_{out}q'_{out} \cos \phi_{out} + \tilde{h}'_{out}\tilde{q}'_{out} \cos \tilde{\phi}_{out} = 0$$

in which  $h'_{out}$  and  $q'_{out}$  are the amplitudes of the pressure and discharge oscillations, and  $\phi_{out}$  is the phase angle between the pressure head and discharge. A tilde ( $\sim$ ) on various variables refers to the branch; other variables are for the main line. (*Hint:*  $E_{in} = E_{out} + \tilde{E}_{out}$ . Substitute expressions for  $E_{in}$ ,  $E_{out}$ , and  $\tilde{E}_{out}$  in terms of the mean and oscillatory parts, integrate over the period  $T$ , and simplify the resulting equation.)

**8-7** Derive a point matrix for a simple surge tank and for an air chamber.

**8-8** Derive a point matrix for a Helmholtz resonator shown in Figure 8-32.

**8-9** A short dead-end pipe, called tuner, is sometimes connected to a pipeline to change its frequency response at a particular frequency. Determine the length, diameter, and wave velocity of a tuner to be connected at the junction of pipes 1 and 2 of the series system of Fig. 8-23 so that the resonating

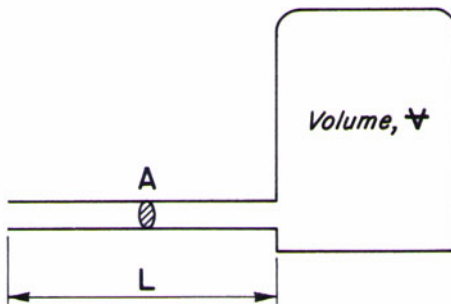


**Fig. 8-32. Helmholtz resonator.**

conditions do not occur at  $\omega_r = 3.0$ . (*Hint:* Arbitrarily select the length, diameter, and wave velocity of a tuner, and analyze the system as a branching system with the branch having a dead end. If the resonating conditions still occur at  $\omega_r = 3.0$ , change the characteristics of the tuner, and repeat the above procedure until a suitable tuner is obtained.)

## References

- Abbott, H. F., Gibson, W. L., and McCaig, I. W., 1963, "Measurements of Auto-Oscillations in a Hydroelectric Supply Tunnel and Penstock System," *Trans., Amer. Soc. of Mech. Engrs.*, vol. 85, Dec., pp. 625-630.
- Allievi, L., 1925, *Theory of Water Hammer* (translated by E. E. Halmos), Riccardo Garoni, Rome, Italy.
- Bergeron, L., 1935, "Etude des variations de regime dans les conduits d'eau: Solution graphique generale," *Revue hydraulique*, vol. I, Paris, pp. 12-25.
- Blackwall, W. A., 1968, *Mathematical Modelling of Physical Networks*, Chapter 14, Macmillan Co., New York, NY.
- Camichel, C., Eydoux, D. and Gariel, M., 1919, "Etude Theorique et Experimentale des Coups de Belier," Dunod, Paris, France.
- Chaudhry, M. H., 1970, "Resonance in Pressurized Piping Systems," *thesis* presented to the University of British Columbia, Vancouver, British Columbia, Canada, in partial fulfillment of the requirements for the degree of doctor of philosophy.
- Chaudhry, M. H., 1970-a, "Resonance in Pressurized Piping Systems," *Jour., Hydraulics Div., Amer. Soc. of Civil Engrs.*, vol. 96, Sept., pp. 1819-1839.

- Chaudhry, M. H., 1970-b, "Resonance in Pipe Systems," *Water Power*, London, UK, July/August, pp.241-245.
- Chaudhry, M. H., 1972, "Resonance in Pipes Having Variable Characteristics," *Jour., Hydraulics Div.*, Amer. Soc. of Civil Engrs., vol. 98, Feb., pp. 325-333.
- Chaudhry, M. H., 1972-a, Closure of Chaudhry [1970-a] *Jour., Hydraulics Div.*, Amer. Soc. of Civ. Engrs., April, pp. 704-707.
- Den Hartog, J. P., 1929, "Mechanical Vibrations in Penstocks of Hydraulic Turbine Installations," *Trans.*, Amer. Soc. of Mech. Engrs., vol. 51, pp. 101-110.
- Fashbaugh, R. H. and Streeter, V. L., 1965, "Resonance in Liquid Rocket Engine System," *Jour., Basic Engineering*, Amer. Soc. of Mech. Engrs., vol. 87, Dec., p. 1011.
- Favre, H., 1942, "La Resonance des Conduites et Characteristiques Lineairement Variables," *Bulletin Technique de la Suisse Romande*, vol. 68, No.5, Mar., pp. 49-54. (Translated into English by Sinclair, D. A., "Resonance of Pipes with Linearly Variable Characteristics," Tech. Translation 1511, National Research Council of Canada, Ottawa, Canada 1972.)
- Hovanessian, S. A. and Pipes, L. A., 1969, *Digital Computer Methods in Engineering*, Chapter 4, McGraw-Hill Book Co., New York, NY.
- Jaeger, C., 1948, "Water Hammer Effects in Power Conduits," *Civil Engineering and Public Works Review*, vol. 23, No. 500-503, London, England, Feb.-May.
- Jaeger, C., "The Theory of Resonance in Hydropower Systems, Discussion of Incidents and Accidents Occuring in Pressure Systems," *Jour. of Basic Engineering*, Amer. Soc. of Mech. Engrs., vol. 85, Dec. 1963, pp. 631-640.
- Jaeger, C., 1977, *Fluid Transients in Hydroelectric Engineering Practice*, Blackie & Sons, Ltd., London, UK.
- Lathi, B. P., 1965, *Signals, Systems and Communication*, John Wiley & Sons, pp. 2,13.
- McCracken, D. D. and Dorn, W. S., 1964, *Numerical Methods and FORTRAN Programming*, John Wiley & Sons, New York, NY, p. 156.
- McCaig, I. W. and Gibson, W. L., 1963, "Some Measurements of Auto-Oscillations Initiated by Valve Characteristics," *Proceedings 10th General Assembly*, International Association for Hydraulic Research, London, pp. 17-24.
- Mohapatra, P. K., Chaudhry, M. H., Kassem, A. A. and Moloo, J., 2006, "Detection of Partial Blockage in Single Pipe Lines", *Jour. of Hyd. Engrg.*, Amer. Soc. Civil Engrs., vol 132, no. 2, pp. 200-206.
- Molloy, C. T., 1957, "Use of Four-Pole Parameters in Vibration Calculations," *Jour. Acoustical Society of America*, vol. 29, No.7, July, pp. 842-853.
- Moloo, J., 2002, Patient Data from the Palmetto Richland Heart Center, Personal communication.
- OHesen, J. T., Olufsen, M. S., and Larsen, J. K., 2004, *Applied Mathematical Models in Human Physiology*, SIAM, Philadelphia, PA.

- Parmakian, J., 1963, *Water Hammer Analysis*, Dover Publications, Inc., New York, NY.
- Paynter, H. M., 1953, "Surge and Water Hammer Problems," *Trans.*, Amer. Soc. of Civ. Engrs., vol. 118, pp. 962-1009.
- Pestel, E. C. and Lackie, F. A., 1963, *Matrix Methods in Elastomechanics*, McGraw-Hill Book Co., New York, NY.
- Press, W. H., Tenkolsky, S. A., Vellerling, W. T., and Flannery, B. P., 1993, *Numerical Recipes in FORTRAN*, 2<sup>nd</sup> ed, Cambridge University Press, Cambridge, UK, pp. 963.
- Reczuch, K., Ponikowski, P., Porada, A., Telichowski, A., Derkacz, A., Kaczmarek, A., Jankowska, E. and Banosiak, W., 2002, "The Usefulness of Fractional Flow Reserve in the Assessment of Intermediate Coronary Stenosis", *Polish Heart Journal*, vol. LVII, no. 7.
- Reed, M. B., 1955, *Electrical Network Synthesis*, Chapter 2, Prentice-Hall, Englewood Cliffs, NJ.
- Rocard, Y., 1937, *Les Phenomenes d'Auto-Oscillation dans les Installations Hydrauliques*, Paris, France.
- Saito, T., 1962, "Self-excited Vibrations of Hydraulic Control Valve Pipelines," *Bull. Japan Soc. of Mech. Engrs.*, vol. 5, no. 19, pp. 437-443.
- Stary, H.C., 1999, *Atlas of Atherosclerosis, Progression and Regression*, The Parthenon Publishing Group, New York, NY.
- Thomson, W. T., 1965, *Vibration Theory and Applications*, Prentice-Hall, Inc., Englewood Cliffs, NJ, p. 5.
- Waller, E. J., 1958, "Prediction of Pressure Surges in Pipelines by Theoretical and Experimental Methods," *Publication No. 101*, Oklahoma State University, Stillwater, Oklahoma, June.
- Wylie, C. R., 1965, *Advanced Engineering Mathematics*, Third Ed., McGraw-Hill Book Co., New York, NY, p. 145.
- Wylie, E. B., 1965-a, "Resonance in Pressurized Piping Systems," *Jour. Basic Engineering*, Amer. Soc. of Mech. Engrs., vol. 87, No.4, Dec., pp. 960-966.
- Wylie, E. B. and Streeter, V. L., 1983, *Fluid Transients*, FEB Press, Ann Arbor, Mich.
- Zielke, W. and Rösl, G., 1971, *Discussion of Chaudhry [1970]*, *Jour., Hydraulics Div.*, Amer. Soc. of Civ. Engrs., July: pp. 1141-1146.

### Additional References

- Blade, R. J. and Goodykootz, J., 1962, "Study of Sinusoidally Perturbed Flow in a Line Including a 90 Elbow with Flexible Supports," *Report No. TN-D-1216*, NASA.
- Chaudhry, M. H., 1970, Discussion of paper by Holley, E. R. [1969], Jan. 1970, pp. 294-296.
- Deriaz, P., 1960, "Contributions to the Understanding of Flow in Draft Tubes in Francis Turbines," *Symposium*, International Assoc. for Hydraulic Research, Paper N-1, Sept.

- D'Souza, A. F. and Oldenburger, R., 1964, "Dynamic Response of Fluid Lines," *Trans.*, Amer. Soc. of Mech. Engrs., Series D, Sept., pp. 589.
- Evangelisti, G., 1940, "Determinazione Operatoria Delle Frequenze di Risoneanza Nei Sistemi Idraulici in Pressione," LeClà Alia R. Accademia Della Scienze Dell 'IsticulO di Bologne, Feb.
- Florio, P. J. and Mueller, W. K., 1968, "Development of a Periodic Flow in a Rigid Tube," *Jour. Basic Engineering*, Sept., p. 395.
- Holley, E. R., 1969, "Surging in a Laboratory Pipeline with Steady Inflow," *Jour., Hyd. Div.*, Amer. Soc. of Civ. Engrs., May, pp. 961-980.
- Jaeger, C., 1939, "Theory of Resonance in Pressure Conduits," *Trans.*, Amer. Soc. of Mech. Engrs., vol. 61, Feb., pp. 109-115.
- Katto, Y., 1960, "Some Fundamental Nature of Resonant Surge," Japan Soc. of Mech. Engrs., pp. 484-495.
- Lewis, W. and Blade, R. J., 1963, "Siudy of the Effect of a Closed-End Side Branch on Sinusoidally Perturbed Flow of a Liquid in a Line," *Report TN-D-1876*, NASA .
- Moshkov, L. V., 1969, "Natural Frequencies of Water Pulsations in a Pipe of Uniform Cross Section in the Case of Aerated Flow," *Trans. Vedeneev All Union Sciemific Res. Instl. of Hyd. Engineering*, vol. 88, pp. 46-54 (translated from Russian Israel Program Sci. Trans., Jerusalem 1971).
- Oldenburger, R. and Donelson, J., 1962, "Dynamic Response of Hydroelectric Plant," *Trans.*, Amer. Inst. of Elecc. Engrs., Power App. and Systems, vol. 81, Oct., pp. 403-418.
- Roberts, W. J., 1963, "Experimental Dynamic Response of Fluid Lines," *M.S. Thesis*, Purdue University.
- Vibrations in Hydraulic Pumps and Turbines, *Symposium*, Inst. of Mech. Engrs., Proc. V, pt. 3A 1966-67.
- Tadaya, I. et al., 1967, "Study of Self-Sustained Oscillations of Piston-Type Valving System," Japan Soc. of Mech. Engrs., pp. 793-807.
- Weng, C., 1966, "Transmission of Fluid Power by Pulsating Flow Concept in Hydraulic Systems," *Jour., Basic Engineering*, Amer. Soc. of Mech. Engrs., June.

## CAVITATION AND COLUMN SEPARATION



**Experimental set-up for tests on water-column separation Instituto Superior Técnico, Lisbon, Portugal.** (Courtesy, A. Betamio de, Almeida and Sandra Martins.)

## 9-1 Introduction

The governing equations and the analysis procedures presented in the previous chapters are based on the assumption that the transient-state pressures throughout the system remain above the vapor pressure of the liquid. However, the transient pressure may be reduced to the vapor pressure of the liquid in low-head systems, systems having high peaks, or systems in which transients are produced rapidly. This may produce vapor cavities in the flow or may cause the liquid to separate. Rejoining of the separated columns or collapse of the cavities increases the pressure significantly, which may damage the pipeline.

The term *transient cavitation* is used herein for the formation and growth of cavities in a liquid due to transient-state pressures dropping to the vapor pressure of the liquid. Depending upon the pipeline geometry and the velocity gradient, the cavity may enlarge to fill the entire pipe cross section. This is called *column separation*. Typically, the liquid is divided into two columns at the location of column separation (see Fig. 9-1) although some authors also refer to the formation of a large cavity at the top of a pipe as *column separation*.

In this chapter, column separation, transient cavitation and various causes that may reduce the liquid pressures to the vapor pressure are discussed. Expressions for the dissipation of the pressure waves and for the wave velocity in a gas-liquid mixture are presented. A number of methods for the analysis of cavitating flows or flows with column separation are discussed. The chapter concludes with a case study.

## 9-2 General Remarks

A small gaseous phase in the form of free bubbles or as nuclei adhering to or hidden in the fissures of solids is present in almost all industrial liquids and especially in natural water. The solids may be present at the liquid boundary as contaminants in the liquid. The nuclei grow as the liquid pressure is reduced and may become bubbles of sufficient size to act as nuclei for cavitation. The growth of a bubble depends upon the forces acting on the bubble, such as, surface tension, ambient liquid pressure, liquid vapor pressure, gas pressure inside the bubble, and the pressure history to which the bubble has been exposed. Furthermore, free gases may enter the bubble, and two or more bubbles may coalesce to form a large cavity. The size of this cavity increases until the difference between its internal pressure and the decreasing external pressure is sufficient to offset the surface tension. Once this critical size is reached, the vapor-filled cavity becomes unstable and expands explosively. This hypothesized sequence of events from the pressure reduction to the onset of explosive cavitation occurs in a very short time period, probably in a few milliseconds [Baltzer, 1967].

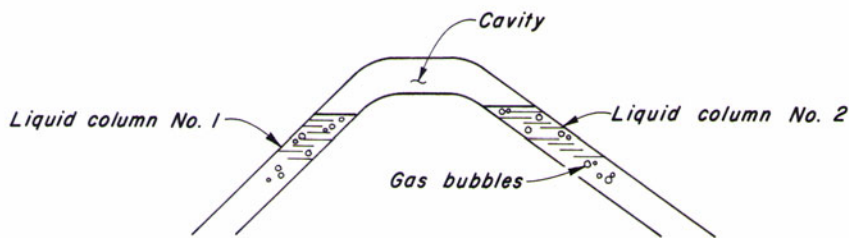


**Fig. 9-1. Column separation.**

The cavity may become so large as to fill the entire cross section of the pipe and thus divide the liquid into two columns. This usually occurs in vertical pipes, pipes having steep slopes, or pipes having "knees" in their profiles. Experimental investigations [Tanahashi and Kasahara, 1970; Weyler et al., 1971; Sharp, 1971] have shown that the bubbles are dispersed in the pipeline over a considerable distance on either side of column separation.

In horizontal pipes or pipes having mild slopes, a thin cavity confined to the top of the pipe and extending over a long distance may be formed. In addition, in this case, cavitation bubbles are produced over a considerable length of the pipe. Such a flow is referred to as *cavitating flow*.

Negative or rarefaction waves result in low pressures that may lead to column separation or cavitating flows. These waves, reflected as positive waves from the system boundaries (e.g., a reservoir), compress the bubbles in the cavitation-flow region and progressively reduce the size of the cavity produced by column separation. Cavities collapse and the rejoining of separated columns may produce very high pressures. These pressures may burst the pipe if not allowed for in the design. The pressure inside a cavity is equal to the sum of the partial pressures of the liquid vapors and that of the released gases. For constant liquid temperature, the partial pressure of the liquid vapors is constant. The partial pressure of the gases, however, increases or decreases if their mole fraction in the cavity increases or decreases. If a cavity forms and collapses several times during a transient, experimental measurements [Weyler, 1971] show that the inside pressure of the cavity increases with successive cavity formations.

If water-column separation occurs at more than one location in a system, experimental results [Tanahashi and Kasahara, 1970] show that the second pressure peak may be higher than the first pressure peak, i.e.,  $H_{max_2} > H_{max_1}$  (Fig. 9-2), although generally the first pressure peak is the highest.

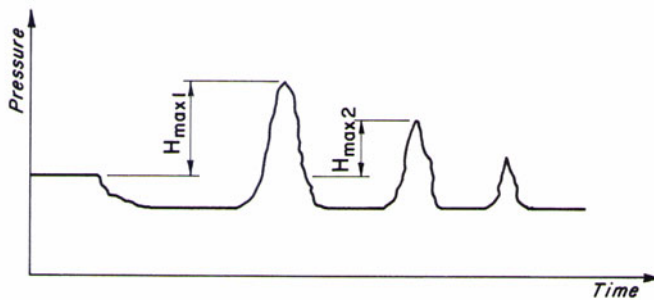


**Fig. 9-2.** Time history of pressure following column separation.

### 9-3 Causes of Column Separation

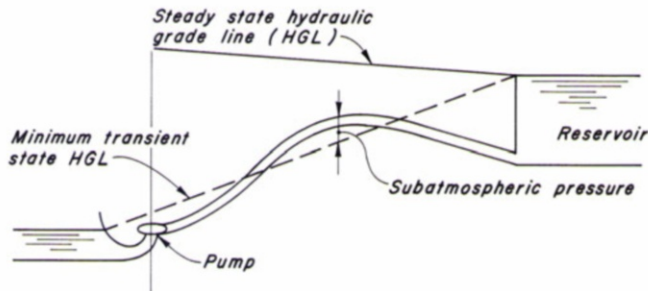
The transient-state pressure in a pipeline may drop to vapor pressure causing cavitation and liquid-column separation following power failure to a pump or rapid closure of a valve. The sequence of events for these cases follows.

Upon power failure, negative-pressure waves generated at the pump travel in the downstream direction. If the pumping head is low and the pump moment of inertia is small, the pressure in the pipeline may be reduced to the vapor pressure of the liquid. For high-head pumping systems, the pressure at the high points of the pipeline may be reduced to the vapor pressure (Fig. 9-3a). If a valve is closed rapidly at the upstream end of a pipeline (Fig. 9-3b), the pressure downstream of the valve may be reduced to the vapor pressure. Similarly, the pressure upstream of a rapidly closing valve at the downstream end of a pipeline generates a positive pressure wave that travels in the upstream direction. This wave is reflected as a negative wave from the reservoir and then this negative wave is reflected again as a negative wave at the closed valve. If the initial steady-state pressure is low or if the magnitude of the pressure waves is large, then the pressures at the valve may be reduced to the vapor pressure.

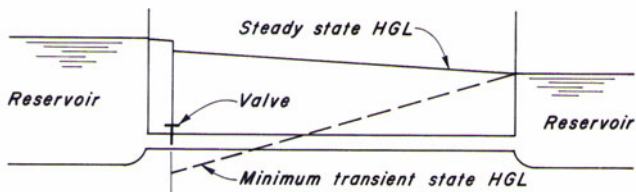
A rapid opening of a valve at the downstream end of a pipeline may reduce the pipeline pressures to the vapor pressure.

### 9-4 Energy Dissipation

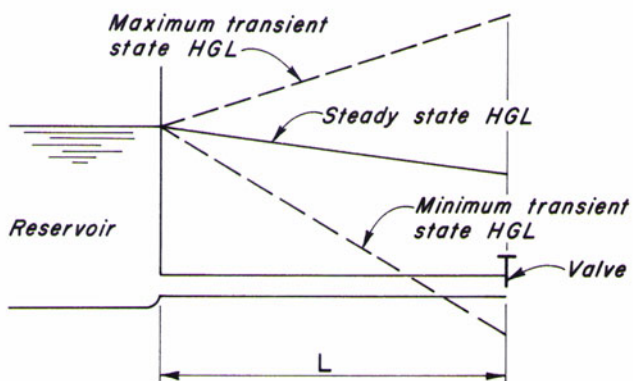
Because of the bubbles, the liquid in a cavitating flow is a mixture of the released gases and the liquid. Experimental investigations have shown that the dissipation of the pressure waves in a gas-liquid mixture is higher than that in a pure liquid. This additional dissipation is due to heat transfer to the liquid when bubbles expand and contract. Bernardinis et al. [1975] showed



(a) Power failure in a pumping system



(b) Upstream valve closure



(c) Downstream valve closure

Fig. 9-3. Reduction of transient pressures to vapor pressure.

how mechanical work is transferred into the liquid in the form of heat energy during each compression-and-expansion cycle of a spherical bubble containing a perfect gas, confined in an unbound incompressible liquid, and subjected to a sudden pressure impulse of short duration.

Weyler et al. [1971] developed the following equation for the shear stress due to non-adiabatic behavior of a spherical bubble

$$\tau_b = C\alpha_o \rho g D |\Delta H| \frac{V}{\Delta x |V|} \quad (9-1)$$

in which  $\alpha_o$  = void fraction at reservoir pressure;  $\rho$  = mass density of the liquid;  $g$  = acceleration due to gravity;  $D$  = inside diameter of the pipe;  $\Delta x$  = fixed length of the pipe;  $\Delta H$  = change in the piezometric head;  $V$  = flow velocity; and  $C$  = an unknown constant. The void fraction,  $\alpha$ , for a gas-liquid mixture is defined as

$$\alpha = \frac{\forall_g}{\forall_g + \forall_l} \quad (9-2)$$

in which  $\forall_g$  and  $\forall_l$  are the volumes of the gas and the liquid in the mixture. Weyler determined the value of  $C$  by trial and error utilizing Baltzer's experimental data [1967]. Since  $C\alpha_o$  varies slightly for a wide range of  $\alpha_o$ , a mean value of  $C\alpha_o = 225$  may be used.

The total shear stress,  $\tau$ , for computing energy dissipation in the cavitating flows is the sum of  $\tau_b$  and the wall shear stress,  $\tau_o$ , i.e.,  $\tau = \tau_b + \tau_o$ .

## 9-5 Wave Velocity in a Gas-Liquid Mixture

The wave velocity in a liquid having a small quantity of undissolved gases is considerably less [Wood, 1955; Silbeman, 1957; Ripken and Olsen, 1958] than that in the pure liquid. Based on the measurements taken at two sewage plants. Pearsall [1965] reported that the wave velocity may be reduced by as much as 75 percent depending upon the gas content.

By making the following assumptions, an expression for the wave velocity in a gas-liquid mixture may be derived [Pearsall, 1965; Raiteri and Siccardi, 1975]:

1. The gas-liquid mixture is homogeneous, i.e., the gas bubbles are uniformly distributed in the liquid.
2. The gas bubbles follow an isothermal law.
3. The pressure inside the bubble is independent of the surface tension and the vapor pressure.

Let us consider a volume of gas-liquid mixture at pressure  $p_o$  confined in an elastic conduit, and let the pressure be instantaneously changed by  $dp$  (pressure increase is positive and pressure drop is negative). Then,

$$d\forall_m = d\forall_g + d\forall_l + d\forall_c \quad (9-3)$$

in which the subscripts  $m$ ,  $g$ ,  $l$ , and  $c$ , respectively, refer to the quantities for the gas-liquid mixture, gas, liquid, and conduit. The symbol  $\nabla$  denotes volume, and the letter  $d$  indicates a change in the volume due to change in pressure,  $dp$ . For example,  $d\nabla_g$  is the change in the volume of gas,  $\nabla_g$ . Now,

$$\nabla_m = \nabla_l + \nabla_g \quad (9-4)$$

Hence, Eq. 9-2 becomes

$$\alpha = \frac{\nabla_g}{\nabla_m} \quad (9-5)$$

Since  $\nabla_g$  is a function of pressure  $p$ , it follows from Eq. 9-5 that  $\alpha$  is also a function of  $p$ . If the bubble expansion follows an isothermal law, then

$$\alpha p = \alpha_o p_o \quad (9-6)$$

in which subscript  $o$  indicates initial conditions, and the variables without a subscript refer to the conditions at pressure  $p$ .

If  $M$  and  $\rho$  are the mass and the mass density, then

$$M_m = M_l + M_g \quad (9-7)$$

It follows from Eq. 9-4 and 9-5 that

$$\nabla_l = (1 - \alpha) \nabla_m \quad (9-8)$$

Dividing Eq. 9-7 by  $\nabla_m$  and making use of Eqs. 9-5 and 9-8, we may write

$$\rho_m = \rho_l(1 - \alpha) + \alpha \rho_g \quad (9-9)$$

On the basis of Eq. 9-6 and the fact that  $p\nabla_g = p_o\nabla_{g_o}$ , Eq. 9-9 becomes

$$\rho_m = \rho_l \left( 1 - \frac{\alpha_o p_o}{p} \right) + \rho_{g_o} \alpha_o \quad (9-10)$$

Let us now write expressions for  $d\nabla_g$ ,  $d\nabla_l$ , and  $d\nabla_c$ . If the conduit walls are thin, then

$$d\nabla_c = -\frac{D_c \nabla_m}{E_c e} dp \quad (9-11)$$

in which  $E_c$  = modulus of elasticity of the conduit walls, and  $D_c$  = diameter of the conduit. If the void fraction is small and  $K_l$  = bulk modulus of elasticity of the liquid, then

$$d\nabla_l = -\nabla_m \frac{dp}{K_l} \quad (9-12)$$

If the gas bubbles follow the isothermal law,  $p\nabla_g = p_o\nabla_{g_o}$ . Differentiating this equation, we obtain

$$d\nabla_g = -\nabla_g \frac{dp}{p} \quad (9-13)$$

Making use of the fact that  $\forall_g = p_o \forall_g / p$  and  $\forall_{go} = \alpha_o \forall_m$ , Eq. 9-13 becomes

$$d\forall_g = -\frac{\alpha_o p_o}{p^2} \forall_m dp \quad (9-14)$$

The bulk modulus of the gas-liquid mixture,  $K_m$ , may be defined as

$$K_m = \frac{dp}{-\frac{d\forall_m}{\forall_m}} \quad (9-15)$$

By substituting expressions for  $d\forall_c$ ,  $d\forall_l$ , and  $d\forall_g$  from Eqs. 9-11, 9-12, and 9-14 into 9-3, substituting the resulting expression for  $d\forall_m$  into Eq. 9-15, and simplifying, we obtain

$$K_m = \frac{1}{\frac{\alpha_o p_o}{p^2} + \frac{1}{K_l} + \frac{D_c}{E_c e}} \quad (9-16)$$

By adding subscript  $m$  to denote values for the gas-liquid mixture in the expression for the wave velocity derived in Chapter 1, we obtain

$$a_m = \sqrt{\frac{K_m}{\rho_m}} \quad (9-17)$$

Substituting expression for  $\rho_m$  from Eq. 9-10 and for  $K_m$  from Eq. 9-16 into Eq. 9-17, yield

$$a_m = \sqrt{\frac{1}{\left[ \rho_l \left( 1 - \frac{\alpha_o p_o}{p} \right) + \rho_{go} p_o \right] \left( \frac{\alpha_o p_o}{p^2} + \frac{1}{K_l} + \frac{D_c}{E_c e} \right)}} \quad (9-18)$$

If the compressibility of the liquid, the elasticity of the conduit walls, and the terms of smaller magnitude are neglected, then the preceding expression, on the basis of Eq. 9-6, may be written as

$$a_m = \sqrt{\frac{\rho}{\rho_l(1-\alpha)\alpha}} \quad (9-19)$$

In this derivation, we assume that the pressure inside the bubble does not depend upon the surface tension and on the vapor pressure of the liquid. Raiteri and Siccardi [1975] derived an expression for the wave velocity without making this assumption. Kalkwijk and Kranenburg [1971] presented a similar, but simplified expression. Fanelli and Reali [1975] and Rath [1981] reported theoretical investigations of the wave velocity in two-phase flows.

## 9-6 Analysis of Cavitation

A system with cavitating flow and column separation may be divided into three phases or regions: waterhammer, cavitation, and column separation.

In the waterhammer region, the void fraction is small and may be neglected. Hence, the wave velocity is not pressure dependent. In the cavitation region, gas bubbles are dispersed throughout the liquid and the liquid behaves like a gas-liquid mixture. As discussed in Section 9-4, there is additional damping due to thermodynamic effects and the wave velocity depends upon the void fraction, which in turn is pressure dependent. At the location of column separation, a cavity is formed which expands and contracts depending upon the flows upstream and downstream of the cavity.

The three regions may be present simultaneously in a piping system: cavitation occurs in one part of the system, liquid column separates at some critical locations, and the remaining system is considered as the waterhammer region. These phases may occur in a sequence as well. For example, the system is initially a waterhammer region, then the void fraction increases due to the reduction of pressure and the flow becomes a cavitating flow. With further reduction of pressure, the column may separate at critical locations. Then, as the transient-state pressure increases due to wave reflections from the boundaries, the separated columns rejoin, the cavities collapse, and the whole system becomes a waterhammer region again.

For the analysis of liquid-column separation or cavitating flow, several parameters, such as the void fraction along the pipeline and hence the wave velocity, the energy dissipation, gas release, etc., are unknown. By making simplifying assumptions, several methods for the analysis of these flows have been reported. We briefly discuss a number of these methods.

In a typical traditional analysis [Parmakian, 1958; Bergeron, 1961 and Sharp, 1965], the cavitation region is neglected, and column separation is considered as an internal boundary. The liquid column is assumed to separate over the entire pipe cross section as soon as the pressure at that location drops to the liquid vapor pressure; the volume of the cavity is calculated from the continuity equation using the velocities of the liquid columns on the upstream and downstream sides of the cavity; and the pressure inside the cavity is assumed to be equal to the liquid vapor pressure. The rest of the system is analyzed as a normal waterhammer analysis. The maximum pressures following rejoining of the separated columns computed by using this approach are found to be higher than those measured on a prototype [Joseph, 1971].

Swaffield [1972] showed that the agreement between the computed and measured results for column separation behind a closing valve in a short pipeline is better when the gas release is considered than with no gas release. In the case of no gas release, referred to as a *vapor-only* case, the pressure inside the cavity is assumed equal to the vapor pressure. When gas release is considered, the pressure inside the cavity is assumed equal to the vapor

pressure plus the partial pressure of the gas. Similar results were obtained by Kranenburg [1972]. Brown [1968] reported that the maximum pressures in the pipelines of two pumping systems computed by assuming column separation only at a critical location were less than those measured on the prototype. However, the agreement between the computed and measured results was better when discrete air cavities were assumed along the pipeline.

For horizontal pipes, Baltzer [1967], Dijkman and Vreugdenhil [1969], and Siemons [1967] assumed that a thin cavity was formed at the top of the pipe, and analyzed the flow below the cavity as an open-channel flow. Vreugdenhil et al. [1972] presented two mathematical models for the analysis of cavitation in long horizontal pipelines: In the first model, a homogeneous gas-liquid mixture was assumed in the cavitation region, while the regular continuity and dynamic equations of waterhammer were used for the waterhammer region. In the second model, called *separated flow model*, a thin cavity was assumed at the top of the pipe in the cavitation region. Gas release into the cavities was neglected in both the models. Based on experimental observations, Weyler et al. [1971] developed a semiempirical formula for predicting additional momentum loss in the cavitation region.

Kranenburg [1974] presented a mathematical model in which all three regions — column separation, cavitation, and waterhammer — were considered. Equations were derived such that they are valid both in the cavitation region and in the waterhammer region. A finite-difference scheme was outlined that is suitable for the analysis of shocks. The computed and measured results showed good agreement.

Several investigations on the propagation of pressure waves in conduits carrying gas-liquid mixtures have been reported [Martin et al., 1976; Wiggert and Sundquist, 1979 and Wylie, 1983]. Although significant advances in the application of numerical methods have been made, the estimation of the quantity of the entrained, entrapped, and released gases is still unresolved.

Experimental investigations of the effects of transient gas release on pressure transients were conducted by Keller and Zielke [1977], Wiggert and Sundquist [1979], Perko and Zielke [1981 and 1983], and Baasiri and Tullis [1983].

## 9-7 Design Considerations

If the analysis of transient conditions caused by normal operations indicates the possibility of liquid-column separation or transient cavitation, then it has to be decided whether the pressures generated by rejoining separated columns or collapse of cavities are acceptable. A pipeline may be designed to withstand these pressures. Such a design, however, may be uneconomical. Therefore, various control devices or appurtenances to prevent cavitation and column separation are considered to obtain an overall economic design.

The following devices are employed to prevent column separation or to reduce the pressure rise when the separated columns rejoin:

- Air chambers;
- Surge tanks;
- One-way surge tanks;
- Flywheels;
- Air-inlet valves; and
- Pressure-relief or pressure-regulating valves.

Air chambers and surge tanks are usually costly. An increase in the inertia of the pump-motor by means of a flywheel increases the space requirements and may require a separate starter for the motor, thus increasing the initial project costs. Caution must be exercised if air-inlet valves are provided because, once activated, air admitted into a pipeline has to be removed from the line prior to refilling since entrapped air may result in very high pressures. By providing a pressure-relief valve or a pressure-regulating valve, the pressure rise following column separation may be reduced by letting the columns rejoin under controlled conditions.

In addition to the initial costs, the cost and ease of maintenance, and the flexibility of operation should be taken into consideration while selecting any of the preceding surge-protection devices for a particular installation.

## 9-8 Case Study

Brown [1968] reported studies and prototype test results on the water-column separation in the discharge lines of two pumping plants. Details of the mathematical model and comparison of the computed and measured results for one of the pumping plants are presented in this section.

### Project Details

The pipeline profile for the 7.2-Mile Pumping Plant is shown in [Fig. 9-4](#). Data for the pumping plant are:

|  |                                   |
|--|-----------------------------------|
| Type of pump                                     | Single stage, double suction      |
| Rated head                                       | 72.24 m                           |
| Flow at rated head                               | 0.237 m <sup>3</sup> /s           |
| Rated speed                                      | 1770 rpm                          |
| Peak efficiency                                  | 86 percent                        |
| Specific speed of equivalent single suction pump | 1270 (gpm units); 0.46 (SI units) |
| Length of pipeline                               | 1078 m                            |
| Diameter of pipeline                             | 0.61 m                            |
| Thickness of steel pipe                          | 4.8 mm                            |
| Output of motors                                 | 224 kW                            |
| Inertia of one motor                             | 10.11 kg m <sup>2</sup>           |
| Inertia of one pump                              | 1.59 kg m <sup>2</sup>            |
| No. pumping units                                | 2                                 |

The pump characteristics reported for a double-suction pump [Stepanoff, 1948 and Swanson, 1953] were used in the analysis. Therefore the specific speed for its equivalent, single-suction, pump is 1270 (gpm units), instead of the listed value of 1800.

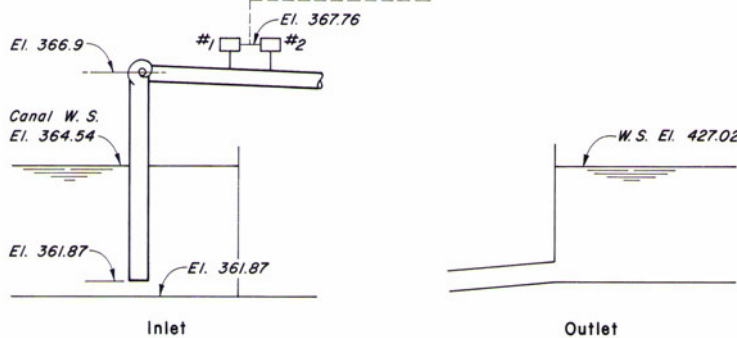
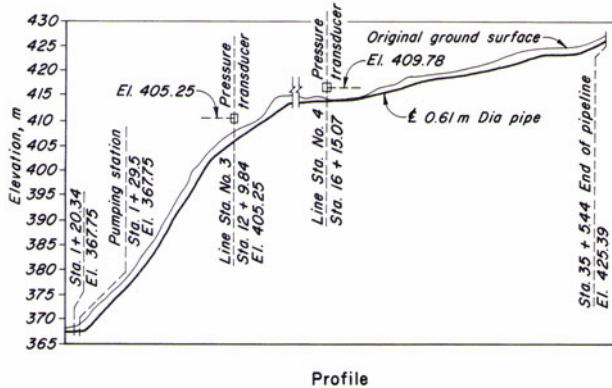


Fig. 9-4. Profile of 7.2-Mile Pumping Plant. (After Brown [1968].)

### Field Tests

The locations of the test stations are shown in Fig. 9-4. The pumping-plant station is located essentially at the pumping units, and station 3 and 4 bracket the “knee” in the pipeline where the water column was expected to separate. The resistance-type pressure cells were used to measure the pressure, and a

photoelectric revolution counter was used for the pump speed. High-speed oscillographs were used to record the data.

## Mathematical Model

A mathematical model based on the method of characteristics was developed. The upstream boundary condition was a centrifugal pump. The pump characteristics for all four zones of operation were stored in the computer. The downstream boundary condition was a constant-head reservoir. The effect of the entrained air and column separation was taken into consideration as outlined below. The notation presented earlier is used herein which is different from that of Brown [1968].

The total volume of the entrained air in the pipeline is assumed to be concentrated at discrete air cavities. Let us consider the air cavity located at the  $i$ th junction (Fig. 9-5). The volume of this air cavity is

$$\forall_i = \alpha A_i L_i \quad (9-20)$$

in which  $\alpha$  = void fraction and  $L_i$  and  $A_i$  are the length and cross-sectional area of the  $i$ th pipe, respectively.

The expansion and contraction of the air pocket is assumed to follow the polytropic equation for a perfect gas

$$(H_{P_{i,n+1}} - h_{l_i}) \forall_{P_i}^m = C \quad (9-21)$$

in which  $\forall_{P_i}$  = volume of the air pocket at the end of time step;  $H_{P_{i,n+1}}$  = piezometric head above the datum at section  $(i, n+1)$  at the end of time step;  $C$  = a constant determined from the initial steady-state conditions for the air pocket; and  $h_{l_i}$  = pressure head between the datum and the lowest possible absolute-pressure head level that a gauge at the top of the pipe at junction  $i$  could measure (Fig. 9-5). The exponent  $m$  is 1.0 for a slow isothermal process, and it is 1.4 for a fast adiabatic process. An average value of  $m = 1.2$  may be used.

The continuity equation at the cavity may be written as

$$\forall_{P_i} = \forall_i + \frac{1}{2} \Delta t [(Q_{P_{i+1,1}} + Q_{i+1,1}) - (Q_{P_{i,n+1}} + Q_{i,n+1})] \quad (9-22)$$

in which  $\Delta t$  = size of the time step;  $\forall_i$  and  $\forall_{P_i}$  are the volumes of the air cavity at the beginning and at the end of the time step;  $Q_{i,n+1}$  and  $Q_{P_{i,n+1}}$  are the flow rates at the upstream end of the air cavity at the beginning and at the end of the time step; and  $Q_{i+1,1}$  and  $Q_{P_{i+1,1}}$  are the flow rates at the downstream end of the air cavity at the beginning and at the end of the time step. Note that the values of the variables at the beginning of the time step are known and, at the end of the time step are unknown.

The method of characteristics presented in Chapter 3 is used for the analysis of transient conditions. The positive and negative characteristic equations (Eqs. 3-17 and 3-18) for the  $(i, n+1)$  and  $(i+1, 1)$  section are

$$Q_{P_{i,n+1}} = C_p - C_{a_i} H_{P_{i,n+1}} \quad (9-23)$$

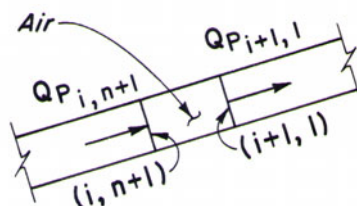
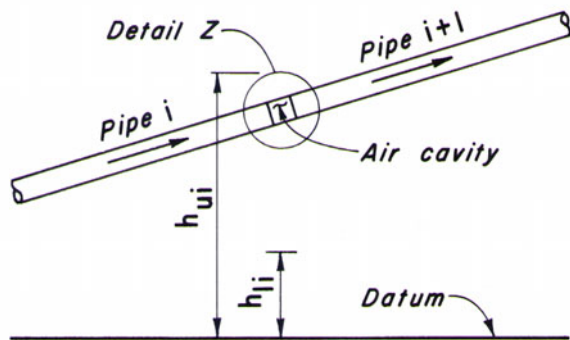
and

$$Q_{P_{i+1,1}} = C_n + C_{a_{i+1}} H_{P_{i+1,1}} \quad (9-24)$$

If the head losses at the junction are neglected, then

$$H_{P_{i,n+1}} = H_{P_{i+1,1}} \quad (9-25)$$

Five unknowns,  $\forall_{P_i}$ ,  $Q_{P_{i,n+1}}$ ,  $Q_{P_{i+1,1}}$ ,  $H_{P_{i,n+1}}$  and  $H_{P_{i+1,1}}$ , may be determined from Eqs. 9-21 through 9-25 by an iterative technique.



Detail Z

**Fig. 9-5.** Notation for air cavity. (After Brown [1968].)

## Comparison of Computed and Measured Results

Brown used  $\alpha = 1 \times 10^{-4}$  at an absolute pressure head of 10.4 m, and exponent  $m = 1.2$ . The pipeline was divided into 30 pipes, and an air cavity was assumed at the end of each pipe. The effects of the entrained air were considered only in the effective head range,  $h_{u_i} - h_{l_i}$ , in which  $h_{u_i}$  is defined as the upper limit of the effective head range. If the hydraulic grade line was above  $h_{u_i}$ , the effects of the air at that location were neglected. An effective head range,  $h_{u_i} - h_{l_i}$ , of 10.4 m was used in the computations. The measured and computed results are shown in Fig. 9-6. For the case shown as Curve No.2, a very small amount of air was considered only at the critical point, i.e., at the knee in the pipeline profile, to determine the effects of the air entrainment. For Curve No.3,  $\alpha = 0.0001$  was assumed. It is clear from these figures that a better agreement between the computed and measured results is obtained if the effects of entrained air are taken into consideration.

## 9-9 Summary

In this chapter, liquid-column separation and cavitating flows are discussed, and the causes of the reduction of pressure that may produce these flows are outlined. The chapter concludes with a case study.

## Problems

**9-1** Derive Eq. 9-19 from first principles.

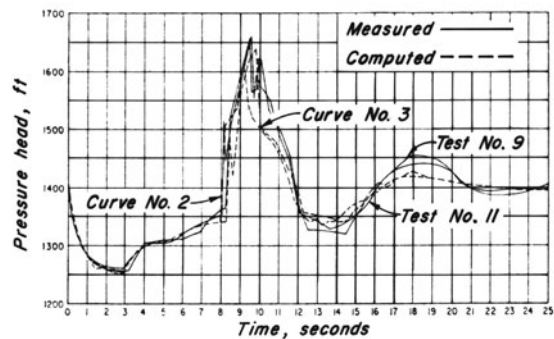
**9-2** At low pressures and temperatures, the expansion of the entrained gases in a gas-liquid mixture is isothermal. Thus, the bulk modulus of the gas,  $K_g$ , is equal to the absolute pressure of the gas,  $p_g$  [Pearsall, 1965]. From first principles, prove that for a low gas content (i.e., void fraction,  $\alpha < 0.001$ ),

$$\frac{a}{a_o} = \sqrt{\frac{p_g}{\alpha K_l + p_g}}$$

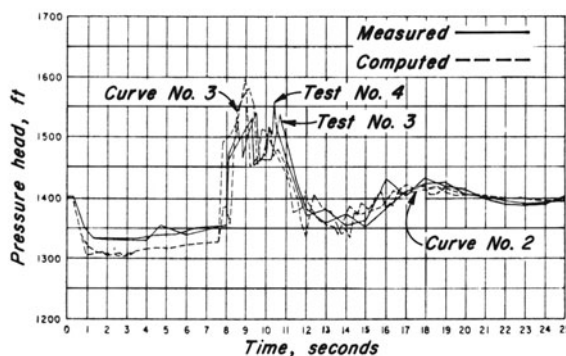
in which  $a_o$  = wave velocity in a gas-free liquid. Neglect the effect of the pipeline anchorage system. (*Hint:* For small values of  $\alpha$ ,  $\alpha p_g \ll (1 - \alpha)\rho_l$  and  $(1 - \alpha)\rho_l \simeq \rho_l$ .)

**9-3** Assuming different values of  $\alpha$ , compute the wave velocity,  $a$ , in an air-water mixture at atmospheric pressure. Plot a graph between  $a$  and  $\alpha$ .

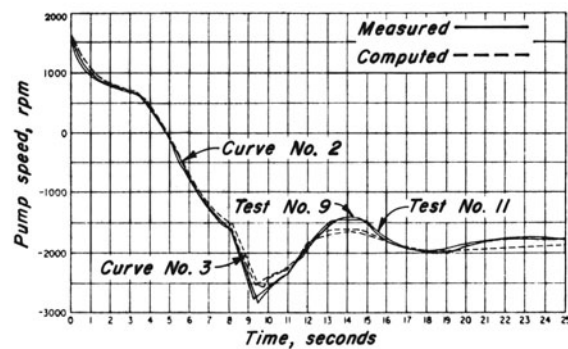
**9-4** Write a computer program for the analysis of the piping system shown in Fig. 9-3a. Transient conditions are produced by power failure to the pump-motors. Assume that the water-column separation occurs as soon as the pressure at the summit of the pipeline is reduced to the vapor pressure of the liquid.



(a) Pumping plant station



(b) Line station 3 - one pump operation



(c) Pump speed

Fig. 9-6. Comparison of computed and measured results. (After Brown [1968].)

**9-5** By using the program of Problem 9-4, investigate the effect of increasing the polar moment of inertia of the pump-motors on the duration of column separation and on the maximum pressures in the pipeline.

## References

- Baasiri, M. and Tullis, J. P. 1983, "Air Release During Column Separation," *Jour. Fluids Engineering*, Amer. Soc. of Mech. Engrs., vol. 105, March, pp. 113-118.
- Baltzer, R. A., 1967, "Column Separation Accompanying Liquid Transients in Pipes," *Jour. of Basic Engineering*, Amer. Soc. of Mech. Engrs., Dec., pp. 837-846.
- Bernardinis, B. D., Federici, G., and Siccardi, F., 1975, "Transient with Liquid Column Separation: Numerical Evaluation and Comparison with Experimental Results," *L'Energia Eletrica*, no. 9, pp. 471-477.
- Bergeron, L., 1961, *Waterhammer in Hydraulics and Wave Surges in Electricity*, John Wiley & Sons, New York, NY. (Translated from original French text published by Dunod, Paris, France [1950].)
- Brown, R. J., 1968, "Water-Column Separation at Two Pumping Plants," *Jour. Basic Engineering*, Amer. Soc. of Mech. Engrs., Dec., pp. 521-531.
- Dijkman, H. K. M. and Vreugdenhil, C. B., 1969, "The Effect of Dissolved Gas on Cavitation in Horizontal Pipe-Lines," *Jour. Hyd. Research*, International Assoc. for Hyd. Research, vol. 7, no. 3, pp. 301-314.
- Fanelli, M. and Reali, M., 1975, "A Theoretical Determination of the Celerity of Water Hammer Waves in a Two-Phase Fluid Mixture," *L'Energia Eletrica*, no. 4, pp. 183-485.
- Joseph, I., 1971, "Design of Protective Facilities for Handling Column Separation in a Pump Discharge Line," in *Control of Flow in Closed Conduits*, edited by Tullis J. P., Fort Collins, CO, pp. 295-313.
- Kalkwijk, J. P. Th. and Kranenburg, C., 1971, "Cavitation in Horizontal Pipelines due to Water Hammer," *Jour., Hyd. Div.*, Amer. Soc. Civ. Engrs., vol. 97, Oct., pp. 1585-1605.
- Keller, A. and Zielke, W., 1977, "Variation of Free Gas Content in Water During Pressure Fluctuations," *Proc. Third Round Table Meeting on Water Column Separation, Royaumont, Bulletin de la Direction des Études et Récherchés*, Series A, no. 2, pp. 255-269.
- Kobori, T., Yokoyama, S., and Miyashiro, H., 1955, "Propagation Velocity of Pressure Waves 10 Pipe Line," *Hitachi Hyoron*, vol. 37, no. 10. Oct.
- Kranenburg, C., 1972, "The Effects of Free Gas on Cavitation in Pipelines," *Proc. First International Conference on Pressure Surges*, British Hydromechanics Research Assoc., England, pp. C4-41 to C4-52.
- Kranenburg, C., 1974, "Gas Release During Transient Cavitation in Pipes," *Jour., Hyd. Div.*, Amer. Soc. of Civ. Engrs., vol. 100, Oct., pp. 1383-1398.

- Martin, C. S., Padmanabhan, M., and Wiggert, D. C., 1976, "Pressure Wave Propagation in TwoPhase Bubbly Air-Water Mixtures," *Proc. Second International Conf. on Pressure Surges*, London, British Hydromechanics Research Association.
- Parmakian, J., 1958, "One-Way Surge Tanks for Pumping Plants," *Trans., Amer. Soc. of Mech. Engrs.*, vol. 80, pp. 1563-1573.
- Pearsall, I. S., 1965, "The Velocity of Water Hammer Waves," *Symposium on Surges in Pipelines. Institution of Mech. Engrs.*, vol. 180. part 3E, Nov., pp. 12-20 (see also discussions, pp. 21-27 and author's reply, pp. 110-111).
- Perko, H. D. and Zielke, W., "Some Further Investigations of Gaseous Cavitation," in Rath [1981], pp. 85-110.
- Perko, H. D. and Zielke, W., 1983, "On the Modeling of Pressure Waves with Gaseous Cavitation," *Proc. Sixth International Symp. and International Assoc. for Hydraulic Research Group*, Meeting on Transients in Cooling-Water Systems, Bamwood, Gloucester, CEGB, England.
- Raiteri, E. and Siccardi, F., 1975, "Transients in Conduits Conveying a Two-phase Bubbly flow: Experimental Measurements of Celerity," *L'Energia Elettrica*, no. 5, pp. 256-261.
- Rath, H. J., 1981, "Nonlinear Propagation of Pressure Waves in Elastic Tubes Containing Bubbly Air-Water Mixtures," *Proc. Fifth International Symp. and International Assoc. for Hydraulic Research Working Group Meeting on Water-Column Separation*, Obemach, Universities of Hanover and Munich, pp. 197-228.
- Ripken, J. F. and Olsen, R. M., 1958, "A Study of the Gas Nuclei on Cavitation Scale Effects in Water Tunnel Tests," *St. Anthony Falls Hyd. Lab. Proj., Report No. 58*, Minneapolis, Univ. of Minnesota.
- Safwat, H. H., 1972, "Photographic Study of Water Column Separation," *Jour., Hyd. Div., Amer. Soc. of Civ. Engrs.*, vol. 98, April, pp. 739-746.
- Safwat, H. H., 1975, "Water-Column Separation and Cavitation in Shon Pipelines," Paper No. 75-FE- 33, presented at the *Joint Fluid Engineering and Lubrication Conference*, Minneapolis, Minn., organized by Amer. Soc. of Mech. Engrs., May.
- Sharp, B. B., 1965, "Rupture of the Water Column," *Proc. Second Australian Conf. of Hydraulics. Fluid Mech.*, Auckland, New Zealand, pp. AI69-176.
- Sharp, B. B., 1971, Discussion of Weyler, et al. [1971], *Jour. Basic Engineering*, Amer. Soc. of Mech. Engrs., March, pp. 7-10.
- Siemons, J., 1967, "The Phenomenon of Cavitation in a Horizontal Pipe-line due to Sudden Pump Failure," *Jour. Hyd. Research*, International Assoc. for Hyd. Research, vol. 5, no. 2, pp. 135-152.
- Silbeman, E., 1957, "Some Velocity Attenuation in Bubbly Mixtures Measured in Standing Wave Tubes," *Jour. Acoust. Soc. of Amer.*, vol. 29, p. 925.
- Stepanoff, A. J., 1948, *Centrifugal and Axial Flow Pumps*, John Wiley & Sons, New York, NY, pp. 271-295.

- Wylie, E. B. and Streeter, V. L., 1967, *Fluid Transients*, Prentise Hall, England Cliffs, NJ.
- Streeter, V. L., 1983, "Transient Cavitating Pipe Flow," *Jour. Hydraulic Engineering*, vol. 109, Nov., pp. 1408-1423.
- Swaffield, J. A., 1972, "Column Separation in an Aircraft Fuel System," *Proc. First International Conference on Pressure Surges*, British Hydromechanics Research Assoc., England, pp. (C2) 13-28.
- Swanson, W. M., 1953, "Complete Characteristic Circle Diagrams for Turbomachinery," *Trans.*, Amer. Soc. of Mech. Engrs., vol. 75, pp. 819-826.
- Tanahashi, T. and Kasahara, E., 1970, "Comparison between Experimental and Theoretical Results of the Waterhammer with Water Column Separations," *Bull. Japan Soc. of Mech. Engrs.*, vol. 13, no. 61, July, pp. 914-925.
- Vreugdenhil, C. B., De Vries, A. H., Kalkwijk, J. P. Th., and Kranenburg, C., 1972, "Investigation into Cavitation in Long Horizontal Pipeline Caused by Water-Hammer," *6th Symposium*, International Assoc. for Hyd. Research, Rome, Italy, Sept. 13 pp.
- Weyler, M. E., Streeter, V. L., and Larsen, P. S., 1971, "An Investigation of the Effect of Cavitation Bubbles on the Momentum Loss in Transient Pipe Flow," *Jour. Basic Engineering*, Amer. Soc. of Mech. Engrs., March, pp. 1-7.
- Whiteman, K. J. and Pearsall, I. S., 1962, "Reflex-Valve and Surge Tests at a Station," *Fluid Handling*, vol. XIII, Sept. and Oct., pp. 248-250 and 282-286.
- Wiggert, D. C. and Sundquist, M. J., 1979, "The Effect of Gaseous Cavitation on Fluid Transients," *Jour. Fluids Engineering*, Amer. Soc. of Mech. Engrs., vol. I, pp. 79-86.
- Wiggert, D. C., Martin, C. S., Naghash, M., and Rao, P. V., 1983, "Modeling of Transient TwoComponent Flow Using a Four-Point Implicit Method," *Proc. Symp. on Numerical Methods for Fluid Transient Analysis*, Amer. Soc. of Mech. Engrs., Houston, June, pp. 23-28.
- Wood, A. B., 1955, *A Textbook of Sound*, Bell & Sons, London, UK.
- Wylie, E. B., 1983, "Simulation of Vaporous and Gaseous Cavitation," *Proc. Symp. on Numerical Methodsfor Fluid Transient Analysis*, Martin, C. S., and Chaudhry, M. H. (eds.), Amer. Soc. of Mech. Engrs., Houston, June, pp. 47-52.

## Additional References

- Carstens, H. R. and Hagler, T. W., 1964, "Water Hammer Resulting from Cavitating Pumps," *Jour., Hyd. Div.*, Amer. Soc. of Civ. Engrs., vol. 90.
- CEGB, 1983, *Proc. Sixth International Symp. and International Assoc. for Hydraulic Research Working Group Meeting on Transients in Cooling Water Systems*, Bamwood, Gloucester, UK.
- Due, J., 1959, "Water Column Separation," *Sulzer Tech. Review*, vol. 41.
- Due, J., 1965, "Negative Pressure Phenomena in Pump Pipelines," *International Symposium on Waterhammer in Pumped Storage Projects*, Amer. Soc. of Mech. Engrs., Nov.

- De Haller, P. and Bedue, A., 1951, "The Break-away of Water Columns as a Result of Negative Pressure Shocks," *Sulzer Tech. Review*, vol. 4, pp. 18-25.
- ENEL, 1971, *Proc. Meeting on Water Column Separation*, Organized by ENEL, Milan, Italy, Oct.
- ENEL, 1980, *Proc. Fourth Round Table and International Assoc. for Hydraulic Research Working Group Meeting on Water Column Separation*, Report No. 382, Cagliari, Italy.
- IAHR, 1981, *Proc. Fifth International Symp. and international Assoc. for Hydraulic Research Working Group Meeting on Water Column Separation*, Obemach, Universities of Hanover and Munich, Germany.
- Kephart, J. T. and Davis, K., 1961, "Pressure Surge Following Water-Column Separation," *Jour., Basic Engineering*, Amer. Soc. of Mech. Engrs., vol. 83, Sept., pp. 456-460.
- Knapp, R. T., Daily, J. W., and Hammitt, F. G., 1970, *Cavitation*, McGraw-Hill Book Co., New York, NY.
- Li, W. H., 1963, "Mechanics of Pipe Flow Following Column Separation," *Trans.*, Amer. Soc. of Civ. Engrs., vol. 128, part 2, pp. 1233-1254.
- Li, W. H. and Walsh, J. P., 1964, "Pressure Generated in a Pipe," *Jour. Engineering Mech. Div.*, Amer. Soc. of Civ. Engrs., vol. 90, no. EM6, pp. 113-133.
- Lupton, H. R., 1953, "Graphical Analysis of Pressure Surges in Pumping Systems," *Jour. Inst. of Water Engrs.*, vol. 7, p. 87.
- Proc. Second Round Table Meeting on Water Column Separation*, Vallombrosa, 1974, ENEL Report 290; also published in *L'Energia Eletrica*, No. 4 1975, pp. 183-485, not inclusive.
- Proc. Third Round Table Meeting on Water Column Separation*, Royaumont, *Bulletin de la Direction des Études et Recherches*, Series A, No. 2 1977.
- Richards, R. T. et al. 1956, "Hydraulic Design of the Sandow Pumping Plant," *Jour., Power Div.*, Amer. Soc. of Civ. Engrs., April.
- Richards, R. T., 1956, "Water Column Separation in Pump Discharge Lines," *Trans.*, Amer. Soc. of Mech. Engrs., vol. 78, pp. 1297-1306.
- Tanahashi, T. and Kasahara, E., 1969, "Analysis of Water Hammer with Water Column Separation," *Bull. Japan Soc. of Mech. Engrs.*, vol. 12, no. 50, pp. 206-214.
- Walsh, J. P. and Li, W. H., 1967, "Water Hammer Following Column Separation," *Jour., Applied Mech. Div.*, Amer. Soc. of Mech. Engrs., vol. 89, pp. 234-236.

---

## TRANSIENT CONTROL



Three 49-m<sup>3</sup> air chambers at Kangbook Intake Pump station, S. Korea.  
Pipeline discharge is 4.34 m<sup>3</sup>/s. (Courtesy, B. Y. Kim, Shinwoo, S. Korea.)

## 10-1 Introduction

A piping system may be designed with a liberal factor of safety to withstand possible maximum and minimum pressures. Such a design, however, is uneconomical. Therefore, to develop an economical project, various devices and/or control procedures are considered to eliminate or to mitigate the effects of undesirable transients, such as excessive pressure rise or drop, column separation, pump or turbine overspeed, etc. Control devices are usually costly and there is no single device that is suitable for universal applications on all systems or to handle all operating conditions. Therefore, to design a piping system, a number of alternatives with and without control devices are considered. The alternative that gives an overall economical system, an acceptable system response, and desired flexibility of operation is selected. An acceptable system response includes meeting the specified limits on the maximum and minimum pressures, maximum turbine or pump speed, preventing liquid-column separation, drainage of surge tank or air chamber, or the development of resonance, etc.

To understand the fundamental principle of transient-control devices or controlled operations, let us consider the basic water hammer equation we derived in Chapter 1. This equation relates the instantaneous change in flow velocity,  $\Delta V$ , to the resulting change in pressure

$$\Delta H = -\frac{a}{g} \Delta V \quad (10-1)$$

in which  $a$  = wave velocity and  $g$  = acceleration due to gravity. This equation indicates that the basic function of a transient-control device used for reducing the magnitude of pressure rise or pressure drop is to reduce  $\Delta V$  and/or  $a$ .

To eliminate or to reduce undesirable transients, such as high or low transient pressures, column separation, and excessive pump or turbine overspeed, control devices such as surge tanks, air chambers, and valves are utilized. The severity of undesirable transients may be reduced by modifying the pipeline profile, by increasing the diameter of the pipeline, by reducing the wave velocity, or by modifying the operating conditions. In addition, the flow conditions may be varied in a controlled manner to keep the pressures within the prescribed limits. Such controlled variation of the flow conditions to have specified system response is referred to as *optimal control of transient flows* (see Section 10-5).

In this chapter, we present various devices commonly used for eliminating undesirable transients. A brief description of surge tanks, air chambers, and valves is presented. Boundary conditions for these devices are then developed. These conditions are required for the analysis of a system by the method of characteristics. The chapter concludes with a case study.

In the derivation of the boundary conditions, the notation of Chapter 3 is used: Two subscripts designate the pressure and flow velocity at a section of a pipe: The first subscript refers to the pipe, while the second refers to the

section. The subscript  $P$  designates an unknown variable at the end of the time step, i.e., at time  $t_o + \Delta t$ , while a variable without the subscript  $P$  refers to its known value at the beginning of the time step, i.e., at time,  $t_o$  (see Fig. 3-1).

## 10-2 Surge Tank

In this section, boundary conditions for a simple surge tank are derived. Proceeding similarly, boundary conditions for other types of surge tanks may be developed. Various types of surge tanks are presented in Section 11-2.

### Description

A surge tank is an open chamber or a tank connected to the pipeline for transient control. This tank reflects the pressure waves, and supplies or stores excess water resulting from the operation of turbines, pumps, or control valves.

Rapid transients, i.e., waterhammer, in a piping system having a surge tank may be analyzed by using the method of characteristics. However, slow transients, e.g., oscillations of the water level in a surge tank following a load change on a turbine, may be analyzed as a lumped system, details of which are presented in Chapter 11.

### Boundary Conditions

Let us consider a surge tank directly connected to the pipeline, as shown in Fig. 10-1. If the pipe connecting the tank to the pipeline is short, it may be neglected in the analysis.

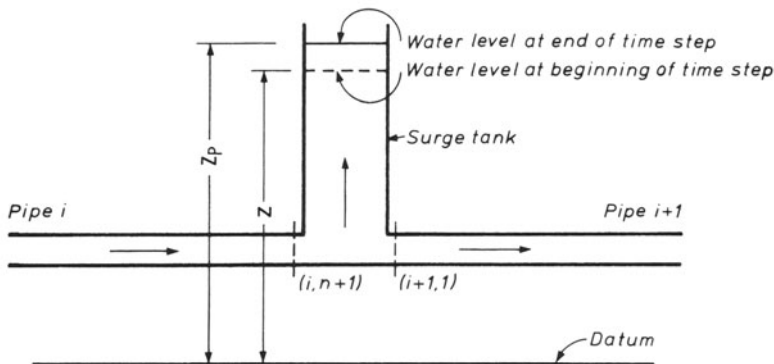


Fig. 10-1. Notation for surge tank.

The following equations may be written for the junction of the surge tank with the pipeline (see Fig. 10-1). The head loss at the junction of the tank and the pipeline is small and is neglected.

*Positive characteristic equation for section ( $i, n + 1$ )*

$$Q_{P_{i,n+1}} = C_p - C_{a_i} H_{P_{i,n+1}} \quad (10-2)$$

*Negative characteristic equation for section ( $i + 1, 1$ )*

$$Q_{P_{i+1,1}} = C_n + C_{a_{i+1}} H_{P_{i+1,1}} \quad (10-3)$$

*Continuity equation*

$$Q_{P_{i,n+1}} = Q_{P_{i+1,1}} + Q_{P_s} \quad (10-4)$$

in which  $Q_{P_s}$  = flow into the tank at the end of the time step (flow into the tank is considered positive);  $Q_P$  = discharge at the end of time step;  $H_P$  = piezometric head above datum;  $C_p$ ,  $C_n$ , and  $C_a$  are constants as defined by Eqs. 3-19 through 3-21. The subscripts  $i$  and  $i + 1$  refer to the pipe numbers, and the subscripts 1 and  $n + 1$  refer to the section numbers.

*Energy equation*

If the losses at the junction are neglected, then

$$H_{P_{i,n+1}} = H_{P_{i+1,1}} = z_P \quad (10-5)$$

*Surge-tank water level*

Let  $z$  and  $z_P$  be the heights of the liquid surface in the tank above the datum at the beginning and at the end of the time step. If the size of the time step,  $\Delta t$ , is small, then we may write

$$z_P = z + \frac{1}{2} \frac{\Delta t}{A_s} (Q_{P_s} + Q_s) \quad (10-6)$$

in which  $A_s$  = horizontal cross-sectional area of the tank, and  $Q_s$  is flow into the tank at the beginning of the time step.

Solving Eqs. 10-2 to 10-6 for  $H_{P_{i,n+1}}$ , we obtain

$$H_{P_{i,n+1}} = \frac{C_p - C_n + Q_s + (2A_s z / \Delta t)}{C_{a_i} + C_{a_{i+1}} + (2A_s / \Delta t)} \quad (10-7)$$

In the above derivation, it was assumed that the length of the standpipe between the pipeline and the tank is short and therefore may be neglected. However, if this is not the case, then the standpipe may be included in the analysis as a pipe or as a lumped mass (see Problem 10-2).

Similarly, the head losses in the orifice of an orifice tank may be included by modifying Eq. 10-5.

## 10-3 Air Chamber

In this section, we briefly describe an air chamber and its operation and develop boundary conditions for analysis by the method of characteristics.

### Description

An air chamber (Fig. 10-2) is a vessel with compressed air at its top and water in its lower part. To restrict the inflow into or outflow from the chamber, an orifice is provided between the chamber and the pipeline. The orifice is usually shaped such that it produces more head loss for inflow into the chamber than for a corresponding outflow from the chamber. Such an orifice is referred to as *differential orifice* (Fig. 10-2). To prevent significant pressure drop in the pipeline and hence column separation, the outflow from the chamber should be as free as possible, while the inflow may be restricted to reduce the size of the chamber. A ratio of 2.5: 1 between the orifice head losses for the same inflow and outflow is common [Evans and Crawford, 1954]. Since the volume of air may be reduced due to leakage or due to solution in the water after a period of operation, an air compressor is provided to keep the volume of the air within the prescribed limits.

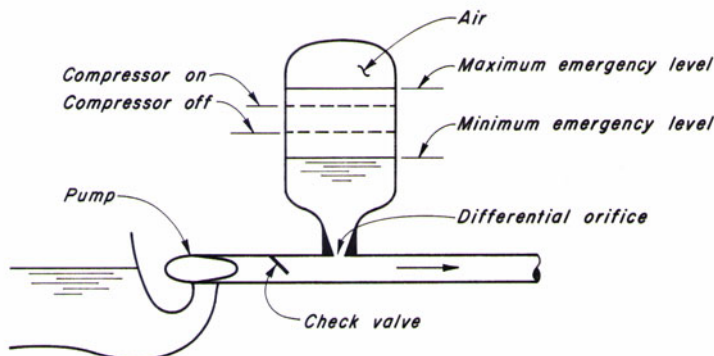


Fig. 10-2. Air chamber.

To prevent reverse flow, a check valve is provided between the pump and the air chamber (Fig. 10-2). Upon power failure, the pressure in the pipeline drops and water outflows from the chamber into the pipeline. When the flow in the pipeline reverses, the check valve closes instantaneously, and water flows into the chamber. Because of the inflow or outflow from the chamber, the air

in the chamber contracts or expands, and the pressure rise and drop in the pipeline are reduced due to gradual variation of the flow velocity.

As compared to a surge tank, an air chamber has the following advantages:

1. The volume of an air chamber required for keeping the maximum and minimum pressures within the prescribed limits is smaller than that of an equivalent surge tank.
2. An air chamber can be installed with its axis parallel to the ground. This reduces the foundation costs and is preferable to withstand both wind and earthquake loads.
3. An air chamber can be located near the pump, which may not be practical for a surge tank because of excessive height. This reduces the pressure rise and the pressure drop in the pipeline.
4. To prevent freezing in cold climates, it costs less to heat an air chamber than a surge tank because of smaller size and because of proximity to the pump house.

The *disadvantage* of an air chamber is that an air compressor and auxiliary control equipment have to be provided. These require constant maintenance and high initial costs.

Engler [1933], Allievi [1937], and Angus [1937] discussed the use of air chambers in pumping systems to control transients generated by power failure to the pumps. Various authors have presented charts to determine the size of an air chamber for a pipeline to keep the maximum and minimum pressures within design limits [Combes and Borot, 1952; Evans and Crowford, 1954 and Ruus, 1977]. These charts (see Appendix A) may be used to determine an approximate size of a chamber for a pipeline. During the final design, however, a detailed transient analysis should be carried out. The method of characteristics incorporating the following boundary conditions may be used for this analysis.

### Boundary Conditions

Referring to Fig. 10-3, the following equations may be written for the junction of the chamber and the pipeline:

*Positive characteristic equation for section ( $i, n+1$ )*

$$Q_{P_{i,n+1}} = C_p - C_{a_i} H_{P_{i,n+1}} \quad (10-8)$$

*Negative characteristic equation for section ( $i+1, 1$ )*

$$Q_{P_{i+1,1}} = C_n + C_{a_{i+1}} H_{P_{i+1,1}} \quad (10-9)$$

*Energy equation*

If the losses at the junction are neglected, then

$$H_{P_{i,n+1}} = H_{P_{i+1,1}} \quad (10-10)$$

*Continuity equation*

$$Q_{P_{i,n+1}} = Q_{P_{i+1,1}} + Q_{P_{\text{orf}}} \quad (10-11)$$

in which  $Q_{P_{\text{orf}}}$  = flow through the orifice (inflow into the chamber is considered positive).

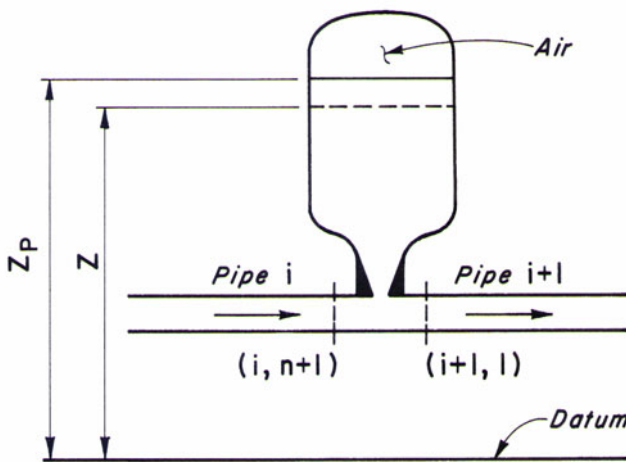


Fig. 10-3. Notation for air chamber.

If we assume the air enclosed at the top of the chamber follows the polytropic relation for a perfect gas, then

$$H_{P_{\text{air}}}^* \nabla_{P_{\text{air}}}^m = C \quad (10-12)$$

in which  $H_{P_{\text{air}}}^*$  and  $\nabla_{P_{\text{air}}}^m$  are the absolute pressure head and the volume of the enclosed air at the end of the time step respectively;  $m$  is the exponent in the polytropic gas equation, and  $C$  is a constant. The value  $C$  is determined from the expression,  $C = \nabla_{P_{\text{air}}}^m H_{P_{\text{air}}}^*$ , in which the subscript  $o$  refers to the initial steady-state conditions. The values of  $m$  is 1.0 for an isothermal and 1.4 for adiabatic expansion or contraction of the air. The expansion or contraction process is almost adiabatic for a small chamber and rapid transients, and it is

almost isothermal for slow transients in large air volumes. An average value of  $m = 1.2$  is recommended because the transients are usually rapid at the beginning but are slow near the end. Graze [1972 and 1976] suggests the use of a differential equation based on rational heat transfer instead of the polytropic equation, Eq. 10-12. The main difficulty in using the equation recommended by Graze is that the rate of heat transfer is not precisely known and has to be estimated.

The head loss for the flow through the orifice may be expressed as

$$h_{P_{\text{orf}}} = C_{\text{orf}} Q_{P_{\text{orf}}} |Q_{P_{\text{orf}}}| \quad (10-13)$$

in which  $C_{\text{orf}}$  = coefficient of orifice losses, and  $h_{P_{\text{orf}}}$  = orifice head loss for a flow of  $Q_{P_{\text{orf}}}$ . Note that for a differential orifice,  $C_{\text{orf}}$  has different values for the inflow into and for outflow from the chamber.

The following equations may be written for the enclosed air volume:

$$H_{P_{\text{air}}}^* = H_{P_{i,n+1}} + H_b - z_P - h_{P_{\text{orf}}} \quad (10-14)$$

$$\forall_{P_{\text{air}}} = \forall_{\text{air}} - A_c (z_P - z) \quad (10-15)$$

$$z_P = z + 0.5 (Q_{\text{orf}} + Q_{P_{\text{orf}}}) \frac{\Delta t}{A_c} \quad (10-16)$$

in which  $H_b$  = barometric pressure head;  $A_c$  = horizontal cross-sectional area of the chamber;  $z$  and  $z_P$  are the heights of the water surface in the chamber above the datum at the beginning and at the end of the time step (measured positive upwards);  $Q_{\text{orf}}$  = orifice flow at the beginning of time step; and  $\forall_{\text{air}}$  = volume of air at the beginning of time step.

We have nine equations, Eq. 10-8 to 10-16, in nine unknowns, namely,  $Q_{P_{i,n+1}}$ ,  $Q_{P_{i+1,1}}$ ,  $Q_{P_{\text{orf}}}$ ,  $H_{P_{i,n+1}}$ ,  $H_{P_{i+1,1}}$ ,  $h_{P_{\text{orf}}}$ ,  $\forall_{P_{\text{air}}}$ ,  $H_{P_{\text{air}}}^*$  and  $z_P$ . To simplify the solution of these equations, some of the unknowns may be eliminated as follows: Substituting Eqs. 10-8 through 10-10 into Eq. 10-11, we obtain

$$Q_{P_{\text{orf}}} = (C_p - C_n) - (C_{a_i} + C_{a_{i+1}}) H_{P_{i,n+1}} \quad (10-17)$$

It follows from Eqs. 10-14 through 10-15 that

$$(H_{P_{i,n+1}} + H_b - z_P - C_{\text{orf}} Q_{P_{\text{orf}}} |Q_{P_{\text{orf}}}|) [\forall_{\text{air}} - A_c (z_P - z)]^m = C \quad (10-18)$$

In Eqs. 10-16 through 10-18, we have three unknowns;  $Q_{P_{\text{orf}}}$ ,  $H_{P_{i,n+1}}$ , and  $z_P$ . The elimination of  $H_{P_{i,n+1}}$  and  $z_P$  from these equations yields a nonlinear equation in  $Q_{P_{\text{orf}}}$  which may be solved by an iterative technique, such as the Newton-Raphson method. The known value,  $Q_{\text{orf}}$ , at the beginning of the time step may be used as a first estimate for starting the iterations.

## 10-4 Valves

In this section, we discuss different types of valves for controlling transients and develop boundary conditions for analysis by the method of characteristics.

## Description

The transients are controlled by the following valve operations:

1. The valve opens or closes to reduce the rate of net change in the pipeline flow velocity.
2. If the pressure exceeds a set limit, the valve opens for rapid outflow which causes the pressure to drop, thus reducing the maximum pressure.
3. The valve opens to admit air into the pipeline, thus preventing the pressure from dropping to the liquid vapor pressure.

Valves commonly used for transient control are:

Safety valves;

Pressure-relief valves;

Pressure-regulating valves;

Air-inlet valves; and

Check valves.

A brief description of the operation of each valve follows.

A *safety valve* ([Fig. 10-4a](#)) is a spring or weight-loaded valve, which opens as soon as the pressure inside the pipeline exceeds the pressure limit set on the valve and closes abruptly when the pressure drops below the specified limit ([Fig. 10-5a](#)). A safety valve is either fully open or fully closed.

The operation of a *pressure-relief valve* or *surge suppressor* ([Fig. 10-4b](#)) is similar to that of a safety valve except that its opening is proportional to the amount by which the pressure in the pipeline at the valve exceeds the specified limit. The valve closes when the pipeline pressure drops and is fully closed when the pressure is below the limit set on the valve. There is usually hysteresis in the opening and the closing of the valve, as shown in [Fig. 10-5b](#) [Evangelisti, 1969].

For a pumping system having multiple pumps discharging into a common header, a battery of smaller relief valves or surge suppressors may be preferred [Lescovich, 1967] instead of one large surge suppressor. A suppressor may be installed on each pump or the entire battery of the suppressors may be mounted on the main discharge line. In the latter arrangement, the overpressure setting of each valve should be set such that the valves open in sequence one after the other rather than simultaneously.

A *pressure-regulating valve* (PRV) is a pilot-controlled throttling valve, which is opened or closed by a servomotor with the opening and closing times set individually. It is installed downstream of a pump in a pumping system and upstream of a turbine in a hydropower plant. Following power failure to the pump-motor, this valve opens rapidly and then closes gradually ([Fig. 10-5c](#)) to reduce the pressure rise. The operation of this valve in a hydropower scheme is as follows: If the power plant is isolated from the electrical grid, the PRV is kept partly open to provide for the maximum anticipated rapid load increase. When accepting rapid load changes, the PRV is closed synchronously

with the wicket gates to maintain an essentially constant flow velocity in the penstock. Following a load rejection, the PRV is opened as the wicket gates are closed, and then the PRV is closed at a slow rate. In such an operation, some water is wasted. However, the amount of wasted water is usually insignificant since isolated operation is an emergency condition. Upon full-load rejection, either in the normal or isolated operation of the turbine, all the turbine flow is switched from the turbine to the PRV. The PRV is then closed slowly.

[Figure 10-6](#) illustrates the synchronous operation of a PRV and a turbine. Ideally, the net change in the penstock flow may be reduced to zero by matching the discharge characteristics of the PRV with that of the turbine. However, this is usually impossible because of the nonlinear flow characteristics of the turbine and the valve and because of the dead or delay time between the opening (closing) of the pressure regulator and the closing (opening) of the wicket gates. This dead time should be as short as possible to minimize pressure rise or drop in the penstock.

An *air-inlet valve* admits air into the pipeline whenever the pressure inside the pipeline drops below the atmospheric pressure. This reduces the pressure difference between the outside atmospheric pressure and the pressure inside the pipeline, thereby preventing the collapse of the pipeline. Air-inlet valves may be used to reduce the generation of high pressures when the liquid columns rejoin following column separation by providing an air cushion in the pipe.

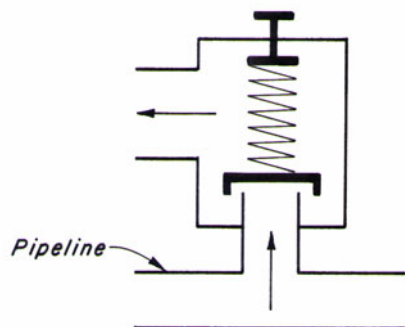
Once air is admitted into the pipeline, extreme care must be exercised while refilling the pipeline. The air should be released slowly from the pipeline because the entrapped air may result in very high pressures [Albertson and Andrews, 1971 and Martin, 1976].

A *check valve* is used to prevent reverse flow through a pump and to prevent inflow into a one-way surge tank from the pipeline. A check valve in its simplest form is a flap valve, although a dashpot or a spring may be provided to prevent slamming of the valve. Such valve slamming may result in a pressure spike and/or vibrations in the piping system.

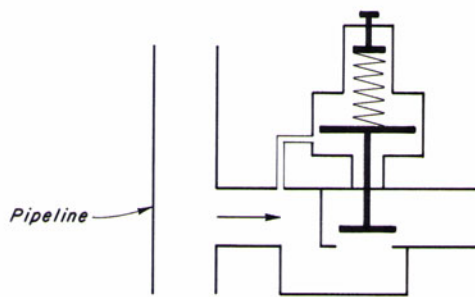
## Boundary Conditions

The boundary conditions developed in Section 3-3 may be used for a safety and for a relief valve. These may also be used for a PRV if the pump is isolated from the pipeline following power failure by a check valve. Boundary conditions for the synchronous operation of a pump and a PRV are derived in this section; and for a Francis turbine and a PRV, in Section 10-6.

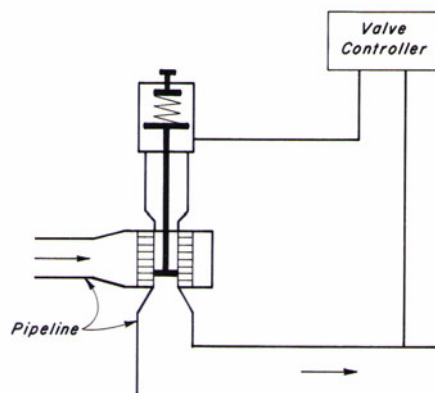
A check valve may be considered a dead end for negative flows, while it may be ignored for positive flows. For a large valve, however, a more elaborate analysis may be necessary. In such analyses, the differential equation of Problem 4-6 describing the closure of a check valve as the flow in the discharge line decelerates is solved.



(a) Safety valve

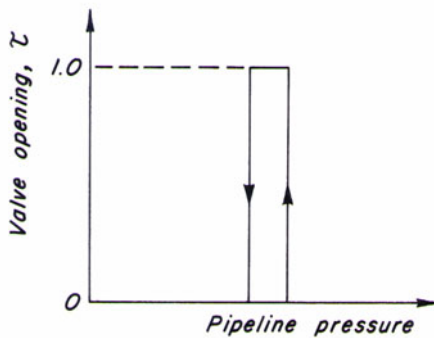


(b) Pressure relief valve

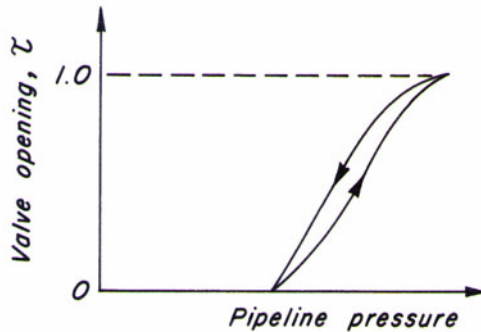


(c) Pressure regulating valve

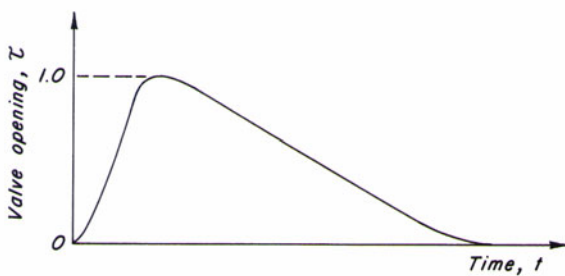
Fig. 10-4. Schematic of safety, relief, and pressure-regulating valves.



(a) Safety valve



(b) Pressure relief valve



(c) Pressure regulating valve

Fig. 10-5. Discharge characteristics of safety, relief, and pressure-regulating valves. (After Evangelisti [1969].)

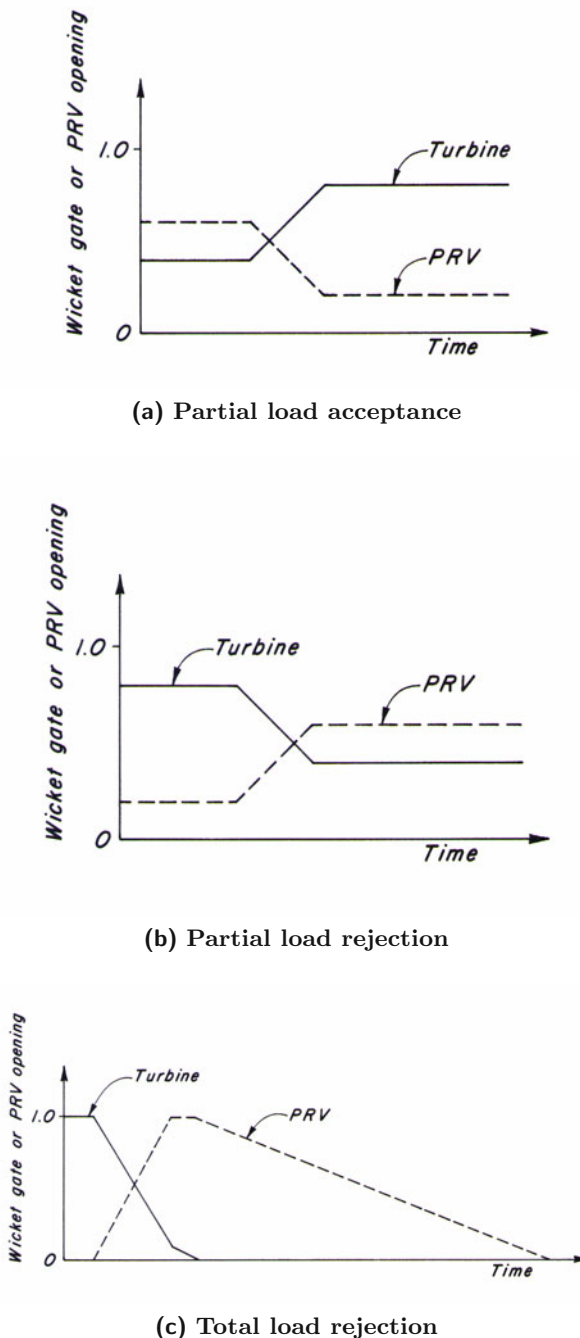


Fig. 10-6. Synchronous operation of turbine and pressure-regulating valve.

To develop the boundary conditions for a valve, the variation of effective valve opening,  $\tau$ , with time should be known. For a pressure relief valve or surge suppressor,  $\tau$  is a function of the pressure in the pipeline at the valve. Therefore,  $\tau$  is determined as the calculations progress. The  $\tau$ -versus-time curve for a PRV is specified a priori. Discrete values on this  $\tau-t$  curve are specified, and the  $\tau$  values at intermediate times are determined by interpolation.

### ***PRV and a Pump***

Let us consider the PRV and pump arrangement shown in Fig. 10-7 in which the pipes between the pump and section  $(i, 1)$  and between the valve and section  $(i, 1)$  are short and therefore neglected. Assuming the downstream flow direction as positive, the continuity equation at section  $(i, 1)$  may be written as

$$Q_{P_{i,1}} = n_P Q_{P_p} - Q_{P_v} \quad (10-19)$$

in which  $Q_P$  = discharge at the end of the time step; the subscripts  $p$ ,  $v$ , and  $(i, 1)$  refer to the pump, PRV, and section  $(i, 1)$ , respectively; and  $n_P$  = number of parallel pumps.

Referring to Fig. 10-7,

$$H_{P_{i,1}} = H_{P_p} + H_{\text{suc}} - \Delta H_{P_d} \quad (10-20)$$

in which  $H_{\text{suc}}$  = height of the suction water level above the datum;  $H_{P_{i,1}}$  = piezometric head at section  $(i, 1)$  above datum;  $\Delta H_{P_d}$  = head losses through the discharge valve; and  $H_{P_p}$  = pumping head.

The PRV flow,  $Q_{P_v}$ , is given by the equation

$$Q_{P_v} = C_{pv}\tau_P \sqrt{H_{P_{i,1}} - z_o} \quad (10-21)$$

in which  $C_{pv} = Q_{ov}/\sqrt{H_o - z_o}$ ;  $Q_{ov}$  = flow through the fully open valve under a head of  $(H_o - z_o)$ ;  $\tau_P$  = effective valve opening at the end of time step =  $(C_d A_v) / (C_d A_v)_o$ ;  $C_d$  = coefficient of discharge;  $A_v$  = area of valve opening;  $z_o$  = height above the datum of the reservoir into which PRV is discharging; and the subscript  $o$  refers to steady-state conditions. For a PRV discharging into the suction reservoir,  $z_o = H_{\text{suc}}$ , and for a PRV discharging into atmosphere,  $z_o$  = height of the PRV above the datum.

The following equations are available at the upstream end of pump-PRV:

- i. Negative characteristic equation for section  $(i, 1)$ , Eq. 4-16;
- ii. Equations for the head and torque characteristics, Eqs. 4-7 and 4-8; and
- iii. Equation for the rotating masses, Eq. 4-14.

Now, we have seven equations in seven unknowns, namely,  $Q_{P_p}$ ,  $Q_{P_v}$ ,  $Q_{P_{i,1}}$ ,  $H_{P_{i,1}}$ ,  $\alpha_P$ ,  $h_P$  and  $\beta_P$ . To simplify the solution of these equations, let us

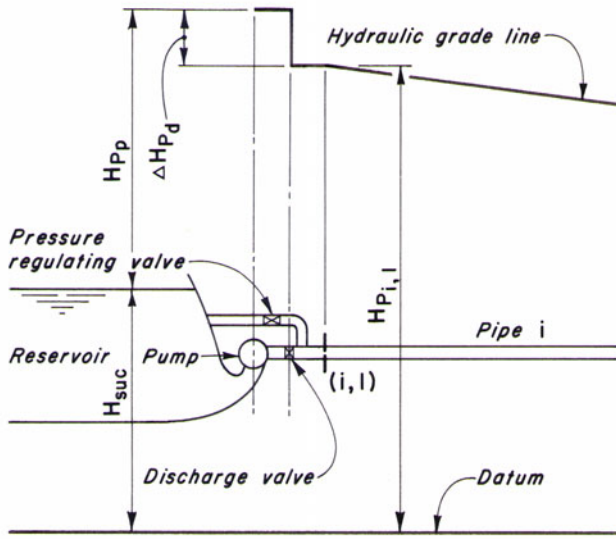


**Fig. 10-7.** Notation for a pressure-regulating valve-centrifugal pump system.

eliminate different variables so that we have two equations in two unknowns and then solve these equations by an iterative technique, such as the Newton-Raphson method. In this section, we derive the expressions for  $F_1$  and  $F_2$  and for their derivatives for the Newton-Raphson method, outlined in Section 4-4.

By eliminating  $Q_{P_{i,1}}$  and  $H_{P_{i,1}}$  from Eqs. 10-19, 10-21, and 4-16, and writing  $\Delta H_{P_d} = C_v Q_{P_p} |Q_{P_p}|$ , we obtain

$$n_P Q_{P_p} = C_{pv} \tau_P \sqrt{H_{P_p} + H_{suc} - C_v Q_{P_p} |Q_{P_p}| - z_o} + C_n \\ + C_{a_i} (H_{P_p} + H_{suc} - C_v Q_{P_p} |Q_{P_p}|) \quad (10-22)$$

By using the relationships,  $v_P = Q_{P_p}/Q_R$  and  $h_P = H_{P_p}/H_R$ , Eq. 10-22 may be written as

$$n_P Q_R v_P = C_{pv} \tau_P \sqrt{H_R h_P + H_{suc} - C_v Q_R^2 v_P |v_P| - z_o} + C_n \\ + C_{a_i} (H_R h_P + H_{suc} - C_v Q_R^2 v_P |v_P|) \quad (10-23)$$

By eliminating  $h_P$  from Eqs. 4-7 and 10-23, and simplifying the resulting equation, we obtain

$$\begin{aligned}
F_1 &= C_{pv}\tau_P \\
&\times \left( a_1 H_R (\alpha_P^2 + v_P^2) + a_2 H_R (\alpha_P^2 + v_P^2) \tan^{-1} \frac{\alpha_P}{v_P} - C_v Q_R^2 v_P |v_P| \right. \\
&+ H_{suc} - z_o \left. \right)^{\frac{1}{2}} + C_{a_i} H_R a_1 (\alpha_P^2 + v_P^2) + C_{a_i} H_R a_2 (\alpha_P^2 + v_P^2) \tan^{-1} \frac{\alpha_P}{v_P} \\
&- C_{a_i} C_v Q_R^2 v_P |v_P| - n_P Q_R v_P + C_n + C_a H_{suc} = 0
\end{aligned} \tag{10-24}$$

Differentiation of Eq. 10-24 with respect to  $\alpha_P$  and  $v_P$  yields

$$\begin{aligned}
\frac{\partial F_1}{\partial \alpha_P} &= \frac{1}{2} \tau_P C_{pv} \left[ a_1 H_R (\alpha_P^2 + v_P^2) + a_2 H_R (\alpha_P^2 + v_P^2) \tan^{-1} \frac{\alpha_P}{v_P} \right. \\
&- C_v Q_R^2 v_P |v_P| + H_{suc} - z_o \left. \right]^{-1/2} \left( 2a_1 \alpha_P H_R + a_2 H_R v_P \right. \\
&+ 2a_2 H_R \alpha_P \tan^{-1} \frac{\alpha_P}{v_P} \left. \right) + 2a_1 C_{a_i} H_R \alpha_P + 2a_2 C_{a_i} H_R \alpha_P \tan^{-1} \frac{\alpha_P}{v_P} \\
&+ a_2 C_{a_i} H_R v_P
\end{aligned} \tag{10-25}$$

$$\begin{aligned}
\frac{\partial F_1}{\partial v_P} &= \frac{1}{2} \tau_P C_{pv} \left[ a_1 H_R (\alpha_P^2 + v_P^2) + a_2 H_R (\alpha_P^2 + v_P^2) \tan^{-1} \frac{\alpha_P}{v_P} \right. \\
&- C_v Q_R^2 v_P |v_P| + H_{suc} - z_o \left. \right]^{-1/2} \times \left[ 2v_P H_R \left( a_1 + a_2 \tan^{-1} \frac{\alpha_P}{v_P} \right) \right. \\
&- a_2 H_R \alpha_P - 2C_v Q_R^2 |v_P| \left. \right] + 2a_1 C_{a_i} H_R v_P + 2a_2 C_{a_i} H_R v_P \tan^{-1} \frac{\alpha_P}{v_P} \\
&- a_2 C_{a_i} H_R \alpha_P - 2C_{a_i} C_v Q_R^2 |v_P| - n_P Q_R
\end{aligned} \tag{10-26}$$

Expressions for  $F_2$ ,  $\partial F_2 / \partial \alpha_P$ , and  $\partial F_2 / \partial v_P$  are given by Eqs. 4-20, 4-27, and 4-28, respectively. The value of  $\tau_P$  is determined from the specified valve-opening-versus-time curve, and then Eqs. 10-24 to 10-26, 4-20, 4-27, and 4-28 are used to determine the values of  $\alpha_P$  and  $v_P$  by following the procedure outlined in Section 4-4. The flowchart of Fig. 10-8 should help in understanding the procedure.

### Air-Inlet Valve

An air-inlet valve admits air into the pipeline when the inside pressure drops below the outside atmospheric pressure. However, this air is entrapped and not allowed to release when the pressure increases above the atmospheric pressure. In a combination air valve, a large orifice is provided for air inflow and a smaller orifice, for air release. In this section, boundary condition for an air-inlet valve is developed. The development of boundary condition for a combination air valve is discussed at the end of this sub-section.

For an air-inlet valve located at the junction of the  $i$ th and  $(i+1)$ th pipe as shown in Fig. 10-9, the positive and negative characteristic equations for sections  $(i, n+1)$  and  $(i+1, 1)$  are

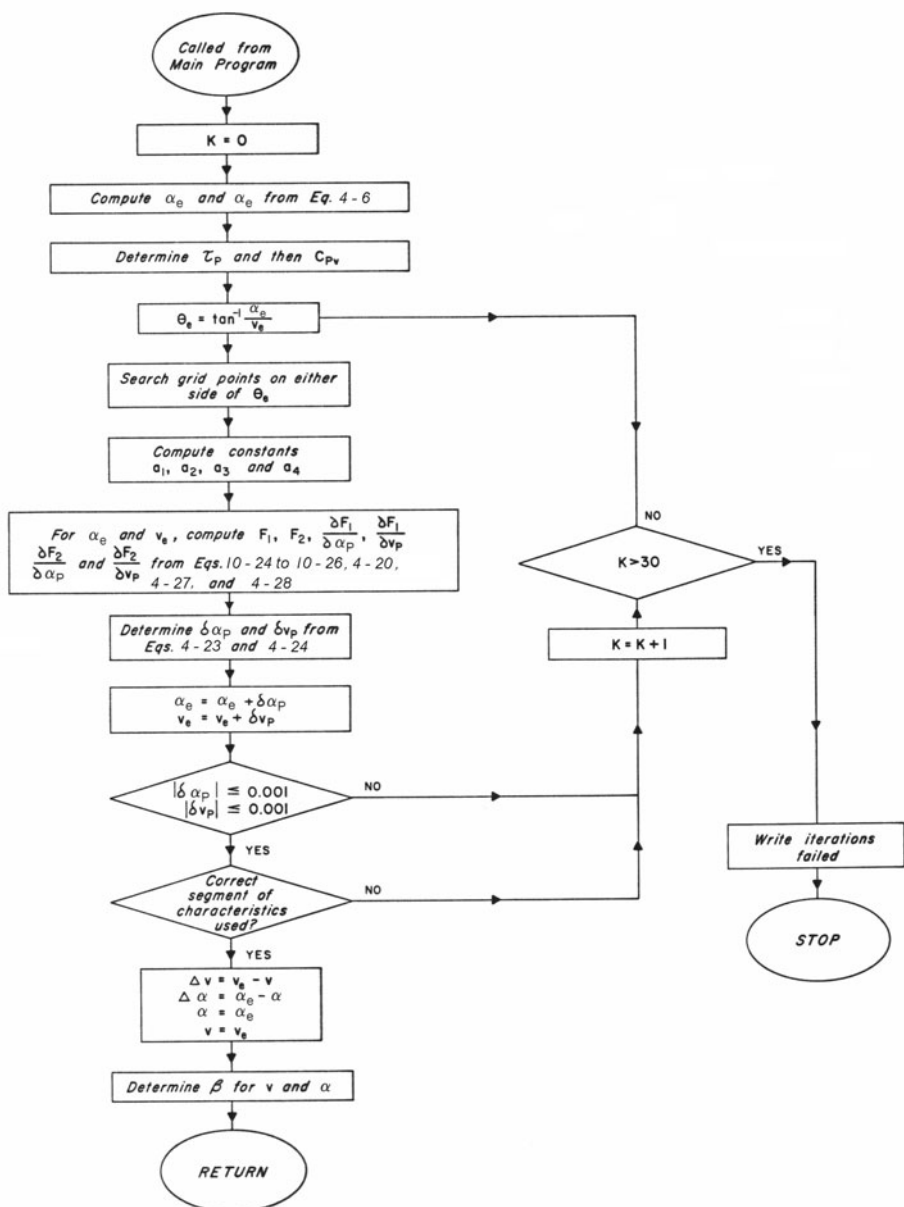


Fig. 10-8. Flowchart for boundary conditions for a pressure-regulating valve-centrifugal pump system.

$$Q_{P_{i,n+1}} = C_p - C_{a_i} H_{P_{i,n+1}} \quad (10-27)$$

$$Q_{P_{i+1,1}} = C_n + C_{a_{i+1}} H_{P_{i+1,1}} \quad (10-28)$$

If the head losses in the pipeline at the valve are neglected, then

$$H_{P_{i,n+1}} = H_{P_{i+1,1}} \quad (10-29)$$

In the subsequent discussion, the piezometric head at the valve is designated as  $H_{P_{i,n+1}}$ .

As  $H_{P_{i,n+1}}$  drops below a predetermined value,  $y$ , set on the valve [Papadakis and Hsu, 1977], the valve opens, and the air flows into the pipeline. Later, when  $H_{P_{i,n+1}} > y$ , the valve closes and the air inside the pipeline is entrapped. Thus, depending upon the time variation of pressure at the valve, the valve may open and close several times during the transient conditions and the mass of the entrapped air increases with each opening of the valve.

The boundary conditions are developed based on the following *assumptions*:

1. The airflow into the pipeline is isentropic;
2. The entrapped air remains at the valve location and is not carried away by the flowing liquid, and
3. The expansion or contraction of the entrapped air is isothermal.

Let  $m_a$  be the mass of the air entrapped in the pipeline at the beginning of the time step. Then, for small  $\Delta t$ , the mass of air,  $m_{P_a}$  at the end of time step is

$$m_{P_a} = m_a + \frac{dm_a}{dt} \Delta t \quad (10-30)$$

in which  $dm_a/dt$  is the time rate of mass inflow of air through the valve into the pipeline.

It follows from the continuity equation that the entrapped air

$$\forall_{P_{\text{air}}} = \forall_{\text{air}} + 0.5 \Delta t [(Q_{P_{i+1,1}} + Q_{i+1,1}) - (Q_{P_{i,n+1}} + Q_{i,n+1})] \quad (10-31)$$

By substituting Eqs. 10-27 through 10-29 into Eq. 10-31, we obtain

$$\forall_{P_{\text{air}}} = C_{\text{air}} + 0.5 \Delta t (C_{a_i} + C_{a_{i+1}}) H_{P_{i,n+1}} \quad (10-32)$$

in which  $C_{\text{air}} = \forall_{\text{air}} + 0.5 \Delta t (C_n + Q_{i+1,1} - C_p - Q_{i,n+1})$ .

For the isothermal expansion and contraction of the air inside the pipeline

$$p \forall_{P_{\text{air}}} = m_{P_a} RT \quad (10-33)$$

in which  $R$  = universal gas constant and  $p$  and  $T$  are the absolute pressure and temperature of the air volume inside the pipeline. Now, the absolute pressure

$$p = \gamma (H_{P_{i,n+1}} - z + H_b) \quad (10-34)$$

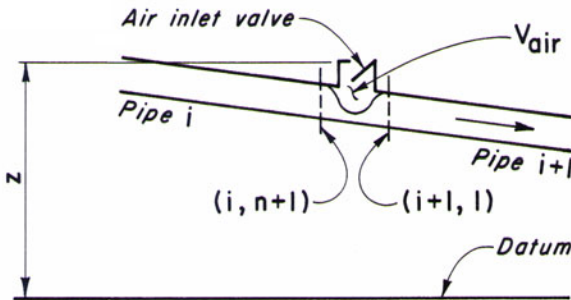


**Fig. 10-9.** Notation for air-inlet valve.

in which  $z$  = height of the valve throat above the datum;  $\gamma$  = specific weight of the liquid inside the pipeline; and  $H_b$  = barometric pressure head.

Substituting  $H_{P_{i,n+1}}$  from Eq. 10-34 into Eq. 10-32, eliminating  $\forall_{P_{\text{air}}}$  from the resulting equation and Eq. 10-33, we obtain

$$m_{P_a} RT = p \left[ C_{\text{air}} + 0.5 \Delta t (C_{a_i} + C_{a_{i+1}}) \left( \frac{p}{\gamma} + z - H_b \right) \right] \quad (10-35)$$

Elimination of  $m_{P_a}$  from Eqs. 10-30 and 10-35 yields

$$\left( m_a + \frac{dm_a}{dt} \Delta t \right) RT = p \left[ C_{\text{air}} + 0.5 \Delta t (C_{a_i} + C_{a_{i+1}}) \left( \frac{p}{\gamma} + z - H_b \right) \right] \quad (10-36)$$

In this equation,  $p$  and  $dm_a/dt$  are the two unknowns. The airflow through the valve is at sonic velocity if the absolute pressure,  $p$ , inside the pipeline is less than  $0.53 p_a$  ( $p_a$  = barometric pressure), while the air velocity through the valve is subsonic if  $p$  is greater than  $0.53 p_a$  but less than  $p_a$ . The expressions for  $dm_a/dt$  are [Streeter, 1966]:

Subsonic air velocity through the valve ( $p_a > p > 0.53 p_a$ )

$$\frac{dm_a}{dt} = C_d A_v \sqrt{7 p_a \rho_a \left( \frac{p}{p_a} \right)^{1.43} \left[ 1 - \left( \frac{p}{p_a} \right)^{0.286} \right]} \quad (10-37)$$

Sonic air velocity through the valve ( $p \leq 0.53 p_a$ )

$$\frac{dm_a}{dt} = 0.686 C_d A_v \frac{p_a}{\sqrt{RT_a}} \quad (10-38)$$

in which  $C_d$  = coefficient of discharge of the valve;  $A_v$  = area of the valve opening at its throat;  $\rho_a$  = mass density of air at absolute atmospheric pressure,  $p_a$ , and absolute temperature,  $T_a$ , outside the pipeline. Equations 10-37 and 10-38 are obtained by substituting  $k = 1.4$  into the equations presented in Streeter [1966] in which  $k$  is the ratio of the specific heats for air.

Substitution of Eq. 10-37 or 10-38 into Eq. 10-36 yields a nonlinear equation in  $p$ , which may be solved by an iterative technique, such as the Newton-Raphson method.  $H_{P_{i,n+1}}, \forall_{P_{\text{air}}}, m_{P_a}, H_{P_{i+1,1}}, Q_{P_{i,n+1}}$ , and  $Q_{P_{i+1,1}}$  may then be determined from Eqs. 10-34, 10-32, 10-33, 10-29, 10-27, and 10-28, respectively.

Prior to the first-time opening of the air-inlet valve,  $m_a = 0$ . Afterward, however, the value of  $m_a$  increases with each subsequent opening of the valve.

Note that, in the development of above boundary conditions, it is assumed that there is no air outflow through the valve. However, a combination air valve has a larger orifice for air inflow and a smaller orifice for air release. In this case, air releases through the air valve when the pressure inside the pipeline exceeds the outside pressure. The air outflow may be included by using the equations for air outflow instead of the equations for air inflow, see Problem 10-6. Since air inflow is considered positive, air outflow is negative.

## 10-5 Optimal Transient Control

The mode of operation of various appurtenances and control devices that results in a desired system response is called *optimal flow control*. A desired system response may involve keeping the maximum and minimum transient-state pressures within specified limits, changing the flow conditions from one steady state to another steady state in minimum time, changing the flow conditions from one steady state to another without flow oscillations, and so on. For example, a valve at the downstream end of a pipeline may be closed such that the pressure remains below a specified limit and the transients in the pipeline vanish as soon as the valve movement ceases. Such a valve operation is referred to as *optimum valve closure* [Ruus, 1966] or *Valve stroking* [Streeter, 1963; Streeter, 1967; Driels, 1974 and 1975; Ikeo and Kobori, 1975]. Optimal flow control is a design or synthesis approach in which the boundary conditions are varied to obtain a desired system response. This approach is different from the usual analysis approach in which the variations of the boundary conditions are specified and the system response is computed.

Typical applications of optimal control of transient flows are:

1. Changing the outflow at different locations in water supply or oil pipelines without affecting the outflow to other clients.
2. Establishing flow in the conduits of a pumped-storage project in minimum time while switching from generation to pumping mode or vice versa.
3. Opening or closing the control valves in a piping system without violating the upper or lower pressure limits.

4. Closing the wicket gates of hydraulic turbines to minimize pressure and speed rise following load rejection.
5. Accepting or rejecting load on hydraulic turbines in minimum time without exceeding the specified pressure drop or pressure rise.
6. Utilizing the storage capacity of sewer systems by properly operating the control devices to obtain constant outflow for treatment.

To conserve space, computational procedures for determining optimal flow control are not presented herein; interested readers should see Streeter and Wylie [1967] and Streeter [1963 and 1967], Ruus [1966], Driels [1974 and 1975] and Ikeo and Kobori [1975] for problem-oriented procedures, and Ikeo and Kobori [1975] and Bell et al., [1974] for the application of various operations-research techniques.

## 10-6 Case Study

Studies carried out for the analysis of transients in the power conduit of the Jordan River Redevelopment [Portfors and Chaudhry, 1972 and Chaudhry and Portfors, 1972] are presented in this section.

### Design

During the design of this power plant, a number of plant layouts [Forster et al., 1970] were considered, and transient analysis was done by using a computer program [Bell, 1969]. During the construction of the project, questions were raised about the accuracy of the results computed during the design. To verify these results, the author developed another program, the details of which are presented in this section.

The project layout shown in Fig. 3-19 was selected because it was the most economical. In the optimization studies, a waterhammer pressure rise equal to 30 percent of the static head was assumed. However, subsequent studies indicated that substantial savings would result from a reduction in the pressure rise without greatly affecting the plant regulation. Therefore, a 20 percent pressure rise was adopted for the final design.

To keep the maximum transient pressures within the design limits, an upstream surge tank and a PRV were considered. The topography at Jordan River is unsuitable for a surge tank located near the powerhouse, as the cost of a tower-type surge tank would be very high. In addition, computer studies indicated that, with a surge tank more than 1.6 km away from the powerhouse, the plant would not be stable up to its full generating capacity under isolated operation.

In comparison to a surge tank, a PRV operating in synchronous operation with the turbine was found to provide good governing characteristics. The estimated cost of the PRV was about the same as that of a 90-m-high

surge tank. However, the PRV was selected because it alone would meet the operational requirements.

### Mathematical Model

A mathematical model was developed [Portfors and Chaudhry, 1972 and Chaudhry and Portfors, 1972] to analyze the transient conditions in the power conduit of the power plant using the method of characteristics and the following boundary conditions developed for the synchronous operation of the turbine and the PRV. (Boundary conditions for the operation of PRV alone are presented in Section 3-11.)

Let us designate the last section on the penstock adjacent to the turbine as  $(i, n + 1)$ . Then, referring to Fig. 10-10, the continuity equation may be written as

$$Q_{P_{i,n+1}} = Q_{P_{\text{tur}}} + Q_{P_v} \quad (10-39)$$

in which  $Q_{P_{\text{tur}}}$  and  $Q_{P_v}$  are the turbine and PRV discharge at the end of time step. The positive characteristic equation for section  $(i, n + 1)$  is

$$Q_{P_{i,n+1}} = C_p - C_a H_{P_{i,n+1}} \quad (10-40)$$

In terms of net head,  $H_n$ , and the height of tailwater above datum,  $H_{\text{tail}}$ , Eq. 10-40 becomes

$$Q_{P_{i,n+1}} = C_p - C_a \left( H_n - \frac{Q_{P_{i,n+1}}^2}{2gA_i^2} + H_{\text{tail}} \right) \quad (10-41)$$

in which  $A_i$  = cross-sectional area of the penstock at turbine inlet.

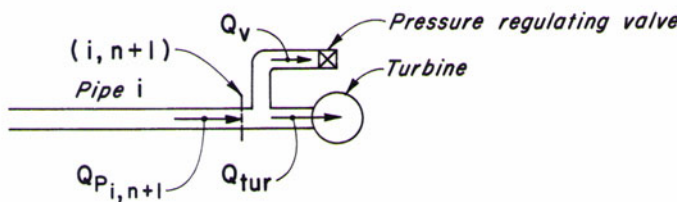


**Fig. 10-10. Schematic of pressure-regulating valve and Francis turbine.**

If the turbine characteristics are used in the analysis as outlined in Section 5-4, then

$$Q_{P_{\text{tur}}} = a_3 + a_2 \sqrt{H_n} \quad (10-42)$$

in which  $a_2$  and  $a_3$  are constants as defined by Eq. 5-3.

The PRV flow

$$Q_{P_v} = Q_r \sqrt{\frac{H_n}{H_r}} \quad (10-43)$$

in which  $Q_r$  and  $Q_{P_v}$  are the PRV discharges, both for valve opening,  $\tau_P$ , under net heads of  $H_r$  and  $H_n$ , respectively; and the subscript  $r$  refers to the rated conditions.

Substituting Eqs. 10-42 and 10-43 into Eq. 10-39, we obtain

$$Q_{P_{i,n+1}} = a_3 + a_4 \sqrt{H_n} \quad (10-44)$$

in which  $a_4 = a_2 + Q_r / \sqrt{H_r}$ .

Elimination of  $H_n$  from Eqs. 10-41 and 10-44 yields

$$a_5 Q_{P_{i,n+1}}^2 + a_6 Q_{P_{i,n+1}} + a_7 = 0 \quad (10-45)$$

in which  $a_5 = C_a [1/(2gA_i^2) - 1/a_4^2]$ ;  $a_6 = 2a_3C_a/a_4^2 - 1$ ; and  $a_7 = C_p - C_a a_3^2/a_4^2$ . Solution of Eq. 10-45 gives

$$Q_{P_{i,n+1}} = \frac{-a_6 - \sqrt{a_6^2 - 4a_5a_7}}{2a_5} \quad (10-46)$$

Now the values of  $H_n$ ,  $Q_{P_{\text{tur}}}$ ,  $Q_{P_v}$ , and  $H_{P_{i,n+1}}$  are determined from Eqs. 10-44, 10-42, and 10-43, and 10-40, respectively.

The iterative procedure of Section 5-6 was used to refine the solution and to determine the turbine speed.

## Results

The transient-state pressures computed by using the preceding mathematical model were compared with those measured on the prototype following 150-MW load rejection. The PRV and the turbine wicket-gate-opening-versus-time curves (Fig. 10-11) recorded during the prototype tests were used in the analysis. The polar moment of inertia of the turbine and generator was taken equal to  $1.81 \times 10^6 \text{ kg m}^2$  to compute the transient-state turbine speed.

A comparison of the computed and measured transient-state pressures at the turbine inlet shows close agreement (Fig. 10-12). However, there is a phase shift, and the measured results show higher dissipation of pressure oscillations than that indicated by the computed results. Probably, the phase shift is caused by incorrect values of the wave velocity, and the difference in the dissipation rate is due to computing the transient-state head losses by using the steady-state friction equation.

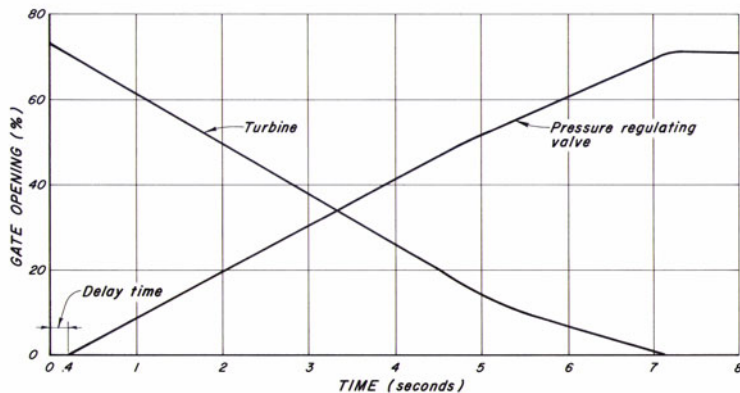


Fig. 10-11. Time history of wicket gates and pressure-regulating valve opening following 150-MW load rejection.

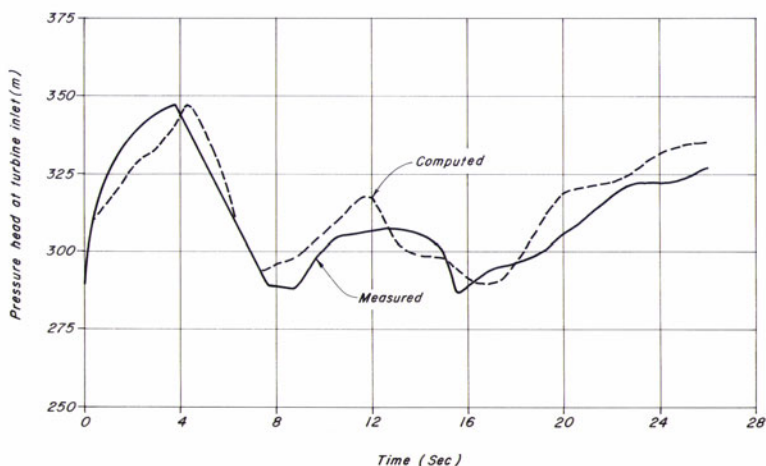


Fig. 10-12. Comparison of computed and measured pressure head at turbine Inlet.

## 10-7 Summary

In this chapter, a number of devices and appurtenances are presented to control the transient conditions in pipelines. A brief description of the operation of these devices is given, and the boundary conditions for these devices are developed. The chapter concludes with a case study.

## Problems

**10-1** Derive the boundary condition for an orifice surge tank. In this tank, an orifice is provided between the pipeline and the surge tank.

**10-2** Develop the boundary conditions for a simple tank and for an air chamber having standpipes between the pipeline and the tank and between the pipeline and the chamber (Figs. 10-13 and 10-14). Include the water in the standpipe as a lumped mass.

**10-3** Write a computer program for the analysis of a piping system having an air chamber as shown in Fig. 10-2. Assume the check valve closes as soon as power fails. The pipeline has a constant-head reservoir at the downstream end.

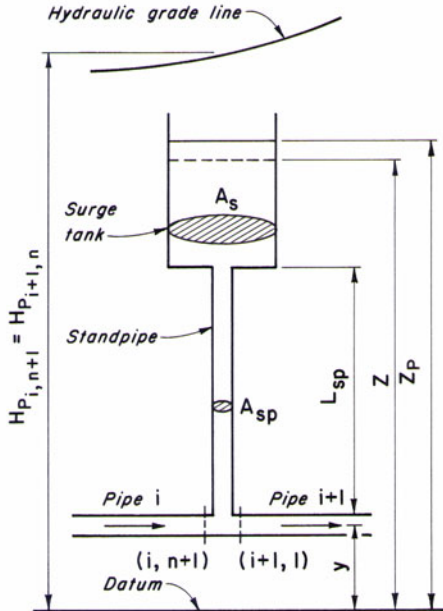
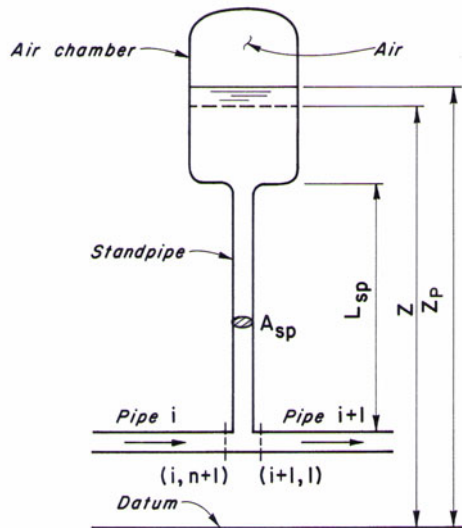


Fig. 10-13. Surge tank with standpipe.



**Fig. 10-14.** Air chamber with standpipe.

**10-4** Prove that an air chamber behaves like a virtual surge tank [Evangelisti, 1969] having cross-sectional area

$$A_s = \frac{1}{m} \frac{\forall_{o_{air}} H_o^{*(1/m)}}{[H_{P_{i,n+1}} + H_b]^{(m+1)/m}}$$

in which the variables are as defined in Section 10-3.

**10-5** Develop the boundary conditions for the centrifugal-pump-PRV system shown in Fig. 10-7. Assume the PRV is discharging into the suction line of the pump. (*Hint:* Equation 10-21 is modified to  $Q_{P_v} = \tau_P Q_o \sqrt{(H_{P_{1,1}} - H_{P_o}) / H_o}$  in which  $H_{P_{1,1}}$ , is the piezometric head on the suction side of the pump, and  $H_o$  = steady-state pumping head.)

**10-6** Develop the boundary conditions for an air-inlet valve that allows outflow of air but not of liquid, from the pipeline when the pressure inside the pipeline exceeds the outside atmospheric pressure. (*Hint:* Use expressions similar to Eqs. 10-37 and 10-38 for the time rate of mass outflow of air through the valve. As the air inflow is assumed positive in Eqs. 10-30 and 10-36,  $dm_a/dt$  for air outflow is considered negative in the corresponding equations.)

## References

- Albertson, M. L. and Andrews, J. S., 1971, "Transients Caused by Air Release," in *Control of Flow in Closed Conduits*, edited by Tullis, J. P., Colorado State University, Fort Collins, CO.
- Allievi, L., 1937, "Air Chamber for Discharge Lines," *Trans.*, Amer. Soc. of Mech. Engrs., vol. 59, Nov., pp. 651-659.
- Angus, R. W., 1937, "Air Chambers and Valves in Relation to Waterhammer," *Trans.*, Amer. Soc. of Mech. Engrs., vol. 59, Nov., pp. 661-668.
- Bell, P. W. W., 1969, "User's Manual for WATHAM," Draft, International Power and Engineering Consultants, Vancouver, Canada.
- Bell, P. W. W., Johnson, G., and Winn, C. B., 1974, "Control Logic for Real Time Control of Flow in Combined Sewers," *Proc., 9th Canadian Symp.*, Water Poll. Res., Canada, pp. 217234.
- Chaudhry, M. H., and Portfors, E. A., 1973, "A Mathematical Model for Analyzing Hydraulic Transients in a Hydro Power Plant," *Proc. First Canadian Hydraulic Conference*, published by the University of Alberta, Edmonton, Alberta, Canada, May, pp. 298-314.
- Combes, G., and Borot, G., 1952, "New Chart for the Calculation of Air Vessels Allowing for Friction Losses," *La Houille Blanche*, pp. 723-729.
- Driels, M., 1974, "Valve Stroking in Separated Pipe Flow," *Jour., Hyd. Div.*, Amer. Soc. of Civ. Engrs., vol. 100, Nov., pp. 1549-1563.
- Driels, M., 1975, "Predicting Optimum Two-Stage Valve Closure," *Paper No. 75-WA/FE-2*, Amer. Soc. of Mech. Engrs., 7 pp.
- Engler, M. L., 1933, "Relief Valves and Air Chambers," *Symposium on Waterhammer*, Amer. Soc. of Mech. Engrs. and Amer. Soc. Civil Engrs., pp. 97-115.
- Evangelisti, G., 1969, "Waterhammer Analysis by the Method of Characteristics," *L' Energia Elettrica*, no. 12, pp. 839-858.
- Evans, W. E. and Crawford, C. C., 1954, "Design Charts for Air Chambers on Pump Lines," *Trans.*, Amer. Soc. of Civil Engrs., vol. 119, pp. 1025-1045.
- Forster, J. W., Kadak, A., and Salmon, G. M., 1970, "Planning of the Jordan River Redevelopment," *Engineering Jour.*, Engineering Inst. of Canada, Oct., pp. 34-43.
- Graze, H. R., 1972, "The imponance of Temperature in Air Chamber Operations," *Proc. First International Conference on Pressure Surges*, British Hydromechanics Research Assoc., England, pp. F2-13-F2-21.
- Graze, H. R., Schübert, J., and Forrest, J. A., 1976, "Analysis of Field Measurements of Air Chamber Installations," *Proc. Second International Conf. on Pressure Surges*, British Hydromechanics Research Association, pp. K2-19-K2-36.
- Ikeo, S. and Kobori, T., 1975, "Waterhammer Caused by Valve Stroking in Pipeline With Two Valves," *Bull.*, Japan Soc. of Mech. Engrs., vol. 18, October, pp. 1151-1157.

- Lescovich, J. E., 1967, "The Control of Water Hammer by Automatic Valves," *Jour. Amer. Water Works Assoc.*, May, pp. 832-844.
- Martin, C. S., 1976, "Entrapped Air in Pipelines," *Proc. Second Conference on Pressure Surges*, British Hydromechanics Research Assoc., England.
- Papadakis, C. N. and Hsu, S. T., 1977, "Transient Analysis of Air Vessels and Air Inlet Valves," *Jour., Fluid Engineering*, Amer. Soc. of Mech. Engrs..
- Portfors, E. A. and Chaudhry, M. H., 1972, "Analysis and Prototype Verification of Hydraulic Transients in Jordan River Power Plant," *Proc. First Conference on Pressure Surges*, British Hydromechanics Research Assoc., England, Sept., pp. E4-57-E4-72.
- Ruus, E., 1966, "Optimum Rate of Closure of Hydraulic Turbine Gates," presented at Amer. Soc. of Mech. Engrs.-Engineering Inst. of Canada Conference, Denver, Colorado, April.
- Ruus, E., 1977, "Charts for Waterhammer in Pipelines with Air Chamber," *Canadian Jour. of Civil Engineering*, vol. 4, no. 3, Sept., pp. 293-313 .
- Streeter, V. L., 1963, "Valve Stroking to Control Water Hammer," *Jour., Hyd. Div.*, Amer. Soc. of Civil Engineers, vol. 89, March, pp. 39-66.
- Streeter, V. L., 1966, *Fluid Mechanics*, 4th edition, McGraw-Hill Book Co., p. 304.
- Streeter, V. L., 1967, "Valve Stroking for Complex Piping Systems," *Jour. Hyd. Div.*, Amer. Soc. of Civ. Engrs., vol. 93, May, pp. 81-98.
- Tucker, D. M. and Young, G. A. J., 1962, "Estimation of the Size of Air Vessels," *Report SP 670*, British Hydromechanics Research Assoc.

### Additional References

- Bechteler, W., 1969, "Surge Tank and Water Hammer Calculations on Digital and Analog Computers," *Water Power*, vol. 21, no. 10, Oct., pp. 386-390.
- Chaudhry, M. H., 1968, "Boundary Conditions for Waterhammer Analysis," *thesis submitted to the Univ. of British Columbia, Vancouver, Canada, in partial fulfillment of the requirements of M.A.Sc.*, April.
- Jacobson, R. S., 1952, "Charts for Analysis of Surge Tanks in Turbine or Pump Installations," *Special Report 104*, Bureau of Reclamation, Denver, Colorado, Feb.
- Kerr, S. L., 1960, "Effect of Valve Operation on Waterhammer," *Jour. Amer. Water Works Assoc.*, vol. 52, Jan.
- Kinno, H., 1968, "Waterhammer Control in Centrifugal Pump Systems," *Jour. Hyd. Div.*, Amer. Soc. of Civ. Engrs., May, pp. 619-639.
- Lindros, E., 1954, "Grand Coulee Model-Pump Investigation of Transient Pressures and Methods for Their Reduction," *Trans.*, Amer. Soc. of Mech. Engrs., p. 775.
- Lundgren, C. W., 1961, "Challs for Determining Size of Surge Suppressors for Pump-Discharge Lines," *Jour. Engineering for Power*, Amer. Soc. of Mech. Engrs., Jan., pp. 43-46.

- Meeks, D. R. and Bradley, M. J., 1970, "The Effect of Differential Throttling on Air Vessel Performance," *Symposium on Pressure Transients*, The City University, London, Nov.
- Parmakian, J., 1950, "Air Inlet Valves for Steel Pipe Lines," *Trans.*, Amer. Soc. of the Civ. Engrs., vol. 115, pp. 438-443.
- Parmakian, J., 1953, "Pressure Surge Control at Tracy Pumping Plant," *Proc.*, Amer. Soc. of Civil Engrs., vol. 79, Separate No. 361, Dec..
- Parmakian, J., 1953, "Pressure Surge at Large Installations," *Trans.*, Amer. Soc. of Mech. Engrs., p.995.
- Parmakian, J., 1958, "One-Way Surge Tanks for Pumping Plants," *Trans.*, Amer. Soc. of Mech. Engrs., pp. 1563-1573.
- Ruus, E. and Chaudhry, M. H., 1969, "Boundary Conditions for Air Chambers and Surge Tanks," *Engineering Jour.*, Engineering Inst. of Canada, , Nov., pp. I-VI.
- Strowger, E. B., 1937, "Relation of Relief Valve and Turbine Characteristics in the Determination of Waterhammer," *Trans.*, Amer. Soc. of Mech. Engrs., vol. 59, Nov., pp. 701-705.
- Whiteman, K. J. and Pearsall, I. S., 1962, "Reflex Valve and Surge Tests at a Pumping Station," *Fluid Handling*, vol. 152, Sept. and Oct., pp. 248-250, 282-286.
- Widmann, R., 1965, "The Interaction Between Waterhammer and Surge Tank Oscillations," *International Symposium on Waterhammer in Pumped Storage Projects*, Amer. Soc. of Mech. Engrs., Chicago Nov., pp. 1-7.
- Wood, D. J., 1970, "Pressure Surge Attenuation Utilizing an Air Chamber," *Jour., Hyd. Div.*, Amer. Soc. of Civil Engrs., vol. 96, May, pp. 1143-1156.

## SURGE TANKS



**Scale model of Vietas surge tank, Swedish Power Authority.** (Courtesy, Swedish Power Board and C. S. Martin [1973].)

## 11-1 Introduction

A *surge tank*, also referred to as a *surge shaft*, *surge chamber*, etc. is an open standpipe or a shaft connected to the conduits of a hydroelectric power plant or to the pipeline of a pumping system. The top of the tank is usually open to the atmosphere. [Figure 11-1](#) shows the schematic of a typical hydropower plant with an upstream surge tank. The conduit between the upstream reservoir and the tank is referred to as a *tunnel* and the conduit between the tank and the turbine is called a *penstock*.

A surge tank reduces the amplitude of pressure fluctuations by reflecting the incoming pressure waves or by storing or providing water, thereby reducing acceleration or deceleration in the tunnel. For example, the waterhammer waves in a penstock produced by the changes in turbine flow ([Fig. 11-1](#)) are reflected back at the surge tank and no transient pressures are transmitted into the tunnel. Due to these reflections, the pressure rise or drop is less than that without a surge tank. Therefore, if there is no surge tank, the tunnel has to be designed to withstand waterhammer pressures.

A surge tank improves the regulation and governing characteristics of a hydraulic turbine. The length of the power conduit for determining the water-starting time (see Section 5-10) is up to the surge tank rather than up to the upstream reservoir. The water-starting time is, therefore, shorter and thus the regulating characteristics of the power plant are improved.

Previous chapters dealt with the analysis of transients by a distributed systems approach which is suitable for rapid transients. However, the oscillations of water level in a surge tank are slow and may thus be computed by using a lumped-system approach. In addition, the stability of these oscillations may be investigated analytically by using the lumped-system approach. This cannot be done by the distributed-system approach.

In this chapter, the analysis of surge-tank oscillations by the lumped-system approach is presented. Various types of surge tanks are first discussed. Differential equations describing the water-level oscillations in simple, orifice, differential, and closed surge tanks are derived, and numerical methods for their solution are discussed. The stability of simple and closed surge tanks by the phase-plane method is presented. The chapter concludes by summarizing the design studies for the Chute-des-Passes surge-tank system.

## 11-2 Types of Surge Tanks

Depending upon the configuration, a surge tank may be classified as *simple*, *orifice*, *differential*, *one-way*, or *closed*. A brief description of each follows.

A *simple surge tank* is an open shaft or standpipe connected to the pipeline with negligible losses at its junction with the pipeline. If an orifice and/or a smaller diameter pipe restricts the entrance to the surge tank, it is called an *orifice tank*. An orifice tank combined with a riser is termed *differential surge*

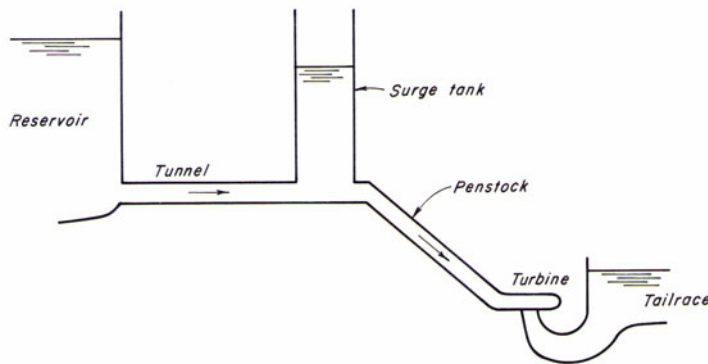


**Fig. 11-1. Schematic of a hydroelectric power plant.**

*tank*. In a *one-way surge tank*, the water flows from the tank into the pipeline only when the pressure in the pipeline drops below the water level in the surge tank. Following the transient conditions, the tank is filled from the pipeline or from another source. A tank with its top closed and with compressed air between the water surface and the top of the tank is called a *closed surge tank*, *air chamber*, a tank with air cushion, etc. A tank may have upper or lower galleries providing additional volume of water or larger cross-sectional area for stability considerations. [Figure 11-2](#) shows a number of typical surge tanks.

If necessary, a combination of different types of surge tanks may be provided in a project. This is usually the case for renovation, rehabilitation or upgrading of existing projects.

### 11-3 Governing Equations

The dynamic and continuity equations describe the oscillations of the water level in a surge tank. The following assumptions are made to simplify the derivation of these equations for analysis by the lumped-system approach:

1. The tunnel walls are rigid, and the water is incompressible. Thus, a flow change at any point in the system is transmitted instantaneously throughout the system, and the water in the tunnel moves like a solid slug.
2. The inertia of the water in the surge tank is negligible as compared to that of the water in the tunnel.
3. The head losses in the system during the transient state may be computed by using the steady-state equations for the corresponding flow velocities.

Because of assumption 1, the flow variables do not vary with distance and are functions of time only. Therefore, there are no spatial derivatives and the resulting equations are ordinary differential equations instead of partial differential equations.

The governing equations for different type of tanks are derived in the following paragraphs.

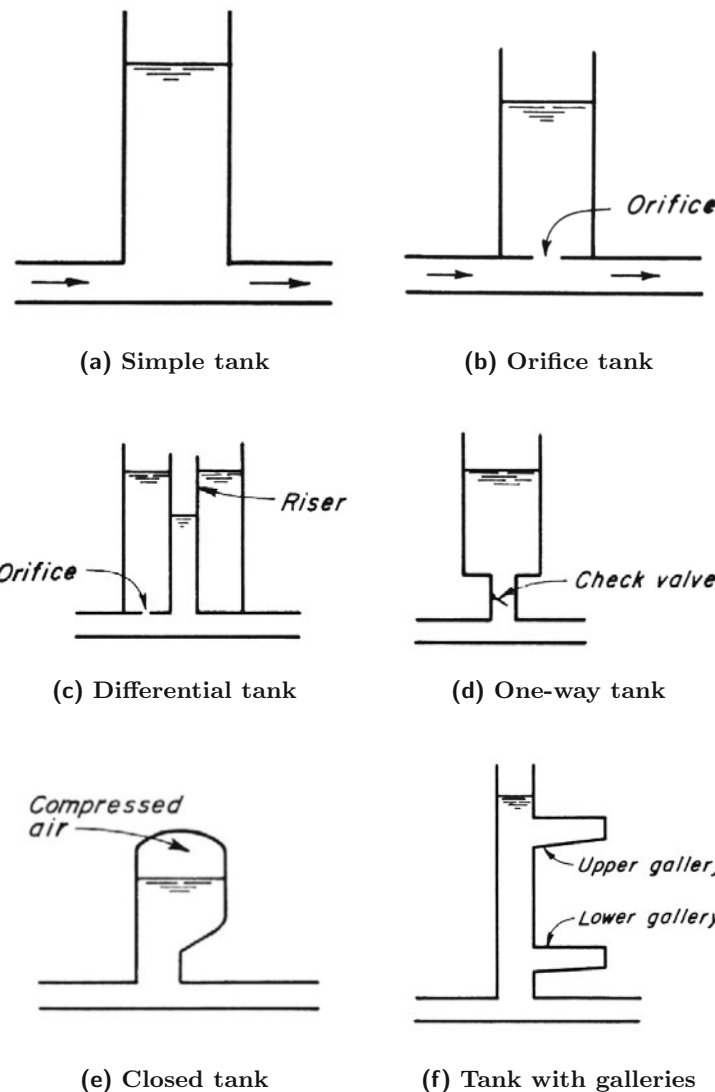


Fig. 11-2. Types of surge tanks.

### Simple Surge Tank

A simple tank is directly connected to the pipeline and the head loss between the tank and the pipeline is negligible.

Figure 11-3a shows a simple, upstream surge-tank with a control valve representing a pump or a hydraulic turbine. A flow change at the valve results in the oscillation of the water level in the tank.

### Dynamic Equation

A freebody diagram of a horizontal tunnel with constant cross-sectional area is shown in Fig. 11-3b. Forces acting on the water in the tunnel are:

$$F_1 = \gamma A_t (H_o - h_v - h_i) \quad (11-1)$$

$$F_2 = \gamma A_t (H_o + z) \quad (11-2)$$

$$F_3 = \gamma A_t h_f \quad (11-3)$$

in which  $A_t$  = cross-sectional area of the tunnel;  $H_o$  = static head;  $\gamma$  = specific weight of liquid;  $h_v$  = velocity head at the intake;  $h_i$  = intake head losses;  $h_f$  = friction and form losses in the tunnel between the intake and the surge tank; and  $z$  = water level in the surge tank above the reservoir level (measured positive upward). Considering the downstream flow direction as positive, the resultant force acting on the water in the positive direction is  $\sum F = F_1 - F_2 - F_3$ . Hence, it follows from Eqs. 11-1 to 11-3 that

$$\sum F = \gamma A_t (-z - h_v - h_i - h_f) \quad (11-4)$$

Now, the mass of the water element is  $\gamma A_t L/g$ , in which  $L$  = length of the tunnel and  $g$  = acceleration due to gravity. If  $Q_t$  is the tunnel flow and  $t$  = time, then

$$\text{Rate of change of momentum of water} = \frac{\gamma A_t L}{g} \frac{d}{dt} \left( \frac{Q_t}{A_t} \right) = \frac{\gamma L}{g} \frac{dQ_t}{dt} \quad (11-5)$$

According to Newton's second law of motion, the rate of change of momentum is equal to the resultant force. Therefore, it follows from Eqs. 11-4 and 11-5 that

$$\frac{\gamma L}{g} \frac{dQ_t}{dt} = \gamma A_t (-z - h_v - h_i - h_f) \quad (11-6)$$

By defining  $h = h_v + h_i + h_f = c Q_t |Q_t|$ , in which  $c$  is a coefficient, Eq. 11-6 may be written as

$$\frac{dQ_t}{dt} = \frac{g A_t}{L} (-z - c Q_t |Q_t|) \quad (11-7)$$

Note that  $h$  is expressed as  $c Q_t |Q_t|$  to account for the reverse flow.

The tunnel in the preceding derivation is horizontal and has constant cross-sectional area throughout its length. It can be shown that Equation 11-7 is also valid for a sloping tunnel (see Problem 11-3) and for a tunnel having  $n$  segments with different cross-sectional areas of various lengths if the term  $A_t/L$  of Eq. 11-7 is replaced by  $\sum_{i=1}^n (A_t/L)_i$  (see Problem 11-5).

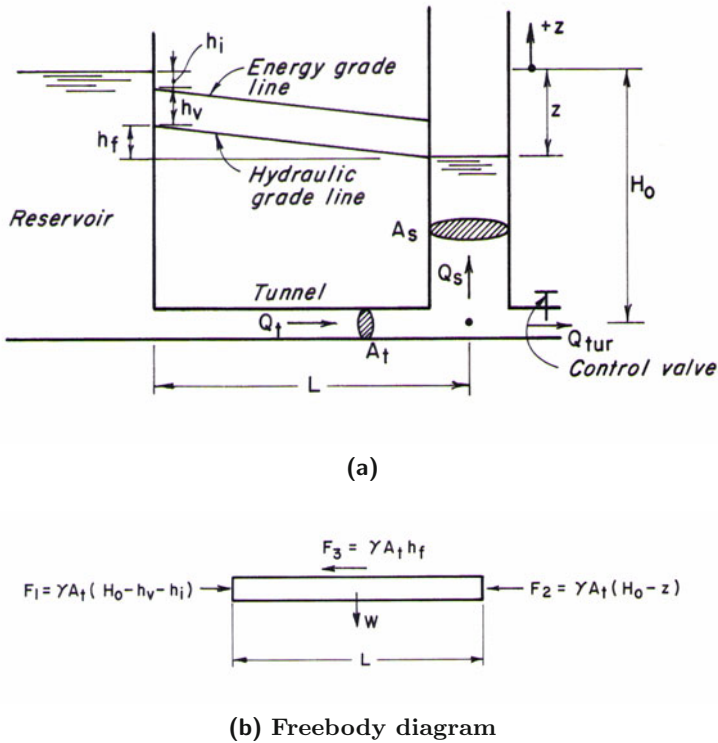


Fig. 11-3. Notation for simple surge tank.

### Continuity Equation

Referring to Fig. 11-3, the continuity equation for the junction of the tunnel and the surge tank may be written as

$$Q_t = Q_s + Q_{tur} \quad (11-8)$$

in which  $Q_s$  = flow into the surge tank (positive into the tank), and  $Q_{tur}$  = turbine flow. Note that Eq. 11-8 is equally valid for a pumping system if the pump flow is designated as  $Q_{tur}$ . Since  $Q_s = A_s (dz/dt)$ , Eq. 11-8 becomes

$$\frac{dz}{dt} = \frac{1}{A_s} (Q_t - Q_{tur}) \quad (11-9)$$

Note that Eqs. 11-7 and 11-9 are valid for an upstream simple surge tank. These equations are valid for a tailrace surge tank (i.e., a tank located downstream of the turbine), if the velocity head,  $h_v$  is properly included.

## Orifice Tank

The orifice of an orifice tank located between the tunnel and the tank (Fig. 11-2b) restricts the flow into or out of an orifice tank. This restriction reduces the amplitude of the water-level oscillations in the tank, develops accelerating or decelerating head on the tunnel more rapidly, and decreases the volume of inflow or outflow from the tank than that for a simple tank. Therefore, the size of tank required for a particular installation is smaller than that for a simple tank. The disadvantages of an orifice tank are: (1) pressure waves are partly reflected back at the tank and partly transmitted into the tunnel which must be considered for tunnel design and (2) the governing of turbines with an orifice tank is inferior to that with a simple surge tank because the accelerating and decelerating heads are developed rapidly following a change in the turbine flow.

## Dynamic Equation

Referring to the freebody diagram of Fig. 11-4b, the following forces are acting on the water in the tunnel

$$F_1 = \gamma A_t (H_o - h_i - h_v) \quad (11-10)$$

$$F_2 = \gamma A_t (H_o + z + h_{\text{orf}}) \quad (11-11)$$

$$F_3 = \gamma A_t h_f \quad (11-12)$$

in which the orifice loss,  $h_{\text{orf}} = c_{\text{orf}} Q_s |Q_s|$ . Considering the downstream direction as positive, the resultant force acting on the water in the tunnel in the positive direction is  $\sum F = F_1 - F_2 - F_3$ . Following Eq. 11-5, the rate of change of momentum of the water in the tunnel is  $(\gamma L/g) (dQ_t/dt)$ . Applying Newton's second law of motion and substituting the expressions for  $F_1$ ,  $F_2$ , and  $F_3$  from Eqs. 11-10 to 11-12, we obtain

$$\frac{\gamma L}{g} \frac{dQ_t}{dt} = \gamma A_t (-z - h_v - h_i - h_f - h_{\text{orf}}) \quad (11-13)$$

By defining  $h = h_v + h_i + h_f = cQ_t |Q_t|$ , substituting expression for  $h_{\text{orf}}$ , and simplifying, Eq. 11-13 becomes

$$\frac{dQ_t}{dt} = \frac{gA_t}{L} (-z - cQ_t |Q_t| - c_{\text{orf}} Q_s |Q_s|) \quad (11-14)$$

in which  $c$  is a coefficient.

The continuity equation for a simple tank (Eq. 11-9) is also valid for an orifice tank.

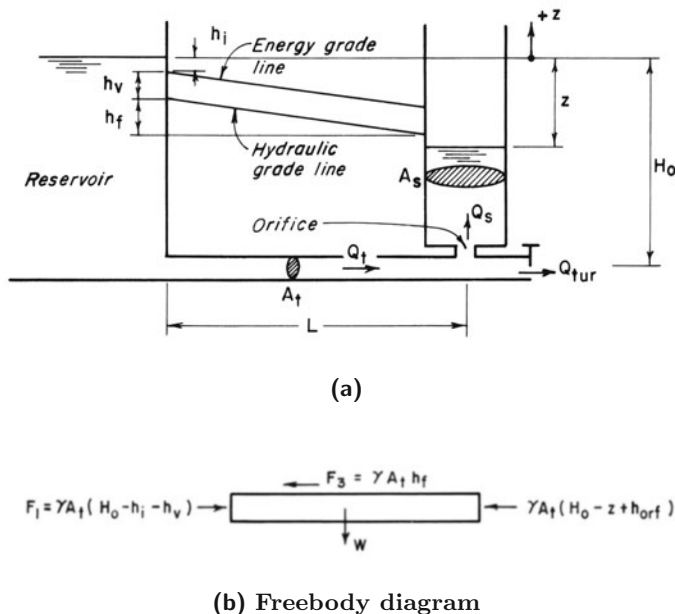


Fig. 11-4. Notation for orifice tank.

### Differential Surge Tank

The riser in a differential tank (Fig. 11-2c) acts like a simple tank while the main tank acts like an orifice tank. Thus, a differential tank is a compromise between a simple tank and an orifice tank. In this tank, following a change in the penstock flow, the accelerating or decelerating head on the tunnel develops slower than that in an orifice tank but faster than in a simple tank. Because of this, the area of the main tank may be smaller as compared to that of an equivalent simple tank, and the regulation characteristics of the turbine are not as adversely affected as that of an orifice tank.

Figure 11-2c shows the schematic of a typical differential tank in which an orifice is provided between the tunnel and the main tank. However, depending upon the topography, the riser and the main tank may not be as close to each other as shown in this figure. The riser may be allowed to spill into the tank. The initial steady state water surface in the riser and in the main tank are at the same level. For load acceptance, the increased water demand is initially provided by the riser. Because of small cross-sectional area, the water level in the riser falls rapidly, thus creating an accelerating head on the tunnel in a short period of time. The water level in the tank, however, falls slowly to supply additional water. Following load rejection, the turbine gates are closed and the water level in the riser rises rapidly to store water. This creates, in a short period of time, a decelerating head on the tunnel and a differential

head on the orifice of the outer tank. The water rejected by the turbine then slowly flows through the orifice into the tank.

### Dynamic and Continuity Equations

Referring to Fig. 11-5 and proceeding similarly as for the simple and orifice tanks, the dynamic equation may be written as

$$\frac{L}{gA_t} \frac{dQ_t}{dt} = -z_r - cQ_t |Q_t| \quad (11-15)$$

in which  $z_r$  = water level in the riser above the reservoir level (positive upwards). The continuity equation at the junction of the tunnel and the tank is

$$Q_t = Q_s + Q_r + Q_{tur} \quad (11-16)$$

in which  $Q_r$  = inflow or outflow from the riser, and  $Q_s$  = inflow or outflow from the main tank.  $Q_s$  depends upon the difference of water levels in the riser and in the tank, and upon the size and characteristics of the orifice at the bottom of the tank, and may be computed from the following equation:

$$Q_s = \pm C_d A_{orf} \sqrt{2g |z_r - z|} \quad (11-17)$$

in which  $C_d$  = coefficient of discharge of the orifice, and  $A_{orf}$  = cross-sectional area of the orifice. If  $z_r > z$ , the flow is into the tank and  $Q_s$  is positive; if  $z_r < z$ , then  $Q_s$  is negative. The coefficient of discharge may have different values for the flow into or out of the tank. In addition, note that it is assumed in Eq. 11-17 that there is no spill from the riser into the tank. However, if water from the riser spills into the tank, then this equation should be modified to take this into account.

For the variation of water level in the riser and in the tank, the following equations are available:

$$A_s \frac{dz}{dt} = Q_s \quad (11-18)$$

and

$$A_r \frac{dz_r}{dt} = Q_t - Q_s - Q_{tur} \quad (11-19)$$

### Closed Surge Tank

As discussed in Chapter 10, closed surge tanks have been used for surge control [Allievi, 1937 and Paramkian, 1963] in pumping plants for about 100 years and are referred to as air chambers, air vessels, air bottles, etc. They have been used as an anti-resonance device in oil pipelines [Lundberg, 1966] and in hydroelectric power plants [Gardner, 1973]. They were used as a surge-control device about 100 yrs ago in small hydro-power plants in the U.S.A,

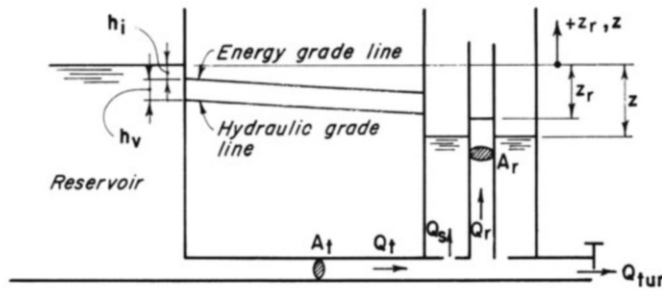


**Fig. 11-5.** Notation for differential tank.

but their use was discontinued because of problems with governing stability [Paramkian, 1981]. These problems were most probably due to the hydraulic governors. Norwegian engineers have used these tanks at several large power plants, which are operating satisfactorily. The U.S. Army Corps of Engineers considered a closed surge tank in the design of Snettisham project [Chaudhry, 1983].

A closed surge tank has the following advantages for application in hydroelectric installations: (1) It may cost less than an ordinary surge tank, e.g., the saving of several million kroners at Driva Power plant, Norway; (2) it can be located near the turbine, thus providing surge-control and improving load-response characteristics of the system; (3) unlike an ordinary surge tank, it can be provided in almost any topographic situation, thus making it attractive for rehabilitation and renovation of old plants; (4) it allows a steeper tunnel slope, which reduces construction costs and provides favorable geological conditions, and (5) in cold climates, it can be protected from freezing more easily than other types of tanks. The main disadvantage of a closed surge tank is that a compressor is needed, which requires maintenance in addition to the initial costs.

Referring to Fig. 11-6 and assuming that the enclosed air expands and contracts according to the polytropic gas equation, we may write the following equations:

### Dynamic Equation

$$\frac{L}{gA_t} \frac{dQ_t}{dt} = z - cQ_t |Q_t| - p \quad (11-20)$$

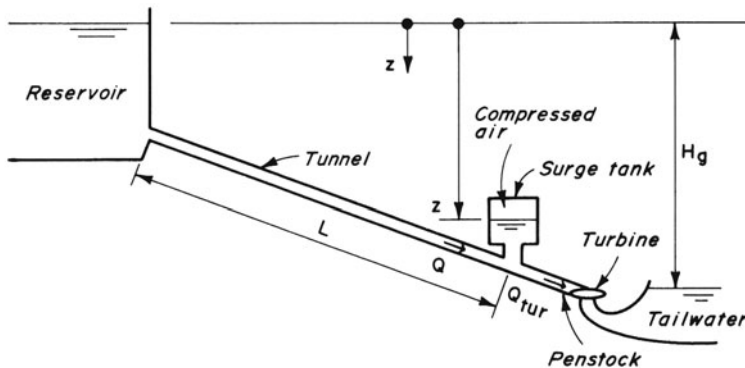


**Fig. 11-6.** Notation for closed surge tank.

### Continuity Equation

$$\frac{dz}{dt} = \frac{1}{A_s} (Q_{tur} - Q_t) \quad (11-21)$$

in which  $Q_t$  = flow in the tunnel;  $z$  = water surface level in the tank below the upstream reservoir, measured positive downwards;  $L$  = tunnel length;  $p$  = gauge pressure of the enclosed air, in m of water;  $c$  = coefficient of head losses in the tunnel; and  $Q_{tur}$  = turbine flow.

For the enclosed air,

$$(p + p_a) \nabla^n = (p_o + p_a) \nabla_o^n \quad (11-22)$$

in which  $p_o$  = atmospheric pressure;  $\nabla$  = volume of the enclosed air;  $n$  = exponent in the polytropic gas equation ( $n$  is 1. and 1.4 for isothermal and adiabatic behavior, respectively) and the subscript  $o$  denotes the initial steady-state values.

## 11-4 Solution of Governing Equations

Since the tunnel walls and the water inside the tunnel are assumed rigid, we do not have spatial derivatives (i.e., variation with respect to  $x$ ) in the dynamic and continuity equations. Therefore, the flow in the tunnel and the water level in the tank vary with respect to time only. Hence, these equations are a set of ordinary differential equations. The dynamic equation is nonlinear because of the term  $cQ_t |Q_t|$ . Also note that the turbine flow may be a function of time.

A closed-form solution of the dynamic and continuity equations is available only for a few special cases [Jaeger, 1961]. Therefore, graphical [Frank and

Schüller, 1938 and Mosonyi, 1957 and 1960] and arithmetical methods suitable for hand computations [Rich, 1963 and Pickford, 1969] were used in the past to integrate these equations or analog simulations [Paynter, 1951] were done. However, with the availability of computers, graphical and arithmetical methods of integration have been superseded by digital computation [MacCracken and Dorn, 1964; Gragg, 1965; Bulirsch and Stoer, 1966 and Chaudhry et al., 1983]. We discuss only these methods herein.

A number of finite-difference techniques are available to solve the dynamic and continuity equations numerically. Although higher-order methods have been used for such analysis, [Bullough and Robbie, 1972; Forrest and Robbie, 1980; Chaudhry et al., 1983 and Chaudhry et al., 1985] the modified Euler method (second-order accurate) may be used with confidence for practical applications [Chaudhry et al., 1983 and 1985] provided computational time interval is short.

## 11-5 Surge Oscillations in Frictionless System

In this section, we develop a closed-form solution of the governing equations for a frictionless system. If the head losses in the system and the velocity head are neglected, then  $c = 0$  and the dynamic equation for a simple tank becomes

$$\frac{dQ_t}{dt} = -\frac{gA_t}{L}z \quad (11-23)$$

Let the initial flow,  $Q_o$ , be instantaneously reduced to zero at  $t = 0$ ; i.e.,  $Q_{tur} = Q_o$  for  $t < 0$ , and  $Q_{tur} = 0$  for  $t \geq 0$ . Therefore, for  $t \geq 0$ , Eq. 11-9 may be written as

$$\frac{dz}{dt} = \frac{1}{A_s}Q_t \quad (11-24)$$

Differentiating Eq. 11-24 with respect to  $t$  and eliminating  $dQ_t/dt$  from the resulting equation and Eq. 11-23, we obtain

$$\frac{d^2z}{dt^2} + \frac{gA_t}{LA_s}z = 0 \quad (11-25)$$

Since the coefficient of  $z$  in Eq. 11-25 is a positive real constant, a general solution of Eq. 11-25 may be written as

$$z = C_1 \cos \sqrt{\frac{gA_t}{LA_s}}t + C_2 \sin \sqrt{\frac{gA_t}{LA_s}}t \quad (11-26)$$

in which arbitrary constants  $C_1$  and  $C_2$  are determined from the initial conditions. At  $t = 0$ ,  $z = 0$  and  $dz/dt = Q_o/A_s$ . Substitution of these conditions into Eq. 11-26 gives

$$C_1 = 0$$

$$C_2 = Q_o \sqrt{\frac{L}{gA_s A_t}} \quad (11-27)$$

Hence, it follows from Eqs. 11-26 and 11-27 that

$$z = Q_o \sqrt{\frac{L}{gA_s A_t}} \sin \sqrt{\frac{gA_t}{LA_s}} t \quad (11-28)$$

Equation 11-28 describes the oscillations of the water surface in the surge tank. The period,  $T$ , and the amplitude,  $Z$ , of these oscillations (Fig. 11-7) are

$$T = 2\pi \sqrt{\frac{L}{gA_s A_t}} \quad (11-29)$$

$$Z = Q_o \sqrt{\frac{L}{gA_s A_t}}$$

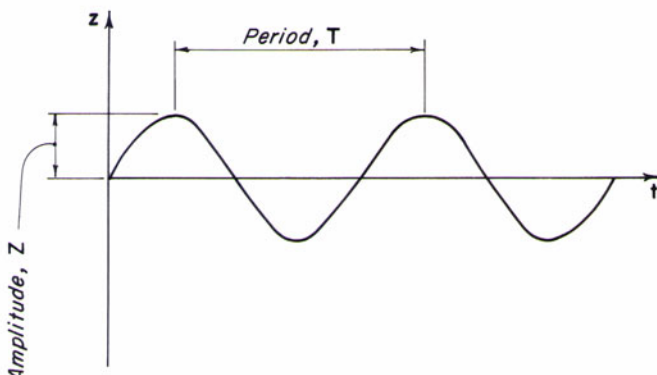


**Fig. 11-7.** Period and amplitude of oscillations of a frictionless system.

## 11-6 Terminology

In this section, a number of terms commonly used in the surge-tank literature are defined.

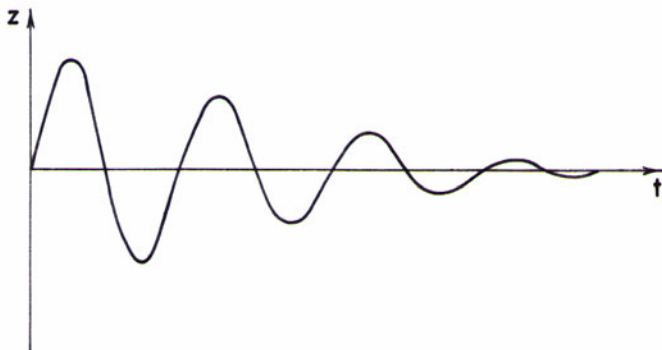
The water level in the surge tank (Fig. 11-3) begins to oscillate following a change in the turbine flow. The amplitude of these oscillations may increase or decrease in time depending upon the system parameters and the magnitude and time variation of the flow change. The oscillations are said to be *stable* if they dampen to the final steady state in a reasonable time and *unstable* if their magnitude increases with time (see Fig. 11-8).

Surge tanks are designed so that the oscillations are stable and the tank does not drain. Tank drainage may be explained as follows: Following a large load increase, tunnel flow does not accelerate fast enough to meet the turbine demand. Therefore, water flows out of the surge tank to make the shortfall and the tank water level continues to fall until the tank drains. This condition usually occurs if the tunnel losses are large.

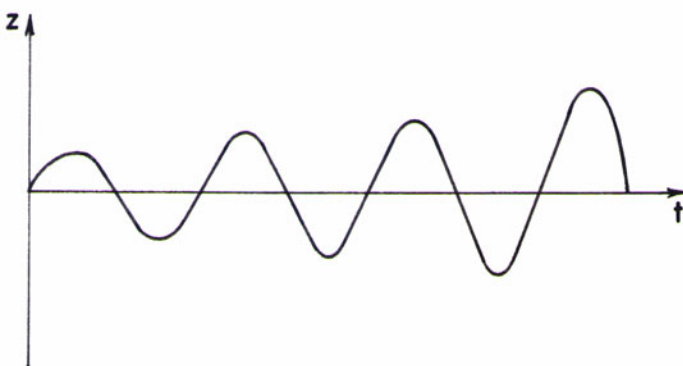
## Turbine Flow

For the analysis of water level oscillations in a surge tank, the variation of turbine flow may be classified into the following four *cases* (Fig. 11-9). The abscissa of this figure is the normalized flow,  $q$ , and the ordinate is the normalized tank water level,  $y$ . The initial steady state discharge,  $Q_o$ , and the amplitude,  $Z$ , of the water-level oscillations in a frictionless system are used as reference values to normalize, i.e.,  $q = Q/Q_o$  and  $y = z/Z$ .

1. *Constant Flow.* In this case, the turbine flow changes from one steady-state discharge,  $Q_1$ , to another steady-state discharge,  $Q_2$ . Since the turbine flow depends upon the surge-tank level, the assumption of constant turbine flow is valid only on very high-head installations where the water-level oscillations in the surge tank may be considered as small as compared to the static head.
2. *Constant-Gate Opening.* For turbine flow, the wicket-gate opening may be assumed constant when the plant is under manual control or under blocked-gate operation when the governor is inoperative or the turbine gates are opened to their maximum position to maintain constant power.
3. *Constant Power.* In this case, it is assumed that an ideal governor maintains constant power input to the turbine (or constant turbine output if the turbine efficiency is considered constant). To meet the increased demand in turbine flow following a load increase, the governor opens the wicket gates. As a result, the water level in the surge tank is lowered which reduces the net head on the turbine. Therefore, the governor opens the gates further to keep the power constant. No restriction on the turbine-gate opening is assumed, which implies that the turbine discharge can be increased to any required amount to maintain constant power. Thus, it is clear the corrective action of the governor is destabilizing and the system may become unstable.
4. *Constant Power Combined with Maximum Gate Opening.* In Case 3, we assumed that the turbine gates can be opened to any value to maintain constant power. On actual power plants, however, gates cannot be opened



(a) Stable oscillations



(b) Unstable oscillations

**Fig. 11-8.** Stable and unstable oscillations.

to more than their fully open position. Therefore, the governor maintains constant power if the net head on the turbine is more than or equal to the rated head. When the net head is less than the rated head, the case of constant-gate opening applies. Note that for the net heads less than the rated head, the turbine power output decreases as the water level in the surge-tank is lowered. As a result, the system frequency decreases if the plant is isolated. Usually the load is tripped if the system frequency drops below a specified value. In our analysis, however, we are assuming that the load is not tripped, and the turbine keeps on generating power irrespective of the system frequency.

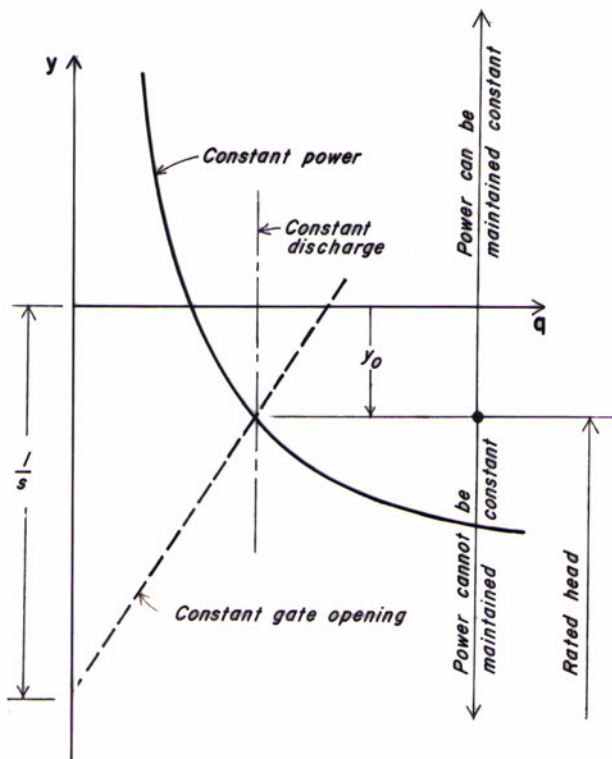


Fig. 11-9. Normalized turbine flow demand.

### Stability

By integrating Eqs. 11-7 and 11-9 graphically, Frank and Schüller [1938] showed that the oscillations are always stable in Case 2 and are stable in Case 1 if the tunnel friction losses are taken into consideration. Case 3 has been studied by a number of investigators: Thoma [1910] linearized the governing differential equations and demonstrated that the oscillations are unstable if the tank area is less than a minimum. This minimum area is called the Thoma area,  $A_{th}$ , [Jaeger, 1960]. Paynter [1949, 1951 and 1953] solved the equations analytically and on an analog computer and presented a stability diagram. Using the phase-plane method, Cunningham and Li [1958]; Marris [1959 and 1961] and Sideriades [1960 and 1962] demonstrated that the Thoma stability criterion does not hold for large oscillations. Ruus [1969] analyzed Case 4 on a digital computer and showed that small, rather than large, oscillations are critical for the stability of a tank. Chaudhry and Ruus [1971] investigated

the stability for all four cases by the phase-plane method and showed that the oscillations are stable, large or small, if the Thoma criterion is satisfied, especially for Case 4 which resemble real-life situations better than the other three cases. To conserve space, a summary of these studies is presented here; for details, see Chaudhry and Ruus [1971]. A number of quantitative results are obtained from the analysis of the singularities, and a number of phase portraits are presented to show the effect of the changes in different parameters on the qualitative behavior of the system.

## 11-7 Normalization of Equations

To normalize the governing equations (Eqs. 11-7 and 11-9) and to reduce the number of parameters, the initial steady state flow,  $Q_o$ , amplitude,  $Z$ , and period  $T$  of the oscillations of a frictionless, simple surge tank are used as reference values as follows:

$$\begin{aligned} y &= z/Z \\ x &= Q_t/Q_o \\ q &= Q_{tur}/Q_o \\ \tau &= 2\pi t/T \end{aligned} \tag{11-30}$$

By substituting these variables into Eqs. 11-7 and 11-9 and simplifying the resulting equations, we obtain

$$\frac{dy}{d\tau} = x - q \tag{11-31}$$

$$\frac{dx}{d\tau} = -y - \frac{1}{2}Rx^2 \tag{11-32}$$

in which  $R = 2h_{f_o}/Z = 2cQ_o^2/Z$ ; and  $h_{f_o}$  = tunnel head loss corresponding to flow  $Q_o$ .

## 11-8 Phase-Plane Method

To facilitate discussion, a summary of the method follows; for a detailed description of the method, see Cunningham [1958].

Let us consider a system described by the following differential equations

$$\frac{dx}{d\tau} = P(x, y) \tag{11-33}$$

and

$$\frac{dy}{d\tau} = Q(x, y) \tag{11-34}$$

in which the functions  $P(x, y)$  and/or  $Q(x, y)$  may be nonlinear. By dividing Eq. 11-34 by Eq. 11-33, we obtain

$$\frac{dy}{dx} = \frac{Q(x, y)}{P(x, y)} \quad (11-35)$$

The points  $(x_s, y_s)$  for which  $dy/dx = 0/0$  are called *singular points* or *singularities*. The location of these points, which are equilibrium points for the system, is obtained by simultaneously solving the equations  $P(x, y) = 0$ , and  $Q(x, y) = 0$ . The type of a particular singularity determines whether the system is stable or unstable at that equilibrium point. This may be done by substituting  $x = x_s + u$  and  $y = y_s + v$  into Eq. 11-35, which after simplification yields

$$\frac{dv}{du} = \frac{Q(x_s, y_s) + c'u + d'v + c''u^2 + d''v^2}{P(x_s, y_s) + a'u + b'v + a''u^2 + b''v^2} \quad (11-36)$$

in which  $a'$ ,  $a''$ ,  $b'$ ,  $b''$ ,  $c'$ ,  $c''$ ,  $d'$ , and  $d''$  are real constants. If both the linear and higher-power terms in  $u$  and  $v$  are present in the denominator and in the numerator, the singularity is called a *simple* singularity. For such a singularity, the higher-power terms can be neglected because their effect on the solution in the neighborhood of the singularity is small compared to that of the linear terms. However, if the linear terms are missing, the singularity is *non-simple*, and the higher-power terms cannot be neglected.

To study the properties of the solution in the neighborhood of a simple singularity, the higher-order terms of Eq. 11-36 are neglected. Thus, this equation may be written as

$$\frac{dv}{du} = \frac{c'u + d'v}{a'u + b'v} \quad (11-37)$$

The characteristic roots,  $\lambda_1$  and  $\lambda_2$ , of the two equations equivalent to the above equation, i.e.,

$$\frac{dv}{dt} = c'u + d'v \quad (11-38)$$

and

$$\frac{du}{dt} = a'u + b'v \quad (11-39)$$

are

$$\lambda_1, \lambda_2 = \frac{1}{2} \left[ (a' + d') \pm \sqrt{(a' + d')^2 + 4(b'c' - a'd')} \right] \quad (11-40)$$

The roots,  $\lambda_1$  and  $\lambda_2$ , determine the type of a singularity, as follows:

*Node*, if both roots are real and have the same sign;

*Saddle*, if both roots are real and have the opposite signs;

*Vortex*, if both roots are imaginary; and

*Focus*, if the roots are complex conjugates.

The node and focus are called *stable* if the real part of the roots is negative; and the singularity is *unstable* if the real part is positive. Note that Eqs. 11-37 through 11-40 are valid only for simple singularities.

## 11-9 Stability of Simple Tank

The stability of a simple surge tank is investigated in this section for different cases of turbine flow by using the phase-plane method [Cunningham, 1958; Marris, 1959 and 1961; Sideriades, 1962 and Chaudhry and Ruus, 1971]. Typical phase portraits are plotted by the method of isolines [Cunningham, 1958 and Chaudhry and Ruus, 1971].

### Constant-Gate Opening

A general head-discharge relationship for a reaction turbine running at constant speed is not available. However, as an approximation, the relationship between the net head and turbine discharge at constant gate opening may be assumed as linear, as shown by the turbine characteristics [Krueger, 1966]. To simplify the analysis, the head-discharge relationship is assumed as shown in Fig. 11-9. Then, the equation for the flow through a reaction turbine may be written as

$$q = b(1 + sy) \quad (11-41)$$

in which  $b = 1/(1 - k)$ ;  $s = Z/H_o$ ;  $k = h_{f_o}/H_o$ ; and  $H_o$  = static head.

From Eqs. 11-31, 11-32, and 11-41, it follows that

$$\frac{dy}{dx} = \frac{x - b(1 + sy)}{-y - \frac{1}{2}Rx^2} \quad (11-42)$$

The coordinates of the singular points are determined by solving simultaneously

$$x - b(1 + sy) = 0 \quad (11-43)$$

and

$$-\frac{1}{2}Rx^2 - y = 0 \quad (11-44)$$

The solution of these two equations give the coordinates of two singular points:  $(1, -\frac{1}{2}R)$  and  $[-1/k, -1/(ks)]$ . The second singular point is virtual because Eqs. 11-31 and 11-32 are valid only for  $x > 0$ . A singular point is *virtual* if it does not lie in the region in which the governing equations are valid. The effect of a virtual singular point on the stability of the system depends upon its distance from the stable singularities.

Let us consider each of these singular points one by one.

#### **Singularity $(1, -\frac{1}{2}R)$**

By substituting  $x = 1 + u$  and  $y = -\frac{1}{2}R + v$  into Eq. 11-42, and following the procedure outlined previously for determining the type of a singular point, the following equation is obtained:

$$\frac{dv}{du} = \frac{u - bsv}{-Ru - v} \quad (11-45)$$

Comparison of Eqs. 11-45 and 11-37 yields  $a' = -R$ ;  $b' = -1$ ;  $c' = 1$ ; and  $d' = -bs$ . Thus,

$$\lambda_1, \lambda_2 = \frac{1}{2} \left[ -(R + bs) \pm \sqrt{(R + bs)^2 - 4(1 + Rbs)} \right] \quad (11-46)$$

Since  $R$ ,  $b$ , and  $s$  are all positive constants, both roots are real and negative if  $(R + bs)^2 > 4(1 + Rbs)$ , i.e.,  $|R - bs| > 2$ . The roots are complex conjugates with negative real part if  $|R - bs| < 2$ . In the former case, the singular point is a *stable node*; in the latter, it is a *stable focus*.

Note that the singular point is a *stable node* for  $|bs| > 2$ , and a *stable focus* for  $|bs| < 2$ , even if the flow is considered frictionless, i.e.,  $R = 0$ . This is because of the damping effect of the turbine gates being held in a fixed position.

### *Singularity* $[-1/k, -1/(ks)]$

Substitution of  $x = -(1/k) + u$ , and  $y = -1/(ks) + v$  into Eq. 11-42 results in

$$\frac{dv}{du} = \frac{u - bsv}{(R/k)u - v} \quad (11-47)$$

Comparison of Eqs. 11-47 and 11-37 yields  $a' = R/k$ ;  $b'd' = -bs$ . Hence,

$$\lambda_1, \lambda_2 = \frac{1}{2} \left[ \left( \frac{R}{k} - bs \right) \pm \sqrt{\left( \frac{R}{k} - bs \right)^2 + 4 \left( -1 + \frac{Rbs}{k} \right)} \right] \quad (11-48)$$

which upon simplification becomes

$$\lambda_1, \lambda_2 = \frac{1}{2} \left[ \left( \frac{R}{k} - bs \right) \pm \sqrt{\left( \frac{R}{k} - bs \right)^2 + 4(2b - 1)} \right] \quad (11-49)$$

Since  $2b > 1$ , both roots are real with opposite signs. Hence, the singularity is a *saddle*. It is a *virtual singularity* because Eqs. 11-31 and 11-32 are not valid for  $x < 0$ . The effect of this singular point on the stability of oscillations depends upon its location. For small friction losses,  $1/k$  and  $1/(ks)$  are large quantities, and thus the point lies far away from the stable singular point  $(1, -\frac{1}{2}R)$ . Hence, its destabilizing effect is negligible. For large friction losses, however, this virtual singularity affects the stability of the system because of its proximity to the stable singularity  $(1, -\frac{1}{2}R)$ . For a frictionless flow, the singular point  $[-1/k, -1/(ks)]$  lies at an infinite distance from the origin and thus has no destabilizing effect on the system.

## Constant Power

In this case, an “ideal governor” is assumed to ensure constant power input to the turbine. It is clear from Fig. 11-9 that, as the water level in the tank drops, the governor has to open the gates to increase the discharge for maintaining constant power. No restriction on turbine-gate opening is assumed, which implies that the turbine discharge can be increased to any required amount to maintain constant power.

Assuming constant turbine efficiency and neglecting penstock friction losses, for constant power,

$$Q_{tur} (H_o + z) = Q_o (H_o - h_{f_o}) \quad (11-50)$$

It follows from Eq. 11-50 that

$$q = \frac{Q_{tur}}{Q_o} = \frac{H_o - h_{f_o}}{H_o + z} \quad (11-51)$$

which upon simplification becomes

$$q = \frac{1 - k}{1 + sy} \quad (11-52)$$

in which  $k$  and  $s$  have the same meaning as defined previously. By substituting Eq. 11-52 into Eq. 11-31, dividing the resulting equation by Eq. 11-32 and simplifying,

$$\frac{dy}{dx} = \frac{x + sxy - 1 + k}{-sy^2 - (1 + kx^2)y - \frac{1}{2}Rx^2} \quad (11-53)$$

To determine the coordinates of the singular points, the following two equations are solved simultaneously:

$$x + sxy - 1 + k = 0 \quad (11-54)$$

$$sy^2 + (1 + kx^2)y + \frac{1}{2}Rx^2 = 0 \quad (11-55)$$

which gives the coordinates of the following three singular points:  $(1, -\frac{1}{2}R)$ ;  $[-\frac{1}{2} + c_1, -\frac{1}{2}R(c_2 - c_1)]$ ; and  $[-\frac{1}{2} - c_1, -\frac{1}{2}R(c_2 + c_1)]$  in which  $c_1 = \sqrt{(1/k) - \frac{3}{4}}$ , and  $c_2 = (1/k) - \frac{1}{2}$ .

By substituting  $x = x_s + u$  and  $y = y_s + v$  into Eq. 11-53, and neglecting the terms in  $u$  and  $v$  of power higher than one, we obtain

$$\frac{dv}{du} = \frac{(1 + sy_s)u + sx_sv}{-(R + 2ky_s)x_su - (kx_s^2 + 2sy_s + 1)v} \quad (11-56)$$

Comparison of Eqs. 11-37 and 11-56 yields

$$\begin{aligned} a' &= -(R + 2ky_s)x_s \\ b' &= -(kx_s^2 + 2sy_s + 1) \\ c' &= (1 + sy_s) \\ d' &= sx_s. \end{aligned} \quad (11-57)$$

**Singularity  $(1, -\frac{1}{2}R)$** 

Substituting  $x_s = 1$  and  $y_s = -\frac{1}{2}R$  into Eq. 11-57, noting that  $k = \frac{1}{2}Rs$ , and simplifying, we obtain:  $a' = R(k-1)$ ;  $b' = k-1$ ;  $c' = 1-k$ ; and  $d' = s$ . Hence,

$$\begin{aligned}\lambda_1, \lambda_2 &= \frac{1}{2} \left\{ R(k-1) + s \right. \\ &\quad \left. \pm \sqrt{[R(k-1) + s]^2 + 4[-(k-1)^2 - sR(k-1)]} \right\} \quad (11-58)\end{aligned}$$

or

$$\lambda_1, \lambda_2 = \frac{1}{2} \left[ R(k-1) + s \pm \sqrt{D_1} \right] \quad (11-59)$$

in which  $D_1 = [R(k-1) + s]^2 + 4[2k(1-k) - (k-1)^2]$ . If  $2k(1-k) - (k-1)^2 > 0$  (i.e.,  $k > \frac{1}{3}$ ), then the singularity is a *saddle* (Fig. 11-12c). For  $k < \frac{1}{3}$ , the singularity is a node if  $D_1 > 0$ , and a spiral if  $D_1 < 0$ . The node or spiral is stable if  $R(k-1) + s < 0$ . For small friction, this inequality takes the form  $s < R$ , or  $2h_{f_o}H_o > Z^2$ . The following expression for the Thoma area,  $A_{th}$ , may be obtained from  $s = R$ :

$$A_{th} = \frac{L}{2cgA_t H_o} \quad (11-60)$$

If  $2h_{f_o}H_o < Z^2$ , the singularity is unstable (Fig. 11-10b).

**Singularity  $[c_1 - \frac{1}{2}, -\frac{1}{2}R(c_2 - c_1)]$** 

Substitution of the coordinates of the singularity into Eq. 11-57 and simplification of the resulting expressions give:  $a' = -R(1-k)$ ;  $b' = -k(\frac{1}{2} + c_1)$ ;  $c' = k(\frac{1}{2} + c_1)$ ; and  $d' = s(c_1 - \frac{1}{2})$ . Hence,

$$\lambda_1, \lambda_2 = \frac{1}{2} \left[ -R(1-k) + s \left( c_1 - \frac{1}{2} \right) \pm \sqrt{D_2} \right] \quad (11-61)$$

in which

$$D_2 = \left[ -R(1-k) + s(c_1 - \frac{1}{2}) \right]^2 + 4 \left[ -k^2 \left( c_1 + \frac{1}{2} \right)^2 + 2k(1-k) \left( c_1 - \frac{1}{2} \right) \right].$$

The singularity is a *saddle* if  $2k(1-k)(c_1 - \frac{1}{2}) > k^2(c_1 + \frac{1}{2})^2$ , which reduces to  $k < \frac{1}{3}$  (Fig. 11-10b). Note that for  $k = \frac{1}{3}$ , this singularity shifts to the previous singular point at  $(1, -\frac{1}{2}R)$ . For  $k > \frac{1}{3}$ , the singular point is a *node* if  $D_2 > 0$ , and a *focus* if  $D_2 < 0$ ; they are stable if  $R(1-k) > s(c_1 - \frac{1}{2})$ , and unstable if  $R(1-k) < s(c_1 - \frac{1}{2})$ .

It is clear from Fig. 11-12c that all trajectories emanating from inside the separatrix (i.e., point corresponding to the initial conditions lies inside the separatrix on the phase portrait) reach the stable node. However, for initial conditions such that the corresponding point on the phase portrait lies outside the separatrix, the tank *drains*.

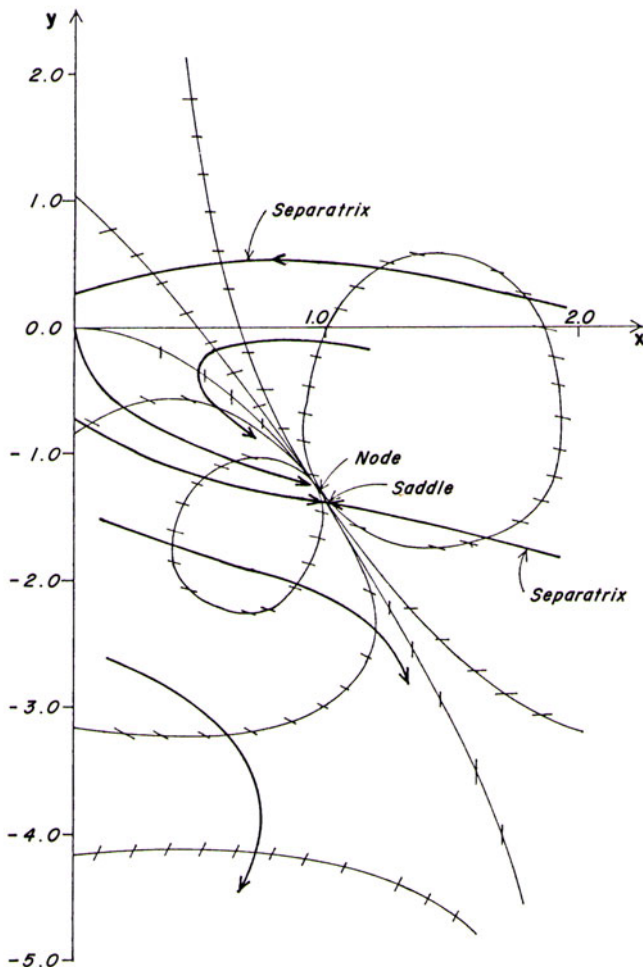
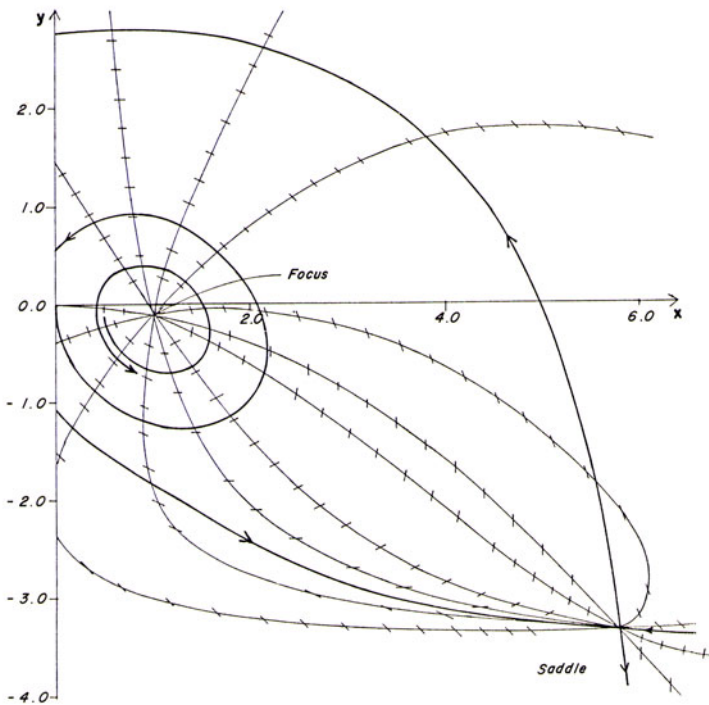
(a)  $k = 0.35, R = 2.8$ 

Fig. 11-10. Phase portrait for constant power.

$$\text{Singularity } \left[ \left( -c_1 - \frac{1}{2} \right), -\frac{1}{2}R(c_2 + c_1) \right]$$

Because Eqs. 11-31 and 11-32 are not valid for  $x < 0$ , the singularity is virtual. By substituting the coordinates of the singularity into Eq. 11-57, we obtain  $a' = R(k - 1)$ ;  $b' = -k\left(\frac{1}{2} - c_1\right)$ ;  $c' = k\left(\frac{1}{2} - c_l\right)$ ; and  $d' = -s\left(c_1 + \frac{1}{2}\right)$ . Hence,

$$\lambda_1, \lambda_2 = \frac{1}{2} \left[ -R(1 - k) - s \left( \frac{1}{2} + c_1 \right) \pm \sqrt{D_3} \right] \quad (11-62)$$

(b)  $k = 0.025, R = 0.2$ **Fig. 11-10.** (*Continued*)

in which

$$D_3 = [R(1 - k) + s \left(\frac{1}{2} + c_1\right)]^2 - 4 \left[k^2 \left(\frac{1}{2} - c_1\right)^2 + 2k(1 - k) \left(\frac{1}{2} + c_1\right)\right].$$

Since  $0 \leq k < 1$ ,  $s > 0$ , and  $R > 0$ , both roots are real and negative if  $D_3 > 0$ , and complex conjugates with negative real part if  $D_3 < 0$ . In the former case, the singularity is a *stable node*; in the latter, a *stable focus*.

### Constant Power Combined With Constant-Gate Opening

In the previous section, it was assumed that the turbine gates can be opened to any value to provide required flow to maintain constant power. On an actual project, however, the gates cannot be opened beyond their fully open position. Therefore, increasing the discharge to maintain constant power as the water level in the surge tank falls is limited.

Referring to Fig. 11-9, for a net head greater than the rated head (i.e., for  $y > -y_o$ , in which  $y_o$  = final steady-state water level in the tank), the governor operates the gates in such a manner that the turbine discharge corresponds

to the constant power. For heads less than the rated head, i.e., for  $y < -y_o$ , the governor keeps the gate open at the maximum value, and the turbine flow is equal to the discharge through the maximum gate opening under this head (Fig. 11-9). The flow in this case is less than that required for constant power. Thus, power output cannot be maintained constant for  $y < -y_o$ , and the oscillations for this condition should be analyzed considering the gate opening as constant at the fully open position.

For this combined governing case, the phase plane is divided into two regions: (1) constant power region for  $y > -y_o$ , and (2) constant-gate-opening region for  $y < -y_o$ . There are five singular points: two each in the constant-gate and in the constant-power regions and one common to both the constant-gate and constant-power regions. The latter, located at  $(1, -\frac{1}{2}R)$ , is called a *compound singularity*. To facilitate discussion, all the singular points for constant-gate opening and constant power are listed in Table 11-1.

For  $k < \frac{1}{3}$ , there is only one real singular point at  $(1, -\frac{1}{2}R)$ , hereafter called the *first singularity*. This is a compound singular point: for  $y < -y_o$  (region of maximum gate opening), it is always stable; for  $y > -y_o$  (region of constant power), it may be stable or unstable whether the Thoma criterion is satisfied or not. Thus, if the Thoma criterion is satisfied, the oscillations are stable *whether they are large or small*. If the tank area is less than the Thoma area, the oscillations may be stable, unstable, or of constant magnitude (called the *limit cycle* in phase-plane terminology) depending upon the stabilizing action of the constant gate opening and the point from which the trajectory emanates, i.e., the starting point on the phase portrait corresponding to the initial conditions. The trajectories emanating inside the limit cycle are unstable, and their amplitude increases until it is equal to that of the limit cycle. The oscillations outside the limit cycle are stable and their amplitude decreases until it is equal to that of the limit cycle.

For  $k > \frac{1}{3}$ , the second singularity becomes real and is either a stable or an unstable *node* or *focus*, while the first singularity is a *saddle*. Since such a high value of friction loss is not economical, this case is usually of little practical importance. Phase portraits for  $k = 0.35$  and  $R = 2.8$ , and  $k = 0.025$  and  $R = 0.2$  are presented in Fig. 11-11. Oscillations in the latter case are unstable (Fig. 11-10b) according to Paynter's stability diagram [1951], if it is assumed that the constant power is always maintained. If, however, it is considered that the governor can open the gates up to a maximum limit, and then the gates remain fully open as long as  $y < -y_o$ , then the oscillations are stable, as shown in Fig. 11-11a.

## 11-10 Stability of Closed Surge Tank

By assuming small perturbations and an ideal governor that always maintains constant power (i.e., the wicket-gate opening may become infinite if necessary), Svee [1972] developed the following equation for the critical area,

$A_{cr}$  for the stability of a closed surge tank:

$$A_{cr} = A_{th} \left( 1 + \frac{np_o}{a_o} \right) \quad (11-63)$$

in which

$$A_{th} = \frac{Q_o^2 L}{2gA_t h_{f_o} (H_g - h_{f_o})} \quad (11-64)$$

and  $a_o$  = distance between the roof of the tank and the initial steady-state tank water level. Replacing  $a_o = -\nabla_o/A_{cr}$  in Eq. 11-63 and solving for  $A_{cr}$ , one obtains

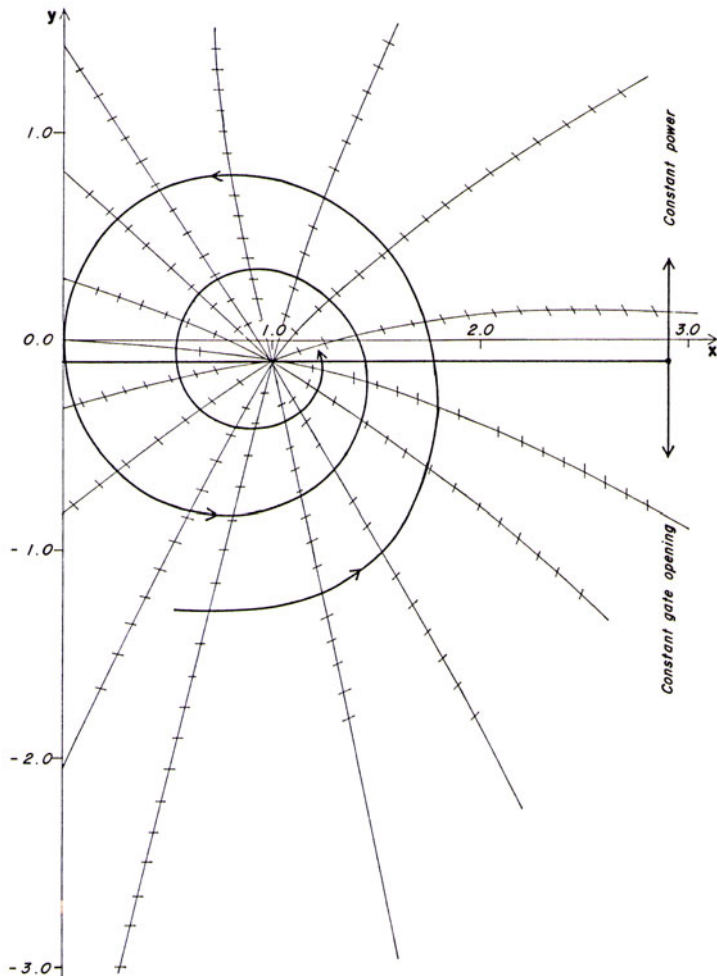
$$A_{cr} = \frac{1}{\frac{1}{A_{th}} - \frac{np_o}{\nabla_o}} \quad (11-65)$$

It is clear from this equation that for an open surge tank, with  $p_o = 0$ ,  $A_{cr} = A_{th}$ . In addition, this equation shows that the range of air pressure and air volume for a particular surge-tank installation is limited; i.e.,  $\nabla_o < np_o A_{th}$  yields a negative value for  $A_{cr}$ .

**Table 11-1. Characteristics of singular points**

| Coordinates of Singularity  | Type     | Stable or<br>Unstable | Required<br>Conditions            | Miscellaneous |
|---|----------|-----------------------|-----------------------------------|---------------|
| <i>Constant gate opening (<math>y &lt; -\frac{1}{2}R</math>):</i> |          |                       |                                   |               |
| (1, $-\frac{1}{2}R$ )   | Node     | Stable                | $ R - bs  > 2$                    | Real          |
|   | Focus    | Stable                | $ R - bs  < 2$                    | Real          |
| ( $-1/k$ , $-1/ks$ )  | Saddle   | —                     | Always                            | Virtual       |
| <i>Constant power (<math>y &gt; -\frac{1}{2}R</math>):</i>        |          |                       |                                   |               |
| (1, $-\frac{1}{2}R$ )   | Saddle   | —                     | $k > \frac{1}{3}$                 | Real          |
|   | Node     | —                     | $k < \frac{1}{3}$ , and $D_1 > 0$ | Real          |
|   | Stable   | —                     | $R(k - 1) + s < 0$                |               |
|   | Unstable | —                     | $R(k - 1) + s > 0$                |               |
|   | Focus    | —                     | $k < \frac{1}{3}$ , and $D_1 < 0$ | Real          |
|   | Stable   | —                     | $R(k - 1) + s < 0$                |               |
|   | Unstable | —                     | $R(k - 1) + s > 0$                |               |
| $[c_1 - \frac{1}{2}, -\frac{1}{2}R(c_2 - c_1)]$                   | Saddle   | —                     | $k < \frac{1}{3}$                 | Real          |
|   | Node     | —                     | $k > \frac{1}{3}$ , and $D_2 > 0$ | Real          |
|   | Stable   | —                     | $R(1 - k) > s(c_1 - \frac{1}{2})$ |               |
|   | Focus    | —                     | $k > \frac{1}{3}$ , and $D_2 < 0$ | Real          |
|   | Stable   | —                     | $R(1 - k) > s(c_1 - \frac{1}{2})$ |               |
|   | Unstable | —                     | $R(1 - k) < s(c_1 - \frac{1}{2})$ |               |
| $[-c_1 - \frac{1}{2}, -\frac{1}{2}R(c_2 + c_1)]$                  | Node     | Stable                | $D_3 > 0$                         | Virtual       |
|   | Focus    | Stable                | $D_3 < 0$                         | Virtual       |

Since this expression is developed by using a linearized analysis and is valid only for small oscillations, the critical tank size determined from this equation

(a)  $k = 0.025, R = 0.2$ 

**Fig. 11-11.** Phase portrait for constant power combined with constant gate opening.

is arbitrarily increased by 50 to 100 percent to allow for the stability of large oscillations. This increases the project costs significantly since these tanks are rather large (e.g., the closed surge tank of Driva Power Plant, Norway, has an area of  $780 \text{ m}^2$ ), and larger-capacity air compressors have to be provided.

By using the phase-plane method, Chaudhry et al. studied [1983 and 1985] the stability of closed tanks for the cases of constant discharge, constant-gate opening, and constant power. It was found that the oscillations are always stable for the first two cases. These two cases, however, normally do not occur

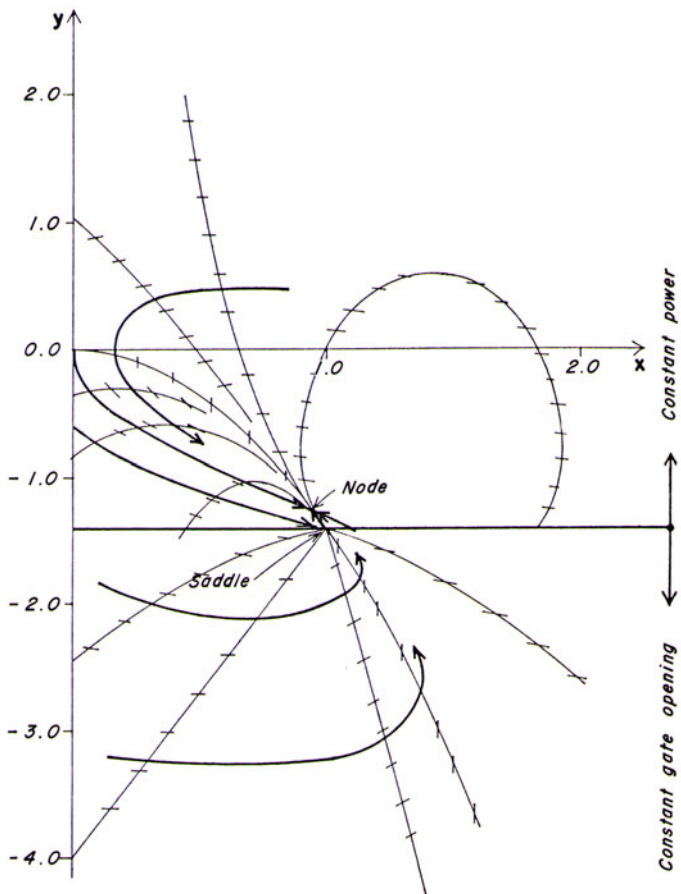
(b)  $k = 0.35, R = 2.8$ 

Fig. 11-11. (Continued)

in real-life projects. For the idealized case of constant power, however, the following two conditions have to be satisfied for large oscillations:

$$A_s > A_{cr} \quad (11-66)$$

and

$$h_{f_o}^3 \left[ 1 - \sqrt{-3 + \frac{4H_g}{h_{f_o}}} \right]^3 + 4Z^2 (H_g - h_{f_o}) \left( 1 + \frac{np_o A_s}{\forall_o} \right) < 0 \quad (11-67)$$

In other words, oscillations may be unstable even if the tank area is greater than the critical area, determined from the expression developed by Svee, if the second condition is not satisfied.

However, if the limit on the wicket gates that they can be opened only up to the full-open position is included in the analysis, then the oscillations are always stable [Chaudhry et al., 1985], whether large or small, if  $A_s > A_{cr}$  since both constant power and constant gate regions are stable. For  $A_s < A_{cr}$ , small oscillations grow until the destabilizing action of the constant-power region is counterbalanced by the stabilizing action of the maximum gate region, and perpetual oscillations are obtained (see Fig. 11-12). In the phase-plane terminology, it is referred to as the *limit cycle*. Large oscillations emanating from outside the limit cycle are damped to the amplitude of the limit cycle because the stabilizing action of the maximum gate region is more than the destabilizing action of the constant-power region.

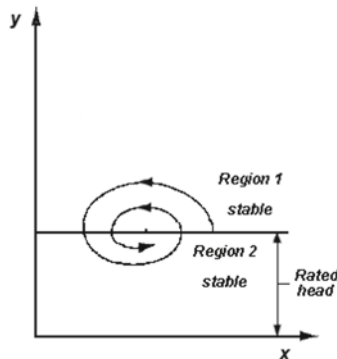
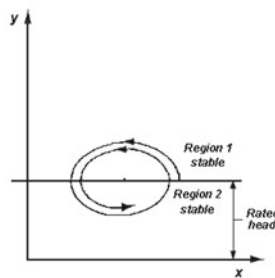
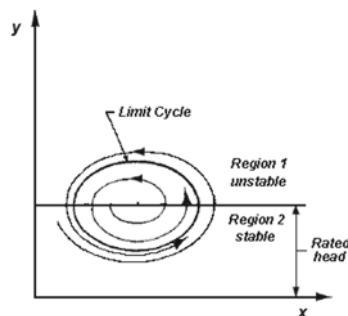
The rate of damping of the oscillations is higher if a limit on the maximum gate opening is included in the analysis as compared to that if an ideal governor with no such limit on the opening is considered.

## 11-11 Multiple Surge Tanks

A project with more than one surge tank is referred to as a *multiple-surge-tank system* or a *system of surge tanks*. Multiple surge tanks may be necessary in the following situations:

- To divert, through adits, additional water from secondary sources into the tunnel upstream of the main surge tank.
- To increase the cross-sectional area of the tank for increasing the turbo-generator output. This may be accomplished more easily by adding a new tank than by increasing the area of an existing tank.
- To provide a tank on the tailrace tunnel of an underground hydroelectric power plant or a pumped storage project to reduce maximum waterhammer pressures and/or to improve the governing characteristics of the power plant.
- To split the main surge tank into two or more shafts for the economy of construction or to suit the rock conditions.

Due to a large number of possible configurations of the multiple-surge-tank systems, the equations describing the tank oscillations are not derived in this section to conserve space. Two typical systems usually found in practice are presented in Problem 11-7. Equations for these systems may be derived in a manner similar to that used for a simple and for an orifice tank in Section 11-3.

(a)  $A_s > A_{cr}$ (b)  $A_s = A_{cr}$ (c)  $A_s < A_{cr}$ 

**Fig. 11-12. Stability of Oscillations for Different Tank Areas.** (After Chaudhry et al. [1985].)

## 11-12 Design Considerations

In this section, a number of guidelines for designing a project are outlined to develop an overall economical project that meets the operational requirements, provides flexibility in operations and keeps the maintenance costs low.

### Necessity of a Tank

The following criteria [Krueger, 1966] may be used to decide whether a surge tank is required in a particular project.

- One or more than one surge tank should be provided that reduce the maximum or minimum waterhammer pressures and results in a more economical penstock-surge-tank installation.
- A surge tank should be provided if the maximum speed rise following rejection of the maximum turbine output cannot be reduced to less than 60 percent of the rated speed by other practical methods, such as increasing the generator inertia or penstock diameter or decreasing the effective wicket-gate closing time. The speed rise is computed assuming one unit operating alone if there are more than one units on the penstock.
- As a rough rule of thumb for governing stability and good regulation, the provision of a surge tank should be investigated if

$$\frac{\sum L_i V_i}{H_n} > \quad 3 \text{ to } 5 \text{ (SI units)} \quad (11-68)$$

in which  $\sum L_i V_i$  is computed from the intake to the turbine, and  $H_n$  is the minimum net head (In the English units,  $\sum L_i V_i / H_n > 10$  to 20.). In general, a surge tank should be preferred to a pressure regulating valve although the latter may be more economical for high-head plants.

### Location

A surge tank should be located as near to the turbine as economically possible for the local topography.

### Size

The cross-sectional area of a tank for a hydroelectric power plant is selected to satisfy the following criteria:

- The tank is stable.
- The tank does not drain (i.e., the water level does not fall to the tunnel crown) following maximum possible load acceptance at the maximum rate with the upstream reservoir at its minimum level and maximum expected head losses.

- The tank does not overflow following load rejection unless an overflow weir is provided.

The minimum cross-sectional area required for stability has been under discussion for a long time. Jaeger [1960] proposed a safety factor  $n$  such that the area of the surge tank should be  $n$  times the Thoma area,  $A_{th}$ , with  $n > 1$ . As a rough guide for preliminary design,  $n$  may be 1.5 for a simple tank, and 1.25 for an orifice and for a differential tank. During the final design when various plant parameters have been selected, the stability of the tank should be checked by computer simulations over the full range of different parameters, such as, reservoir level, friction factors, etc. In these investigations, the variation of the turbine efficiency with head and with gate opening and the fact that the turbine gates cannot be opened more than their maximum opening should be taken into consideration. If these calculations show that the tank is unstable or that the dissipation of the tank oscillations is very slow, then the above procedure is repeated with an increased tank area. If, however, the tank is stable, and the rate of dissipation of oscillations is high, then a reduction in the tank area may be considered.

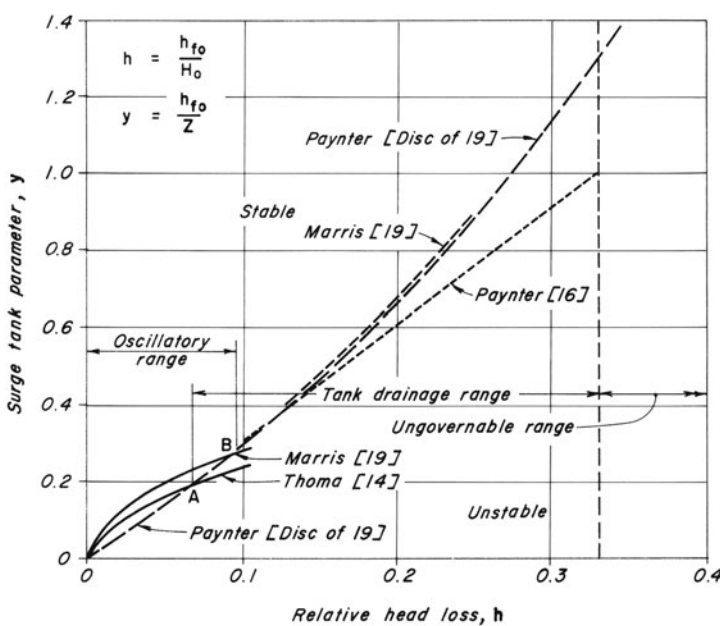


**Fig. 11-13.** Types of instability for various values of  $h$  and  $y$ . (After J. W. Forster [1962].)

[Figure 11-13](#) may be used to determine the type of instability to be expected, i.e., oscillatory or drainage. In this figure, compiled by Forster [1962] using results of various investigators, the abscissa,  $h$ , is  $h_{f_o}/H_o$ , and the ordinate,  $y$ , is  $h_{f_o}/Z$ . The curves represent the condition of critical stability where oscillations, once begun, continue with constant amplitude. This figure should be used for the most critical operating conditions, i.e., minimum reservoir level and maximum possible turbine output at that level. In general, if  $h$  and  $y$  for a system plot above the upper envelope of curves, the system is free of both oscillatory instability and tank drainage for all conditions, including full-load acceptance from zero load. A system plotting below the lower envelope is subject to instability or tank drainage, or both.

The maximum water level in a surge tank is computed for the turbine to reject maximum possible load. For a penstock, with multiple units, all units are assumed to reject load simultaneously which is possible if there is a fault on the transmission line. Experience with the operation of large grid systems shows that such severe unloading conditions occur a number of times during the life of the project.

The selection of the critical loading conditions is more complex and difficult than the unloading conditions. Some authors suggest a load acceptance of 50 to 100 percent of the rated load to determine the maximum downsurge. In the author's opinion, however, the maximum load and the rate of load acceptance should be selected in consultation with the engineers responsible for grid operation. For this selection, the following items are taken into consideration: the size of the grid system, the size and the rate of maximum load that the plant may be required to accept because of isolation from the grid system, and the maximum load that can be added to the system at a given rate.

The most critical multiple operations, i.e., load acceptance following load rejection or load rejection following load acceptance, are determined by simulations with the second operation starting at different points on the tank water-level oscillations cycle. Usually the second operation starting at the peak or the lowest level do not produce the worst conditions but rather at the mid-point of the surge cycle.

The *minimum probable* friction factor should be used for computing the *maximum upsurge*, and the maximum probable friction factor, for computing the *maximum downsurge*.

Instead of increasing the tank area to keep the maximum upsurge or the minimum downsurge within acceptable limits, the provision of an upper or lower gallery may be more economical.

For an orifice tank, the orifice is usually designed [Ruus, 1966] so that the initial retarding head for full-load rejection is approximately equal to the maximum upsurge. Johnson's charts [1908 and 1915] may be used to determine the approximate dimensions of the tank, riser, and the ports.

## 11-13 Case Study

Design studies for the Chute-des-Passes surge-tank system [Forster, 1962] are presented in this section for illustration purposes.

### Project Details

Figures 11-14 and 11-15 show the plant layout and the details of the hydraulic elements. The upstream tunnel is 9.82-km long, is concrete-lined, and has a diameter of 10.46 m. The 2.73-km-long downstream tunnel is also pressurized, is unlined, and has a diameter of 14.63 m. The maximum and minimum reservoir elevations are 378.2 m and 347.7 m, respectively. There are five units rated at 149.2 MW each at a net head of 164.6 m.

The plant supplies power to 746-MW electric smelters that are used for the production of aluminum. The nature of the smelters is such that power shutdown of a few hours could impose great operating difficulties in addition to large monetary losses. The plant could be isolated from the system due to major system disturbances, although the possibility of such an event occurring was considered remote.

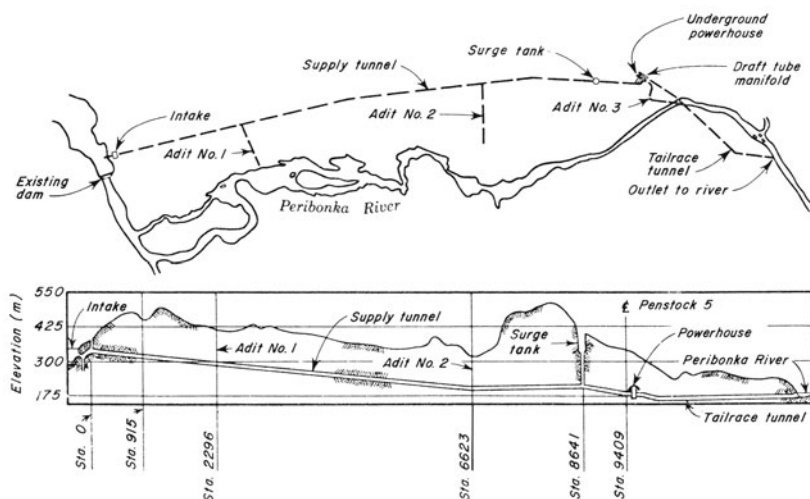


**Fig. 11-14. Project layout of Chute-Des-Passes development. (After J. W. Forster [1962].)**

At the upstream end of the tailrace tunnel, the 144.9-by-14.64-m tailrace manifold running parallel to the 144.9-m-long powerhouse served as the downstream surge tank.

## Program of Investigations

For the assumed range of various parameters, computations were done for the following:

1. Maximum and minimum water levels in the upstream and in the downstream surge tank.
2. Stability of the system and the rate of surge damping.
3. Discharge and volume of overflow over the spillway of the upstream tank.
4. Permissible load acceptance for different tank sizes over full operating range of the reservoir.

## Range of Various Variables

The selection of the range of various variable is discussed in the following paragraphs.

### *Size of Upstream and Downstream Tanks*

For the downstream surge tank comprising the tailrace manifold, the area was assumed to be fixed at 144.9 by 14.64 m.

Preliminary analysis had indicated that the diameters of the upstream tank should range from 33.5 to 52 m. Based on preliminary computer investigations, three tank diameters, 33.5, 39.7, and 45.75, were selected for a detailed analysis.

### *Tunnel Resistance*

From the data published on the Niagara Falls Development [Bryce and Walker, 1959], Appalachia tunnel [Elder, 1956], and Swedish unlined tunnels [Rahm, 1953], the maximum and minimum values for Manning  $n$  are listed in Table 11-2. (For more data on head losses in tunnels, see *Report of the Task Force on flow in Large Conduits of the Committee on hydraulic Structures*, [1965].)

**Table 11-2. Manning  $n$**

| <i>Tunnel</i>                  | <i>Maximum</i> | <i>Minimum</i> |
|--------------------------------|----------------|----------------|
| Concrete-lined upstream tunnel | 0.013          | 0.011          |
| Unlined downstream tunnel      | 0.038          | 0.035          |

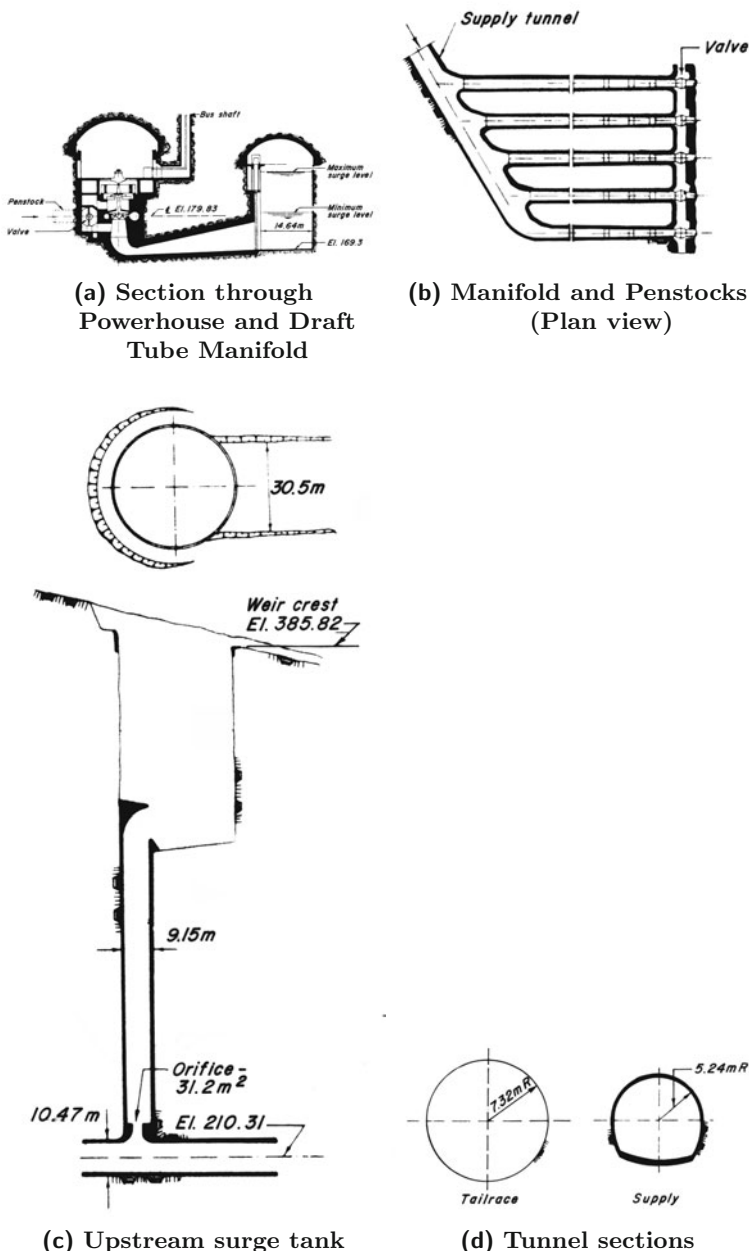


Fig. 11-15. Hydraulic elements of the Chute-Des-Passes Power Plant.  
(After J. W. Forster [1962].)

### *Orifice Size*

The orifice size was selected such that the maximum transient pressure head in the tunnel did not exceed one half the height of the rock cover.

The orifice loss coefficient for the flow into the tank was computed from the expansion losses for the flow from the orifice into the standpipe and from the standpipe into the tank. The loss coefficient for the outflow from the tank was determined from the contraction losses for the flow from the tank into the standpipe, from the standpipe into the orifice, and a 45° cone-diffuser expansion. Doubling these estimated loss coefficients or assuming them as zero had a negligible effect on the stability of the system.

### *Reservoir Levels*

Four reservoir levels — El. 347.7, 356.8, 366.0 and 378.2 m — were selected for determining the permissible amounts of load acceptance.

**Table 11-3** summarizes the assumptions made regarding the reservoir level and the tunnel losses for determining different critical conditions.

**Table 11-3. Assumed conditions**

| <b>Critical Condition</b>  | <b>Assumption</b>              |                        |
|--|--------------------------------|------------------------|
|  | <b>Tunnel Loss Coefficient</b> | <b>Reservoir Level</b> |
| Stability  | Minimum                        | Minimum                |
| Possibility of drainage of upstream tank following load acceptance | Maximum                        | Minimum                |
| Maximum upstream tank level following full load rejection          | Minimum                        | Maximum                |

### *Upstream Tank*

Increasing the tank diameter from 33.55 to 39.65 m increases the firm capacity of the isolated plant at low reservoir levels by about 37.3 MW. This advantage decreases rapidly as the tank diameter is increased above 39.65 m and disappears entirely at higher reservoir levels. Considering such factors as permissible amount of load acceptance, degree of surge damping, and effective plant capacity, a tank diameter of 39.65 m was selected. The bottom elevation of the tank was set at El. 321.5 m. This level allowed sudden acceptance of one unit or a small amount of load acceptance following full-load rejection. A

surge tank-level indicator was installed in the control room so that the operators could avoid accepting the load during that part of the surge cycle that would cause excessive downsurge.

Overflow from the tank would have been carried by a stream course through the permanent town site for the project. Because of the potential danger associated with sudden rushes of water through an inhabited area, it was later decided to excavate a basin in rock at the upper level to retain the overflow until it could discharge back into the surge tank.

### ***Downstream Tank***

The tailrace manifold was selected to act as the tailrace surge tank. For normal operation, the maximum and minimum water levels in this tank were computed to be at El. 192.15 m and El. 181.2 m, respectively. The floor was set at El.170.5 m. To avoid letting the water level fall so low as to unwater the draft tubes following total-load rejection, a weir was constructed in the tailrace tunnel downstream of the manifold.

## **11-14 Summary**

In this chapter, the description and analysis of various types of surge tanks are presented. The phase-plane method is used to investigate the stability of a simple surge tank. Design criteria for determining the necessity of a surge tank and for selecting the tank size are presented, and the details of the studies carried out for the design of the Chute-des-Passes surge-tank system are outlined.

## **Problems**

**11-1** Compute the free surge and the period of oscillations of a simple surge tank following sudden total rejection if the initial steady flow is  $1200 \text{ m}^3/\text{s}$ . The length of the tunnel is 1760 m, and the cross-sectional area of the tunnel and of the tank are  $200 \text{ m}^2$  and  $600 \text{ m}^2$ , respectively.

**11-2** Prove that dynamic equation (Eq. 11-7) is valid for an inclined surge tank (Fig. 11-16) if  $A_s$  = horizontal area of the tank.

**11-3** Derive the dynamic equations for simple, orifice, and differential tanks assuming that the tunnel is inclined at an angle  $\theta$  to the horizontal. (Hint: Draw a freebody diagram of the tunnel, and apply Newton's second law of motion. Because of the cancellation of the component of the weight of water in the tunnel by the difference in the datum head on the ends of tunnel, Eqs. 11-7, 11-14, and 11-15 are valid.)

**11-4** Prove that the oscillations of the tunnel flow and the water level in a simple tank following load rejection are  $90^\circ$  out of phase. Is the flow leading the water level or vice versa? Assume the system is frictionless.

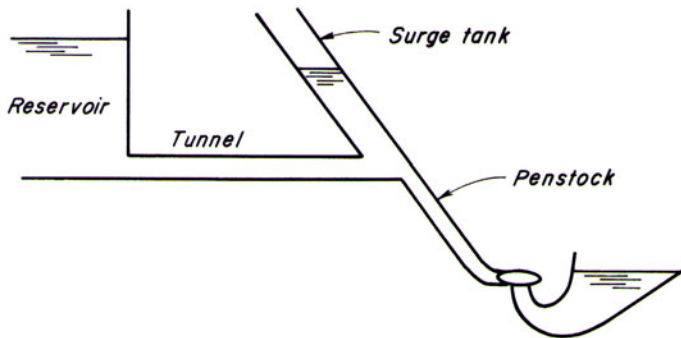


**Fig. 11-16.** Inclined surge tank.

**11-5** If the cross-sectional area of a tunnel varies in steps along its length, prove that the actual tunnel may be replaced by an equivalent tunnel having length,  $L_e$ , and area,  $A_e$  such that

$$\frac{L_e}{A_e} = \sum_{i=1}^n \frac{L_i}{A_i}$$

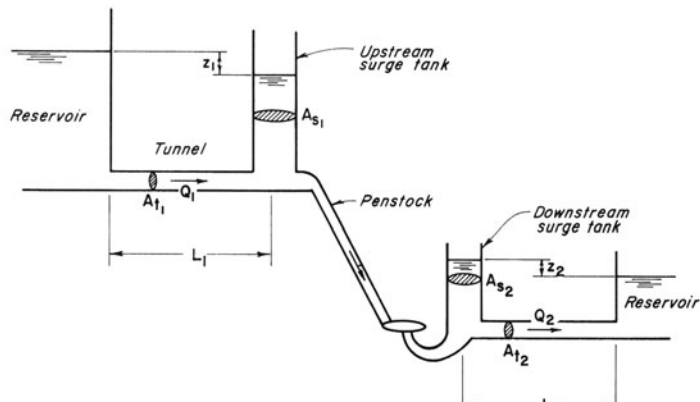
in which  $L_i$  and  $A_i$  are the length and the cross-sectional area of the  $i$ th section of the tunnel ( $i = 1$  to  $n$ ).

**11-6** If the inertia of the water in the tank is taken into consideration, prove that the expression for the free surge (Eq. 11-29) for a simple tank is valid; however, the expression for the period,  $T$ , becomes

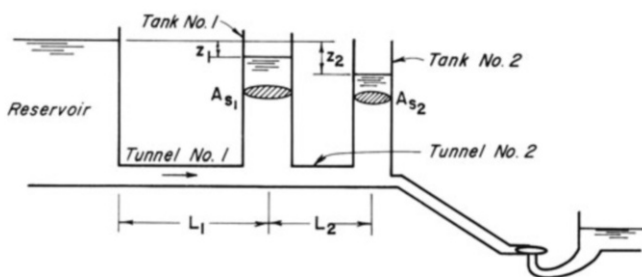
$$T = 2\pi \sqrt{\frac{\lambda A_s}{g A_t}}$$

in which  $\lambda = L + H_a A_t / A_s$ , and  $H_a$  = height of the tank.

**11-7** Figure 11-17 shows two typical multiple-surge-tank systems. Derive the dynamic and continuity equations for these systems.



(a)



(b)

Fig. 11-17. Multiple surge tanks.

**11-8** Prove that the critical area,  $A_{cr}$ , for perpetual oscillations in a closed surge tank (Fig. 11-18) is [Svee, 1972]

$$A_{cr} = A_{sc} \left( 1 + n \frac{p_o}{\gamma z_{a_o}} \right)$$

in which  $A_{sc}$  is critical area for an open surge tank and is given by the expression

$$A_{sc} = \frac{LA_t}{2g \left( \frac{h_{f_o}}{V_o^2} + \frac{1}{2g} \right) \left( H_o - h_{f_o} + \frac{V_o^2}{2g} \right) + 2 \frac{V_o^2}{2g}}$$

$p_o$  = steady-state air pressure, and  $z_{a_o}$  = distance between the roof of the tank and the initial steady-state water surface in the tank. Assume the

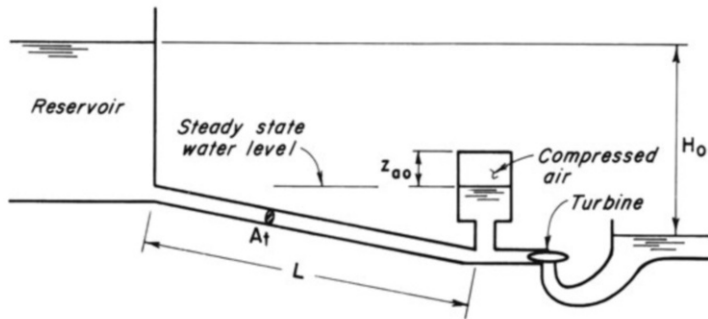


**Fig. 11-18.** Closed surge tank.

expansion and contraction of the air follow the law,  $p v_{air}^n = \text{constant}$ ; the governor maintains constant power; and the efficiency of turbine is constant. (Hint: Write the dynamic equation for the tunnel, the continuity equation, and the governor equation in terms of small deviations,  $\Delta z$ ,  $\Delta Q_t$  and  $\Delta Q_{tur}$  from the steady-state values; neglect terms of second and higher order, and combine the resulting equations by eliminating  $\Delta Q_t$  and  $\Delta Q_{tur}$ . For perpetual oscillations, the coefficient of the term  $d[\Delta z]/dt$  of this equation should be equal to zero.)

**11-9** Write a computer program for determining the water-level oscillations in a simple tank following a load acceptance or rejection. Using this program, compute the minimum downsurge for a surge-tank system in which flow is suddenly increased from 56 to 112 m<sup>3</sup>/s. The length of the tunnel is 1964 m, the cross-sectional area of the tunnel and the surge tank are 23.25 and 148.8 m<sup>2</sup> and the initial steady-state tunnel losses are equal to 1.22 m.

**11-10** By using the energy principles, prove that the amplitude of surge oscillations following a sudden reduction of flow from  $Q_o$  to zero in a frictionless, simple, surge-tank system is  $Q_o \sqrt{L/(gA_s A_t)}$ .

## Answers

**11-1** Free surge,  $Z = 46.42$  m; period  $T = 145.84$  s.

**11-9** 15.38 m below the reservoir level.

## References

- Allievi, L. 1937, "Air Chamber for Discharge Lines." *Trans.*, Amer. Soc. of Mech. Engrs., vol. 59, Nov., pp. 651-659.
- Bryce, J. B. and Walker, R. A., 1959, "Head Loss Coefficients for Niagara Water Supply Tunnels." *Engineering Journal*, Engineering Inst. of Canada. July.
- Bulirsch, R. and Stoer, J., 1966, "Numerical Treatment of Ordinary Differential Equations by Extrapolation Methods." *Numerische Mathematik*. vol. 8, pp. 1-13.
- Bullough, J. B. B. and Robbie, J. F., 1972, "The Accuracy of Certain Numerical Procedures when Applied to the Solution of Ordinary Differential Equations of the Type Used in the Digital Computer Prediction of Mass Oscillation in Closed Conduits," *Proc. First Conf. on Pressure Surges*. British Hydromechanics Research Association. Bedford. England, pp. A6-53 - A6-75.
- Chaudhry, M. H. 1983, "Review of Hydraulic Transient Studies, Snettisham Project," *Report*, prepared for the U. S. Army Corps of Engineers, Alaska District, Anchorage, Alaska, May.
- Chaudhry, M. H. and Ruus, E., 1971, "Surge Tank Stability by Phase Plane Method." *Jour. Hyd. Div.*, Amer. Soc. of Civ. Engrs., April, pp. 489-503.
- Chaudhry, M. H., Sabbah, M. A. and Fowler, J. E., 1983, "Analysis and Stability of Closed Surge Tanks," *Proc. Fourth International Conf. on Pressure Surges*, British Hydromechanics Research Association. Bedford. England. Sept., pp. 133-146.
- Chaudhry, M. H., Sabbah, M. A. and Fowler, J. E., 1985, "Analysis and Stability of Closed Surge Tanks," *Jour. Hyd. Engg.*, Amer. Soc. of Civ. Engrs., July, pp. 1079-1096.
- Cunningham, W. J., 1958, *Introduction to Nonlinear Analysis*. McGraw-Hill Book Company, Inc., New York, NY.
- Elder, R. A., 1956, "Friction Measurements in Appalachia Tunnel." *Jour. Hyd. Div.*, Amer. Soc. of Civ. Engrs., vol. 82, June.
- Forrest, J. A. and Robbie, J. F., 1980, "Mass Oscillation Prediction-A Comparative Study of Mass Surge and Waterhammer Methods." *Proc. Third International Conf. on Pressure Surges*. British Hydromechanics Research Association. Bedford. England, March, pp. 333-360.
- Forster, J. W., 1962, "Design Studies for Chute des-Passes Surge-Tank System." *Jour. Power Div.*, Amer. Soc. of Civ. Engrs., vol. 88, May, pp. 121-152.
- Frank, J. and Schüller, J., 1938, *Schwingungen in den Zuleitungs-und Ableitungskanal von Wasserkraftanlagen*, Springer, Berlin, Germany.
- Gardner, P. E. J., 1973, "The Use of Air Chambers to Suppress Hydraulic Resonance," *Water Power*, Mar., pp. 102-105, Apr., pp. 135-139.
- Gear, C. W., 1971, *Numerical Initial Value Problems in Ordinary Differential Equations*. Prentice-Hall. Englewood Cliffs, NJ.
- Gragg, W. B., 1965, "On Extrapolation Algorithms for Ordinary Initial-Value Problems." *SIAM Jour. Numerical Analysis*, pp. 384-403.

- Jaeger, C., 1960, "A Review of Surge Tank Stability Criteria." *Jour. Basic Engg.*, Amer. Soc. of Mech. Engrs., Dec., pp. 765-775.
- Jaeger, C., 1961, *Engineering Fluid Mechanics*, translated from German by Wolf, P.O., Blackie and Sons Ltd., London, UK.
- Johnson, R. D., 1908, "The Surge Tank in Water Power Plants." *Trans.*, Amer. Soc. of Mech. Engrs., vol. 30, pp. 443-501.
- Johnson, R. D., 1915, "The Differential Surge Tank." *Trans.*, Amer. Soc. of Civ. Engrs., vol. 78, pp. 760-805.
- Krueger, R. E., 1966, "Selecting Hydraulic Reaction Turbines." *Engineering Monograph No. 20*. Bureau of Reclamation, Denver, CO.
- Lundberg, G. A. 1966, "Control od Surges in Liquid Pipelines." *Pipeline Engineer*, Mar., pp. 84-88.
- Li, W. H., *Differential Equations of Hydraulic Transients*, Dispersion, and Ground-water Flow. Prentice-Hall, Inc., Englewood Cliffs, NJ, pp. 22-36.
- Marris, A. W., 1959, "Large Water Level Displacements in the Simple Surge Tank." *Jour. Basic Eng*, Amer. Soc. of Mech. Engrs., vol. 81.
- Marris, A. W., 1961, "The Phase-Plane Topology of the Simple Surge Tank Evaluation." *Jour. Basic Engg.*, Amer. Soc. of Mech. Engrs., pp. 700-708.
- Martin, C. S., 1973, "Status of Fluid Transients in Western Europe and the United Kingdom Report on Laboratory Visits by Freeman Scholar." *Jour. Fluids Engineering*, June, pp. 301-318.
- Matthias, F. T., Travers. F. J. and Duncan. J. W. L., 1960, "Planning and Construction of the Chute des-Passes Hydroelectric Power Project." *Engineering Journal*, Engineering Insl. of Canada. vol. 43, Jan.
- McCracken, D. D. and Dorn, W. S., 1964, *Numerical Methods and FORTRAN Programming*, John Wiley & Sons, Inc., New York, NY.
- Mosonyi, E., 1957 1960, *Water Power Development*, Vol. I and II, Publishing House of Hungarian Academy of Sciences. Budapest, Hungary.
- Parmakian, J., 1963, *Waterhammer Analysis*, Dover Publications, Inc., New York, NY.
- Parmakian, J., 1981, "Surge Control." *Closed-Conduit Flow*, M. H. Chaudhry and V. Yevjevich, eds., Water Resources Publications, Littleton, CO, pp. 206.
- Paynter, H. M., "A Palimpsest on the Electronic Analogue Art," A. Philbrick. Researches, Inc., Boston, MA.
- Paynter, H. M., 1949, "The Stability of Surge Tanks." *thesis* presenled to Massachusetts Insititute of Technology, Cambridge. Mass., in panial fulfillment of the requirements of degree of Master of Science.
- Paynter, H. M., 1951, "Transient Analysis of Cenain Nonlinear Systems in Hydroelectric Plants." *thesis* presenled to Massachusells Institute of Tech-nology, Cambridge. Mass. in panial fulfillment of the requirements of degree of Doctor of Philosophy.
- Paynter, H. M., 1953, "Surge and Water Hammer Problems." Electrical Analogies and Electronic Computers Symposium, *Trans.*, Amer. Soc. Civ. Engrs., vol. 118, pp. 962-1009.

- Pickford, J., 1969, *Analysis of Surge*. MacMillan and Co. Ltd. London, UK.
- Rahm, S. L., 1953, "Flow Problems with Respect to Intake and Tunnels of Swedish Hydroelectric Power Plants." *Bulletin No. 36*, Inst. of Hydraulics. Royal Inst. of Tech., Stockholm, Sweden.
- Rich, G. R., 1963, *Hydraulic Transients*. Dover Publications. New York, NY.
- Ruus, E. 1966, "The Surge Tank," *Lecture Notes*, University of British Columbia, Vancouver, Canada.
- Ruus, E., 1969, "Stability of Oscillation in Simple Surge Tank." *Jour., Hyd. Div.*, Amer. Soc. of Civ. Engrs., Sept., pp. 1577-1587.
- Sideriades, L., 1960, Discussion of "A Review of Surge Tank Siability Criteria," *Jour. Basic Engg.*, Amer. Soc. of Mech. Engrs., Dec., pp. 778-781.
- Sideriades, L., 1962, "Qualitative Topology Methods: Their Applications to Surge Tank Design." *La Houille Blanche*, Sept., pp. 569-80.
- Stoer, J. and Oulirsch. R., 1980, *Introduction to Numerical Analysis*, Springer Verlag, New York, NY.
- Svee, R., 1972, "Surge Chamber with an Enclosed Compressed Air Cush-  
ion." *Proc. International Conf. on Pressure Surges*, British Hydromechanics Research Association, Bedford, England, Sept., pp. G2-15-G2-24.
- Task Force, 1965, "Factors Influencing Flow in Large Conduits." Report of the Task Force on Flow in Large Conduits of The Committee on Hydraulic Structures. *Jour. Hyd. Div.*, Amer. Soc. of Civ. Engrs., vol. 91, Nov., pp. 123-152.
- Thoma, D., 1910, *Zur Theorie des Wasserschlossers bei Selbsttaetig Geregelten Turbinenmanlagen*, Oldenburg, Munchen, Germany.
- Verner, J. H., 1968, "Explicit Runge-Kutta Methods with Estimates of Local Trunction Error." *SIAM Jour. Numerical Analysis*. vol. 15. no. 4. Aug., pp. 772-787.

## LEAK AND PARTIAL BLOCKAGE DETECTION \*



**Partial blockage of ten-year old steel pipe due to deposition of calcium carbonate; diameter is reduced by 40 percent.** (Courtesy, B. Brunone.)

---

\* This chapter is authored by Pranab K Mohapatra

## 12-1 Introduction

Leak and partial blockage are common in pipelines, typically at junctions, joints and connections. Huge losses of drinking water due to leaks in pipelines are well documented [AWWA 1990; Weil 1993]. In addition to reduced flows, there may be economical losses and environmental issues. A pipeline, on the other hand, may be partially blocked due to chemical or physical deposition. Deposition of solid wastes in sewers, freezing of water in water pipelines and a jammed valve in an industrial piping system are typical examples of partial blockage in a piping system. The flow area is decreased due to a partial blockage, there is energy loss and the flow may separate on the downstream side. The energy loss is a function of the blockage size and mean flow. Both leak and partial blockage are considered abnormalities in a piping system. It is important to determine the position and size of leakage/partial blockage in a pipeline to develop remedial measures to mitigate their adverse effects.

Conventional practices for determining the location and magnitude of any abnormalities in a piping system are based on the measurements taken or inspections made throughout or on a major part of the system. A distributed set of pressure sensors, flow meters and valve sensors are used for this purpose. These methods are time consuming and costly. Therefore, economical methods are needed to detect leaks and partial blockages. Transient flows in a pipe show different characteristics with and without an abnormality, such as a leak or a partial blockage. Thus, transients may be used to detect the location and size of these abnormalities. Detection of partial blockage and leak in a pipeline by the transfer matrix method of Chapter 8 is presented in this chapter.

Several research articles on the detection of leak [Covas and Ramos 1999; Brunner 1999; Brunone and Ferrante 2001; Wang et al. 2002; Sattar and Chaudhry 2008; Haghghi et al. 2012] and partial blockage [Jiang et al. 1996; De Salis and Oldham 1999; Mohapatra et al. 2006; Sattar et al. 2008; Meniconi et al. 2010] in pipes have been published. Sattar [2006] presented an excellent review of literature on the detection of leak and partial blockage in pipelines.

In this chapter, terminology is outlined first and then the methodologies for the detection of leak and blockage are presented.

## 12-2 Terminology

All examples considered in this chapter are for a single pipeline connected to a constant-head upstream reservoir and an oscillating valve at the downstream end ([Fig. 1-1](#)). The pipe diameter is  $D$ , and length,  $L$ . The leak is of circular shape, while a partial blockage is an orifice. A leak is characterized by its size (opening diameter of leak),  $D_L$  and location by the distance from the upstream reservoir,  $X_L$ . Similarly, a partial blockage is defined by its size,  $D_B$  and location,  $X_B$ . The size and the location may be non-dimensionalized by using  $D$  and  $L$  as the reference parameters. Pressure frequency response

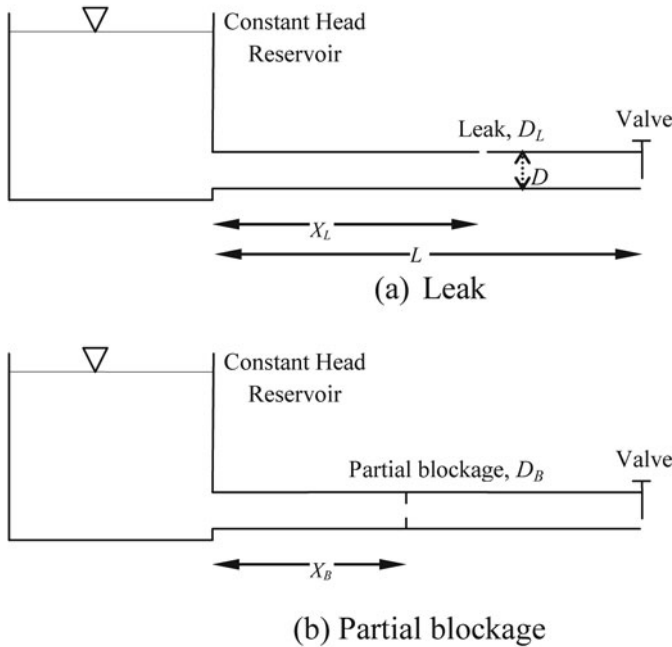


**Fig. 12-1. Definition sketch.**

(PFR) is the frequency response of pressure head at the specified location in the pipeline (see Chapter 8 for details). Non-dimensional pressure fluctuation is presented as a function of the non-dimensional frequency. Shape of PFR depends on the location where pressure is measured. PFR near the exit valve is considered in all examples presented in this chapter. Peak pressure frequency response (PPFR) is obtained from the PFR by joining the peaks. Similarly, trough pressure frequency response (TPFR) is obtained by joining the troughs in PFR. PFR and PPFR near the exit valve with and without a partial blockage are presented in Fig. 12-2. Note that the PPFRs are flat and curved lines for without and with partial blockage cases, respectively. Similar to PFR and PPFR, discharge frequency response (DFR) and peak discharge frequency response (PDFR) may be obtained for any location in the pipe. These frequency responses may be used to detect a leak/partial blockage in the piping system. Two non-dimensional parameters, damage and reflection are used in leak detection. Damage,  $\delta$ , is defined as  $\delta = \sqrt{(C_d A_L / A)}$ , where,  $A_L$  and  $A$  are leak and pipe area, respectively and  $C_d$  = coefficient of discharge of leak. The reflection,  $\psi$ , is given by  $\psi = \Delta |h_r|$ .

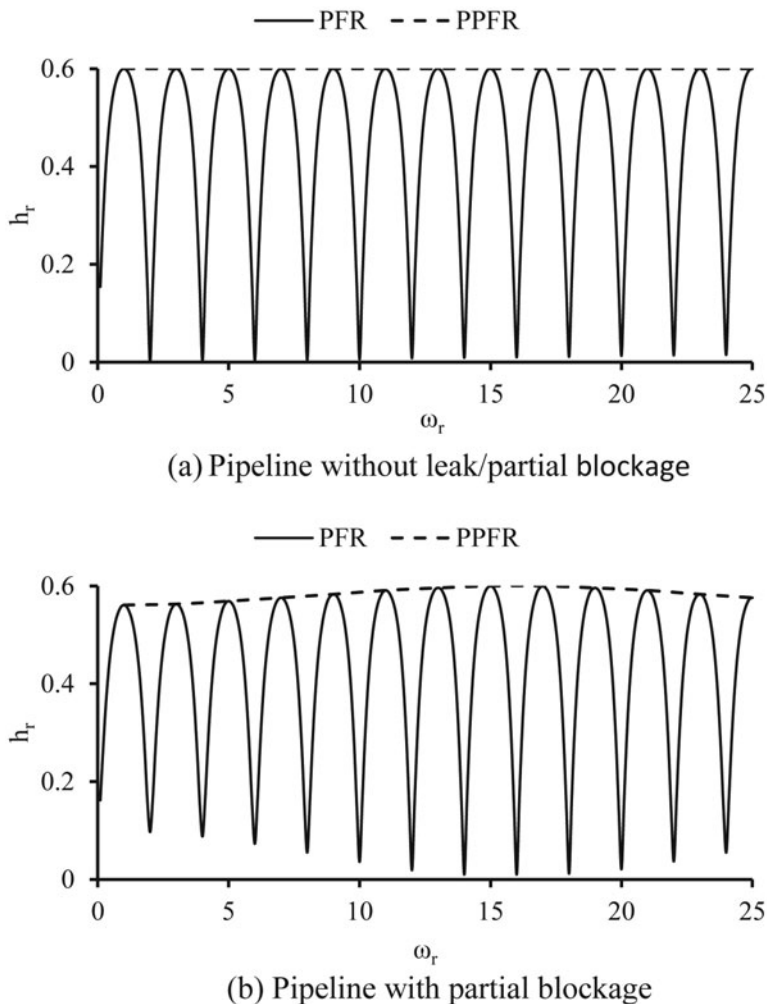


**Fig. 12-2.** Pressure frequency response at the downstream valve.

### 12-3 Partial Blockage Detection

A procedure for the detection of a partial blockage based on Mohapatra et al. [2006] is discussed in this section.

#### Frequency Analysis

A transfer matrix describes each component of a fluid system. Eqs. 8-33, 8-67 and 8-71 may be written in extended matrix form as

*Field matrix*

$$\mathbf{F}_i = \begin{bmatrix} \cosh(\mu_i L_i) & -\frac{1}{Z_c} \sinh(\mu_i L_i) & 0 \\ -Z_c \sinh(\mu_i L_i) & \cosh(\mu_i L_i) & 0 \\ 0 & 0 & 1 \end{bmatrix} \quad (12-1)$$

*Point matrix for a downstream oscillating valve*

$$\mathbf{P}_{ov} = \begin{bmatrix} 1 & 0 & 0 \\ -\frac{2H_0}{Q_0} & 1 & \frac{2kH_0}{\tau_0} \\ 0 & 0 & 1 \end{bmatrix} \quad (12-2)$$

*Point matrix for a partial blockage*

$$\mathbf{P}_B = \begin{bmatrix} 1 & 0 & 0 \\ -\frac{2\Delta H_0}{Q_0} & 1 & 0 \\ 0 & 0 & 1 \end{bmatrix} \quad (12-3)$$

A single pipeline is considered in the following examples to explain the procedure for the detection of partial blockage. For such a pipeline, the overall transfer matrix may be written as

$$\mathbf{U} = \mathbf{F}_2 \mathbf{P}_B \mathbf{F}_1 \quad (12-4)$$

By using the point matrix for an oscillating valve, the frequency responses for pressure and discharge are obtained (see Eqs. 8-129 through 8-131).

The absolute values of  $h_{n+1}^L$  and  $q_{n+1}^L$  are the amplitudes of the pressure and discharge fluctuations at the downstream valve, respectively. Equation 12-4 is used to obtain  $\mathbf{U}$  and the frequency responses are obtained by using Eqs. 8-129 through 8-131. The PFR and/or the DFR are developed by repeating this procedure for different frequencies.

## System Parameters

Transient flow in a piping system is affected by the size and the location of the partial blockage. As presented in the point matrix for partial blockage (Eq. 12-3), the blockage size is defined in terms of the associated head loss. The size of the partial blockage and the associated head loss may be correlated for a given flow. The pipeline parameters for the study presented here are: Pipe length,  $L = 1,600$  m; pipe diameter,  $D = 0.3$  m; amplitude of the valve oscillation,  $k = 0.1$ ; mean pressure head in pipe,  $H_0 = 50$  m; wave speed,  $a = 1,200$  m/s;  $Q_0 = 0.1$   $m^3/s$ , and friction parameter,  $f = 0.0$ . The normalized blockage size,  $z = D_B/D$ , and the location of the blockage,  $X_B/L$ , are varied. An ideal system, i.e., a frictionless pipe, is used here to demonstrate the use of frequency response method to detect the partial blockage in a pipeline.

In addition, in the absence of experimental data, the numerical results may be verified by comparing with the analytical results for simplified cases. Note that the pipe friction affects the PPFR, i.e., the amplitude of PPFR decreases while the periodicity remains same. The procedures for using the PPFR for partial blockages and the results are discussed in the following sections. The frequency response method (FRM) is validated by comparing the results with those obtained by the method of characteristics (MOC).

### PPFR for Partial Blockage

The PPFRs for the downstream end of the pipe computed by MOC and FRM are compared in Fig. 12-3. The peak pressure fluctuations by FRM are overpredicted as compared to that by MOC. However, the overall shape is similar. Because of the nonlinearities, the amplitude of the positive swings in pressure oscillations is larger than the negative swings in the MOC simulations. In the transfer matrix method, however, the amplitudes of the positive and negative swings are equal. Thus, the amplitudes from the trough to peak are approximately the same in both methods and a good comparison is indicated.

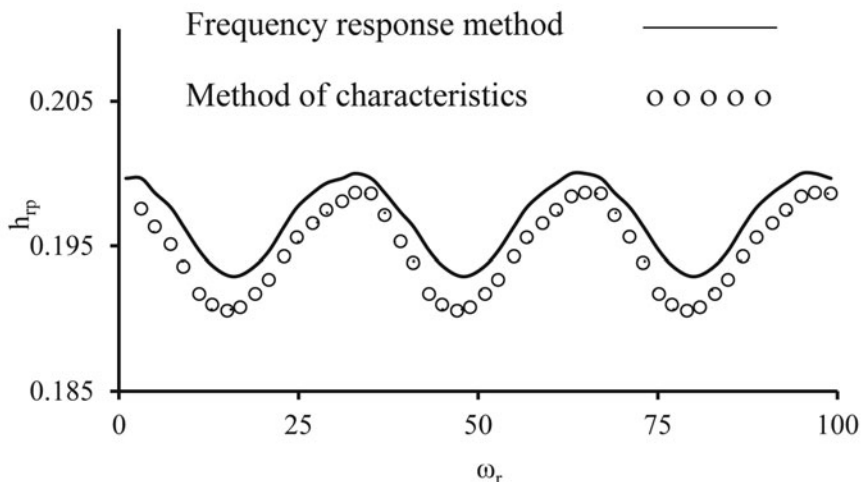


**Fig. 12-3.** Peak pressure frequency response.

The effect of the location of the partial blockage is shown in Fig. 12-4. Five different locations for the partial blockage are considered. In the PPFR, the nondimensional frequency,  $\omega_r$ , ranges from 1 to 100. The number of peaks or troughs in the PPFR increases when the position of the partial blockage is moved from the upstream end towards the middle of the pipe. A similar trend

is also seen when the partial blockage position is changed from the valve end towards the midlength. A comparison of the trends of these responses shows that if the size remains constant, a partial blockage produces mirror images in their PPFR at equal distances from both the ends. In addition, the number of peaks has a definite correlation with the location of the partial blockage. For example, the numbers of peaks are 3 and 9 when the partial blockage is located 100 and 300 m, respectively, from the upstream end. This correlation is also seen for other locations of the partial blockage. PPFR for these cases are not presented here to conserve space. It is observed in the PPFR that the peak pressure fluctuation attains a constant value when the partial blockage is located at the midlength of the pipeline. In addition, the mean value of the peak pressure fluctuation is constant in all the cases considered in [Fig. 12-4](#). Thus, the mean peak pressure fluctuation may be used to estimate the partial blockage size.

The effect of partial blockage size on the PPFR is shown in [Fig. 12-5](#) for three different sizes of partial blockages ( $z = 0.60, 0.45$ , and  $0.40$ ) for  $X_B = 200$  m.

A large partial blockage resulting in more head losses is reflected as higher amplitude in the PPFR. Mean peak pressure fluctuation for different sizes of blockage is presented in [Fig. 12-6](#) in which the variation of non-dimensional pressure fluctuation with partial blockage size,  $z = D_B/D$ , is presented. As expected, a lower value of the mean peak pressure indicates a greater head loss and a larger blockage (lower value of  $z$ ). The variation in PFR is insignificant for small blockage sizes  $z > 0.8$ . Note that [Fig. 12-6](#) is valid only for a particular value of  $Q_0$  (It is  $0.1 \text{ m}^3/\text{s}$  in this case).

Based on the preceding analysis, the following procedure may be used to determine the size and location of a partial blockage.

1. A PPFR is obtained for a range of  $\omega_r$  from 0 to  $\omega_{max}$  and the number of peaks,  $N$ , is counted.
2. Check if a peak, P, or a trough, T, occurs first.
3. Distance of the partial blockage is calculated from

$$\frac{X_B}{L} = \frac{2N}{\omega_{max}} \quad (12-5)$$

if P is first or

$$1 - \frac{X_B}{L} = \frac{2N}{\omega_{max}} \quad (12-6)$$

if T is first.

4. The mean peak pressure,  $\bar{h}_{rp}$ , is calculated from the PPFR and  $PR$  is obtained by dividing  $\bar{h}_{rp}$  by  $\bar{h}_{rp0}$ . The size of the blockage,  $z$ , may then be determined from [Fig. 12-6](#).

Note that N can be only an integer value and the value of  $X_B/L$  obtained by using Eq 12-8 indicates a range, i.e. For example, for  $L=1,600$  m,  $\omega_{max}=100$

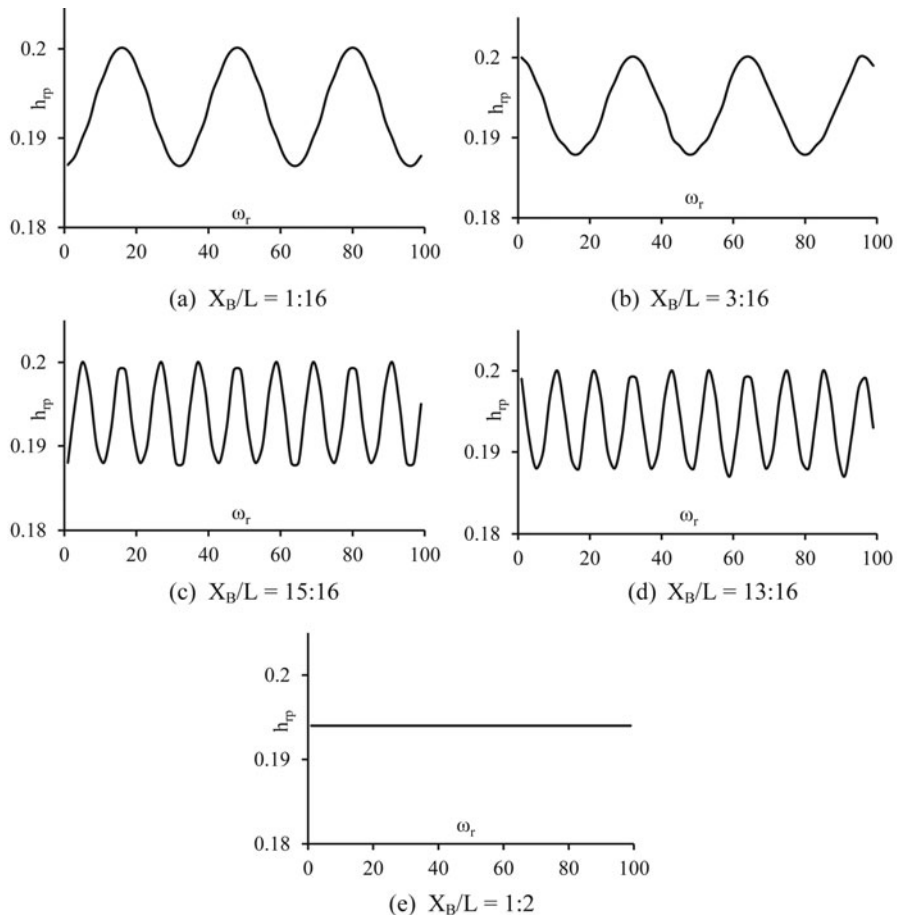


**Fig. 12-4.** Effect of blockage location on PPFR,  $z=0.5$ .

and  $N=6$ ,  $X_B$  lies between 200 m and 233.33 m.  $\omega_{max}$  has to be increased to achieve greater accuracy for  $X_B$ .

## 12-4 Leak Detection

In this section, a computational procedure is outlined for leak detection utilizing the frequency domain analysis, presented by Sattar and Chaudhry [2008].

A leak in a pipeline may be detected by using the frequency response of pressure. Note that PPFR is based on the frequencies related to the odd harmonics whereas TPFR is obtained from the frequencies of even harmonics.

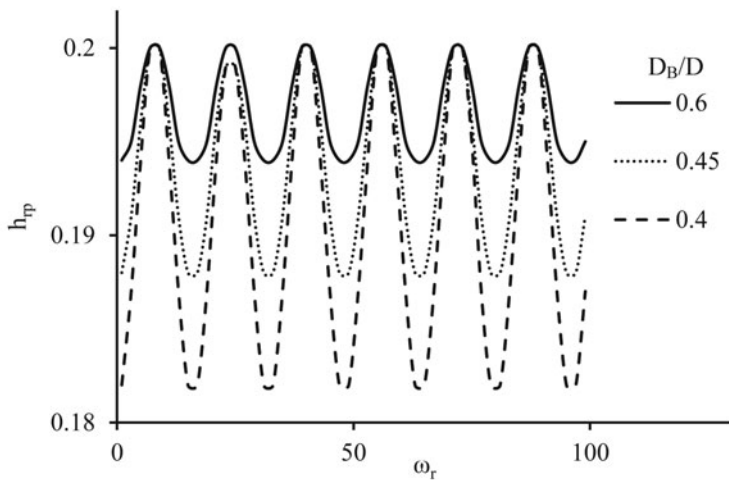


**Fig. 12-5.** Effect of blockage size on PPFR,  $X_B/L = 1/8$ .

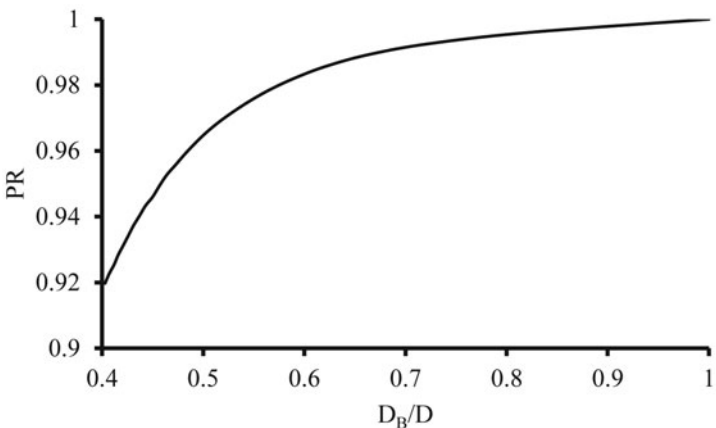


**Fig. 12-6.** Effect of blockage size on pressure fluctuation ratio.

In other words,  $\omega_r=1, 3, 5, \dots$  for PPFR and  $\omega_r=2, 4, 6, \dots$  for TPFR. In this section, TPFR is used for detecting leak in a pipeline. Note that a leak increases the amplitude of pressure oscillations in the system frequency response at the even harmonics. Such an increase in amplitude has an oscillatory pattern. The frequency and amplitude of this pattern is utilized to predict the leak location/discharge. The procedure is discussed in the following paragraphs.

## Frequency Response

A leak is modeled as an orifice with the opening size and the pressure determining the leak discharge. Following orifice equation is used to calculate the leak discharge:

$$Q_L = C_d A_L \sqrt{2gH_L} \quad (12-7)$$

where  $Q_L$  is the steady leak discharge for head,  $H_L$  and  $C_d$  is the discharge coefficient.

The frequency response for discharge and pressure fluctuation is computed as described in the previous section. However, the point matrix for the leak,  $\mathbf{P}_L$ , as given below, is used in Eq. 12-4 in stead of  $\mathbf{P}_B$ .

$$\mathbf{P}_L = \begin{bmatrix} 1 - \frac{Q_L}{2H_L} & 0 \\ 0 & 1 \\ 0 & 0 & 1 \end{bmatrix} \quad (12-8)$$

As stated earlier, the TPFR at the downstream end of the pipeline is constructed by using the same system parameters as those used in the previous section. Fig. 12-7 represents the effect of the leak location for four different locations,  $X_L/L$ . The TPFR follows a specific pattern depending on the leak location. The oscillatory pattern is due to the reflection of pressure waves at the leak and the generation of secondary leak-induced standing waves in the system. Note that, unlike the partial blockage, TPFR is almost the same when the leak is located symmetrically about the pipe midlength, e.g.,  $X_L/L=1:16$  and  $X_L/L=15:16$  result in identical TPFR. Thus, TPFR predicts two possible locations of a leak. In addition, similar to the partial blockage detection, TPFR results in a poor signal when the leak is located at the midlength of the pipeline, i.e., at  $X_L/L = 0.5$ . It can be proven theoretically that the TPFR results in a zero line when  $X_L/L$  is either 0 or 1.

The effect of the leak size on TPFR is shown in Fig. 12-8. There are three different leak sizes but the leak location is constant. Note that the point matrix for a leak has a term with leak discharge. Thus, the leak size,  $D_L/D$  is used to calculate the leak discharge,  $Q_L$ , in the formulation. The legend of Fig. 12-8 shows  $D_L/D$ , but not the leak discharge,  $Q_L$ . As indicated in Fig. 12-8, the amplitude of oscillations in the TPFR is proportional to the leak discharge. The amplitude increases as the leak discharge increases. However, the pattern frequency is constant since the leak is at the same location.

## Leak Detection Procedure

A transient signal generated at the downstream end of a pipeline by a valve propagates in the pipeline until it reaches a leak where it is partially reflected back. The reflected wave, which depends upon the leak discharge and location, travels back to the valve carrying information about the leak. As this process

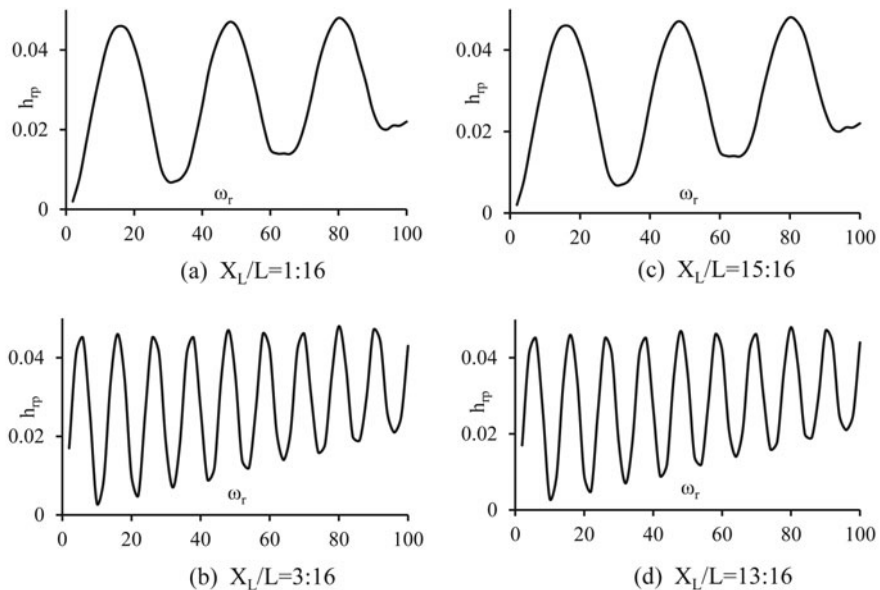


**Fig. 12-7.** Effect of leak location on TPFR.

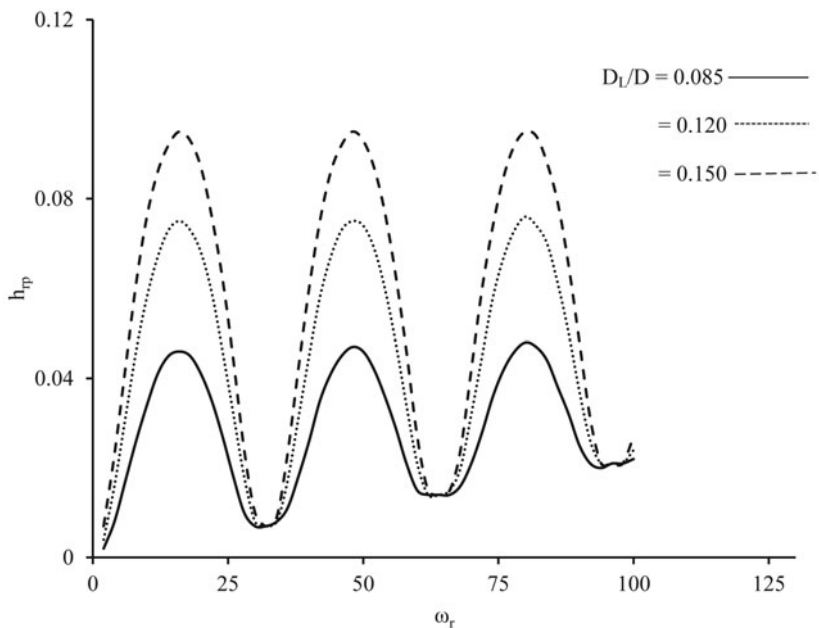


**Fig. 12-8.** Effect of leak size on TPFR,  $X_L/L = 1 : 16$ .

of reflection repeats, a series of traveling and standing waves are generated in the system. These waves can be used to detect the location of the leak by interpreting the frequency response of the entire system. It is observed that the presence of a leak in a pipeline modifies the shape of the TPFR. The increase in the amplitude has an oscillatory pattern along the frequency axis, which tends to repeat in a periodic manner at a frequency and amplitude directly related to the location and discharge of the leak.

A wave generated at the downstream valve travels to the leak where it is partially reflected back to the valve with an opposite sign. A leak reflection time may be defined as  $T_L = 2(L - X_L)/a$  which depends directly on the location of the leak in the system with respect to the valve. Accordingly, one can interpret the periodic increase in the amplitude of pressure oscillations at even harmonics in the frequency response of a system with a leak to be directly dependent on the leak reflection time. This oscillatory pattern has a period  $\Delta\omega_r^{even}$ . This is related to the leak-induced reflection frequency,  $\omega_L = 2\pi/T_L$ , where  $T_L$  is the leak reflection time as defined earlier. Since frequencies are normalized by using  $\omega_{th}$  as a reference, the oscillation period of the leak-induced pattern,  $\Delta\omega_r^{even}$ , may be defined as

$$\Delta\omega_r^{even} = \frac{\omega_L}{\omega_{th}} = \frac{2\pi/T_L}{2\pi/TW_{th}} = \frac{T_{th}}{\omega_L} = \frac{4L/a}{2(L - X_L)/a} = \frac{2L}{L - X_L} \quad (12-9)$$

This equation may be used to predict  $X_L$ . Note that  $\Delta\omega_r^{even}$  is the difference between  $\omega_r$  values corresponding to consecutive peaks in the TPFR.

Thus the procedure for leak detection may be summarized as follows:

1. Compute the frequency response of the piping system at the downstream valve.
2. Compute the frequency of the leak-induced pattern by applying spectral analysis to a set of data containing only the amplitude of head oscillations at the even harmonics in the system frequency response. To ensure a high resolution spectrum and a correct frequency extraction, a significant number of head responses at the even harmonics are needed.
3. Use Eq. 12-9 to compute the leak location.

Note that, in the above procedure, it is not necessary to know the pipe frequency response prior to the leak for detecting the existence of a leak and for determining its location.

To estimate the leak discharge, compute the non-dimensional damage,  $\delta$ , and nondimensional reflection,  $\psi$  as defined in Section 12-2. A relationship between  $\psi$  and  $\delta$  is developed for the given system. This relationship helps in estimating the leak discharge based on the magnitude of the oscillatory pattern of the TPFR. Alternatively, the leak discharge may be computed iteratively from the transform matrix equations after knowing the leak location.

## 12-5 Real-life Application

The procedures for the detection of a partial blockage and leak presented in this chapter may be utilized in real-life applications. The operation time of the valve depends on the length of the pipe and wave velocity and should not be less than the theoretical time period,  $T_{th}$ . At the location of the oscillating valve, the amplitudes of the pressure fluctuations are recorded. This procedure is repeated for a range of frequencies by varying the period of oscillating valve. The PPFR/TPFR is obtained from the recorded values of pressure fluctuation and the corresponding frequency of the oscillating valve. The PPFR/TPFR may be used to estimate the location and the size of partial blockage or leak. However, for real-life application of the method, there are a number of uncertainties associated with the friction factor, demand, pipe properties, and system topologies. A decision on the range of frequencies should consider the safety of the system and constraints on the valve operation. Valve operation for continuous opening and closing may require specialized instrumentation. The amplitude of the fluctuation of valve opening should be kept low, say about 0.1, so that the assumption of linear relationships is valid. Leak or partial blockage shape affects the PPFR/TPFR.

## 12-6 Summary

Detection of partial blockage and leak in pipelines by using the transfer matrix method is presented in this chapter. Procedures and associated uncertainties with real-life application are outlined.

## Problems

**12-1** Can the frequency response of discharge be used to detect leak and/or partial blockage in pipelines?

**12-2** Is it necessary that the pressure be recorded at the downstream valve? Can the pressure signal at mid-length of the pipe be used for leak/partial blockage detection?

**12-3** Equation 12-3 is for a point partial blockage. However, a partial blockage may extend over a length. Assume a line partial blockage in a pipeline and derive the point matrix for this.

**12-4** Use the point matrix in Prob 12-3 to plot the frequency responses (PPFR/TPFR).

**12-5** Develop the PPFR for two partial blockages and verify if Eq. 12-5 is still valid.

## References

- AWWA, 1990, *Manual of Water Supply Practices: Water Audits and Leak Detection* 1st edition, AWWA M36, American Water Works Association, Denver, CO.
- Brunner, B., 1999, "Transient Test-based Technique for Leak Detection in Outfall Pipes." *Jour. Water Resour. Plan. Manage.*, Vol. 125, No. 5, pp. 302-306.
- Brunone, B., and Ferrante, M., 2001, "Detecting Leaks in Pressurized Pipes by Means of Transients." *J. Hydraul. Res.*, Vol. 39, No. 5, pp. 539-547.
- Chaudhry, M. H., 1987, *Applied Hydraulic Transients*, 2nd edition, Van Nostrand Reinhold, NY.
- Covas, D., and Ramos, H., 1999, "Leakage Detection in Single Pipelines using Pressure Wave Behaviour." *Proc. CCWI99 (Computing and Control for the Water Industry)*, Dragan A. S. and Godfrey A. W., eds., Univ. of Exeter, U.K, pp. 287-299.
- De Salis, M. H. F., and Oldham, D. J., 2001, "Development of a Rapid Single Spectrum Method for Determining the Blockage Characteristics of a Finite Length Duct." *Jour. Sound Vib.*, Vol. 243, No. 4, pp. 625-640.
- Haghghi, A., Covas, D., and Ramos, H., 2012, "Direct Backward Transient Analysis for Leak Detection in Pressurized Pipelines: from Theory to Real Application." *Jour. Wat. Supply: Research and Technology — AQUA*, 61.3, pp. 189-200.
- Jiang, Y., Chen, H., and Li, J., 1996, "Leakage and Blockage Detection in Water Network of District Heating System." *Trans. ASHRAE*, Vol. 102, No.1, pp. 291-296.
- Meniconi, S., Brunone, B., Ferrante, M., and Massari, C., 2010, "Fast Transients as a Tool for Partial Blockage Detection in Pipes: First Experimental Results." *Water distribution systems analysis 2010 — WDSA2010*, Tucson, AZ, USA, pp. 144-153.
- Mohapatra, P. K., Chaudhry, M. H., Kassem, A. A., and Moloo, J., 2006, "Detection of Partial Blockage in Single Pipeline." *Jour. Hydraul. Engrg.*, Vol. 132, No. 2, pp. 200-206.
- Sattar, A. M., 2006, *Leak and Blockage Detection in Pipelines, PhD thesis*, Dept. of Civil and Env. Engg., Univ. of South Carolina.
- Sattar, A. M., and Chaudhry, M.H., 2008, "Leak Detection in Pipelines by Frequency Response Method." *Jour. Hydraul. Res.*, Vol. 46, Extra Issue 1, pp. 138-151.
- Sattar, A. M., Chaudhry, M. H., and Kassem, A. A., 2008, "Partial Blockage Detection in Pipelines by Frequency Response Method." *Jour. Hydraul. Engrg.*, Vol. 134, No. 1, pp. 76-89.
- Wang, X., Lambert, M. F., Simpson, A. R., Liggett, J. A., and Vitkovsky, J. P., 2002, "Leak Detection in Pipelines Using the Damping of Fluid Transients." *Jour. Hydraul. Eng.*, Vol. 128, No. 7, pp. 697-711.

- Weil, G. J., 1993, "Non-contract Remote Sensing of Buried Water Pipeline Leaks using Infrared Thermograph." *Water Resources Planning management*, Proceedings of 20th Anniversary Congress on Water Management in the '90s. ASCE, Seattle, Washington, pp. 404-407.

## TRANSIENT OPEN-CHANNEL FLOWS



Flow through the breach in the Elm Point levee in St. Charles, MO. Breach occurred on June 23, 2008; with most of the flooded area being agricultural land. (<http://chl.erdc.usace.army.mil>)

## 13-1 Introduction

In the previous chapters, we considered transient flows in the closed conduits. In this chapter, we discuss transient flows in open channels. A flow having a free surface is considered open-channel flow even though the channel may be closed at the top, e.g., a tunnel flowing partially full.

A number of common terms are defined, and the examples of transient flows are presented. The dynamic and continuity equations describing these flows are derived, and a number of methods for their solution are discussed. Details of explicit finite-difference and implicit finite-difference method are then presented. This is followed by a discussion of a number of special topics on open-channel transients. The chapter concludes with a case study.

## 13-2 Terminology

The flow is called *unsteady flow* if the depth and/or velocity varies at a point with time. Typical examples of unsteady flow are: floods in rivers, tides in estuaries, surges in power canals, and storm runoff in sewers.

Unsteady flow may be classified as *rapidly varied* or *gradually varied* flow [Chow, 1959] depending upon the temporal (i.e., with respect to time) and/or spatial (i.e., with respect to distance) rate of variation of the flow depth. This classification allows the assumption of hydrostatic pressure distribution in gradually varied flow. The water-surface variation in rapidly varied flow is rapid and usually the water surface has a discontinuity, called a *bore* or a *shock*. Examples of such flows are surges in power canals caused by load changes on turbines or tidal bores in estuaries. In the gradually varied flow, the variation of the free surface is gradual, e.g., river floods, tides without bore formation.

Transient flow in an open channel involves the propagation of waves. A *wave* is defined as a temporal or spatial variation of flow or water surface. The *wavelength*,  $\lambda$ , is the distance from one crest to the next, and the *amplitude* of a wave is the difference between the maximum level and the still water level (see Fig. 13-1).

The wave speed *relative* to the medium in which it is traveling is called *wave celerity*,  $c$ . Note that it is different from the flow velocity,  $V$ , with which the particles of the fluid move. The *absolute wave velocity*,  $\mathbf{V}_w$ , of a wave is equal to the vectorial sum of the wave celerity and the flow velocity, i.e.,

$$\mathbf{V}_w = \mathbf{V} + \mathbf{c} \quad (13-1)$$

in which boldface type indicates that the variables are vectors. In one-dimensional flow, there is only one flow direction. Therefore, the wave celerity is either in the direction of flow (downstream), or it is opposite to the flow (upstream). Equation 13-1 may be written as

$$V_w = V \pm c \quad (13-2)$$

in which, the positive sign is for a wave traveling in the downstream direction,

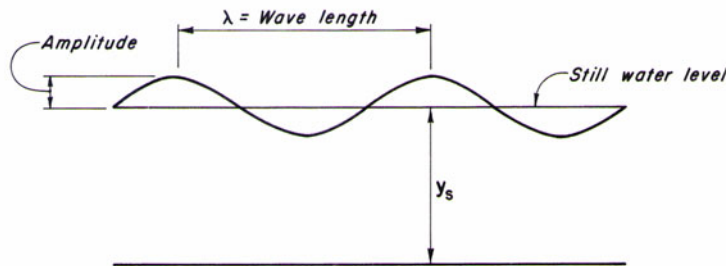


**Fig. 13-1. Wavelength and amplitude.**

and the negative is for a wave traveling upstream.

Based on different characteristics, the waves may be classified as follows: A wave having a wavelength more than 20 times the flow depth is termed a *shallow-water wave*, and a wave having a wavelength less than twice the flow depth is called a *deep-water wave*. Note that it is the ratio of the wavelength,  $\lambda$ , to the depth,  $y_s$ , and not the flow depth alone, which defines the type of a wave [Rouse, 1961]. For example, depending upon the ratio of the wavelength to the flow depth, a short wave, such as a ripple, can be a deep-water wave in an otherwise shallow water; and a long wave, such as a tide, in the deepest part of an ocean can be a shallow-water wave.

In a shallow-water wave, the fluid particles at a cross-section have the same flow velocity, the wave celerity depends upon the flow depth, and the vertical acceleration of the fluid particles is usually negligible compared to the horizontal acceleration. In a deep-water wave, the particle motion is negligible at depths equal to the wavelength from the surface, the horizontal and vertical accelerations are comparable in magnitude but decrease rapidly with distance from the surface, and the wave celerity depends on the wavelength,

A wave is called a *positive wave* if the wave surface is higher than the initial steady-state surface, and it is called a *negative wave* if the wave surface is lower than the steady-state surface.

If the fluid particles translate spatially with the wave, the wave is called *translatory*, e.g., surges, tides, floods; while, if there is no such translation, the wave is called a *stationary wave*, e.g., a sea wave.

A wave having just one rising or falling limb is called a *monoclinal wave*. A *solitary wave* has gradually rising and falling (or recession) limbs. A number of waves traveling in succession are called a *wave train*.

### 13-3 Examples of Transient Flows

Transient flow in an open channel is produced whenever the flow or the depth of flow or both are changed at a section. These changes may be planned or accidental, or these may be natural or produced by human action. Typical examples of open-channel transients are:

- Floods in the rivers, streams, and lakes produced by snow-melt or rain-storm; by opening or closing of control gates, or due to failure of dams, levees or other control structures;
- Surges in the channels caused by loading or unloading the turbines, starting or stopping the pumps, opening or closing the control gates;
- Surges in the navigation canals caused by the operation of locks;
- Waves in a river or a reservoir generated by a landslide;
- Lake and reservoir circulation caused by wind or density currents;
- Storm runoff in sewers, drainage channels, culverts and tunnel, and
- Tides in estuaries or inlets.

Depending upon the rate at which the flow or the depth changes, a bore or a shock may be formed during the transient conditions.

### 13-4 Surge Height and Celerity

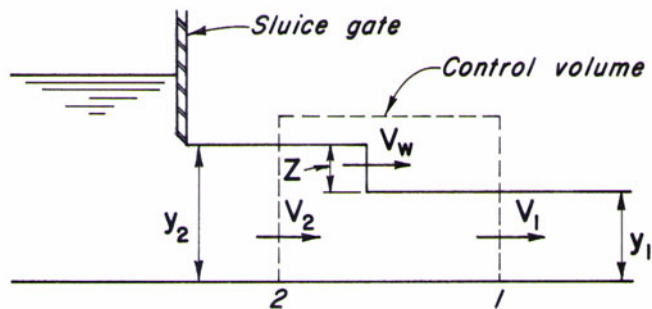
Expressions for the height and celerity of a surge wave generated by the opening of a sluice gate are derived in this section.

Let the channel flow be steady at time  $t = 0$  when a sluice gate located at the upstream end of the channel ([Fig. 13-2a](#)) is suddenly opened. This increases the flow suddenly from  $Q_1$  to  $Q_2$  and the flow increase produces a surge wave of height,  $z$ , which travels in the downstream direction. Let us designate the flow depth and the flow velocity to the right of the wave front (i.e., undisturbed conditions) by  $y_1$  and  $V_1$ , and the corresponding variables to the left of the wave front by  $y_2$  and  $V_2$  ([Fig. 13-2a](#)). If  $V_w$  is the *absolute wave velocity* and we assume that the wave shape does not change as it propagates in the channel, then the unsteady flow ([Fig. 13-2a](#)) may be converted into steady flow by superimposing velocity  $V_w$  on the control volume in the upstream direction ([Fig. 13-2b](#)). The velocity in the downstream direction is considered positive.

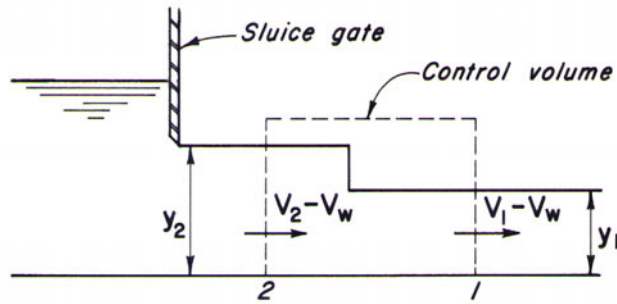
Referring to [Fig. 13-2b](#), the continuity equation may be written as

$$A_1 (V_1 - V_w) = A_2 (V_2 - V_w) \quad (13-3)$$

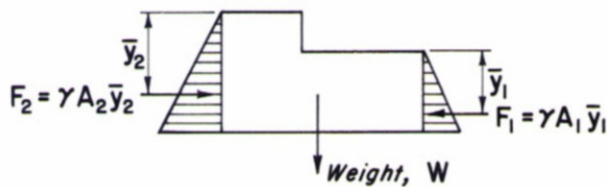
Let us assume the pressure distribution at sections 1 and 2 is hydrostatic and the channel bottom is horizontal, and frictionless. Then, the forces acting on the control volume ([Fig. 13-2c](#)) are:



(a) Unsteady flow



(b) Equivalent steady flow



(c) Freebody diagram of control volume

Fig. 13-2. Surge height and celerity.

$$\text{Force in the upstream direction, } F_1 = \gamma \bar{y}_1 A_1 \quad (13-4)$$

$$\text{Force in the downstream direction, } F_2 = \gamma \bar{y}_2 A_2 \quad (13-5)$$

in which  $\bar{y}_1$  and  $\bar{y}_2$  are the depths of the centroids of areas  $A_1$  and  $A_2$ .

The rate of change of momentum of the water in the control volume

$$\begin{aligned} &= \frac{\gamma}{g} A_1 (V_1 - V_w) [(V_1 - V_w) - (V_2 - V_w)] \\ &= \frac{\gamma}{g} A_1 (V_1 - V_w) (V_1 - V_2) \end{aligned} \quad (13-6)$$

The resultant force,  $F$ , acting on the water in the control volume in the downstream direction, is

$$F = F_2 - F_1 = \gamma (A_2 \bar{y}_2 - A_1 \bar{y}_1) \quad (13-7)$$

Applying Newton's second law of motion,

$$\frac{\gamma}{g} A_1 (V_1 - V_w) (V_1 - V_2) = \gamma (A_2 \bar{y}_2 - A_1 \bar{y}_1) \quad (13-8)$$

Eliminating  $V_2$  from Eqs. 13-3 and 13-8 and rearranging the resulting equation, we obtain

$$(V_1 - V_w)^2 = \frac{g A_2}{A_1 (A_2 - A_1)} (A_2 \bar{y}_2 - A_1 \bar{y}_1) \quad (13-9)$$

Since the wave is moving in the downstream direction, its velocity must be greater than the initial flow velocity  $V_1$ . Hence, it follows from Eq. 13-9 that

$$V_w = V_1 + \sqrt{\frac{g A_2}{A_1 (A_2 - A_1)} (A_2 \bar{y}_2 - A_1 \bar{y}_1)} \quad (13-10)$$

If there is no initial flow in the channel (i.e.,  $V_1 = 0$ ), then the absolute wave velocity  $V_w$  is equal to the radical term of Eq. 13-10. Transposing  $V_1$  to the left-hand side,

$$V_w - V_1 = \sqrt{\frac{g A_2}{A_1 (A_2 - A_1)} (A_2 \bar{y}_2 - A_1 \bar{y}_1)} \quad (13-11)$$

We previously defined the celerity,  $c$ , of a wave as its velocity relative to the medium in which it is traveling. Since  $V_w - V_1$  is the velocity of the wave relative to the initial flow velocity  $V_1$ , the following general expression for  $c$  is obtained from Eq. 13-11

$$c = \pm \sqrt{\frac{g A_2}{A_1 (A_2 - A_1)} (A_2 \bar{y}_2 - A_1 \bar{y}_1)} \quad (13-12)$$

A positive sign is used if the wave is traveling in the downstream direction, and a negative sign is used if it is traveling upstream.

The relationship between the velocities and the depths of flow at sections 1 and 2 is obtained by eliminating  $V_w$  from Eqs. 13-3 and 13-8, i.e.,

$$(A_2\bar{y}_2 - A_1\bar{y}_1) = \frac{A_1A_2}{g(A_2 - A_1)}(V_1 - V_2)^2 \quad (13-13)$$

The wave height,  $z$ , is equal to  $y_2 - y_1$ . If  $y_2 > y_1$ , then the wave is a positive wave, and if  $y_2 < y_1$ , then it is a negative wave.

There are five variables namely,  $y_1$ ,  $V_1$ ,  $y_2$ ,  $V_2$  and  $V_w$ , in Eqs. 13-3 and 13-13. The value of  $V_2$  or  $y_2$  may be determined by trial and error from these equations if the values of other three independent variables are known.

Note that Eqs. 13-12 and 13-13 are general and may be used for channels having any cross section. Let us now discuss how these equations are simplified for a rectangular channel.

### Rectangular Channel

For a rectangular channel having width,  $B$ ,  $\bar{y}_1 = \frac{1}{2}y_1$ ;  $\bar{y}_2 = \frac{1}{2}y_2$ ;  $A_1 = By_1$ ; and  $A_2 = By_2$ . Substituting these expressions into Eq. 13-12 and simplifying the resulting equation,

$$c = \sqrt{\frac{gy_2}{2y_1}(y_1 + y_2)} \quad (13-14)$$

If the wave height is small as compared to the flow depth,  $y$ , then  $y_1 \approx y_2 \approx y$ . Hence, it follows from Eq. 13-14 that

$$c = \sqrt{gy} \quad (13-15)$$

For a rectangular channel, the continuity equation (Eq. 13-3) may be written as

$$By_1(V_1 - V_w) = By_2(V_2 - V_w) \quad (13-16)$$

from which it follows that

$$V_w = \frac{y_1V_1 - y_2V_2}{y_1 - y_2} \quad (13-17)$$

Noting that for a wave traveling in the downstream direction,  $V_w = V_1 + c$ , substituting expression for  $c$  from Eq. 13-14 and eliminating  $V_w$  from the resulting equation and Eq. 13-17, we obtain

$$(V_1 - V_2)^2 = \frac{g(y_1 - y_2)}{2y_1y_2}(y_1^2 - y_2^2) \quad (13-18)$$

This equation, derived by Johnson [1922], may be solved by trial and error to determine the surge height.

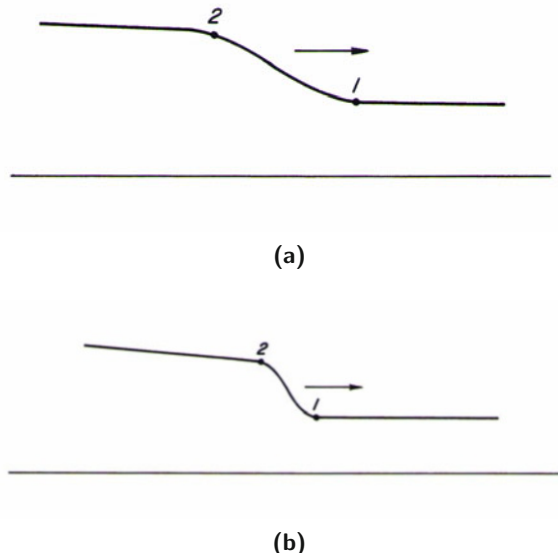


**Fig. 13-3.** Variation of the wave front of a positive wave.

Figure 13-3 shows a positive wave traveling in the downstream direction. Because the depth at the leading edge of the wave front (point 1) is smaller than at the trailing edge (point 2), it follows from Eq. 13-15 that the wave celerity is higher at point 2 than that at point 1. Thus, as the wave travels, the trailing edge of the wave front tends to overtake the front edge. Therefore, the wave front gradually becomes steeper until a bore forms. Using a similar argument, it is clear that a negative wave front flattens as it travels in a channel.

For the subcritical flows, the Froude number,  $F < 1$ , i.e.,

$$\frac{V}{\sqrt{gy}} < 1 \quad (13-19)$$

or

$$V < \sqrt{gy} \quad (13-20)$$

On the basis of Eq. 13-15, Eq. 13-20 may be written as

$$V < c \quad (13-21)$$

Hence, it follows from Eq. 13-2 and 13-21 that  $V_w$  is negative if the wave is traveling in the upstream direction; i.e., a disturbance travels both in the upstream and in the downstream direction. For supercritical flows ( $F > 1$ ), however, a wave travels only in the downstream direction, since the flow velocity is greater than the wave celerity and  $V_w$  is always positive.

## 13-5 Governing Equations

The dynamic and continuity equations usually referred to as Saint-Venant equations [de Saint-Venant, 1871, 1949] describing the one-dimensional transient flows are derived in this section. For a general derivation of these equations, see Strelkoff [1969]; Yen [1973]; Mahmood and Yevjevich [1975]; and Cunge et al. [1980].

The following assumptions are made in deriving these equations [de Saint-Venant, 1949; Henderson, 1966]:

1. The channel bottom slope is small so that  $\sin \theta \simeq \tan \theta \simeq \theta$  and  $\cos \theta \simeq 1$ , where  $\theta$  is the angle between the channel bottom and the horizontal axis.
2. The pressure distribution at a channel section is hydrostatic. This is true if the vertical acceleration is small, i.e., if the variation of water surface with distance is gradual.
3. The transient-state friction losses may be computed by using the equations for the steady-state friction losses.
4. The velocity distribution at a channel section is uniform.
5. The channel is straight and prismatic.

Let us consider the control volume shown in Fig. 13-4. The  $x$ -axis lies along the bottom of the channel and is positive in the downstream direction. The depth of flow,  $y$ , is measured vertically from the channel bottom. Thus, the  $x$  and  $y$  axes are not orthogonal. However, as the channel is assumed to have a small bottom slope, the error due to this discrepancy is insignificant.

### Continuity Equation

Let us consider the inflow into and outflow from the control volume of Fig. 13-4 in which  $\gamma$  is the specific weight of the water.

The rate of mass inflow into the control volume

$$= \frac{\gamma}{g} AV \quad (13-22)$$

The rate of mass outflow from the control volume

$$= \frac{\gamma}{g} \left( A + \frac{\partial A}{\partial x} \Delta x \right) \left( V + \frac{\partial V}{\partial x} \Delta x \right) \quad (13-23)$$

Hence, the net rate of mass inflow

$$= \frac{\gamma}{g} AV - \frac{\gamma}{g} \left( A + \frac{\partial A}{\partial x} \Delta x \right) \left( V + \frac{\partial V}{\partial x} \Delta x \right)$$

Neglecting the second-order terms,

$$\text{Net rate of mass inflow} = -\frac{\gamma}{g} V \frac{\partial A}{\partial x} \Delta x - \frac{\gamma}{g} A \frac{\partial V}{\partial x} \Delta x \quad (13-24)$$

The rate of increase of the mass of the control volume

$$= \frac{\gamma}{g} \frac{\partial A}{\partial t} \Delta x \quad (13-25)$$

The time rate of increase of the mass of the control volume must equal the net rate of mass inflow into the control volume. Hence, it follows from Eqs. 13-24 and 13-25 that

$$\frac{\gamma}{g} \frac{\partial A}{\partial t} \Delta x = -\frac{\gamma}{g} V \frac{\partial A}{\partial x} \Delta x - \frac{\gamma}{g} A \frac{\partial V}{\partial x} \Delta x \quad (13-26)$$

Dividing both sides by  $(\gamma/g)\Delta x$  and rearranging, Eq. 13-26 becomes

$$\frac{\partial A}{\partial t} + V \frac{\partial A}{\partial x} + A \frac{\partial V}{\partial x} = 0 \quad (13-27)$$

Since the channel is assumed prismatic, the flow area,  $A$ , is a known function of depth,  $y$ . Therefore, the derivatives of  $A$  may be expressed in terms of  $y$  as follows:

$$\begin{aligned} \frac{\partial A}{\partial x} &= \frac{dA}{dy} \frac{\partial y}{\partial x} = B(y) \frac{\partial y}{\partial x} \\ \frac{\partial A}{\partial t} &= \frac{dA}{dy} \frac{\partial y}{\partial t} = B(y) \frac{\partial y}{\partial t} \end{aligned} \quad (13-28)$$

For a channel having continuous side slopes,  $dA/dy$  is equal to the channel width  $B$  at depth  $y$ . If the values of  $A(y)$  and  $B(y)$  are obtained by independent measurements, the measurement error may cause  $B(y)$  to be different from the values of channel width obtained by differentiating area  $A(y)$  with respect to depth,  $y$ . For numerical stability, [Amein and Fang, 1970] it is important that  $A(y)$  and  $B(y)$  are compatible, i.e., if either  $A(y)$  or  $B(y)$  is obtained by measurement, then the other is determined by calculus.

Substituting Eq. 13-28 into Eq. 13-27, we obtain

$$\frac{\partial y}{\partial t} + D \frac{\partial V}{\partial x} + V \frac{\partial y}{\partial x} = 0 \quad (13-29)$$

in which hydraulic depth,  $D = A/B$ . Since discharge  $Q = VA$ , we can write

$$\frac{\partial Q}{\partial x} = V \frac{\partial A}{\partial x} + A \frac{\partial V}{\partial x} \quad (13-30)$$

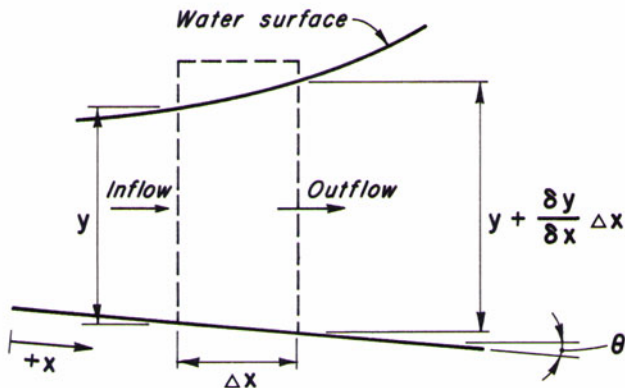
On the basis of Eq. 13-28, Eq. 13-30 becomes

$$\frac{\partial Q}{\partial x} = BV \frac{\partial y}{\partial x} + A \frac{\partial V}{\partial x} \quad (13-31)$$

Hence, it follows from Eqs. 13-29 and 13-31 that

$$\frac{\partial Q}{\partial x} + B \frac{\partial y}{\partial t} = 0 \quad (13-32)$$

This equation is referred to as the *continuity equation*.

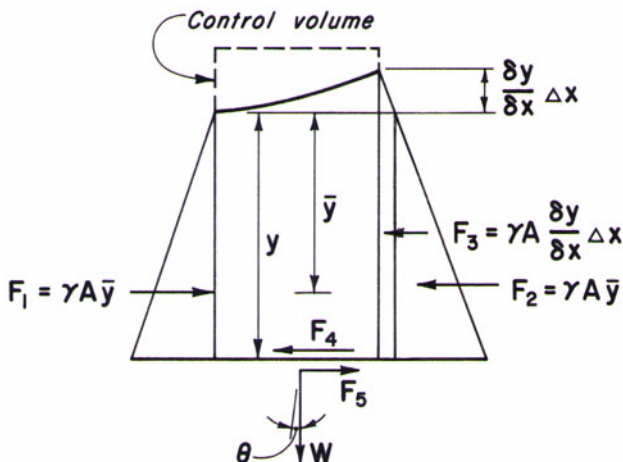


$$\text{Distance : } x \quad x + \Delta x$$

$$\text{Flow area : } A \quad A + \frac{\partial A}{\partial x} \Delta x$$

$$\text{Velocity : } V \quad V + \frac{\partial V}{\partial x} \Delta x$$

(a)



(b) Freebody diagram

Fig. 13-4. Notation for dynamic and continuity equations.

## Dynamic Equation

The following forces are acting on the water in the control volume, shown in Fig. 13-4b:

$$\begin{aligned} F_1 &= F_2 = \gamma A \bar{y} \\ F_3 &= \gamma A \frac{\partial y}{\partial x} \Delta x \\ F_4 &= \gamma A S_f \Delta x \end{aligned} \quad (13-33)$$

Note that the pressure force acting on the downstream face is divided into two parts,  $F_2$  and  $F_3$ , and the terms of higher order are not included in the expression for  $F_3$ . In Fig. 13-4b,  $F_1$ ,  $F_2$ , and  $F_3$  are the pressure forces;  $F_4$  is the friction force;  $F_5$  is the  $x$ -component of the weight of the water in the control volume;  $\theta$  is the angle between the channel bottom and horizontal axis (positive downward); and  $S_f$  is the slope of the energy grade line.

The value of  $S_f$  may be computed by using any standard equation for the steady-state losses, such as Manning or Chezy equation. Since  $\theta$  is assumed to be small,  $\sin \theta \simeq \theta \simeq S_o$ , in which  $S_o$  = bottom slope. Hence,

$$F_5 = \gamma A \Delta x S_o \quad (13-34)$$

Referring to Fig. 13-4b, the resultant force acting on the water in the control volume in the positive  $x$ -direction is  $F = \sum F_i = F_1 - F_2 - F_3 - F_4 + F_5$ . Substituting expressions for  $F_1$  to  $F_5$  from Eqs. 13-33 to 13-34, we obtain

$$F = -\gamma A \frac{\partial y}{\partial x} \Delta x + \gamma A S_o \Delta x - \gamma A S_f \Delta x \quad (13-35)$$

$$\text{Momentum entering the control volume} = \frac{\gamma}{g} A V^2 \quad (13-36)$$

$$\text{Momentum leaving the control volume} = \frac{\gamma}{g} \left[ A V^2 + \frac{\partial}{\partial x} (A V^2) \Delta x \right] \quad (13-37)$$

Therefore, net influx of momentum into the control volume

$$= -\frac{\gamma}{g} \frac{\partial}{\partial x} (A V^2) \Delta x \quad (13-38)$$

The time rate of increase of momentum

$$= \frac{\partial}{\partial t} \left( \frac{\gamma}{g} A V \Delta x \right) \quad (13-39)$$

According to the law of conservation of momentum, the time rate of increase of momentum is equal to the net rate of momentum influx plus the sum of

the forces acting on the water in the control volume. Hence, it follows from Eqs. 13-35, 13-38, and 13-39 that

$$\frac{\partial}{\partial t} \left( \frac{\gamma}{g} A V \Delta x \right) = -\frac{\gamma}{g} \frac{\partial}{\partial x} (AV^2) \Delta x - \gamma A \frac{\partial y}{\partial x} \Delta x + \gamma A S_o \Delta x - \gamma A S_f \Delta x \quad (13-40)$$

Dividing throughout by  $(\gamma/g)\Delta x$  and simplifying, Eq. 13-40 becomes

$$\frac{\partial}{\partial t} (AV) + \frac{\partial}{\partial x} (AV^2) + gA \frac{\partial y}{\partial x} = gA (S_o - S_f) \quad (13-41)$$

Expanding the two terms on the left-hand side, dividing by  $A$ , and rearranging the terms yield

$$g \frac{\partial y}{\partial x} + V \frac{\partial V}{\partial x} + \frac{\partial V}{\partial t} + \frac{V}{A} \left( \frac{\partial A}{\partial t} + V \frac{\partial A}{\partial x} + A \frac{\partial V}{\partial x} \right) = g (S_o - S_f) \quad (13-42)$$

On the basis of Eq. 13-27, the sum of the terms within the parentheses on the left-hand side of Eq. 13-42 is equal to zero. Hence, Eq. 13-42 becomes

$$g \frac{\partial y}{\partial x} + \frac{\partial V}{\partial t} + V \frac{\partial V}{\partial x} = g (S_o - S_f) \quad (13-43)$$

The terms of Eq. 13-43 may be rearranged as follows to indicate the significance of each term for a particular type of flow [Henderson, 1966]:

$$\underbrace{S_f = S_o}_{\text{Steady, uniform}} - \underbrace{\frac{\partial y}{\partial x} - \left( \frac{V}{g} \right) \frac{\partial V}{\partial x}}_{\text{Steady, nonuniform}} - \underbrace{\left( \frac{1}{g} \right) \frac{\partial V}{\partial t}}_{\text{Unsteady, nonuniform}} \quad (13-44)$$

Equations 13-29 and 13-43 are referred to as the St. Venant equations. Note that these equations are derived assuming the channel to be prismatic having no lateral inflow or outflow. Proceeding similarly, these equations may be derived for non-prismatic channels having lateral inflow or outflow (Problem 13-7).

The equations presented above are in non-conservation form. For the numerical schemes requiring the equations to be in the conservation form, the continuity and momentum equations for prismatic channels [Cunge et al., 1980] may be written as

$$\frac{\partial A}{\partial t} + \frac{\partial Q}{\partial x} = 0 \quad (13-45)$$

$$\frac{\partial Q}{\partial t} + \frac{\partial}{\partial x} \left( \frac{Q^2}{A} + gI \right) = gA (S_o - S_f) \quad (13-46)$$

where

$$I = \int_0^{y(x)} (y - \eta) \sigma(\eta) d\eta \quad (13-47)$$

in which  $\sigma(\eta)$  = width of the cross section and  $\eta$  = depth integration variable. Strictly speaking, these equations are not in the conservation form because of the presence of the source terms. The conservation form of equations is superior in conserving the mass and momentum as compared to the non-conservation form and should be preferred.

## 13-6 Methods of Solution

By neglecting different terms of the governing equations depending on their magnitude relative to the other terms, several analytical procedures have been developed to analyze unsteady flows [Cunge, 1969, Ponce and Simon, 1977; Ponce and Yevjevich, 1978 and Cunge et al., 1980]. However, if all the terms are retained, then the following numerical methods may be used for the solution of the governing equations:

- Method of characteristics.
- Finite-difference methods.
- Finite-element method.

As discussed in Chapter 3, the equations in the method of characteristics [Stoker, 1957; Abbott, 1966; Cunge, et al., 1980], are first converted into characteristic form, which are then solved by a finite-difference scheme. In the finite-difference methods [Henderson, 1966; Abbott, 1979; Katopodes and Strelkoff, 1978 and Cunge et al., 1980], the partial derivatives are replaced by finite-difference quotients, and the resulting algebraic equations are then solved to determine the transient conditions. In the finite-element method [Partridge and Brebbia, 1976; Cooley and Moin, 1976; Katopodes and Strelkoff, 1979 and Katopodes, 1984], the system is divided into a number of elements, and the partial differential equations are integrated at the nodal points of the elements.

The application of the finite-element method in open-channel transients is limited and is not discussed further herein. The method of characteristics fails due to the convergence of the characteristic curves once a bore forms. Therefore, the bore has to be isolated and treated separately in the computations. The isolation of a bore is cumbersome, especially if there are several geometrical changes in the channel system since the transmission and reflection of the bore at each change has to be considered. Therefore, a computational procedure is desirable in which the formation of a bore does not require special treatment. Based on the advances made in gas dynamics, a number of finite-difference schemes that do not require isolation of the bore have been proposed. Such schemes are presented in Sections 13-8, 13-10, and 13-11.

Depending on the finite-difference approximation used to replace the partial derivatives, two types of finite-difference schemes are obtained. If the

finite-difference approximations for the spatial derivatives (i.e., partial derivatives with respect to  $x$ ) are in terms of the quantities at the known time level, then the resulting equations may be directly solved for each computational node one at a time. In other words, the unknown variables are explicitly expressed in terms of the known variables. Such methods are referred to as explicit methods [ Richtmyer and Morton, 1967; Cunge et al., 1980; Anderson et al., 1984]. In the implicit methods, the finite-difference approximations for the spatial derivatives are in terms of the unknown variables, and the algebraic equations for the entire system are solved simultaneously. Details of these methods are presented in the following sections.

### 13-7 Method of Characteristics

As described previously, in this method, the St. Venant equations are first converted into the characteristic equations, which are then solved along the characteristic curves. The method is unsuitable for systems having numerous geometrical changes, and it fails because of the convergence of the characteristic curves whenever a bore or a shock forms. Although quite popular in the 1960s, this method has been replaced by the finite-difference methods. However, in some finite-difference methods, the characteristic equations are utilized to develop the boundary conditions. Herein, only equations that are used in the next section are presented; readers interested in the details of the method should see Stoker [1957]; Abbott [1966] and Mahmood and Yevjevich [1975].

Multiplying Eq. 13-29 by an unknown multiplier,  $\lambda$ , and adding it to Eq. 13-43, we obtain

$$\left[ \frac{\partial V}{\partial t} + (V + \lambda D) \frac{\partial V}{\partial x} \right] + \lambda \left[ \frac{\partial y}{\partial t} + \left( V + \frac{g}{\lambda} \right) \frac{\partial y}{\partial x} \right] = g(S_o - S_f) \quad (13-48)$$

Now, if we define the unknown multiplier  $\lambda$  such that  $V + \lambda D = dx/dt = V + g/\lambda$ , we obtain  $\lambda = \pm\sqrt{gB/A}$ . The celerity of a gravity wave in free-surface flows is given by the expression

$$c = \sqrt{\frac{gA}{B}} \quad (13-49)$$

Therefore, by defining  $\lambda = g/c$ , the preceding expression for  $dx/dt$  may be written as

$$\frac{dx}{dt} = V + c \quad (13-50)$$

By utilizing Eq. 13-50 and the expressions for the total derivatives of  $V$  and  $y$ , we may write Eq. 13-48 as

$$\frac{dV}{dt} + \frac{g}{c} \frac{dy}{dt} = g(S_o - S_f) \quad (13-51)$$

Similarly, by defining  $\lambda = -g/c$ , we may write

$$\frac{dx}{dt} = V - c \quad (13-52)$$

Then, by using Eq. 13-52 and the expressions for the total derivatives, Eq. 13-48 becomes

$$\frac{dV}{dt} - \frac{g}{c} \frac{dy}{dt} = g(S_o - S_f) \quad (13-53)$$

Note that Eq. 13-51 is valid if Eq. 13-50 is satisfied, and Eq. 13-53 is valid if Eq. 13-52 is satisfied. Equations 13-50 and 13-52 plot as characteristic curves (Fig. 13-5) in the  $x-t$  plane. Referring to this figure and noting the preceding conditions for the validity of Eqs. 13-51 and 13-53, it is clear that Eq. 13-51 is valid along the positive characteristic curve,  $C^+$ , and Eq. 13-53 is valid along the negative characteristic curve,  $C^-$ .

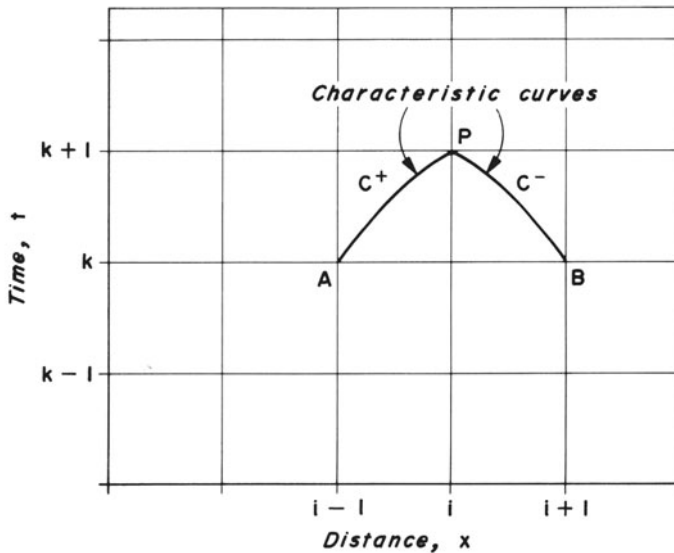


**Fig. 13-5.** Notation for positive and negative characteristic equations.

Multiplying Eqs. 13-51 and 13-53 by  $dt$  and integrating along the characteristic curves  $AP$  and  $BP$ , we obtain

$$\int_A^P dV + \int_A^P \frac{g}{c} dy = \int_A^P g(S_o - S_f) dt \quad (13-54)$$

and

$$\int_B^P dV - \int_B^P \frac{g}{c} dy = \int_B^P g (S_o - S_f) dt \quad (13-55)$$

Note that, we have not made any approximation whatsoever in the derivation of Eqs. 13-54 and 13-55. However, approximations become necessary for the integration of various terms of these equations, as discussed in the following paragraphs.

To evaluate the integrals of the second term on the left-hand side and the term on the right-hand side of Eqs. 13-54, the variation of  $V$  and  $y$  along the characteristic curves should be known. However,  $V$  and  $y$  are the unknowns we want to compute. Therefore, the integrals of these terms cannot be directly computed. We may, however, integrate these terms by making an approximation. For example, we may use the values of  $c$  and  $S_f$  computed by using values of  $V$  and  $y$  at the known time level, and assume that these computed values of  $c$  and  $S_f$  are constant from  $A$  to  $P$  and from  $B$  to  $P$  (Fig. 13-5). Hence, Eqs. 13-54 may be written as

$$V_P - V_A + \left(\frac{g}{c}\right)_A (y_P - y_A) = g (S_o - S_f)_A \Delta t \quad (13-56)$$

and

$$V_P - V_B - \left(\frac{g}{c}\right)_B (y_P - y_B) = g (S_o - S_f)_B \Delta t \quad (13-57)$$

in which subscripts  $P$ ,  $A$ , and  $B$  refer to the values at the corresponding grid points in the  $x$ - $t$  plane (Fig. 13-5).

Let us assume that the characteristics pass through the grid point adjacent to the boundary node. As discussed in later sections, accuracy considerations dictate that the spatial grid spacing,  $\Delta x$ , and the time interval,  $\Delta t$ , be selected such that the characteristics pass as near to the adjacent spatial nodes as possible.

To use the characteristics equations in the development of the boundary conditions, we will use the following notation: A subscript is used to denote the grid point in the  $x$ -direction and, a superscript to denote the grid point in the  $t$ -direction. For example,  $V_i^k$  refers to the flow velocity at the  $i$ th section and at the  $k$ th time level (Fig. 13-6). The superscript  $k$  is used for the time level at which the flow conditions are known (referred to as the “known time level”) and superscript  $k+1$ , for the time level at which the flow conditions are unknown (referred to as the “unknown time level”).

By using this notation and combining the known quantities, Eqs. 13-56 and 13-57 may be written as

$$V_i^{k+1} = C_p - C_{a_{i-1}} y_i^{k+1} \quad (13-58)$$

and

$$V_i^{k+1} = C_n + C_{a_{i+1}} y_i^{k+1} \quad (13-59)$$

in which

$$\begin{aligned}
 C_p &= V_{i-1}^k + C_{a_{i-1}} y_{i-1}^k + g (S_o - S_f)_{i-1} \Delta t \\
 C_n &= V_{i+1}^k - C_{a_{i+1}} y_{i+1}^k + g (S_o - S_f)_{i+1} \Delta t \\
 C_a &= \frac{g}{c}
 \end{aligned} \tag{13-60}$$

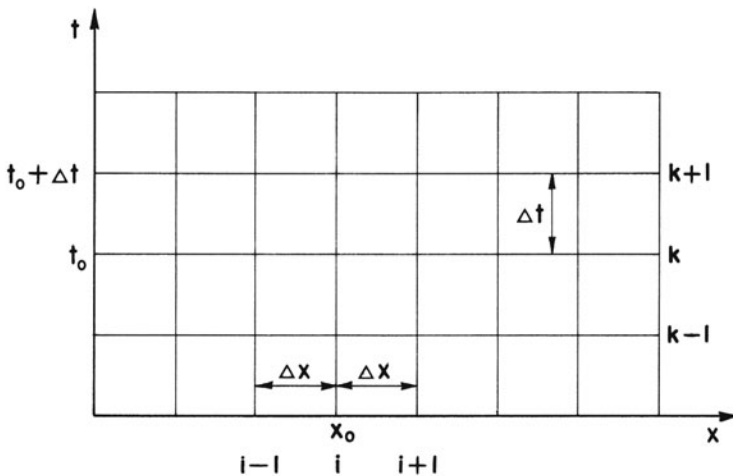


**Fig. 13-6.** Notation for computational grid.

### 13-8 Explicit Finite-Difference Methods

Several explicit finite-difference methods have been used for the analysis of unsteady, free-surface flows. We present details of one of these methods, called the Lax diffusive scheme [Martin and DeFazio, 1969; Mahmood and Yevjevich, 1975; and Chaudhry, 1976]; readers interested in more schemes should see Strelkoff, [1970]; Cunge et al. [1980]; Fennema and Chaudhry [1986], and Chaudhry [2008].

Lax scheme is very simple to program and yields satisfactory results. In addition, a bore does not have to be isolated in the computations. However, the main limitation of the scheme is that short time intervals may be needed for stability and steep wave fronts may be diffused.

In this scheme, the partial derivatives and coefficients  $D$  and  $S_f$  of the governing equations are approximated as follows:

$$\begin{aligned}
\frac{\partial y}{\partial t} &= \frac{y_i^{k+1} - y_i^*}{\Delta t} \\
\frac{\partial V}{\partial t} &= \frac{V_i^{k+1} - V_i^*}{\Delta t} \\
\frac{\partial y}{\partial x} &= \frac{y_{i+1}^k - y_{i-1}^k}{2\Delta x} \\
\frac{\partial V}{\partial x} &= \frac{V_{i+1}^k - V_{i-1}^k}{2\Delta x} \\
D_i^* &= 0.5(D_{i-1}^k + D_{i+1}^k) \\
S_f^* &= 0.5(S_{f_{i-1}}^k + S_{f_{i+1}}^k)
\end{aligned} \tag{13-61}$$

in which

$$\begin{aligned}
y_i^* &= 0.5(y_{i-1}^k + y_{i+1}^k) \\
V_i^* &= 0.5(V_{i-1}^k + V_{i+1}^k)
\end{aligned} \tag{13-62}$$

Replacing the partial derivatives of the governing equations (Eqs. 13-29 and 13-43) by these finite-difference approximations and the coefficient  $D$  and the slope  $S_f$  by the expressions of Eq. 13-61 and simplifying, we obtain

$$\begin{aligned}
y_i^{k+1} &= y_i^* - 0.5 \frac{\Delta t}{\Delta x} D_i^* (V_{i+1}^k - V_{i-1}^k) \\
&\quad - 0.5 \frac{\Delta t}{\Delta x} V_i^* (y_{i+1}^k - y_{i-1}^k)
\end{aligned} \tag{13-63}$$

$$\begin{aligned}
V_i^{k+1} &= V_i^* - 0.5 \frac{\Delta t}{\Delta x} g (y_{i+1}^k - y_{i-1}^k) \\
&\quad - 0.5 \frac{\Delta t}{\Delta x} V_i^* (V_{i+1}^k - V_{i-1}^k) + g \Delta t (S_o - S_f^*)
\end{aligned} \tag{13-64}$$

Note that the  $x$ -derivatives of the St. Venant equations are replaced by finite-difference approximations evaluated at time  $t_o$  (Fig. 13-6) and the coefficients,  $D$  and  $S_f$ , are also evaluated at time  $t_o$ . Thus, we have two linear algebraic equations relating the two unknowns  $V_i^{k+1}$  and  $y_i^{k+1}$  at point  $(i, k+1)$  to the known conditions at points  $(i-1, k)$ ,  $(i, k)$ , and  $(i+1, k)$ . Because of this explicit relationship, the method is called *explicit finite-difference method*.

It is clear (Fig. 13-6) that the coordinates of points  $(i, k+1)$ ,  $(i, k)$ ,  $(i-1, k)$ , and  $(i+1, k)$  are  $(x_o, t_o + \Delta t)$ ,  $(x_o, t_o)$ ,  $(x_o - \Delta x, t_o)$ , and  $(x_o + \Delta x, t_o)$ , respectively. By expanding the terms of Eqs. 13-63 and 13-64 in a Taylor series, e.g.,  $y_i^{k+1} = y(x_o, t_o) + \Delta t \partial y / \partial t + [(\Delta t)^2 / 2!] (\partial^2 y / \partial t^2)$ , and comparing with Eqs. 13-29 and 13-43, it can be shown that this difference

scheme introduces additional diffusion-like terms,  $\frac{1}{2} \left[ (\Delta x)^2 / \Delta t \right] (\partial^2 y / \partial x^2)$  and  $\frac{1}{2} \left[ (\Delta x)^2 / \Delta t \right] (\partial^2 V / \partial x^2)$ . Therefore, this scheme is called a *diffusive scheme*.

Note that Eqs. 13-63 and 13-64 are for the interior nodes only, i.e., at  $i = 2, 3, \dots, n$ . Boundary nodes need special treatment, as discussed in the following paragraphs.

## Boundary Conditions

As discussed earlier, Eqs. 13-63 and 13-64 are used to determine the conditions at the interior nodes. At the boundaries, however, special boundary conditions are developed by solving the positive or negative characteristic equations, or both, simultaneously with the conditions imposed by the boundary. The positive characteristic equation, Eq. 13-58, is used for a downstream boundary, and the negative characteristic equation, Eq. 13-59, is used for an upstream boundary.

Two subscripts are used herein to designate variables at various sections. The first subscript refers to the channel, and the second refers to the section number. For example, subscript  $(i, 1)$  refers to the first section on the  $i$ th channel and subscript  $(i, n + 1)$  is for the last section on the  $i$ th channel divided into  $n$  reaches. Note that superscript  $k + 1$  designates the unknown quantities at time  $t_o + \Delta t$  (Fig. 13-6).

Four common boundary conditions are derived in this section; other boundary conditions may be developed similarly.

### **Constant-Head Upstream Reservoir**

If the entrance loss at the reservoir is  $C_u (V_{i,1}^{k+1})^2 / (2g)$ , then referring to Fig. 13-7a,

$$y_{res} = y_{i,1}^{k+1} + (1 + C_u) \frac{(V_{i,1}^{k+1})^2}{2g} \quad (13-65)$$

Substituting for  $y_{i,1}^{k+1}$  from Eq. 13-59 into Eq. 13-65 and solving for  $V_{i,1}^{k+1}$ , we obtain

$$V_{i,1}^{k+1} = \frac{-1 + \sqrt{1 + 4C_r(C_n + C_a y_{res})}}{2C_r} \quad (13-66)$$

in which

$$C_r = C_a (1 + C_u) / (2g) \quad (13-67)$$

Now  $y_{i,1}^{k+1}$  can be determined from Eq. 13-59.

If the head losses and the velocity head at the channel entrance are negligible, then  $y_{i,1}^{k+1} = y_{res}$  and  $V_{i,1}^{k+1}$  may be computed from Eq. 13-59. Note that Eqs. 13-65 and 13-66 are valid for the positive flows only; similar equations may be written for the negative flows.

### **Constant-Head Downstream Reservoir**

If the head loss at the reservoir entrance is  $C_v (V_{i,n+1}^{k+1})^2 / 2g$ , then, referring to Fig. 13-7b,

$$y_{i,n+1}^{k+1} = y_{res} - \frac{(1 - C_v) (V_{i,n+1}^{k+1})^2}{2g} \quad (13-68)$$

in which  $y_{res}$  = reservoir depth above the channel bottom, and  $C_v$  = entrance-loss coefficient. Simultaneous solution of Eqs. 13-58 and 13-68 yields

$$V_{i,n+1}^{k+1} = \frac{1 - \sqrt{1 - 4C_r (C_p - C_a y_{res})}}{2C_r} \quad (13-69)$$

in which  $C_r = (1 - C_v) C_a / 2g$ .

If the velocity head is lost at the reservoir entrance, then  $C_v = 1$ , and Eq. 13-69 cannot be used since it results in division by zero. In such a case, the following equation may be used:

$$y_{i,n+1}^{k+1} = y_{res} \quad (13-70)$$

$V_{i,n+1}^{k+1}$  is then determined from Eq. 13-58.

### **Specified Discharge at Channel End**

Discharge may be changed at the upstream or at the downstream end of the channel due to load acceptance or rejection by hydraulic turbines, starting or stopping of pumps, or opening or closing of control gates; or, it may be constant with respect to time.

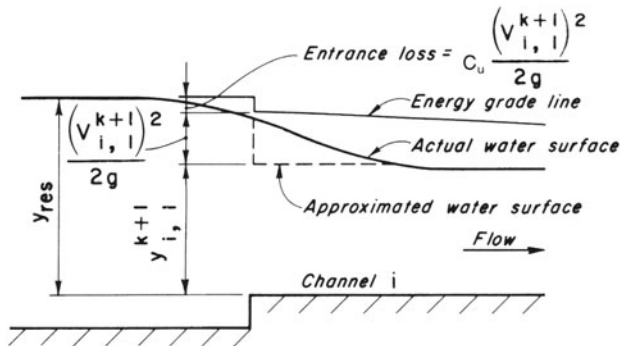
The discharge at the channel ends may be specified at discrete times in a tabular form or as a function of time, i.e.,  $Q = Q(t)$ . Thus, discharge  $Q_{i,j}^{k+1}$  at the end of time step is known. Now,

$$Q_{i,j}^{k+1} = A (y_{i,j}^{k+1}) V_{i,j}^{k+1} = Q (t^{k+1}) \quad (13-71)$$

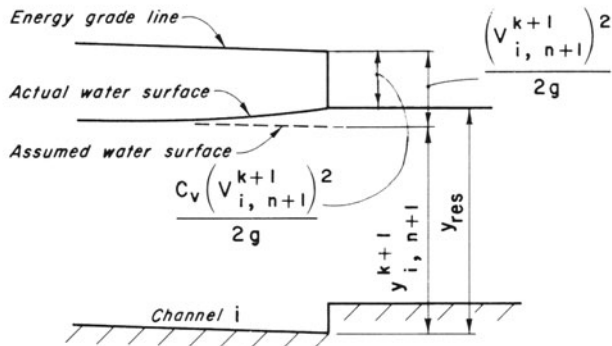
in which  $A (y_{i,j}^{k+1})$  denotes the flow area at depth  $y_{i,j}^{k+1}$  and  $Q (t^{k+1})$  denotes the discharge at time  $t^{k+1}$  and section  $(i, j)$  refers to the sections at the upstream or at the downstream end of the channel. To determine  $y_{i,j}^{k+1}$  and  $V_{i,j}^{k+1}$ , Eqs. 13-58 and 13-71 are solved by an iterative procedure for the downstream end and Eqs. 13-59 and 13-71, for the upstream end.

### **Junction of Two Channels**

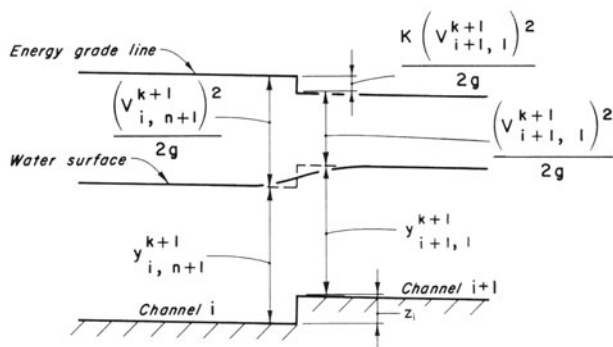
A junction of two channels where outflow of the channel upstream of the junction is inflow into the channel downstream of the junction is called a series junction.



(a) Upstream reservoir



(b) Downstream reservoir



(c) Junction of two channels

Fig. 13-7. Notation for boundary conditions.

To develop the boundary conditions for a series junction, we solve the energy and continuity equations at the junction with the positive and negative characteristic equations.

Referring to Fig. 13-7c, the energy equation at the junction may be written as

$$y_{i,n+1}^{k+1} + \frac{(V_{i,n+1}^{k+1})^2}{2g} = z_i + y_{i+1,1}^{k+1} + (1+K) \frac{(V_{i+1,1}^{k+1})^2}{2g} \quad (13-72)$$

in which  $K$  is the coefficient of head losses at the junction, and  $z_i$  = rise or drop in the channel bottom = (invert elevation of the  $(i+1)^{th}$  channel) - (invert elevation of the  $i^{th}$  channel).

The negative characteristic equations for section  $(i+1, 1)$

$$V_{i+1,1}^{k+1} = C_n + C_{a_{i+1}} y_{i+1,1}^{k+1} \quad (13-73)$$

The positive characteristic equation for  $(i, n+1)$

$$V_{i,n+1}^{k+1} = C_p - C_{a_i} y_{i,n+1}^{k+1} \quad (13-74)$$

The continuity equation at the junction may be written as

$$A(y_{i,n+1}^{k+1}) V_{i,n+1}^{k+1} = A(y_{i+1,1}^{k+1}) V_{i+1,1}^{k+1} \quad (13-75)$$

There are four unknowns, namely,  $y_{i,n+1}^{k+1}$ ,  $y_{i+1,1}^{k+1}$ ,  $V_{i,n+1}^{k+1}$  and  $V_{i+1,1}^{k+1}$ , in Eqs. 13-72 to 13-75. These unknowns may be determined by solving these equations by the Newton-Raphson method as follows:

To simplify the presentation, let us designate

$$\begin{aligned} y_{i,n+1}^{k+1} &= x_1 \\ y_{i+1,1}^{k+1} &= x_2 \\ V_{i,n+1}^{k+1} &= x_3 \\ V_{i+1,1}^{k+1} &= x_4 \end{aligned} \quad (13-76)$$

Equations 13-72 to 13-75 may then be written as

$$F_1 = x_1 - x_2 + \frac{x_3^2}{2g} - (1+K) \frac{x_4^2}{2g} - z_i = 0 \quad (13-77)$$

$$F_2 = -C_{a_{i+1}} x_2 + x_4 - C_n = 0 \quad (13-78)$$

$$F_3 = C_{a_i} x_1 + x_3 - C_p = 0 \quad (13-79)$$

$$F_4 = A_i(x_1) x_3 - A_{i+1}(x_2) x_4 = 0 \quad (13-80)$$

in which  $F_1$ ,  $F_2$ ,  $F_3$ , and  $F_4$  are functions of  $x_1$ ,  $x_2$ ,  $x_3$  and  $x_4$ , and  $A_i(x_1)$  and  $A_{i+1}(x_2)$  denote that  $A_i$  and  $A_{i+1}$  are functions of  $x_1$  and  $x_2$ , respectively.

Neglecting the second- and higher-order terms,  $F$  may be expanded in the Taylor series as

$$F = F^{(0)} + \left\{ \frac{\partial F}{\partial x_1} \Delta x_1 + \frac{\partial F}{\partial x_2} \Delta x_2 + \frac{\partial F}{\partial x_3} \Delta x_3 + \frac{\partial F}{\partial x_4} \Delta x_4 \right\}^{(o)} = 0 \quad (13-81)$$

or

$$\left\{ \frac{\partial F}{\partial x_1} \Delta x_1 + \frac{\partial F}{\partial x_2} \Delta x_2 + \frac{\partial F}{\partial x_3} \Delta x_3 + \frac{\partial F}{\partial x_4} \Delta x_4 \right\}^{(o)} = -F^{(o)} \quad (13-82)$$

in which the derivatives  $\partial F / \partial x_1$ ,  $\partial F / \partial x_2$ ,  $\partial F / \partial x_3$ ,  $\partial F / \partial x_4$  and the function  $F^{(o)}$  are evaluated for the estimated values of  $x_1^{(o)}$  to  $x_4^{(o)}$ .

On the basis of Eq. 13-82, Eqs. 13-77 through 13-80 may be written as

$$\Delta x_1 - \Delta x_2 + \frac{x_3^{(o)}}{g} \Delta x_3 - \frac{(1+K)x_4^{(o)}}{g} \Delta x_4 = -F_1^{(o)} \quad (13-83)$$

$$-C_{a_{i+1}} \Delta x_2 + \Delta x_4 = -F_2^{(o)} \quad (13-84)$$

$$C_{a_i} \Delta x_1 + \Delta x_3 = -F_3^{(o)} \quad (13-85)$$

$$B_i x_3^{(o)} \Delta x_1 - B_{i+1} x_4^{(o)} \Delta x_2 + A_i \Delta x_3 - A_{i+1} \Delta x_4 = -F_4^{(o)} \quad (13-86)$$

In Eq. 13-86, areas  $A_i$  and  $A_{i+1}$  are computed for  $x_1^{(o)}$  and  $x_2^{(o)}$ , and it is assumed that  $\partial A_i / \partial x_1 = B_i$  and  $\partial A_{i+1} / \partial x_2 = B_{i+1}$

The coefficients of Eq. 13-86 are significantly larger than the coefficients of Eq. 13-83 through 13-85. To reduce their magnitude, both the left- and the right-hand sides of Eq. 13-86 may be divided by  $B_i$ . Thus, Eq. 13-86 becomes

$$x_3^{(o)} \Delta x_1 - \frac{B_{i+1}}{B_i} x_4^{(o)} \Delta x_2 + \frac{A_i}{B_i} \Delta x_3 - \frac{A_{i+1}}{B_i} \Delta x_4 = -\frac{1}{B_i} F_4^{(o)} \quad (13-87)$$

Equations 13-83 to 13-85 and 13-87 are a set of four linear equations in four unknowns, namely,  $\Delta x_1$  to  $\Delta x_4$ . These equations may be solved by any standard numerical technique, such as the Gauss elimination scheme [McCracken and Dorn, 1967]. Then,

$$\begin{aligned} x_1^{(1)} &= x_1^{(o)} + \Delta x_1 \\ x_2^{(1)} &= x_2^{(o)} + \Delta x_2 \\ x_3^{(1)} &= x_3^{(o)} + \Delta x_3 \\ x_4^{(1)} &= x_4^{(o)} + \Delta x_4 \end{aligned} \quad (13-88)$$

in which  $x_1^{(1)}$  to  $x_4^{(1)}$  are better approximations of the solution of the nonlinear equations, Eqs. 13-72 through 13-75, than the initial estimated values of  $x_1^{(o)}$

to  $x_4^{(o)}$ . If  $|\Delta x_1|$ ,  $|\Delta x_2|$ ,  $|\Delta x_3|$ , and  $|\Delta x_4|$  are smaller than a specified tolerance, then  $x_1^{(o)}$  to  $x_4^{(o)}$  are solutions of Eqs. 13-72 through 13-75; otherwise, assume

$$\begin{aligned} x_1^{(1)} &= x_1^{(o)} \\ x_2^{(1)} &= x_2^{(o)} \\ x_3^{(1)} &= x_3^{(o)} \\ x_4^{(1)} &= x_4^{(o)} \end{aligned} \quad (13-89)$$

and repeat the foregoing procedure until a solution is obtained. To avoid an unlimited number of iterations in the case of divergence, introduce a counter in the iterative loop so that the computations are stopped if the number of iterations exceed a specified value, e.g., 30. To start the iterations, the first estimated values of  $x_1^{(o)}$  to  $x_4^{(o)}$  may be specified equal to the known values at the beginning of the time step.

## Stability Conditions

The finite-difference scheme presented above is said to be stable [Richtmyer and Morton, 1967; Mahmood and Yevjevich, 1975; and Cunge et al., 1980] if small numerical errors due to round-off introduced at time  $t_o$  are not amplified during successive applications of the difference equations, and the error at subsequent time do not grow so large as to obscure the valid part of the solution. Using the technique presented by Courant et al. [1928], it has been shown [Strelkoff, 1970, and Mahmood, and Yevjevich, 1975] that the Lax diffusive scheme is stable if

$$\Delta t \leq \frac{\Delta x}{|V| \pm c} \quad (13-90)$$

This is called the *Courant-Friedrichs-Lowy* condition or simply the *Courant condition*.

## Computational Procedure

To determine the transient conditions, the channel is divided into  $n$  equal-length reaches; the first section is numbered as 1, and thus the last section is  $n + 1$  (see Fig. 13-8). The initial steady-state conditions (i.e.,  $V$ ,  $y$ , and  $Q$ ) at these sections are computed. The time step,  $\Delta t$ , is selected so that Eq. 13-90 is satisfied. Equations 13-63 and 13-64 are used to determine  $y_i^{k+1}$  and  $V_i^{k+1}$  at sections 2 to  $n$ , and the appropriate boundary conditions are used to compute  $V_i^{k+1}$  and  $y_i^{k+1}$  at the upstream and at the downstream ends, i.e., at sections 1 and  $n + 1$ . Thus,  $y_i^{k+1}$  and  $V_i^{k+1}$  at time  $t = \Delta t$ , are known at all the sections, and the value of  $Q_i^{k+1}$  is computed by multiplying  $V_i^{k+1}$  by

the flow area corresponding to  $y_i^{k+1}$ . Now, assuming these computed values of  $V_i^{k+1}$ ,  $y_i^{k+1}$ , and  $Q_i^{k+1}$  as  $V_i^k$ ,  $y_i^k$ , and  $Q_i^k$ , the values of  $y_i^{k+1}$  and  $V_i^{k+1}$  at time  $2\Delta t$  are computed. This procedure is continued until the transient conditions for the required time are computed.

If there are two or more channels in the system, then the time step  $\Delta t$  is selected for the shortest channel, and each remaining channel is divided into equal-length reaches such that Eq. 13-90 is satisfied.

It is necessary that the Courant stability condition (Eq. 13-90) is satisfied at all grid points at each time step. If it is not satisfied, then the time step is reduced (e.g., 0.75 of the previous value), and the conditions at the end of the time step are recomputed before incrementing the time. To avoid making  $\Delta t$  too small in this process, its current value is compared at each time step to the value required for stability, and, if permissible,  $\Delta t$  is increased (e.g., by 15 percent) for the next time step.

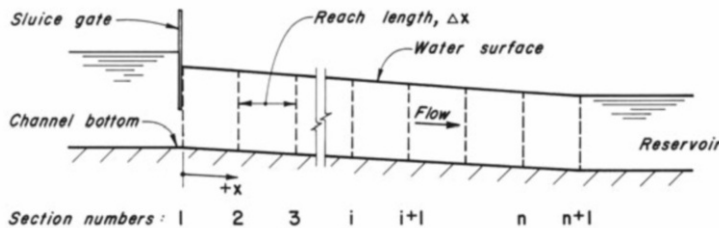


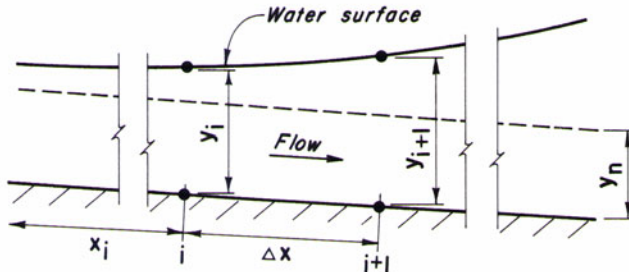
Fig. 13-8. Division of channel into  $n$  reaches.

### 13-9 Initial Conditions

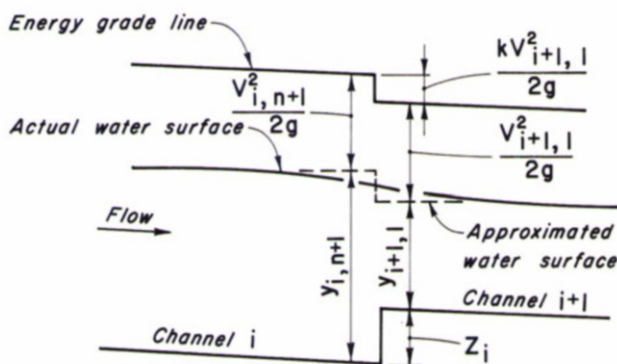
To compute the transient-state conditions, it is necessary that the initial steady-state flow depth and velocity are known at all the channel sections. If these conditions are not compatible with the St. Venant equations, then small disturbances are generated at each section as the transient conditions are computed and these hypothetical disturbances may mask the actual solution of the system. To avoid this, either of the following procedures may be utilized:

1. Any initial conditions, such as zero velocity and a constant depth, throughout the system are assumed, and the boundary conditions are set to the initial steady-state conditions. Using the St. Venant equations, the system conditions are computed for a sufficient length of time until the variation of flow variables at all grid points is negligible and the conditions have

converged to the steady values corresponding to the initial boundary conditions. The boundary conditions are then set equal to the values for which transient conditions are to be computed.



(a) Along channel



(b) Junction of two channels

**Fig. 13-9.** Notation for computing steady-state conditions.

2. The initial conditions are determined by solving either the ordinary differential equation or the energy equation describing the gradually varied flow in open channels [Henderson, 1966; Schulte and Chaudhry, 1987 and Chaudhry, 2008].

The former procedure requires a large amount of computer time. In addition, the solution by some finite-difference schemes may converge to incorrect initial conditions, especially if the numerical scheme is inconsistent. Therefore, the second procedure for determining the initial conditions is recommended. Details of this procedure follow.

The steady-state gradually varied flow in open channels is described by the following equation [Chaudhry, 2008]:

$$\frac{dy}{dx} = \frac{S_o - S_f}{1 - \frac{Q^2 B}{g A^3}} \quad (13-91)$$

Equation 13-91 is a first-order differential equation defining the rate of change of flow depth with distance. The flow depth along the channel may be computed by integrating this equation. For this purpose, the fourth-order Runge-Kutta method may be used as follows:

Let the depth of flow,  $y_i$  at  $x = x_i$ , be known (Fig. 13-9a). Then, the depth of flow at  $x = x_{i+1}$ ,

$$y_{i+1} = y_i + \frac{1}{6} (a_1 + 2a_2 + 2a_3 + a_4) \quad (13-92)$$

in which

$$\begin{aligned} a_1 &= \Delta x f(x_i, y_i) \\ a_2 &= \Delta x f\left(x_i + \frac{1}{2} \Delta x, y_i + \frac{1}{2} a_1\right) \\ a_3 &= \Delta x f\left(x_i + \frac{1}{2} \Delta x, y_i + \frac{1}{2} a_2\right) \\ a_4 &= \Delta x f(x_i + \Delta x, y_i + a_3) \end{aligned} \quad (13-93)$$

$$f(x, y) = \frac{dy}{dx}$$

By starting from the known depth at a control section, and by repeated application of Eq. 13-92, the flow depth and velocity along the entire channel are computed in steps of length,  $\Delta x$ .

The above procedure is used to determine the water surface profile in a prismatic channel. However, at the junction of two channels, the depth in one of the channels is initially known, and the depth in the other channel may be calculated from the energy equation as follows:

Let us assume that  $y_{i+1,1}$  is known at the junction of channels  $i$  and  $i + 1$  and  $y_{i,n+1}$  has to be determined (Fig. 13-9b). Let the head losses at the junction be given by  $kV_{i+1,1}^2/2g$ . In this expression, the first subscript represents the number of the channel, while the second subscript represents the number of the section on the channel. Unlike the actual water-surface profile, the computed water-surface profile has a sudden rise or drop at the junction because the losses and the velocity head are assumed to change abruptly at the junction.

Energy equation at the junction may be written as

$$y_{i,n+1} + \frac{V_{i,n+1}^2}{2g} = Z_i + y_{i+1,1} + (1 + k) \frac{V_{i+1,1}^2}{2g} \quad (13-94)$$

in which  $Z_i$  = drop in channel bottom at junction  $i$ . In this equation, a rise is considered positive, and a drop, as negative. Equation 13-94 may be written as

$$y_{i,n+1} = Z_i + y_{i+1,1} + (1+k) \frac{V_{i+1,1}^2}{2g} - \frac{V_{i,n+1}^2}{2g} \quad (13-95)$$

and solved by an iterative technique to determine  $y_{i,n+1}$ .

## 13-10 Implicit Finite-Difference Methods

In the finite-difference method presented in this section, we replace the  $x$ -derivatives in terms of the finite differences evaluated at time  $t_o + \Delta t$  instead of the finite differences at time  $t_o$  in the explicit method of Section 13-8. Thus, the unknown quantities appear implicitly (hence, the name, *implicit finite-difference method*) in the resulting algebraic equations, which are usually nonlinear. Solution of these algebraic equations is more complex than that in the explicit method. However, the implicit method is unconditionally stable and thus allows longer computational time step,  $\Delta t$ . The advantages and disadvantages of the explicit and implicit methods are outlined in Section 13-12.

### Implicit Schemes

In an implicit scheme, the spatial derivatives are replaced by the finite-difference approximations in terms of the variables at the unknown time level. Depending on the finite-difference approximations and the evaluation of coefficients of the governing equations, several schemes [Cunge and Wegner, 1964; Vasiliev et al., 1965; Amein and Chu, 1975; and Chaudhry, 2008] have been reported in the literature. Of these schemes, the Preissmann scheme has been used extensively for the analysis of unsteady free-surface flows and is presented herein. This scheme has the following advantages:

1. Variable spatial grid may be used since variables at only two adjacent nodes are used.
2. It yields an exact solution for the linearized form of the governing equations for a special choice of  $\Delta x$  and  $\Delta t$ . This property allows verification of the method for simple cases for which analytical solutions are available.
3. Both flow variables,  $V$  and  $y$ , are computed at the same nodes.
4. By varying the weighting coefficient for the spatial derivatives, steep wave fronts may be simulated.

### Preissmann Scheme

In the Preissmann scheme, the partial derivatives and other variables are approximated as follows ([Fig. 13-6](#)):

$$\frac{\partial f}{\partial t} = \frac{(f_i^{k+1} + f_{i+1}^{k+1}) - (f_i^k + f_{i+1}^k)}{2\Delta t} \quad (13-96)$$

$$\frac{\partial f}{\partial x} = \frac{\alpha [f_{i+1}^{k+1} - f_i^{k+1}]}{\Delta x} + \frac{(1-\alpha) [f_{i+1}^k - f_i^k]}{\Delta x} \quad (13-97)$$

$$f(x, t) = \frac{\alpha (f_{i+1}^{k+1} + f_i^{k+1})}{2} + (1-\alpha) \frac{(f_{i+1}^k + f_i^k)}{2} \quad (13-98)$$

in which  $\alpha$  = weighting coefficient,  $0.5 < \alpha \leq 1$ . For brevity,  $f$  in Eqs. 13-96 and 13-97 refers to both  $y$  and  $V$ ; and  $f(x, t)$  in Eq. 13-98 refers to  $D$ ,  $S_f$  and  $V$ . Substituting these equations into Eqs. 13-29 and 13-43 and simplifying the resulting equations, we obtain

$$\begin{aligned} & \left[ (y_i^{k+1} + y_{i+1}^{k+1}) + \frac{\Delta t}{\Delta x} [\alpha (D_{i+1}^{k+1} + D_i^k) + (1-\alpha) (D_{i+1}^k + D_i^k)] \right. \\ & \cdot \left. [\alpha (V_{i+1}^{k+1} - V_i^{k+1}) + (1-\alpha) (V_{i+1}^k - V_i^k)] \right] \\ & + \frac{\Delta t}{\Delta x} [\alpha (V_{i+1}^{k+1} + V_i^{k+1}) + (1-\alpha) (V_{i+1}^k + V_i^k)] \\ & \cdot [\alpha (y_{i+1}^{k+1} - y_i^{k+1}) + (1-\alpha) (y_{i+1}^k - y_i^k)] \\ & = y_i^k + y_{i+1}^k \end{aligned} \quad (13-99)$$

$$\begin{aligned} & V_i^{k+1} + V_{i+1}^{k+1} + 2g \frac{\Delta t}{\Delta x} [(\alpha y_{i+1}^{k+1} - y_i^{k+1}) + (1-\alpha) (y_{i+1}^k - y_i^k)] \\ & + \frac{\Delta t}{\Delta x} [\alpha (V_{i+1}^{k+1} + V_i^{k+1}) + (1-\alpha) (V_{i+1}^k + V_i^k)] \\ & \cdot [\alpha (V_{i+1}^{k+1} - V_i^{k+1}) + (1-\alpha) (V_{i+1}^k - V_i^k)] \\ & = V_i^k + V_{i+1}^k + 2g \Delta t S_o \\ & - g \Delta t [\alpha (S_{f_{i+1}}^{k+1} + S_{f_i}^{k+1}) + (1-\alpha) (S_{f_{i+1}}^k + S_{f_i}^k)] \end{aligned} \quad (13-100)$$

There are four unknowns, namely  $V_i^{k+1}$ ,  $y_i^{k+1}$ ,  $V_{i+1}^{k+1}$ , and  $y_{i+1}^{k+1}$ , in Eqs. 13-99 and 13-100. By writing similar equations for grid points  $i = 1, 2, \dots, n$ , we have a total of  $2n$  equations. Note that we cannot write Eqs. 13-97 for node

$n + 1$  since we do not have node  $n + 2$ . However,  $V$  and  $y$  are two unknowns at each node. Therefore, we have  $2(n + 1)$  unknowns, and to obtain a unique solution, we need two more equations. These two equations are provided by the boundary conditions, as discussed in the following paragraphs.

## Boundary Conditions

Unlike the explicit methods, equations representing the conditions imposed by the boundary are directly included in the system of equations and not in combination with the characteristic equations. For example, Eq. 13-65 is used for a constant-level upstream reservoir, and Eq. 13-68 is used for a constant-level downstream reservoir. Similarly, other conditions at the upstream and downstream ends may be specified.

## Solution Procedure

The resulting equations for the interior nodes and boundaries are nonlinear algebraic equations. These may be solved by using the Newton-Raphson method. For this purpose, Eqs. 13-99 and 13-100 for the interior nodes  $1, 2, 3, \dots, n$  and equations for conditions imposed by the boundaries are linearized in terms of the known quantities  $y_i^k$ ,  $V_i^k$ , etc. For example, for the  $i$ th node, this process results in the following two equations:

$$a_i \Delta y_i + b_i \Delta V_i + d_i \Delta y_{i+1} + e_i \Delta V_{i+1} = f_i \quad (13-101)$$

$$a_{i+1} \Delta y_{i+1} + b_{i+1} \Delta V_i + d_{i+1} \Delta y_{i+1} + e_{i+1} \Delta V_{i+1} = f_{i+1} \quad (13-102)$$

in which the coefficients  $a_i$ ,  $b_i$ ,  $d_i$ ,  $e_i$ ,  $f_i$ ,  $a_{i+1}$ ,  $b_{i+1}$ ,  $d_{i+1}$ ,  $e_{i+1}$ , and  $f_{i+1}$  are functions of the known quantities, and  $\Delta y_i$ ,  $\Delta V_i$ ,  $\Delta y_{i+1}$ , and  $\Delta V_{i+1}$  are corrections for the iterative procedure. These equations for the system may be written as

$$\mathbf{A}\mathbf{x} = \mathbf{b} \quad (13-103)$$

in which  $\mathbf{A}$  is a coefficient matrix,  $\mathbf{x}$  is a column vector comprised of the corrections, and  $\mathbf{b}$  is a column vector comprised of the constants on the right-hand side of Eqs. 13-101 and 13-102. In an expanded form, Eq. 13-103 may be written as

$$\left[ \begin{array}{cccccc} + & + & & & & \\ + & + & + & & & \\ + & + & + & + & (0) & \\ & + & + & + & + & \\ & + & + & + & + & \\ & + & + & + & + & \\ & & + & + & + & \\ & & : & & & \\ & & : & & & \\ & & + & + & + & \\ (0) & & + & + & + & \\ & & + & + & + & \\ & & + & + & + & \\ & & + & + & + & \end{array} \right] \left\{ \begin{array}{c} V_1 \\ y_1 \\ V_2 \\ y_2 \\ V_3 \\ y_3 \\ \vdots \\ \vdots \\ V_n \\ y_n \\ V_{n+1} \\ y_{n+1} \end{array} \right\} = \left\{ \begin{array}{c} + \\ + \\ + \\ + \\ + \\ + \\ \vdots \\ \vdots \\ + \\ + \\ + \\ + \end{array} \right\} \quad (13-104)$$

in which + is a non-zero element and all other elements are zero. A close examination of Eq. 13-104 shows that the nonzero elements of matrix  $\mathbf{A}$  lie near the diagonal, and thus  $\mathbf{A}$  is a banded matrix. Special computational procedures are available for the solution of such a system of linear equations. These procedures save computer time and storage requirements, and are more accurate.

### Systems Having Branch and Parallel Channels

The coefficient matrix,  $\mathbf{A}$ , is banded only for a system of channels connected in series. For a branching system (Fig. 13-10), a number of coefficients do not lie near the diagonal, and the procedure for solving a banded matrix cannot be used. In such cases, however, if the channel sections are numbered as shown in Fig. 13-10, the resulting matrix is a banded matrix [Kao, 1977]. Note that the numbering of the channel sections on the branch channel increases in the upstream direction and the difference between the consecutive section numbers of a channel is 2. These factors have to be properly taken into consideration in the computations.

Similarly, a matrix for systems having parallel channels (Fig. 13-11) is not banded. For such systems, a procedure [Kamphuis, 1970] may be used in which the matrix  $\mathbf{A}$  is first reduced to the upper triangular form, and then back substitution is done to solve the system of equations; or the sections may be numbered as shown in Fig. 13-11, which results in a banded matrix [Kao, 1977].

### Stability

A von Neumann stability analysis of linearized St. Venant equations shows that the Preissmann scheme is unconditionally stable. This means there is no restriction on the size of the grid spacing  $\Delta x$  and  $\Delta t$  for the stability of the numerical scheme. However, accuracy considerations dictate that a

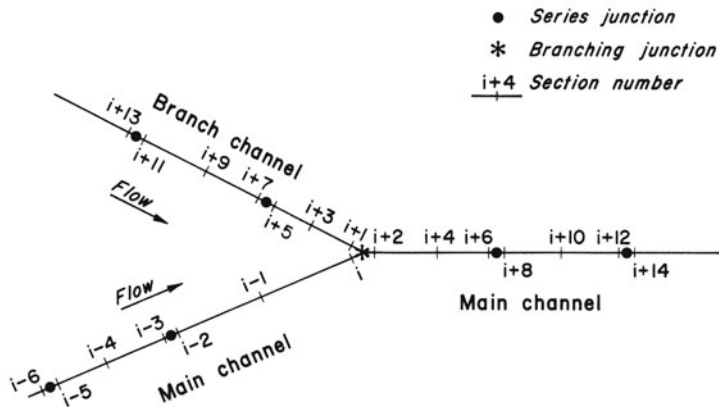


Fig. 13-10. Designation of channel sections on a branch system.

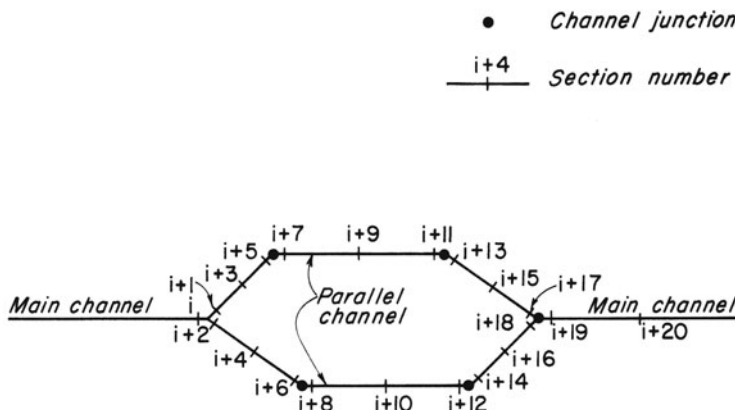


Fig. 13-11. Designation of channel sections on a parallel system.

computational time step nearly equal to that given by the Courant condition be used in the computations.

Since the scheme is unconditionally stable, the time step may be varied during the computations, i.e., a shorter  $\Delta t$  may be used to increase accuracy when the conditions are varying rapidly, and, the time step may be increased when the conditions are varying slowly.

Note that the computational time step,  $\Delta t$ , cannot be arbitrarily increased even though the numerical scheme is unconditionally stable. Actually, the time step,  $\Delta t$ , is selected by considering both the accuracy and the stability of the scheme. For a large time step, the finite differences do not approximate the partial derivatives of the original equations and sharp peaks are truncated. Therefore, the accuracy of the results should be checked by comparing the computed results obtained by using reduced values of  $\Delta t$ . If the difference is negligible, then a larger value of  $\Delta t$  may be used with confidence.

### 13-11 Second-Order Explicit Schemes

Several explicit schemes that are second-order accurate in both space and time have been developed for the solution of hyperbolic systems for application in computational fluid dynamics [Anderson et al., 1984]. A number of these schemes have been applied in hydraulic engineering [Chaudhry and Hussaini, 1985; Fennema and Chaudhry, 1986; and Chaudhry, 2008].

These methods are more accurate than the first-order methods and are easier to apply than most of the implicit methods. Since fewer mesh points are used in the higher-order methods as compared to the first-order methods to achieve the same accuracy, the use of these methods becomes economical, even though slightly more computations per time step are required. The higher-order methods are superior in reproducing shocks and bores as compared to the first-order methods.

Details of one of these schemes are presented here; readers interested in other schemes may refer to Chaudhry and Hussaini [1985]; Fennema and Chaudhry [1986]; and Chaudhry [2008].

#### MacCormack Scheme

The MacCormack scheme is second-order accurate both in space and time, and is suitable for analyzing flows having shocks and bores. It is comprised of the predictor and corrector parts [MacCormack, 1969]. A backward finite difference is used in the predictor part, and a forward difference is used in the corrector part (another alternative is to use the forward finite difference in the predictor part and a backward difference in the corrector part). Only the first alternative is presented here. In this alternative, the following finite-difference approximations are employed:

#### Predictor Part

$$\begin{aligned}\frac{\partial f}{\partial t} &= \frac{(f_i^* - f_i^k)}{\Delta t} \\ \frac{\partial f}{\partial x} &= \frac{f_i^k - f_{i-1}^k}{\Delta x}\end{aligned}\tag{13-105}$$

### Corrector Part

$$\begin{aligned}\frac{\partial f}{\partial t} &= \frac{(f_i - f_i^*)}{\Delta t} \\ \frac{\partial f}{\partial x} &= \frac{f_{i+1}^* - f_i^*}{\Delta x}\end{aligned}\quad (13-106)$$

In these equations,  $f$  is used for brevity to represent both  $V$  and  $y$  and an asterisk,  $*$ , refers to the predicted values.

### Predictor Part

By substituting the above approximations for the partial derivatives and simplifying the resulting equations, we obtain

$$\begin{aligned}y_i^* &= y_i^k - \frac{\Delta t}{\Delta x} D_i^k (V_i^k - V_{i-1}^k) - \frac{\Delta t}{\Delta x} V_i^k (y_i^k - y_{i-1}^k) \\ V_i^* &= V_i^k + g \frac{\Delta t}{\Delta x} (y_i^k - y_{i-1}^k) - V_i^k \frac{\Delta t}{\Delta x} (V_i^k - V_{i-1}^k) \\ &\quad + g (S_o - S_f)_i^k \Delta t\end{aligned}\quad (13-107)$$

in which  $y_i^*$  and  $V_i^*$  are the predicted values. By using Eq. 13-107, we determine the predicted values of  $y$  and  $V$  at  $i = 2, 3, \dots, n$  from the known values at  $k$  time level.

### Corrector Part

Now, using  $V^*$  and  $y^*$ , computed during the predictor part, and the values of coefficients  $D$  and  $S_f$  corresponding to these values, the “corrected” values of  $V$  and  $y$  are determined from the following equations

$$y_i = y_i^* - D_i^* \frac{\Delta t}{\Delta x} (V_{i+1}^* - V_i^*) - V_i^* \frac{\Delta t}{\Delta x} (y_{i+1} - y_i^*) \quad (13-108)$$

$$\begin{aligned}V_i &= V_i^* - g \frac{\Delta t}{\Delta x} (y_{i+1}^* - y_i^*) - V_i^* \frac{\Delta t}{\Delta x} (V_{i+1}^* - V_i^*) \\ &\quad + g (S_o - S_f)_i^* \Delta t\end{aligned}\quad (13-109)$$

By using these equations for one node at a time, we compute the corrected values of  $V$  and  $y$  at nodes,  $i = 2, 3, \dots, n$ .

The values of  $V$  and  $y$  at the  $k+1$  time level are obtained from the following equations:

$$\begin{aligned}y_i^{k+1} &= 0.5 (y_i^k + y_i) \\ V_i^{k+1} &= 0.5 (V_i^k + V_i)\end{aligned}\quad (13-110)$$

## Boundary Conditions

The equations presented in the previous paragraphs are for the flow conditions at the interior nodes. At the boundaries, positive or negative characteristic equations (Eqs. 13-58, 13-59) or both are solved simultaneously with the conditions imposed by the boundary. The procedure is similar to that used for the Lax diffusive scheme.

## Artificial Viscosity

Modified-equation analysis [Warming and Hyett, 1974] of the above scheme shows that the higher-order terms are introduced which are not present in the governing partial differential equations. These terms represent the truncation errors. Generally, the solution has dissipative errors if the leading term in the truncation error has even derivatives, and it has dispersive errors if the leading term has odd derivatives. The dispersive errors usually result in numerical oscillations. Therefore, artificial viscosity is added in the scheme to smooth these oscillations. Several procedures have been reported for this purpose. The procedure, developed by Jameson et al., [1981], has the advantage of smoothing regions where the solution has steep gradients while leaving relatively smooth areas undisturbed. A parameter,  $\xi$ , is first computed using the normalized form of the gradients of one variable. For free-surface flows, for example, flow depth may be used to determine the parameter,

$$\xi_i = \frac{|y_{i+1} - 2y_i + y_{i-1}|}{|y_{i+1}| + 2|y_i| + |y_{i-1}|}$$

$$\xi_{i+1/2} = \kappa \frac{\Delta x}{\Delta t} \max(\xi_{i+1}, \xi_i) \quad (13-111)$$

in which  $\kappa$  is used to regulate the amount of dissipation. The computed variables are then modified by

$$\begin{aligned} \alpha_i &= \xi_{i+1/2} (U_{i+1} - U_i) - \xi_{i-1/2} (U_i - U_{i-1}) \\ U_i &= U_i + \alpha_i \end{aligned} \quad (13-112)$$

## Stability

For the stability of the above scheme, the following condition must be satisfied at all computational nodes:

$$\Delta t = C_n \frac{\Delta x}{\max [|V| + \sqrt{gD}]} \quad (13-113)$$

in which  $C_n$  is the desired Courant number. The denominator is the maximum of the quantity  $|V| + \sqrt{gD}$  evaluated at all the grid points. The known values

of  $V$  and  $D$  at the beginning of the time interval may be used to compute  $\Delta t$ . The above condition is then checked at the end of the time interval for the computed values of  $V$  and  $D$ . Von Neumann stability analysis shows that  $C_n \leq 1$  for the stability of the MacCormack scheme [Anderson et al., 1984 and Fennema and Chaudhry, 1986].

### Example

*By using the above numerical schemes, simulate the transient flow in a 5-km long, rectangular, frictionless, horizontal channel. The transient conditions are produced by reducing the flow instantaneously at the downstream end to zero at  $t = 0$ . Compare the computed results with the analytical solution. The initial flow velocity and flow depth are 3.125 m/s and 6 m, respectively.*

### Solution

By using the above numerical schemes and the boundary conditions, the transient flows in the channel are modeled [Fennema and Chaudhry, 1986]. A bore is produced by the instantaneous reduction of flow at the downstream end. This bore travels in the upstream direction.

The computed flow depths are compared with the analytical solution in Fig. 13-12. Analytical computations show that the bore should be at midlength of the channel at  $t = 354$  s. The computed profiles are at the nearest computed time to 354 s.

The oscillations near the bore are due to truncation errors. The MacCormack scheme produces wiggles on the back side of the wave front. Fig. 13-12b shows the flow depths with the addition of artificial viscosity. The bore is slightly smeared, although the oscillations near the bore are significantly reduced.

It is clear from Fig. 13-12 that the MacCormack scheme simulates steep wave fronts and that the computed wave height and speed agree satisfactorily with the analytical results.

## 13-12 Comparison of Finite-Difference Methods

The finite-difference methods presented in the previous sections are compared in this section.

**Stability.** Courant stability condition (Eq. 13-90) must be satisfied in the explicit methods., i.e.,  $\Delta t \leq \Delta x / (|V| \pm c)$ . There is no such restriction on  $\Delta t$  in the implicit method.

**Ease of Programming.** The explicit methods are easier to program than the implicit methods. Therefore, if the time available for developing a program is limited, the explicit methods should be preferred.

**Economy.** Because the size of  $\Delta t$  for an implicit scheme is not restricted for stability, a larger value of  $\Delta t$  is permissible, thus requiring less computer time as compared to an explicit scheme in which  $\Delta t$  is restricted by the Courant stability condition. However, recent investigations show that, for accuracy and to simulate the physics of the process properly,  $\Delta t$  in an implicit scheme should be nearly the same as that required by the Courant condition.

**Computer-Memory Requirements.** The computer storage required in an implicit method is usually more than that in an explicit method. This may be a problem if the system is large and the computer memory is limited.

**Simulation of Special Systems.** Explicit methods may be unsuitable for conduits having closed tops in which the transient water surface either primes or reaches the top of the conduit. In such a situation, the free-water-surface width becomes zero or very small, and the size of  $\Delta t$  allowed for stability is reduced to a very small value. Examples of such systems are sewers and tailrace tunnels in hydroelectric power plants. The implicit method should be preferred for the analysis of these systems.

**Simulation of Sharp Peaks.** Because of smaller  $\Delta t$ , the explicit methods are more suitable for the analysis of transients with sharp peaks of short duration. In the implicit methods, such peaks are usually smoothed out. If, however, time steps of the same size as that in the explicit method are used, the peaks would be reproduced, but the computer time required in the implicit method would be greater than that in the explicit method.

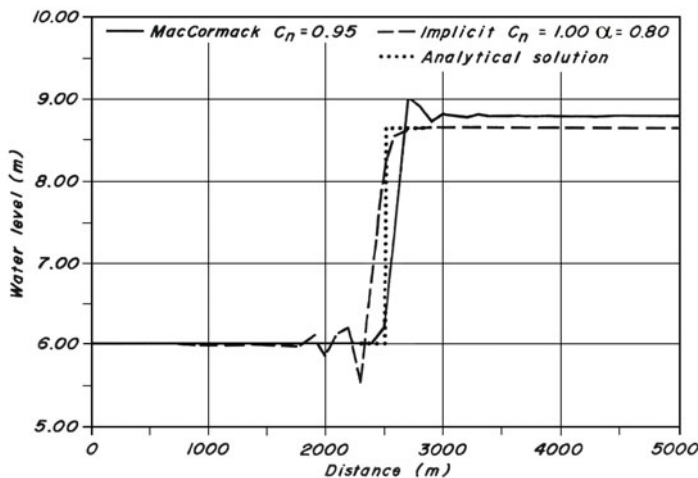
**Formation of Bores and Shocks.** The explicit methods are more suitable than the implicit methods for the analysis of transients in which a bore is formed.

## 13-13 Special Topics

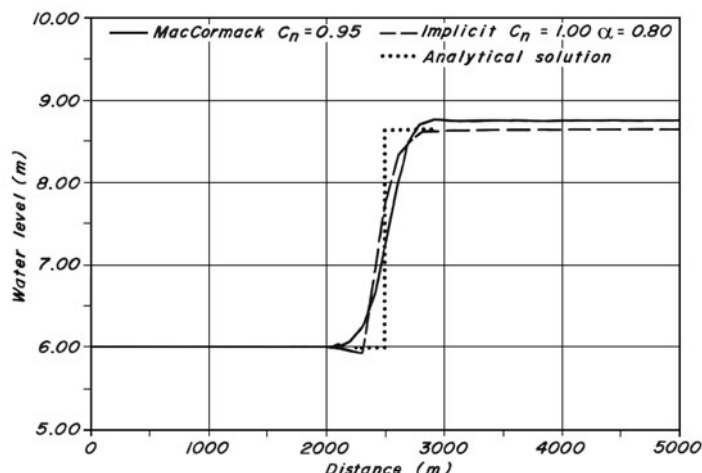
A number of special topics are discussed in this section.

### Dam-break Flows

The computation of the dam-break flows is similar to that of open-channel transients in which a bore forms. Stoker [1948, 1957] studied these flows in a rectangular, horizontal, and frictionless channel with water in the channel downstream of the dam. He assumed an instantaneous failure of the dam. Ritter [1982], Dressler [1952, 1954], and Whitham [1955] investigated analytically the propagation of the bore produced by dam failure with dry condition downstream of the dam. Dronkers [1964] used the method of characteristics to determine the gradually varied flows on both sides of the bore, and applied the conservation equations at the bore. Different finite-difference



(a) No artificial viscosity.



(b) Artificial viscosity added.

**Fig. 13-12. Comparison of computed water levels.** (After Fennema and Chaudhry [1986].)

schemes have been used by various investigators [Cunge, 1970; Martin and Zovne, 1971; Sakkas and Strelkoff, 1973], and the finite-element method by Katopodes [1984]. Terzidis and Strelkoff [1970] showed that the Lax diffusive scheme and the two-step Lax-Wendroff-Richtmyer explicit scheme may be used for the analysis of flows in which a bore forms without isolation of

the bore. The results computed by using these schemes and measured in the laboratory show good agreement. It is also shown that the solution of St. Venant equations in their usual form, without inclusion of special dissipation terms, gives erroneous results when applied to flows with bores of height greater than one-half the flow depth. For a bore of smaller height, however, the St. Venant equation yielded satisfactory results. Fennema and Chaudhry [1986] presented two finite-difference schemes which allow the analysis of supercritical flows downstream of the breached dam. Martin and Zovne [1971] showed that the propagation and reflection of bores from a solid wall may be analyzed by the diffusive explicit scheme, and that the isolation of the bore and its treatment as an internal boundary is more of an academic interest than that required in real-life applications.

The size of the breach and the time in which it develops when the dam fails have to be estimated for the computation of dam-break flows. However, very limited information is available for the estimation of these parameters. Instantaneous failure of the entire dam appears to be rather unrealistic for real-life applications for emergency preparedness.

Following a dam failure, a positive wave propagates in the downstream channel, and a negative wave travels in the upstream reservoir. While using a finite-difference method, the boundary conditions at the breached-dam site have to be developed. For this purpose, the relationships for various opening sizes [Mahmood and Yevjevich, 1975, Chap. 15] in the dam may be used. The computer program DAMBRK distributed by National Weather Service, NOAA, has been used extensively for the preparation of emergency plans downstream of large dams.

### Tidal Oscillations

River reaches influenced by tides may be analyzed by solving the St. Venant equation by the finite-difference methods. An important decision in such investigations is whether a one-dimensional or a two-dimensional model is appropriate for the particular application.

Unlike the analysis of transients in canals, rivers, etc., it is not necessary to determine the initial conditions for computing tidal oscillations. The computations are started with any assumed initial conditions, and the system is analyzed with the tidal water levels for a number of tidal cycles as a boundary until periodic flows are established. This is similar to the computation of steady-oscillatory flows in pipes by the method of characteristics (see Section 8-4).

### Secondary Oscillations

We discussed in Section 13-4 that the front of a positive wave becomes steep as it propagates in a channel. A wave having large energy breaks and becomes a moving hydraulic jump or a bore ([Fig. 13-13a](#)) while the front of a wave

with small energy assumes an undular form, as shown in [Fig. 13-13b](#). In other words, this is similar to a stationary hydraulic jump in which a strong jump is formed for Froude number  $F > 9$  and an undular jump for  $F < 1.7$ . These secondary water-surface oscillations are called Favre waves, described first by Favre in 1935.

The discontinuity in the water surface of a bore occurs over a very short distance and the flow upstream and downstream of the bore may be assumed to be gradually varied. Consequently, the length of this discontinuity is usually smaller than the reach length into which the channel is divided. Since the St. Venant equations are valid on both sides of the bore, satisfactory results are obtained using these equations, as long as the details of wave front is not of primary interest. However, if the wave front has secondary oscillations, the water surface has undulations for a long distance, the validity of hydrostatic-pressure distribution is questionable, and the maximum water levels computed by using the St. Venant equations are not necessarily the highest levels. In addition, experience has shown that these oscillations are higher near the banks than in the middle of the channel. Photographs of [Figure 13-14](#) taken during the prototype tests (For a description of these tests, see Section 13-14.) show the secondary oscillations of the water surface near the wave front.

For the design of power canals or other channels in which the wave front has secondary oscillations, the maximum water level near the banks should be known to determine the top elevation of the banks. However, very limited data on these oscillations have been reported in the literature. [Figure 13-15](#) taken from Benet and Cunge [1971] may be used to estimate the height of these water surface undulations.

### **Free-Surface-Pressurized Flow**

Free-surface flow in which the conduit is pressurized during the transient state is called *free-surface-pressurized flow*. Such flows occur in sewers and in the conduits of hydroelectric power plants or pumped-storage projects.

Meyer-Peter [1932] and Calame [1932] studied this flow while investigating surges in the tailrace tunnel of Wettingen Hydroelectric Power Plant. Their computed results were in close agreement with those measured on a hydraulic model. In 1937, Drioli reported his observations on the translation of waves in an industrial canal. Jaeger [1956] discussed this problem and presented a number of expressions for various possible cases. Preissmann [1961], Cunge [1966], Cunge and Wegner [1964], Amoroch and Strelkoff [1965], and Wiggett [1970 and 1972] analyzed these flows using computers. Song et al. [1983] investigated the flows experimentally and by using numerical techniques.

To facilitate discussion, let us re-write the equations describing the transient flows in open channels and in closed conduits:

*Open channels:*

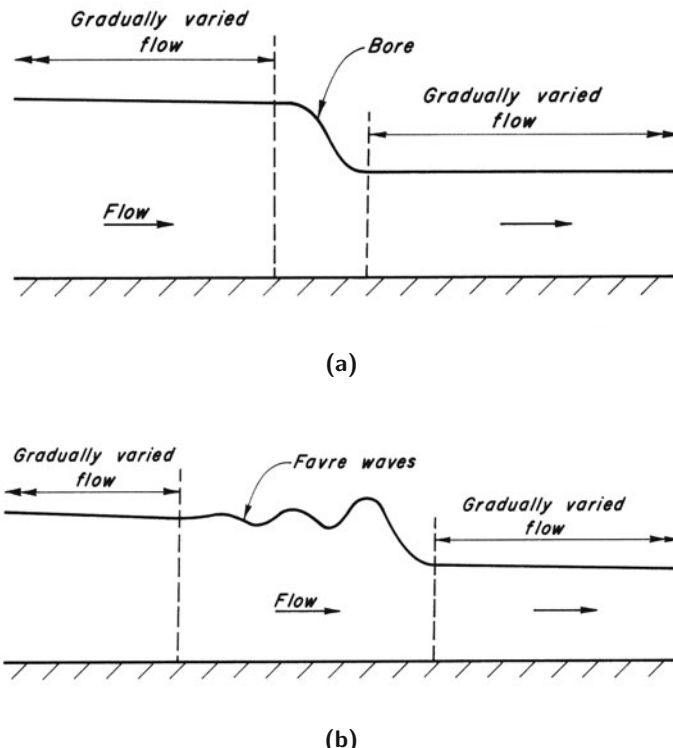


**Fig. 13-13.** Variation of water surface at wave front.

Continuity equation

$$\frac{\partial y}{\partial t} + V \frac{\partial y}{\partial x} + D \frac{\partial V}{\partial x} = 0 \quad (13-29)$$

Dynamic equation

$$g \frac{\partial y}{\partial x} + \frac{\partial V}{\partial t} + V \frac{\partial V}{\partial x} = g (S_o - S_f) \quad (13-43)$$

*Closed conduits:*

Continuity equation

$$\frac{\partial H}{\partial t} + V \frac{\partial H}{\partial x} + \frac{a^2}{g} \frac{\partial V}{\partial x} = 0 \quad (13-114)$$

Dynamic equation

$$g \frac{\partial H}{\partial x} + \frac{\partial V}{\partial t} + V \frac{\partial V}{\partial x} = g (S_o - S_f) \quad (13-115)$$

in which  $H$  = piezometric head and  $a$  = wave velocity. A comparison of Eqs. 13-29 and 13-114, and 13-43 and 13-115 shows that these equations are identical if the depth of flow,  $y$ , is assumed equal to the piezometric head,  $H$ , and if  $a = \sqrt{gA/B} = c$ , in which  $c$  = the celerity of the surface waves. Therefore, we may analyze pressurized flow by solving the St. Venant equations by using an interesting technique proposed by Preissmann [1961]. In this technique, a very narrow slot or piezometer with its top open to atmosphere is assumed at the crown of the conduit (Fig. 13-16). It is assumed that the water level in the piezometer represents the pressure in the conduit but the slot does not increase the cross-sectional area as well as the hydraulic radius of the pressurized conduit. The width of the piezometer is selected such that  $c = a$ . Thus, the free-surface and the pressurized flows do not have to be analyzed separately. Once the conduit primes, the depth determined by solving the St. Venant equation is the pressure in the conduit at that location. This technique has been successfully used for the analysis of sewers [Mahmood and Yevjevich, 1975] and for the analysis of surges in the tailrace tunnels of a hydroelectric power plant [Chaudhry and Kao, 1976].

### Landslide-Generated Waves

If a landslide mass falls or moves into a body of water, waves are generated due to displacement of water and due to impact of the landslide. These waves, sometimes referred to as impulse waves, have caused destruction [Miller, 1960; Kiersch, 1964; McCulloch, 1966; Kachadoorian, 1965 and Forstad, 1968] and loss of human life. For example, the waves generated by the Vajont slide, in Italy, killed about 2300 people.

Wiegel [1955], Prins [1958], Law and Brebner [1968], Kamphuis and Bowering [1970], Noda [1970], Das and Wiegel [1972], and Babcock [1975] conducted tests on landslide-generated waves in laboratory flumes and presented empirical relationships and graphs for various wave characteristics, such as the initial wave height, wavelength, etc.

Tests on scale hydraulic model were conducted to study the waves generated by the movement of slides into reservoirs of the Mica [Anonymous, 1970], Libby [Davidson and McCartney, 1975], Revelstoke [Mercer et al., 1979; Chaudhry and Cass, 1976 and Chaudhry et al., 1983], and Morrow Point [Pugh, 1982] dams. The diffusive scheme of Section 13-8 was used [Chaudhry and Cass, 1976 and Chaudhry et al., 1983] for the propagation of slide-generated waves approximately 67 km in the reservoir in both the upstream and downstream directions from the slide site.

The empirical relationships reported by Kamphuis and Bowering [1970] are presented herein; for similar relationships, see Wiegel, [1955], Prins, [1958], Law and Brebner, [1968]; Kamphuis and Bowering, [1970] and Noda, [1970]. These relationships were derived from data for waves generated by loaded trays sliding down an inclined roller ramp into a 45-m-long, 1-m wide laboratory flume. The slides were simulated in the direction of the longitudinal axis



(a)



(b)

**Fig. 13-14.** Seton Canal, secondary oscillations at wave front. (Courtesy, B. C. Hydro and Power Authority, Canada.)

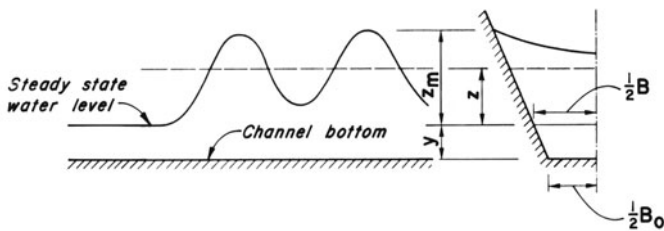


(c)

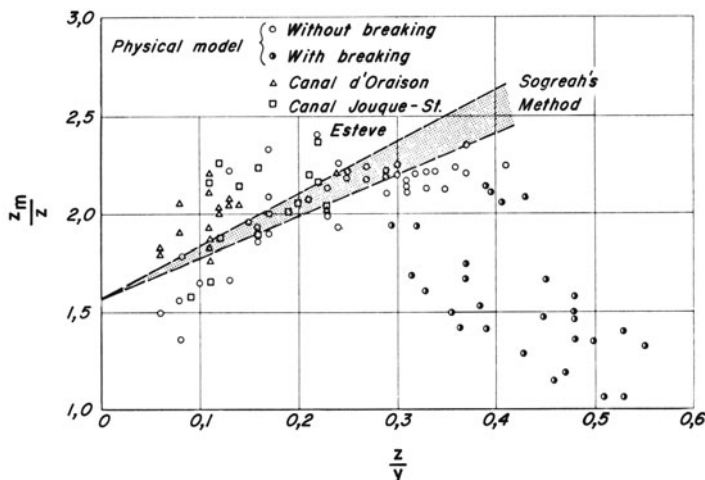


(d)

**Fig. 13-14.** (*Continued*)



(a) Notation



(b)

**Fig. 13-15. Amplitude of secondary oscillations.** (After Benet and Cunge, [1971].)

of the flume from various heights and various slide angles. These waves varied from a pure oscillatory wave train to a wave approaching a solitary wave, followed by an oscillatory wave train and bores. The waves became stable at or upstream of a point located about 17 m from the point of slide impact. The following equations were presented:

*Maximum height of the stable wave*

$$\frac{H_c}{d} = F^{0.7} (0.31 + 0.2 \log q) \quad (13-116)$$

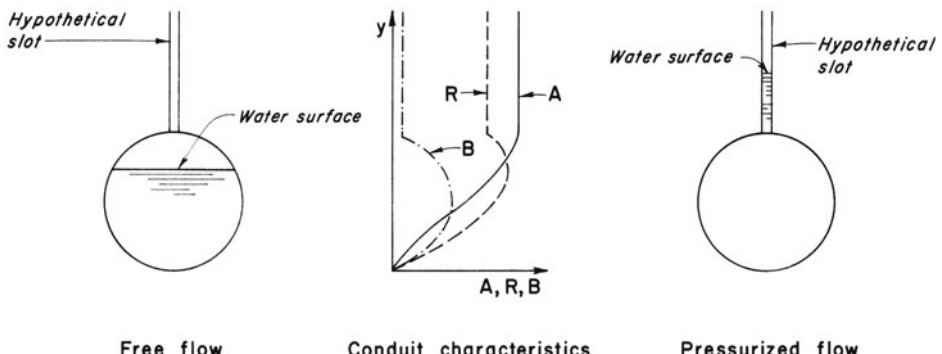


**Fig. 13-16.** Hypothetical slot.

in which  $h_c$  = maximum stable wave height above the still water level;  $d$  = water depth;  $V_s$  = slide velocity upon impact with water;  $g$  = acceleration due to gravity;  $q$  = slide volume per unit width in dimensionless form,  $(l/d), (h/d)$ ;  $l$  = length of slide up the slope;  $h$  = thickness of slide normal to the slope; and  $F = V_s/\sqrt{gd}$ .

*Wave-height attenuation*

$$\frac{H}{d} = \frac{H_c}{d} + 0.35e^{-0.08x/d} \quad (13-117)$$

in which  $H$  = maximum wave height above still water level at distance  $x$  from the slide; and  $x$  = distance downstream from the point of slide impact.

For a given slide, the maximum stable wave height,  $H_e$  may be determined from Eq. 13-116 and height,  $H$ , at any point downstream from the slide impact may then be computed by using Eq. 13-117.

*Wave period*

$$\frac{T_1}{\sqrt{gd}} = 11 + 0.225 \frac{x}{d} \quad (13-118)$$

in which  $T_1$  = period of the first wave (i.e., the time required by the wave to pass a point).

Eq. 13-116 estimates satisfactorily the stable wave height for  $0.05 \leq q \leq 1.0$ , as long as the slide is thick (i.e.,  $h/d > 0.5$ ), the front angle,  $\beta$ , of the slide is  $90^\circ$  or greater, and the angle of the slide plane,  $\theta$  is about  $30^\circ$ . However, the wave heights determined from Eq. 13-116 are higher for  $\beta < 90^\circ$  and  $\theta > 30^\circ$  but low for  $\theta < 30^\circ$ .

Raney and Butler [1975] developed a two-dimensional mathematical model to determine the characteristics of the slide-generated waves. Comparison of

the computed results with those measured on a hydraulic model [Davidson and McCartney, 1975] showed satisfactory agreement. Koutitas [1977] used finite-element method and Chiang et al. [1981] used a finite-difference method to predict landslide-generated waves in a reservoir.

## 13-14 Case Study

A brief description of the mathematical model, prototype tests, and a comparison of the computed and measured results [Chaudhry, 1976] are presented in this section.

### Mathematical Model

The mathematical model was based on the equations derived in Section 13-8. The following boundary conditions were included in the model: flow or stage changes at the upstream or at the downstream end; constant-head reservoir at the upstream or at the downstream end; and junction of two channels having different cross sections, friction factors, and/or bottom slopes.

The model was designed to analyze transient conditions in a system having up to 20 prismatic channels in series. As outlined in Section 13-8, the value of  $\Delta t$  was checked at each time step and its value was increased by 15 percent or decreased by 25 percent so that the Courant stability condition was always satisfied and at the same time  $\Delta t$  unnecessarily did not become too small.

### Prototype Tests

To verify the model, prototype tests were conducted on Seton Canal, B.C., Canada. Relevant information on the project, owned and operated by B.C. Hydro, and the test program follow.

#### *Project Data*

Seton Canal, concrete-lined, 3.82-km long and designed for a flow of  $113 \text{ m}^3/\text{s}$ , conveys water from Seton Lake to Seton Generating Station. The alignment and typical cross sections of the canal are shown in Fig. 13-17. The hydropower plant has one 44-MW, vertical reaction turbine. The effective wicket-gate opening and closing times are 15 and 13 s, respectively. While starting the turbine from rest, wicket gates are opened to 15 percent (breakaway gate). At this opening, the turbine runner begins to rotate, and the gates are then closed to speed-no-load gate of 9 percent. The wicket gates are kept at this opening until the unit is synchronized to the system.

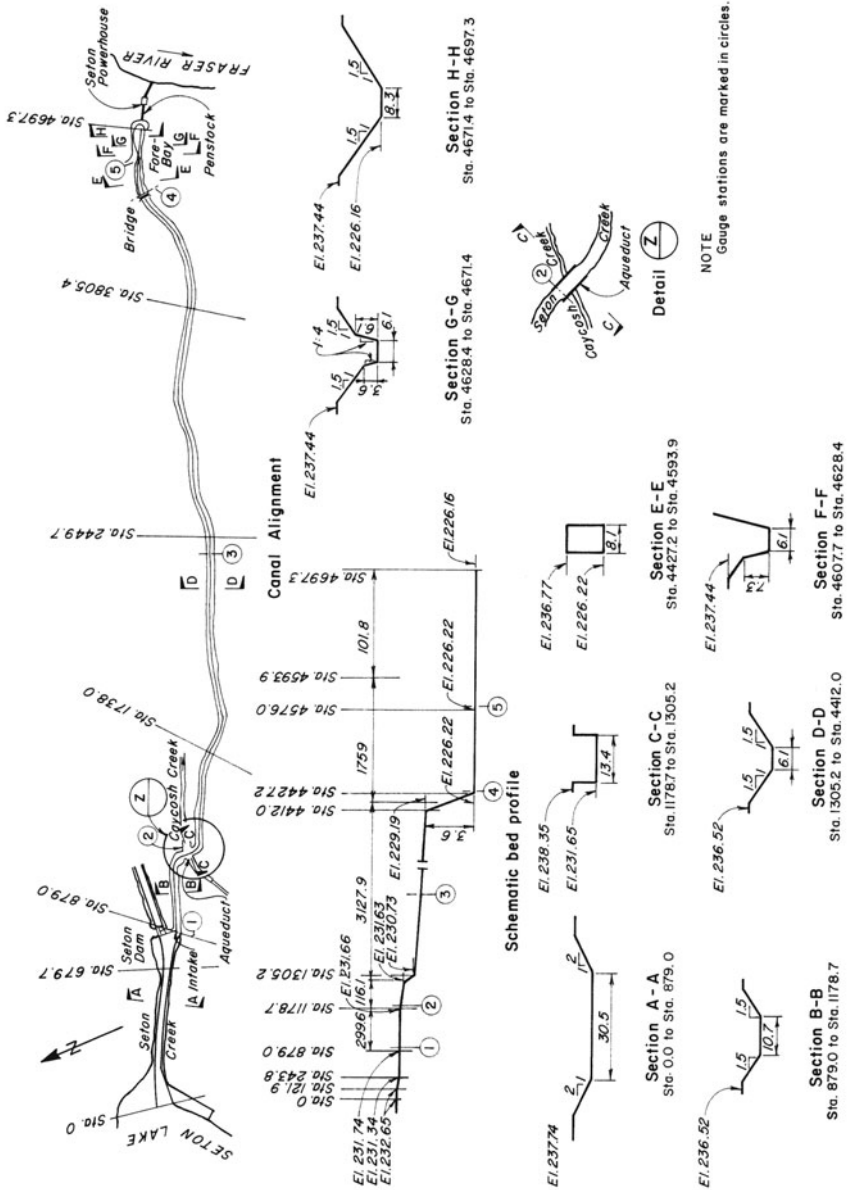


Fig. 13-17. Plan and profile of the Seton project

### **Tests**

Transient flows were produced in the canal by accepting or rejecting load on the turbine. The following tests were conducted:

Acceptance of 44 MW;

Rejection of 44 MW;

Acceptance of 44 MW followed by rejection of 44 MW after 42 min and then acceptance of 44 MW after 37 min.

After total-load rejection, turbine gates were kept open at speed-no-load gate of 9 percent.

Transient-state water levels were read at intervals of 30 s to 1 min from the gauge plates attached to the vertical or inclined side walls. Countdown for the start of the test was given over a VHF/UHF radio. At the beginning of each test, steady-state water levels were observed at 19 locations along the canal length.

Transient water levels were recorded at five stations along the length of the canal ([Fig. 13-17](#)).

### **Comparison of Computed and Measured Results**

The computed water levels at various stations are compared with those measured on the prototype in [Figs. 13-18](#) and [13-19](#). In the computations, the canal was represented by six channels, each having a constant cross section along its length. The Manning equation was used to calculate friction losses, and the load acceptance or rejection on the turbine was simulated by assuming a linear discharge variation at the downstream end of the canal. Seton Lake was represented by a constant-head reservoir at the upstream end.

The secondary fluctuations of the water surface (Favre waves) are not computed by the program because the governing equations (Eqs. 13-29 and 13-43) are based on hydrostatic pressure distribution. Therefore, to determine the maximum water levels, the amplitude of the secondary fluctuations were computed using the data presented by Benet and Cunge [1971] and were superimposed on the maximum-water levels computed by the model. The maximum level of the computed surge fluctuations is marked in [Fig. 13-19a](#) to [13-19c](#).

It is clear from these figures that the computed and the measured water levels agree closely following the initial surge and for maximum water level of the secondary fluctuations at the upper end of the canal. The computed maximum water level of the fluctuations at Station 3 are, however, too high, because the fluctuations were not developed in the prototype as the initial wave propagated upstream.

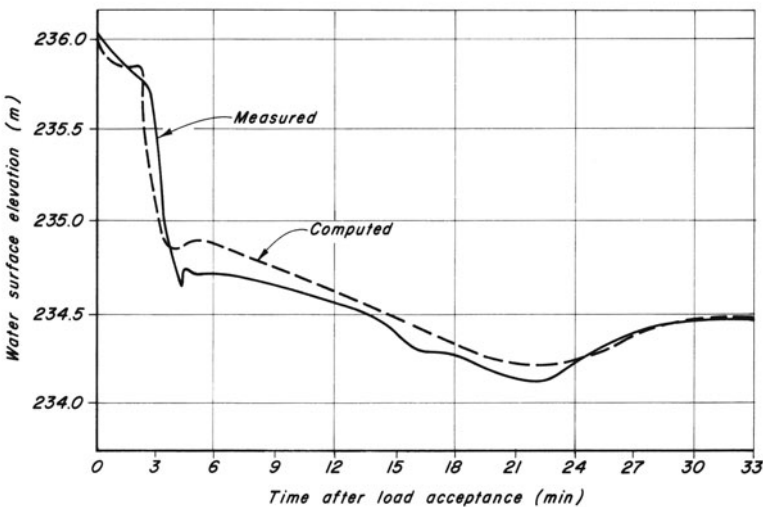


**Fig. 13-18.** Comparison of computed and measured transient-state water levels at Station 5 following 44-MW load acceptance.

### 13-15 Summary

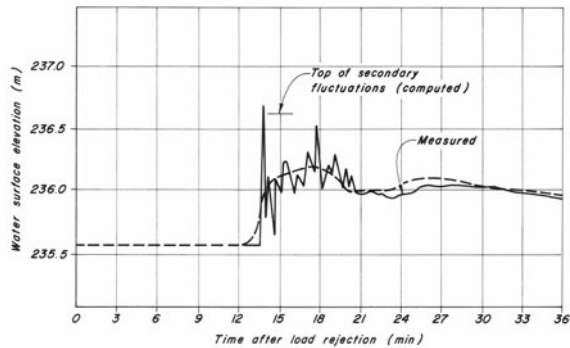
In this chapter, transient flows in open channels are discussed. A number of terms are defined, the continuity and dynamic equations are derived, and numerical methods available for their solution are discussed. Details of the explicit and implicit finite-difference methods are presented. The chapter concludes with a case study.

## Problems

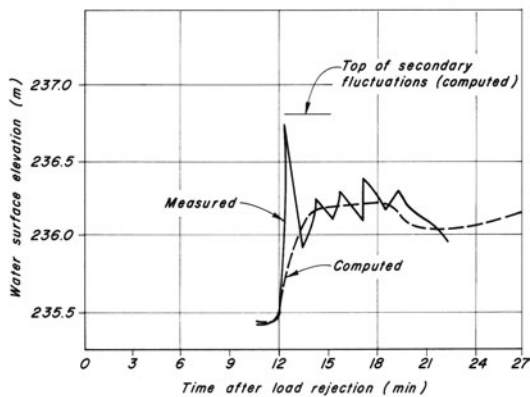
**13-1** A 6.1-m-wide rectangular canal is carrying  $28 \text{ m}^3/\text{s}$  at a depth of 3.04 m. The gates at the downstream end are suddenly closed. Determine the initial surge height,  $z$ , and the velocity,  $V_w$ , of the surge wave.

**13-2** An initial steady-state flow of  $16.8 \text{ m}^3/\text{s}$  in a 3-m-wide rectangular power canal is suddenly reduced to  $11.2 \text{ m}^3/\text{s}$  at the downstream end. If the initial depth was 1.83 m, determine the height and the velocity of the initial surge wave.

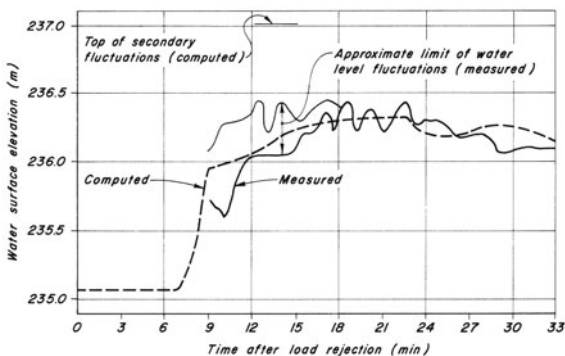
**13-3** A trapezoidal canal having a bottom width of 6.1 m and side slopes of 1.5 horizontal to 1 vertical is carrying  $126 \text{ m}^3/\text{sec}$  at a depth of 5.79 m. If the flow is suddenly stopped at the downstream end, compute the surge height and the wave velocity.



(a) At station 1

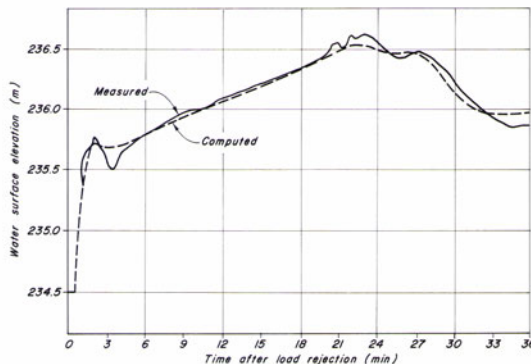


(b) At station 2

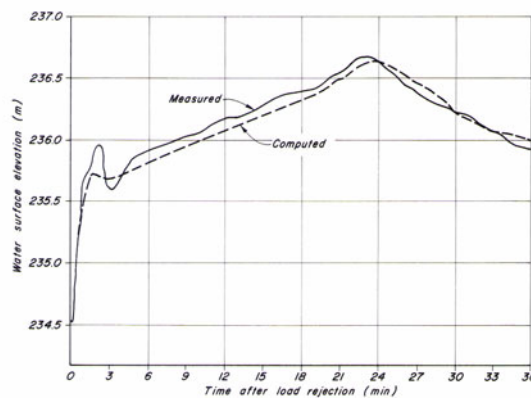


(c) At station 3

**Fig. 13-19.** Comparison of computed and measured transient-state water levels following 44-MW load rejection.



(d) At station 4



(e) At station 5

Fig. 13-19. (Continued)

**13-4** Prove that if the surge height,  $z$ , is small as compared to the initial flow depth,  $y_o$ , then

$$c = \sqrt{g \left( \frac{A_o}{y_o} + 1.5z \right)}$$

in which  $A_o$  = initial steady-state flow area.

**13-5** Develop the boundary conditions for the junction of three channels for Lax diffusive scheme. Neglect the friction losses and difference in the velocity heads at the junction.

**13-6** Plot the variation of water surface at the downstream end of a canal with time following sudden closure of the control gates at the downstream end. Assume the canal is short, horizontal, and frictionless.

**13-7** Derive the dynamic and continuity equations for non-prismatic channels having lateral outflow  $q$  per unit length of channel. Assume (1) gradual bulk outflow, e.g., over a side spillway; (2) outflow has negligible velocity, e.g., seepage; and (3) gradual inflow, e.g., from tributaries, having velocity component,  $u_l$ , in the positive  $x$ -direction.

**13-8** Write a computer program to compute the transient-state conditions in a rectangular channel by using the Lax diffusive scheme. Use the data given in the example of Section 13-11 and compare the computed results with those determined by using the MacCormack scheme. (These results are presented in [Fig. 13-12](#).)

**13-9** Lax scheme becomes unstable if the time derivative is replaced by  $\partial f / \partial t = (f_i^{k+1} - f_i^k) / \Delta t$  instead of that given by Eq. 13-61 ( $f$  stands for both  $y$  and  $V$ ) even if the grid spacing satisfies the Courant stability condition. By modifying the computer program of Problem 13-8, prove that this is true.

**13-10** [Fig. 13-20](#) shows the tailrace system of the G. M. Shrum Generating Station [Chaudhry and Kao, 1976], and [Table 13-1](#) lists the essential data for the project. Results of tests conducted on the prototype and on the hydraulic model are presented in [Figs. 13-21](#) to [13-23](#). By using different explicit and implicit finite-difference schemes, compute the transient conditions in the system and compare the computed and measured results. Note that the tailrace tunnel may prime following large load changes during periods of high tailwater levels.

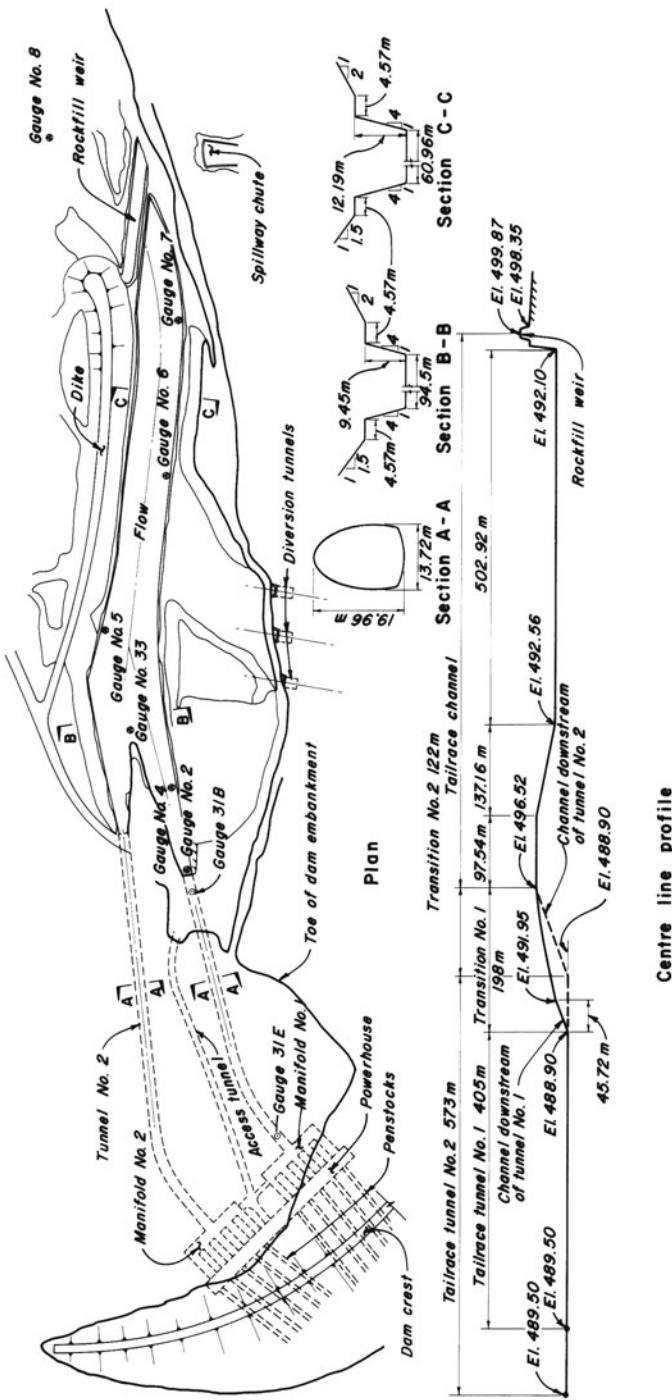
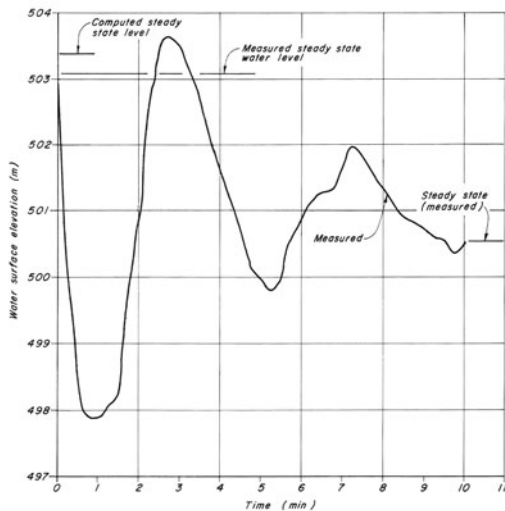


**Fig. 13-20.** Tailrace system of G. M. Shrum Generating Station.

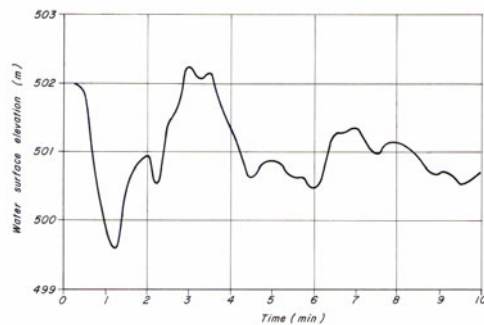
**Table 13-1. Data for tailrace system**

| General   |                                     |   |
|---|-------------------------------------|---|
| No. of tailrace tunnels   | 2                                   |   |
| No. of manifolds  | 2                                   |   |
| Units on Manifold No.1  | 1 to 5                              |   |
| Units on Manifold No.2  | 6 to 10                             |   |
| Tailrace Tunnels  |                                     |   |
| Shape   | Modified horseshoe                  |   |
| Size  | 19.96 m high, 13.72 m wide          |   |
| Lining  | Concrete                            |   |
| Length  | Tunnel 1, 405 m; 2, 573 m           |   |
| Manifold size   | 13.71 by 99.67 m                    |   |
| Tailrace Channel  |                                     |   |
| For the length and cross sections of the channel, see <a href="#">Fig. 13-20</a> .      |                                     |   |
| Weir length = 192 m.  |                                     |   |
| Turbines  |                                     |   |
| Turbines  | Maximum output <sup>a</sup><br>(MW) | Discharge <sup>a</sup> per turbine<br>(m <sup>3</sup> /s) |
| 1 to 5  | 261                                 | 178   |
| 6 to 8  | 275                                 | 190   |
| 9 and 10  | 300                                 | 204   |
| Prototype Test  |                                     |   |
| Inflow to manifold No.1 reduced from 810 to 133 m <sup>3</sup> /s in 8 s.               |                                     |   |
| Inflow to manifold No.2 remained steady at 240 m <sup>3</sup> /s.                       |                                     |   |
| Model Test  |                                     |   |
| <a href="#">Fig. 13-22:</a>   |                                     |   |
| Inflow to both manifolds reduced simultaneously from 990 to 0 m <sup>3</sup> /s in 8 s. |                                     |   |
| Initial steady-state water level at Gauge No.8 = El. 507.5 m.                           |                                     |   |
| <a href="#">Fig. 13-23:</a>   |                                     |   |
| Initial steady-state water level at Gauge No.8 = El. 507.5 m.                           |                                     |   |
| Inflow to manifold No.2 varied in 8 s as follows:                                       |                                     |   |
| (a) 990 to 0 m <sup>3</sup> /s;   |                                     |   |
| (b) 990 to 0 m <sup>3</sup> /s and then 0 to 396 m <sup>3</sup> /s after 20 s and       |                                     |   |
| (c) 990 to 0 m <sup>3</sup> /s and then to 396 m <sup>3</sup> /s after 127 s.           |                                     |   |

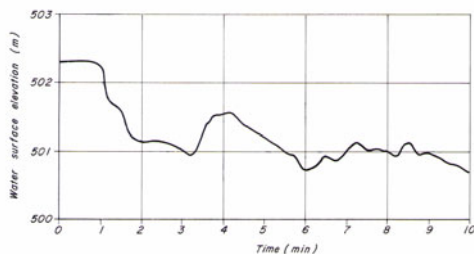
<sup>a</sup> At a net head of 164.6 m.



(a) Manifold No. 1

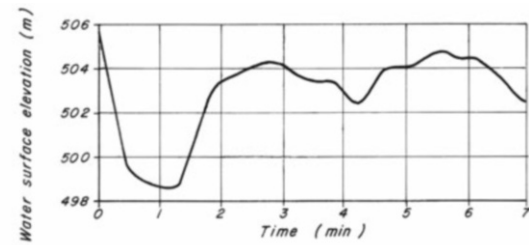


(b) Gauge no. 2

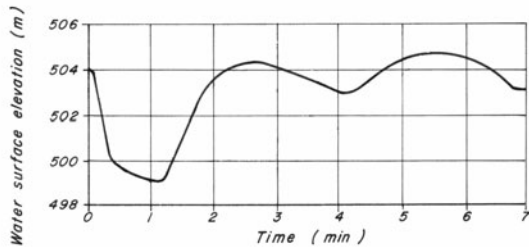


(c) Gauge no. 5

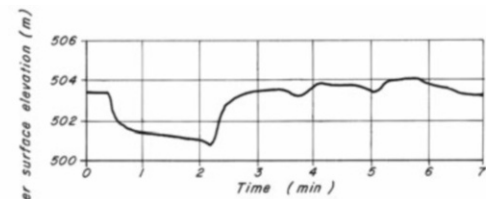
Fig. 13-21. Measured prototype water levels.



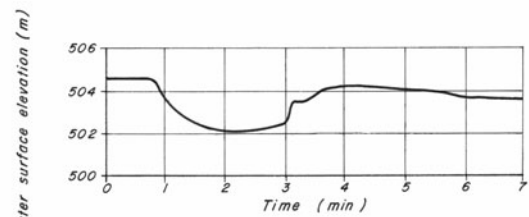
(a) Manifold No. 1



(b) Tunnel 1 (31E)

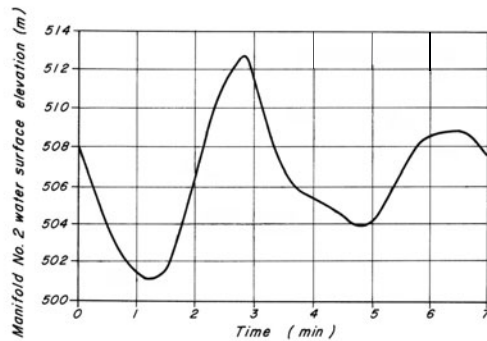


(c) Tunnel 1 (31B)

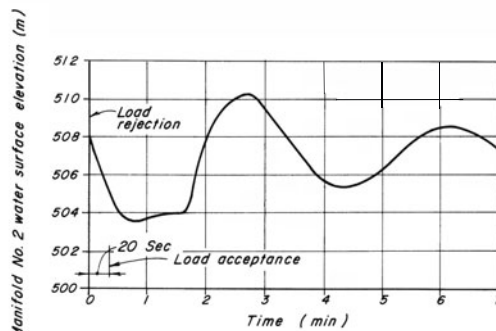


(d) Gauge 33

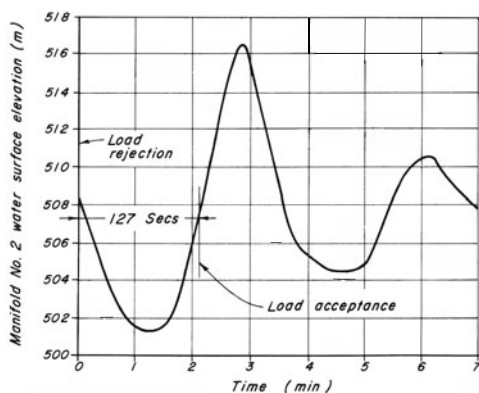
Fig. 13-22. Measured water levels on hydraulic model.



(a)



(b)



(c)

Fig. 13-23. Measured water levels on hydraulic model.

## Answers

**13-1**  $z = 0.9$  m;  $V_w = -5.13$  m/s.

**13-3**  $z = 0.93$  m;  $V_w = -5.52$  m/s.

**13-7**

Continuity equation:

$$A \frac{\partial V}{\partial x} + BV \frac{\partial y}{\partial x} + B \frac{\partial y}{\partial t} + V \frac{\partial A(x, y)}{\partial x} + q = 0$$

Dynamic equation:

$$\frac{\partial V}{\partial t} + V \frac{\partial V}{\partial x} + g \frac{\partial y}{\partial x} = g(S_o - S_f) + D_1$$

in which

$$D_1 = 0 \quad \text{for case 1}$$

$$D_1 = \frac{V}{2A} \quad \text{for case 2}$$

$$D_1 = \frac{(V - u_l)q}{A} \quad \text{for case 3}$$

## References

- Abbott, M. B., 1966, *An Introduction to the Method of Characteristics*, American Elsevier, New York.
- Abbott, M. B. and Verwey, A., 1970, "Four-Point Method of Characteristics," *Jour. Hydr. Div.*, Amer. Soc. of Civil Engrs., vol. 96, Dec., pp. 2549-2564.
- Amein, M. and Fang, C. S., 1970, "Implicit Flood Routing in Natural Channels," *Jour. Hyd. Div.*, Amer. Soc. of Civil Engrs., vol. 96, Dec., pp. 2481-2500.
- Anderson, D. A., Tannehill, J. C. and Pletcher, R. H., 1984, *Computational Fluid Mechanics and Heat Transfer*, McGraw-Hill, New York, NY.
- Babcock, C. I., 1975, "Impulse Wave and Hydraulic Bore Inception and Propagation as Resulting from Landslides," a *research problem* presented to Georgia Inst. of Tech., Atlanta, Georgia, in partial fulfillment of the requirements for the degree of M.Sc. in civil engineering, Oct..
- Balloffet, A., Cole, E. and Balloffet, A. F., 1974, "Dam Collapse Wave in a River," *Jour. Hyd. Div.*, Amer. Soc. of Civil Engrs., vol. 100, No. HY5, May, pp. 645-665.
- Baltzer, R. A. and Lai, C., 1968, "Computer Simulation of Unsteady Flows in Waterways," *Jour. Hyd. Div.*, Amer. Soc. of Civil Engrs., vol. 94, July, pp. 1083-1117.

- Benet, F. and Cunge, J. A., 1971, "Analysis of Experiments on Secondary Undulations Caused by Surge Waves in Trapezoidal Channels," *Jour. of Hydraulic Research*, Inter. Assoc. for Hyd. Research, vol. 9, no. I, pp. 11-33.
- Calame, J., 1932, "Calcul de l'onde translation dans les canaux d'usines," Editions la Concorde, Lausanne, Switzerland.
- Chaudhry, M. H., 1976, "Mathematical Modelling of Transient Stale Flows in Open Channels," *Proc. International Symposium on Unsteady Flow in Open Channels*, Newcastle-upon-Tyne, published by British Hydromechanics Research Assoc., Cranfield, Bedford, England, pp. C1-1 C1-18.
- Chaudhry, M. H. and Kao, K. H., 1976, "G. M. Shrum Generating Station: Tailrace Surges and Operating Guidelines During High Tailwater Levels," *Report*, British Columbia Hydro and Power Authority, Vancouver, B.C., November.
- Chaudhry, M. H., Mercer, A. G. and Cass, D. E., 1983, "Modeling of Slide-Generated Waves in a Reservoir," *Jour. Hydraulic Engineering*, Amer. Soc. of Civil Engrs., vol. 109, Nov., pp. 1505-1520.
- Chaudhry, M. H. and Hussaini, M. Y., 1985, "Second-Order Accurate Explicit Finite Difference Schemes for Waterhammer Analysis," *Jour. of Fluids Engineering*, Amer. Soc. Mech. Engrs., Dec., pp. 523-529.
- Chaudhry, M. H. 2008, "Open-Channel Flow," 2nd ed., Springer, New York, NY.
- Chen, C. L., 1980, "Laboratory Verification of a Dam-Break Flood Model," *Jour. Hyd. Div.*, Amer. Soc. of Civil Engrs., April, pp. 535-556.
- Chiang, W. L., Divoky, D., Parnicky, P. and Wier, W., 1981, "Numerical Model of LandslideGenerated Waves," Prepared for U.S. Bureau of Reclamation by Tetra Tech., Inc., California, Nov..
- Chow, V. T., 1959, *Open-Channel Hydraulics*, McGraw-Hili Book Co., New York, NY.
- Cooley, R. L. and Moin, S. A., 1976, "Finite Element Solution of Saint-Venant Equations," *Jour., Hyd. Div.*, Amer. Soc. of Civil Engrs., vol. 102, June, pp. 759-775.
- Courant, R., Friedrichs, K. and Lewy, H., 1928, "Über die partiellen Differenzengleichungen der Mathematischen Physik," *Math. Ann.*, vol. 110, pp. 32-74 (in German).
- Cunge, J. A. and Wegner, M., 1964, "Integration Numerique des equations d'ecoulement de Barre de Saint Venant par un schema Implicite de differences finies," *La Houille Blanche*, No. I, pp. 33-39.
- Cunge, J. A., 1966, "Comparison of Physical and Mathematical Model Test Results on Translation Waves in the Oraison-Manosque Power Canal," *La Houille Blanche*, no. I, Grenoble, France, pp. 55-69, (in French).
- Cunge, J. A., 1969, "On the Subject of a Flood Propagation Computation Method (Muskingum Method)," *Jour. of Hydraulic Research*, vol. 7, no. 2, pp. 205-230.
- Cunge, J. A., 1970, "Calcul de Propagation des Ondes de Rupture de Barrage," *La Houille Blanche*, no. I, pp. 25-33.

- Cunge, J. A., Holley, F. M. and Verwey, A., 1980, *Practical Aspects of Computational River Hydraulics*, Pitman, London, UK.
- Das, M. M. and Wiegel, R. L., 1972, "Waves Generated by Horizontal Motion of a Wall," *Jour., Waterways, Harbors and Coastal Engineering Div.*, Amer. Soc. of Civ. Engrs., vol. 98, no. WWI, Feb., pp. 49-65.
- Davidson, D. D. and McCartney, B. L., 1975, "Water Waves Generated by Landslides in Reservoirs," *Jour., Hyd. Div.*, Amer. Soc. of Civ. Engrs., vol. 101, Dec., pp. 1489-1501.
- De Saint-Venant, B., 1871, "Theorie du mouvement non-permanent des eaux avec application aux crues des vivieres et a l'introduction des mareas dans leur lit," *Acad. Sci. Comptes Rendus, Paris*, vol. 73, pp. 148-154, 237-240 (translated into English by U.S. Corps of Engineers, No. 49-g, Waterways Experiment Station, Vicksburg, Miss., 1949).
- Dressler, R. F., 1952, "Hydraulic Resistance Effect upon the Dam Break Functions," *Jour. of Research, U.S. Bureau of Standards*, vol. 49, No. 3, Sept., pp. 217-225.
- Dressler, R. F., 1954, "Comparison of Theories and Experiments for the Hydraulic Dam-Break Wave," *Intern. Assoc. of Scientific Hydrology*, no. 38, vol. 3, pp. 319-328.
- Drigli, C., 1937, "Esperienze sul moto perturbato nei canali industriali," *L'Energie Elettrica*, no. IV-V, vol. XIV, Milan, Italy, April-May.
- Dronkers, J. J., 1964, *Tidal Computations in Rivers and Coastal Waters*, North Holland Publishing Co., Amsterdam, the Netherlands.
- Favre, H., 1935, Ondes de translation dans les canaux de couverts, Dunod.
- Fennema, R. J. and Chaudhry, M. H., 1986, "Explicit Numerical Schemes for Unsteady FreeSurface Flows with Shocks," *Water Resources Research*, vol. 22(13).
- Fennema, R. J. and Chaudhry, M. H., 1986, "Simulation of One-Dimensional Dam-Break Flows" *Jour. of Hydraulic Research.*, Intern. Assoc. for Hydraulic Research, vol. 25(1), pp. 41-51.
- Forstad, F., 1968, "Waves Generated by Landslides in Norwaygias Fjords and Lakes," *Publication No. 79*, Norwegian Geotechnical Institute, Oslo, pp. 13-32.
- Fread, D. L. and Harbaugh, T. E., 1973, "Transient Simulation of Breached Earth Dams," *Jour., Hyd. Div.*, Amer. Soc. of Civil Engrs., Jan., pp. 139-154.
- Fread, D. L., 1974, "Numerical Properties of Implicit Four-Point Finite-Difference Equations of Unsteady Flow," *Tech. Memo NWS HYDRO-18*, NOAA, U.S. National Weather Service.
- Fread, D. L., 1977, "The Development and Testing of a Dam-Break Flood Forecasting Model," *Proc., Dam Break Flood Routing Model Workshop*, U.S. Dept. of Commerce, National Tech. Service, Oct., pp. 164-197.
- Henderson, F. M., 1966, *Open Channel Flow*, MacMillan, New York, NY.
- Jaeger, C., 1956, *Engineering Fluid Mechanics*, Blackie & Son Limited, London, UK, pp. 381-392.

- Jameson, A., Schmidt, W. and Turkel, E., 1981, "Numerical Solutions of the Euler Equations by Finite Volume Methods Using Runge-Kutta Time-Stepping Schemes," *AIAA 14th Fluid and Plasma Dynamics Conf.*, Palo Alto, Calif., AIAA-81-1259.
- Johnson, R. D., 1922, "The Correlation of Momentum and Energy Changes in Steady Flow with Varying Velocity and the Application of the Former to Problems of Unsteady Flow or Surges in Open Channels," *Engineers and Engineering*, The Engineers Club of Philadelphia, p.233.
- Kachadoorian, R., 1965, "Effects of the Earthquake of March 27 1964, at Whittier, Alaska," *Professional Paper, No. 542-B*, U.S. Geological Survey.
- Kamphuis, J. W., 1970, "Mathematical Tidal Study of St. Lawrence River." *Jour., Hyd. Div.*, Amer. Soc. of Civil Engrs., vol. 96, No. HY3, March, pp. 643-664.
- Kamphuis, J. W. and Bowering, R. J., 1970, "Impulse Waves Generated by Landslides," *Proc., Twelfth Coastal Engineering Conference*, Amer. Soc. of Civ. Engrs., Washington, DC., Sept., pp. 575-588.
- Kao, K. H., 1977, "Numbering of a Y-Branch System to Obtain a Banded Matrix for Implicit Finite-Difference Scheme," B.C. Hydro interoffice memorandum, Hydraulic Section, November.
- Katopodes, N. D. and Strelkoff, T., 1978, "Computing Two-Dimensional Dam-Break Flood Waves," *Jour., Hyd. Div.*, Amer. Soc. of Civil Engrs., Sept., pp. 1269-1287.
- Katopodes, N. D. and Strelkoff, T., 1979, "Two-Dimensional Shallow Water-Wave Models," *Jour. Engineering Mechanics Div.*, Amer. Soc. of Civil Engrs., vol. 105, No. EM2, Proc. Paper 14532, pp. 317-334.
- Katopodes, N. D. and Schamber, D. R., 1983, "Applicability of Dam-Break Flood Wave Models," *Jour. Hydraulic Engineering*, Amer. Soc. of Civil Engrs., vol. 109, May, pp. 702-721.
- Katopodes, N. D., 1984, "A Dissipative Galerkin Scheme for Open-Channel Flow," *Jour. Hydraulic Engineering*, Amer. Soc. of Civil Engrs., vol. 110, HY4, Proc. Paper 18743, April.
- Katopodes, N. D., 1984, "Two-Dimensional Surges and Shocks in Open Channels," *Jour. Hydraulic Engineering*, Amer. Soc. of Civil Engrs., vol. 110, June, pp. 794-812.
- Kiersch, G. A., 1964, "Vaiont Reservoir Disaster," *Civ. Engineering*, Amer. Soc. of Civ. Engrs., vol. 34, no. 3, March, pp. 32-47.
- Koutitas, C. G., 1977, "Finite Element Approach to Waves due to Landslides." *Jour., Hyd. Div.*, Amer. Soc. of Civ. Engrs., vol. 103, Sept., pp. 1021-1029.
- Law, L. and Brebner, A., 1968, "On Water Waves Generated by Landslides," *Third Australasian Conference on Hydraulics and Fluid Mechanics*, Sidney, Australia, Nov., pp. 155159.
- Lax, P. D., 1954, "Weak Solutions of Nonlinear Hyperbolic Partial Differential Equations and Their Numerical Computation," *Communications on Pure and Applied Mathematics*, vol. 7, pp. 159-163.

- Lax, P. D. and Wendroff, B., 1960 , "Systems of Conservation Laws," *Communications on Pure and Applied Mathematics*, vol. 13, pp. 217-237.
- Leendertse, J. J., 1967, "Aspects of a Computational Model for Long Period Water-Wave Propagation," *Memo RM-5294-PR*, Rand Corporation, May.
- Liggett, J. A. and Woolhiser, D. A., 1967, "Difference Solutions of the Shallow-Water Equation," *Jour. Engineering Mech. Div.*, Amer. Soc. of Civil Engrs., vol. 93, April, pp. 39-71.
- MacCormack, R. W., 1969, "The Effect of Viscosity in Hypervelocity Impact Cratering," *Paper No. 69-354*, Amer. Inst. Aero. Astro., Cincinnati, OH, April 30/May 2.
- Mahmood, K. and Yevjevich, V. (ed.), 1975, *Unsteady Flow in Open Channels*, Water Resources Publications, Fort Collins, CO.
- Martin, C. S. and Zovne, J. J., 1971, "Finite-Difference Simulation of Bore Propagation," *Jour., Hyd. Div.*, Amer. Soc. of Civ. Engrs., vol. 97, No. HY7, July, pp. 993-1010.
- Martin, C. S. and DeFazio, F. G., 1969, "Open Channel Surge Simulation by Digital Computers," *Jour., Hyd. Div.*, Amer. Soc. of Civil Engrs., vol. 95, Nov., pp. 2049-2070.
- McCracken, D. D. and Dorn, W. S., 1967, *Numerical Methods and FORTRAN Programming*, John Wiley & Sons, New York, NY.
- McCulloch, D. S., 1966, "Slide-Induced Waves, Seiching and Ground Fracturing Caused by the Earthquakes of March 27 1964, at Kenai Lake, Alaska," *Professional Paper 543-A*, U.S. Geological Survey.
- Mercer, A. G., Chaudhry, M. H. and Cass, D. E., 1979, "Modeling of Slide-Generated Waves," *Proc, Fourth Hydrotechnical Conference*, vol. 2, Canadian Society for Civil Engineering, May, pp. 730-745.
- Meyer-Peter, E. and Favre, H., 1932, "Ueber die Eigenschaften von Schwallen und die Berechnung von UnteIWasserstollen," *Schweizerische Bauzeitung*, Nos. 4-5, vol. 100, Zurich, Switzerland, July, pp. 43-50, 61-66.
- Miller, D. J., 1960 "Giant Waves in Lituya Bay, Alaska," *Professional Paper 354-L*, U.S. Geological Survey.
- Noda, E., 1970, "Water Waves Generated by Landslides," *Jour., Waterways, Harbors and Coastal Engineering Div.*, Amer. Soc. of Civ. Engrs., vol. 96, no. WW4, Nov., pp. 835-855.
- Patridge, P. W. and Brebbia, C. A., 1976, "Quadratic Finite Elements in Shallow Water Problems," *Jour., Hyd. Div.*, Amer. Soc. of Civil Engrs., vol. 102, Sept., pp. 1299-1313.
- Ponce, V. M. and Yevjevich, V., 1978, "Muskingum-Cunge Method with Variable Parameters," *Jour., Hyd. Div.*, Amer. Soc. of Civil Engrs., vol. 104, Dec., pp. 1663-1667.
- Preissmann, A. and Cunge, J. A., 1961, "Calcul des intumescences sur machines electroniques," *Proc. IX Meeting*, International Assoc. for Hydraulic Research, Dubrovnik.
- Price, R. K., 1974, "Comparison of Four Numerical Methods for Flood Routing," *Jour., Hyd. Div.*, Amer. Soc. of Civil Engrs., vol. 100, July, pp. 879-899.

- Prins, J. E., 1958, "Characteristics of Waves Generated by a Local Disturbance," *Trans., Amer. Geophysical Union*, vol. 39, no. 5, Oct., pp. 865-874.
- Proceedings 1977, Dam-Break Flood Routing Model Workshop*, U.S. National Technical Information Service, Oct..
- Pugh, C. A., 1982, "Hydraulic Model Studies of Landslide-Generated Water Waves-Morrow Point Reservoir," *Report No. REC-ERC-82-9*, Bureau of Reclamation, Denver, Colo., April.
- Rajar, R., 1978, "Mathematical Simulation of Dam-Break Flow," *Jour. Hyd. Div.*, Amer. Soc. of Civil Engrs., July, pp. 1011-1026.
- Rajar, R., 1983, "Two-Dimensional Dam-Break Flow in Steep Curved Channels," *XX Congress*, Intern. Assoc. for Hydraulic Research, Moscow, Sept., pp. 199-200.
- Raney, D. C. and Butler, H. L., 1975, "A Numerical Model for Predicting the Effects of Landslide- Generated Water Waves," *Research Report H-75-1*, U.S. Army Engineer Waterways Experiment Station, Vicksburg, Miss., Feb..
- Richtmyer, R. D. and Morton, K. W., 1967, *Difference Methods for Initial-Value Problems*, 2nd ed., Interscience Publishers, New York, NY.
- Ritter, A., 1982, "Die Fortpflanzung der Wasserwellen," *Zeitschrift des Vereines Deutscher Ingenieure*, vol. 36, No. 33, Aug., pp. 947-954.
- Rouse, H. (ed.), 1961, *Engineering Hydraulics*, John Wiley & Sons, New York, NY.
- Sakkas, J. G. and Strelkoff, T., 1973, "Dam-Break Flood in a Prismatic Dry Channel," *Jour., Hyd. Div.*, Amer. Soc. of Civil Engrs., Dec., pp. 2195-2216.
- Schamber, D. R. and Katopodes, N. D., 1984, "One-Dimensional Models for Partially Breached Dams," *Jour. Hydraulic Engineering*, Amer. Soc. of Civil Engrs., vol. 110, August, pp. 1086-1102.
- Schulte, A. M. and Chaudhry, M. H., 1987, "Gradually-Varied Flows in Open-Channel Networks," *Jour. Hydraulic Research*, vol. 25(3), pp. 357-371.
- Song, C. S. S., Cardle, J. A. and Leung, K. S., 1983, "Transient Mixed-Flow Models for SIOrm Sewers," *Jour. Hydraulic Engineering*, Amer. Soc. of Civil Engrs., vol. 109, Nov., pp. 1487-1504.
- Stoker, J. J., 1948, "The Formation of Breakers and Bores," *Communications on Pure and Applied Mathematics*, vol. I, pp. 1-87.
- Stoker, J. J., 1957, *Water Waves*, Interscience, New York, NY.
- Strelkoff, T., 1969, "One-Dimensional Equations of Open Channel Flow," *Jour., Hyd. Div.*, Amer. Soc. of Civil Engrs., vol. 95, May, pp. 861-876.
- Strelkoff, T., 1970, "Numerical Solution of Saint-Venant Equations," *Jour., Hyd. Div.*, Amer. Soc. of Civil Engrs., vol. 96, January, pp. 223-252.
- Terzidis, G. and Strelkoff, T., 1970, "Computation of Open Channel Surges and Shocks," *Jour., Hyd. Div.*, Amer. Soc. of Civil Engrs., vol. 96, Dec., pp. 2581-2610.
- Vasiliev, O. F. et al. 1965, "Numerical Methods for the Calculation of Shock Wave Propagation in Open Channels," *Proc. 11th Congress*, International Assoc. for Hyd. Research, Leningrad, vol. III, l3 pp.

- Warming, R. F. and Hyett, B. J., 1974, "The Modified Equation Approach to the Stability and Accuracy Analysis of Finite-Difference Methods," *Jour. of Computational Physics*, vol. 14, pp. 159-179.
- Whitham, G. B., 1955, "The Effects of Hydraulic Resistance in the Dam-Break Problem," *Proc., Royal Society*, No. 1170, Jan..
- Wiegel, R. L., 1955, "Laboratory Studies of Gravity Waves Generated by the Movement of a Submerged Body," *Trans. Amer. Geophysical Union*, vol. 36, no. 5, Oct., pp. 759-774.
- Wiggert, D. C., 1970, "Prediction of Surge Flows in the Batiaz Tunnel," *Research Report*, Laboratory for Hydraulics and Soil Mechanics, Federal Institute of Technology, Zurich, Switzerland, no. 127, June.
- Wiggert, D. C., 1972, "Transient Flow in Free-Surface, Pressurized Systems," *Jour., Hyd. Div.*, Amer. Soc. of Civ. Engrs., Jan., pp. 11-27.
- Yen, B. C., 1973, "Open-Channel Flow Equations Revisited," *Jour., Engineering Mech. Div.*, Amer. Soc. of Civ. Engrs., vol. 99, Oct., pp. 979-1009.
- "Wave Action Generated by Slides into Mica Reservoir, Hydraulic Model Studies," *Report*, Western Canada Hydraulic Laboratories, Port Coquitlam, B.C., Canada, Nov. 1970.

## ERRATUM

# Applied Hydraulic Transients

M. Hanif Chaudhry

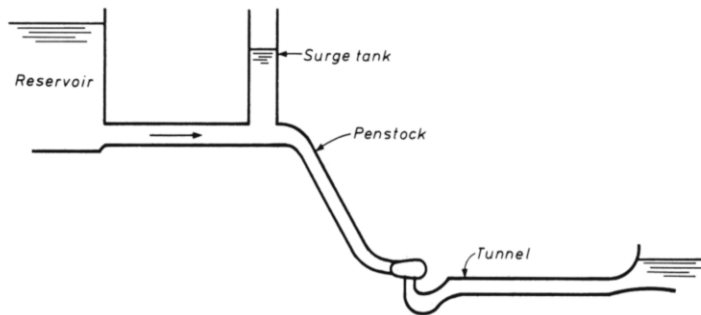
M.H. Chaudhry, *Applied Hydraulic Transients*, DOI 10.1007/978-1-4614-8538-4,  
© Author 2014

---

**DOI 10.1007/978-1-4614-8538-4\_14**

- p. 38 Add the following titles to (a) and (b) in Fig. 2.1: (a) At time  $t$ , (b) At time  $t + \Delta t$
- p. 98 Line 7 of section 3-10 should read, four-point-centered...
- p. 104 Fig. 3-23 should read as  $a = 1100$  m/s and  $a = 900$  m/s
- p. 121 In the footnote, the numerator of the second equation for  $N_s$ , should read  $\sqrt{Q_R}$ ....
- p. 122 Line 5 from the top should read Appendix C
- p. 126 Eq. 4-13: The right-hand side, should read: - 60.....
- p. 129 Line 7 from the bottom: should read Appendix C
- p. 141 Third line from the bottom should read  $Q_{P_{i,1}}$ .

- p. 158 Fig. 5-1 (e): Tailrace channel should be a full-flow, pressurized tunnel, as shown in the figure below.



p. 243 Eq. 7-12 should read  $H_B$  and not  $H_A$ .

p. 317 Last paragraph, the second and third lines should read "...time domain in the plots on the left-hand side of Figs. 8-30 a and b and the respective transformed series in the frequency domain are shown in the plots on the right-hand side of Figs. 8-30 a and b."

p. 466 Eq. 13-100, the first line should read  $\propto (y_{i+1}^{k+1} - y_i^{k+1})$  and the second line should read ...  $\propto (V_{i+1}^{k+1} - V_i^{k+1})$

p. 483 The top line of the should read  $H_c =$   
The second paragraph, first line should read  $H_c$

p. 524 For  $\theta = 245$ , the last column should read -.97  
For  $\theta = 270$ , the second column should read .68

# A

---

## DESIGN CHARTS

Design charts, approximate formulas and typical data needed for transient analysis are presented in this appendix. These may be used for quick computations for planning, feasibility studies, or preliminary design when a large number of alternatives are considered to develop an economical design or to select the parameters of a system for a detailed analysis.

### A-1 Equivalent Pipe

A pipeline with step changes in the diameter, wall thickness, or wall material along its length may be replaced by an “equivalent pipe” for an approximate analysis. If an equivalent pipe is used in the analysis instead of the actual pipeline, the partial wave reflections and the spatial variation of the friction losses and of the elastic and inertial effects are not properly taken into consideration. This approximation is satisfactory for small spatial variations in the pipeline properties.

The total friction losses, the wave travel time, and the inertial effects of the equivalent pipe should be equal to those of the actual pipeline. These characteristics for the equivalent pipe of a pipeline having  $n$  pipes in series may be determined from the following equations:

$$A_c = \frac{L_e}{\sum_{i=1}^n \frac{L_i}{A_i}} \quad (\text{A-1})$$

$$a_c = \frac{L_e}{\sum_{i=1}^n \frac{L_i}{a_i}} \quad (\text{A-2})$$

$$f_c = \frac{D_e A_e^2}{L_e} \sum_{i=1}^n \frac{f_i L_i}{D_i A_i^2} \quad (\text{A-3})$$

in which  $a$  is the wave velocity, and  $A$ ,  $L$ ,  $D$ , and  $f$  are the cross-sectional area, length, diameter, and Darcy-Weisbach friction factor for the pipe, respectively.

The subscripts  $e$  and  $i$  refer to the equivalent pipe and to the  $i$ th pipe of the pipeline.

## A-2 Valve Closure

[Figures A-1](#) and [A-2](#) show the maximum pressure rise at the valve and at the midlength of a pipeline above the upstream reservoir level caused by the closure of a downstream valve discharging into atmosphere. The valve closure is assumed to be uniform, i.e., valve-opening versus time curve is a straight line.

The following notation is used:  $\rho = aV_o/(2gH_o)$ ;  $K = T_c/(2L/a)$ ;  $a$  = wave velocity;  $g$  = acceleration due to gravity;  $H_o$  = static head (elevation of the reservoir level – elevation of the valve);  $L$  = length of the pipeline;  $V_o$  = initial steady-state velocity in the pipeline;  $T_c$  = valve closure time;  $\Delta H_m$  = maximum pressure rise at midlength above the reservoir level;  $\Delta H_d$  = maximum pressure rise at the valve above the reservoir level;  $h_{f_o}$  = initial steady-state head loss in the pipeline for velocity  $V_o$ ;  $h = h_{f_o}/H_o$ ;  $H_{\max}$  = maximum pressure head at the valve =  $H_o + \Delta H_d$  and  $H_{\max}$  = maximum pressure head at midlength of the pipeline =  $H_o + \Delta H_m$ .

## A-3 Valve Opening

Minimum pressure head,  $H_{\min}$ , at the valve caused by *uniformly* opening a downstream valve from the completely closed position may be determined from the following equation [Parmakian, 1963]:

$$H_{\min} = H_o \left( -k + \sqrt{k^2 + 1} \right)^2 \quad (\text{A-4})$$

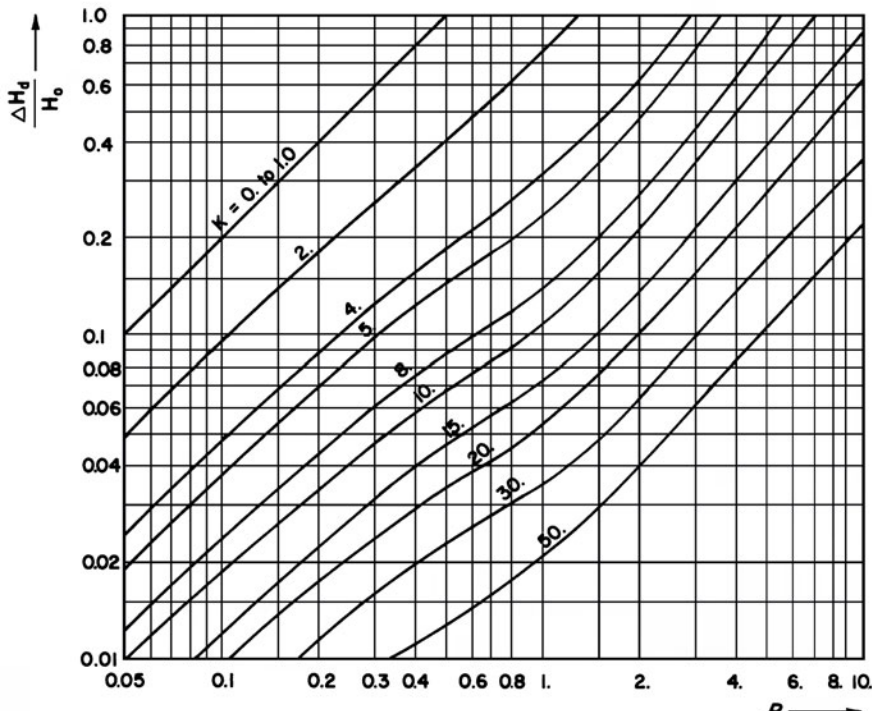
in which  $k = LV_f/(gH_oT_o)$ ;  $L$  = length of the pipeline;  $V_f$  = final steady-state velocity in the pipeline;  $T_o$  = valve opening time; and  $H_o$  = static head. The minimum pressure occurs  $2L/a$  seconds after the start of the valve movement. Equation A-4 is applicable if  $T_o > 2L/a$ . For  $T_o \leq 2L/a$ ,

$$H_{\min} = H_o - \frac{a}{g} \Delta V \quad (\text{A-5})$$

in which  $\Delta V$  = change in the flow velocity due to valve opening.

## A-4 Power Failure to Centrifugal Pump

Graphs are presented in [Figs. A-3](#) through [A-8](#) [Kinno and Kennedy, 1965] for the minimum and maximum pressure heads at the pump, and at the



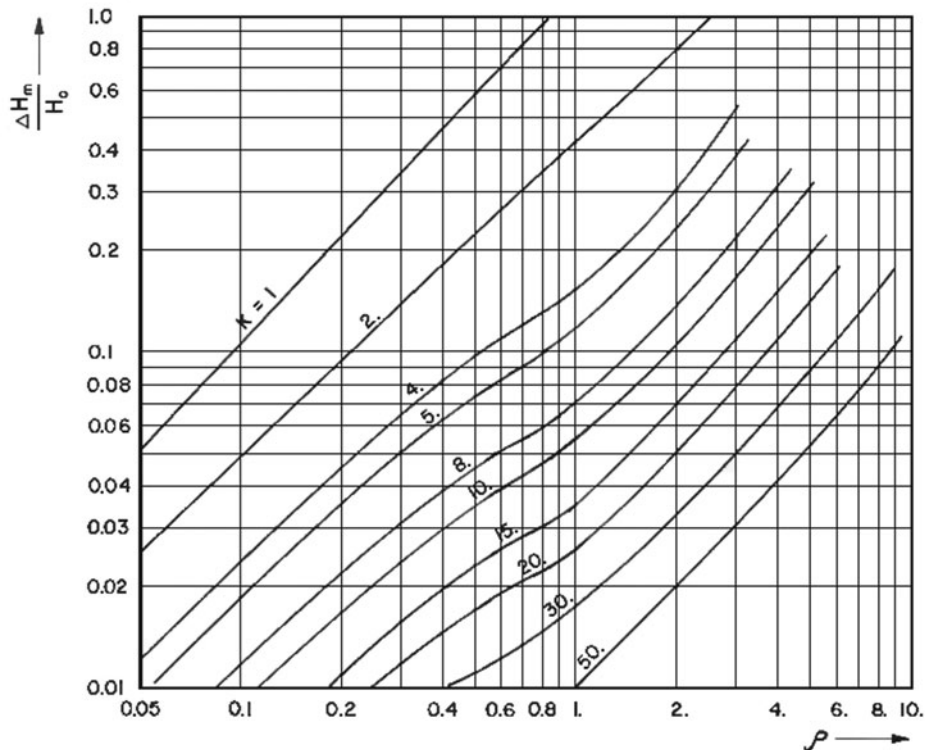
(a) At valve

**Fig. A-1.** Maximum pressure rise due to uniform valve closure; frictionless system ( $h = 0$ ).

midlength of a pipeline, and for the time of flow reversal following power failure to the centrifugal pump units. In Fig. A-5, numbers on the curves refer to the maximum downsurge or maximum upsurge divided by  $H_o^*$ .

The graphs are applicable to pumps with specific speed of less than 0.46 (SI units), i.e., 2700 (gpm units); they are not applicable to systems in which there is a valve closure during the transient state or to systems with waterhammer control devices other than large surge tanks. In the analysis, the latter are considered as the upstream reservoirs.

The following notation is used:  $a$  = wave velocity;  $E_R$  = pump efficiency at rated conditions;  $g$  = acceleration due to gravity;  $H_R$  = rated head of the pump;  $H_f$  = friction losses in the discharge line;  $h_f = H_f/H_R$ ;  $H_d$  = minimum transient-state head at the pump;  $h_d = H_d/H_R$ ;  $H_m$  = minimum transient-state head at midlength of the discharge line;  $h_m = H_m/H_R$ ;  $H_{mr}$  = maximum transient-state head at midlength of the discharge line;  $h_{mr} = H_{mr}/H_R$ ;  $H_r$  = maximum transient-state head at the pump;  $h_r = H_r/H_R$ ;  $L$  = length of the



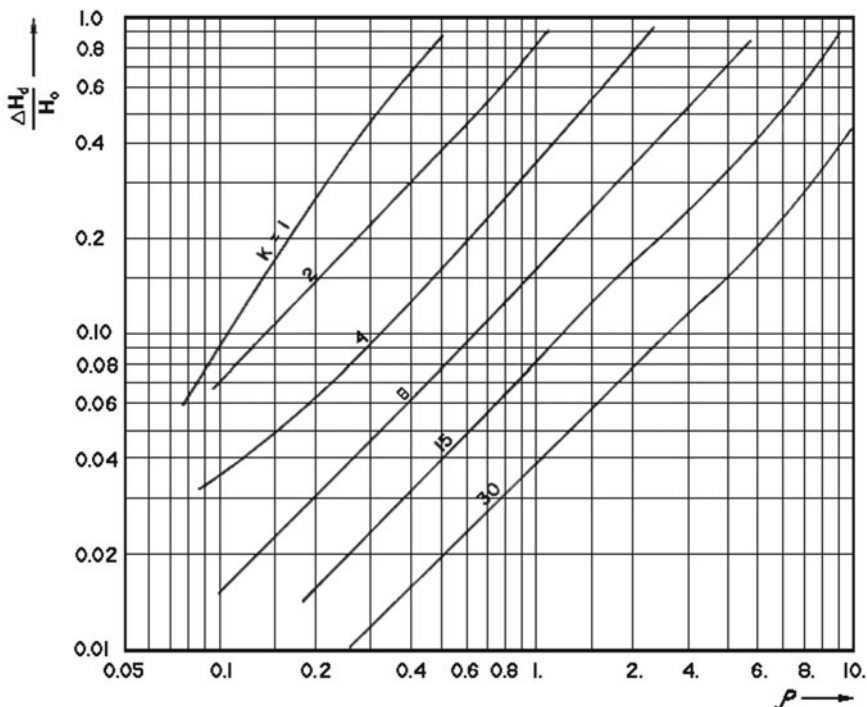
(b) At mid-length

Fig. A-1. (Continued)

discharge line;  $N_R$  = rated pump speed;  $Q_R$  = rated pump discharge;  $t$  = time;  $t_o$  = elapsed time from power failure to flow reversal at the pump;  $V_R$  = fluid velocity in the discharge line for rated pump discharge;  $WR^2$  = moment of inertia of the pump impeller and motor, and entrained fluid;  $\rho = aV_R / (2gH_R)$ ;  $\tau = 0.5 / (kL/a)$ ; and, in the SI units,  $k = (892770H_RQ_R)/(E_RIN_R^2)$  in which  $Q_R$ ,  $H_R$ ,  $WR^2$ , and  $N_R$  are in  $\text{m}^3/\text{s}$ ,  $\text{m}$ ,  $\text{kg m}^2$ , and rpm, respectively, and  $E_R$  is in the fractional form e.g., 0.8; and, in the English units,  $k = (183200H_RQ_R)/(E_RWR^2N_R^2)$  in which  $Q_R$ ,  $H_R$ ,  $WR^2$ , and  $N_R$  are in  $\text{ft}^3/\text{s}$ ,  $\text{ft}$ ,  $\text{lb-ft}^2$ , and rpm respectively, and  $E_R$  is in the fractional form, e.g., 0.8.

## A-5 Air Chamber

Charts are presented in Fig. A-9 [Ruus, 1977] for the maximum upsurge and downsurge at the pump end, at the midlength, and at the quarter point on the



(a) At valve

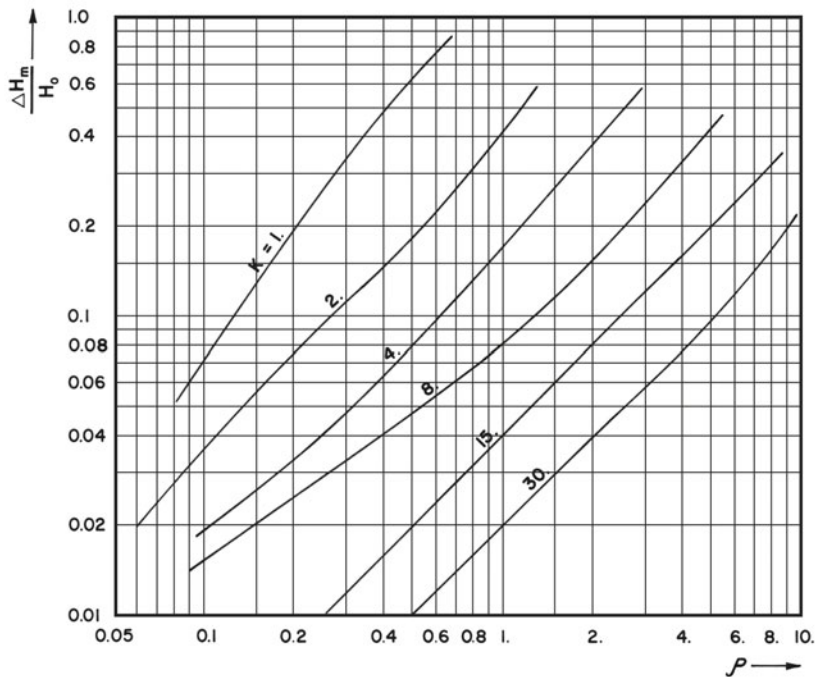
**Fig. A-2.** Maximum pressure rise due to uniform valve closure; friction losses taken into consideration ( $h = 0.25$ ).

reservoir side of a discharge line following power failure to the pumps. These charts may be used to determine the required air volume for a discharge line.

The charts are based on the following assumptions: Air chamber is located near the pump; check valve closes simultaneously with the power failure; Darcy-Weisbach formula for computing the steady-state friction losses is valid during the transient state; the absolute pressure head,  $H^*$ , and the volume of air,  $C$ , inside the air chamber follow the relationship  $H^*C^{1.2} = \text{constant}$ .

The following notation is used:  $a$  = wave velocity;  $V_o$  = initial steady-state velocity in the discharge pipe;  $g$  = acceleration due to gravity;  $H_o$  = static head (Elevation of the reservoir – Elevation of the air chamber);  $H_o^*$  = absolute static head =  $H_o + 10.36$  (in the English units,  $H_o + 34$ );  $H_{f_o}$  = initial steady-state head losses in the discharge line =  $fLV_o^2/(2gD)$ ;  $C_o$  = initial steady-state air volume in the chamber;  $Q_o$  = initial steady-state discharge in the pipe;  $L$  = length of the discharge line;  $D$  = diameter of the discharge line; and  $\rho^* = aV_o/[2g(H_o^* + H_{f_o})]$ .

The maximum *upsurge* and *downsurge* are *above* and *below* the downstream reservoir level, and the absolute pressure heads are obtained by sub-

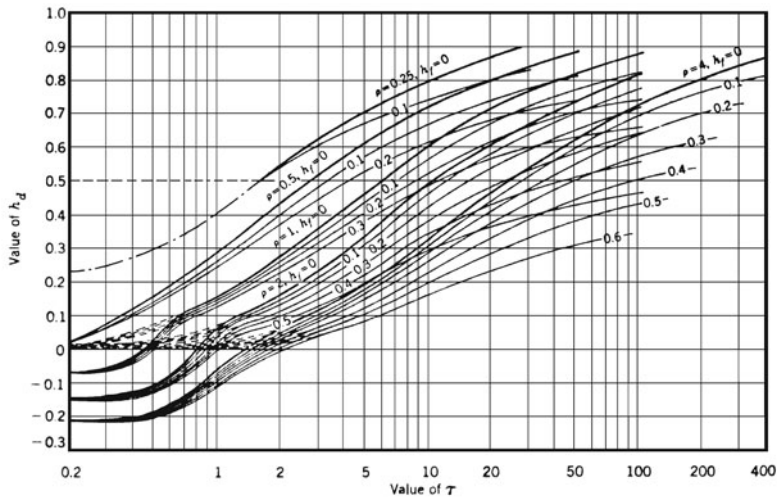


(b) At midlength

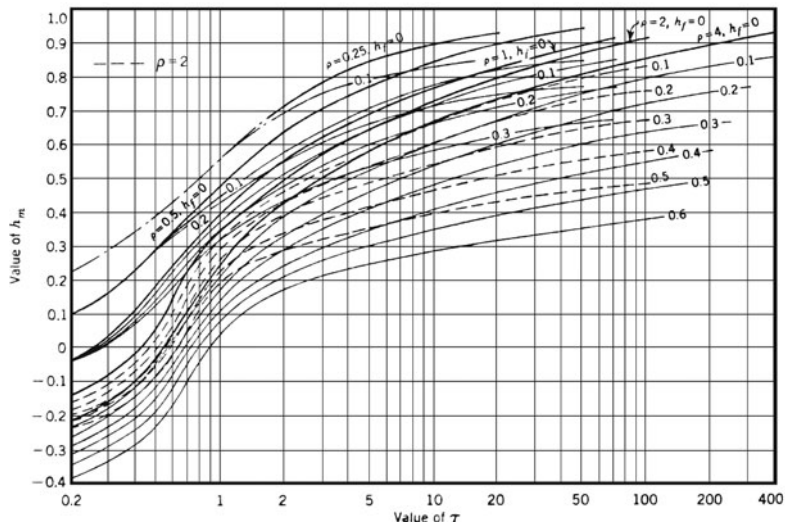
Fig. A-2. (Continued)

tracting or adding the downsurge or upsurge to the reservoir level plus the barometric head.

The size of air chamber required for a pipeline may be determined as follows: Determine  $2C_o a / (Q_o L)$  from Fig. A-9 for the maximum allowable downsurge at any critical point along the pipeline, e.g., a vertical bend. Linear interpolation may be used if the bend is not located either at the midlength or at the quarterpoint. From the expression  $2C_o a / (Q_o L)$ , compute the minimum initial steady-state air volume,  $C_{o\min}$ . This volume corresponds to the upper emergency level in the air chamber. Then, add the volume of the chamber between the upper and the lower emergency levels to the minimum air volume. For this volume between the upper and lower emergency levels, ten percent is suggested for large size chambers and 20 percent, for small chambers. For this new air volume,  $C_{o\max}$ , determine the maximum downsurge at the pump end from Fig. A-9, and then determine the absolute minimum head,  $H_{\min}$ , at the pump end by subtracting the maximum downsurge at the pump from the absolute static head,  $H_o^*$ . The maximum transient-state air volume,  $C_{\max}$  may then be determined from the equation



(a) At pump



(b) At midlength of discharge line

**Fig. A-3.** Minimum head following power failure, including friction.  
(After Kinno and Kennedy, [1965].)

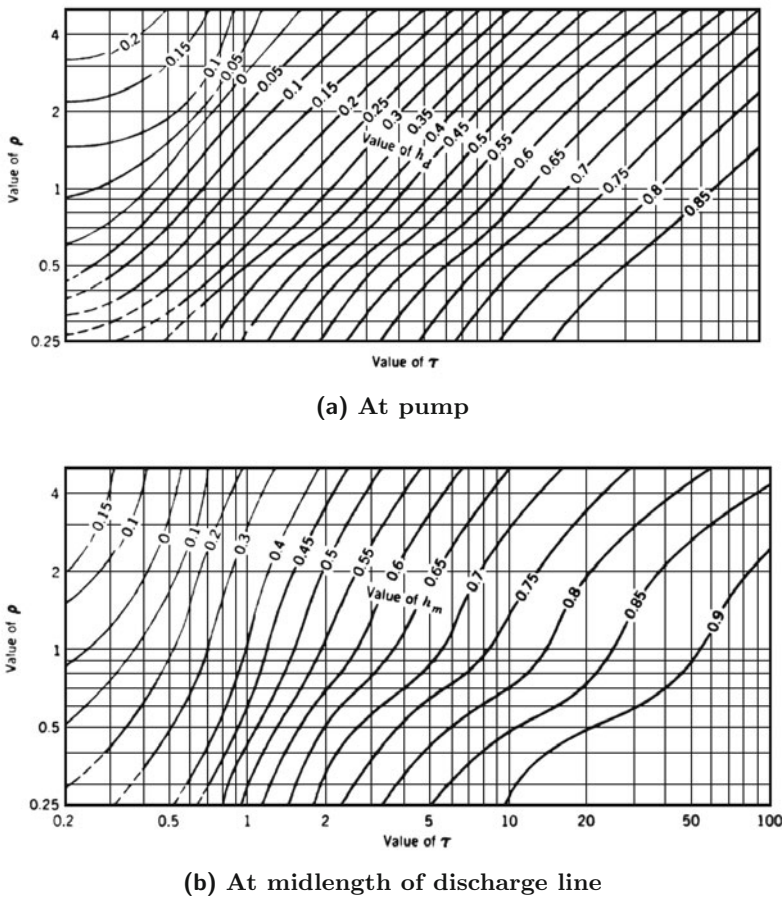


**Fig. A-4.** Minimum head following power failure, no friction losses.  
(After Kinno and Kennedy, [1965].)

$$C_{\max} = C_{o\max} \left( \frac{H_o^* + H_{f_o}}{H_{\min}^*} \right)^{1/1.2} \quad (\text{A-6})$$

in which  $H_o^* + H_{f_o}$  is the absolute initial steady-state head. To prevent air from entering the pipeline, a suitable amount of submergence should be provided at the chamber bottom. For this purpose, the chamber volume may be selected about 120 percent of the maximum air volume,  $C_{\max}$ , for small air chambers and about 110 percent, for large air chambers.

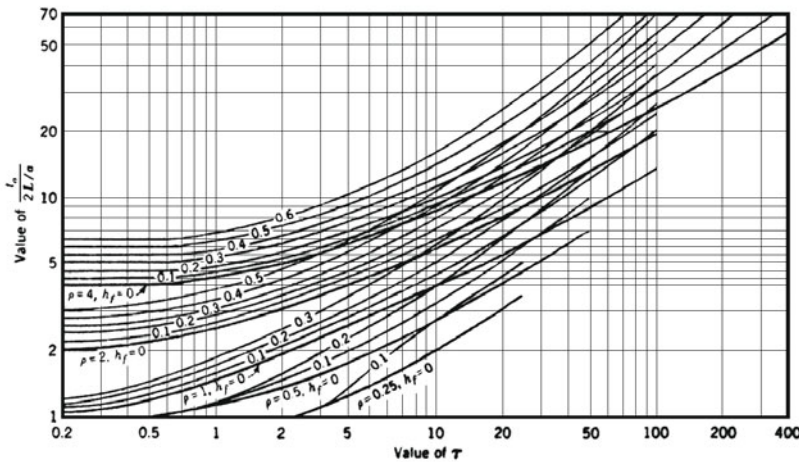


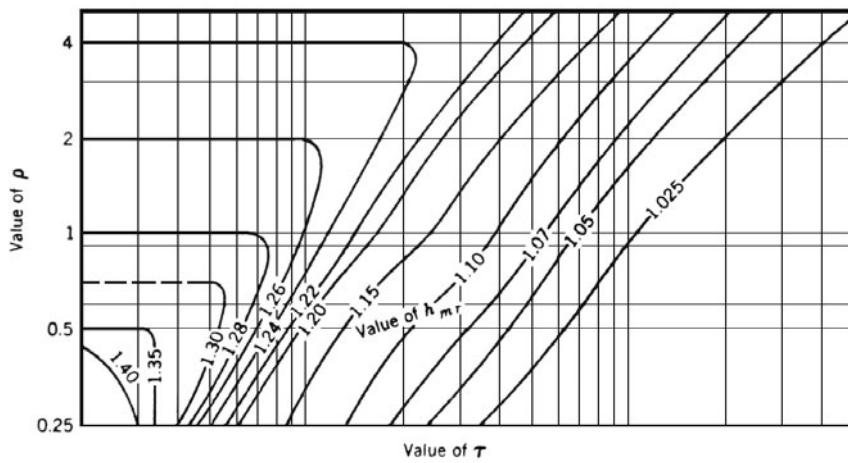
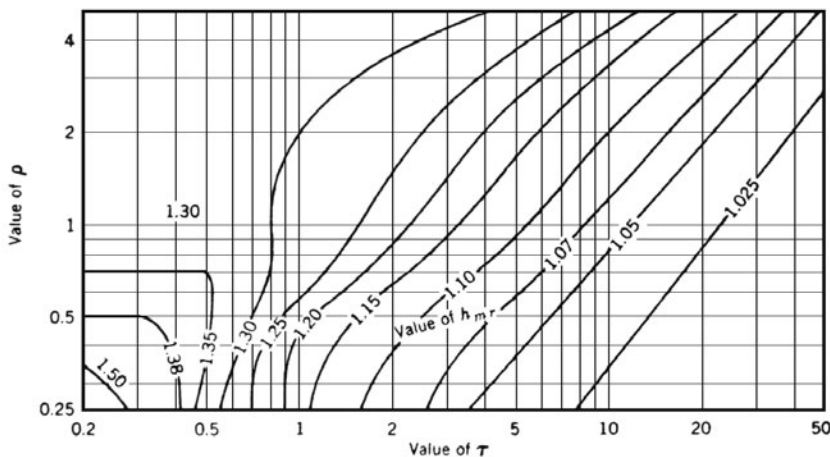
**Fig. A-5.** Time of flow reversal at pump following power failure. (After Kinno and Kennedy, [1965].)

## A-6 Simple Surge Tank

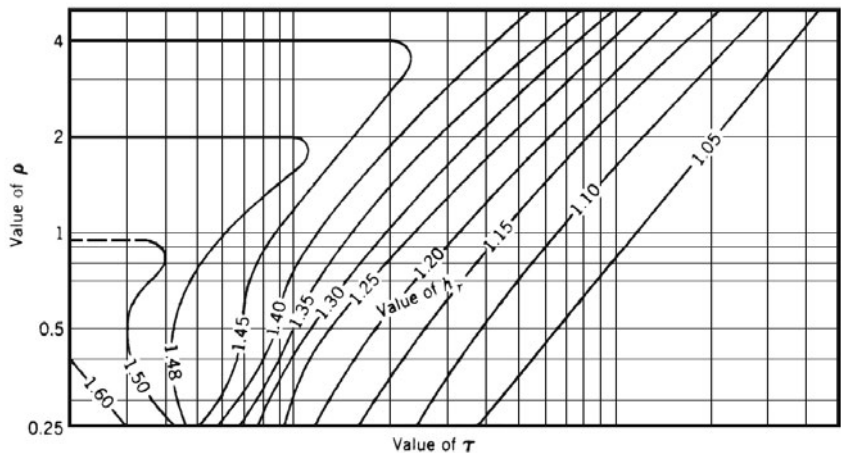
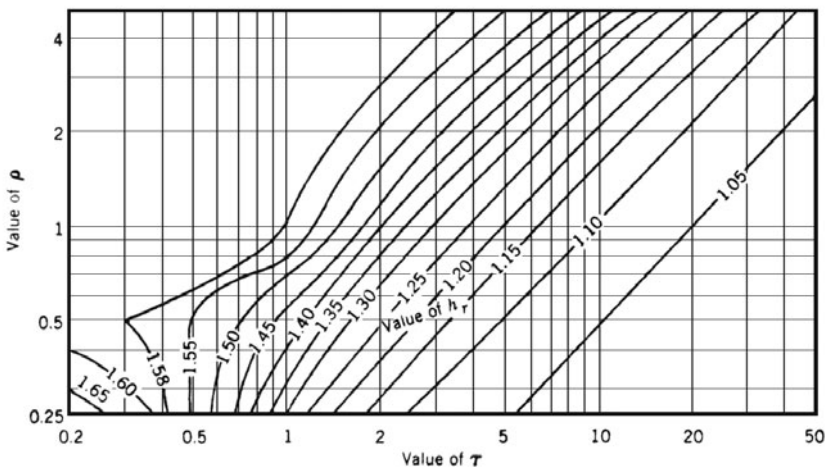
Figure A-10 shows the maximum upsurge in a simple surge tank following uniform gate closure from 100 to 0 percent, and Fig. A-11 shows the maximum downsurge in a tank following uniform gate opening from 0 to 100 percent and from 50 to 100 percent [Ruus, 1977].

In these figures, there are three regions: In region *A*, there is only one maximum that occurs after the end of the gate movement; in region *B*, the second maxima is the highest that occurs after the end of the gate operation; and in region *C*, the first of the two maxima is the largest that occurs prior to the end of the gate movement.

The following notation is used in these figures:  $A_t$  = cross-sectional area of the tunnel;  $A_s$  = cross-sectional area of the surge tank;  $g$  = acceleration due to gravity;  $h_o$  = head losses plus velocity head in the tunnel for a steady flow of  $Q_o$ ;  $L$  = length of the tunnel from the upstream reservoir to the surge tank;  $T_c$  = gate-closing time;  $T_o$  = gate-opening time;  $T^* = 2\pi\sqrt{LA_s/(gA_t)}$  = period of surge oscillations following instantaneously stopping a flow of  $Q_o$  in a corresponding frictionless system;  $Z_{\max}$  = maximum *upsurge* (or *downsurge*) above (or below) the upstream reservoir level; and  $Z^* = Q_o\sqrt{L/(gA_tA_s)}$  = maximum surge following instantaneously stopping a flow of  $Q_o$  in a corresponding frictionless system.

(a)  $E_R = 0.8$ (b)  $E_R = 0.9$ 

**Fig. A-6.** Maximum head following power failure at midlength of discharge line. (After Kinno and Kennedy, [1965].)

(a)  $E_R = 0.8$ (b)  $E_R = 0.9$ 

**Fig. A-7.** Maximum head at pump following power failure. (After Kinno and Kennedy, [1965].)

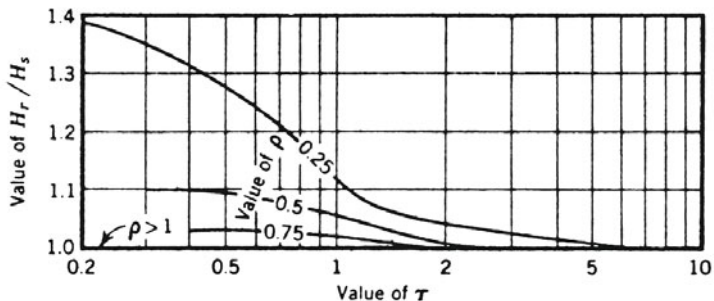


**Fig. A-8.** Maximum head at pump, reverse pump rotation prevented.  
(After Kinno and Kennedy, [1965].)

## A-7 Surges in Open Channels

The height and the celerity of a surge in a trapezoidal or rectangular open channel [Wu, 1970] produced by instantaneously reducing the flow at the downstream end of the channel may be computed from Fig. A-12. The height of this wave is reduced as it propagates upstream. Figure A-13 may be used to determine the wave height at any location along the channel.

For the selection of the top elevation of the channel banks, the water surface behind the wave front may be assumed horizontal (see Section 7-2).

The following notation is used in Figs. A-12 and A-13:  $b_o$  = bottom width of channel;  $c$  = celerity of surge wave;  $F_o$  = Froude number corresponding to initial steady-state conditions,  $V_o / \sqrt{gy_o}$ ;  $g$  = acceleration due to gravity;  $k$  = dimensionless parameter =  $b_o / (my_o)$ ;  $m$  = channel side slope,  $m$  horizontal to 1 vertical;  $Q_o$  = initial steady-state discharge;  $Q_f$  = final steady-state discharge;  $S_o$  = channel bottom slope;  $V_o$  = initial steady-state flow velocity;  $V_w$  = absolute wave velocity =  $V + c$ ;  $V_{wo}$  = initial steady-state absolute wave velocity;  $x$  = distance along the channel bottom from the control gates;  $y_o$  = initial steady-state flow depth;  $z$  = surge wave height at distance  $x$ ;  $z_o$  = initial surge wave height at downstream end;  $\beta$  = dimensionless parameter =  $z_o / y_o$ ;  $\lambda$  = dimensionless parameter =  $V_{wo} / V_o$ ; and  $K$  = dimensionless parameter =  $1 + 1/(1 + k)$ .

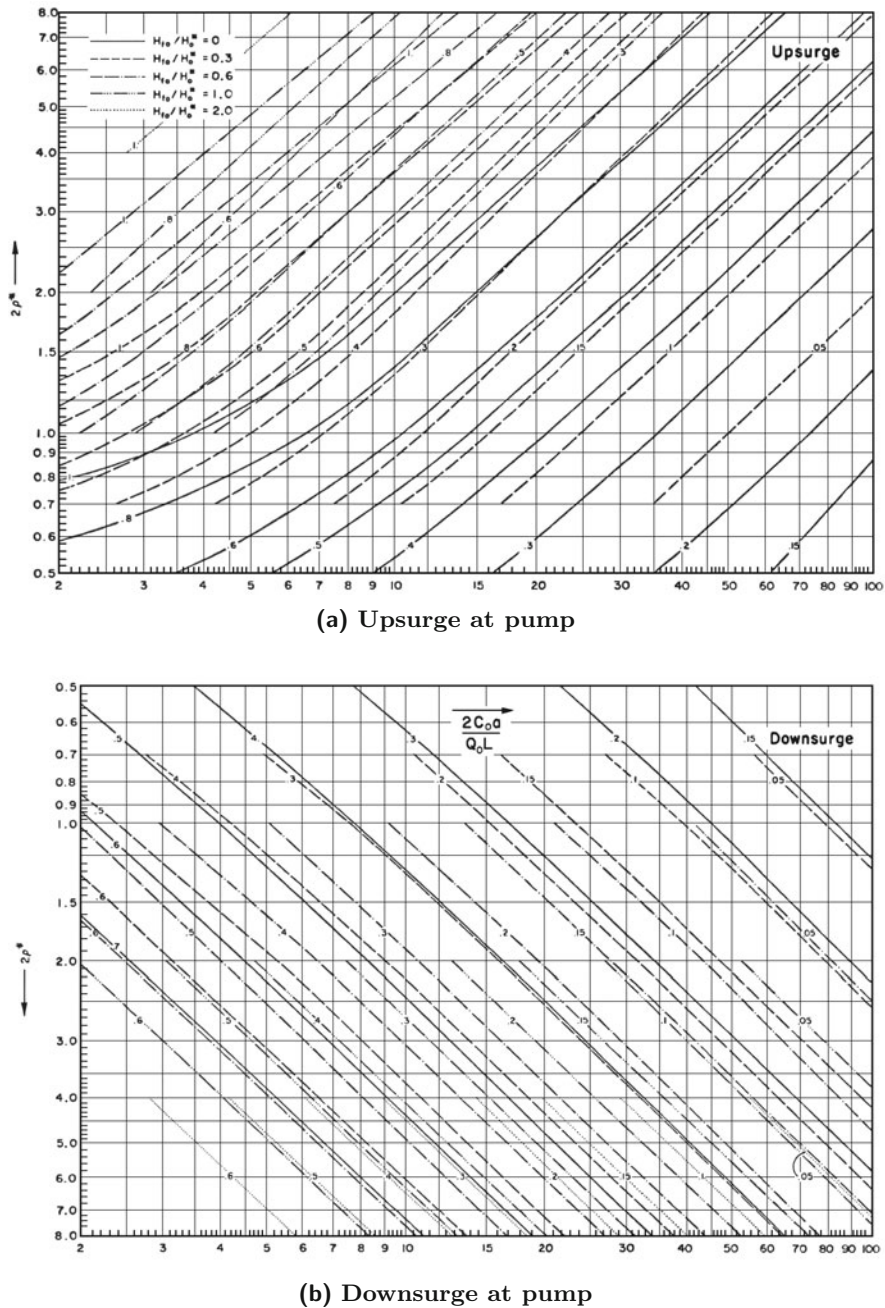
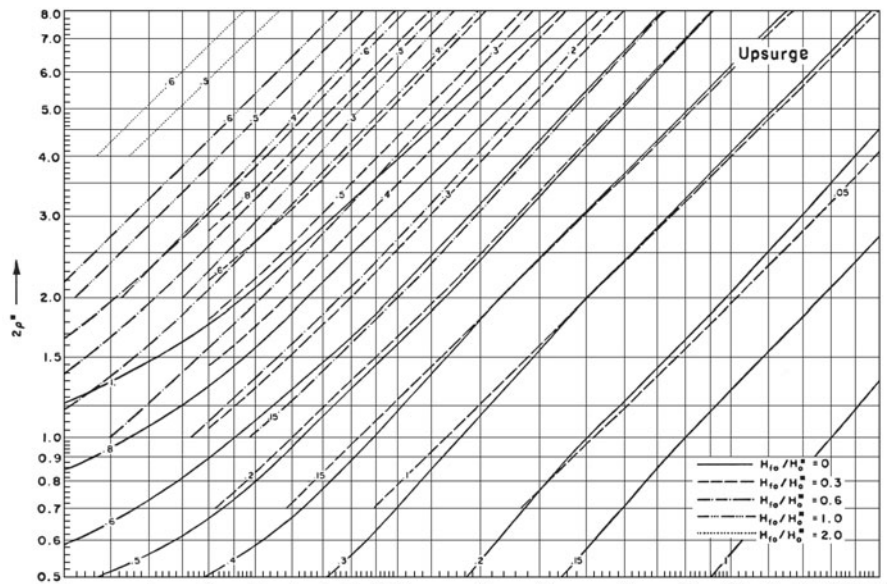
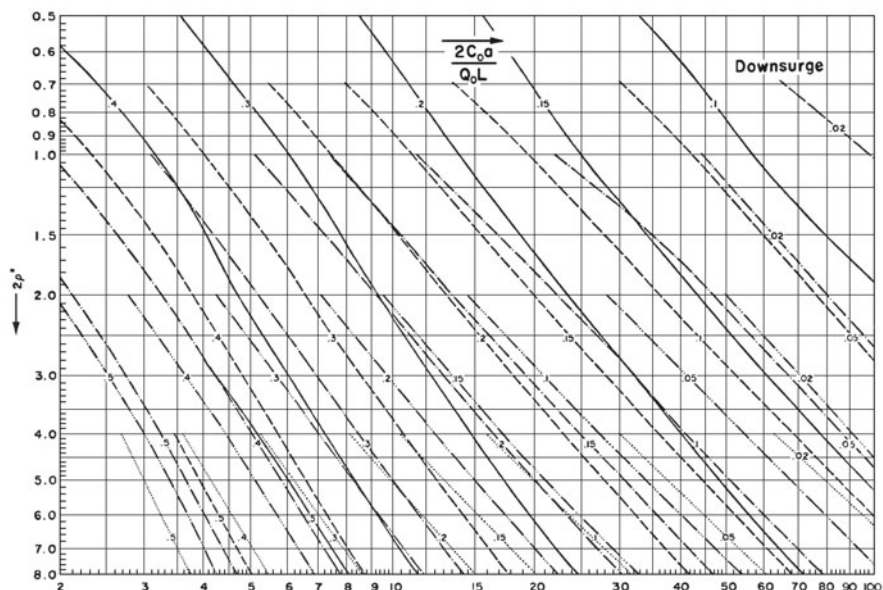


**Fig. A-9.** Maximum upsurge and downsurge in a discharge line having an air chamber. (After Ruus, [1977].)

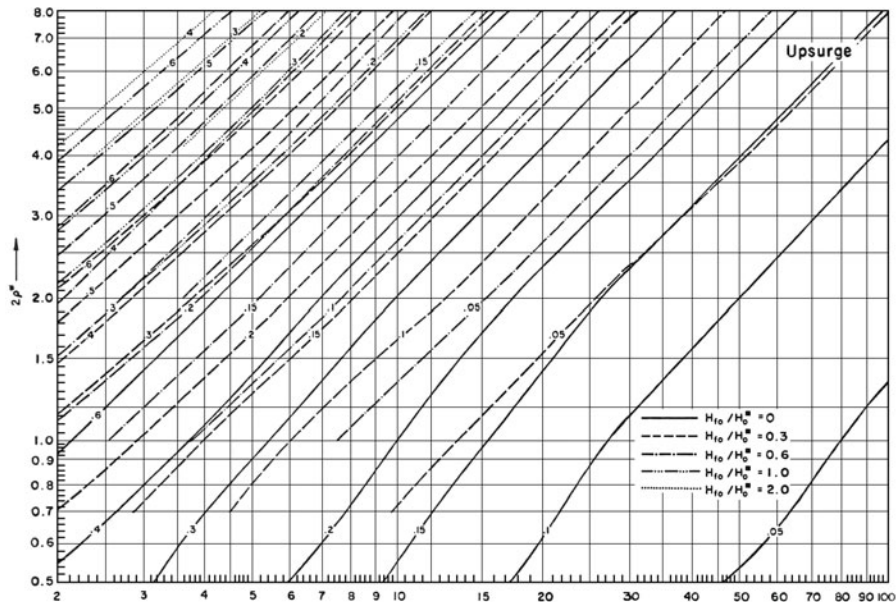


(c) Upsurge at midlength of discharge line

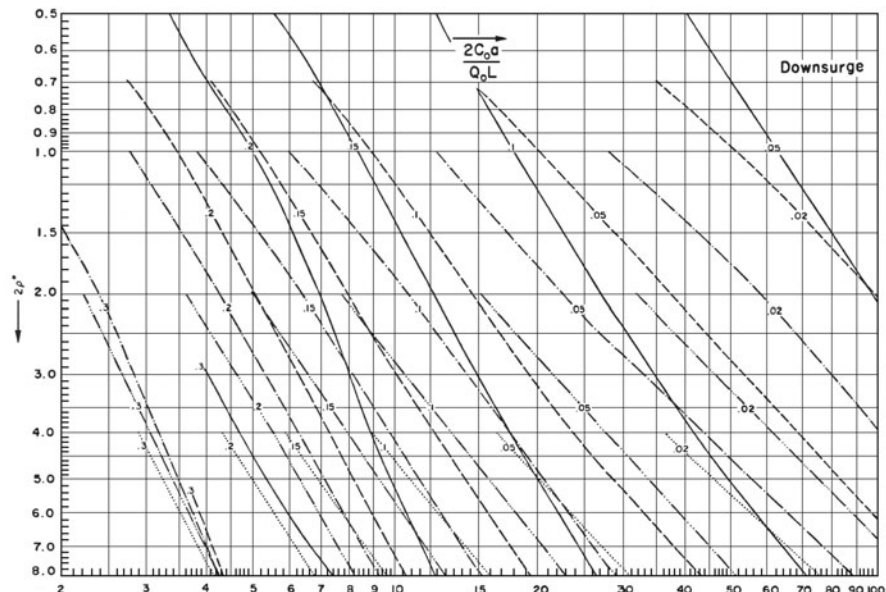


(d) Downsurge at midlength of discharge line

Fig. A-9. (Continued)



(e) Upsurge at quarter point of discharge line (reservoir side)



(f) Downsurge at quarter point of discharge line (reservoir side)

Fig. A-9. (Continued)

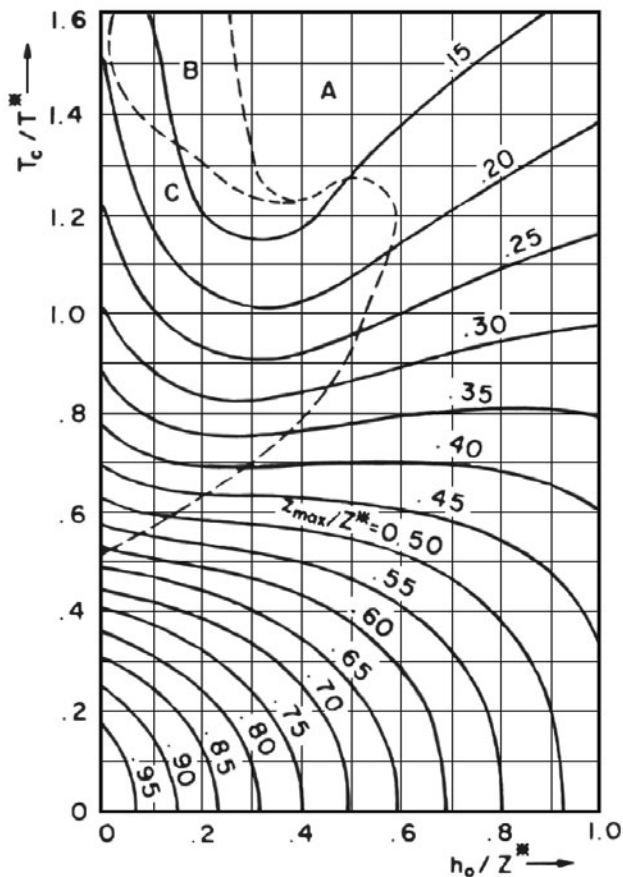


**Fig. A-10.** Maximum upsurge in a simple surge tank for uniform gate closure from 100 to 0 percent. (After Ruus and El-Fitiany, [1977].)

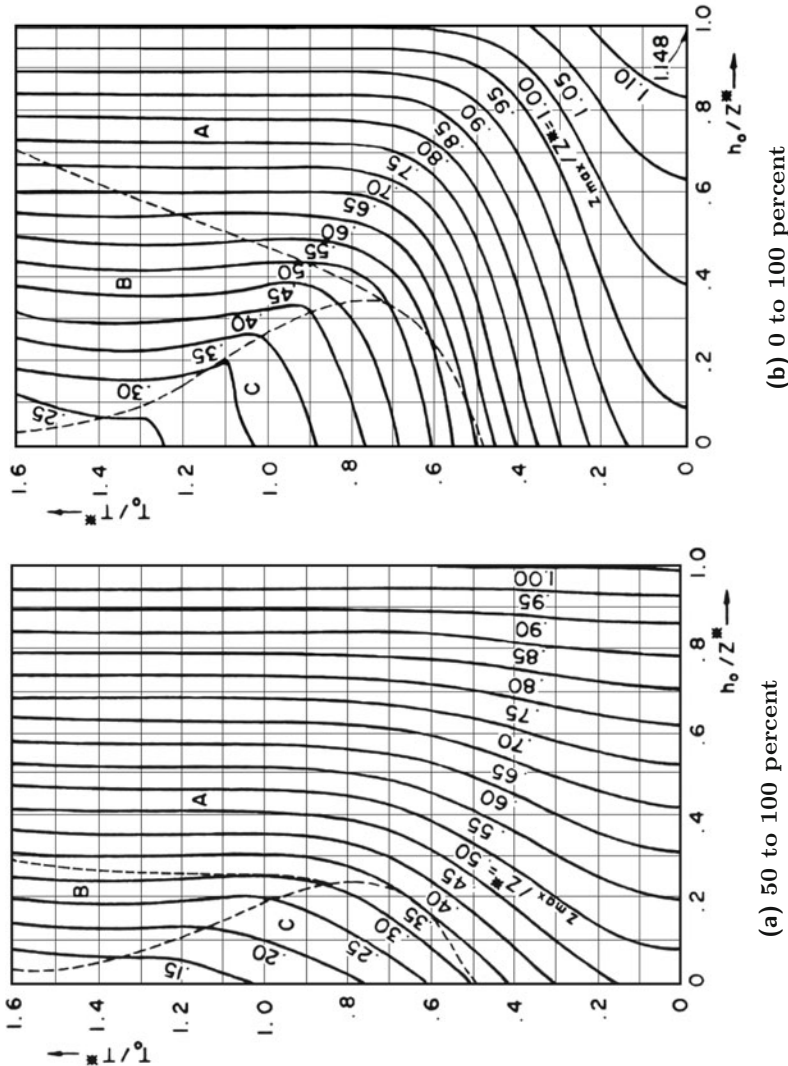
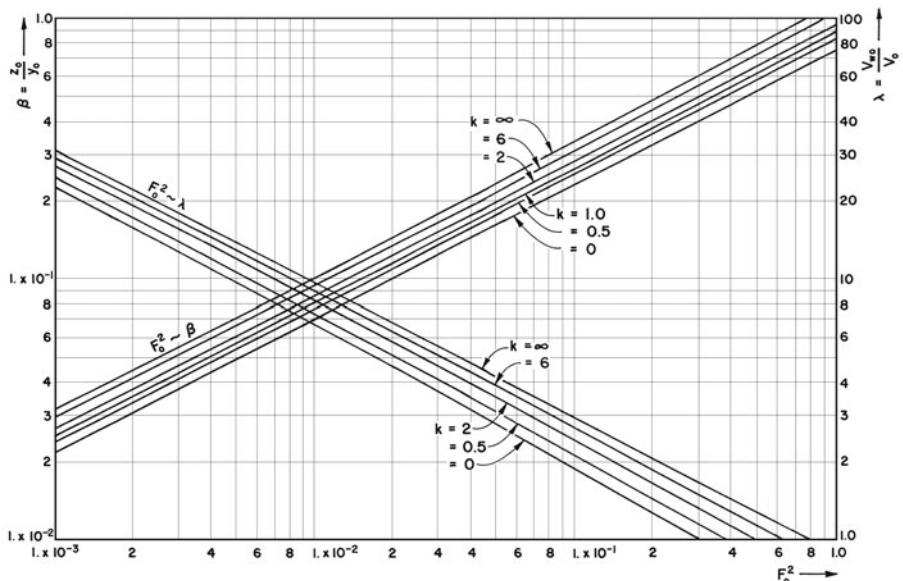
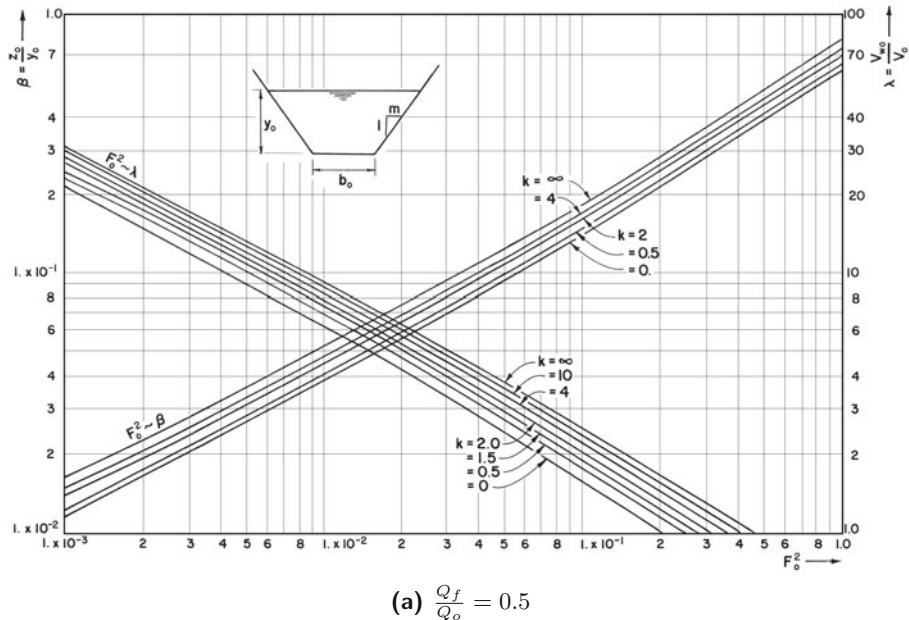


Fig. A-11. Maximum downsurge in a simple surge tank for uniform gate opening from 0 to 100 percent and from 50 to 100 percent. (After Ruus and El-Fitiary, [1977].)



**Fig. A-12.** Height and absolute velocity of a surge wave caused by instantaneous flow reduction at the downstream end. (After Wu, [1970].)

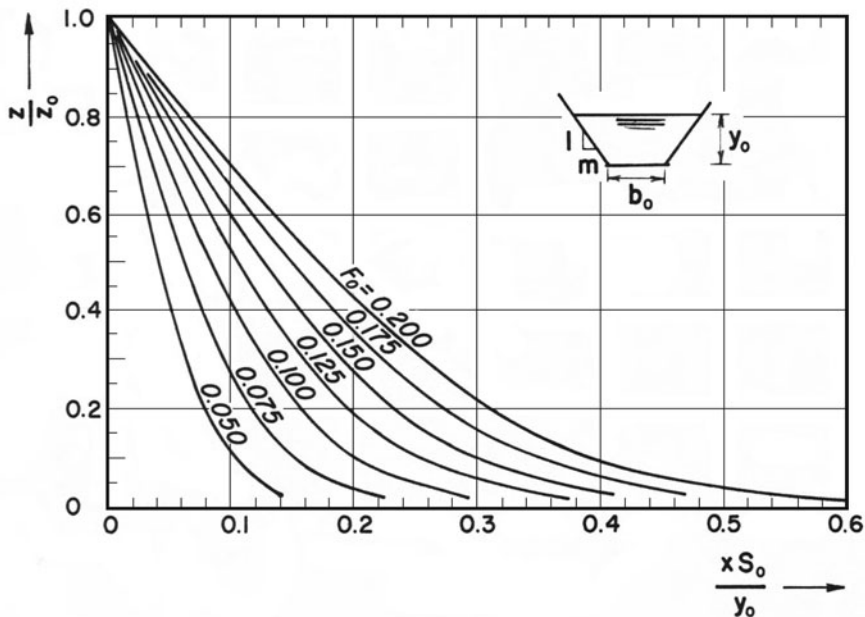
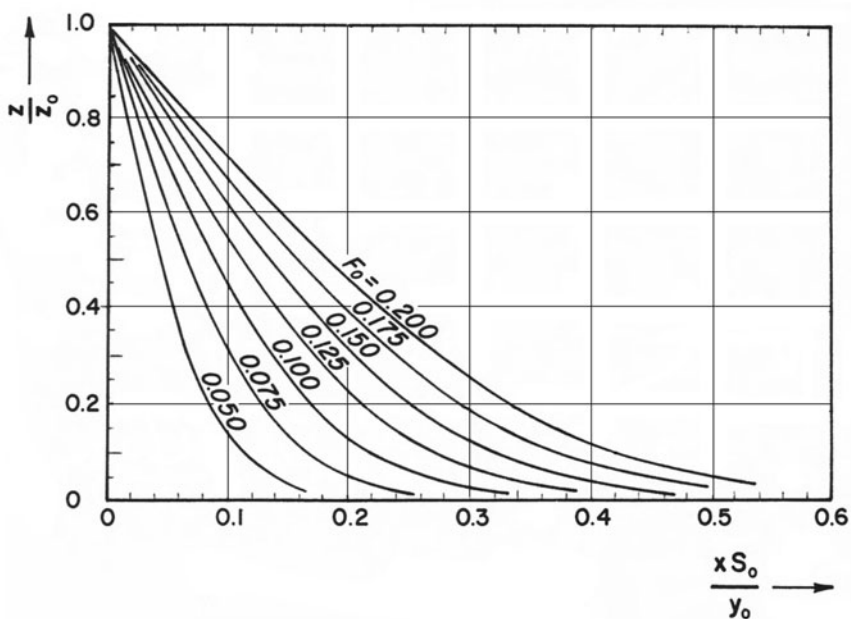
(a)  $K = 1.75$ (b)  $K = 1.50$ 

Fig. A-13. Variation of wave height of a positive surge propagating in a trapezoidal channel. (After Wu, [1970].)

## A-8 Data for Pumping Systems

It is necessary to know the values of polar moment of inertia and characteristics of the pumps for analyzing transient-state conditions caused by power failure to the electric motors of the pumping systems. If this data is not available, then empirical equations and pump data presented in this appendix may be used as an initial estimate until more precise data for the project are available.

### Polar Moment of Inertia

The following equations derived for the graph presented in the Report of the Design Team on Pumps and Drivers [1975] may be used to estimate the inertia of induction motors:

1200 rpm:

$$I = k_1 P^{1.38} \quad (\text{A-7})$$

1800 rpm:

$$I = k_2 P^{1.38} \quad (\text{A-8})$$

in which  $I$  = polar moment of inertia of the motor,  $P$  = rated power output of the motor, and  $k_1$  and  $k_2$  are empirical constants. In SI units,  $I$  is in kg m<sup>2</sup>,  $P$  is in kW,  $k_1 = 0.0045$  and  $k_2 = 0.00193$ . In U.S. customary units,  $I$  is in Ib-ft<sup>2</sup>,  $P$  is in horsepower,  $k_1 = 0.07$ , and  $k_2 = 0.03$ .

Eqs. A-7 and A-8 are valid for motors having output between 7.5 watts and 375 watts (10-500 hp). They are not valid for synchronous or wound-rotor induction motors. Inertia of the pump is not included; this is usually about 10 percent of the inertia of the motor.

### Pump Characteristic Data

Pump characteristic data for four pumps, taken from Brown (1980), is presented in [Table A-1](#).

**Table A-1. Pump Characteristic Data**

| $\theta = \tan^{-1}(\alpha/v)$ | $N_s = 0.46$ |         | $N_s = 1.61$ |         | $N_s = 2.78$ |         | $N_s = 4.94$ |         |
|--------------------------------|--------------|---------|--------------|---------|--------------|---------|--------------|---------|
|                                | $h$          | $\beta$ | $h$          | $\beta$ | $h$          | $\beta$ | $h$          | $\beta$ |
| 0°(360°)                       | -.55         | -.43    | -1.22        | -1.35   | -1.62        | -1.38   | -.97         | -.57    |
| 5                              | -.48         | -.26    | -1.07        | -1.14   | -1.34        | -1.08   | -.92         | -.61    |
| 10                             | -.38         | -.11    | -.90         | -.91    | -1.10        | -.82    | -.97         | -.73    |
| 15                             | -.27         | -.05    | -.74         | -.69    | -.82         | -.57    | -.88         | -.66    |
| 20                             | -.17         | .04     | -.54         | -.40    | -.59         | -.37    | -.67         | -.54    |
| 25                             | -.09         | .14     | -.36         | -.15    | -.35         | -.16    | -.46         | -.38    |
| 30                             | .06          | .25     | -.15         | .05     | -.14         | .06     | -.24         | -.15    |
| 35                             | .22          | .34     | .06          | .21     | .11          | .22     | -.02         | .06     |
| 40                             | .37          | .42     | .29          | .38     | .31          | .37     | .24          | .30     |
| 45                             | .50          | .50     | .50          | .50     | .50          | .50     | .50          | .50     |
| 50                             | .64          | .55     | .70          | .60     | .81          | .59     | .80          | .64     |
| 55                             | .78          | .59     | .89          | .69     | .86          | .68     | 1.06         | .76     |
| 60                             | .91          | .61     | 1.04         | .74     | .89          | .71     | 1.30         | .88     |
| 65                             | 1.03         | .61     | 1.19         | .79     | .93          | .73     | 1.50         | .94     |
| 70                             | 1.13         | .60     | 1.30         | .81     | 1.14         | .83     | 1.73         | 1.11    |
| 75                             | 1.21         | .58     | 1.40         | .84     | 1.42         | .98     | 1.99         | 1.39    |
| 80                             | 1.27         | .55     | 1.49         | .87     | 1.64         | 1.20    | 2.26         | 1.66    |
| 85                             | 1.33         | .50     | 1.53         | .91     | 1.84         | 1.36    | 2.54         | 1.89    |
| 90                             | 1.35         | .44     | 1.57         | .99     | 1.98         | 1.47    | 2.83         | 2.10    |
| 95                             | 1.36         | .41     | 1.60         | 1.06    | 2.09         | 1.53    | 3.05         | 2.28    |
| 100                            | 1.34         | .37     | 1.63         | 1.13    | 2.16         | 1.52    | 3.33         | 2.52    |
| 105                            | 1.31         | .35     | 1.67         | 1.22    | 2.18         | 1.51    | 3.51         | 2.68    |
| 110                            | 1.28         | .34     | 1.70         | 1.30    | 2.22         | 1.55    | 3.67         | 2.83    |
| 115                            | 1.22         | .34     | 1.73         | 1.39    | 2.31         | 1.63    | 3.81         | 3.03    |
| 120                            | 1.17         | .36     | 1.75         | 1.45    | 2.39         | 1.69    | 3.87         | 3.24    |
| 125                            | 1.13         | .40     | 1.72         | 1.50    | 2.53         | 1.83    | 3.80         | 3.23    |
| 130                            | 1.09         | .47     | 1.68         | 1.56    | 2.59         | 1.95    | 3.67         | 3.15    |
| 135                            | 1.04         | .54     | 1.64         | 1.61    | 2.70         | 2.17    | 3.46         | 2.90    |
| 140                            | .99          | .62     | 1.60         | 1.64    | 2.71         | 2.35    | 3.18         | 2.59    |
| 145                            | .96          | .70     | 1.56         | 1.65    | 2.85         | 2.53    | 2.85         | 2.39    |
| 150                            | .91          | .77     | 1.52         | 1.66    | 2.95         | 2.71    | 2.47         | 2.09    |
| 155                            | .89          | .82     | 1.49         | 1.66    | 3.05         | 2.82    | 2.25         | 1.82    |
| 160                            | .85          | .86     | 1.46         | 1.66    | 3.03         | 2.87    | 1.97         | 1.57    |
| 165                            | .82          | .89     | 1.42         | 1.67    | 2.88         | 2.73    | 1.70         | 1.32    |
| 170                            | .79          | .91     | 1.39         | 1.66    | 2.74         | 2.61    | 1.50         | 1.11    |
| 175                            | .75          | .90     | 1.35         | 1.63    | 2.54         | 2.39    | 1.28         | .92     |
| 180                            | .71          | .88     | 1.30         | 1.57    | 2.30         | 2.16    | 1.09         | .65     |
| 185                            | .68          | .85     | 1.25         | 1.48    | 1.92         | 1.84    | .90          | .49     |
| 190                            | .65          | .82     | 1.18         | 1.37    | 1.55         | 1.45    | .77          | .52     |
| 195                            | .61          | .74     | 1.10         | 1.23    | 1.15         | 1.22    | .70          | .66     |
| 200                            | .58          | .67     | .98          | 1.08    | .84          | .96     | .71          | .67     |
| 205                            | .55          | .59     | .80          | .91     | .63          | .74     | .68          | .64     |
| 210                            | .54          | .50     | .65          | .75     | .51          | .53     | .58          | .51     |

**Table A-1.** (*Continued*)

| $\theta = \tan^{-1}(\alpha/v)$ | $N_s = 0.46$            |                             | $N_s = 1.61$            |                             | $N_s = 2.78$            |                             | $N_s = 4.94$            |                             |
|--------------------------------|-------------------------|-----------------------------|-------------------------|-----------------------------|-------------------------|-----------------------------|-------------------------|-----------------------------|
|                                | $h$<br>$\alpha^2 + v^2$ | $\beta$<br>$\alpha^2 + v^2$ |
| 215                            | .53                     | .42                         | .55                     | .60                         | .41                     | .36                         | .41                     | .32                         |
| 220                            | .52                     | .33                         | .44                     | .42                         | .28                     | .18                         | .26                     | .12                         |
| 225                            | .52                     | .24                         | .37                     | .27                         | .19                     | -.03                        | .03                     | -.15                        |
| 230                            | .53                     | .16                         | .30                     | .11                         | .12                     | -.17                        | -.18                    | -.39                        |
| 235                            | .55                     | .07                         | .24                     | -.01                        | .08                     | -.28                        | -.37                    | -.61                        |
| 240                            | .57                     | .01                         | .24                     | -.13                        | .03                     | -.43                        | -.59                    | -.81                        |
| 245                            | .59                     | -.12                        | .27                     | -.26                        | -.14                    | -.53                        | -.74                    | -.97                        |
| 250                            | .61                     | -.21                        | .29                     | -.37                        | -.20                    | -.72                        | -.91                    | -.117                       |
| 255                            | .63                     | -.22                        | .31                     | -.49                        | -.42                    | -1.03                       | -1.19                   | -1.46                       |
| 260                            | .64                     | -.35                        | .32                     | -.60                        | -.49                    | -1.20                       | -1.52                   | -1.75                       |
| 265                            | .66                     | -.51                        | .33                     | -.69                        | -.55                    | -1.31                       | -1.86                   | -2.03                       |
| 270                            | .66                     | -.68                        | .33                     | -.77                        | -.75                    | -1.43                       | -2.20                   | -2.30                       |
| 275                            | .62                     | -.85                        | .31                     | -.86                        | -.94                    | -1.61                       | -2.50                   | -2.54                       |
| 280                            | .51                     | -1.02                       | .29                     | -.96                        | -.96                    | -1.75                       | -2.79                   | -2.79                       |
| 285                            | .32                     | -1.21                       | .22                     | -1.10                       | -.92                    | -1.77                       | -2.93                   | -2.93                       |
| 290                            | .23                     | -1.33                       | .15                     | -1.30                       | -.94                    | -1.77                       | -3.08                   | -3.08                       |
| 295                            | .11                     | -1.44                       | .05                     | -1.67                       | -1.04                   | -1.86                       | -3.10                   | -3.10                       |
| 300                            | -.20                    | -1.56                       | -.10                    | -1.93                       | -1.23                   | -2.00                       | -3.19                   | -3.19                       |
| 305                            | -.31                    | -1.65                       | -.27                    | -2.04                       | -1.55                   | -2.10                       | -3.11                   | -3.11                       |
| 310                            | -.39                    | -1.67                       | -.40                    | -2.15                       | -1.75                   | -2.22                       | -3.10                   | -3.10                       |
| 315                            | -.47                    | -1.67                       | -.50                    | -2.25                       | -1.85                   | -2.42                       | -2.97                   | -2.97                       |
| 320                            | -.53                    | -1.63                       | -.60                    | -2.35                       | -2.01                   | -2.54                       | -2.85                   | -2.85                       |
| 325                            | -.59                    | -1.56                       | -.70                    | -2.33                       | -2.15                   | -2.67                       | -2.62                   | -2.62                       |
| 330                            | -.64                    | -1.44                       | -.80                    | -2.20                       | -2.28                   | -2.75                       | -2.31                   | -2.31                       |
| 335                            | -.66                    | -1.33                       | -.90                    | -2.05                       | -2.28                   | -2.78                       | -2.07                   | -2.07                       |
| 340                            | -.68                    | -1.18                       | -1.00                   | -1.95                       | -2.30                   | -2.75                       | -1.80                   | -1.78                       |
| 345                            | -.67                    | -1.00                       | -1.10                   | -1.80                       | -2.21                   | -2.63                       | -1.56                   | -1.46                       |
| 350                            | -.66                    | -.83                        | -1.20                   | -1.65                       | -2.04                   | -2.33                       | -1.33                   | -1.15                       |
| 355                            | -.61                    | -.64                        | -1.30                   | -1.50                       | -1.86                   | -1.94                       | -1.12                   | -.85                        |

Notes: Specific speed,  $N_s$  is in SI units. Conversion factors are as follows: 1 SI unit = 52.9 mertic units = 2733 gpm units.

## References

- Brown, R. J., and Rogers, D.C., 1980, "Development of Pump Characteristics from Field Tests," *Jour. of Mech. Design*, Amer. Soc. of Mech. Engineers, vol. 102, October, pp. 807-817 .
- Kinno, H. and Kennedy, J. F., 1965, "Water-Hammer Charts for Centrifugal Pump Systems," *Jour., Hyd. Div.*, Amer. Soc. of Civ. Engrs., vol. 91, May, pp. 247-270.
- Parmakian, J., 1963, *Waterhammer Analysis*, Dover Publications, Inc., New York, p. 72.
- Ruus, E., 1977, "Charts for Waterhammer in Pipelines with Air Chamber," *Canadian Jour. Civil Engineering*, vol. 4, no. 3, September.
- Ruus, E. and El-Fitiany, F. A., 1977, "Maximum Surges in Simple Surge Tanks," *Canadian Jour. Civil Engineering*, vol. 4, no. 1, pp. 40-46.
- Wu, H., 1970, "Dimensionless Ratios for Surge Waves in Open Canals," *thesis*, presented to the University of British Columbia in partial fulfillment of the requirements for the degree of Master of Applied Science, April.
- "Pumps and Drivers," Report of the Design Team on Pumps and Drivers, Bureau of Reclamation, Denver, Colorado, Feb. 1975.

## B

---

# TRANSIENTS CAUSED BY OPENING OR CLOSING A VALVE

## B-1 Program Listing

```
C ANALYSIS OF TRANSIENTS IN A PIPELINE CAUSED BY OPENING OR
C CLOSING OF A DOWNSTREAM VALVE

C FREE FORMAT IS USED FOR READING THE INPUT DATA.
C PIPELINE MAY HAVE UPTO 10 PIPES IN SERIES AND EACH PIPE MAY
C HAVE UPTO 100 COMPUTATIONAL NODES; THESE LIMITS MAY BE
C INCREASED BY MODIFYING THE DIMENSION STATEMENT.
C WAVE VELOCITY IS ADJUSTED, IF NECESSARY, TO AVOID INTERPOLATION
C ERROR.
C RELATIVE VALVE OPENING VS TIME CURVE IS SPECIFIED AT DISCRETE
C POINTS; VALUES AT INTERMEDIATE TIMES ARE DETERMINED BY PARABOLIC
C INTERPOLATION.
C SI UNITS ARE USED.

C***** NOTATION *****
C
C A = WAVE SPEED (M/S);
C AR = PIPE CROSS-SECTIONAL AREA (M2);
C D = PIPE DIAMETER (M);
C DT = COMPUTATIONAL TIME INTERVAL (S);
C DXT = TIME INTERVAL FOR STORING TAU VS TIME CURVE (S);
C F = DARCY-WEISBACH FRICTION FACTOR;
C H = PIEZOMETRIC HEAD AT BEGINNING OF TIME INTERVAL (M);
C HMAX = MAXIMUM PIEZOMETRIC HEAD (M);
C HMIN = MINIMUM PIEZOMETRIC HEAD (M);
C HP = PIEZOMETRIC HEAD AT END OF TIME INTERVAL (M);
C HRES = RESERVOIR LEVEL ABOVE DATUM (M);
C HS = VALVE HEAD LOSS FOR FLOW OF QS (M);
```

---

The author or publisher shall have no liability, consequential or otherwise, of any kind arising from the use of the computer programs or any parts thereof presented in Appendixes B through E.

```

C   IPRINT = NUMBER OF TIME INTERVAL AFTER WHICH CONDITIONS
C   ARE TO BE PRINTED;
C   L = PIPE LENGTH (M);
C   M = NUMBER OF POINTS ON TAU VS TIME CURVE;
C   N = NUMBER OF REACHES INTO WHICH PIPE IS SUB-DIVIDED;
C   NP = NUMBER OF PIPES;
C   NRLP = NUMBER OF REACHES ON LAST PIPE;
C   Q = DISCHARGE AT BEGINNING OF TIME INTERVAL (M3/S);
C   QO = STEADY-STATE DISCHARGE (M3/S);
C   QP = DISCHARGE AT END OF TIME INTERVAL (M3/S);
C   QS = VALVE DISCHARGE (M3/S);
C   T = TIME (S);
C   TAU = RELATIVE VALVE OPENING;
C   TAUF = FINAL VALVE OPENING;
C   TAUO = INITIAL VALVE OPENING;
C   TLAST = TIME UPTO WHICH CONDITIONS ARE TO BE COMPUTED (S);
C   TV = VALVE OPENING OR CLOSING TIME (S);
C   Y = STORED TAU VALUES.
C
C*****REAL L
C*****DIMENSION Q(10,100),H(10,100),QP(10,100),HP(10,100),CA(10),F(10),
C 1 CF(10),AR(10),A(10),L(10),N(10),D(10),Y(20),HMAX(10,100),
C 2 HMIN(10,100)
C
C   READING AND WRITING OF INPUT DATA
C
C   GENERAL DATA
READ(1,*) NP,NRLP,IPRINT,G,QO,HRES,TLAST
WRITE(2,20) NP,NRLP,QO,HRES,TLAST
20 FORMAT(8X,'NUMBER OF PIPES =',I3/8X,'NUMBER OF REACHES ON LAST '
1'PIPE =',I3/8X,'STEADY STATE DISCH. =',F6.3,' M3/S' /8X,'RESERVOIR
2 LEVEL =',F6.1,' M'/8X,'TIME FOR WHICH TRANSIENTS ARE TO BE '
3'COMPUTED =',F6.1,' S'/)
C
C   DATA FOR VALVE
C
READ(1,*) M,TV,DXT,TAUO,TAUF,QS,HS,(Y(I),I=1,M)
WRITE(2,30) M,TV,DXT,HS,QS,(Y(I),I=1,M)
30 FORMAT(8X,'NUMBER OF POINTS ON TAU VS TIME CURVE =',I2/8X,
1'VALVE OPERATION TIME =',F6.2,' S'/8X,'TIME INTERVAL FOR STORING'
2' TAU CURVE =',F6.3,' S'/8X,'VALVE LOSS =',F6.2,' M FOR QS =',
3 F6.3,' M3/S'/8X,'STORED TAU VALUES :'/8X,15F8.3/)
C
C   DATA FOR PIPES
C
READ(1,*) (L(I),D(I),A(I),F(I),I=1,NP)
WRITE(2,40)
40 FORMAT(/8X,'PIPE NO', 5X, 'LENGTH',5X,'DIA',5X,'WAVE VEL.',5X,'FRI
2C FACTOR'/21X,'(M)',7X,'(M)',7X,'(M/S)')
WRITE(2,50)(I,L(I),D(I),A(I),F(I),I=1,NP)
50 FORMAT(10X,I3,6X,F7.1,3X,F5.2,5X,F7.1,11X,F5.3)
DT=L(NP)/(NRLP*A(NP))
WRITE(2,51)
51 FORMAT(/8X,'PIPE NO',5X,'ADJUSTED WAVE VEL'/27X,'(M/S ')
C
C   CALCULATION OF PIPE CONSTANTS
C
DO 60 I=1,NP
AR(I)=0.7854*D(I)**2

```

```

AUNADJ=A(I)
AN=L(I)/(DT*A(I))
N(I)=AN
ANI=N(I)
IF((AN-ANI).GE.0.5) N(I)=N(I)+1
A(I)=L(I)/(DT*N(I))
WRITE(2,55) I,A(I)
55 FORMAT(10X,I3,12X,F7.1)
56 CA(I)=G*AR(I)/A(I)
CF(I)=F(I)*DT/(2.*D(I)*AR(I))
F(I)=F(I)*L(I)/(2.*G*D(I)*N(I)*AR(I)**2)
60 CONTINUE
C
C CALCULATION OF STEADY STATE CONDITIONS
C
H(1,1)=HRES
DO 80 I=1,NP
NN=N(I)+1
DO 70 J=1,NN
H(I,J)=H(I,1)-(J-1)*F(I)*QO**2
Q(I,J)=QO
70 CONTINUE
H(I+1,1)=H(I,NN)
80 CONTINUE
NN=N(NP)+1
IF (QO.NE.0.) HS=H(NP,NN)
DO 85 I=1,NP
NN=N(I)+1
DO 85 J=1,NN
HMAX(I,J)=H(I,J)
HMIN(I,J)=H(I,J)
85 CONTINUE
NP1=NP-1
T=0.0
TAU=TAU0
WRITE(2,88)
88 FORMAT(/8X,'TIME',2X,'TAU',2X,'PIPE',7X,'HEAD (M)',7X,'DISCH. ',
1'(M3/S)'/20X,'NO',5X,'(1)',5X,'(N+1)',5X,'(1)',5X,'(N+1) '/')
90 K=0
I=1
NN=N(I)+1
WRITE(2,100) T,TAU,I,H(I,1),H(I,NN),Q(I,1),Q(I,NN)
100 FORMAT(F12.1,F6.3,I4,2F9.2,F9.3,F10.3)
IF (NP.EQ.1) GO TO 150
DO 140 I=2,NP
NN=N(I)+1
WRITE(2,120) I,H(I,1),H(I,NN),Q(I,1),Q(I,NN)
120 FORMAT(20X,I2,2F9.2,F9.3,F10.3)
140 CONTINUE
150 T=T+DT
K=K+1
IF(T.GT.TLAST) GO TO 240
C
C UPSTREAM RESERVOIR
C
HP(1,1)=HRES
CN=Q(1,2)-H(1,2)*CA(1)-CF(1)*Q(1,2)*ABS(Q(1,2))
QP(1,1)=CN+CA(1)*HRES
C
C INTERIOR POINTS
C

```

```

DO 170 I=1,NP
NN=N(I)
DO 160 J=2,NN
JP1=J+1
JM1=J-1
CN=Q(I,JP1)-CA(I)*H(I,JP1)-CF(I)*Q(I,JP1)*ABS(Q(I,JP1))
CP=Q(I,JM1)+CA(I)*H(I,JM1)-CF(I)*Q(I,JM1)*ABS(Q(I,JM1))
QP(I,J)=0.5*(CP+CN)
HP(I,J)=(CP-QP(I,J))/CA(I)
160 CONTINUE
170 CONTINUE
C
C SERIES JUNCTION
C
IF (NP.EQ.1) GO TO 178
DO 175 I=1,NP1
IP1=I+1
N1=N(I)
NN=N(I)+1
CN=Q(IP1,2)-CA(IP1)*H(IP1,2)-CF(IP1)*Q(IP1,2)*ABS(Q(IP1,2))
1) CP=Q(I,N1)+CA(I)*H(I,N1)-CF(I)*Q(I,N1)*ABS(Q(I,N1))
HP(I,NN)=(CP-CN)/(CA(I)+CA(IP1))
HP(IP1,1)=HP(I,NN)
QP(I,NN)=CP-CA(I)*HP(I,NN)
QP(IP1,1)=CN+CA(IP1)*HP(IP1,1)
175 CONTINUE
C
C VALVE AT DOWNSTREAM END
C
178 NN=N(NP)+1
NM1=N(NP)
CP=Q(NP,NM1)+CA(NP)*H(NP,NM1)-CF(NP)*Q(NP,NM1)*ABS(Q(NP,NM1))
IF(T.GE.TV) GO TO 180
CALL PARAB(T,DXT,Y,TAU)
GO TO 190
180 TAU=TAUF
IF(TAU.LE.0.0) GO TO 200
190 CV=(QS*TAU)**2/(HS*CA(NP))
QP(NP,NN)=0.5*(-CV+SQRT(CV*CV+4.*CP*CV))
HP(NP,NN)=(CP-QP(NP,NN))/CA(NP)
GO TO 210
200 QP(NP,NN)=0.0
HP(NP,NN)=CP/CA(NP)
C
C STORING VARIABLES FOR NEXT TIME STEP
C
210 DO 230 I=1,NP
NN=N(I)+1
DO 220 J=1,NN
Q(I,J)=QP(I,J)
H(I,J)=HP(I,J)
IF (H(I,J).GT.HMAX(I,J)) HMAX(I,J)=H(I,J)
IF (H(I,J).LT.HMIN(I,J)) HMIN(I,J)=H(I,J)
220 CONTINUE
230 CONTINUE
IF(K.EQ.IPRINT) GO TO 90
GO TO 150
240 WRITE(2,250)
250 FORMAT(/8X,'PIPE NO',3X,'SECTION NO',3X,'MAX PRESS.',3X,
1 'MIN. PRESS./')

```

```

DO 270 I=1,NP
NN=N(I)+1
DO 270 J=1,NN
WRITE(2,260) I,J,HMAX(I,J),HMIN(I,J)
260 FORMAT(9X,I2,13X,I2,2F13.2)
270 CONTINUE
STOP
END
SUBROUTINE PARAB(X,DX,Y,Z)
DIMENSION Y(20)
I=X/DX
R=(X-I*DX)/DX
IF(I.EQ.0) R=R-1.
I=I+1
IF(I.LT.2) I=2
Z=Y(I)+0.5*R*(Y(I+1)-Y(I-1))+R*(Y(I+1)+Y(I-1)-2.*Y(I)))
RETURN
END

```

## B-2 Input Data

```

2,2,2,9.81,1.0,67.7,10.0
7,6.0,1.0,1.0,0.0,1.,60.05,1.0,0.9,0.7,0.5,0.3,0.1,0.0
550.0,0.75,1100.0,0.01
450.0,0.60,900.0,0.012

```

## B-3 Program Output

```

NUMBER OF PIPES = 2
NUMBER OF REACHES ON LAST PIPE = 2
STEADY STATE DISCH. = 1.000 M3/S
RESERVOIR LEVEL = 67.7 M
TIME FOR WHICH TRANSIENTS ARE TO BE COMPUTED = 10.0 S

NUMBER OF POINTS ON TAU VS TIME CURVE = 7

```

## 532 B TRANSIENTS CAUSED BY OPENING OR CLOSING A VALVE

VALVE OPERATION TIME = 6.00 S

TIME INTERVAL FOR STORING TAU CURVE = 1.000 S

VALVE LOSS = 60.05 M FOR QS = 1.000 M3/S

STORED TAU VALUES :

1.000 .900 .700 .500 .300 .100 .000

| PIPE NO | LENGTH<br>(M) | DIA<br>(M) | WAVE VEL.<br>(M/S) | FRICTION FACTOR |
|---------|---------------|------------|--------------------|-----------------|
| 1       | 550.0         | .75        | 1100.0             | .010            |
| 2       | 450.0         | .60        | 900.0              | .012            |

| PIPE NO | ADJUSTED WAVE VEL<br>(M/S) |
|---------|----------------------------|
|---------|----------------------------|

|   |        |
|---|--------|
| 1 | 1100.0 |
| 2 | 900.0  |

| TIME | TAU | PIPE<br>NO | HEAD<br>(1) | HEAD<br>(N+1) | DISCH.<br>(1) | DISCH.<br>(N+1) |
|------|-----|------------|-------------|---------------|---------------|-----------------|
|------|-----|------------|-------------|---------------|---------------|-----------------|

|      |       |   |        |        |       |       |
|------|-------|---|--------|--------|-------|-------|
| .0   | 1.000 | 1 | 67.70  | 65.78  | 1.000 | 1.000 |
|      |       | 2 | 65.78  | 60.05  | 1.000 | 1.000 |
| .5   | .962  | 1 | 67.70  | 65.78  | 1.000 | 1.000 |
|      |       | 2 | 65.78  | 63.46  | 1.000 | .989  |
| 1.0  | .900  | 1 | 67.70  | 68.73  | 1.000 | .988  |
|      |       | 2 | 68.73  | 69.78  | .988  | .970  |
| 1.5  | .813  | 1 | 67.70  | 74.16  | .977  | .967  |
|      |       | 2 | 74.16  | 79.88  | .967  | .937  |
| 2.0  | .700  | 1 | 67.70  | 79.93  | .935  | .922  |
|      |       | 2 | 79.93  | 95.83  | .922  | .884  |
| 2.5  | .600  | 1 | 67.70  | 88.25  | .867  | .847  |
|      |       | 2 | 88.25  | 110.41 | .847  | .814  |
| 3.0  | .500  | 1 | 67.70  | 94.96  | .761  | .755  |
|      |       | 2 | 94.96  | 125.13 | .755  | .722  |
| 3.5  | .400  | 1 | 67.70  | 99.19  | .643  | .633  |
|      |       | 2 | 99.19  | 139.20 | .633  | .609  |
| 4.0  | .300  | 1 | 67.70  | 104.41 | .506  | .496  |
|      |       | 2 | 104.41 | 149.14 | .496  | .473  |
| 4.5  | .200  | 1 | 67.70  | 108.47 | .350  | .344  |
|      |       | 2 | 108.47 | 158.61 | .344  | .325  |
| 5.0  | .100  | 1 | 67.70  | 111.20 | .183  | .177  |
|      |       | 2 | 111.20 | 165.65 | .177  | .166  |
| 5.5  | .038  | 1 | 67.70  | 113.07 | .006  | .004  |
|      |       | 2 | 113.07 | 149.46 | .004  | .059  |
| 6.0  | .000  | 1 | 67.70  | 96.01  | -.175 | -.106 |
|      |       | 2 | 96.01  | 114.27 | -.106 | .000  |
| 6.5  | .000  | 1 | 67.70  | 63.25  | -.217 | -.157 |
|      |       | 2 | 63.25  | 61.79  | -.157 | .000  |
| 7.0  | .000  | 1 | 67.70  | 34.25  | -.139 | -.085 |
|      |       | 2 | 34.25  | 12.33  | -.085 | .000  |
| 7.5  | .000  | 1 | 67.70  | 23.55  | .047  | .035  |
|      |       | 2 | 23.55  | 6.74   | .035  | .000  |
| 8.0  | .000  | 1 | 67.70  | 47.63  | .208  | .126  |
|      |       | 2 | 47.63  | 34.76  | .126  | .000  |
| 8.5  | .000  | 1 | 67.70  | 82.89  | .205  | .148  |
|      |       | 2 | 82.89  | 88.45  | .148  | .000  |
| 9.0  | .000  | 1 | 67.70  | 105.95 | .088  | .054  |
|      |       | 2 | 105.95 | 130.93 | .054  | .000  |
| 9.5  | .000  | 1 | 67.70  | 108.02 | -.097 | -.071 |
|      |       | 2 | 108.02 | 123.44 | -.071 | .000  |
| 10.0 | .000  | 1 | 67.70  | 78.39  | -.229 | -.139 |
|      |       | 2 | 78.39  | 85.13  | -.139 | .000  |

| PIPE NO | SECTION NO | MAX PRESS. | MIN. PRESS. |
|---------|------------|------------|-------------|
| 1       | 1          | 67.70      | 67.70       |
| 1       | 2          | 91.18      | 44.05       |
| 1       | 3          | 113.07     | 23.55       |
| 2       | 1          | 113.07     | 23.55       |
| 2       | 2          | 140.26     | 9.53        |
| 2       | 3          | 165.65     | 5.40        |

# C

---

## TRANSIENTS CAUSED BY POWER FAILURE TO PUMPS

### C-1 Program Listing

```
C ANALYSIS OF TRANSIENTS IN A PIPELINE CAUSED BY POWER
C FAILURE TO PUMPS
C
C PIPELINE MAY HAVE SEVERAL SIMILAR PUMPS IN PARALLEL; UPTO
C 10 PIPES IN SERIES; AND EACH PIPE MAY HAVE UPTO
C 100 COMPUTATIONAL NODES. THESE LIMITS MAY BE INCREASED
C BY MODIFYING THE DIMENSION STATEMENT.
C FREE FORMAT IS USED FOR READING THE INPUT DATA.
C WAVE VELOCITY IS ADJUSTED, IF NECESSARY, TO AVOID INTERPOLATION
C ERROR. ,
C DATA FOR PUMP CHARACTERISTICS IS STORED AT DISCRETE POINTS IN
C A FORM PRESENTED IN CHAPTER 4.
C SIMULATION OF LIQUID-COLUMN SEPARATION IS NOT INCLUDED.

C.....***** NOTATION *****
C
C      A = WAVE VELOCITY (M/S);
C      ALPHA =NON-DIMENSIONAL PUMP SPEED =N/NR;
C      AR = PIPE CROSS-SECTIONAL AREA (M2);
C      BETA = NON-DIMENSIONAL TORQUE = TORQUE/RATED TORQUE;
C      D = PIPE DIAMETER (M);
C      DT = COMPUTATIONAL TIME INTERVAL (S);
C      DTH = THETA INTERVAL FOR STORING PUMP CHARACTERISTICS;
C      ER = PUMP EFFICIENCY;
C      F = DARCY-WEISBACH FRICTION FACTOR;
C      FB = POINTS ON TORQUE CHARACTERISTIC OF PUMP;
C      FH = POINTS ON HEAD CHARACTERISTIC OF PUMP;
C      H = PIEZOMETRIC HEAD AT BEGINNING OF TIME INTERVAL (M);
C      HMAX = MAXIMUM PIEZOMETRIC HEAD (M);
C      HMIN = MINIMUM PIEZOMETRIC HEAD (M);
```

```

C      HP = PIEZOMETRIC HEAD AT END OF TIME INTERVAL (M);
C      HR = RATED HEAD (M);
C      HRES = RESERVOIR LEVEL ABOVE DATUM (M);
C      IPRINT = NUMBER OF TIME INTERVAL AFTER WHICH CONDITIONS
C      ARE TO BE PRINTED;
C      L = PIPE LENGTH (M);
C      N = NUMBER OF REACHES INTO WHICH PIPE IS DIVIDED;
C      NO = STEADY STATE PUMP SPEED (RPM);
C      NP = NUMBER OF PIPES;
C      NPC = NUMBER OF POINTS ON PUMP CHARACTERISTIC CURVE;
C      NPP = NUMBER OF PARALLEL PUMPS;
C      NR = RATED PUMP SPEED (RPM);
C      NRLP = NUMBER OF REACHES ON LAST PIPE;
C      Q = DISCHARGE AT BEGINNING OF TIME INTERVAL (M3/S1);
C      QO = STEADY-STATE DISCHARGE (M3/S);
C      QP = DISCHARGE AT END OF TIME INTERVAL (M3/S);
C      QR = RATED DISCHARGE (M3/S);
C      T = TIME (S);
C      TLAST = TIME UPTO WHICH TRANSIENT CONDITIONS ARE
C      TO BE COMPUTED;
C      TR = RATED TORQUE (N-M);
C      V = NON-DIMENSIONAL PUMP DISCHARGE (Q/QR).
C
C*****REAL L,NR,NO
C*****DIMENSION Q(10,100),H(10,100),QP(10,100),HP(10,100),CA(10),F(10),
C*****1CF(10),AR(10),A(10),L(10),N(10),D(10),FH(60),FB(60),HMAX(10),
C*****2HMIN(10)
C*****COMMON /CP/ALPHA,QR,V,CN,DALPHA,DV,BETA,C5,C6,NPP,T
C*****COMMON /PAR/FH,FB,DTH
C
C      READING AND WRITING OF INPUT DATA
C
C      GENERAL DATA
C      Read(1,*) NP,NRLP,IPRINT,NPP,G,QO,NO,TLAST
C      Write(2,10) NP,NRLP,QO,NO,TLAST,NPP
10     FORMAT(8X,'NUMBER OF PIPES =',I3/8X,'NUMBER OF REACHES ON LAST PIP
1E =',I3/8X,'STEADY STATE DISCH. =' ,F6.3,' M3/S'/8X,'STEADY STATE
2 PUMP SPEED =',F6.1,' RPM'/8X,'TIME FOR WHICH TRANS. STATE COND.
3ARE TO BE COMPUTED =' ,F5.1,' S'/8X,'NUMBER OF PARALLEL PUMPS =' 
4,I3/)
C
C      READING AND WRITING OF PUMP DATA
C
C      Read(1,*) NPC,DTH,QR,HR,NR,ER,WR2, (FH(I),I=1,NPC)
C      Read(1,*) (FB(I),I=1,NPC)
C      Write(2,20) NPC,DTH,QR,HR,NR,ER,WR2, (FH(I),I=1,NPC)
20     FORMAT(8X,'NUMBER OF POINTS ON CHARACTERISTIC CURVE =',I4/
18X,'THETA INTERVAL FOR STORING CHARACTERISTIC CURVE =',F4.0/8X,
2'RATED DISCH. =',F5.2,' M3/S'/8X,'RATED HEAD =' ,F6.1,' M'/8X,
3'RATED PUMP SPEED =',F6.1,' RPM'/8X,'PUMP EFFICIENCY =',F6.3/8X,
4'WR2=',F7.2,' KG-M2'//8X,'POINTS ON HEAD CHARACT. CURVE'/
5 (8X,10F7.3))
C      Write(2,30) (FB(I) ,I=1,NPC)
30     FORMAT(/8X,'POINTS ON TORQUE CHARACT. CURVE'/(8X,10F7.3))
C
C      DATA FOR PIPES
C
C      READ (1,*) (L(I),D(I),A(I),F(I), I=1,NP)
C      Write(2,40)

```

```

40  FORMAT(/8X,'PIPE NO',5X,'LENGTH',5X,'DIA',5X,'WAVE VEL.',5X,'FRI
2C FACTOR'/22X,'(M)',6X,'(M)',7X,'(M/S)' )
   Write(2,50)(I,L(I),D(I),A(I),F(I),I=1,NP)
50  FORMAT(10X,I3,6X,F7.1,3X,F5.2,5X,F7.1,11X,F5.3)
   DT=L(NP)/(NRLP*A(NP))
   Write(2,51)
51  FORMAT(/8X,'PIPE NO',5X,'ADJUSTED WAVE VEL'/26X,'(M/S)')
C CALCULATION OF PIPE CONSTANTS
   DO 60 I=1,NP
   AR(I)=0.7854*D(I)**2
   AUNADJ=A(I)
   AN=L(I)/(DT*A(I))
   N(I)=AN
   AN1=N(I)
   IF((AN-AN1).GE.0.5) N(I)=N(I)+1
   A(I)=L(I)/(DT*N(I))
   Write(2,55) I,A(I)
55  FORMAT(10X,I3,12X,F7.1)
   CA(I)=G*AR(I)/A(I)
   CF(I)=F(I)*DT/(2.*D(I)*AR(I))
   F(I)=F(I)*L(I)/(2.*G*D(I)*N(I)*AR(I)**2)
   CONTINUE
C COMPUTATION OF CONSTANTS FOR PUMP
C THE FOLLOWING CONSTANTS ARE FOR SI UNITS (HR IN M, QR IN
C M3/S; AND NR IN RPM). FOR ENGLISH UNITS (HR IN FT, QR IN
C CFS, AND NR IN RPM), REPLACE 93604.99 BY 595.875 AND
C 4.775 BY 153.744.
   TR=(93604.99*HR*QR)/(NR*ER)
   C5=CA(1)*HR
   C6=-(4.775*TR*DT)/(NR*WR2)
   ALPHA=NO/NR
   V=QO/(NPP*QR)
   DV=0.0
   DALPHA=0.0
C CALCULATION OF STEADY STATE CONDITIONS
C
   IF(V.EQ.0.0) GO TO 65
   TH=ATAN2(ALPHA,V)
   TH=57.296*TH
   GO TO 68
65  TH=0.0
68  CALL PARAB(TH,1,Z)
   HO=Z*HR*(ALPHA**2+V**2)
   H(1,1)=HO
   CALL PARAB(TH,2,Z)
   BETA=Z*(ALPHA**2+V**2)
   DO 80 I=1,NP
   NN=N(I)+1
   DO 70 J=1,NN
   H(I,J)=H(I,1)-(J-1)*F(I)*QO**2
   IF(I.NE.NP.AND.J.EQ.NN) H(I+1,1)=H(I,NN)
   Q(I,J)=QO
70  CONTINUE
   HMAX(I)=H(I,1)
   HMIN(I)=H(I,1)
80  CONTINUE
   NN=N(NP)+1
   HRES=H(NP,NN)
   T=0.0

```

```

NP1=NP-1
Write(2,85)
85 FORMAT(/8X,'TIME',2X,'ALPHA',4X,'V',4X,'PIPE',7X,
  1'HEAD (M)',7X,'DISCH. (M3/S)'/29X,'NO.',5X,'(1)',5X,'(N+1)'
  1,5X,'(1)',5X,'(N+1)')
90 K=0
  I=1
  NN=N(I)+1
  Write(2,86) T,ALPHA,V,I,H(1,1),H(1,NN),Q(1,1),Q(1,NN)
  DO 89 I=2,NP
  NN=N(I)+1
  Write(2,87) I,H(I,1),H(I,NN),Q(I,1),Q(I,NN)
86 FORMAT(F12.1,F7.2,F7.2,I5,F9.1,F9.1,F9.3,F10.3)
87 FORMAT(26X,I5,2F9.1,F9.3,F10.3)
89 CONTINUE
150 T=T+DT
  K=K+1
  IF(T.GT.TLAST) GO TO 240
C
C      PUMP AT UPSTREAM END
C
CN=Q(1,2)-H(1,2)*CA(1)-CF(1)*Q(1,2)*ABS(Q(1,2))
CALL PUMP
QP(1,1)=NPP*V*QR
HP(1,1)=(QP(1,1)-CN)/CA(1)
C
C      INTERIOR POINTS
C
DO 170 I=1,NP
NN=N(I)
DO 160 J=2,NN
JP1=J+1
JM1=J-1
CN=Q(I,JP1)-CA(I)*H(I,JP1)-CF(I)*Q(I,JP1)*ABS(Q(I,JP1))
CP=Q(I,JM1)+CA(I)*H(I,JM1)-CF(I)*Q(I,JM1)*ABS(Q(I,JM1))
QP(I,J)=0.5*(CP+CN)
HP(I,J)=(CP-QP(I,J))/CA(I)
160 CONTINUE
170 CONTINUE
C
C      SERIES JUNCTION
C
IF(NP.EQ.1) GO TO 178
DO 175 I=1,NP1
N1= N(I)
NN=N(I)+1
IP1=I+1
CN=Q(IP1,2)-CA(IP1)*H(IP1,2)-CF(IP1)*Q(IP1,2)*ABS(Q(IP1,2))
CP=Q(I,N1)+CA(I)*H(I,N1)-CF(I)*Q(I,N1)*ABS(Q(I,N1))
HP(I,NN)=(CP-CN)/(CA(I)+CA(IP1))
HP(IP1,1)=HP(I,NN)
QP(I,NN)=CP-CA(I)*HP(I,NN)
QP(IP1,1)=CN+CA(IP1)*HP(IP1,1)
175 CONTINUE
C
C      RESERVOIR AT DOWNSTREAM END
C
178 NN=N(NP)+1
NN1=N(NP)
HP(NP,NN)=HRES
CP=Q(NP,NN1)+CA(NP)*H(NP,NN1)-CF(NP)*Q(NP,NN1)*ABS(Q(NP,NN1))

```

```

QP(NP,NN)=CP-CA(NP)*HP(NP,NN)
C
C      STORING MAX. AND MIN. PRESSURES AND VARIABLES FOR NEXT TIME STEP
C
210 DO 230 I=1,NP
      NN=N(I)+1
      DO 220 J=1,NN
      Q(I,J)=QP(I,J)
      H(I,J)=HP(I,J)
220 CONTINUE
      IF (H(I,1).GT.HMAX(I)) HMAX(I)=H(I,1)
      IF (H(I,1).LT.HMIN(I)) HMIN(I)=H(I,1)
230 CONTINUE
      IF(K.EQ.IPRINT) GO TO 90
      GO TO 150
240 Write(2,250)
250 FORMAT(//10X,'PIPE NO.',5X,'MAX. PRESS. ',5X,'MIN. PRESS./27X
     1,'(M)',16X,'(M)')
      Write(2,260) (I,HMAX(I),HMIN(I),I=1,NP)
260 FORMAT(12X,I3,7X,F7.1,9X,F7.1)
      STOP
      END
      SUBROUTINE PUMP
      DIMENSION FH(60),FB(60)
      COMMON /CP/ALPHA,QR,V,CN,DALPHA,DV,BETA,C5,C6,NPP,T
      COMMON /PAR/FH,FB,DTH
      KK=0
      JJ=0
C
C      COMPUTATION OF PUMP DISCHARGE
C
      VE=V+DV
5       ALPHAE=ALPHA+DALPHA
8       JJ=JJ+1
10      IF (VE.EQ.0.0.AND.ALPHAE.EQ.0.0) GO TO 20
      TH=ATAN2(ALPHAE,VE)
      TH1=TH
      TH=TH*57.296
      IF (TH.LT.0.0) TH=TH+360.
      IF (TH1.LT.0.0) TH1=TH1+6.28318
      GO TO 30
20      TH= 0.0
      TH1=0.0
30      M=TH/DTH+1.
      A1=FH(M)*M-FH(M+1)*(M-1)
      A2=(FH(M+1)-FH(M))/(DTH*0.017453)
      A3=FB(M)*M-FB(M+1)*(M-1)
      A4=(FB(M+1)-FB(M))/(DTH*0.017453)
      ALPSQ=ALPHAE*ALPHAE
      VESQ=VE*VE
      ALPV=ALPSQ+VESQ
      F1=C5*A1*ALPV+C5*A2*ALPV*TH1-QR*VE*NPP+CN
      F2=ALPHAE-C6*A3*ALPV-C6*A4*ALPV*TH1-ALPHA-C6*BETA
      F1AL=C5*(2.*A1*ALPHAE+A2*VE+2.*A2*ALPHAE*TH1)
      F1V=C5*(2.*A1*VE-A2*ALPHAE+2.*A2*VE*TH1)-QR*NPP
      F2AL=1.-C6*(2.*A3*ALPHAE+A4*VE+2.*A4*ALPHAE*TH1)
      F2V=C6*(-2.*A3*VE+A4*ALPHAE-2.*A4*VE*TH1)
      DENOM=F1AL*F2V-F1V*F2AL
      DALPHA=(F2*F1V-F1*F2V)/DENOM
      DV=(F1*F2AL-F2*F1AL)/DENOM
      ALPHAE=ALPHAE+DALPHA

```

```

VE=VE+DV
IF (ABS(DV).LE.0.001.AND.ABS(DALPHA).LE.0.001) GO TO 50
IF (JJ.GT.30) GO TO 70
GO TO 8
50 TH=ATAN2(ALPHAE,VE)
TH=57.296*TH
IF (TH.LT.0.0) TH=TH+360.
CALL PARAB(TH,2,BETA)
MB=TH/DTH+1
BETA= BETA * (ALPHA*ALPHA+V*V)
IF (MB.EQ.M) GO TO 60
GO TO 8
60 DALPHA=ALPHAE-ALPHA
DV=VE-V
ALPHA=ALPHAE
V=VE
RETURN
70 Write(2,80) T,ALPHAE,VE
80 FORMAT(8X,'***ITERATIONS IN PUMP SUBROUTINE FAILED'/8X,'T=',F8.2
2/8X,'ALPHAE =',F6.3/8X,'VP =',F6.3)
STOP
END
SUBROUTINE PARAB(X,J,Z)
COMMON /PAR/FH,FB,DX
DIMENSION FH(60),FB(60)
I=X/DX
R=(X-I*DX)/DX
IF(I.EQ.0) R=R-1.
I=I+1
IF(I.LT.2) I=2
GO TO (10,20),J
10 Z=FH(I)+0.5*R*(FH(I+1)-FH(I-1)+R*(FH(I+1)+FH(I-1)-2.*FH(I)))
RETURN
20 Z=FB(I)+0.5*R*(FB(I+1)-FB(I-1)+R*(FB(I+1)+FB(I-1)-2.*FB(I)))
RETURN
END

```

## C-2 Input Data

```

2,2,2,2,9.81,0.5,1100.0,15.0
55,5.0,0.250,60.0,1100.0,0.84,16.85
-0.53,-0.476,-0.392,-0.291,-0.150,-0.037,0.075,0.200,0.345,
0.500,0.655,0.777,0.9,1.007,1.115,1.188,1.245,1.278,1.290,1.287,

```

1.269,1.240,1.201,1.162,1.115,1.069,1.025,0.992,0.945,0.908,0.875,  
 0.848,0.819,0.788,0.755,0.723,0.690,0.656,0.619,0.583,0.555,0.531,  
 0.510,0.502,0.500,0.505,0.520,0.539,0.565,0.593,0.615,0.634,0.640,  
 0.638,0.630  
 -0.350,-0.474,-0.180,-0.062,0.037,0.135,0.228,0.320,0.425,0.500,0.548,  
 0.588,0.612,0.615,0.600,0.569,0.530,0.479,0.440,0.402,0.373,0.350,0.34,  
 0.34,0.35,0.38,0.437,0.52,0.605,0.683,0.75,0.802,0.845,0.872,0.883,0.878,  
 0.86,0.823,0.78,0.725,0.66,0.58,0.49,0.397,0.31,0.23,0.155,0.085,0.018,  
 -0.052,-0.123,-0.22,-0.348,-0.49,-0.68  
 450.0,0.75,900.0,0.01  
 550.0,0.75,1100.0,0.012

### C-3 Program Output

NUMBER OF PIPES = 2  
 NUMBER OF REACHES ON LAST PIPE = 2  
 STEADY STATE DISCH. = .500 M3/S  
 STEADY STATE PUMP SPEED =1100.0 RPM  
 TIME FOR WHICH TRANS. STATE COND. ARE TO BE COMPUTED = 15.0 S  
 NUMBER OF PARALLEL PUMPS = 2

NUMBER OF POINTS ON CHARACTERISTIC CURVE = 55  
 THETA INTERVAL FOR STORING CHARACTERISTIC CURVE = 5.  
 RATED DISCH. = .25 M3/S  
 RATED HEAD = 60.0 M  
 RATED PUMP SPEED =1100.0 RPM  
 PUMP EFFICIENCY = .840  
 WR2= 16.85 KG-M2

|       | POINTS ON HEAD CHARACT. CURVE |       |       |       |       |       |       |       |       |
|-------|-------------------------------|-------|-------|-------|-------|-------|-------|-------|-------|
|       | -.530                         | -.476 | -.392 | -.291 | -.150 | -.037 | .075  | .200  | .345  |
| .500  | .655                          | .777  | .900  | 1.007 | 1.115 | 1.188 | 1.245 | 1.278 | 1.290 |
| 1.287 | 1.269                         | 1.240 | 1.201 | 1.162 | 1.115 | 1.069 | 1.025 | .992  | .945  |
| .908  | .875                          | .848  | .819  | .788  | .755  | .723  | .690  | .656  | .619  |
| .583  | .555                          | .531  | .510  | .502  | .500  | .505  | .520  | .539  | .565  |
| .593  | .615                          | .634  | .640  | .638  | .630  |       |       |       |       |

## 542 C TRANSIENTS CAUSED BY POWER FAILURE TO PUMPS

|      | POINTS ON TORQUE CHARACT. CURVE |                            |             |                    |              |      |               |                 |        |
|------|---------------------------------|----------------------------|-------------|--------------------|--------------|------|---------------|-----------------|--------|
|      | -.350                           | -.474                      | -.180       | -.062              | .037         | .135 | .228          | .320            | .425   |
| .500 | .548                            | .588                       | .612        | .615               | .600         | .569 | .530          | .479            | .440   |
| .402 | .373                            | .350                       | .340        | .340               | .350         | .380 | .437          | .520            | .605   |
| .683 | .750                            | .802                       | .845        | .872               | .883         | .878 | .860          | .823            | .780   |
| .725 | .660                            | .580                       | .490        | .397               | .310         | .230 | .155          | .085            | .018 - |
| .052 | -.123                           | -.220                      | -.348       | -.490              | -.680        |      |               |                 |        |
|      | PIPE NO                         | LENGTH<br>(M)              | DIA<br>(M)  | WAVE VEL.<br>(M/S) |              | FRI  | C FACTOR      |                 |        |
|      | 1                               | 450.0                      | .75         | 900.0              |              |      | .010          |                 |        |
|      | 2                               | 550.0                      | .75         | 1100.0             |              |      | .012          |                 |        |
|      | PIPE NO                         | ADJUSTED WAVE VEL<br>(M/S) |             |                    |              |      |               |                 |        |
|      | 1                               | 900.0                      |             |                    |              |      |               |                 |        |
|      | 2                               | 1100.0                     |             |                    |              |      |               |                 |        |
| TIME | ALPHA                           | V                          | PIPE<br>NO. | HEAD<br>(1)        | (M)<br>(N+1) |      | DISCH.<br>(1) | (M3/S)<br>(N+1) |        |
| .0   | 1.00                            | 1.00                       | 1           | 60.0               | 59.6         |      | .500          | .500            |        |
|      |                                 |                            | 2           | 59.6               | 59.0         |      | .500          | .500            |        |
| .5   | .69                             | .69                        | 1           | 28.3               | 59.6         |      | .347          | .500            |        |
|      |                                 |                            | 2           | 59.6               | 59.0         |      | .500          | .500            |        |
| 1.0  | .52                             | .57                        | 1           | 14.8               | 24.9         |      | .283          | .363            |        |
|      |                                 |                            | 2           | 24.9               | 59.0         |      | .363          | .500            |        |
| 1.5  | .42                             | .56                        | 1           | 7.6                | 10.0         |      | .279          | .305            |        |
|      |                                 |                            | 2           | 10.0               | 59.0         |      | .305          | .227            |        |
| 2.0  | .36                             | .55                        | 1           | 4.0                | 36.6         |      | .276          | .139            |        |
|      |                                 |                            | 2           | 36.6               | 59.0         |      | .139          | .111            |        |
| 2.5  | .31                             | .00                        | 1           | 7.4                | 47.5         |      | -.002         | .066            |        |
|      |                                 |                            | 2           | 47.5               | 59.0         |      | .066          | .050            |        |
| 3.0  | .29                             | -.24                       | 1           | 8.7                | 24.7         |      | -.121         | -.085           |        |
|      |                                 |                            | 2           | 24.7               | 59.0         |      | -.085         | .020            |        |
| 3.5  | .26                             | -.32                       | 1           | 9.4                | 15.2         |      | -.159         | -.152           |        |
|      |                                 |                            | 2           | 15.2               | 59.0         |      | -.152         | -.221           |        |
| 4.0  | .21                             | -.36                       | 1           | 9.2                | 38.8         |      | -.181         | -.300           |        |
|      |                                 |                            | 2           | 38.8               | 59.0         |      | -.300         | -.324           |        |
| 4.5  | .11                             | -.73                       | 1           | 24.6               | 48.0         |      | -.367         | -.367           |        |
|      |                                 |                            | 2           | 48.0               | 59.0         |      | -.367         | -.379           |        |
| 5.0  | -.09                            | -.89                       | 1           | 31.3               | 41.4         |      | -.446         | -.447           |        |
|      |                                 |                            | 2           | 41.4               | 59.0         |      | -.447         | -.409           |        |
| 5.5  | -.34                            | -.96                       | 1           | 34.5               | 39.6         |      | -.479         | -.484           |        |
|      |                                 |                            | 2           | 39.6               | 59.0         |      | -.484         | -.514           |        |
| 6.0  | -.58                            | -.97                       | 1           | 39.0               | 49.6         |      | -.485         | -.549           |        |
|      |                                 |                            | 2           | 49.6               | 59.0         |      | -.549         | -.558           |        |
| 6.5  | -.81                            | -1.06                      | 1           | 53.3               | 56.3         |      | -.529         | -.566           |        |
|      |                                 |                            | 2           | 56.3               | 59.0         |      | -.566         | -.584           |        |
| 7.0  | -1.02                           | -1.05                      | 1           | 64.7               | 62.0         |      | -.523         | -.569           |        |
|      |                                 |                            | 2           | 62.0               | 59.0         |      | -.569         | -.574           |        |
| 7.5  | -1.19                           | -1.00                      | 1           | 75.5               | 67.8         |      | -.502         | -.537           |        |
|      |                                 |                            | 2           | 67.8               | 59.0         |      | -.537         | -.554           |        |
| 8.0  | -1.31                           | -.93                       | 1           | 82.7               | 74.0         |      | -.463         | -.492           |        |
|      |                                 |                            | 2           | 74.0               | 59.0         |      | -.492         | -.499           |        |
| 8.5  | -1.37                           | -.86                       | 1           | 87.1               | 76.1         |      | -.428         | -.430           |        |

|      |       |      |   |      |      |       |       |
|------|-------|------|---|------|------|-------|-------|
|      |       |      | 2 | 76.1 | 59.0 | -.430 | -.431 |
| 9.0  | -1.39 | -.76 | 1 | 86.5 | 74.9 | -.379 | -.367 |
|      |       |      | 2 | 74.9 | 59.0 | -.367 | -.361 |
| 9.5  | -1.37 | -.66 | 1 | 82.1 | 72.1 | -.332 | -.308 |
|      |       |      | 2 | 72.1 | 59.0 | -.308 | -.304 |
| 10.0 | -1.32 | -.59 | 1 | 75.2 | 68.5 | -.293 | -.266 |
|      |       |      | 2 | 68.5 | 59.0 | -.266 | -.256 |
| 10.5 | -1.26 | -.53 | 1 | 68.1 | 63.7 | -.267 | -.237 |
|      |       |      | 2 | 63.7 | 59.0 | -.237 | -.228 |
| 11.0 | -1.20 | -.50 | 1 | 61.4 | 59.5 | -.248 | -.226 |
|      |       |      | 2 | 59.5 | 59.0 | -.226 | -.218 |
| 11.5 | -1.15 | -.48 | 1 | 56.0 | 56.9 | -.242 | -.226 |
|      |       |      | 2 | 56.9 | 59.0 | -.226 | -.223 |
| 12.0 | -1.10 | -.50 | 1 | 52.3 | 55.2 | -.248 | -.238 |
|      |       |      | 2 | 55.2 | 59.0 | -.238 | -.234 |
| 12.5 | -1.07 | -.52 | 1 | 50.3 | 53.7 | -.261 | -.254 |
|      |       |      | 2 | 53.7 | 59.0 | -.254 | -.253 |
| 13.0 | -1.06 | -.55 | 1 | 49.4 | 53.2 | -.275 | -.275 |
|      |       |      | 2 | 53.2 | 59.0 | -.275 | -.275 |
| 13.5 | -1.05 | -.58 | 1 | 49.7 | 53.7 | -.291 | -.295 |
|      |       |      | 2 | 53.7 | 59.0 | -.295 | -.297 |
| 14.0 | -1.06 | -.62 | 1 | 50.9 | 54.5 | -.308 | -.314 |
|      |       |      | 2 | 54.5 | 59.0 | -.314 | -.315 |
| 14.5 | -1.08 | -.64 | 1 | 52.8 | 55.4 | -.322 | -.328 |
|      |       |      | 2 | 55.4 | 59.0 | -.328 | -.331 |
| 15.0 | -1.10 | -.66 | 1 | 54.9 | 56.6 | -.330 | -.339 |
|      |       |      | 2 | 56.6 | 59.0 | -.339 | -.342 |

| PIPE NO. | MAX. PRESS.<br>(M) | MIN. PRESS.<br>(M) |
|----------|--------------------|--------------------|
| 1        | 87.4               | 4.0                |
| 2        | 76.1               | 10.0               |

# D

---

## FREQUENCY RESPONSE OF A SERIES PIPING SYSTEM

### D-1 Program Listing

```
C
C FREQUENCY RESPONSE OF A SERIES PIPING SYSTEM HAVING RESERVOIR AT
C THE UPSTREAM END AND AN OSCILLATING VALVE AT THE DOWNSTREAM END
C CCTRANSFER-MATRIX METHOD IS USED TO COMPUTE THE FREQUENCY RESPONSE.
C PIPING SYSTEM MAY HAVE UPTO 20 PIPES IN SERIES; THIS LIMIT MAY
C BE INCREASED BY MODIFYING THE DIMENSION STATEMENT.
C FRICTION LOSSES ARE NEGLECTED.
C FREE FORMAT IS USED FOR DATA INPUT.
C SI UNITS ARE USED.
C
C***** NOTATION *****
C     AMP=AMPLITUDE OF VALVE OSCILLATIONS;
C     AR=PIPE CROSS-SECTINAL AREA (M2);
C     D=PIPE DIAMETER (M);
C     HO=STATIC HEAD (M);
C     L=PIPE LENGTH (M);
C     M1,M2,M3=INTEGERS FOR
C     OSCILLATIONS;
C     N=NUMBER OF PIPES;
C     Q0=MEAN DISCHARGE (M3/S);
C     TAU0=MEAN VALVE OPENING
C     THPER=THEORETICAL PERIOD OF THE PIPELINE
C     W=FREQUENCY OF VALVE OSCILLATIONS;
C     WR=W/WT;
C     WV=WAVE VELOCITY (M/S);
C     WT=THEORETICAL FREQUENCY OF PIPELINE.
C
C***** 
C
COMPLEX A,B,C,HV,QV,CC,CMPLX
```

```

REAL L
DIMENSION L(20),WV(20),D(20),AR(20),P(20),CP(20),A(2,2),B(2,2),
1C(2,2),F(20)
READ(1,*) N,M1,M2,M3,FRAC
10 FORMAT(4I3,F10.2)
READ(1,*) TAUO,HO,QO,AMP,THPER
20 FORMAT(7F10.3)
WRITE(2,30) TAUO,HO,QO,AMP,THPER,N
30 FORMAT(8X,'MEAN VALVE OPENING = ',F5.3/8X,'STATIC HEAD = ',F7.2,
1' M'/8X,'MEAN DISCHARGE = ',F7.3,' M3/S'/8X,'AMPLITUDE OF VALVE
2OSCILLATIONS = ',F5.3 /8X,'THEORETICAL PERIOD OF THE PIPELINE =',
3F6.3,' S'/8X,'NUMBER OF PIPES = ',I3)
READ(1,*) (L(I),D(I),WV(I),I=1,N)
40 FORMAT(3F10.2)
WRITE(2,50)
50 FORMAT(8X,'LENGTH (M)',3X,'DIA (M)',2X,'WAVE VEL. (M/S)')
DO 60 I=1,N
WRITE(2,55) L(I),D(I),WV(I)
55 FORMAT(F16.2,F11.2,F14.2)
P(I)=L(I)/WV(I)
CP(I)=7.7047*D(I)**2/WV(I)
C IN ENGLISH UNITS, REPLACE 7.7047 BY 25.2898
60 CONTINUE
VC=-(2.*HO*AMP)/TAUO
TW=6.2832/THPER
WRITE(2,65)
65 FORMAT(/8X,'WF/WT',8X,'H/HO',6X,'Q/QO',4X,'PHASE H',3X,'PHASE Q')
DO 80 J=M1,M2,M3
AJ=J
W=FRAC*AJ*TW
A(1,1)=CMPLX(1.,0.)
A(1,2)=CMPLX(0.0,0.0)
A(2,1)=CMPLX(0.0,0.0)
A(2,2)=CMPLX(1.0,0.0)
DO 70 I=1,N
G=W*P(I)
B(1,1)=CMPLX(COS(G),0.0)
B(1,2)=CMPLX(0.0,-(1./CP(I))*SIN(G))
B(2,1)=CMPLX(0.0,-CP(I)*SIN(G))
B(2,2)=CMPLX(COS(G),0.0)
CALL MULT(B,A,C,2,2)
CALL COPY(C,A,2,2)
70 CONTINUE
CC=VC/(C(1,2)-2.*HO*C(2,2)/QO)
HV=CC*C(1,2)
QV=CC*C(2,2)
WR=W/TW
H=CABS(HV)/HO
Q=CABS(QV)/QO
ANGH=57.29578*ATAN2(AIMAG(HV),REAL(HV))
ANGQ=57.29578*ATAN2(AIMAG(QV),REAL(QV))
WRITE(2,85) WR,H,Q,ANGH,ANGQ
80 CONTINUE
85 FORMAT(3X,5F10.3)
STOP
END
SUBROUTINE MULT(A,B,C,N,M)
COMPLEX A,B,C,CMPLX
DIMENSION A(N,N),B(N,N),C(N,N)
DO 6 I=1,N
DO 6 J=1,N

```

```

C(I,J)=CMPLX(0.0,0.0)
DO 6 K=1,N
6 C(I,J)=A(I,K)*B(K,J)+C(I,J)
RETURN
END
SUBROUTINE COPY(C,A,N,M)
COMPLEX A,C
DIMENSION A(N,N),C(N,N)
DO 6 I=1,N
DO 6 J=1,N
6 A(I,J)=C(I,J)
RETURN
END

```

## D-2 Input Data

```

2,1,20,1,0.5
1.0,30.48,0.0089,0.2,3.0
609.5,0.61,1219.0
228.6,0.3,914.4

```

## D-3 Program Output

```

MEAN VALVE OPENING =1.000
STATIC HEAD = 30.48 M
MEAN DISCHARGE = .009 M3/S
AMPLITUDE OF VALVE OSCILLATIONS = .200
THEORETICAL PERIOD OF THE PIPELINE = 3.000 S
NUMBER OF PIPES = 2

LENGTH (M)    DIA (M)    WAVE VEL. (M/S)
 609.50        .61        1219.00
 228.60        .30        914.40

```

## 548 D FREQUENCY RESPONSE OF A SERIES PIPING SYSTEM

| WF/WT  | H/HO | Q/QO | PHASE H  | PHASE Q |
|--------|------|------|----------|---------|
| .500   | .037 | .199 | -95.257  | -5.257  |
| 1.000  | .123 | .190 | -107.887 | -17.887 |
| 1.500  | .076 | .196 | 100.897  | 10.897  |
| 2.000  | .046 | .199 | -96.552  | -6.552  |
| 2.500  | .149 | .186 | -111.940 | -21.940 |
| 3.000  | .400 | .000 | 179.998  | 89.998  |
| 3.500  | .149 | .186 | 111.940  | 21.940  |
| 4.000  | .046 | .199 | 96.551   | 6.551   |
| 4.500  | .076 | .196 | -100.898 | -10.898 |
| 5.000  | .123 | .190 | 107.886  | 17.886  |
| 5.500  | .037 | .199 | 95.257   | 5.257   |
| 6.000  | .000 | .200 | -90.000  | .000    |
| 6.500  | .037 | .199 | -95.258  | -5.258  |
| 7.000  | .123 | .190 | -107.888 | -17.888 |
| 7.500  | .076 | .196 | 100.896  | 10.896  |
| 8.000  | .046 | .199 | -96.552  | -6.552  |
| 8.500  | .149 | .186 | -111.941 | -21.941 |
| 9.000  | .400 | .000 | 179.995  | 89.995  |
| 9.500  | .149 | .186 | 111.939  | 21.939  |
| 10.000 | .046 | .199 | 96.551   | 6.551   |

# E

---

## WATER LEVEL OSCILLATIONS IN A SIMPLE SURGE TANK

### E-1 Program Listing

```
C*****
C
C      COMPUTATION OF WATER-LEVEL OSCILLATIONS IN A SIMPLE SURGE TANK
C
C      FREE FORMAT IS USED FOR READING THE INPUT DATA.
C      SURGE TANK MAY HAVE UPTO FIVE DIFFERENT CROSS-SECTIONAL AREAS;
C      THIS LIMIT MAY BE INCREASED BY MODIFYING THE DIMENSION
C      STATEMENT.
C      LUMPED SYSTEM APPROACH IS USED TO COMPUTE THE OSCILLATIONS.
C      ORDINARY DIFFERENTIAL EQUATIONS DESCRIBING THE MOMENTUM AND
C      CONTINUITY EQUATIONS ARE SOLVED EITHER BY AN ITERATIVE MODIFIED
C      EULER METHOD OR BY FOURTH-ORDER RUNGE-KUTTA METHOD. SELECTION
C      OF THE METHOD IS DONE BY SPECIFYING THE INPUT VARIABLE 'METHOD'.
C      SI UNITS ARE USED.
C      PROGRAM EXECUTION IS STOPPED: (1)IF THE WATER LEVEL IN THE TANK
C      DROPS BELOW THE TANK INVERT LEVEL AFTER PRINTING "TANK IS
C      DRAINED"; AND IF THE WATER LEVEL RISES ABOVE THE TOP OF THE
C      TANK AFTER PRINTING :"TANK IS OVERFLOWING."
C*****
C      ***** NOTATION *****
C
C      ASUR = HORIZONTAL TANK AREA AT ELEVATION EL (M2);
C      AT = TUNNEL CROSS-SECTIONAL AREA (M2);
C      DT = COMPUTATIONAL TIME INTERVAL (S);
C      EINV = TANK INVERT LEVEL (M);
C      ELUR = UPSTREAM REAERVOIR LEVEL (M);
C      ETOP = ELEVATION OF TANK TOP (M);
C      HFO = TUNNEL HEAD LOSS CORRESPONDING TO DISCHARGE Q0 (M);
C      L = PIPE LENGTH (M);
C      METHOD = PARAMETER FOR SPECIFYING THE METHOD OF SOLUTION;
C      Q1 = TUNNEL DISCHARGE AT BIGGINING OF TIME INTERVAL (M3/S);
C      Q2 = TUNNEL DISCHARGE AT END OF TIME INTERVAL (M3/S);
```

```

C      QTI = INITIAL TURBINE FLOW (M3/S);
C      QTF = FINAL TURBINE FLOW (M3/S);
C      QTUR1 = TURBINE FLOW AT BIGGINING OF TIME INTERVAL (M3/S);
C      QTUR2 = TURBINE FLOW AT END OF TIME INTERVAL (M3/S);
C      Z1 = TANK WATER LEVEL ABOVE UPSTREAM RESRVOIR LEVEL AT BIGGINING
C      TG = TIME FOR LINEARLY CHANGING FLOW QTI TO QTF (S);
C      TSTOP = TIME UPTO WHICH OSCILLATIONS ARE TO BE COMPUTED (S);
C          OF TIME INTERVAL (M);
C      Z2 = TANK WATER LEVEL ABOVE UPSTREAM RESERVOIR LEVEL AT END OF
C          TIME STEP (M);
C      ZMAX = MAXIMUM SURGE LEVEL (M);
C      ZMIN = MINIMUM SURGE LEVEL (M);
C*****
C
C      REAL L
C      DIMENSION EL(5),ASUR(5)
C      COMMON /ST/N,EL,ASUR,ELUR,EINV,ETOP
C      READ (5,*) METHOD,IPRINT,G,DT,TSTOP,QTI,QTF,TG,ELUR,EINV,ETOP
C      READ (5,*) L,AT,QO,HFO,N,(EL(I),ASUR(I),I=1,N)
C      GO TO (4,7),METHOD
4     READ (5,*) TOLER
5     WRITE (6,6) TOLER
6     FORMAT(10X,'ITERATIVE MODIFIED EULER METHOD'/5X,
1           'TOLERANCE FOR ITERATIONS =', F7.4,' M'//)
    GO TO 9
7     WRITE (6,8)
8     FORMAT (10X,'FOURTH-ORDER RUNGE-KUTTA METHOD'//)
9     WRITE(6,10) L,AT,HFO,QO,QTI,QTF,TG,DT,IPRINT,ELUR,EINV,ETOP,
1           (EL(I),ASUR(I),I=1,N)
10    FORMAT(5X,'LENGTH =',F8.1,' M'/5X,'TUNNEL AREA =',F6.2,' M2'
1     /5X,'TUNNEL HEAD LOSS =',F6.2,
2     ' M FOR DISCHARGE =',F8.2,' M3/S'/5X,'INITIAL TURBINE FLOW =',
3     F8.2,' M3/S'/5X,'FINAL TURBINE FLOW =',F8.2,' M3/S'/
4     5X,'GATE TIME =',F6.2,' S'/
5     5X,'COMPUTATIONAL TIME INTERVAL =',F6.2,' S'/
6     5X,'IPRINT =',I3/5X,'UPSTREAM RESER. LEVEL =',F9.2,' M'/
7     5X,'TANK INVERT LEVEL =',F9.2,' M'/5X,'ELEV. OF TANK TOP =',
8     F9.2,' M'//5X,'ELEV.',3X,'TANK AREA'/(F10.2,F10.2)/)
C      C = HFO/(QO*QO)
Z1 = -C*QTI*QTI
Q1 = QTI
C1 = G*AT/L
T = 0.0
ZMIN = Z1
ZMAX = Z1
QTUR1=QTI
WRITE (6,14)
14   FORMAT(7X,'T',9X,'Z',8X,'Q',8X,'QTUR'/6X,'(S)',
1           7X,'(M)',5X,'(M3/S)',4X,'(M3/S)')
15   KK = 0
WRITE(6,18) T,Z1,Q1,QTUR1
18   FORMAT(5F10.3)
30   T = T+DT
KK = KK+1
TT=T-TG
IF (TT) 110,112,112
110  QTUR2=QTI+(QTF-QTI)*(T/TG)

```

```

      GO TO 113
112  QTUR2=QTF
113  CONTINUE
      IF (T .GT. TSTOP) GO TO 400
      GO TO (120,150),METHOD

C
C   ITERATIVE MODIFIED EULER METHOD
C
120  JJ=0
      DQDT1=C1*(-Z1-C*Q1*ABS(Q1))
      CALL STA(Z1,AS)
      DZDT1 = (Q1-QTUR1)/AS
      Q2S = Q1 + DQDT1*DT
      Z2S = Z1 + DZDT1 *DT
130  DQDT2 = C1*(-Z2S - C*Q2S*ABS(Q2S))
      CALL STA(Z2S,AS)
      DZDT2 = (Q2S - QTUR2)/AS
      Q2 = Q1 + 0.5*DT*(DQDT1 + DQDT2)
      Z2 = Z1 + 0.5*DT*(DZDT1 + DZDT2)
      IF (ABS(Z2-Z2S).LE.TOLER) GO TO 200
      JJ=JJ+1
      Z2S=Z2
      Q2S=Q2
      IF (JJ.GT.40) GO TO 600
      GO TO 130

C
C   FOURTH-ORDER RUNGE-KUTTA METHOD
C
150  A11=C1*(-Z1-C*Q1*ABS(Q1))
      CALL STA(Z1,AS)
      B11=(Q1-QTUR1)/AS
      Q11=Q1+0.5*DT*A11
      Z11=Z1+0.5*DT*B11
      QTURM=0.5*(QTUR1+QTUR2)
      A21=C1*(-Z11-C*Q11*ABS(Q11))
      CALL STA(Z11,AS)
      B21=(Q11-QTURM)/AS
      Q21=Q1+0.5*DT*A21
      Z21=Z1+0.5*DT*B21
      A31=C1*(-Z21-C*Q21*ABS(Q21))
      CALL STA(Z21,AS)
      B31=(Q21-QTURM)/AS
      Q31=Q1+DT*A31
      Z31=Z1+DT*B31
      A41=C1*(-Z31-C*Q31*ABS(Q31))
      CALL STA(Z31,AS)
      B41=(Q31-QTUR2)/AS
      Q2=Q1+(A11+2.*A21+2.*A31+A41)*DT/6.
      Z2=Z1+(B11+2.*B21+2.*B31+B41)*DT/6.

200  Q1 = Q2
      Z1 = Z2
      QTUR1 = QTUR2
      IF (Z1 .GT. ZMAX) ZMAX = Z1
      IF (Z1 .LT. ZMIN) ZMIN = Z1
      IF (KK .EQ. IPRINT) GOTO 15
      GOTO 30
400  ZMAX=ZMAX+ELUR

```

```

ZMIN=ZMIN+ELUR
WRITE(6,450) ZMAX, ZMIN
450 FORMAT(5X, 'MAX. SURGE LEVEL = ',F9.2,' M'/
1      5X,'MIN. SURGE LEVEL =',F8.2,' M')
1F9.2/)
GO TO 700
600 WRITE(6,650) T,Z2S,Z2
650 FORMAT(10X,'ITERATIONS FAILED',3F10.2)
700 STOP
END
SUBROUTINE STA(Z,AS)
DIMENSION EL(5),ASUR(5)
COMMON /ST/N,EL,ASUR,ELUR,EINV,ETOP
EWS=Z+ELUR
IF (EWS.LT.EINV) GO TO 120
IF (EWS.GT.ETOP) GO TO 130
DO 100 J=1,N
IF (EWS.LT.EL(J)) GO TO 110
100 CONTINUE
110 AS=ASUR(J-1)
RETURN
120 WRITE(6,125)
125 FORMAT(5X, 'TANK IS DRAINED')
STOP
130 WRITE (6,135)
135 FORMAT(5X,'TANK IS OVERFLOWING')
STOP
RETURN
END

```

## E-2 Input Data

```

1,10,9.81,.1,80.,56.,112.,5.,523.,478.,550.
1964.,23.25,56.,1.22,2,478.,148.8,505.,148.8
*.001

```

## E-3 Program Output

```

ITERATIVE MODIFIED EULER METHOD
TOLERANCE FOR ITERATIONS = .0010 M

LENGTH = 1964.0 M

```

TUNNEL AREA = 23.25 M<sup>2</sup>  
 TUNNEL HEAD LOSS = 1.22 M FOR DISCHARGE = 56.00 M<sup>3</sup>/S  
 INITIAL TURBINE FLOW = 56.00 M<sup>3</sup>/S  
 FINAL TURBINE FLOW = 112.00 M<sup>3</sup>/S  
 GATE TIME = 5.00 S  
 COMPUTATIONAL TIME INTERVAL = .10 S  
 IPRINT = 10  
 UPSTREAM RESER. LEVEL = 523.00 M  
 TANK INVERT LEVEL = 478.00M  
 ELEV. OF TANK TOP = 550.00 M

| ELEV.  | TANK AREA |
|--------|-----------|
| 478.00 | 148.80    |

|        |        |
|--------|--------|
| 505.00 | 148.80 |
|--------|--------|

| T<br>(S) | Z<br>(M) | Q<br>(M <sup>3</sup> /S) | QTUR<br>(M <sup>3</sup> /S) |
|----------|----------|--------------------------|-----------------------------|
| .000     | -1.220   | 56.000                   | 56.000                      |
| 1.000    | -1.258   | 56.001                   | 67.200                      |
| 2.000    | -1.370   | 56.012                   | 78.400                      |
| 3.000    | -1.559   | 56.039                   | 89.600                      |
| 4.000    | -1.822   | 56.093                   | 100.800                     |
| 5.000    | -2.159   | 56.181                   | 112.000                     |
| 6.000    | -2.534   | 56.310                   | 112.000                     |
| 7.000    | -2.908   | 56.483                   | 112.000                     |
| 8.000    | -3.280   | 56.697                   | 112.000                     |
| 9.000    | -3.651   | 56.954                   | 112.000                     |
| 10.000   | -4.020   | 57.252                   | 112.000                     |
| 11.000   | -4.387   | 57.591                   | 112.000                     |
| 12.000   | -4.751   | 57.971                   | 112.000                     |
| 13.000   | -5.113   | 58.391                   | 112.000                     |
| 14.000   | -5.472   | 58.850                   | 112.000                     |
| 15.000   | -5.827   | 59.349                   | 112.000                     |
| 16.000   | -6.179   | 59.885                   | 112.000                     |
| 17.000   | -6.528   | 60.460                   | 112.000                     |
| 18.000   | -6.872   | 61.071                   | 112.000                     |
| 19.000   | -7.212   | 61.718                   | 112.000                     |
| 20.000   | -7.548   | 62.402                   | 112.000                     |
| 21.000   | -7.879   | 63.119                   | 112.000                     |
| 22.000   | -8.205   | 63.871                   | 112.000                     |
| 23.000   | -8.525   | 64.656                   | 112.000                     |
| 24.000   | -8.841   | 65.473                   | 112.000                     |
| 25.000   | -9.151   | 66.322                   | 112.000                     |
| 26.000   | -9.455   | 67.201                   | 112.000                     |
| 27.000   | -9.753   | 68.109                   | 112.000                     |
| 28.000   | -10.045  | 69.047                   | 112.000                     |
| 29.000   | -10.330  | 70.011                   | 112.000                     |
| 30.000   | -10.609  | 71.003                   | 112.000                     |
| 31.000   | -10.881  | 72.020                   | 112.000                     |
| 32.000   | -11.146  | 73.061                   | 112.000                     |
| 33.000   | -11.404  | 74.126                   | 112.000                     |
| 34.000   | -11.655  | 75.213                   | 112.000                     |
| 35.000   | -11.899  | 76.321                   | 112.000                     |
| 36.000   | -12.135  | 77.450                   | 112.000                     |
| 37.000   | -12.363  | 78.597                   | 112.000                     |
| 38.000   | -12.584  | 79.763                   | 112.000                     |
| 39.000   | -12.796  | 80.945                   | 112.000                     |
| 40.000   | -13.001  | 82.142                   | 112.000                     |
| 41.000   | -13.198  | 83.354                   | 112.000                     |
| 42.000   | -13.386  | 84.579                   | 112.000                     |

|        |         |         |         |
|--------|---------|---------|---------|
| 43.000 | -13.566 | 85.817  | 112.000 |
| 44.000 | -13.738 | 87.065  | 112.000 |
| 45.000 | -13.901 | 88.322  | 112.000 |
| 46.000 | -14.056 | 89.588  | 112.000 |
| 47.000 | -14.202 | 90.861  | 112.000 |
| 48.000 | -14.340 | 92.140  | 112.000 |
| 49.000 | -14.469 | 93.424  | 112.000 |
| 50.000 | -14.590 | 94.712  | 112.000 |
| 51.000 | -14.702 | 96.002  | 112.000 |
| 52.000 | -14.805 | 97.294  | 112.000 |
| 53.000 | -14.899 | 98.585  | 112.000 |
| 54.000 | -14.985 | 99.876  | 112.000 |
| 55.000 | -15.062 | 101.164 | 112.000 |
| 56.000 | -15.131 | 102.449 | 112.000 |
| 57.000 | -15.191 | 103.730 | 112.000 |
| 58.000 | -15.242 | 105.005 | 112.000 |
| 59.000 | -15.285 | 106.273 | 112.000 |
| 60.000 | -15.319 | 107.534 | 112.000 |
| 61.000 | -15.345 | 108.786 | 112.000 |
| 62.000 | -15.362 | 110.028 | 112.000 |
| 63.000 | -15.371 | 111.260 | 112.000 |
| 64.000 | -15.372 | 112.480 | 112.000 |
| 65.000 | -15.365 | 113.687 | 112.000 |
| 66.000 | -15.350 | 114.880 | 112.000 |
| 67.000 | -15.326 | 116.059 | 112.000 |
| 68.000 | -15.295 | 117.223 | 112.000 |
| 69.000 | -15.256 | 118.370 | 112.000 |
| 70.000 | -15.210 | 119.500 | 112.000 |
| 70.999 | -15.155 | 120.612 | 112.000 |
| 71.999 | -15.094 | 121.705 | 112.000 |
| 72.999 | -15.025 | 122.779 | 112.000 |
| 73.999 | -14.949 | 123.833 | 112.000 |
| 74.999 | -14.866 | 124.865 | 112.000 |
| 75.999 | -14.776 | 125.876 | 112.000 |
| 76.999 | -14.680 | 126.865 | 112.000 |
| 77.999 | -14.576 | 127.831 | 112.000 |
| 78.999 | -14.467 | 128.774 | 112.000 |
| 79.999 | -14.351 | 129.693 | 112.000 |

MAX. SURGE LEVEL = 521.78 M

MIN. SURGE LEVEL = 507.63 M

# F

---

## SI AND ENGLISH UNITS AND CONVERSION FACTORS

SI (Système Internationale) units for various physical quantities are listed in Section F-1, and the factors for converting them to the English units are presented in Section F-2.

### F-1 SI Units

| Physical Quantity          | Name of Unit | Symbol | Definition           |
|----------------------------|--------------|--------|----------------------|
| Length                     | Meter        | m      | —                    |
| Mass                       | Kilogram     | kg     | —                    |
| Force                      | Newton       | N      | $1 \text{ kg m/s}^2$ |
| Energy                     | Joule        | J      | $1 \text{ N m}$      |
| Pressure, stress           | Pascal       | Pa     | $1 \text{ N/m}^2$    |
| Power                      | Watt         | W      | $1 \text{ J/s}$      |
| Bulk modulus of elasticity | Pascal       | Pa     | $1 \text{ N/m}^2$    |

The multiples and fractions of the preceding units are denoted by the following letters:

|           |       |   |
|-----------|-------|---|
| $10^{-3}$ | milli | m |
| $10^{-1}$ | deci  | d |
| $10^3$    | kilo  | k |
| $10^6$    | mega  | M |
| $10^9$    | Giga  | G |

For example,  $2.1 \text{ GPa} = 2.1 \times 10^9 \text{ Pa}$ ;  $1.95 \text{ Gg m}^2 = 1.95 \times 10^6 \text{ kg m}^2$ .

## F-2 Conversion Factors

The conversion factors are listed in [Table F-1](#).

**Table F-1. Conversion Table**

| <b>Quantity</b>                | <b>To Convert</b>        |  |                          |
|--------------------------------|--------------------------|--|--------------------------|
|                                | <b>From SI unit</b>      | <b>To English unit</b>                 | <b>Multiply by</b>       |
| Acceleration                   | $\text{m}/\text{s}^2$    | $\text{ft}/\text{sec}^2$               | 3.28084                  |
| Area                           | $\text{m}^2$             | $\text{ft}^2$                          | 10.7639                  |
| Density                        | $\text{kg}/\text{m}^3$   | $\text{lb}/\text{ft}^3$                | $62.4278 \times 10^{-3}$ |
|                                | $\text{kg}/\text{m}^3$   | $\text{slug}/\text{ft}^3$              | $1.94032 \times 10^{-3}$ |
| Discharge                      | $\text{m}^3/\text{s}$    | $\text{ft}^3/\text{sec}$               | 35.3147                  |
|                                | $\text{m}^3/\text{s}$    | gal/min (U.S.)                         | $15.8503 \times 10^3$    |
|                                | $\text{m}^3/\text{s}$    | gal/min (Imperial)                     | $13.1981 \times 10^3$    |
| Force                          | N                        | $\text{lb}_f$                          | $224.809 \times 10^{-3}$ |
| Length                         | m                        | ft                                     | 3.28084                  |
| Mass                           | kg                       | lb                                     | 2.20462                  |
|                                | kg                       | slug                                   | $68.5218 \times 10^{-3}$ |
| Moment of inertia              | $\text{kg m}^2$          | $\text{lb}\cdot\text{ft}^2$            | 23.7304                  |
| Momentum (Angular)<br>(Linear) | $\text{kg m}^2/\text{s}$ | $\text{lb}\cdot\text{ft}^2/\text{sec}$ | 23.7304                  |
|                                | kg m/s                   | $\text{lb}\cdot\text{ft/sec}$          | 7.23301                  |
| Power                          | W                        | $\text{ft-lb}_f/\text{sec}$            | 0.737561                 |
|                                | W                        | hp                                     | $1.34102 \times 10^{-3}$ |
| Torque                         | Nm                       | $\text{lb}_f\cdot\text{ft}$            | $737.562 \times 10^{-3}$ |
| Velocity                       | m/s                      | ft/sec                                 | 3.28084                  |
|                                | m/s                      | mile/hr                                | 2.23694                  |
| Volume                         | $\text{m}^3$             | $\text{ft}^3$                          | 35.3147                  |
|                                | $\text{m}^3$             | $\text{yd}^3$                          | 1.30795                  |
|                                | $\text{m}^3$             | $\text{in.}^3$                         | $61.0237 \times 10^3$    |
| Specific weight                | $\text{N}/\text{m}^3$    | $\text{lb}_f/\text{ft}^3$              | $6.36587 \times 10^{-3}$ |
| Temperature                    | $^\circ\text{C}$         | $^\circ\text{F}$                       | 1.8; and add 32          |

## Author Index

- Abbott, H. F., 255, 322  
 Abbott, M. B., 55, 66, 110, 450,  
     451, 496  
 Abu Morshedi, 221  
 Albertson, M. L., 356, 373  
 Allievi, L., 6, 7, 29, 255, 260, 323,  
     352, 373, 385, 418  
 Almeida, A. B., 29, 236  
 Almeida, L., 7  
 Almeras, P., 219  
 Amein, M., 446, 465, 496  
 Amorocho, J., 477  
 Anderson, A., 5, 29, 33, 56, 60  
 Anderson, D. A., 451, 470, 473, 496  
 Anderson, S., 3, 5  
 Andrews, J. S., 356, 373  
 Angus, R. W., 352, 373  
 Araki, M., 219  
 AWWA, 422, 434  
 Axworthy, D., 61  
  
 Baasiri, M., 336, 343  
 Babcock, C. I., 479, 496  
 Bagwell, M. U., 241, 247, 248  
 Baker, A. J., 55, 60  
 Ballofet, A., 496  
 Ballofet, A. F., 496  
 Baltzer, R. A., 328, 332, 336, 343,  
     496  
 Banosiak, W., 325  
 Barlett, P. E., 152  
 Bates, C. G., 219  
 Baumeister, T., 60  
 Bechteler, W., 374  
 Bedue, A., 346  
 Bell, P. W. W., 150, 367, 373  
 Belonogoff, G., 111  
 Benet, F., 477, 482, 486, 497  
 Bergant, A., 56, 60, 63, 64  
 Bergeron, L., 7, 30, 54, 60, 255,  
     260, 323, 335, 343  
 Bernardinis, B. D., 330, 343  
  
 Binnie, A. M., 248  
 Blackwall, W. A., 261, 323  
 Blade, R. J., 325, 326  
 Blair, P., 219  
 Boari, M., 247  
 Boldy, A. P., 204, 207, 216  
 Bonin, C. C., 20–22, 30  
 Borga, A., 62  
 Borot, G., 352, 373  
 Bowering, R. J., 479, 499  
 Bradley, M. J., 375  
 Braun, E., 7, 30  
 Brebbia, C. A., 450, 500  
 Brebner, A., 479, 499  
 Brekke, H., 219  
 Brown, F. T., 113  
 Brown, J. M. B., 56, 63  
 Brown, R. J., 150, 336–341, 343  
 Brunner, B., 422, 434  
 Brunone, B., 56, 60, 421, 422, 434  
 Bryce, J. B., 411, 418  
 Bughazem, M., 56, 60  
 Bulirsch, R., 388, 418  
 Bullough, J. B. B., 388, 418  
 Burnett, R. R., 247  
 Butler, H. L., 483, 501  
 Byrne, R. M., 152  
  
 Cabrera, E., 30  
 Calame, J., 477, 497  
 Camichel, C., 7, 30, 250, 260, 301,  
     304, 323  
 Cardle, J. A., 501  
 Carpenter, R. C., 6, 30  
 Carsten, M. R., 56  
 Carstens, H. R., 345  
 Carstens, M. R., 60  
 Cass, D. E., 150, 479, 497, 500  
 Caves, J. L., 235  
 Chaudhry, M. H., 7, 19, 30, 31,  
     55, 56, 60, 61, 63, 85, 87,  
     90, 92, 101, 104, 111, 112,

- 142, 143, 150, 153, 161,  
170, 171, 192, 216–218,  
222, 234, 235, 242, 247,  
262, 268, 271, 272, 301,  
323–325, 367, 368, 373–  
375, 386, 388, 392, 393,  
395, 403, 405, 418, 422,  
428, 434, 454, 463–465,  
470, 473, 475, 476, 479,  
484, 490, 497, 498, 500,  
501
- Chen, C. L., 497
- Chen, H., 434
- Chiang, W. L., 484, 497
- Chow, V. T., 438, 497
- Chung, T. J., 55
- Cole, E., 496
- Collatz, L., 83, 111
- Combes, G., 352, 373
- Concordia, C., 219
- Constantinescu, G., 7, 30
- Contractor, D. N., 113
- Cooley, R. L., 450, 497
- Cooper, P., 152
- Courant, R., 461, 462, 469, 472–  
474, 484, 490, 497
- Covas, D., 62, 422, 434
- Crawford, C. C., 351, 352, 373
- Crowe, C. T., 36, 41, 62
- Cunge, J. A., 445, 449–451, 454,  
461, 465, 475, 477, 482,  
486, 497, 498, 500
- Cunningham, W. J., 392, 395, 418
- Curtis, E. M., 150
- D’Azzo, J. J., 170, 171, 217
- D’Souza, A. F., 325
- Daigo, H., 117, 150
- Daily, J. W., 346
- Das, M. M., 479, 498
- Davidson, D. D., 479, 484, 498
- Davis, K., 346
- Davison, B., 234
- De Haller, P., 346
- De Saint-Venant, B., 445, 449, 451,  
455, 462, 468, 476, 477,  
479, 498
- De Salis, M. H. F., 422, 434
- De Vries, A. H., 235, 345
- DeClemente, T. J., 222, 224, 235
- Defazio, F. G., 454, 500
- Den Hartog, J. P., 255, 323
- Dennis, N. G., 219
- Deriaz, P., 325
- Derkacz, A., 325
- Dijkman, H. K. M., 336, 343
- Divoky, D., 497
- Donelson, J., 326
- Donsky, B., 150, 152
- Dorn, W. S., 175, 218, 272, 301,  
324, 388, 419, 460, 500
- Dresser, T., 248
- Dressler, R. F., 474, 498
- Driels, M., 366, 367, 373
- Drioli, C., 477, 498
- Dronkers, J. J., 474, 498
- Due, J., 345
- Duncan, J. W. L., 419
- Eagleson, P. S., 62, 112
- El-Fitiany, F. A., 518, 519, 525
- Elder, R. A., 411, 418
- Enever, K. J., 217
- Engler, M. L., 352, 373
- Euler, L., 4, 5, 30
- Evangelisti, G., 49, 55, 61, 66, 102,  
111, 113, 242, 247, 325,  
355, 358, 372, 373
- Evans, W. E., 351, 352, 373
- Eydoux, D., 30, 323
- Föllmer, B., 35, 61
- Faibes, O. N., 236
- Fanelli, M., 334, 343
- Fang, C. S., 446, 496
- Fashbaugh, R. H., 255, 324
- Favre, H., 316, 324, 477, 486, 498,  
500
- Federici, G., 343

- Fennema, R. J., 454, 470, 473, 475, 476, 498  
 Ferrante, M., 434  
 Fett, G. H., 220  
 Fischer, S. G., 108, 111, 179, 217  
 Fishburn J. D., 151  
 Flammer, G. H., 64  
 Flannery, B. P., 324  
 Flesch, G., 151  
 Florio, P. J., 325  
 Forrest, J. A., 373, 418  
 Forstad, F., 479, 498  
 Forster, J. W., 367, 373, 408–410, 412, 418  
 Fowler, J. E., 418  
 Fox, J. A., 7, 30, 113  
 Frank, J., 387, 392, 418  
 Fread, D. L., 498  
 Free, J. G., 153  
 Friedrichs, K., 497  
 Frizell, J. P., 6, 30  
 Gardel, A., 7, 30  
 Gardner, P. E. J., 385, 418  
 Gariel, M., 30, 323  
 Gear, C. W., 418  
 Ghidaoui, M. S., 56, 61, 64  
 Gibson, N. R., 7, 30, 31  
 Gibson, W. L., 255, 322, 324  
 Goda, K., 217  
 Goldberg, D. E., 88, 111  
 Goldwag, E., 219  
 Golia, U. M., 60  
 Goodykootz, J., 325  
 Gordon, J. L., 191, 193, 211, 217  
 Gottlieb, D., 55  
 Gould, B. W., 7, 33  
 Gragg, W. B., 388, 418  
 Gray, C. A. M., 66, 111  
 Graze, H. R., 354, 373  
 Greco, M., 60  
 Green, J. E., 248  
 Gromeka, I. S., 6, 31  
 Guerrini, P., 247  
 Guymer, G., 53, 63  
 Haghghi, A., 422, 434  
 Hagibara, S., 192, 217  
 Hagler, T. W., 345  
 Halliwell, A. R., 50, 52, 61  
 Hamill, F., 141, 150  
 Hammitt, F. G., 346  
 Harbaugh, T. E., 498  
 Hassan, J. M., 217  
 Helmholtz, H. L., 5, 322  
 Henderson, F. M., 445, 449, 450, 463, 498  
 Henson, D. A., 113  
 Hill, E. F., 192, 218  
 Hirose, M., 61  
 Holley, E. R., 325  
 Holley, F. M., 498  
 Hollingshead, D. F., 227, 235  
 Holloway, M. B., 55, 61, 85, 101, 111, 242, 247  
 Hooker, D. G., 234, 235  
 Houpis, C. H., 170, 171, 217  
 Hovanessian, S. A., 261, 324  
 Hovey, L. M., 168, 192, 194–196, 217  
 Hsu, S. T., 364, 374  
 Humbel, M., 25  
 Hussaini, M. Y., 55, 60, 61, 92, 111, 234, 470, 497  
 Hwang, K., 56, 63  
 Hyett, B. J., 472, 502  
 Hyman, M. A., 112  
 Ikeo, S., 366, 367, 373  
 Ince, S., 32  
 Ippen, A. T., 62, 112  
 Isobe, K., 217  
 Iwakiri, T., 235  
 Jacob, M. C., 151  
 Jacobson, R. S., 374  
 Jaeger, C., 7, 20, 31, 152, 153, 250, 251, 254, 298, 301, 324, 326, 387, 392, 408, 419, 477, 498  
 Jameson, A., 472, 499

- Jankowska, E., 325  
 Jenkner, W. R., 53, 61  
 Jensen, P., 219  
 Jeppson, R. W., 64  
 Jiang, Y., 422, 434  
 Jimenez, O., 88  
 Johnson, G., 373  
 Johnson, R. D., 409, 419, 443, 499  
 Johnson, S. P., 238, 241, 247  
 Jolas, C., 235  
 Jones, W. G., 222, 235  
 Joseph, I., 141, 150, 343  
 Joukowski, N. E., 6, 7, 31  
 Joukowsky, N., 61  
 Kachadoorian, R., 479, 499  
 Kaczmarek, A., 325  
 Kadak, A., 373  
 Kagawa, T., 56, 61  
 Kalkwijk, J. P. Th., 334, 343, 345  
 Kamath, P. S., 151  
 Kamphuis, J. W., 468, 479, 499  
 Kanupka, G. J., 151  
 Kao, K. H., 468, 479, 490, 497, 499  
 Kaplan, M., 88, 110, 111, 238, 247,  
     248  
 Kaplan, S., 112  
 Karam, J. T., 61  
 Karney, B., 7, 32  
 Kasahara, E., 329, 345, 346  
 Kassem, A. A., 324, 434  
 Katopodes, N. D., 450, 475, 499,  
     501  
 Katto, Y., 326  
 Keller, A., 336, 343  
 Kennedy, J. F., 153, 525  
 Kennedy, W. G., 151  
 Kennison, H. F., 61  
 Kephart, J. T., 346  
 Kerensky, G., 20, 31  
 Kerr, S. L., 7, 32, 248, 374  
 Kersten, R. D., 248  
 Kiersch, G. A., 479, 499  
 Kinno, H., 153, 374, 525  
 Kirchmayer, L. K., 219  
 Kitagawa, A., 61  
 Kittredge, C. P., 151  
 Klabukov, V. M., 217  
 Knapp, R. T., 122, 151, 346  
 Kobori, T., 49, 151, 343, 366, 367,  
     373  
 Koelle, E., 7, 29, 31, 153  
 Kohara, I., 235  
 Kolyshkin, A. A., 61  
 Kondo, M., 151  
 Korteweg, D. J., 5, 31  
 Koutitas, C. G., 484, 499  
 Kovats, A., 153  
 Kranenburg, C., 334, 336, 343, 345  
 Krivehenko, G. I., 159, 217  
 Krueger, R. E., 191, 210, 211, 218,  
     395, 407, 419  
 Kuwabara, T., 219  
 Löwy, R., 7, 31  
 Lackie, F. A., 262, 268, 272, 324  
 Lagrange, I. L., 5, 31  
 Lai, C., 55, 63, 66, 112, 496  
 Lambert, M. F., 63, 64, 434  
 Langley, P., 225, 227, 235  
 Laplace, P. S., 31  
 Larsen, J. K., 324  
 Larsen, P. S., 64, 345  
 Lathi, B. P., 170, 171, 218, 261,  
     276, 324  
 Law, L., 479, 499  
 Lax, P. D., 229, 235, 499, 500  
 Lee, I., 61  
 Leendertse, J. J., 500  
 Lein, G., 219  
 Leonard, R. G., 61  
 Lescovich, J. E., 355, 374  
 Lesmez, M., 236  
 Leung, K. S., 501  
 Levshakoff, M., 237  
 Lewis, W., 326  
 Lewy, H., 497  
 Li, J., 434  
 Li, W. H., 346, 392, 419  
 Liggett, J. A., 55, 62, 434, 500

- Lindros, E., 374  
 Lindvall, G. K. E., 62  
 Linton, P., 153  
 Lister, M., 55, 62, 66, 111  
 Loureiro, D., 62  
 Loureiro, D., 57, 62  
 Ludwig, M., 238, 241, 242, 246, 247  
 Lundberg, G. A., 241, 245, 247,  
     385, 419  
 Lundgren, C. W., 374  
 Lupton, H. R., 346  
 MacCormack, R. W., 470, 473,  
     490, 500  
 Mahmood, K., 445, 451, 454, 461,  
     476, 479, 500  
 Marchal, M., 120, 151  
 Marey, M., 5, 31  
 Marris, A. W., 392, 395, 419  
 Martin, C. S., 118–121, 151, 204,  
     207, 218, 222, 224, 226–  
     229, 235, 236, 336, 344,  
     345, 356, 374, 419, 454,  
     475, 476, 500  
 Martinez, F., 30  
 Massari, C., 434  
 Matthias, F. T., 419  
 Mays, L. W., 92  
 McCaig, I. W., 255, 322, 324  
 McCartney, B. L., 479, 484, 498  
 McCracken, D. D., 175, 218, 272,  
     301, 324, 388, 419, 460,  
     500  
 McCulloch, D. S., 479, 500  
 McInnis, D., 61  
 Meeks, D. R., 375  
 Menabrea, L. F., 5, 31  
 Meniconi, S., 422, 434  
 Mercer, A. G., 479, 497, 500  
 Meyer-Peter, E., 477, 500  
 Michaud, J., 5, 31  
 Miller, D. J., 479, 500  
 Miyashiro, H., 113, 137, 151, 153,  
     343  
 Moen, A. I., 5  
 Mohapatra, P. K., 317, 324, 422,  
     424, 434  
 Moin, S. A., 450, 497  
 Molloy, C. T., 262, 274, 324  
 Moloo, J., 317, 324, 434  
 Monge, G., 5, 31  
 Morton, K. W., 451, 461, 501  
 Moshkov, L. V., 326  
 Mosonyi, E., 388, 419  
 Mueller, W. K., 325  
 Naghash, M., 236, 345  
 Newey, R. A., 219  
 Newton, I., 3, 32  
 Noda, E., 479, 500  
 O'Brien, G. G., 84, 112  
 Ogawa, Y., 235  
 Ohashi, H., 117, 150–152  
 OHesen, J. T., 316, 324  
 Oldenburger, R., 219, 325, 326  
 Oldham, D. J., 422, 434  
 Olsen, R. M., 332, 344  
 Olson, D. J., 151  
 Olufsen, M. S., 324  
 Orszag, S. A., 55  
 Oulirsch, R., 420  
 Padmanabhan, M., 344  
 Papadakis, C. N., 227, 235, 364,  
     374  
 Parmakian, J., 7, 32, 52–54, 62,  
     107, 112, 116, 120, 151,  
     153, 182, 183, 211, 218,  
     255, 324, 335, 344, 375,  
     385, 386, 419, 525  
 Parmley, L. J., 149, 151  
 Parnicky, P., 497  
 Parzany, K., 219  
 Patridge, P. W., 450, 500  
 Paynter, H. M., 152, 153, 192, 204,  
     218, 250, 262, 324, 388,  
     392, 401, 419  
 Pearsall, I. S., 49, 62, 332, 341, 344,  
     345, 375

- Perkins, F. E., 55, 62, 66, 67, 112, 159, 218  
 Perko, H. D., 336, 344  
 Pestel, E. C., 262, 268, 272, 324  
 Petry, B., 219  
 Pezzinga, G., 56, 62  
 Phillips, R. D., 241, 247  
 Pickford, J., 7, 32, 62, 388, 420  
 Pipes, L. A., 324  
 Pletcher, R. H., 496  
 Ponce, V. M., 450, 500  
 Ponikowski, P., 325  
 Porada, A., 325  
 Portfors, E. A., 25, 87, 104, 111, 112, 161, 217, 218, 367, 368, 373, 374  
 Preissmann, A., 465, 468, 477, 479, 500  
 Press, W. H., 317, 324  
 Price, R. K., 500  
 Prins, J. E., 479, 501  
 Pugh, C. A., 479, 501  
 Pulling, W. T., 20, 32  
 Rösl, G., 300, 325  
 Rachford, H. H., 88, 112  
 Rahm, S. L., 62, 411, 420  
 Raiteri, E., 332, 334, 344  
 Rajar, R., 501  
 Ralston, A., 112  
 Ramos, H., 56, 62, 422, 434  
 Raney, D. C., 483, 501  
 Rao, P. V., 345  
 Rath, H. J., 334, 344  
 Rayleigh, J. W. S., 5, 32  
 Reali, M., 334, 343  
 Reczuch, K., 317, 325  
 Reddy, P. H., 56, 62, 90, 112  
 Reed, M. B., 262, 325  
 Resal, H., 5, 32  
 Rich, G. R., 7, 32, 54, 62, 153, 388, 420  
 Richards, R. T., 225, 235, 346  
 Richtmyer, R. D., 451, 461, 475, 501  
 Riemann, B., 5, 32  
 Ripken, J. F., 332, 344  
 Ritter, A., 474, 501  
 Ritter, H. K., 153  
 Roark, R. J., 62  
 Robbie, J. F., 388, 418  
 Roberson, J. A., 36, 41, 62  
 Roberts, W. J., 326  
 Rocard, Y., 20, 32, 255, 262, 325  
 Rogers, D. C., 150  
 Rohling, T. A., 153  
 Roller, J. E., 56, 60  
 Rossi, R., 247  
 Rouse, H., 32, 439, 501  
 Ruus, E., 7, 32, 192, 217, 352, 366, 367, 374, 375, 392, 393, 395, 418, 420, 506, 511, 515, 518, 519, 525  
 Sabbah, M. A., 418  
 Safwat, H. H., 62, 344  
 Saito, T., 255, 325  
 Sakkas, J. G., 475, 501  
 Salmon, G. M., 373  
 Sato, S., 63  
 Sattar, A. M., 422, 428, 434  
 Scarborough, E. C., 225, 235  
 Schübert, J., 373  
 Schüller, J., 388, 392, 418  
 Schamber, D. R., 499, 501  
 Schleif, F. R., 219  
 Schmidt, W., 499  
 Schnyder, O., 7, 32, 153  
 Schohl, G. A., 56  
 Schohl, G. A., 62  
 Schulte, A. M., 463, 501  
 Serkiz, A. W., 20, 32  
 Sharp, B. B., 7, 32, 329, 335, 344  
 Sheer, T. J., 225, 227, 236  
 Shiers, P. F., 236  
 Shiraishi, T., 235  
 Siccardi, F., 236, 332, 334, 343, 344  
 Sideriades, L., 392, 395, 420  
 Siemons, J., 336, 344  
 Silbeman, E., 332, 344

- Silva-Araya, W. F., 56, 62, 63, 90, 112  
 Simon, D. B., 450  
 Simpson, A. R., 60, 63, 64, 434  
 Smith, G. D., 55, 63, 82, 83, 112  
 Song, C. S. S., 477, 501  
 Sprecher, J., 152  
 Stary, H. C., 319, 325  
 Stein, T., 190, 192, 218, 219  
 Stepanoff, A. J., 116, 117, 120, 121, 152, 344  
 Stepanoff, A. M., 338  
 Stephens, M., 64  
 Stephenson, D., 148, 152  
 Stoer, J., 388, 418, 420  
 Stoker, J. J., 450, 451, 474, 501  
 Stoner, M. A., 112  
 Streeter, V. L., 7, 9, 32, 34, 46, 49, 52, 55, 63, 64, 66, 112, 113, 152, 159, 218, 238, 247, 248, 255, 324, 325, 345, 365-367, 374  
 Strelkoff, T., 445, 450, 454, 461, 475, 477, 499, 501  
 Strowger, E. B., 7, 32, 375  
 Stuckenbruck, S., 47, 63  
 Sundquist, M. J., 88, 110, 112, 336, 345  
 Suter, P., 151, 152  
 Suzuki, K., 63  
 Suzuki, T., 56  
 Svee, R., 401, 420  
 Swaffield, J. A., 63, 335, 345  
 Swaminathan, K. V., 63  
 Swanson, W. M., 122, 152, 338, 345  
 Swift, W. L., 151  
 Tadaya, I., 326  
 Takenaka, T., 61  
 Taketomi, T., 63  
 Tanahashi, T., 329, 345, 346  
 Tannehill, J. C., 496  
 Techo, R., 248  
 Tedrow, A. C., 62, 112  
 Telichowski, A., 325  
 Tenkolsky, S. A., 324  
 Terzidis, G., 475, 501  
 Thoma, D., 151, 152, 392, 420  
 Thomas, G., 122  
 Thomson, W. T., 250, 325  
 Thorley, A. R. D., 53, 54, 63, 262  
 Thorne, D. H., 192, 218  
 Tijsseling, A. S., 3, 5, 33  
 Timoshenko, S., 41, 63  
 Todd, D., 88, 112  
 Tognola, S., 152  
 Tournès, D., 65, 112  
 Travers, F. J., 419  
 Trenkle, C. J., 20, 22, 24, 33  
 Trikha, A. K., 56, 63  
 Tsukamoto, H., 117, 152  
 Tucker, D. M., 374  
 Tullis, J. P., 7, 33, 336, 343  
 Turkel, E., 499  
 Twyman, J. W. R., 54, 63  
 Vardy, A. B., 63  
 Vardy, A. E., 56, 88, 110, 112  
 Vasiliev, O. F., 465, 501  
 Vaughan, D. R., 220  
 Vellerling, W. T., 324  
 Verner, J. H., 420  
 Verwey, A., 496, 498  
 Vitkovsky, J. P., 56, 60, 63, 64, 434  
 Von Neumann, 84, 85, 468, 473  
 Vreugdenhil, C. B., 343, 345  
 Vreughenhill, C. B., 336  
 Wahanik, R. J., 235, 236  
 Walker, R. A., 411, 418  
 Waller, E. J., 248, 262, 325  
 Walmsley, N., 204, 216  
 Walsh, J. P., 346  
 Wang, X., 422, 434  
 Warming, R. F., 472, 502  
 Watters, G. Z., 7, 33, 53, 64  
 Webb, K. A., 225, 235  
 Webb, T., 7, 33  
 Weber, W., 5, 33  
 Wegner, M., 465, 477, 497

- Weil, G. J., 422, 435  
Wendroff, B., 229, 235, 500  
Weng, C., 326  
Wentworth, R. C., 111  
Weston, E. B., 6, 33  
Weyler, M. E., 64, 329, 332, 336, 345  
White, F. M., 64  
Whitehouse, J. C., 151  
Whiteman, K. J., 345, 375  
Whitham, G. B., 474, 502  
Widmann, R., 375  
Wiegel, R. L., 479, 498, 502  
Wier, W., 497  
Wiggert, D. C., 47, 63, 88, 110, 112, 222, 224, 226–229, 235, 236, 336, 344, 345, 477, 502  
Wiley, H. S., 112  
Winks, R. W., 152  
Winn, C. B., 373  
Wood, A. B., 332, 345  
Wood, D. J., 375  
Wood, F. M., 3, 5, 7, 33, 54, 64  
Woolhiser, D. A., 500  
Wostl, W. J., 248  
Wozniak, L., 204, 219, 220  
Wu, H., 514, 525  
Wylie, C. R., 40, 46, 52, 55, 64, 251, 276, 285, 289, 325  
Wylie, E. B., 7, 32, 34, 64, 71, 85, 88, 111–113, 152, 236, 238, 247, 248, 262, 268, 269, 301, 325, 336, 345, 367  
Yen, B. C., 445, 502  
Yevjevich, V., 55, 60, 92, 111, 445, 450, 451, 454, 461, 476, 479, 500  
Yokota, H., 217  
Yokoyama, S., 343  
Young, G. A. J., 374  
Young, T., 5, 34  
Yow, W., 88, 113, 236  
Zeller, H., 35, 61  
Zhao, M., 56, 61, 64  
Zielke, W., 56, 64, 228, 236, 300, 325, 336, 343, 344  
Zolotov, L. A., 217  
Zovne, J. J., 475, 476, 500

# Subject Index

- Accidents, 20
- Actuator, 172
- Adenosin, 317
- Adiabatic process, 5, 339, 353, 387
- Air cavity, 339–341
- Air chamber, 143, 245, 337, 351, 353, 372, 379
  - boundary conditions for, 352
  - charts for, 506, 507, 516, 517
  - point matrices, 322
- Air compressor, 351
- air content, 49
- Air pocket, 339
  - air pocket, 234
- Air release, 228, 229
- Air valve, 132, 142, 147, 234, 255, 337, 355, 366
  - boundary conditions for, 362, 372
  - combination, 362
- Air, entrapped, 228, 232, 242, 337, 356, 364, 374
  - boundary conditions for, 232
- Air-water mixture, 49
- Allievi's constant, 7
- Allievi's parameter, 212, 260
- Amplitude, 5, 166, 186, 238, 240, 242, 250, 256, 257, 260, 261, 277, 289, 290, 298, 301, 302, 307, 314, 321, 322, 378, 383, 389
- Angio-plasty, 316
- Anti-resonance, 385
- Antinode, 256, 298, 299
- Antiresonance device, 319–321
- Appalachia tunnel, 411
- Area, Thoma, 392, 398, 401, 408
- Arequipa Power Plant, 25
- Arithmetical method, 388
- Artery, 316
- Atherosclerosis, 318
- Attenuation, 86, 87, 100, 240
- Automatic-control, 244
- Axial stress, 41
- Azambuja Pump Station, 20, 25
- Backfitting, 223
- Barometric pressure head, 354, 365
  - barometric pressure head, 508
- Bersimiss II Power Plant, 255
- Big Creek No. 3 Hydropower Plant, 20, 22
- Block diagram, 171, 263, 266
  - for a permanent-droop governor, 171
  - for a proportional-integral-derivative (PID) governor, 214
  - for simple governor, 170
  - of branch system, 280
  - of dashpot governor, 172
  - of parallel system, 274
- Booster pumping station, 139, 144
- Bore, 19, 55, 438, 440, 444, 450, 451, 470, 473, 474, 476, 477
- Boundary conditions
  - for air chamber, 352, 371
  - for air inlet valve, 362, 372
  - for branching junction, 80
  - for condenser, 230
  - for cooling water system, 230
  - for dead end, 77
  - for downstream reservoir, 76, 457
  - for entrapped air, 232
  - for Francis turbine, 81, 110, 161, 163, 176, 214
  - for junction of three channels, 468, 489
  - for junction of two channels, 457
  - for open channels, 456

- for pressure regulating valve, 356
- and Francis turbine, 368
- and pump, 356
- for pumped-storage schemes, 201
- for pumps, 79, 109, 122, 127
  - parallel, 133
  - series, 137
- for series junction, 79
- for surge tanks, 349
- for upstream reservoir, 74, 456, 457
- for valve, 356
  - at intermediate location, 109
- turbine, 162
- Boyle's law, 5
- Branch channels, 468
- Branch lines, 280
- Branch, with dead end, 280
  - with oscillating valve, 283
  - with reservoir, 281
- Bubbles, 228, 328–330, 332, 335
- Bulk modulus of elasticity, 9, 10, 41, 49, 50, 244, 333
- Bypass valve, 245, 255, 319, 321
- Canals, 3, 4, 20, 239, 477
  - navigation, 440
  - power, 19, 438
- Capacitances, 230
- Cardiovascular system, 316
- Cavitated flow, 328–330, 335
- Cavitation, transient, 327–329, 335, 336
- Cavity, 328
- Cayley-Hamilton theorem, 268
- Characteristic curves, 109, 122, 159, 162, 450–453
- Characteristic data, 120
- Characteristic equations, 66, 77, 78, 95, 100, 232, 233, 339, 362, 451, 452, 456, 467, 472
- Characteristic grid, 72
- Characteristic impedance, 269, 270
- Characteristic lines, 67, 68, 84
- Characteristic method. See Method of characteristics, 65
- Characteristic roots, 394
- Chattering of valves, 19
- Check valve, 142, 143, 148, 149, 246, 247, 255, 351, 355, 356, 371, 507
- Chezy's formula, 448
- Chute-des-Passes Hydroelectric plant, 378, 410, 411
- Closed surge tank, 378, 379, 385, 386, 416
  - Stability, 401
- Coefficient of discharge, 29, 76, 277, 360, 366, 385
- Column separation, 2, 117, 143–145, 147, 148, 227, 246, 327–329, 335–337, 339
- Column vector, 263, 264
- Combine and once-through recirculating system, 222
- Compatibility equations, 67
- Complex variable, 251, 300, 302
- Computational procedure, 95, 367, 450
- Computer
  - analog, 192, 388, 392
  - digital, 120, 388
- Condenser, 222, 223, 225, 227
  - boundary condition for, 222
- Condenser tubes, 222, 225
- Conduit, 19
  - closed, 19, 36, 45
  - elastic, 47
  - inlet, 225
  - noncircular, 53
  - rigid, 50
  - thick-walled, 50
  - thin-walled, 52
- Conservation of mass, 36, 39
- Conservation of momentum, 36, 448
- Consistency, 83

- Continuity equation, 5, 39, 42, 45, 54, 77, 78, 88, 127, 133, 232, 242, 261, 267, 277, 335, 339, 350, 353, 360, 364, 368, 379, 382, 383, 385, 387, 440, 443, 445, 446, 478
- Control device, 20, 73, 143–145, 183, 238, 336, 348, 366, 505
- Control gate, 440, 457
- Control surface, 36–39
- Control system, 171, 255
- Control valves, 241, 366
- Control volume, 36–40, 44, 440, 442, 445, 446, 448 approach, 36
- Convective acceleration, 48
- Convergence of finite difference scheme, 83
- Conversion factors, SI and English units, 555, 556
- Coolant, 222
- Cooling pond, 222–225
- Cooling tower, 222–225
- Cooling water, 222 once-through, 223 recirculating, 223 systems, 143, 221, 222, 224, 225, 227, 228
- Courant number, 84
- Courant stability condition, 84, 88, 181, 229, 230, 242, 462, 473, 474, 484
- Cushioning stroke, 183, 191, 211
- Dam failure, 474
- Damping, 167, 168, 171, 229, 335, 396, 405
- Darcy-Weisbach friction equation, 49, 507
- Darcy-Weisbach friction factor, 45, 49, 267, 503
- Dashpot, 149, 168, 170, 174, 356 saturation limit, 172
- spring, 170 time constant, 168, 172
- Datum, 48
- Dead band, 192
- Dead end, 356 boundary conditions for, 76
- Degree of freedom, 252, 256
- Delay time, 356
- Density, 8–11, 47, 50 of common liquids, 54
- Design charts, 503
- Design criteria, 116 for penstock, 182, 407 for pipelines, 116, 142
- Dewatering and filling, 228
- Differential equation, 168 first-order partial, 46 hyperbolic partial, 46, 54, 83 ordinary, 19, 67, 252, 253, 387, 463 partial, 4, 5, 19, 36, 67, 82, 83, 253, 261, 450, 472 third-order, 194
- Differential orifice, 351
- Differential surge tank, 384, 385, 408
- Diffuser, 121, 222, 224, 225, 227, 228, 413
- Diffusive scheme, 454, 456, 461, 472, 475
- Discharge coefficient of, 29, 76, 277, 360, 366, 385 fluctuating, 286, 288 instantaneous, 250 mean, 250, 276, 279
- Discharge fluctuation, 291, 314
- Discharge line, 245, 254, 337
- Discharge manifold, 129, 133
- Discharge valve, 116, 125, 132, 133, 147, 225, 360
- Discretization error, 82
- Dispersion, 86, 87, 100
- Dissipative error, 472
- Dissolved gases, 49

- Distal pressure, 317
- Distributed system, 19, 253, 270, 271, 321
- Distributing valve, 167, 172, 174
- Downstream boundary, 68, 339, 456
- Downsurge, 409, 414, 506–508, 511
- Draft tube, 158, 159, 181, 191, 211, 216, 414
- Drainage, surge tank, 409
- Driva power plant, 386, 403
- Dynamic equation, 5, 6, 36, 267, 336, 381, 383, 385–388, 417, 448, 478, 487, 496
- Efficiency, 55, 79, 117, 126, 159, 165, 337, 390, 397, 408, 417
- Eigen values, 46, 254
- Elastic
  - conduit, 39, 42, 47, 50, 332
  - Energy, 11
  - linearly, 41
  - properties, 49, 50, 228
- Elasticity, 5
  - bulk modulus of, 9, 10, 41, 49, 50
  - mechanical, 7
  - Young's modulus of, 50, 52, 53, 230, 333, 334
- Elm Point levee, 437
- Energy
  - dissipation, 116, 118, 256, 259, 330, 335
  - elastic, 11
  - grade line, 448
  - kinetic, 3, 11
- Energy equation, 77, 79, 459, 463, 464
- Entrained gases, 86, 341
- Entrance losses, 73, 74
- Equation of motion, 5, 36
- Equilibrium point, 394
- Equivalent pipe, 228, 230, 503, 504
- Equivalent thickness, 52
- Exact solution, 82, 83, 465
- Exciter, 254, 285, 286, 299
- Exit losses, 75
- Expansion joint, 41, 51, 52, 59
- Experience curves, governing, 191
- Explicit finite-difference method, 92, 100, 229, 230, 438, 454, 455
  - second order, 470
- Exponential formula, 49
- Extensive property, 20, 36, 43
- External constraints, 49
- Extrapolation, 124, 141, 176
  - linear, 124
  - parabolic, 163, 176
- Factor of safety, 142, 143, 182, 183, 238, 245, 348
- Fast Fourier Transform, 317
- Favre's waves, 477, 486
- Feedback, 171, 174
- Field matrix, 264–270, 425
  - for conduit having variable characteristics, 272
  - for parallel loops, 274
  - for single conduits, 267, 269
- Field test, 304, 338
- Finite difference form, 48
  - backward, 470
  - forward, 470
- Finite difference method, 54, 55, 65, 66, 92, 98, 100, 229, 230, 438, 450, 451, 454, 465, 473, 476, 484
  - convergence, 82, 83
- First order approximations, 69, 70, 85, 242, 243
- Flood, 88, 438–440
  - wave, 19
- Flow
  - cavitating, 328–330, 335
  - combined free-surface pressurized, 19, 477, 479
  - free-surface, 158, 451, 454, 465, 472, 479

- laminar, 268
- nonuniform, 2, 7
- one-dimensional, 38, 39, 438, 445, 476
- periodic, 2, 3, 250, 256, 476
- steady, 2, 3, 10, 11, 45, 47, 67, 76, 108, 414, 438, 440
- steady-oscillatory, 2, 3, 250, 254, 256, 257, 261, 262, 266, 310
- subcritical, 444
- supercritical, 444, 476
- transient, 2, 3, 19, 35, 36, 45, 66, 76, 179, 271, 438, 445, 473
  - optimal control of, 348, 366
- turbulent, 2, 267, 268
- two-phase, 229, 242, 334
- uniform, 2, 7
- unsteady, 2, 8, 47, 261, 438, 440, 465
- unsteady, nonuniform, 47
- varied
  - gradually, 19, 438, 463, 464, 474
  - rapidly, 438
- Flow velocity, 2, 3, 6, 11, 15, 36, 38, 45, 48, 229, 238, 239, 260, 332, 348, 352, 355, 356, 438–440, 442, 444, 453, 473, 504
- Flowchart
  - for boundary for Francis turbine, 176
  - for boundary for pump, 130
  - for pump-pressure regulating valve, 362
  - for series piping system, 103
- Flowmeter
  - leading-edge, 108, 179
- Fluid
  - compressibility, 49, 228, 230, 252, 256, 334
  - compressible, 5, 10, 39, 42, 47, 48
  - density, 8–11, 47, 50, 54, 244, 262, 332, 333, 366, 440
  - incompressible, 5, 6, 48, 332, 379
  - pseudo, 228, 229
- Flyballs, 169
- Flywheel, 148, 337
- Focus, 394
- Forcing boundary, 283, 285
- Forcing function, 254, 256, 261, 277, 283–286, 291, 292, 295, 299, 307
- fluctuating discharge, 286, 288
- fluctuating pressure head, 286, 307
- oscillating valve, 276, 277, 279, 283, 284, 286, 290–292, 296, 301, 307, 314
- Fourier analysis, 261, 276, 285, 289, 290, 292
- Francis turbine, 81, 159, 161, 179, 204, 255, 356, 368
- boundary conditions for, 81, 110, 161, 163, 176, 214
- charts for, 160
- Free air, 228, 229
- Free gases, 49, 328
- Freezing, 352
- Frequency, 2, 182, 189, 254, 256, 261, 262, 283, 285, 286, 288–292
  - circular, 2, 252
  - forcing, 256
  - fundamental, 252
  - natural, 107, 250, 253–256, 302
  - resonant, 252, 299–302, 316
  - system, 156, 186, 391
- Frequency analysis, 424
- Frequency domain, 261
- Frequency response, 250, 252, 261, 285, 288, 291, 292, 300, 307, 309, 310, 314, 315
- diagram, 252, 292, 307
  - of branch system, 292, 307

- of parallel system, 307
- of series system, 307
- for fluctuating pressure head, 286
- for oscillating valve, 292
- for pipeline with variable characteristics, 315
  - for reciprocating pump, 288
- Frequency response method, 317
- Friction factor, 46, 77, 85, 107, 147, 181, 244, 409, 484
- Darcy-Weisbach, 45, 49, 267, 503
- Hazen-William, 49
- Friction losses, 49, 69, 108, 159, 160, 181, 182, 228, 238, 240, 242, 261, 267, 307, 392, 396, 397, 445, 486, 503, 507
- Friction term, 70, 71, 84, 85, 100, 242, 243, 261
- Froude number, 444, 477, 514
- Fully pipeline, 303
- G. M. Shrum Generating Station, 179, 182, 490
- Gas
  - liquid mixtures, 49, 328, 330, 332–336
  - dissolved, 49
  - dynamics, 450
  - entrained, 49, 86, 228, 336, 339, 341
  - free, 49, 228, 229, 328, 341
  - perfect, 232, 332, 339, 353
  - released, 228, 229, 330, 335, 336
  - undissolved, 332
  - universal constant, 364
- Generation mode, 201
- Generator, 156, 165–167, 200, 207, 209, 210, 213, 369
  - efficiency of, 165
  - inertia, 213, 407
  - load, 165, 166, 176
- output power, 156, 188
- rated output, 170
- tachometer, 179
- torque, 165
- Gordon's curves, 193, 211, 213
- Governing characteristics, 190, 367, 405
- Governing equations, 47–49, 88, 127, 133, 171, 379, 395, 450, 454, 455, 465, 486
- Governing stability, 156, 186, 187, 207
  - isolated stable, 213
- Governor, 156, 162, 166, 167, 170–172, 175, 176, 186, 192, 194, 198, 390, 391, 397, 400, 401
  - accelerometric, 169
  - block diagram, 170–172, 214
  - dashpot, 168, 169, 171, 192
  - Droop
    - temporary, 169
    - hunting, 255
    - ideal, 390, 397, 401, 405
    - proportional-integral-derivative (PID), 169, 192
  - saturation limits, 172
  - settings, 156, 192, 201, 213
    - optimum, 186, 199, 200, 213
  - temporary-droop, 169, 171
  - times, 191, 213
- Graphical analysis, 7
- Graphical method, 5, 7
- Grid points, 72, 82, 86, 87, 91, 95, 102, 124, 125, 144, 453, 466, 472
  - interior, 72
- Grid system, 202, 409
- Grid, characteristics, 453
- Guide vane, 202, 207, 255
  - curves, 207
  - openings, 207
- Harmonics, 251, 256, 260, 261, 276, 285, 288–290, 292

- even, 256, 260
- higher, 251, 252, 256, 298, 301, 304, 316
- odd, 256, 257, 260, 301–303
- Hat Creek Project, 143
  - pipeline profile, 145
- Head
  - absolute pressure, 232, 339, 341, 353, 507
  - accelerating, 383, 384
  - barometric, 233, 354, 365, 508
  - decelerating, 383, 384
  - differential, 385
  - fluctuating pressure, 286, 307
  - initial retarding, 409
  - initial steady-state, 29
  - instantaneous pressure, 250
  - intake, 381
  - mean pressure, 250, 251, 267, 286
  - net, 105, 159–162, 368, 369, 390, 391, 395, 407, 410
  - oscillatory pressure, 262, 309
  - piezometric, 48, 49, 75, 162, 231, 332, 339, 350, 360, 364, 372, 479
  - pressure, 6, 7, 11, 14, 15, 102, 129, 186, 187, 251, 260, 261, 286, 287, 289, 291, 296, 307, 311, 322, 339, 369, 413, 504
  - pumping, 116, 117, 125, 132, 137, 141, 142, 148, 238, 244, 330, 360, 372
  - rated, 79, 105, 129, 145, 147, 200, 209, 337, 391, 400, 401, 505
  - shut-off, 79, 245
  - static, 7, 141, 142, 181, 183, 213, 260, 276, 367, 381, 390, 395, 504, 507, 508
  - transient-state, 73
  - velocity, 74, 75, 77, 79, 125, 162, 381, 382, 456, 457, 464, 489
- Head loss, 45, 49, 75, 77, 79, 107, 110, 125, 137, 138, 147, 191, 209, 228, 230, 257, 279, 322, 340, 351, 354, 360, 364, 369, 379, 387, 393, 411, 456, 457, 459, 464, 504, 507
- Heart attack, 316
- Heat transfer, 330, 354
- Heat transfer, rational, 354
- Helmholtz resonator, 322
- Higher-order
  - approximation, 70
  - interpolations, 86
  - methods, 388, 470
  - schemes, 229
  - terms, 268, 460, 472
- Hill charts, for turbine, 159, 160
- Homologous relationships, 120
- Hoop stress, 41
- Hovey's stability curve, 195
- Hydraulic engineering, 48
- Hydraulic grade line, 117, 145, 147, 240, 341
- Hydraulic jump, 476, 477
- Hydraulic model, 477, 479, 484, 490, 492
- Hydraulic servo, 167, 169
- Hydraulic transients, 2, 3, 143
  - causes, 19
  - in closed conduits, 19
  - in nuclear power plants, 221
  - in oil pipelines, 237, 241
  - in open channels, 19, 437, 440
  - methods of controlling, 347, 348, 366
- Hydraulic turbine, 7, 168, 186, 255
  - characteristics of, 159, 378, 381
  - efficiency of, 7, 390, 397, 408, 417
  - load rejection, 457
  - motoring of, 160
  - operations

- load acceptance, 176, 179, 356, 407, 409, 411, 413, 457
- load rejection, 7, 171, 176, 179, 181, 183, 190, 194, 211, 213, 214, 356, 367, 369, 408, 409, 413, 414
- start-up, 176, 320, 321
- overspeed, 176, 178
- rated head, 105, 391, 400, 401
- rated output, 170
- runaway, 178
- runaway discharge, 178
- runner, 20, 159, 255
- speed rise, 190, 211–214, 367, 407
- types
  - Francis, 81, 105, 159, 161, 163, 175, 176, 178, 179, 191, 204, 207, 255, 356
  - Kaplan, 159, 161, 178, 191
  - Pelton, 162
  - Propeller, 191
  - reaction, 395, 484
- Hydroelectric Power Plant, 19, 57, 155–157, 176, 192, 378, 405, 474, 477
- Bersimiss II, 255
- Big Creek No. 3, 20, 22
- Chute-des-passes, 378, 410, 411
- Driva, 403
- G. M. Shrum, 179, 182, 490
- Kootenay Canal, 57, 207
- Oigawa, 21, 22
- transients in, 155
- Wettingen, 477
- Hysteresis, 192, 355
- Impedance
  - characteristic, 269, 270
  - diagram, 262
  - method, 261, 262
  - terminal, 262
- Implicit finite-difference method, 66, 98, 100, 101, 229, 230, 438, 465, 473, 490
- Incident pressure wave, 16
- Induction motors, 522
- Inertia
  - generator, 191, 210, 213, 407
  - normal, 147, 191, 209–211
  - pump, 116
  - pump-motor, 117, 118, 125, 142, 144, 145, 148, 337
  - turbine and generator, 156, 165, 190, 191, 200, 209, 369
  - water, 168, 228
- Inflow, lateral, 449
- Initial conditions, 47, 68, 170, 197, 333, 388, 398, 462, 463, 476
- Inlet conduit, 225
- Intake, 144, 179, 187, 207, 225, 228, 254, 381, 407
- Integration
  - arithmetic, 388
- Intensive property, 36, 40, 43
- Interior grid points, 72, 95
- Interior nodes, 72, 88, 98, 456, 467, 472
- Interior sections, 72, 102, 456
- Interpolation, 84, 86–88, 100, 144, 162, 360
  - higher-order, 86
  - linear, 86, 105, 204, 508
  - parabolic, 102
- Isoclines, 395
- Isothermal
  - conditions, 5
  - law, 332, 333
  - process, 339, 353, 387
- Johnson's chart for differential tank, 409
- Jordan River Redevelopment, 104, 318, 367
- Kandergrund tunnel, 298

- Kaplan turbine, 159, 161, 191  
 Kinetic energy, 3, 6, 11  
 Kootenay Canal hydroelectric power plant, 57, 207
- Lütschinen Power Plant, 25  
 Lac Blanc-Lac Noir pumped storage plant, 255  
 Lake, 16  
 Landslide, 440, 479  
 Landslide-generated waves, 479, 484  
     height, 479, 482, 483  
     period, 483  
     wavelength, 479
- Lax Diffusive scheme, 92  
 Lax scheme, 93  
 Lax-Wendroff finite-difference scheme, 229  
 Lax-Wendroff-Richtmyer explicit scheme, 475  
 Leading edge flowmeter, 108, 179  
 Leak detection, 428  
 Leak discharge, 430  
 Leaking seals, 228, 254  
 Leaking valve, 254–256  
 Leibnitz's rule, 40, 43  
 Limit cycle, 401, 405  
 Line packing, 239–241, 246  
 Line regulation, 241  
 Liquid column, 2, 328, 335, 336, 356  
 Liquid column separation, *see* column separation; Water-column separation  
 Liquid-vapor mixture, 229  
 Load  
     acceptance, 19, 176, 179, 356, 407, 409, 411, 413, 457, 486  
     isolated, 192, 196  
     rejection, 7, 19, 171, 176, 179, 181, 183, 190, 194, 211, 213, 214, 356, 367, 369, 408, 409, 413, 414, 457, 486, 487  
 Lumped air, 228, 229  
 Lumped-system approach, 19, 253, 270
- MacCormack scheme, 93, 470, 473, 490  
 Mach number, 47  
 Magnetic alternator, 166  
 Manning  $n$ , 411  
 Manning formula, 448, 486  
 Mathematical model, 108, 122, 132, 133, 156, 181, 191, 204, 214, 228, 336, 337, 339, 368, 369, 483, 484
- Matrices  
     banded, 468  
     field, 250, 264–270, 272, 274, 276, 280, 291, 292, 294, 296  
     point, 265, 266, 274, 276, 279–281, 283, 285, 290, 294  
     transfer, 250, 261–264, 266, 273, 274, 276, 280, 283–286, 288, 292, 295, 300–304, 307, 309, 314, *see* Transfer matrices  
 Maximum pressure charts, 507  
 Mean value theorem, 40  
 Mechanical starting time, 170, 187, 209  
 Method of characteristics, 5, 54, 55, 65, 66, 100, 116, 129, 132, 158, 181, 222, 229, 230, 238, 242, 261, 304, 307, 309, 310, 339, 349, 352, 368, 450, 451, 474, 476  
 Methods  
     analytical, 191  
     bisection, 233  
     boundary integral, 55  
     energy, 304, 310  
     Euler, 388

- explicit finite-difference, 66, 92, 100, 229, 230, 438, 454, 455, 473
- finite-element, 450, 475, 484
- Gauss elimination, 460
- graphical, 5, 7, 388
- impedance, 261, 262
- implicit finite-difference, 66, 98, 100, 101, 229, 230, 438, 465, 473
- Newton-Raphson, 128, 139, 141, 242, 301, 354, 361, 366, 459, 467
- phase-plane, 378, 392, 393, 395, 403
- predictor-corrector, 242, 243, 470
- Runge-Kutta, 175, 176, 272, 464
- separation of variable, 268
- transfer matrix, 250, 261, 262, 285, 288, 300, 304, 309, 314, 316
- Minimum pressure, due to valve opening, 504
- Models, *see also* Mathematical models
  - arithmetical, 388
  - homogeneous-flow, 229
  - hydraulic, 477, 479, 484, 490, 492
  - lumped-system, 253, 270
  - one-dimensional, 476
  - separated-flow, 336
  - tests, 159, 161, 214
  - three-dimensional, 479
  - two-dimensional, 476, 483
- Modulus of rigidity, 52, 107
- Mole fraction, 329
- Moment of inertia, 117, 132, 142, 144, 145, 148, 149, 170, 187, 200, 330
- polar, 125, 141, 165, 191, 200, 369, 522
- Momentum equation, 36, 43, 45, 54, 88, 267, 449
- Moody formula, 159
- Morrow Point Reservoir, 479
- Needle valve, 168
- Net head, 105, 159–162, 368, 369, 390, 391, 395, 407, 410
- Newton's second law of motion, 8, 28, 36, 43, 186, 381, 383, 414, 442
- Niagara Falls Development, 411
- Node, 72, 85, 256, 257, 298, 299, 394, 396, 398, 400, 401, 451, 453
- Non-adiabatic process, 332
- Non-reflecting boundary, 81
- Normal mode, 253, 302
- Nuclei, 328
- Oigawa Power Plant, 21, 22
- Oil batch, 244
- Oil pipeline, 237, 238, 241, 242, 244, 366
- Oil-hammer, 3, 238
- Ok Menga Power Plant, 25
- One Coefficient Model, 90
- One-dimensional flow, 38, 39, 438, 445, 476
- One-way surge tank, 144, 145, 148, 337, 356, 379
- Open channels, 19, 437
  - boundary conditions for, 456
  - surface profile, 464
  - transients in, 19, 437, 438, 440, 477
- Operating conditions
  - catastrophic, 183, 245
  - emergency, 142, 143, 147, 182, 183, 245, 356
  - exceptional, 142, 143, 182
  - normal, 20, 117, 142, 143, 182, 183, 245, 356, 414
- Operating guidelines, 20, 244
- Operation

- float-tank, 241
- isolated, 190, 210, 211, 356, 367
- put-and-take, 241
- synchronous, 356, 367, 368
- tight-line, 241
- Operations-research techniques, 367
- Optimal control of transient flows, 348, 366
- Optimum values, 172, 198, 200
- Optimum valve closure, 366
- Orifice, 109, 277
  - air chamber, 351, 353
  - differential, 351, 354
  - equivalent, 228
  - head loss, 110, 228, 351, 354
  - point matrices, 267, 274, 276, 279, 285
  - surge tank, 371, 378, 380, 383, 385, 405, 408, 409
- Oscillating valve, 276, 277, 283, 284, 286, 290–292, 296, 301, 302, 307, 314
  - point matrices for, 279
  - transfer matrix for, 314
- Oscillations
  - auto- or self-excited, 254–256
  - free-damped, 300
  - stable, 187, 192, 195, 197, 390, 392, 401, 403, 405
  - tidal, 476
  - unstable, 187, 197, 390, 392, 401, 405
- Outflow, lateral, 449
- Parabolic
  - extrapolation, 163, 176
- Parallel channels, 468
- Parallel loops, 262, 274
- Parallel pipes, 266
- Parallel pumps, 129, 132, 133, 360
- Parallel system, 273, 274, 307, 468
- Partial blockage detection, 424
- Peak pressure frequency response, 423
- Pelton turbine, 162
- Penstock, 6, 20, 22, 57, 105, 107, 158, 179, 183, 186, 187, 191, 192, 207, 209, 211, 213, 318–321, 356, 368, 378, 384, 397, 407, 409
  - design criteria for, 182, 407
- Perfect gas, 332
  - law, 232, 339, 353
- Period, 2, 73, 147, 179, 242, 250, 252, 288, 289, 310, 314, 321
  - fundamental, 251, 252
  - natural, 254, 256, 288
  - of flow oscillations, 250
  - of fundamental, 304
  - of higher harmonics, 251, 252, 304
  - of oscillations of frictionless system, 388
  - of pressure oscillations, 108
  - of surface waves, 254
  - of surge tank oscillations, 389, 414
  - theoretical, 15, 251, 252, 314
- Periodic flow, 2, 3, 249, 250, 256, 476
- Phase angle, 277, 289, 291, 307, 309, 311, 314, 322
- Phase portraits, 393, 395, 398, 401, 402
- Pilot valve, 167, 169, 355
- Pipe
  - concrete, 8, 52, 53
  - metal, 8
  - PVC, 53
  - rigid, 8, 10
  - thick-walled, 50, 53
  - water supply, 366
  - wood-stave, 53
- Pipeline, 16
  - design criteria for, 116, 142
  - rupture, 242, 245
  - Toulouse, 303

- with variable characteristics, 271, 314
- Piping systems
  - branch, 266, 280
  - flowchart, 102
  - parallel, 262, 273, 274
  - series, 251, 265, 274, 276, 286
- Point matrices, 250, 265, 266, 274, 290
  - extended, 279, 285
  - for air chamber, 322
  - for branch junction, 274, 280, 281
  - for orifice, 267, 274
  - for oscillating valve, 279, 290
  - for series junction, 267, 274
  - for simple surge tank, 322
  - for valve, 267, 274
- Point matrix, leak, 430
- Point matrix, partial blockage, 425
- Poisson's ratio, 41, 50, 51
- Polytropic law, 232, 339, 353
- Positive surge, 514
- Potential energy, 6
- Potential surge, 238–240, 246
- Potentiometer, 108
- Power failure, 20, 116, 118, 122, 125, 132, 143–145, 147, 225, 229, 240, 241, 245, 246, 330, 351, 352, 355, 504–507, 522
- Power intake, 179, 207
- Power plant
  - hydroelectric, 19, 57, 155, 156, 176, 192, 195, 207, 378, 405, 410, *see also* Hydroelectric power plants
  - nuclear, 222
- Preissmann implicit scheme, 465
- Pressure, 2
  - charts for maximum and minimum, 504
  - fluctuating, 286
  - partial, 329, 336
- Pressure controllers, 241, 244
- Pressure drop, 242, 332, 348, 351, 352, 355, 362, 367, 378
- Pressure frequency response, 423
- Pressure gradient, 47
- Pressure regulator, 356
- Pressure rise, 3, 6, 10, 142, 145, 147, 212, 213, 238–242, 246, 276, 337, 348, 355, 367, 378, 504
- Pressure transducer, 132
- Pressure wave, 2, 3, 5–8, 11, 15, 16, 50, 57, 96, 116, 228, 252, 298, 328, 330, 336
  - negative, 16
  - positive, 16
- Pressure-regulating valve, 105, 109, 183, 318, 337, 355, 356, 360, 362, 368, 369
- Pressure-relief valve, 244, 355, 356, 360
- Primary compensation, 168
- Principle of superposition, 276
- Propeller turbine, 191
- Protective devices, 117
- Prototype, 105, 107, 161, 335, 336, 369
  - efficiency, 159
  - pump characteristics, 120
  - tests, 49, 50, 105, 108, 131, 156, 175, 214, 244, 337, 477, 484, *see also* Field test
- Proximal pressure, 317, 318
- Prudhoe Bay, 237
- Pulsation dampeners, 246
- Pump
  - centrifugal, 116
- Pumped-storage projects, 201, 202, 366
- Pumping head, 116, 117, 125, 132, 137, 238, 244, 330
- Pumping mode, 201
- Pumps, 19, 55, 73, 117
  - axial flow, 121
  - booster, 137, 139

- boundary conditions, 127, 133
- centrifugal, 7, 79, 80, 117, 120
- characteristic curve, 122
- characteristics, 7, 116, 117, 122, 138, 141, 147, 338, 339
- diffuser, 121
- discharge line, 133, 135, 141, 144, 245
- double suction, 122, 338
- flowchart for, 129
- impeller, 117, 120, 121
- inertia, 116, 227
- main, 137
- mixed flow, 121
- multiplex, 245
- overspeed, 348
- parallel, 129, 132, 133
- performance curve, 79, 117
- power failure, 20, 55, 116, 118, 125, 132, 144, 145, 147, 225, 229, 240, 241, 245, 246, 330, 351, 355, 504, 505
- put-and-take operation, 241
- pyramidal effect, 240
- quadrants, 118
- radial flow, 121
- rated conditions
  - discharge, 117, 136
  - head, 117, 136
  - speed, 117
- reciprocating, 241, 245, 254, 288
- rotational speed, 116
- runaway speed, 117
- runaway test, 132
- series, 133, 137
- shutoff head, 245
- shutoff valve, 202
- specific speed, 121, 122
- start-up, 116, 141, 144
- start-up time, 141
- starting and stopping, 19, 116
- suction line, 117, 122, 129, 132, 133, 135, 136, 138, 141, 144, 288
- torque characteristics, 124, 125
- tripping of, 142, 201, 225
- vacuum, 225
- zones of operation, 121, 144
- Radial contraction, 39
- Radial expansion, 39
- Radial velocity, 39
- Rapidly varied flow, 19, 438
- Rarefaction control, 241, 246
- Rarefaction waves, 329
- Rated
  - conditions, 117
- Recirculating system
  - combine and once-through, 222, 223
  - cooling water, 223
- Reference speed, 166
- Reflected wave, 16
- Reflection coefficient, 15, 16
- Regulating characteristics, 378
- Regulation
  - line, 241
  - speed, 6
  - station, 241
- Reinforced concrete pipe, 52
- Reservoir, 16
  - constant level, 11, 16, 75, 85, 181, 302, 314, 467
  - downstream, 75, 467
  - upstream, 11, 467
- Residual, 302, 303, 307
- Resonance, 242, 245, 249, 250, 254, 298, 299, 318, 319, 321
- Resonant
  - conditions, *see* Resonance
  - frequency, 252, 262, 299, 302, 316
- Resonator, Helmholtz, 322
- Retrofitting, 223
- Revelstoke Reservoir, 479
- Reynolds number, 46

- Reynolds transport theorem, 36, 39, 40, 43
- Rhythmic opening and closing, of a valve, 7
- Rigid water-column theory, 192
- Riser, surge tank, 378, 384
- Rivers, 19
- Rocket-engine-propellant feed system, 255
- Root locus technique, 262
- Round-off errors, 83
- Routh-Hurwitz criteria, 194
- Runge-Kutta method, 175, 176, 272, 464
- Runner turbine, 20, 159, 255, 484
- Safety valve, 6, 355, 356
- Saint-Venant equations, 445, 449, 451, 455, 462, 468, 476, 477, 479
- conservation form, 450
  - nonconservation, 449
- Scale effects, 159
- Scroll case, turbine, 158, 181, 192, 216
- Seal-well weir, 222, 224, 225
- Second-order approximation, 71, 85, 242, 243
- Secondary compensation, 168
- Secondary water-surface fluctuations, 486
- Self-excited oscillations, 254, 256
- Self-regulation coefficient, 189
- load, 189
  - turbine, 189
- Self-regulation constant, 181
- Separatrix, 398
- Series junction, 17, 77, 78, 109, 265, 267
- Series system, 109, 286, 299, 303
- Servomechanism, 166
- Servomotor, 174, 181, 202, 355
- Seton Project, 479, 484, 486
- Sewer, 19
- Sewers, 438, 440, 474, 477, 479
- Shear force, 44
- Shear modulus, 53
- Shear stress, 44, 45, 332
- Shock, 55, 96, 229, 438, 440, 451, 470, 474
- Simple harmonic motion, 171
- Singular point (or singularity), 393–395
- compound, 401
  - nonsimple, 394
  - simple, 394
  - types
    - focus (or spiral), 394, 398, 400–402
    - node, 394, 396, 398, 400–402
    - saddle, 396, 398, 401
    - virtual, 395, 396, 399
- Singularity, 394
- Siphon, 132
- Slope, 48, 67, 92, 189, 205, 254
- energy grade line, 448
  - side, 446
- Sluice gate, 239, 440
- Smoothening procedure, 229
- Snettisham project, 386
- Sonic velocity, 365
- Specific heat, 366
- Specific speed
- pump, 121, 122
  - turbine, 207
- Specific weight, 54, 126, 186, 231, 311, 365, 381, 445
- Speed
- oscillation, 172
  - regulation, 6
  - rise, 166, 190, 211–214, 407
  - sensing device, 166
- Speed droop, 167
- permanent, 167, 171, 172
  - temporary, 167, 168, 172
- Speed-no-load gate, 159, 179, 183, 204, 484, 486
- Spray ponds, 223, 224
- Spring constant, 168

- Spring-mass system, 252, 255, 256  
 St. Lawrence River, 499  
 Stability  
     criteria, 82, 83, 186, 192, 195  
     diagram of surge tanks, 392  
     limit, 85  
         curve, 192, 195  
     numerical, 83  
 Standpipe, 350, 371, 372, 378, 413  
 Starting time  
     mechanical, 170, 186, 187  
     pump, 141  
     water, 186, 187, 211  
 State vector, 262–264, 273, 276, 291, 296  
     extended, 264, 279  
     intermediate, 301  
 Static head, 7, 141, 181, 183, 213, 260, 276, 367, 381, 390, 395, 504, 507  
 Steady flow, 2, 10, 11, 45, 47, 108, 250, 440  
 Steady-oscillatory flow, 2, 3, 250, 254, 256, 257, 261, 262, 266, 310  
 Steady-state conditions, 15, 19, 49, 72, 76, 102, 129, 222, 225, 229, 232, 243, 339, 353, 360, 461, 462, 514  
 Steamhammer, 3  
 Steamy generator, 222  
 Steel-lined tunnel, 52, 58  
 Stenosis, 316, 318  
     intermediate-grade, 317  
 Stent, 316  
 Strain, 41  
 Strain gauge pressure cell, 107  
 Stress, 41  
 Subcritical flow, 444  
 Subsonic velocity, 365  
 Suction line, 117, 122, 127, 129  
 Supercritical flow, 444, 476  
 Support conditions, 42  
 Surface profile, open channels, 464  
 Surface tension, 328, 332, 334  
 Surge  
     absolute velocity of, 514  
     analysis, 238  
     differential, 379, 384, 385, 408  
     free, 414  
     height, 440, 443  
     potential, 238–240, 246  
     protection, 225  
     suppressor, 142, 143, 355, 360  
 Surge tanks (or surge chambers), 6, 19, 73, 142, 143, 156, 158, 183, 246, 298, 337, 348, 349, 352, 377, 378  
     boundary conditions, 349  
     charts for upsurges or down-surges in, 507, 511  
     closed, 378, 385, 386, 416  
     design criteria, 407  
     differential, 378, 384, 408  
     downstream, 410, 411  
     drainage, 409  
     dynamic and continuity equations, 379, 381, 382  
     for closed tank, 385–387  
     for differential tank, 384, 385  
     for orifice tank, 383  
     for simple tank, 381  
 gallery, 409  
 governing equations, 379  
 inclined, 415  
 multiple, 405, 416  
 one-way, 144, 145, 148, 337, 356, 378  
 open, 402  
 orifice, 371, 378, 405, 408  
 period of oscillations, 511  
 simple, 349, 378, 381, 511  
 stability of, 395  
 stability of, 378, 401  
 system of, 405  
 tailrace, 382, 414  
 tower-type, 367  
 types of, 380  
 upstream, 367, 378, 411

- virtual, 372
  - with standpipe, 371
- Surge wave
  - absolute velocity, 514
  - celerity of, 440, 514
  - negative, 439
  - positive, 439
  - velocity of, 487
- Synchronous operation, 356, 367
- Synchronous speed, 159, 160, 166, 167, 170–172, 176, 179, 181, 191, 209, 216
- Systems, *see also* Cooling water systems; piping systems
  - boundaries, 36
  - branch, 280, 292, 301, 307, 314, 322, 468
  - closed, 241
  - control, 25, 255
  - distributed, 19, 253, 267, 270, 271, 378
  - lumped, 19, 253, 267, 270, 349, 378
  - parallel, 273, 274, 468
  - parameters, 45
  - pressure-regulating-centrifugal pump, 360, 362
  - response, 20, 261, 276, 285, 286, 290, 348, 366
  - series, 109, 286, 299, 307
  - spring-mass, 252, 255, 256
  - surrounding, 36
- Tachometer generator, 179
- Tailrace channel, 179, 492
- Tailrace manifold, 179, 411, 414
- Tailrace tunnel, 19, 179, 405, 410, 414, 474, 477, 479, 490, 492
- Tailwater level, 162, 490
- Temporary speed droop, 168
- Thermodynamic effects, 335
- Thoma area, 392, 398, 401, 408
- Thoma criterion, 393
- Throughput, 244
- Tidal oscillations, 476
- Tides, 438–440, 476
- Tight-line operation, 241
- Time constant, 171
  - actuator, 172
  - dashpot, 168, 181
  - distributing valve, 172
- Time domain, 261, 317
- Time increment, 102, 176, 462
- Time interval, 2, 37, 71, 86–88, 91, 100, 162, 453
  - computation, 88
- Toulouse pipeline, 303, 307
- Transfer matrix, 250, 262–264
  - extended, 286, 292
  - overall, 283, 291
  - field, 264, *see also* Field matrix
    - overall, 263, 265, 274, 276, 280, 292, 300, 303
    - overall, 265
    - point, 250, *see also* Point matrices, 265, 280
- Transfer matrix method, 261, 262, 286, 304, 309, 311, 316, 321
- transfer matrix method, 422
- transient, 422
- Transient analysis, 57, 116, 120, 352, 367, 503
- Transient cavitation, 328, 336
- Transient conditions, 19, 47, 102, 116, 129, 144, 162, 225, 241, 336, 368, 379, 461
  - for opening or closing a valve, 67, 96, 105
- Transient flow, 2, 3, 11, 19, 36
  - optimal control of, 348, 366
- Transient state, 45, 73
  - energy losses, 45
- Transient time, 100, 102
- Transients, *see also* Hydraulic transients
  - caused by pumps, 115, 116
  - causes of, 19, 225, 241

- controlling, methods for, 347, 348  
 in closed conduits, 19  
 in cooled water systems, 221  
 in hydroelectric power plants, 19, 20, 155  
 in long oil pipelines, 237  
 in nuclear power plants, 221  
 in open channels, 19, 437, 438  
 in power canals, 19, 438  
 in pumped-storage projects, 201  
 methods of controlling, 347  
 pressures, 55, 68, 108, 143, 179, 227  
 Transmission coefficient, 15  
 Transmission line, 19  
 Transmitted wave, 16  
 Traveling waves, 5  
 Trough pressure frequency response, 423  
 Truncation error, 82  
 Tuner, 322  
 Tunnel, 105, 158, 378  
     free-flow, 187  
     free-surface flow, 158  
     lined, 52  
     rock, 8, 52  
     steel-lined, 52  
     tailrace, 179, 474, 479  
     unlined, 52, 411  
     unlined rock, 52, 85  
 Turbine, *see also* Hydraulic turbine  
     boundary conditions, 162  
     characteristics of, 159, 161–163, 181, 182, 202, 204  
     discharge, 159  
     efficiency, 390, 397  
     gate closing time, 170  
     gate deviation, 170  
     gate opening, 156, 159–162, 167, 170, 183, 191, 194  
     hill charts for, 159  
     motoring, 160  
     net head, 159, 368, 390, 407, 410  
     operations  
         load acceptance, 55, 156, 176, 356, 411, 413, 457  
         load rejection, 7, 25, 55, 171, 176, 181, 183, 213, 356, 408, 413  
         start-up, 156, 176, 320  
     overspeed, 181, 348  
     power output, 159, 188, 391  
     rated head, 181, 200, 209, 391  
     rated output, 170, 188, 209  
     reference speed, 166  
     relative gate opening, 167  
     rotational speed, 156, 159, 165, 166, 170, 187  
     runaway speed, 161  
     runner, 20, 159, 181, 484  
     runner blade, 255  
         angle, 159  
     scroll case, 158, 181, 192  
     shutdown, 202  
     speed, 156, 162, 183  
         deviation, 169, 170  
         rise, 166  
     stability, 156  
     types  
         Francis, 81, 105, 159, 175, 204, 207, 255, 356  
         impulse, 159  
         Kaplan, 159, 161, 191  
         Pelton, 162  
         Propeller, 191  
         pump, 117, 202  
         reaction, 395, 484  
     unit discharge, 161, 162, 202, 204  
     unit flow, 159  
     unit power, 159, 161  
     unit speed, 159, 178, 181, 202  
     unit torque, 202  
 Turbine flow-demand characteristics  
     constant flow, 390

- constant gate opening, 390
- constant power, 390, 397
  - combined with full gate, 390, 400
- Turbo-machine, 201
- Turbogenerator, 156, 160, 165, 170, 172, 186, 405
- TVA curves, 211
- Two-coefficient model, 91
- Two-phase flow, 334
  - homogeneous, 229
  - homogenous, 229
  - separated, 229
- U.S. Geological Survey, 499
- Undissolved gases, 332
- United States Bureau of Reclamation, 191, 210
- Universal gas constant, 364
- Unsteady flow, 2, 3, 8, 261, 438
- Upsurge, 409, 506, 507
- Vacuum breakers, 225, 228
- Vaiont slide, 479
- Valve
  - Air-inlet, 356
- Valves, 3, *see also* Oscillating valve, 8, 11
  - air, 132, 142, 147, 255, 337, 355, 362
  - boundary conditions for, 76, 354
  - bypass, 255, 318, 319, 321
  - characteristics, 254
  - chattering of, 19
  - check, 116, 142, 143, 145, 148, 246, 255, 351, 355, 356, 507
  - closing time, 145
  - control, 141, 241, 245, 366
  - discharge, 116, 122, 125, 132, 133, 147, 360
  - distributing, 167, 172, 174
  - downstream, 3, 76
  - leaking, 254–256
- opening or closing, 105, 143, 225, 229, 241, 257, 366
- optimum closure, 366
- pilot, 167, 169
- point matrices for, 267
- pressure-regulating, 105, 183, 318, 337, 355, 356, 362
- pump, flowchart, 362
- pressure-relief, 244, 337, 355
- rhythmic or periodic movements, 7
- safety, 6
- siphon, 133
- stroking, 366
- turbine inlet, 318–320
- uniform closure, 504
- Vapor cavities, 328
- Vapor pressure, 46, 49, 117, 328, 330, 355
- Vapors, 4
- Velocity
  - of pressure waves, *see* Waterhammer, wave velocity
  - subsonic, 365
- Velocity gradient, 47, 328
- Vibrations, 250, 255
  - mechanical, 262
  - self-excited, 255
  - steady, 255, 256
- Viscosity
  - artificial, 472–474
  - kinematic, 268
- Void fraction, 229, 332, 333, 335, 339
- Von Neumann stability analysis, 84, 85, 468, 473
- Vortices, 225
- Water boxes, 225, 228, 230
- Water starting time, 186, 187
- Water-column separation, 2, *see also* Column separation, 117, 143, 144, 227, 329, 337
- Waterhammer, 2, 3, 8, 98

- pressure, 6, 7, 191, 211
- wave velocity, 6, 211
  - in air-water mixture, 49
  - in gas-liquid mixture, 49, 328, 330, 332
  - in noncircular conduits, 53
  - in PVC pipes, 53
  - in reinforced concrete pipes, 52
  - in rock tunnels, 52
  - in steel-lined tunnels, 52
  - in thick-walled conduits, 50
  - in thin-walled conduits, 52
  - in wood-stave, 53
- waves, 6, 378
- Wave
  - reflected, 17
  - transmitted, 17
- Wave front, 8, 9, 11, 16, 86, 87, 239, 240, 440, 444
- Wave reflection, 15
- Wave(s), 438, *see also* Pressure wave
  - absolute velocity of, 514
  - amplitude, 5
  - attenuation, 483
  - celerity, 5, 438–440, 442, 444, 479, 514
  - Favre's, 477, 486
  - propagation, 2, 3, 5, 11, 15, 45, 86
  - reflection, 2, 6, 11, 15, *see* wave reflection
  - types
    - deep-water, 50, 439
    - flood, 19
    - impulse, 479
    - landslide-generated, 479
    - monoclinal, 439
    - negative, 11, 16, 330, 439
    - positive, 17, 439, 443, 444
    - rarefaction, 329
    - shallow-water, 439
    - solitary, 439, 482
    - sound, 3
- standing, 254
- stationary, 439
- train, 439, 482
- translatory, 439
- traveling, 5
- water, 3
  - waterhammer, 6, 211, 378
- velocity, 2, 5, 6, 8, 36, 42, 46, 49, 129
- Wavelength, 4, 438, 439
- Wettingen Hydroelectric Power Plant, 477
- Wicket gates, 105, 108, 156, 169, 356
  - breakaway gate, 178
  - effective closing time, 167, 174, 183, 191, 211, 407, 484
  - effective opening time, 167, 174, 183, 484
  - opening, 159, 162, 163
  - speed-no-load gate, 159, 179, 183, 204, 484, 486
  - windage losses, 159, 160
- Wind Gap Pumping Plant, 131, 133, 144
- Young's modulus of elasticity, 50, 51, 334
- Zomming, 110
- Zone
  - of energy dissipation, 116, 118
  - of pump operation, 118
  - of turbine operation, 118
- Zones and quadrants, 118